Karlsruher Institut für Technologie

Entsorgungsforschung

2nd Chinese-German Workshop on Radioactive Waste Disposal

Karlsruhe Institute of Technology (KIT)
Campus North, Building 418
October y 15-16, 2012

A joint workshop organized by

Beijing Research Institute of Uranium Geology, (BRIUG), China
Federal Institute for Geosciences and Natural Resources (BGR), Germany
Project Management Agency Karlsruhe (PTKA) - Karlsruhe Institute of Technology, Germany

Ed. W. Steininger

Projektträger Karlsruhe
Wassertechnologie und Entsorgung (PTKA-WTE)

Projektträger für das

Bundesministerium
für Wirtschaft
und Energie

Herausgeber:
Projektträger Karlsruhe
Wassertechnologie und Entsorgung (PTKA-WTE)
Karlsruher Institut für Technologie (KIT)
Hermann-von-Helmholtz-Platz 1
76344 Eggenstein-Leopoldshafen
Internet: www.ptka.kit.edu

neu zusammengestellt Juli 2017

PTKA
Projektträger Karlsruhe
Karlsruher Institut für Technologie

Der vorliegende Materialienband dient der aktuellen Unterrichtung der auf dem Gebiet der Entsorgung radioaktiver Abfälle arbeitenden Institutionen und der zuständigen Behörden.
Verantwortlich für den Inhalt sind die Autoren. Das Karlsruher Institut für Technologie (KIT) übernimmt keine Gewähr insbesondere für die Richtigkeit, Genauigkeit und Vollständigkeit der Angaben sowie die Beachtung privater Rechte Dritter.

Eine auszugsweise oder vollständige Vervielfältigung ist erlaubt, wenn die Zustimmung der betroffenen Autoren vorliegt.

Berichte und Publikationen zu
Projektstatusgesprächen, Kolloquien und Fachgesprächen
sind über die Internetseite

www.ptka.kit.edu/wte/171.php

des PTKA zu finden.

Foreword

Most countries using nuclear power face the problem of safe disposal of the radioactive wastes. Although for highly radioactive wastes (spent fuel, high-level waste, and some types of long-lived radioactive waste) a repository is still pending, there is international consensus that the preferred solution is disposal in deep geological repositories in the three most favored host-rock media crystalline rocks, evaporitic / salt rocks and argillaceous rocks.

Both China and Germany are well aware that the management of radioactive waste is necessary and indispensable. It is well known that the disposal of these waste types is a challenge in a multifold way and demands sound technical and scientific knowledge and expertise to do it safely and securely.
Against this background, the common *1st Chinese-German Workshop on Radioactive Waste Disposal* was successfully held in Beijing, May 2007. The main purpose of the then workshop was to present ideas, exchange information, and to foster discussion among the experts. AND: It was recognized that the exchange of information is the crucial point.

Since then in both countries progress was made and changes occurred concerning the topic “Disposal of Radioactive Waste”. It was recognized that the purpose of the first workshop still was very important. Therefore it was considered essential to inform mutually on new developments and advancements in the national HLW-disposal programs and to exchange current R&D outcomes and the progress made focusing esp. on results regarding crystalline and argillaceous host rock.

Considering this and the bilateral common interests PTKA, BGR, and BRIUG decided to organize jointly the *2nd Chinese-German Workshop on Radioactive Waste Disposal* in Karlsruhe, Germany.
Twenty four Chinese and twenty two German attendants participated in the workshop. They all represented academia, industry, research, state-owned organizations and other important institutions involved in radioactive waste management activities.
In total twenty three presentations were given focusing on following topics:

- Geology of potential formation
- Geomechanics and rock mechanics
- Long-term safety analysis
- Radionuclide migration
- Behavior of vitrified waste

It was agreed to collect the excellent presentations and to make it available both to document the outcomes of this event and also to have it at the disposal for the attendees and for a larger interested community.

We greatly acknowledge the contributions of all workshop participants.

Hua Shao Walter Steininger Ju Wang

TABLE OF CONTENT

Introductory presentations **2**

KIT Overview **3**

Geological disposal of high-level radioactive waste in China: update 2012 **16**
Wang, J., BRIUG

A new approach for siting a repository for HLW in Germany **62**
Bräuer, V., BGR

Topic: Host rock characterization (rock mechanics / hydrogeology) **89**

Rock mass characterization for the preselected Beishan area, Gansu province of China´s HLW radioactive waste repository **90**
Wang, G., CAS, Institute of Soil & Rock Mechanics

Multi-scale applications of electrical resistivity tomography in the site characterization for HLW disposal **131**
Zhou, Y., Nanjing University

Characterization of fracture networks on different scales **222**
Li, X., Nanjing University

German experience and investigations regarding host rock characterization **265**
Shao, H. Sönnke, J.,BGR

German experience and investigations regarding host rock characterization **290**
Schäfer, T., KIT/INE

A fractional derivative approach to creep of rock salt **321**
Zhou, H.W., CU of Mining & Technology

Basic principles of rock salt disposal **359**
Lux, K.-H., TU Clausthal

Topic: Technical / geotechnical barriers **402**

THMC-testing of expandable clays for potential use in HLW disposal repository **403**
Liu, X., East China Institute of Technology

Experimental investigation on thermo-hydraulic behavior of compacted GMZ02-bentonite **429**
Ye, W., Tongji University

Initial results on stability of natural GMZ Ca-Bentonite and modified Na-Bentonite under thermal/radiation aging **476**
Yang, Z., China Institute for Radiation Protection

THM-behavior of clay **505**
Zhang, C-L.,GRS

Bentonit characterization / behavior **524**
Kaufhold, St., Dohrmann, R., BGR

Project “PEBS” **553**
Wieczorek, K., GRS

Modeling of bentonite behavior **574**
Li, X.,TU Clausthal, et al.

Topic: Radionuclide behavior **593**

Study on the long-term behavior of HLW glass in geological conditions **594**
Wang, B., CAEA

German experiences on HLW glass systems **612**
Kienzler, B., KIT/INE

RN migration research to support geological disposal of HLW in China (Zhou, CAEA) 14:30 Critical issues for Pu239 in geological disposal **636**
Zhuo, D., et al., Chengdu University

Chemical behavior of Pu239 in the groundwater solution **660**
Xu, J., et al., Chengdu University

Topic: Technical / Engineering **681**

Feasibility of CS canister used for HLW geological disposal **682**
Dong, J., CAS, Institute of Metal Research

German concepts for containers / casks for HLW-disposal **728**
Biurrun, E., et al., DBE Technology GmbH

Annex **752**

Agenda
List of participants
Picture

Karlsruhe Institute of Technology

2nd- Chinese-German Workshop on Radioactive Waste Disposal

Karlsruhe, October 15 -16, 2012

PTKA
Project Management Agency Karlsruhe
Karlsruhe Institute of Technology

BGR Bundesanstalt für Geowissenschaften und Rohstoffe

BRIUG

Federal Ministry of Economics and Technology

Monday, October 15, 2012

INTRODUCTORY PRESENTATIONS

Karlsruhe Institute of Technology

Karlsruhe Institute of Technology

The Merger of Forschungszentrum Karlsruhe and Universität Karlsruhe

RESEARCH – TEACHING – INNOVATION

The KIT Vision

Feature of uniqueness:
KIT eliminates the pillar structure!

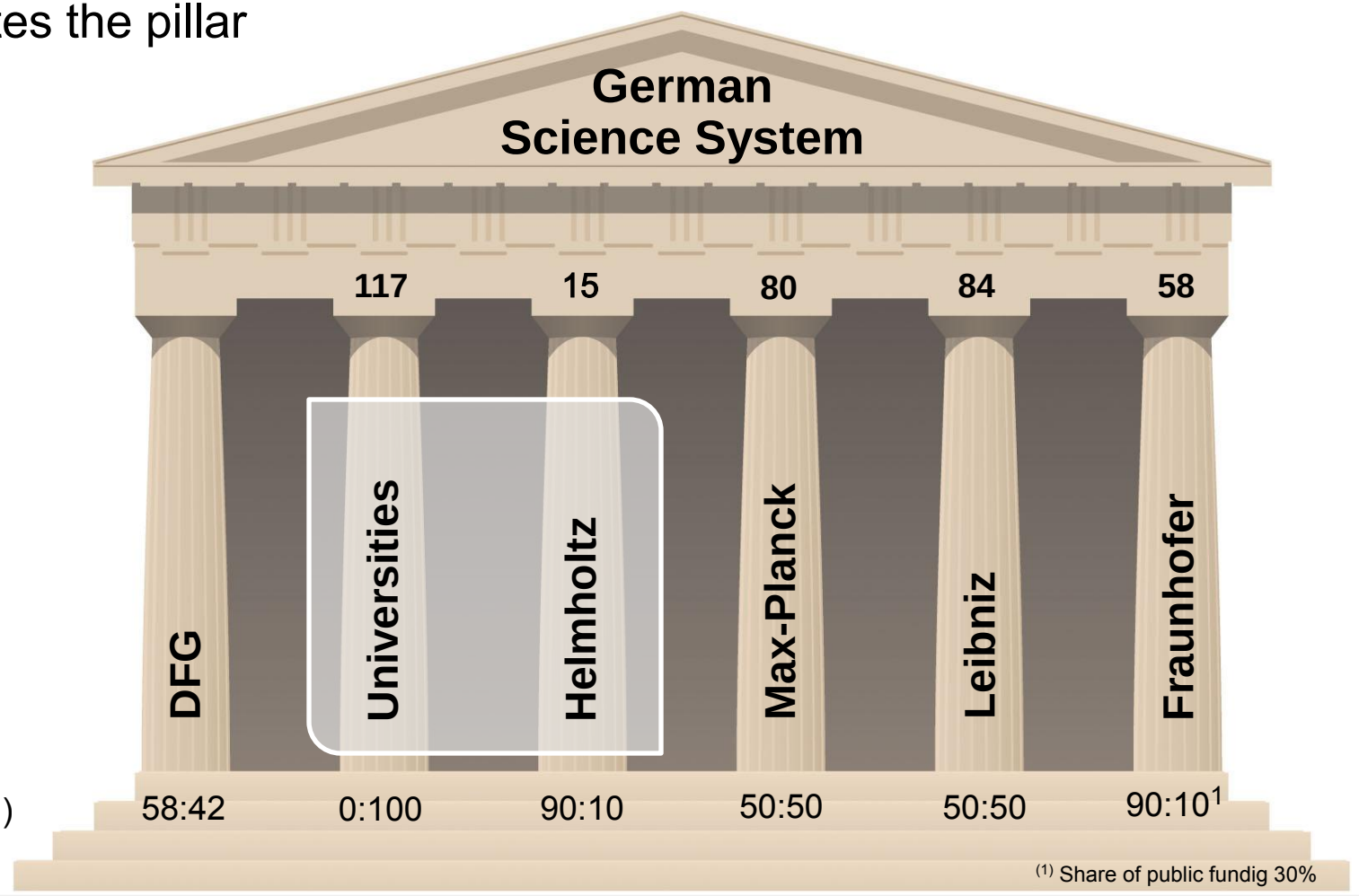

Common Objective

Positioning as an institution of excellent research and teaching in natural and engineering sciences on an international scale, with scientific excellence and worldwide top level in

- Research

- Teaching

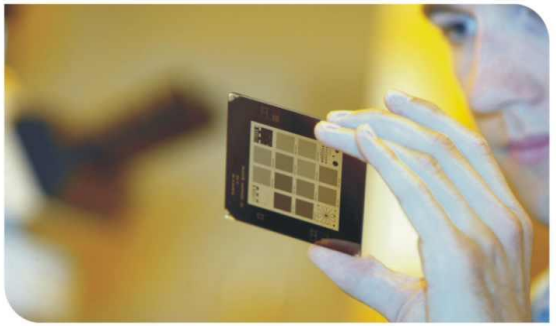

- Innovation

Prerequisite:
Excellent infrastructure and service units.

Staff

Employees	**9,139**
Teaching and research	5,636
Infrastructure and services	3,503
Professors	364
Foreign scientists	777
Trainees	509
Students (WS 2011/2012)	**22,552**

Status 2011

Strong Teaching: 364 Professors

Internationally Attractive: 777 Foreign scientists

Excellent Training: 509 Trainees

22,552 Students

Centers and Focuses

KIT - Zentren

- **Energy** 01.01.08
- **NanoMikro** 01.01.08
- **Elementary particle and astro particle physics** 01.01.08
- **Climate and environment** 01.01.09
- **Mobility systems** 01.01.11

KIT-Schwerpunkte

- **COMMputation** 01.05.08
- **Humans and Technology** 15.07.09
- **Optics and Photonics** 01.01.10
- **Anthropomatics and Robotics** 01.07.2010

KIT - Schools

- **School of Optics and Photonics** 13.10.06
- **School of Energy** *2011*
- **…** **Schools**

Example: KIT Energy Center

Research Topics

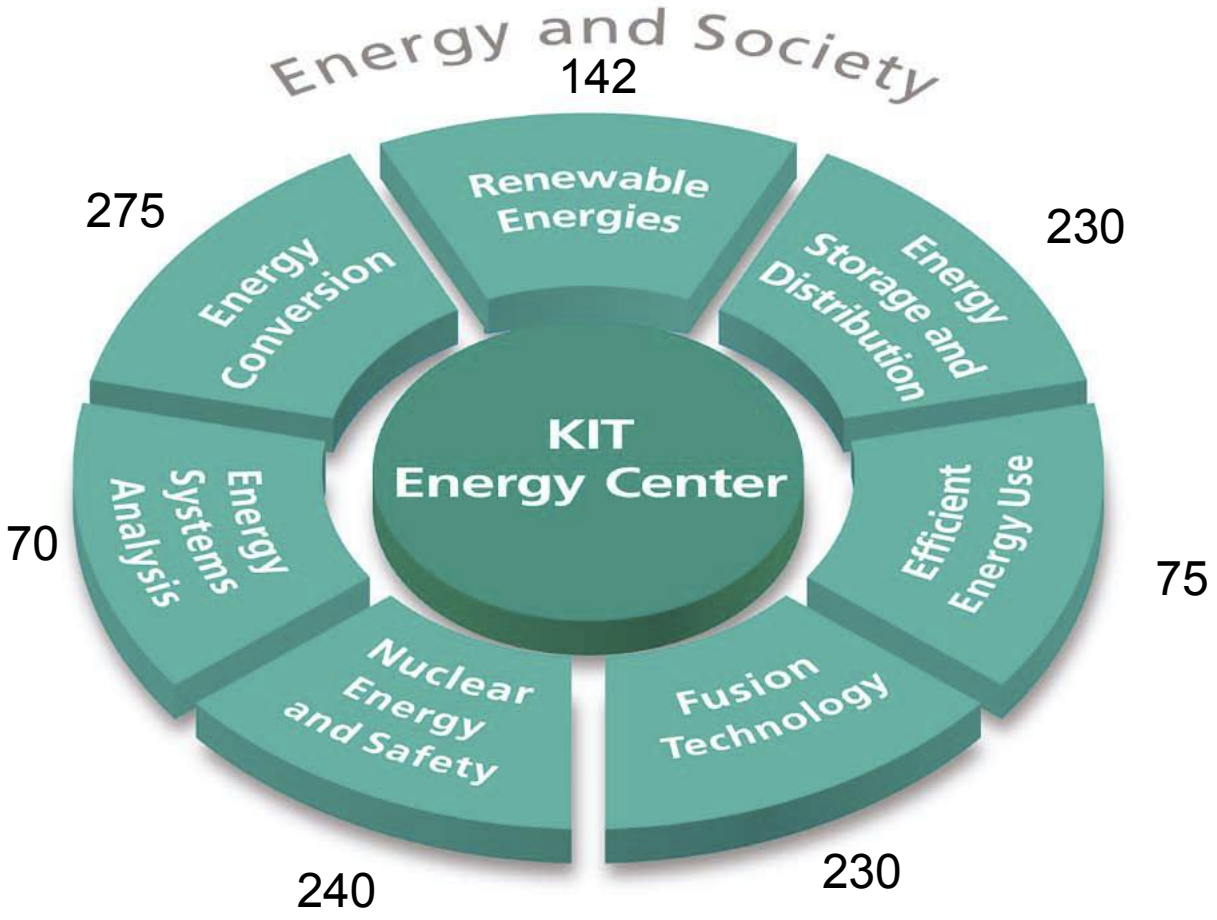

Employees: 1250
Budget: 250 M€

New orientation of the programme nuclear safety research

Nuclear waste disposal and safety

- FZJ, HZDR, KIT
- Reduction of personnel: 11%
- Concentration on topic in the field of nuclear waste disposal

Research programme 2010 - 2014: Total staff: 272 FTE

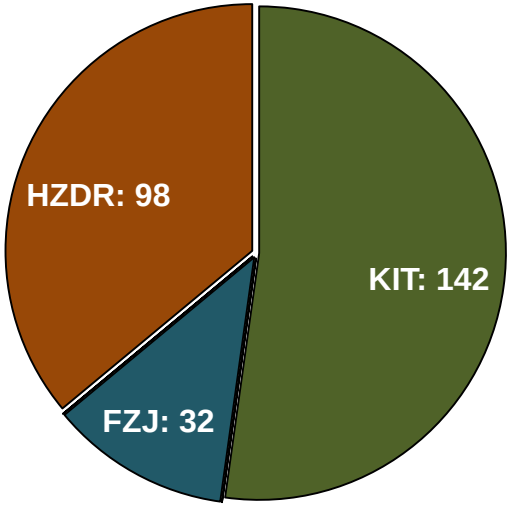

KIT Helmholtz
FZJ Helmholtz
HZDR Helmholtz

-29.5 FTE
-11%

Research programme 2015 - 2019: Total staff: 242,5 FTE

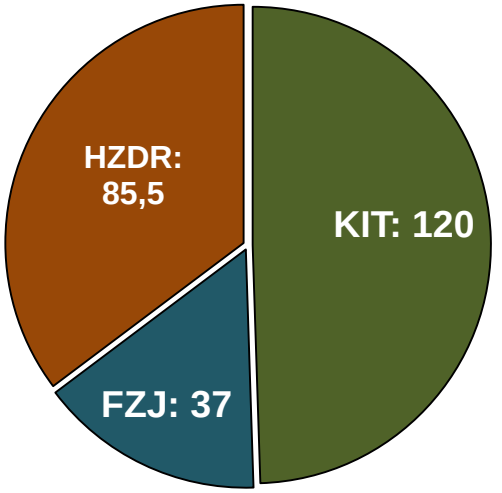

KIT - Institute for Nuclear Waste Disposal (INE)

Research on nuclear waste disposal

Fundamental research

Understanding processes on a molecular level

Aquatic chemistry of actinides and long-lived fission products

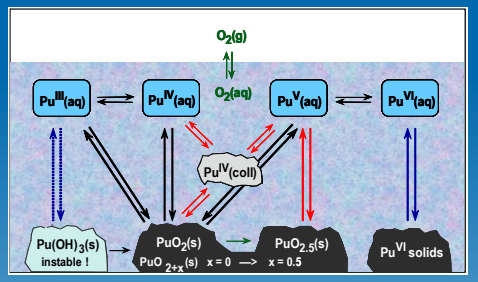

Elucidation and quantification of complex geochemical reactions (example: Plutonium chemistry)

Understanding of radionuclide speciation In repository systems on a molecular level

Colour of plutonium solutions at different redox states

Application oriented research

Radionuclide retention in the multi-barrier system

Investigation of radionuclide migration in the laboratory …

… and under natural conditions (in underground laboratories)

Spent fuel corrosion experiments

Experimental setup under remote control in shielded boxes.

Development and adaption of speciation methods

Structural informations at trace level

Elucidation of radionuclide speciation by laser spectroscopy …

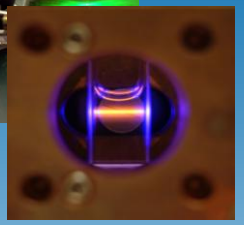

… and by x-ray spectroscopy at the INE-beamline for actinide research at ANKA

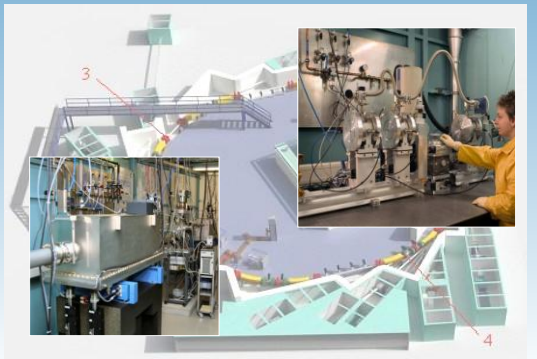

Vitrification technology

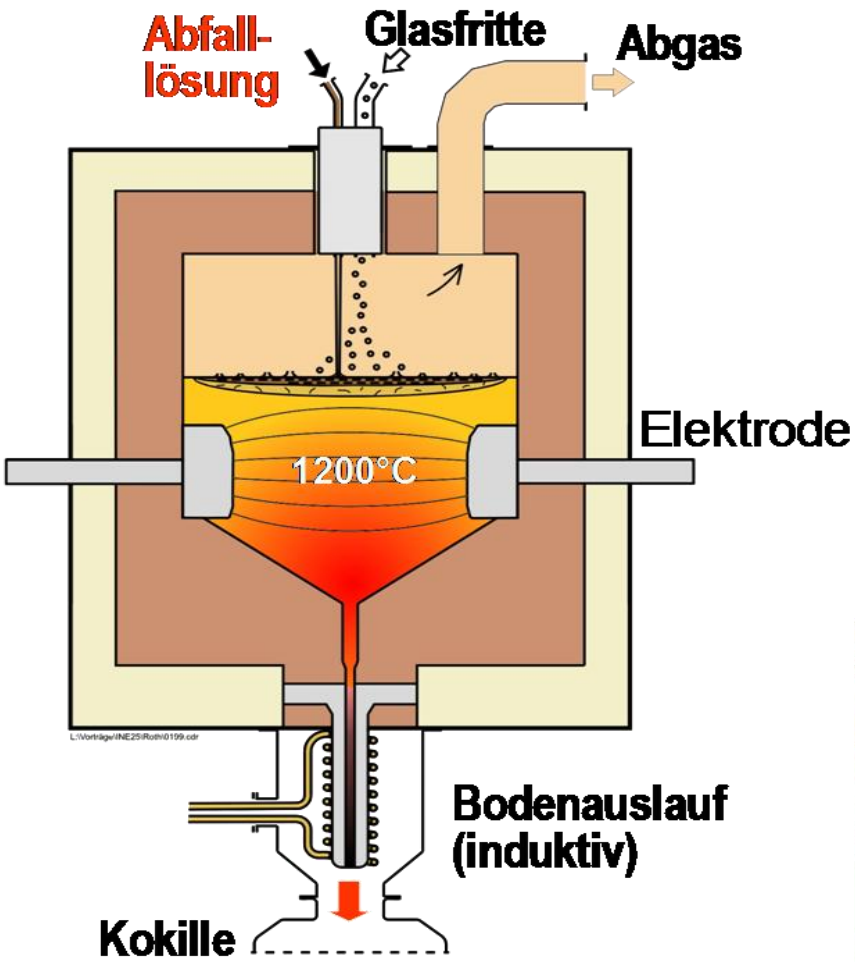

Vitrification Plant China (VPC)

- Governmental environmental protection project
- Location near Guangyuan/Sichuan province
- Project duration 6 years
- HLLW design throughput 50 l/h
- Glass production rate 31 kg/h
- Approx. 1300 Glass canisters

Location of VPC

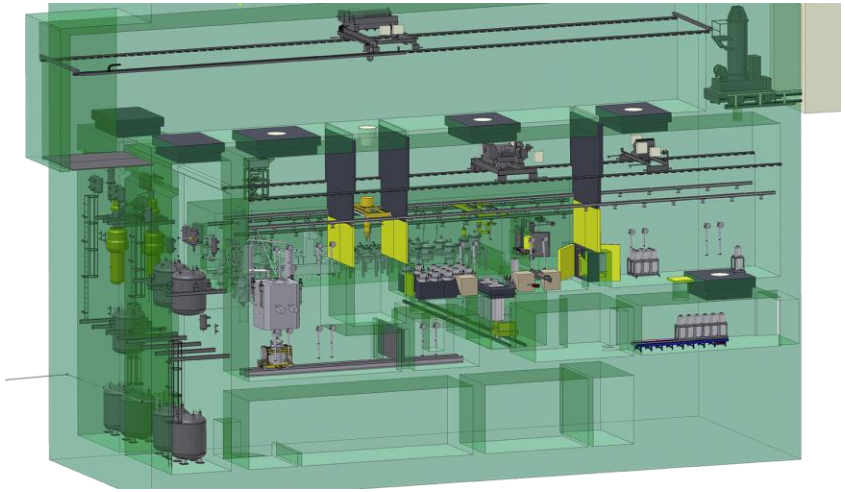

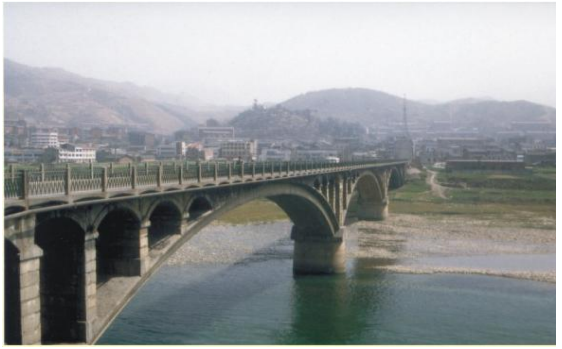

MIGRATION 2011

13th International Conference on the Chemistry and Migration Behaviour of Actinides and Fission Products in the Geosphere

Migration 2011

Beijing, China

September 18 – 23, 2011

Local Organization:

Peking University
China Institute of Atomic Energy (CIAE)
Committee on Nuclear Chemistry & Radiochemistry, Chinese Nuclear (Chemical) Society(CNRCS)
Committee on Radiation Protection, Chinese Nuclear Society(CRP,CNS)
Beijing Nuclear Society(BNS)
Radiochemistry & Radiation Chemistry Key Laboratory for Fundamental Science(RCKLFS)

Supported by

Migration 2011 is being organized by Peking University and supported by:

- National Natural Science Foundation of China (NSFC)
- Ministry of Education (Through 111 and FRFCU projects) , PRC
- Beijing National Laboratory for Molecular Sciences
- Chinese Academy of Engineering Physics (CAEP)
- Institute of High Energy Physics, Chinese Academy of Sciences
- Lanzhou University
- Sichuan University

111 Project

Migration is also supported by the:
European Commission through ACTINET-I3
Karlsruhe Institute for Technology (KIT)

230 presentations
(61 oral; 169 poster)

270 participants from
19 countries

BRIUG

PTKA
Projektträger Karlsruhe
Karlsruher Institut für Technologie

BGR
Bundesanstalt für
Geowissenschaften
und Rohstoffe

KIT
Karlsruhe Institute of Technology

2nd Chinese-German Workshop on Radioactive Waste Disposal, Karlsruhe, Oct. 15-16, 2012

Welcome !

Migration 2011

Oral + poster contributions (230)

China	43	Korea	6
Germany	42	Sweden	6
France	27	India	5
USA	27	Russia	5
Japan	18	EU	4
Spain	14	Australia	3
Switzerland	10	Taiwan	3
Belgium	6	UK	3
Finland	6	Austria	1
		Czech Republic	1

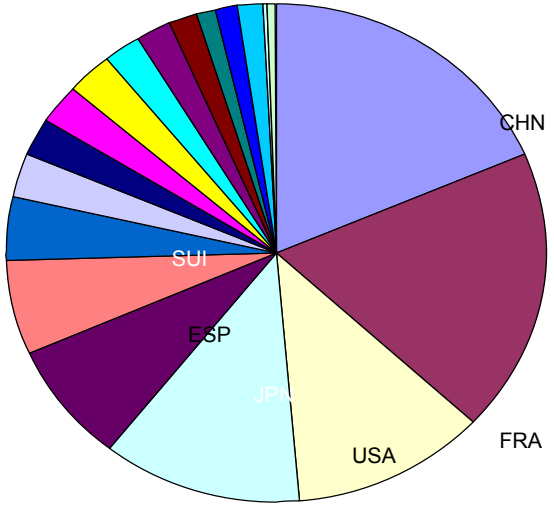

2nd Chinese-German Workshop on Radioactive Waste Disposal,
Karlsruhe, Germany, 15-18, Oct. 2012

Geological Disposal of High Level Radioactive Waste in China: update 2012

Ju WANG
Beijing Research Institute of Uranium Geology,
China National Nuclear Corporation

Outlines

- Nuclear power plants in China
- Policies and regulations related to geological disposal
- Highlights
- Challenges

Nuclear power plants in China

- 15 reactors in operation in 2012
- 26 reactors under construction in 2012
- although the Fukushima accident happened in 2011, the milestone for NPP development by 2020 remains unchanged:
  - 40 GW in operation
  - 18 GW under construction

Development of NPP in China

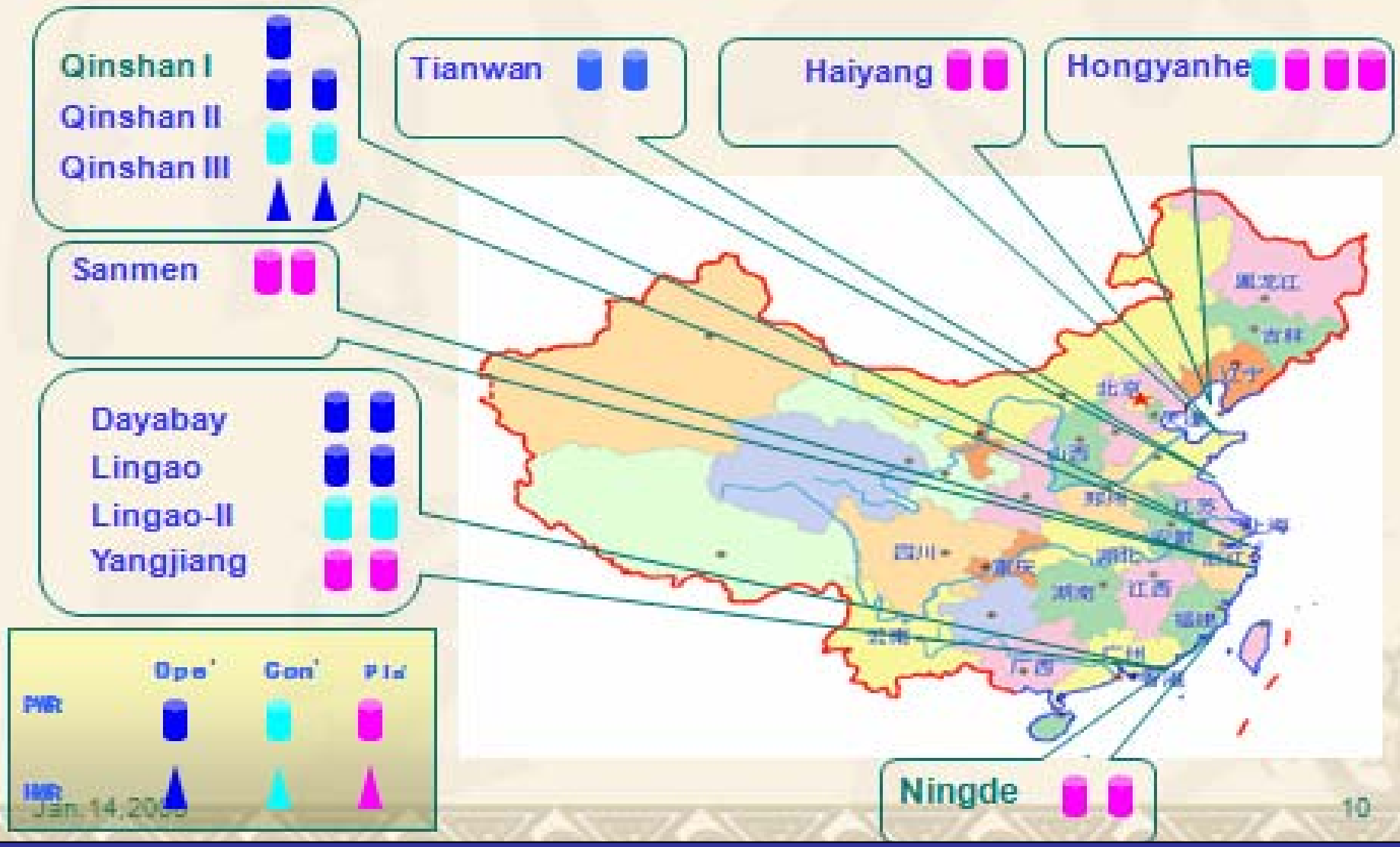

Nuclear power plants in Chinese Mainland in 2011:

15 reactors in operation, 26 under construction

Law for waste management

2003: Law on Prevention of Radioactive Pollution:

“high level radioactive waste should be disposed in a centralized geological repository”

Policies for nuclear fuel cycle

- A closed nuclear fuel cycle policy
- spent fuel should be reprocessed
- waste form for final geological disposal:
  vitrified waste, CANDU SF
- deep geological repository is used
- host rock: granite or clay
- repository concept:
  - multi-barrier concept
  - shaft--tunnel-disposal vault
  - located in saturated zone

Regulations

- **2006: R&D Guidelines for Geological Disposal of High Level Radioactive Waste**

jointly published by China Atomic Energy Authority, Ministry of Sci. &Tech., Ministry of Environ. Prot.

Major contents of the Guidelines

3 main stages for HLW disposal

- 2006--2020 :
  Laboratory Study and Site Selection
- 2020--2040
  In Situ R&D in Underground Research Laboratory
- 2040--middle of 21st Century
  Repository construction

A 3-step strategy for HLW disposal

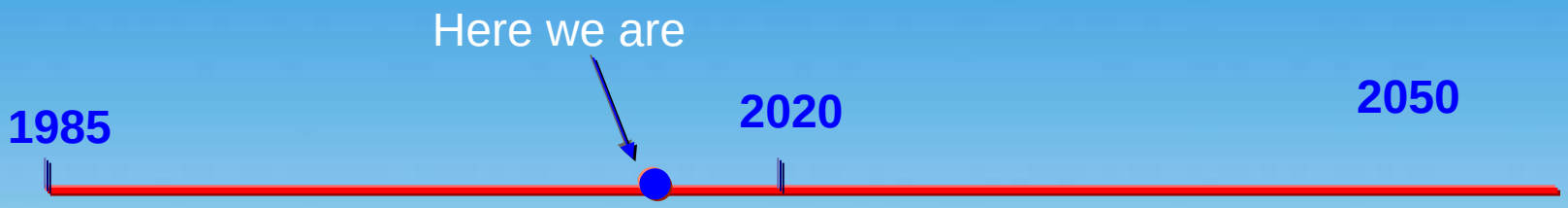

Site → URL → Repository

China plans to build an URL before 2020

France: Bure, Tournemire
Belgium: Mol
Germany: Gorleben, Asse
Czech: Joseph

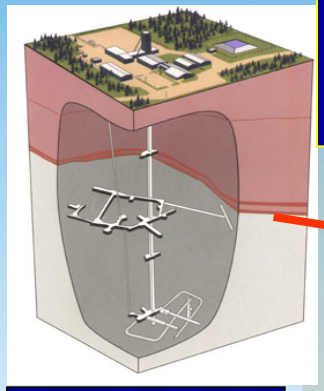

Canada

USA

Sweden

Korea: URT

Japan:
Kamaishi, Tono
Mizunami, Honorobe

Switzerland

China:
2020

Goal in 2050:

Construction of China's National geological repository for high level waste is completed

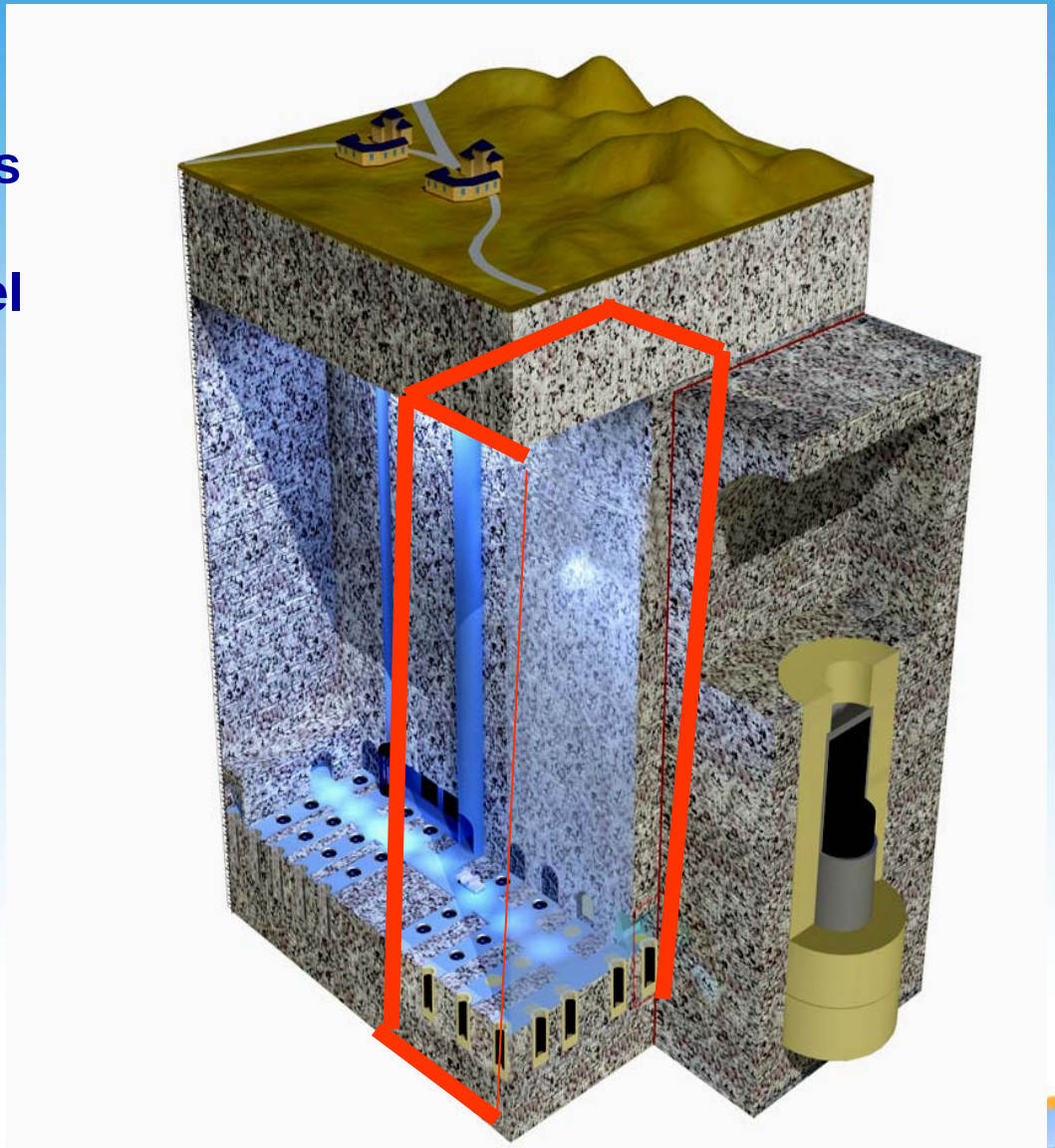

A multi-barrier concept

Regulations

- **2007: the Long Term Development Plan for NPP in China (2006-2020) approved by the State Council:**

  -- The construction of an underground research laboratory (URL) for high level radioactive waste in China should be completed by 2020

Regulations

- **2012: The Long-term plan for nuclear safety and prevention of radioactive pollution (2012-2020) approved by the State Council, the same words:**

  -- The construction of an underground research laboratory (URL) for high level radioactive waste in China should be completed by 2020

Regulation for fund

- 2010: Waste Fund approved by the State Council:
- Rate: 0.026 Yuan/KWh.
- Used for:
  - Geological disposal
  - Spent fuel transportation & storage
  - reprocessing

Regulation

- **2011: the new "Regulation of safe management of radioactive waste" approved by the State Council:**
  - **The China Atomic Energy Authority is responsible for implementing R&D, site selection, URL and repository construction**

Organizational structure

国家原子能机构

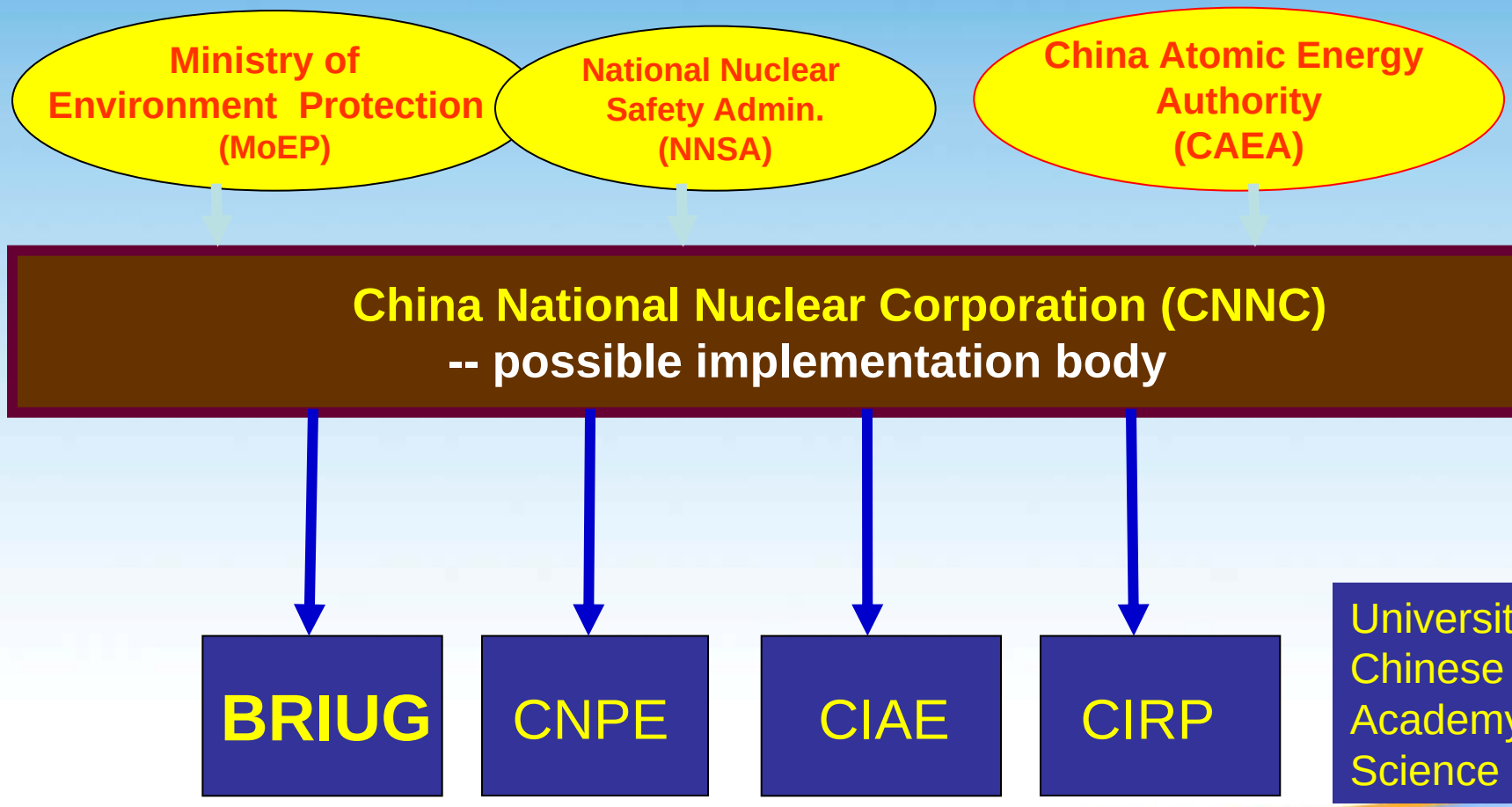

Site selection--History

1986: Site selection started

1989: Six regions selected for high level radioactive waste repository

1990: sub-area selection in Beishan site, Northwest China's Gansu province

2000: systematical site characterizaiton in Northwest China's Beishan site

Highlights since 2007---Site selection

- New strategy for Site selection
- Select 12 sites in all China, after comparison, then select 3 sites equally good for repository
- host rock: granite & clay
  priority: granite

Site selection process

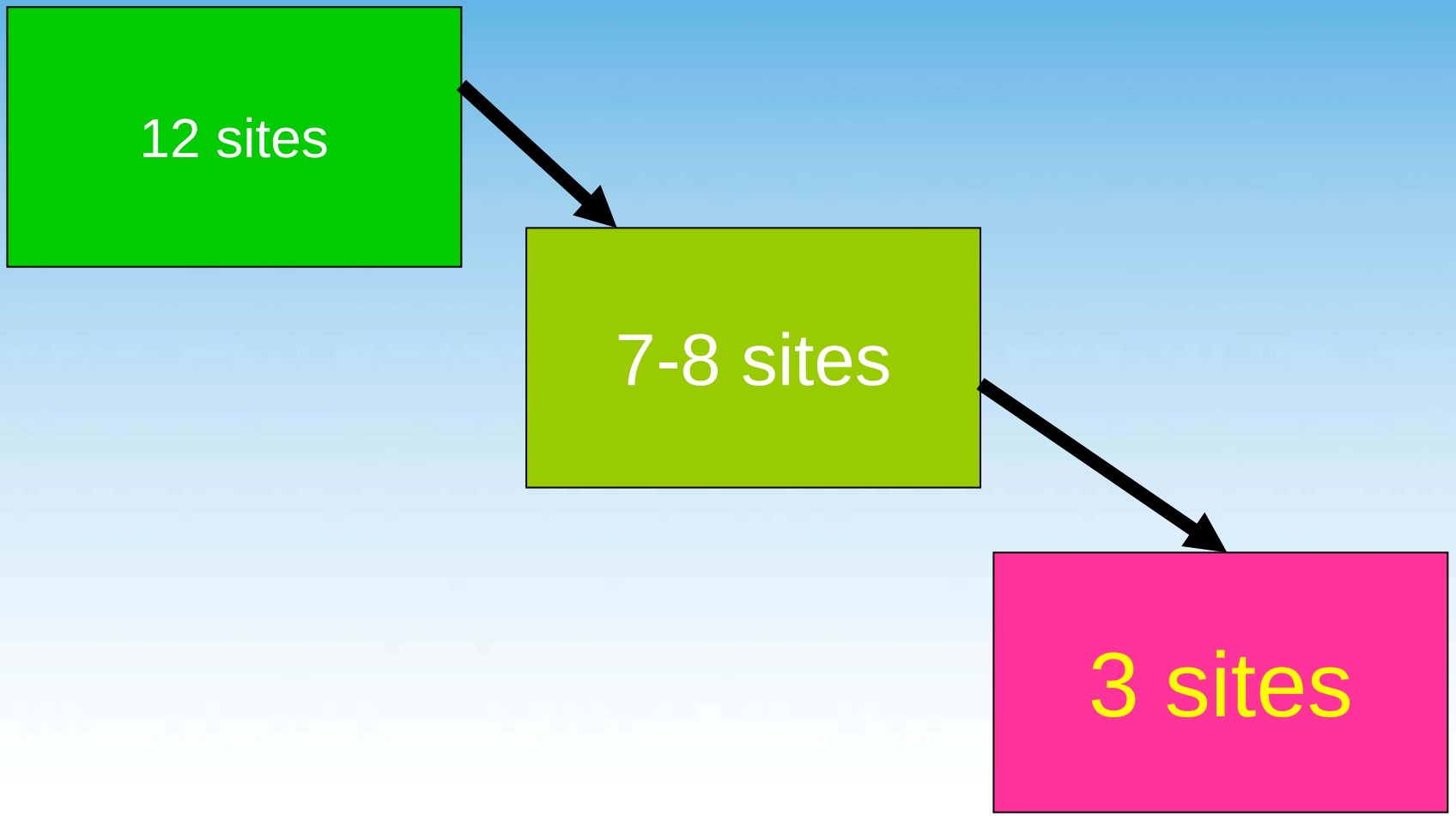

6 regions selected for repository

1- South China; 2- East China; 3- Southwest China

4- Inner mongolia; 5- Xinjiang; 6- NW China—Beishan area

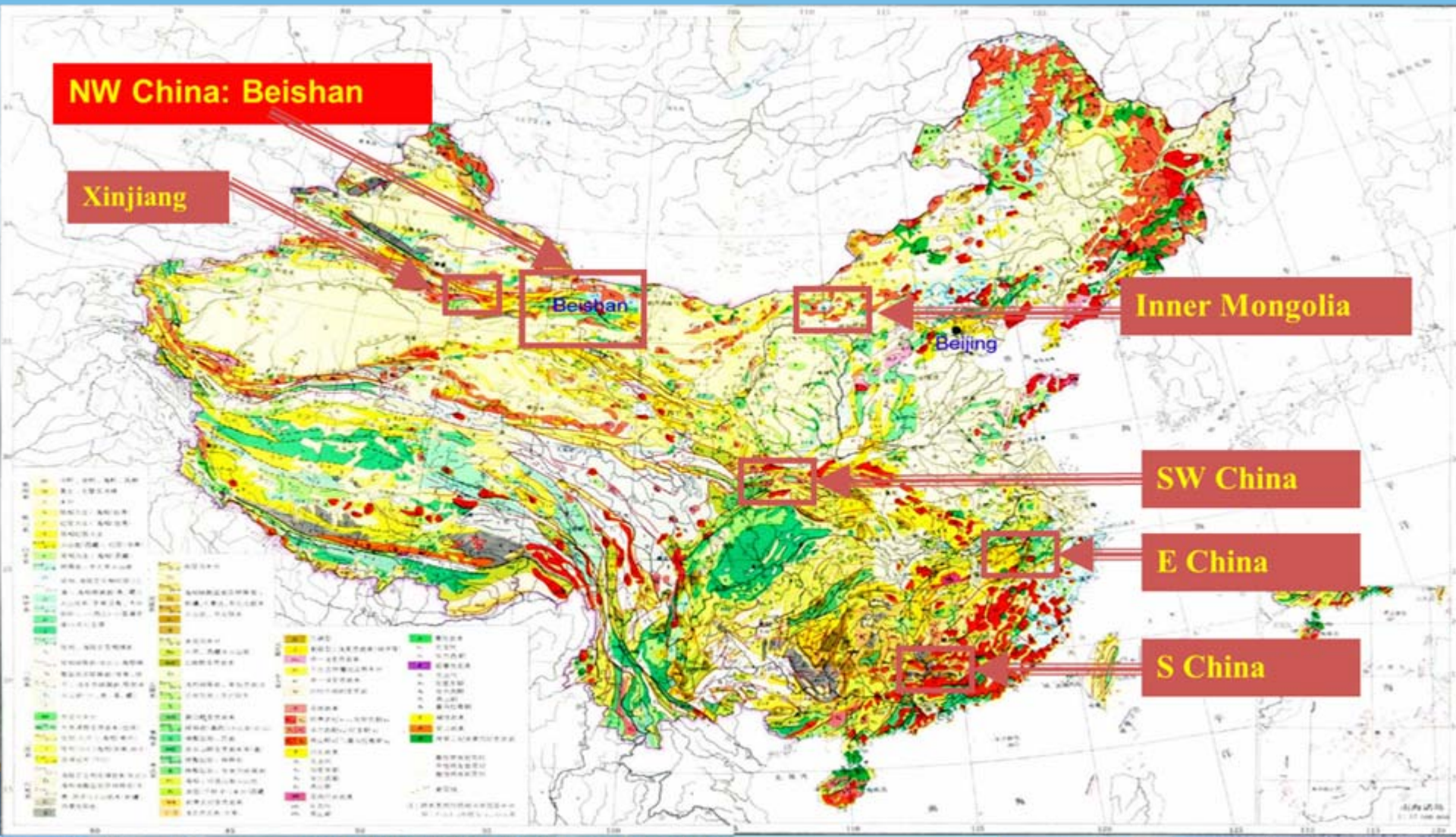

Aqishan

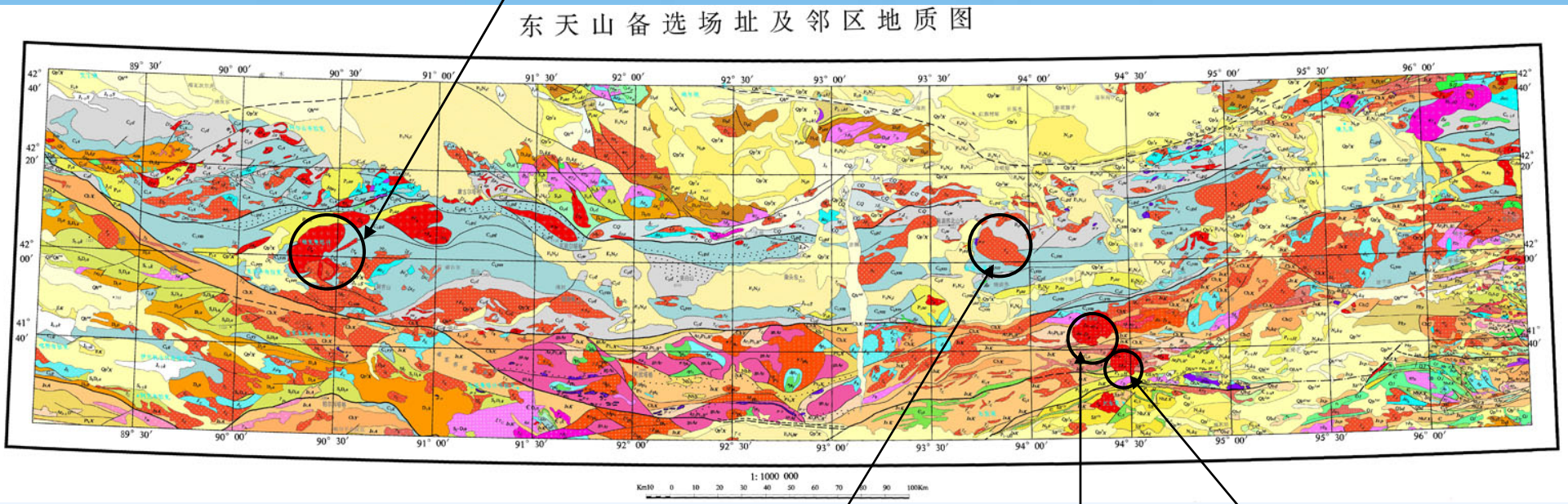

Yamansu

Weiya

Tianhu

Highlights since 2007---Site selection

- Beishan site: considered as the first priority site for China's high level radioactive waste repository
- site characterization continued in the Gibi desert Beishan site in NW China's Gansu province
- 15 boreholes drilled in the site.

Beishan: the most potential site

NW China's Beishan area has been selected as the most potential site

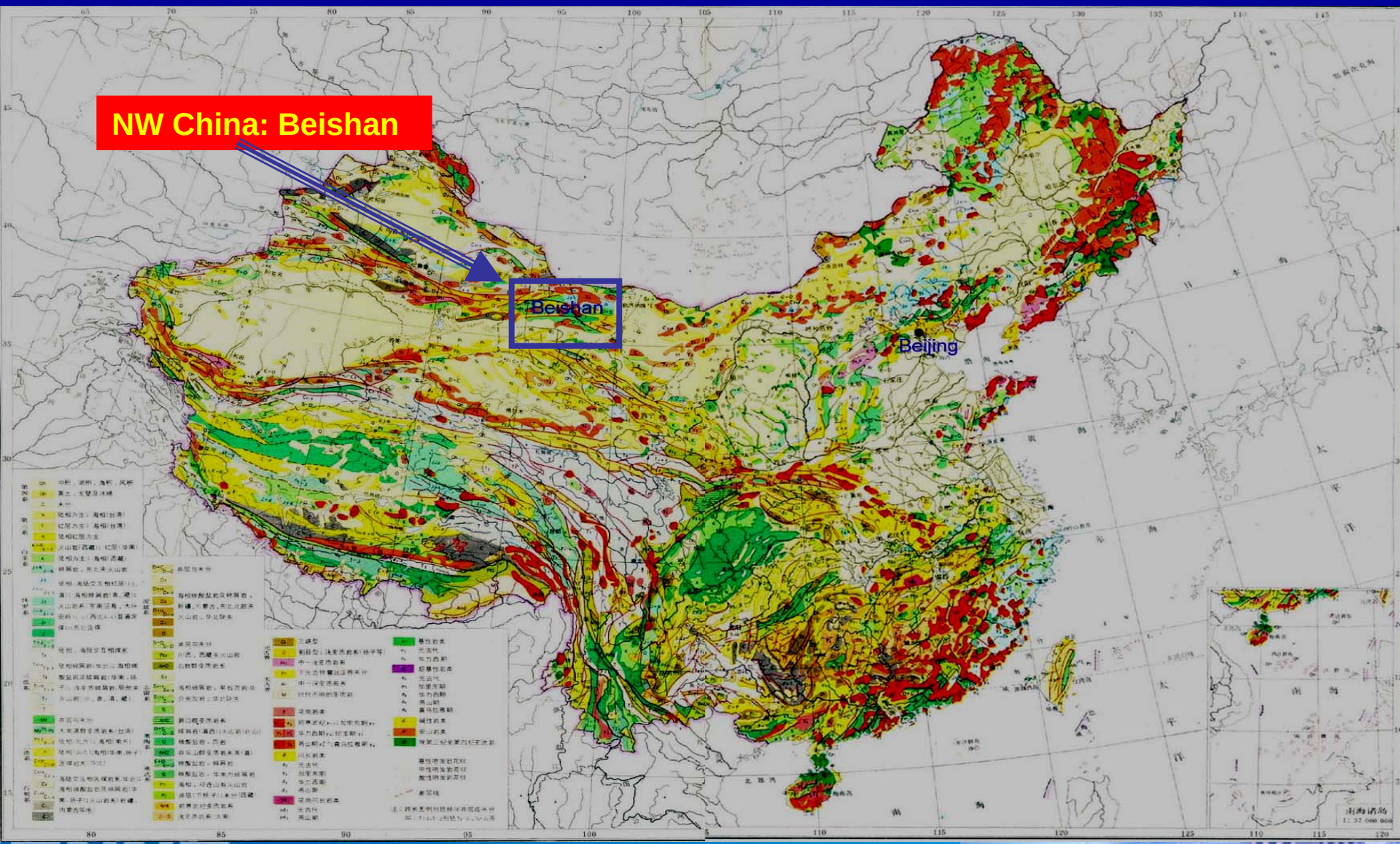

15 bore holes drilled in Beishan site since 2007

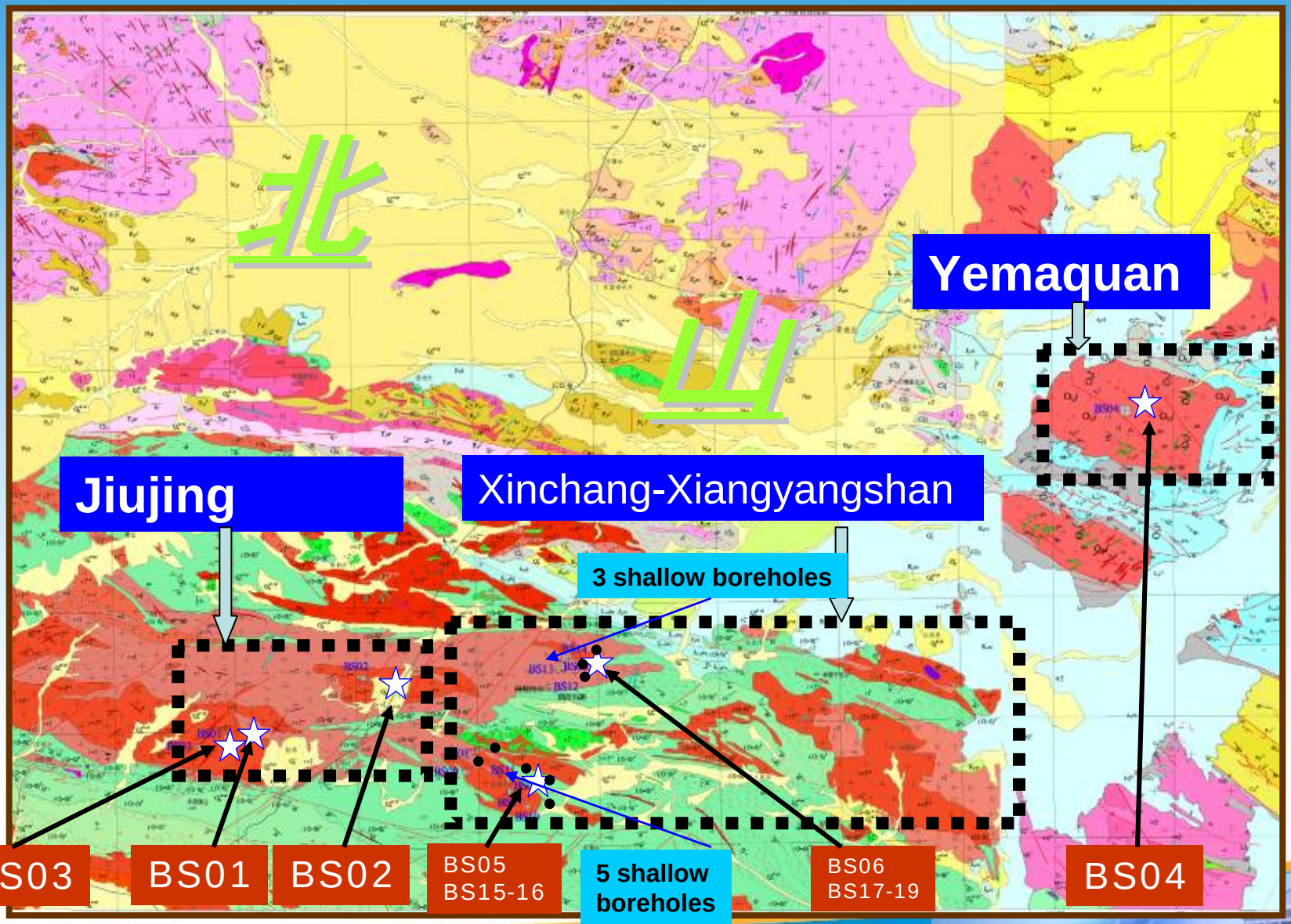

Opening Ceremony for borehole BS16（March 18, 2011）

Core samples from BS 16

Surface geophysical survey: to investigation the faults

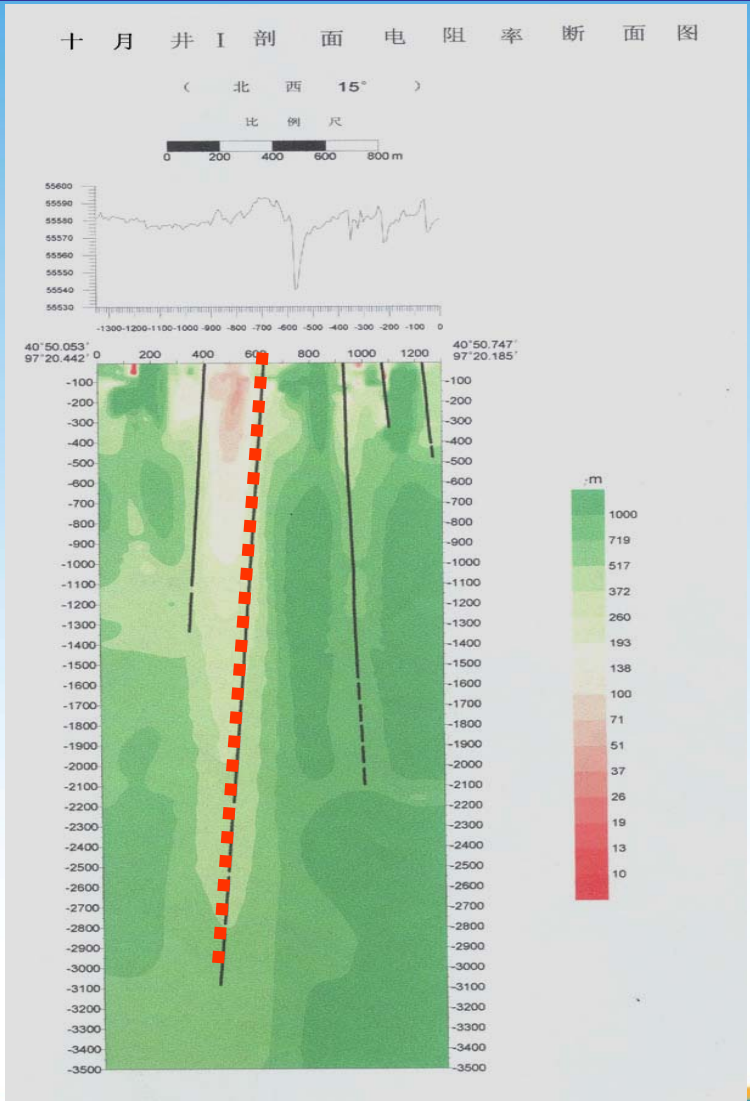

3-D image of faults in granite

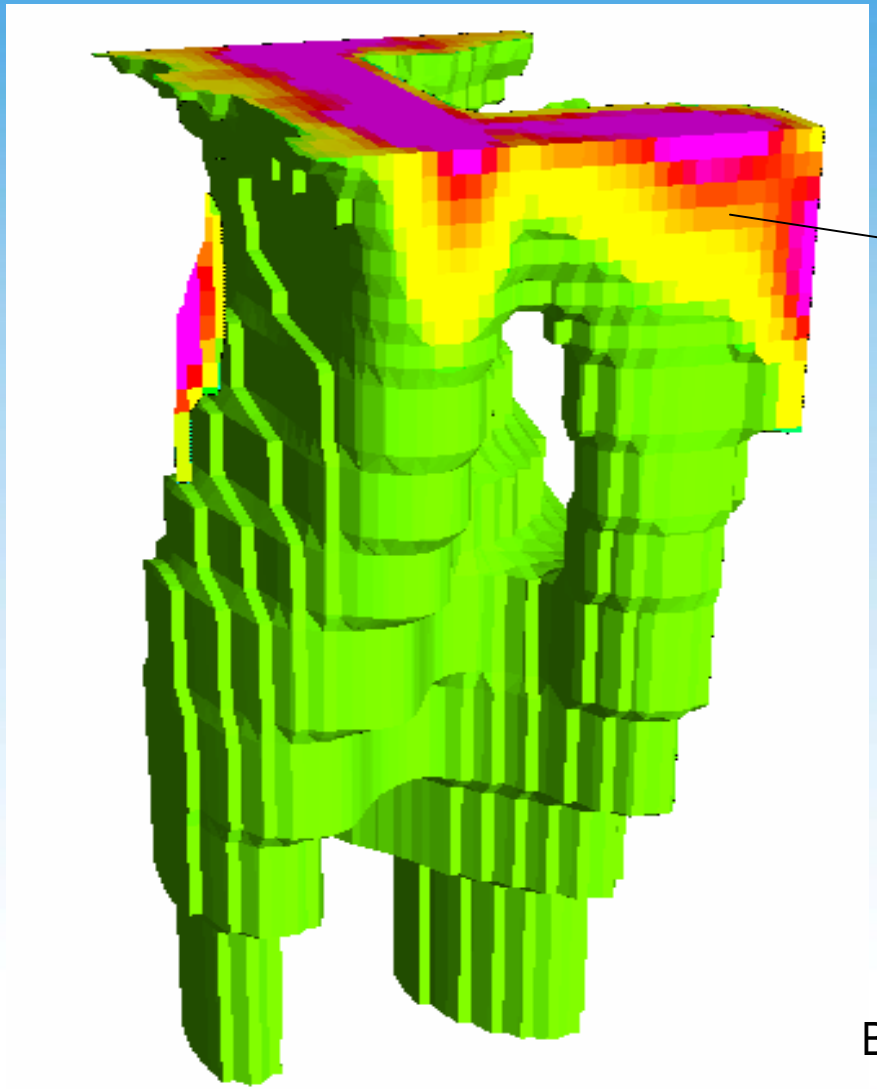

Blocks with less than 700 Ω·m

Groundwater modeling

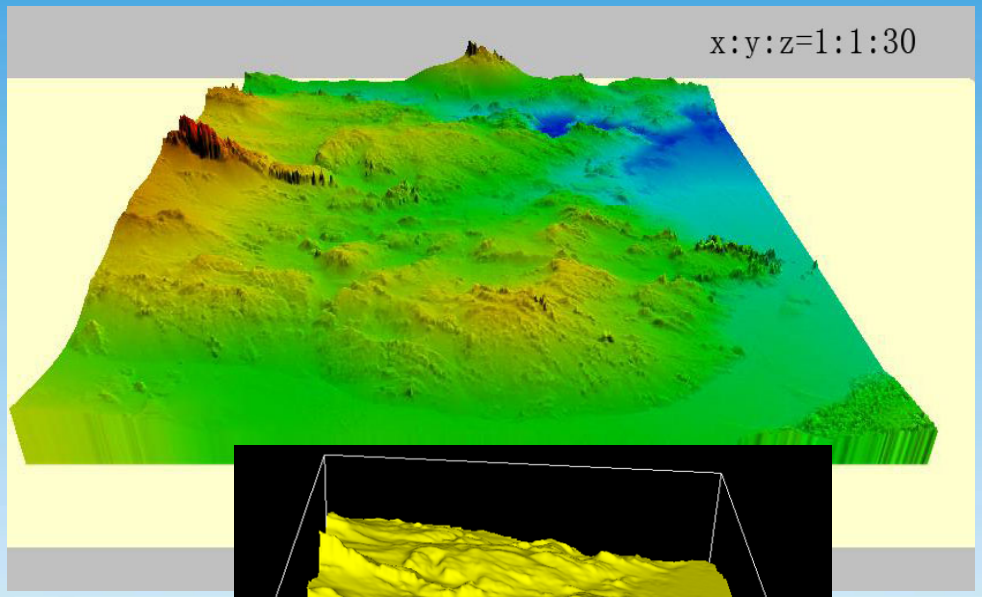

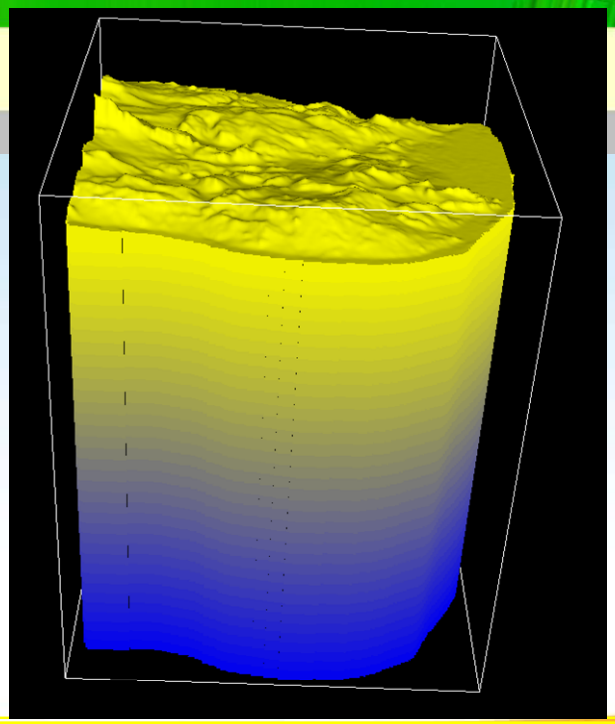

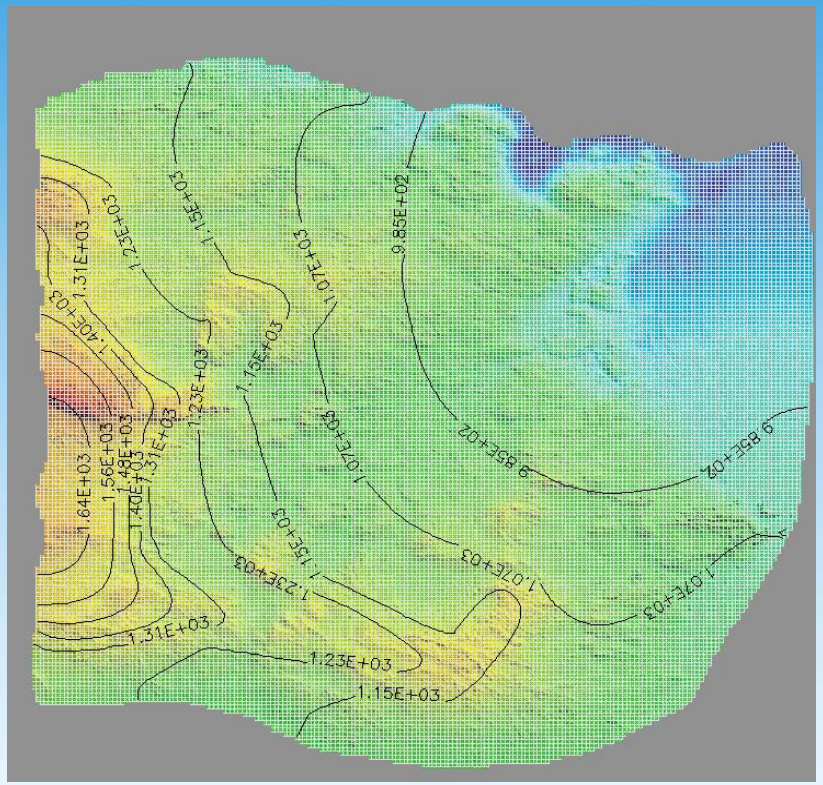

模拟水头等值线

Beishan site: Preliminary conclusion

- located in Northwestern China's Gobi desert area
- low population density
- low precipitation : 60--80 mm/a
- high evaporation: 2900-3200 mm/a
- no economical prospect
- no important mineral resources
- convenient transportation
- stable crust
- favorable hydrogeological conditions
- favorable host rock: granite and diorite

the most potential site for China's HLW repository

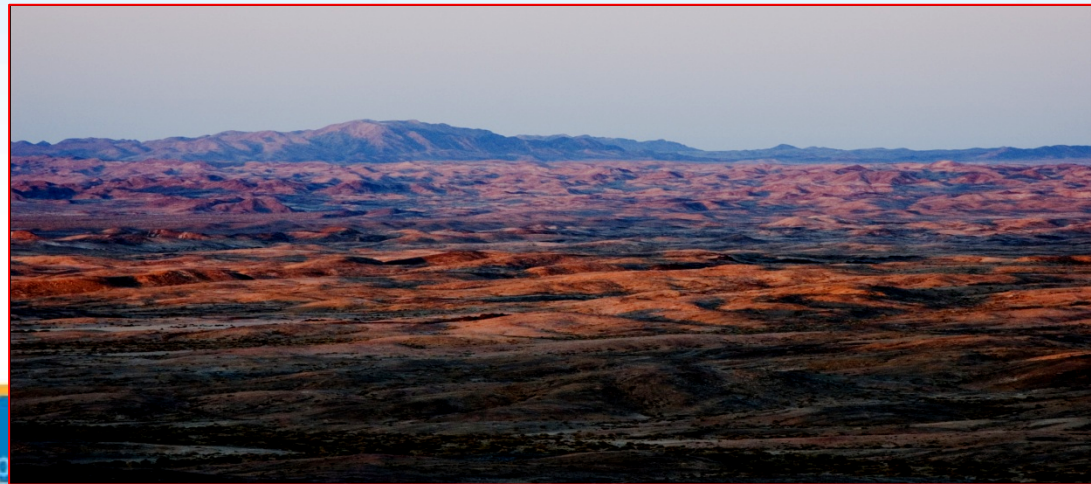

Highlight---Engineering design

A preliminary concept design for China's high level radioactive waste repository has been proposed. It is a multi-barrier system, with bentonite as buffer material.

Preliminary repository concept

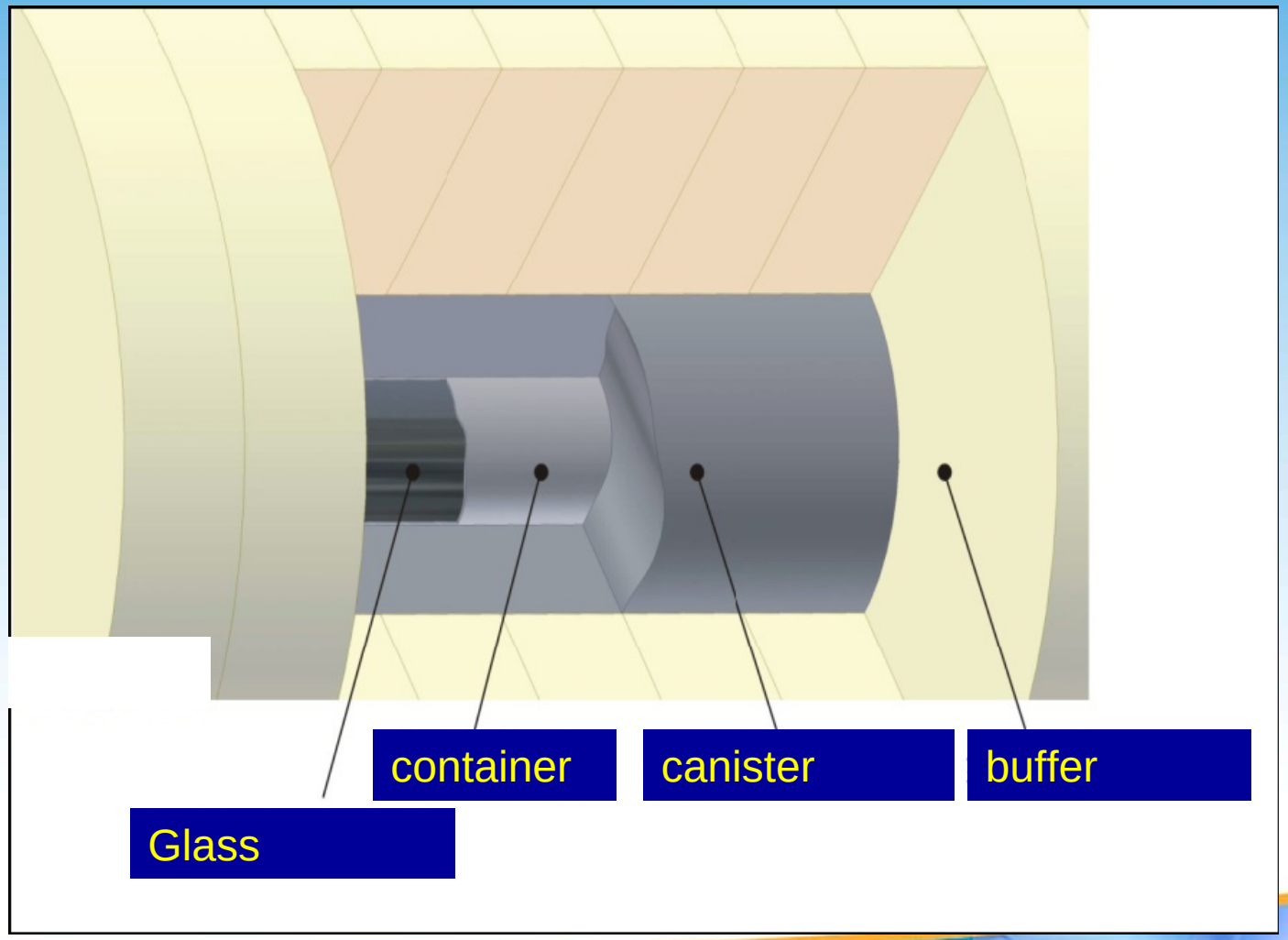

Engineering Design--thermal analysis

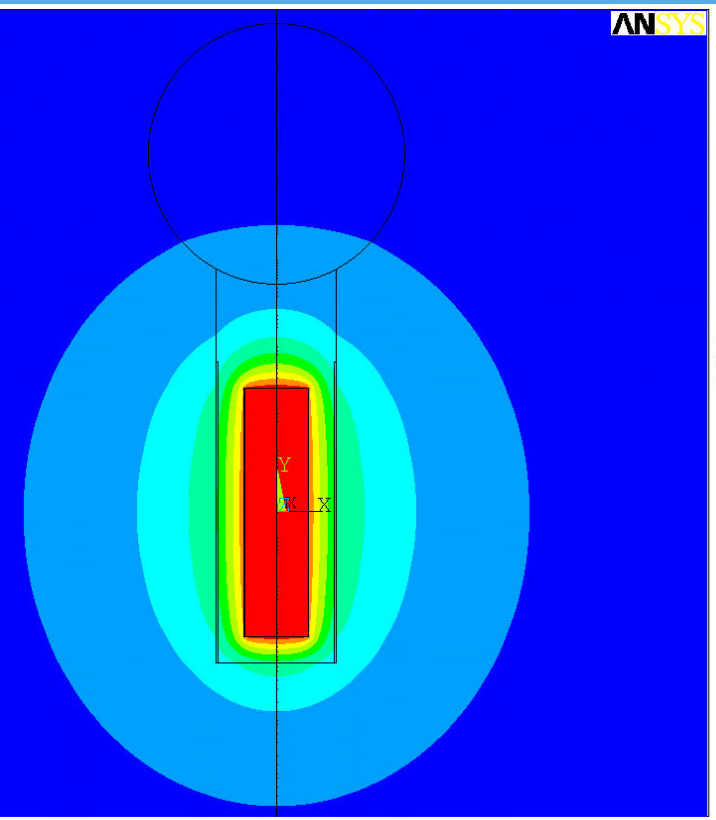

单个废物罐热分析

处置库热分析

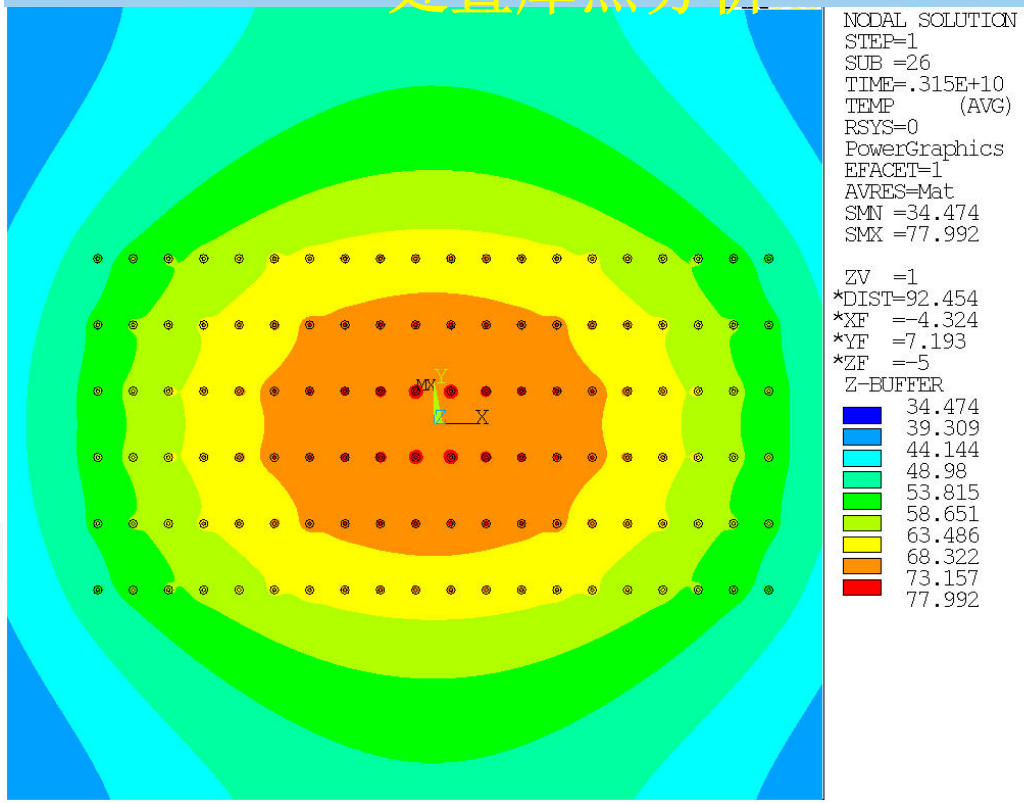

Highlights

Engineered barrier system development

- The GMZ bentonite deposit, located in Inner Mongolia, is selected as the most potential supplier for buffer material.

- tonnage: 160 M ton.
-
- A large-scale mock-up established in order to study the behaviour of GMZ bentonite under simulated repository conditions.

Outcrops of the GMZ bentonite deposits

Super large:

160 M T

China-Mock-Up for Bentonite Study

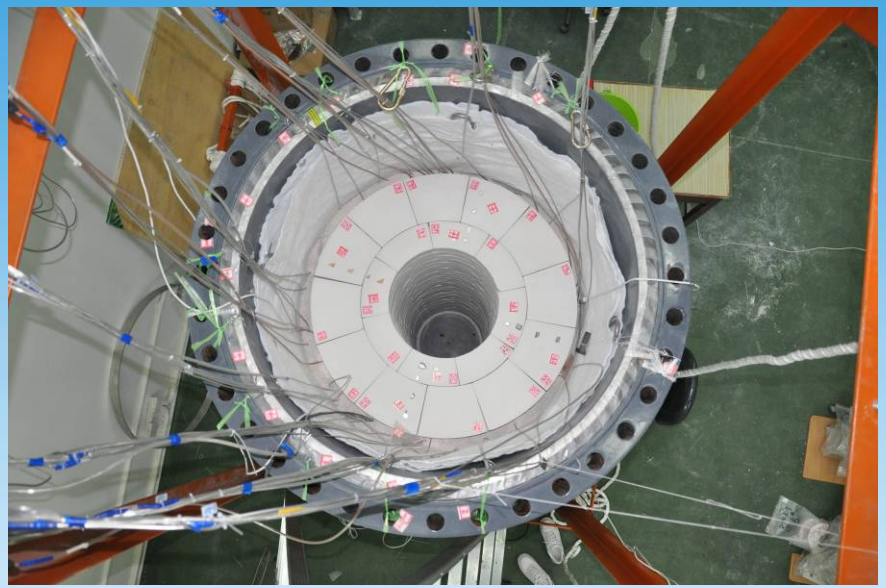

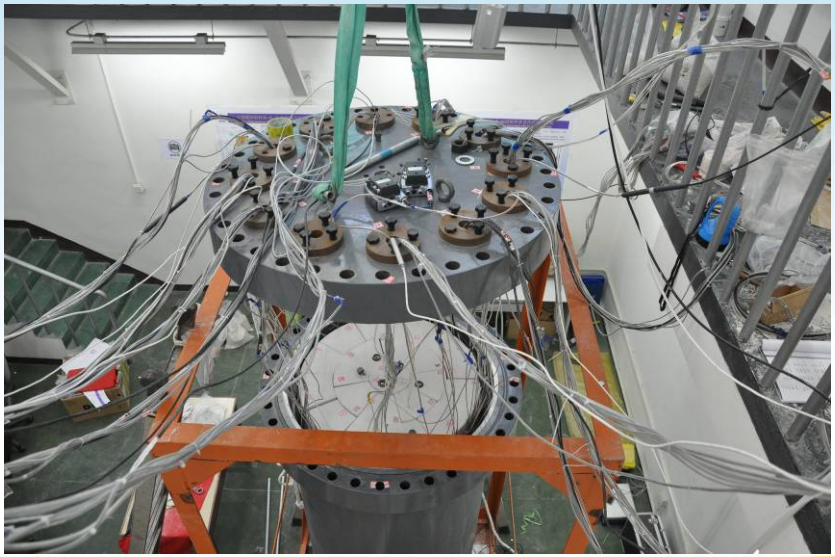

PEBS Project Meeting in Beijing 23-27,May 2011

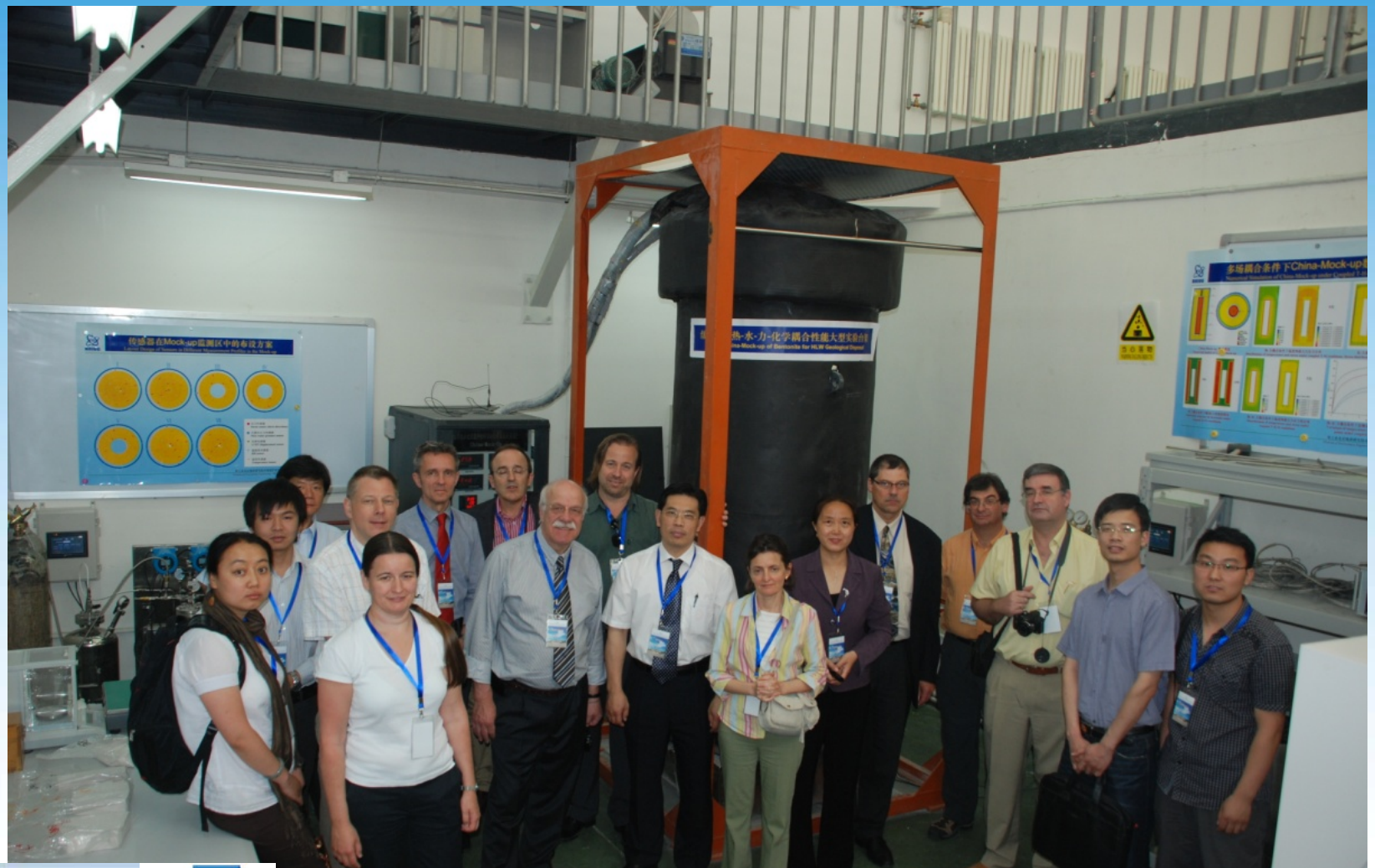

Long-term performance of Engineered Barrier Systems

Workpackage B: China-Mock-Up (2010-2014)

EUROPEAN COMMISSION

SEVENTH FRAMEWORK PROGRAMME

Highlight:

Safety assessment

- **Preliminary safety assessment has been conducted for China's repository concept, by using Beishan site as a reference site.**

Safety assessment: case study

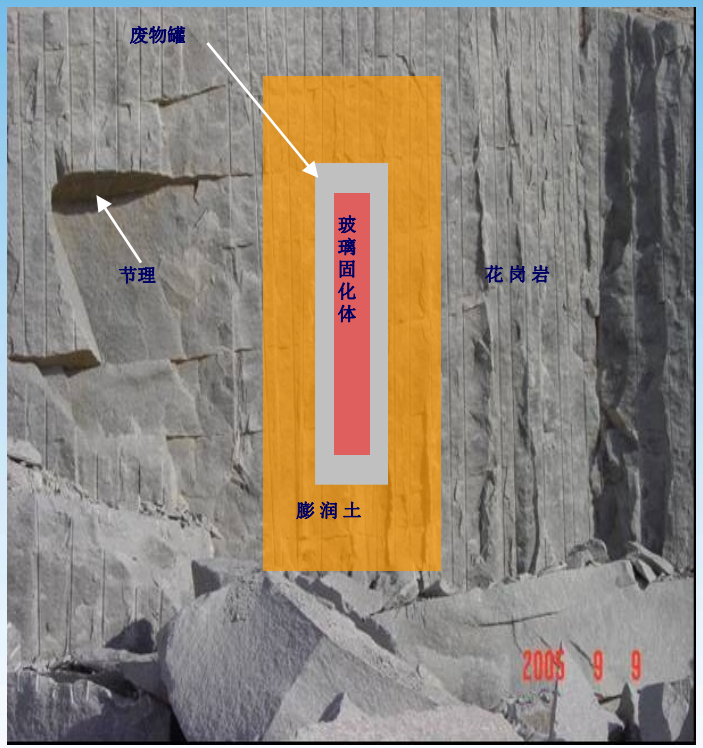

工程屏障概念模型
Conceptual model of engineered barrier

性能评价过程
Procedure of performance assessment

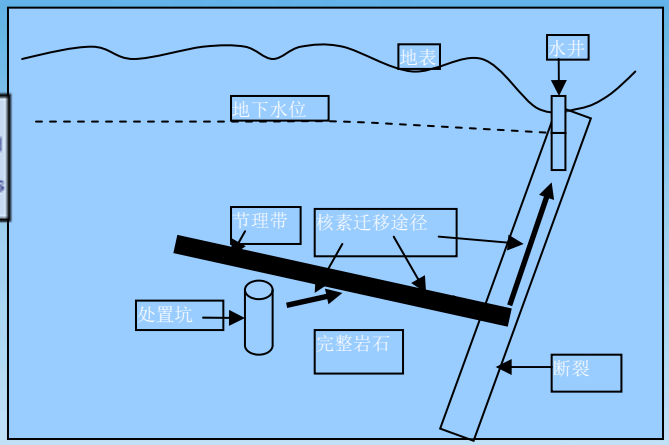

北山预选区地质屏障概念模型
Conceptual model of geological barrier for Beishan site

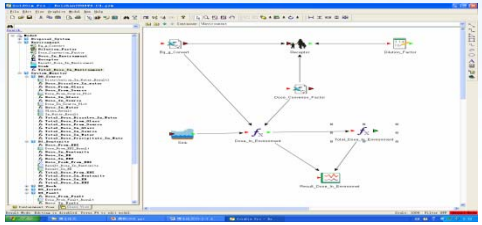

GOLDSIM，a PA software

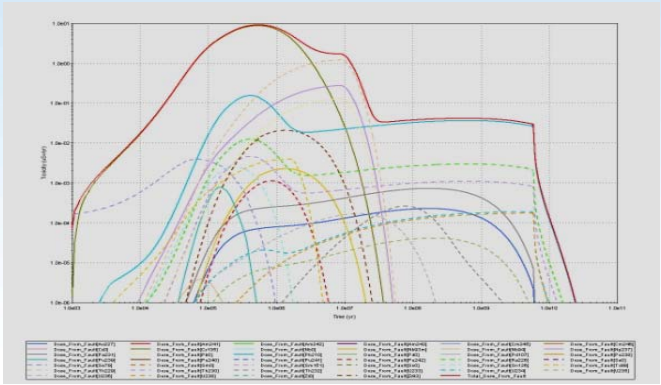

处置库系统毒性释放率
Toxicity release rate from repository system

International Exchange and Cooperation

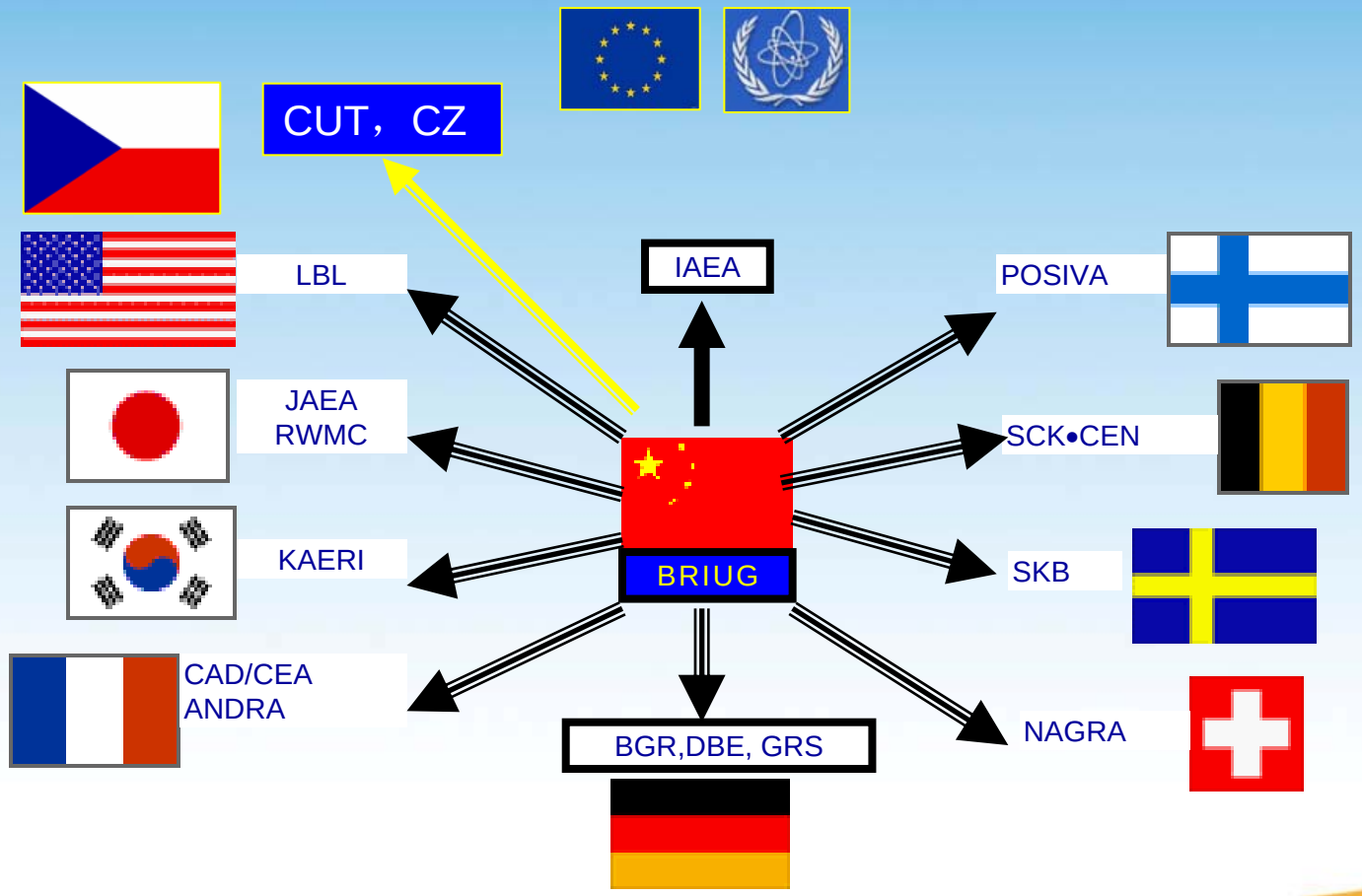

1st Chinese-Germany Workshop on Radioactive Waste Disposal, May 28-31, 2007, Beijing

CAEA delegation visits Ministry of Economics, Germany, 2007-09

IAEA experts visit Beishan, 9 Sept.,2011

next 5 year

- Site selection for the URL
- Site characterization will be continued at Beishan site
- Other sites in Xinjiang, Inner Mongolia will also be investigated
- Site selection for Underground Research Laboratory will be started soon
- Engineering design and engineered barrier system study will continue
- The behaviour of key radionuclides will further studied
- The safety assessment for the proposed disposal system will continue.

Challenges

For geological disposal of high level radioactive waste, the following challenges are still facing the Chinese program:

- **Social**
- **Economic**
- **Public acceptance**
- **Scientific & technological**
- **Engineering**

Thank you

A new approach for siting a repository for HLW in Germany ?

Volkmar Bräuer

Federal Institute for Geosciences and Natural Resources

GEOZENTRUM HANNOVER

Stilleweg 2

30655 Hannover

www.bgr.bund.de

Agenda

1. Political background

2. Scientific background
   - Criteria
   - Host rocks
   - Disposal concepts
   - Retrievability

3. Outlook

BGR Bundesanstalt für Geowissenschaften und Rohstoffe
GEOZENTRUM HANNOVER

Federal Government and State Governments: Roadmap for selection of a repository site, December, 15th 2011

1. Phase to mid 2012
determination of the decision making process by federal law

2. and 3. Phase from end of 2012 to mid 2013
development of bases for decisions and decision on the developed proposals by federal law

4. Phase from 2014 to end of 2019
site selection and above surface exploration

5. Phase to end of 2027 ?
underground exploration und site decision

6. Phase
Licensing, construction und operation

BGR Bundesanstalt für Geowissenschaften und Rohstoffe
GEOZENTRUM HANNOVER

The waste management concept in Germany of **1998**

- **Coalition agreement 1998**
  - Doubt about the suitability of the Gorleben site
  - Definition of an new waste management plan

- **Consensus Federal Government / energy supply companies 2000**
  - Moratorium on Gorleben site
    (max. 3-10 years)
  - Minimisation of transports
    - Last Transport of SF for reprocessing 2005
    - Licensing of interim waste storage facilities at NPP
  - Consensus with utilities regarding life time limits for NPP
  - Adaption of the national atomic act

AkEnd
1999 - 2002

Procedure development
Development of a site selection procedure for a deep radwaste repository

Procedure implementation
Investigation of further sites from 2005 on

BGR Bundesanstalt für Geowissenschaften und Rohstoffe
GEOZENTRUM HANNOVER

Agenda

1. Political background

2. Scientific background
   - Criteria
   - Host rocks
   - Disposal concepts
   - Retrievability

3. Outlook

BGR Bundesanstalt für Geowissenschaften und Rohstoffe
GEOZENTRUM HANNOVER

Factors to be considered for the site selection

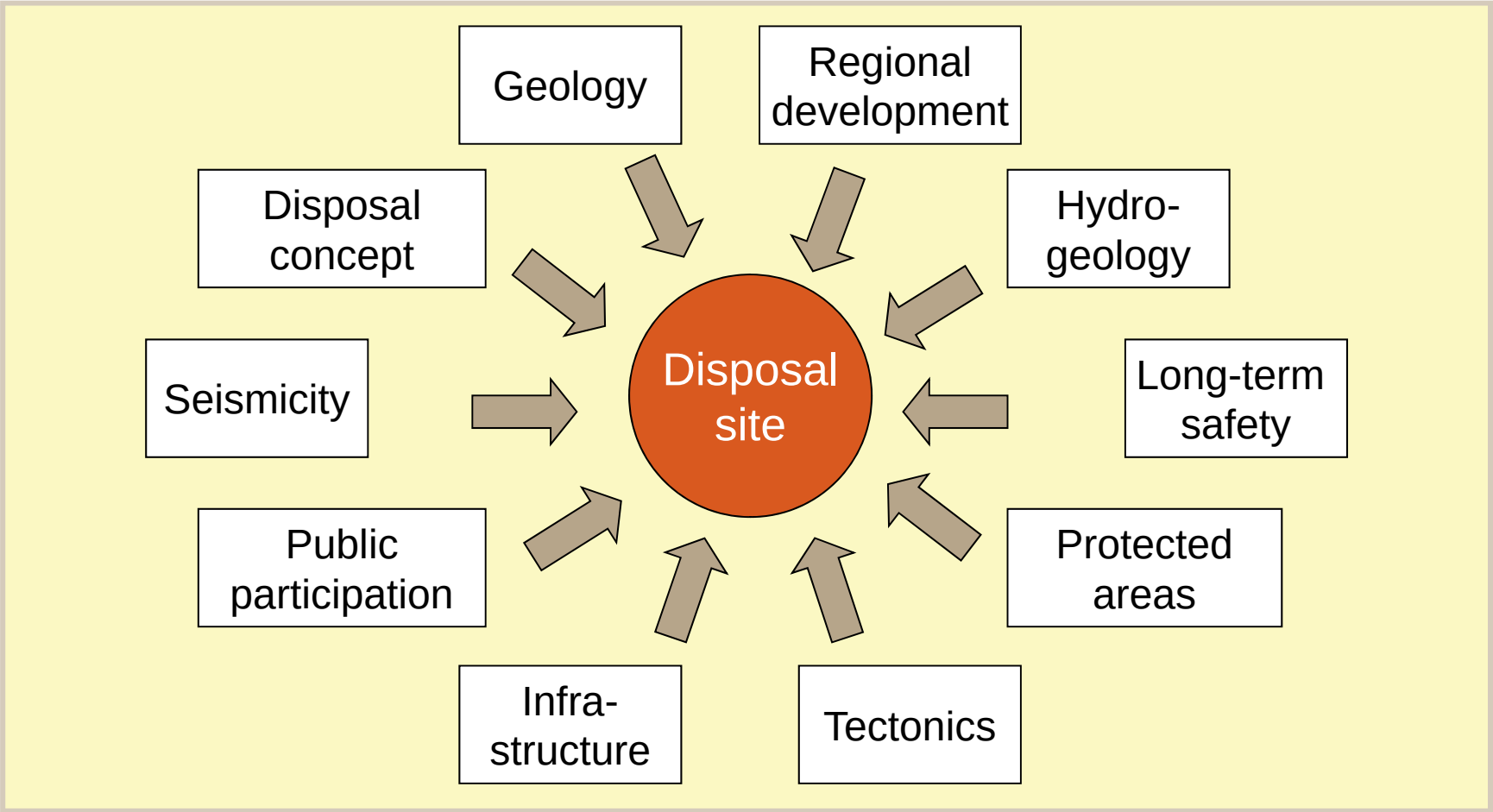

BGR Bundesanstalt für Geowissenschaften und Rohstoffe
GEOZENTRUM HANNOVER

AkEnd Arbeitskreis Auswahlverfahren Endlagerstandorte www.akend.de

Definition of criteria for site selection

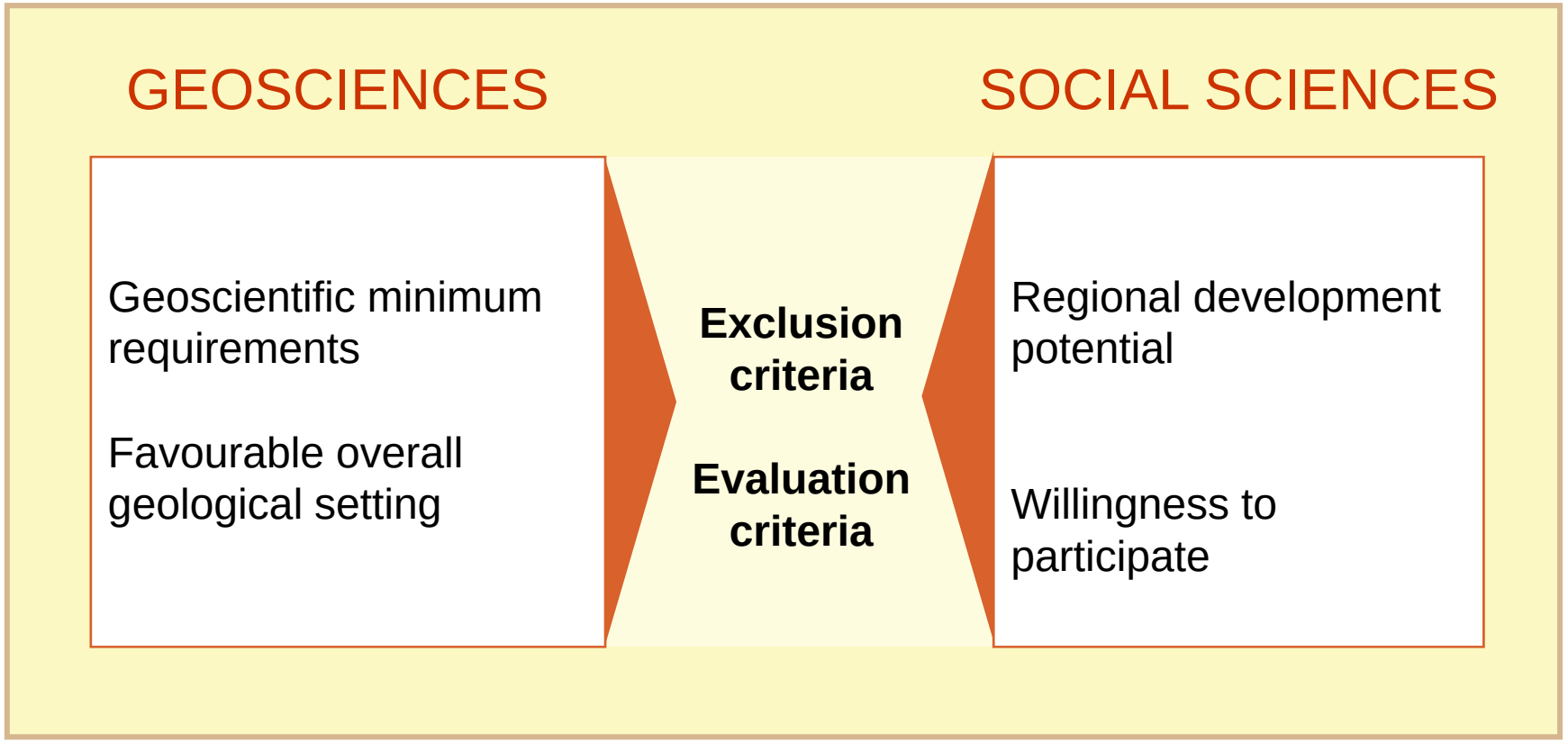

BGR Bundesanstalt für Geowissenschaften und Rohstoffe
GEOZENTRUM HANNOVER

AkEnd Arbeitskreis Auswahlverfahren Endlagerstandorte
www.akend.de

STEPS

in the selection procedure

(Dec. 2002)

↑ Step backwards, if required

	Procedure steps
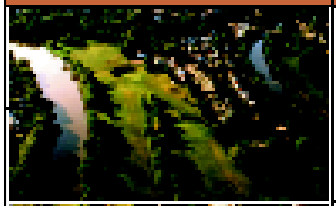	**STEP 1** Identification of **areas** fulfilling specific minimum requirements
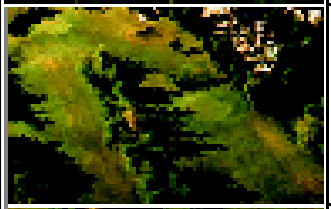	**STEP 2** Selection of **partial areas** with particularly favourable overall geological setting ↑
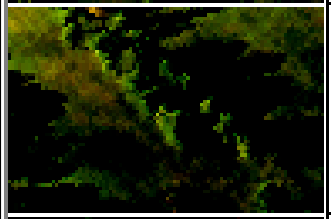	**STEP 3** Identification and selection of **site regions** for exploration from the surface ↑
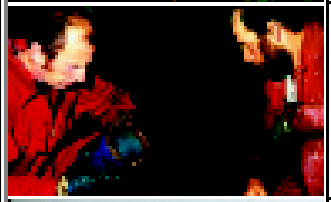	**STEP 4** Determination of **sites** for underground exploration ↑
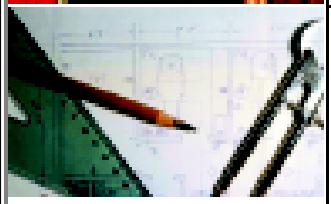	**STEP 5** Decision on a site
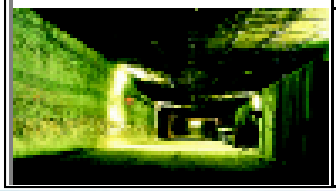	**Repository Site** Licensing procedure

BGR Bundesanstalt für Geowissenschaften und Rohstoffe
GEOZENTRUM HANNOVER

AkEnd Arbeitskreis Auswahlverfahren Endlagerstandorte www.akend.de

Procedural step 1

Exclusion criteria geoscientific

Determination of areas fulfilling specific minimum requirements

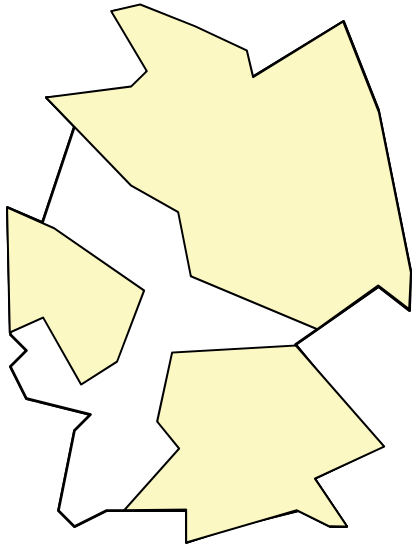

- Large-area vertical movements
- Active fault zones
- Seismic activity
- Volcanic activity
- Groundwater age

areas

BGR Bundesanstalt für Geowissenschaften und Rohstoffe
GEOZENTRUM HANNOVER

AkEnd Arbeitskreis Auswahlverfahren Endlagerstandorte www.akend.de

Procedural step 1

Minimum requirements geoscientific

Determination of areas fulfilling specific minimum requirements

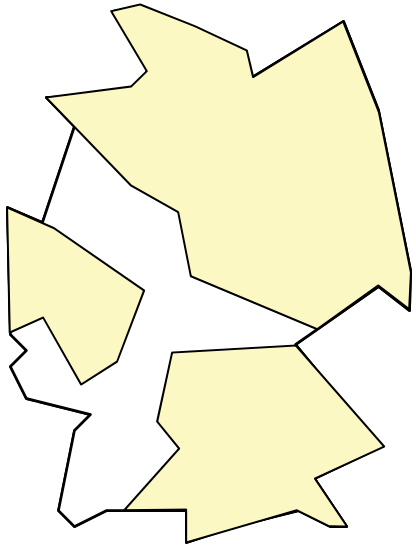

areas

Thickness of isolating rock zone at least: 100 m

Depth at least: 300 m

Mine no deeper than: 1,500 m

Spatial extension:
e.g. salt: 3 km²
e.g. clay/granite: 10 km²

Rock permeability:
$< 10^{-10}$ m/s

No findings which give rise to doubt about adherence of rock permeability, thickness and extension for 1 million years

No risk from rock burst

BGR Bundesanstalt für Geowissenschaften und Rohstoffe
GEOZENTRUM HANNOVER

Agenda

1. Political background

2. Scientific background
   - Criteria
   - Host rocks
   - Disposal concepts
   - Retrievability

3. Outlook

BGR Bundesanstalt für Geowissenschaften und Rohstoffe
GEOZENTRUM HANNOVER

Repository relevant properties of potential host rocks

Property	Rock salt	Clay/claystone	Crystalline rock (e.g. granite)
heat conductivity	high	low	medium
permeability	practically impermeable	very low to low	very low (unfractured) to permeable (fractured)
strength	medium	low to medium	high
deformation behaviour	visco-plastic (creep)	plastic to brittle	brittle
stability of cavities	self-supporting	artificial reinforcement required	high (unfractured) to low (strongly fractured)
in situ stresses	lithostatically isotropic	anisotropic	anisotropic
dissolution behaviour	high	very low	very low
sorption behaviour	very low	very high	medium to high
heat resistance	high	low	high

favorable unfavorable medium

BGR Bundesanstalt für Geowissenschaften und Rohstoffe
GEOZENTRUM HANNOVER

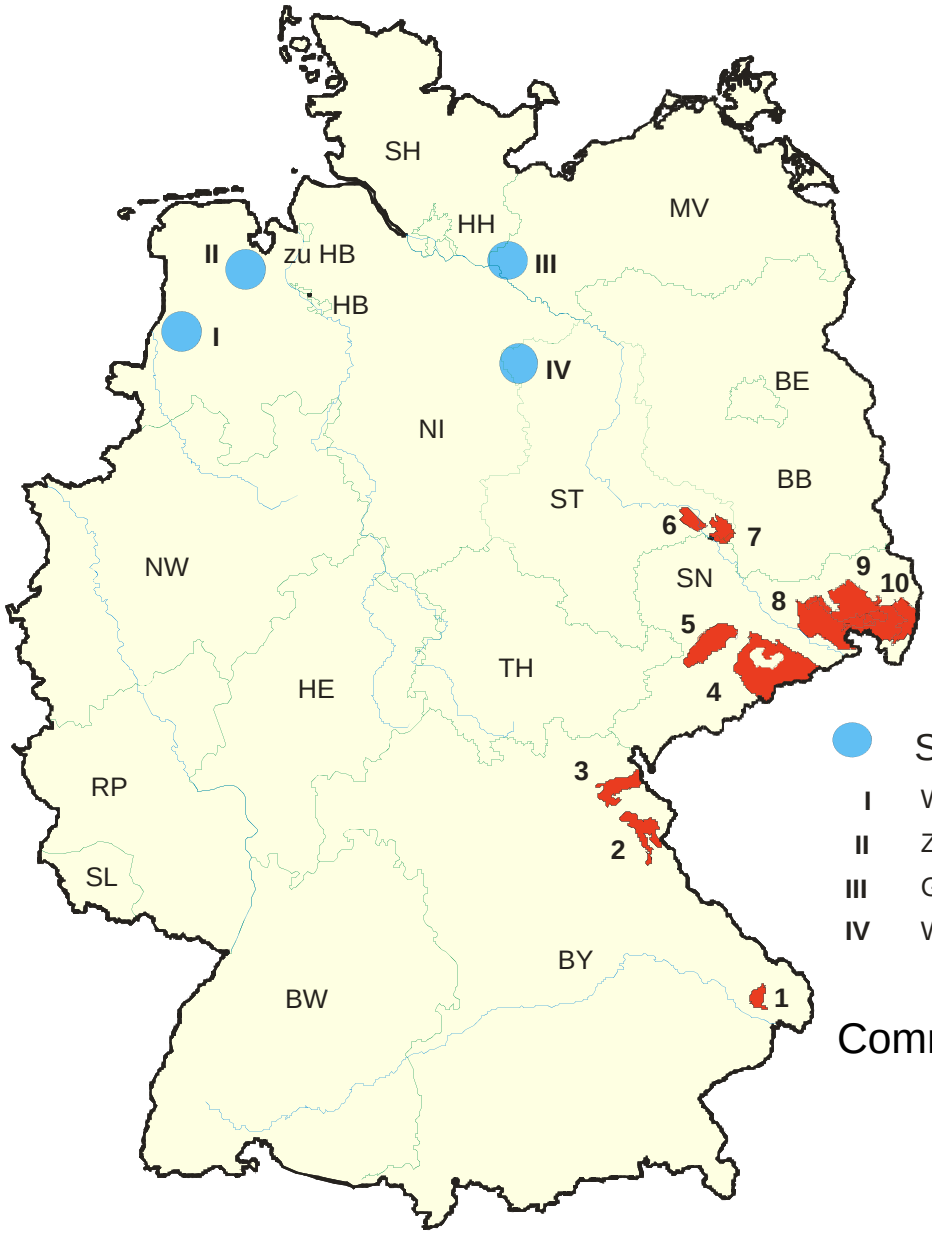

Regions worthy of investigation for the geologic disposal of heat-generating high-level radioactive waste in Germany

KOCKEL & KRULL 1995,
BRÄUER et al. 1994

Salt structures

I	Wahn
II	Zwischenahn
III	Gülze - Sumte
IV	Waddekath

Crystalline rocks

1	Saldenburg	6	Pretzsch
2	Nördl. Oberpf. Wald	7	Prettin
3	Fichtelgebirge	8	Pulsnitz
4	Graugneis	9	Radeberg - Löbau
5	Granulitgebirge	10	Zawidow

Comment: Numbering does not indicate any ranking

BGR Bundesanstalt für Geowissenschaften und Rohstoffe
GEOZENTRUM HANNOVER

Exclusion and selection criteria (Clay study)

1. International fundamental requirements (IAEO, Nagra (CH), Andra (F))
   - long-term geological stability
   - favorable host rock properties
   - sufficient extent of host rock body
   - avoidance of, and insensitivity to, detrimental phenomena and perturbations
   - explorability
   - predictability
2. Exclusion criteria / minimum requirements (AkEnd 2002)
3. Regional restrictions in Germany
4. Specific criterias of argillaceous rock formations

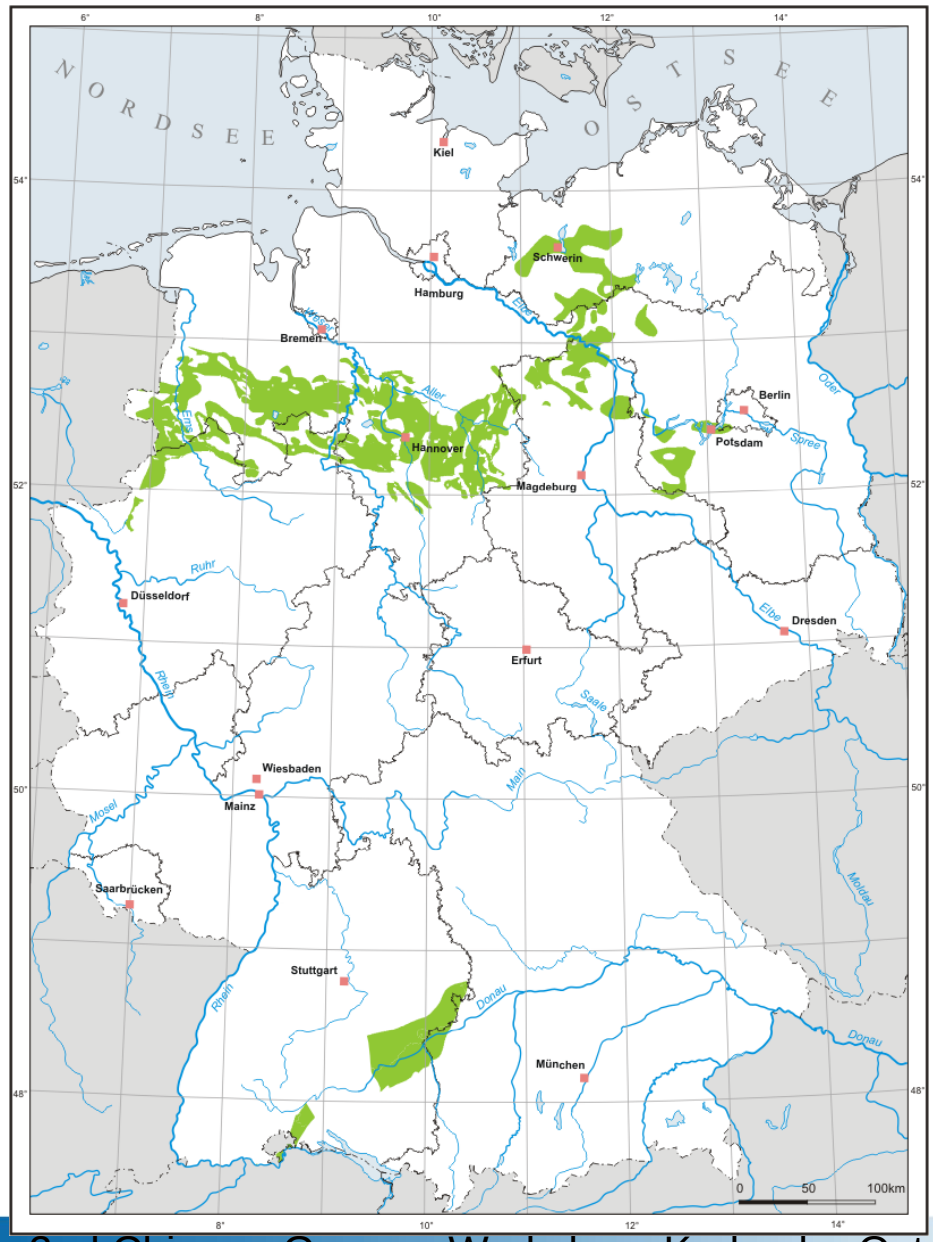

Radioactive Waste Disposal

Argillaceous rock formations in Germany

BGR 2007

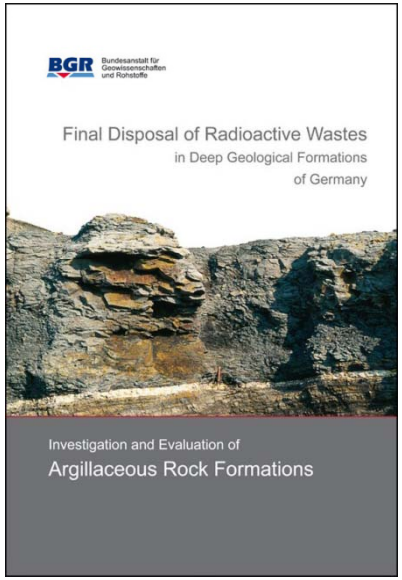

BGR-„Clay report“ by order of the German Federal Ministry of Economics and Technology

BGR Bundesanstalt für Geowissenschaften und Rohstoffe
GEOZENTRUM HANNOVER

Agenda

1. Political background

2. Scientific background
   - Criteria
   - Host rocks
   - Disposal concepts
   - Retrievability

3. Outlook

BGR Bundesanstalt für Geowissenschaften und Rohstoffe
GEOZENTRUM HANNOVER

Disposal concepts (barrier significance)

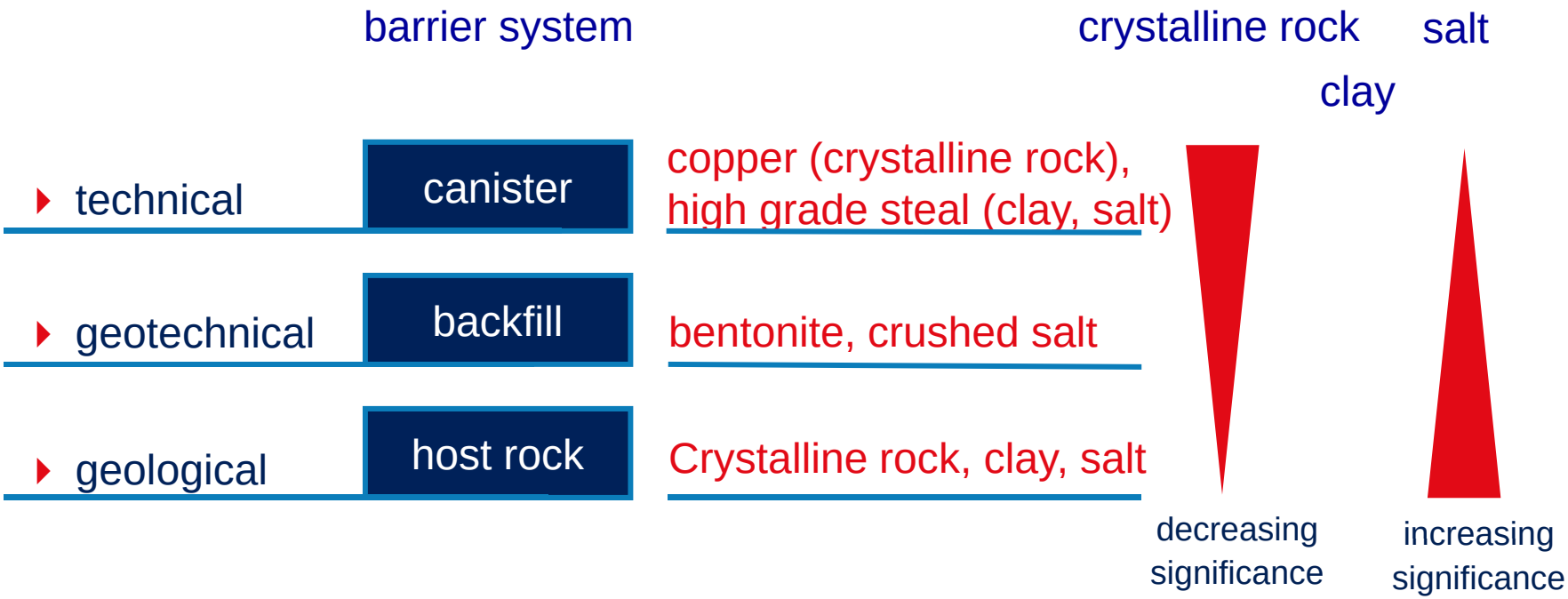

BGR Bundesanstalt für Geowissenschaften und Rohstoffe
GEOZENTRUM HANNOVER

Main criteria for repository concepts in different host rocks

Components	Rock salt	Clay/claystone	Crystalline rock
maximum emplacement depth	approx. 900 m	approx. 500 m	500 - 1200 m
storage technique*	drifts and deep boreholes	drifts and/or short boreholes	boreholes or drifts
design temperature	max. 200 °C	max. 100 °C	max. 100 °C (bentonite backfill)
backfill*	crushed salt	bentonite	bentonite
temporary storage period (fuel rods and HAW coquilles)	min. 15 years	min. 30 - 40 years	min. 30 - 40 years
drift reinforcement	not necessary	necessary and potentially very complicated	necessary in strongly fractured zones
container concept	established	new development required for Germany	new development required for Germany
mining experience	very large (salt mines)	almost none	large (ore mining)

* adapted to each type of host rock

favorable unfavorable medium

BGR Bundesanstalt für Geowissenschaften und Rohstoffe
GEOZENTRUM HANNOVER

Agenda

1. Political background

2. Scientific background
   - Criteria
   - Host rocks
   - Disposal concepts
   - Retrievability

3. Outlook

BGR Bundesanstalt für Geowissenschaften und Rohstoffe
GEOZENTRUM HANNOVER

Retrievability - Factors to be considered

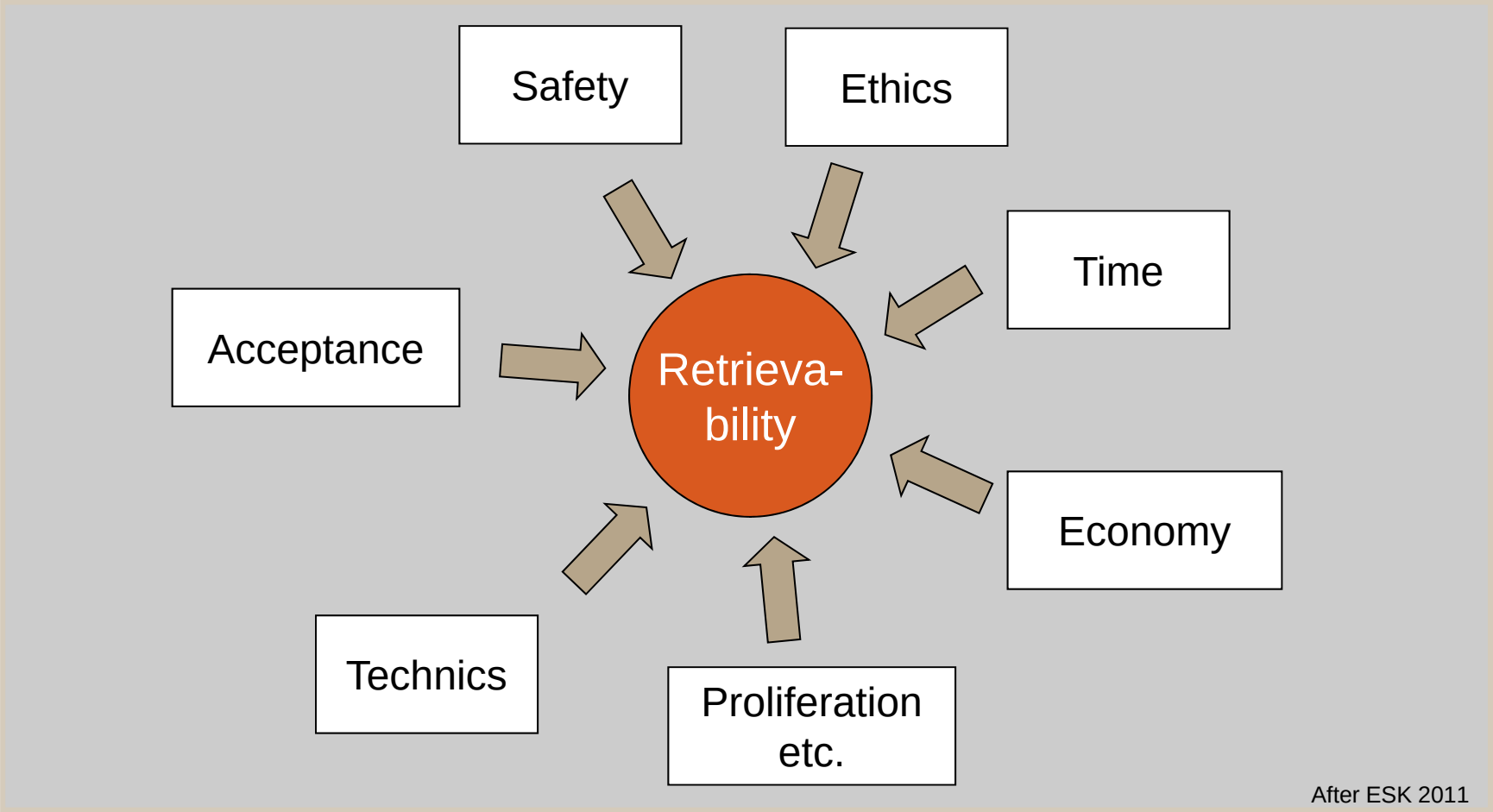

BGR Bundesanstalt für Geowissenschaften und Rohstoffe
GEOZENTRUM HANNOVER

Retrievability

1. During the operating phase (Reversibility)
   Time: several decades

2. Retrieval (recover) pursuant to BMU safety stipulations (2010)
   – Containers must make it possible to retrieve the waste
   Time: up to 500 years after sealing the repositor

3. Retrievability (s. s.)
   Time: Permanent retrievable emplacement

BGR Bundesanstalt für Geowissenschaften und Rohstoffe
GEOZENTRUM HANNOVER

Retrievability

Pro:

- Retrieval of the waste after water influx, escape of toxins
- Regression feasibility in response to failures in construction, long term forecast deficits
- Flexibility in the light of new scientific-technological developments
- Recycling of the waste
- Permanent control and surveillance capacity (enhancing safety, technical/societal)
- Self-determination by future generations
- Enhancing acceptance by ability to retrieve

BGR Bundesanstalt für Geowissenschaften und Rohstoffe
GEOZENTRUM HANNOVER

Retrievability

Contra:

- Permanent access to the waste must be maintained
- Potential radiation exposure during recovery
- Safety deficits (greater hazard)
  - technical: inflow/outflow of fluids
  - societal: access possible/misuse
- Surveillance/maintenance measures over long periods of time
- Shifting responsibility to future generations
- Long term societal development is not predictable
- Costs of surveillance/maintenance have to be borne over a long period

Radioactive Waste Disposal (international overview)

Country	Repository MAW/LAW	HAW Host rock	est. operation
Germany	yes (no operation)	**Rock salt, (Alternatives)**	approx. 2030 ?
France	yes	**Claystone**	2025
Belgium	no	**Clay**	approx. 2040
Finland	yes	**Granite**	2020
Great Britain	yes (LLW)	**n. d.**	approx. 2040
Sweden	yes	**Granite**	2023
Spain	yes	**n. d.**	Not before 2050
Netherlands	(yes) 100 years	**n. d.**	approx. in 100 years
Italy	no	**n. d.**	n.d.
Lithuania	yes	**Clay, Anhydrite, Rock salt, Crystalline r.**	n.d.
Slowakia	yes	**Granite, Claystone, Clay**	n.d.
Slowenia	no	**Sedimentary rocks, Granite**	2065
Czech. Republic	yes	**Granite ?**	approx. 2065
Hungary	yes	**Claystone, Granite?**	approx. 2050
Switzerland	no	**Claystone, (Granite)**	2050
Bulgaria	no	**Claystone, Granite?**	n.d.
Romania	yes	**Rock salt?**	2055
USA	yes	**Tuff?, Rock salt?**	n.d.
Japan	yes	**Granite**	2030

BGR Bundesanstalt für Geowissenschaften und Rohstoffe
GEOZENTRUM HANNOVER

Agenda

1. Political background

2. Scientific background
   - Criteria
   - Host rocks
   - Disposal concepts
   - Retrievability

3. Outlook

BGR Bundesanstalt für Geowissenschaften und Rohstoffe
GEOZENTRUM HANNOVER

Federal Government and State Governments: Roadmap for selection of a repository site, December, 15th 2011

Phase 1 : selection procedure steps • which procedure steps • how are the Federal Government and the State Governments involved • who pays • which institutions are involved	to mid 2012 §
Phase 2 + 3: scientific basics • scientific basis is compiled and specified	to mid 2013 §
Phase 4: Site selection and surface exploration • site regions are localized •regions (in different geological formations/host rocks) for surface exploration are selected and specified • surface exploration is implemented • site for the underground exploration is specified	to mid 2014 to end of 2014 § to end of 2019 §
Phase 5: Underground exploration and siting • Assessment of alternatives and site nomination • site is confirmed	to end of 2027?§
Phase 6: Administrative procedure • repository is approved, constructed and under operation	?

§ legislated/stipulated by federal law

BGR Bundesanstalt für Geowissenschaften und Rohstoffe
GEOZENTRUM HANNOVER

2nd Chinese-German Workshop, Karlsruhe Oct. 15-16, 2012

BGR Bundesanstalt für Geowissenschaften und Rohstoffe

GEOZENTRUM HANNOVER

Monday, October 15

TOPIC: HOST ROCK CHARACTERIZATION (ROCK MECHANICS / HYDROGEOLOGY)

Rock Mass Characterization for the Preselected Beishan area, Gansu, of China's High-level Radioactive Waste Repository

Wang Guibin

Institute of Rock and Soil Mechanics,
the Chinese Academy of Sciences

2012.10.15

CONTENTS

- Introduction
- Field survey and sampling
- Joint characteristics
- Mechanical properties
- In-situ testing results
- Conclusions

Introduction

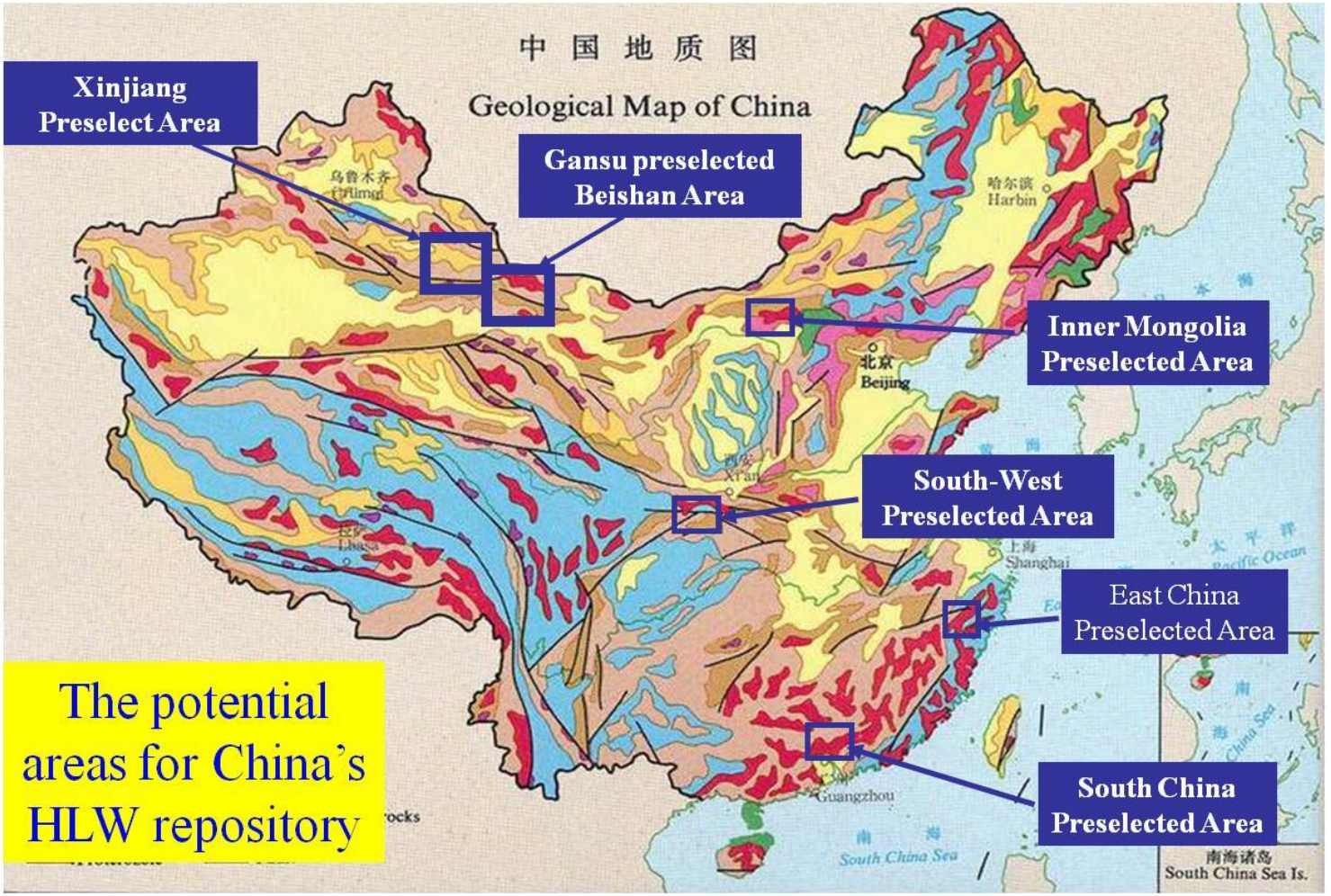

Introduction

- Jiujin section, Jijicao quarry and Xinchang are candidates in Beishan-the preselected area **(most preferred area)** for China′s HLW deep geological disposal

- Since 2002, a series of investigations were performed by Institute of Rock and Soil mechanics, CAS

Rock mass characterization for the preselected Beishan area

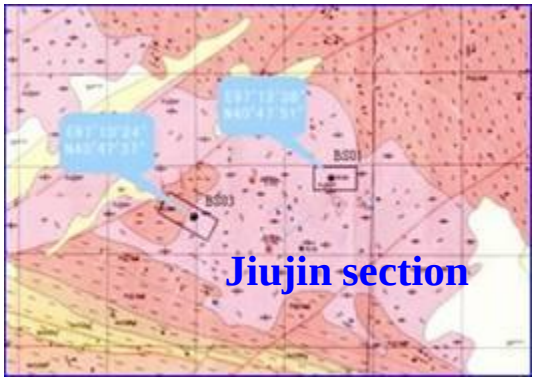

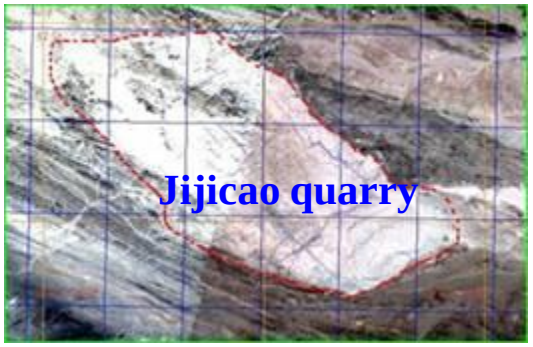

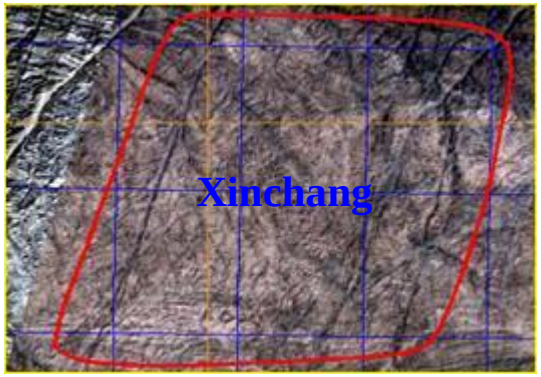

- Introduction
- **Field survey and sampling**
- Joint characteristics
- Mechanical properties
- In-situ testing results
- Conclusions

Field Joint Survey

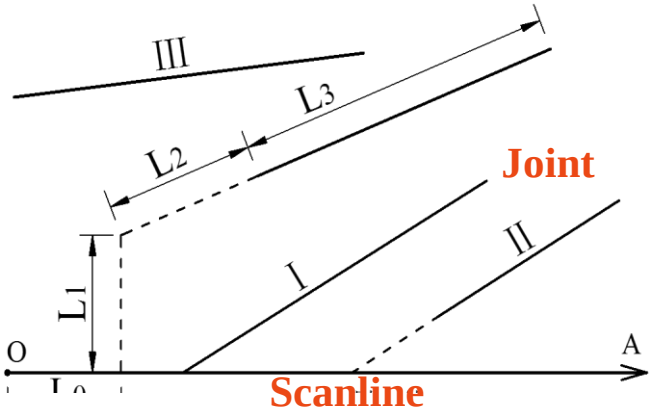

Schematic Joint Survey Method

Rock Sampling and Test Machines

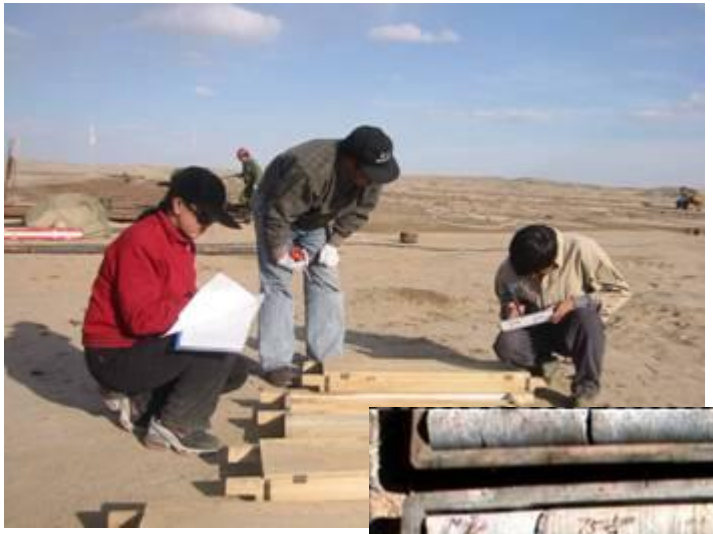

Rock mass characterization for the preselected Beishan area

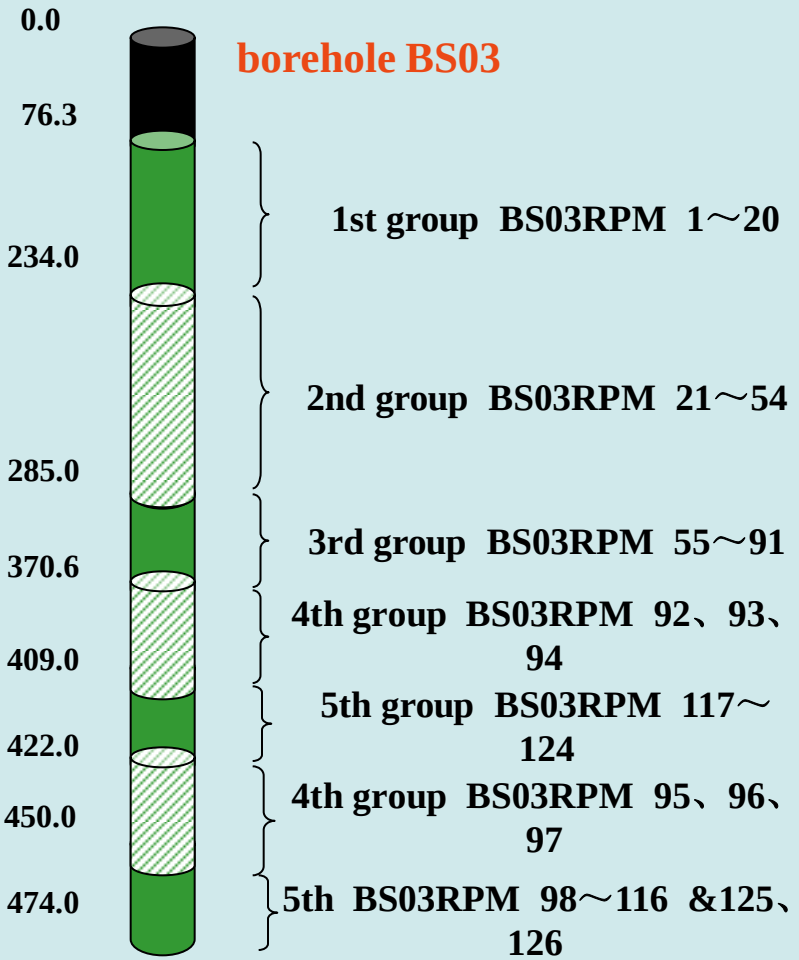

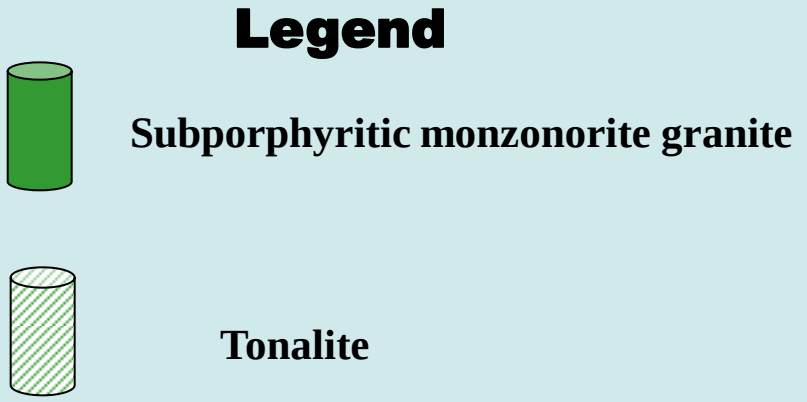

The lithology is mainly monzonite granite and partially tonalite .

Five group of rock sample were chosen from different depth

- Introduction
- Field survey and sampling
- **Joint characteristics**
- Mechanical properties
- In-situ testing results
- Conclusions

Rock mass characterization for the preselected Beishan area

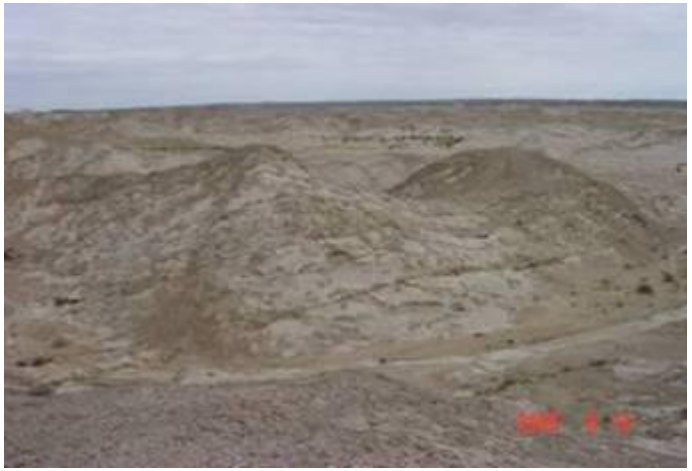

- ✓ **Joints are principally steep shear joints.**
- ✓ **Joints ,which dip angle greater than 60° , are about 91%.**
- ✓ **“X” type shear joints can be observed in some outcrops.**
- ✓ **Only one set of joint can be observed for most outcrops.**
- ✓ **Joints are flat, smooth, with stable strike and long extension.**

Rock mass characterization for the preselected Beishan area

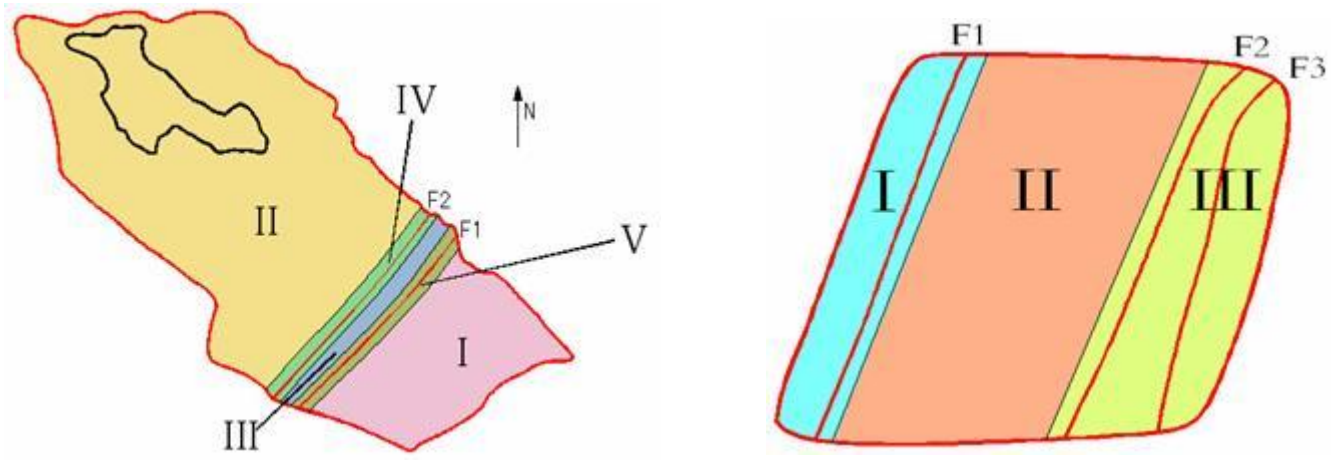

According to the faults, Jijicao quarry (left) and Xinchang (right) are roughly divided into statistical homogeneities and the region which is influenced by the faults.

Rock mass characterization for the preselected Beishan area

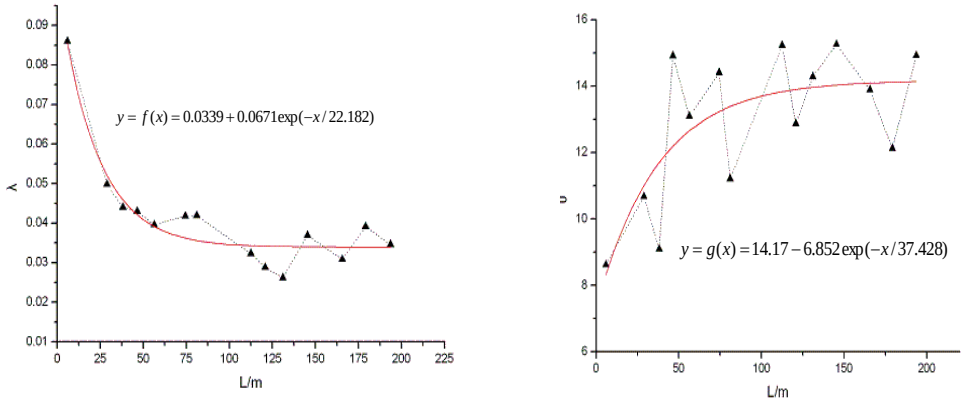

Mean trace length and trace midpoint density vs.L in Jiji quarry

L is the distance that a outcrop leaves from the fault

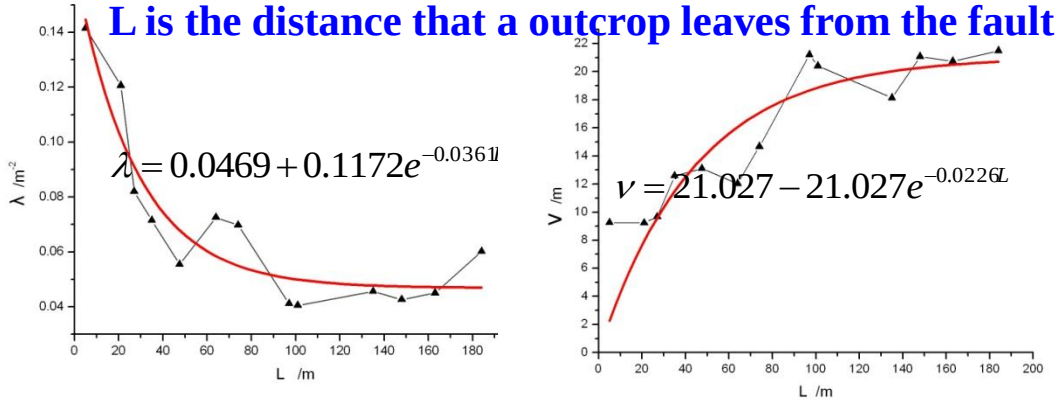

Mean trace length and trace midpoint density vs. L in Xingchang

➢**The boundary of the statistical homogeneities is determined.**

Statistic of joint orientation

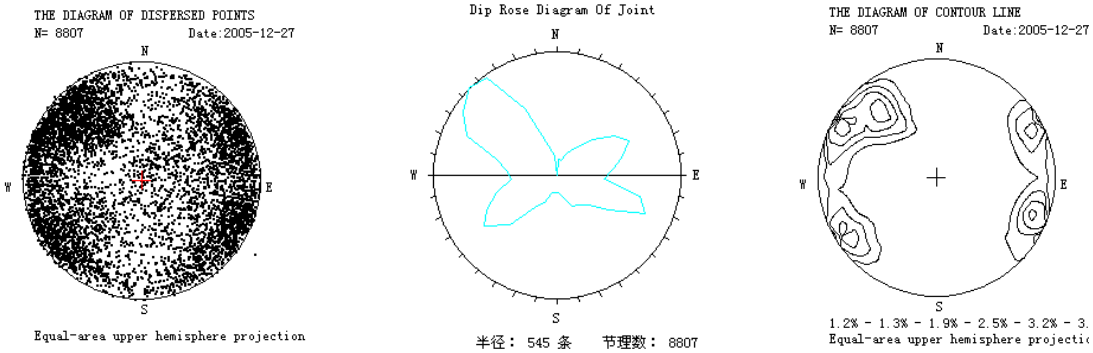

Joint polar points and Dip rose diagram of statistical homogeneity II of Jiji quarry

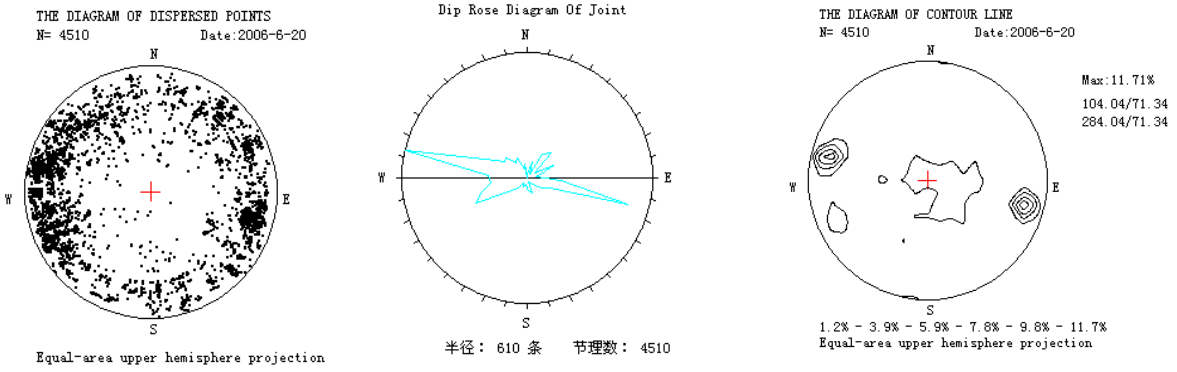

Joint polar points and Dip rose diagram of statistical homogeneity II of Xingchang

Probability analysis of joint orientation

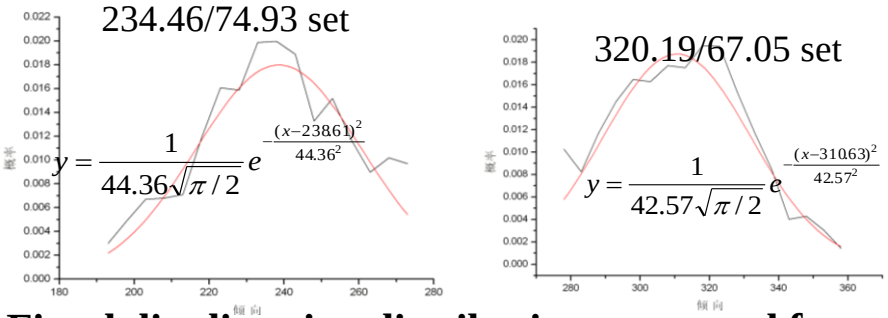

Fitted dip direction distribution curve and formula of statistical homogeneity II of Jiji quarry

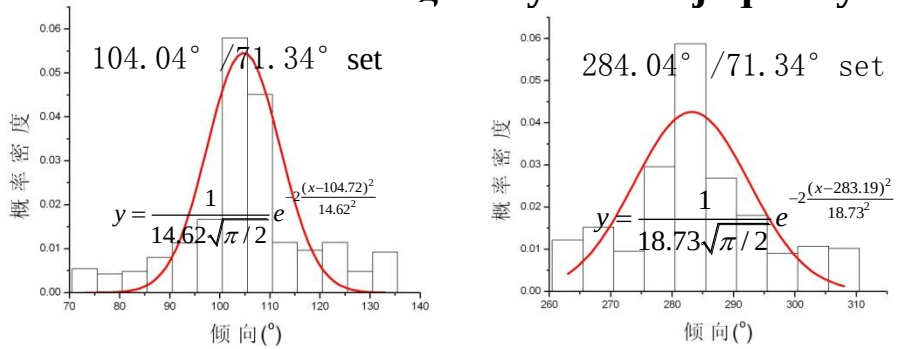

Fitted dip direction distribution curve and formula of statistical homogeneity II of Xingchang

➢**Dip direction can be fitted by Gaussian (normal) distribution**

Statistics of joint spacing

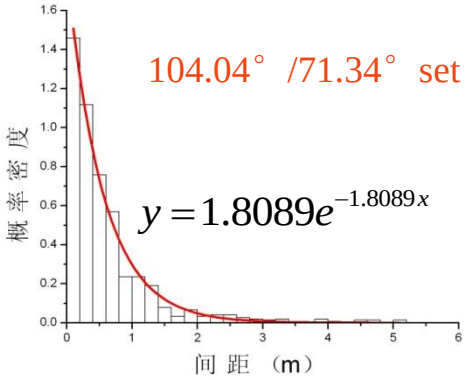

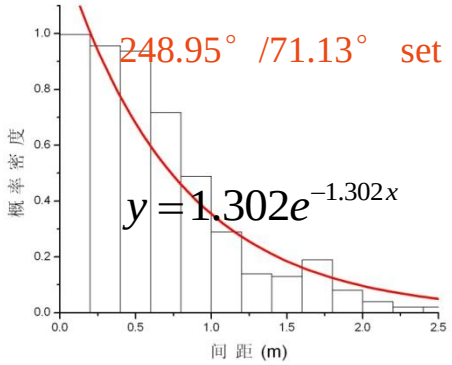

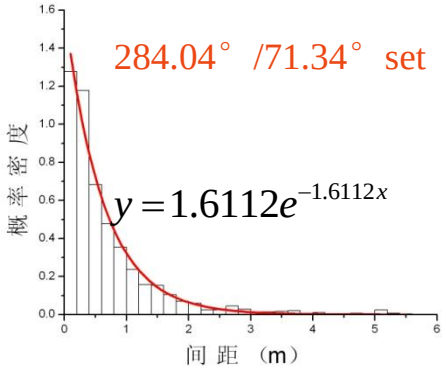

Fitted joint space distribution (negative exponential distribution) and formula of statistical homogeneity II of xingchang

According to *ISRM suggested method* joint spacing of the 104.04 /71.34 set of Xinchang is moderate spacing and the others are wide spacing.

Joint spacing of Xingchang

	SET	ORIENTATION	SPACING (m)
II	1	104.04 ° /71.34 °	0.55
	2	248.95 ° /71.13 °	0.77
	3	284.04 ° /71.34 °	0.62

Estimation of mean trace length and midpoint density

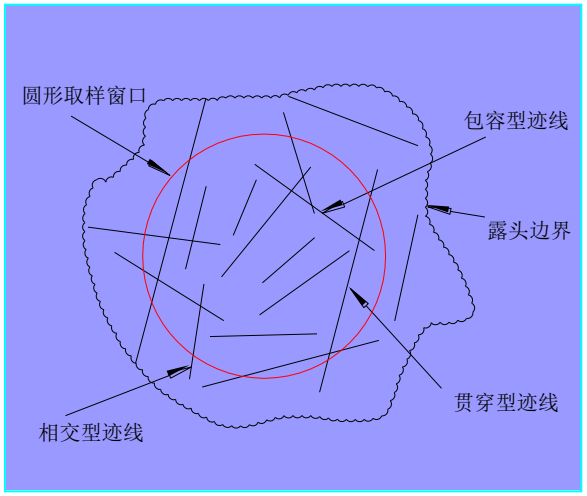

Schematic circular sample window

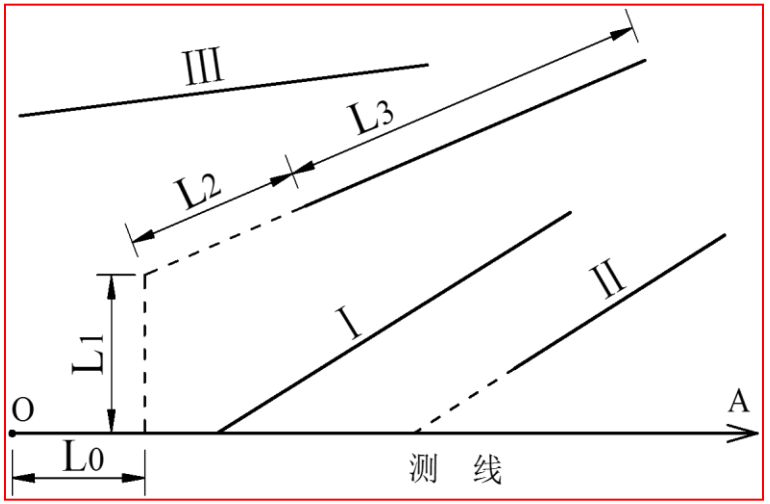

Types of the endpoints of joint traces

Mean trace length $\nu = \dfrac{\pi(N + N_2 - N_0)}{2(N - N_2 + N_0)}c$

Midpoint density $\lambda = \dfrac{N - N_2 - N_0}{2\pi c^2}$

Estimation of mean trace length and midpoint density (continued)

Concentric circles method

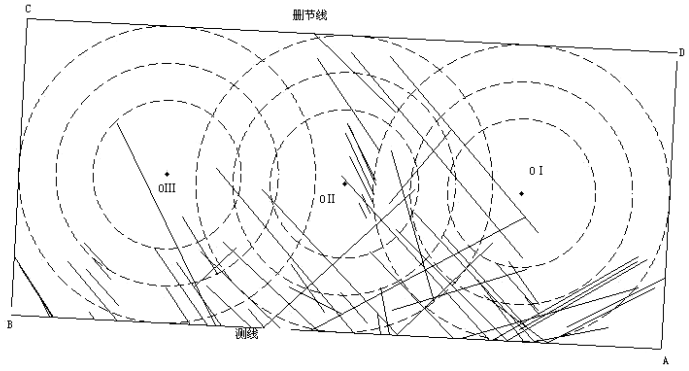

Results of Concentric circles

同心圆法所得路关P90平均迹长和迹线中点的面密度

窗口半径/m	窗口编号	各类迹线条数			迹线中点面密度 λ	平均迹长估计值 υ/m
		N_0	N_1	N_2		
13.5287	O Ⅰ	7	16	4	0.0261	17.001
	O Ⅱ	12	16	3	0.0348	11.688
	O Ⅲ	5	10	0	0.0174	10.625
10.1465	O Ⅰ	0	14	0	0.0216	15.938
	O Ⅱ	6	13	2	0.0386	10.838
	O Ⅲ	1	9	0	0.0170	13.040
6.7644	O Ⅰ	0	5	0	0.0174	10.625
	O Ⅱ	6	7	1	0.0661	5.033
	O Ⅲ	0	3	0	0.0104	10.625

Tangent circles method

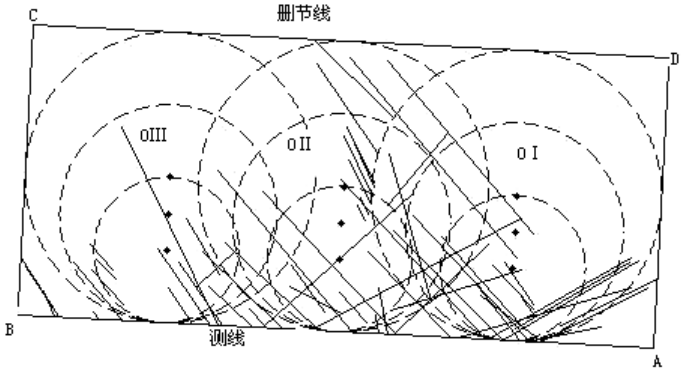

Results of tangent circles

相切圆法所得路关P90平均迹长和迹线中点的面密度

窗口半径/m	窗口编号	各类迹线条数			迹线中点面密度 λ	平均迹长估计值 υ/m
		N_0	N_1	N_2		
13.5287	O Ⅰ	7	16	4	0.0261	17.001
	O Ⅱ	12	16	3	0.0348	11.688
	OIII	5	10	0	0.0174	10.625
10.1465	O Ⅰ	4	11	5	0.0294	17.6158
	O Ⅱ	9	14	3	0.0495	9.9613
	O Ⅲ	5	10	0	0.0309	7.9691
6.7644	O Ⅰ	3	9	6	0.0522	14.8756
	O Ⅱ	5	8	6	0.0626	11.8060
	O Ⅲ	3	8	1	0.0487	7.5896

➢**Stable and reasonable results can be obtained from Tangent Circles Method**

Estimation of mean trace length and midpoint density (continued)

Trace length and midpoint density for each statistical homogeneity of Jiji quarry

NO.	I	II	III	IV	V
/m	14.834	14.398	15.167	15.667	12.184
$/m^{-2}$	0.034	0.0387	0.034	0.0408	0.0414

Trace length and midpoint density for each statistical homogeneity of Xingchang

NO.	I	II	III
/m	14.129	18.671	14.173
$/m^{-2}$	0.1058	0.0586	0.0827

➢**Mean trace length is smaller and midpoint density is greater in the region that is influenced by faults than that in statistical homogeneities**

JSR---Jointing Structure Rate

$$JSR = W_n \overline{D}_a \overline{L}$$

W_n is the weight determined by the joint set number.

$\overline{D}_a$ is the weight determined by mean density of trace midpoints

$\overline{L}$ is the weight determined by mean trace length

- JSR is a general index which can be used for evaluating both the block size and the connectivity of joints networks

Description and grade for jointing structure characterization according to JSR

JSR	Description
0-200	Very slightly jointed
200-400	Slightly jointed
400-600	Moderate jointed
600-800	Strongly jointed
800-1000	Very Strongly jointed

Jointing structure characterization for the sections of the Beishan area

Section		W_n	R_1	R_2	*JSR*	Description
BS01		2.5	9	5	112.5	**Very slightly jointed**
BS03		4	7.5	7	210	**slightly jointed**
Jijicao	I	4	10.5	1.5	63	**Very slightly jointed**
	II	4	10.5	1.5	63	**Very slightly jointed**
	III	2	11	1.5	33	**Very slightly jointed**

Development of 3-D joint simulation system

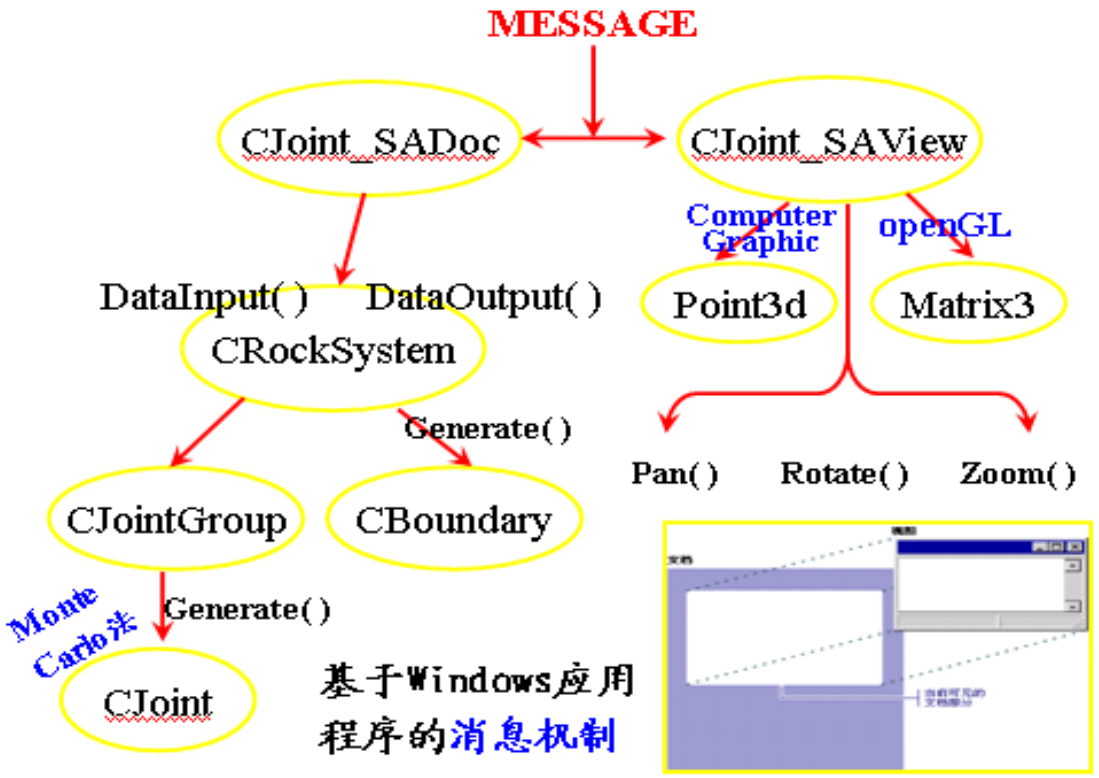

Development of 3-D joint simulation system (continued)

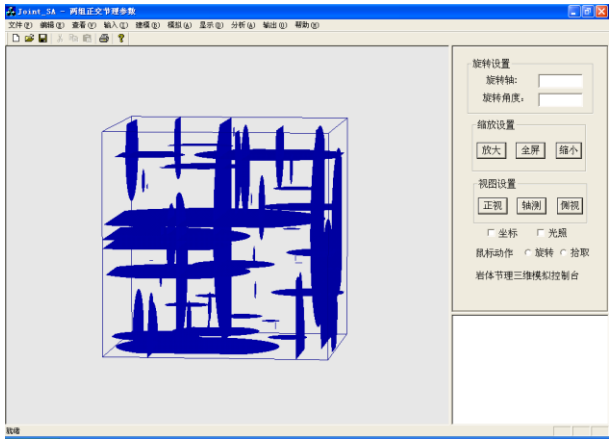

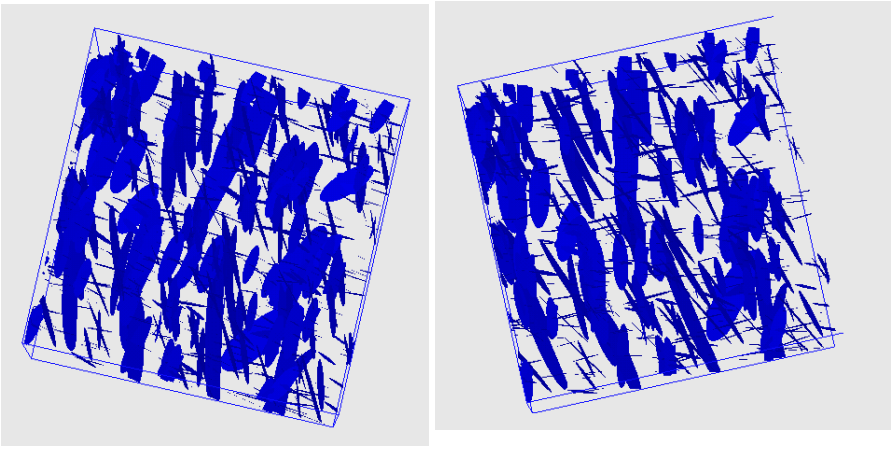

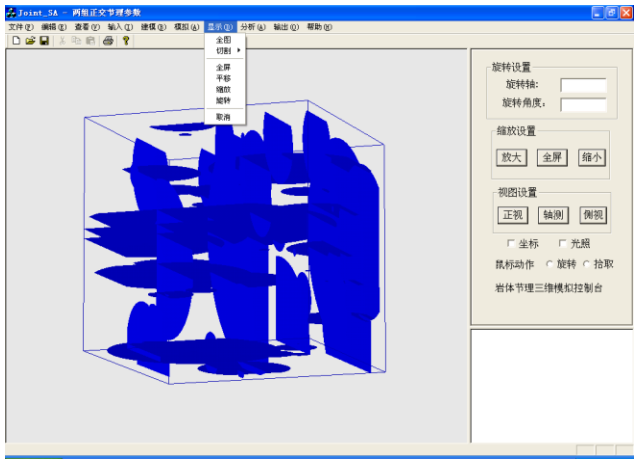

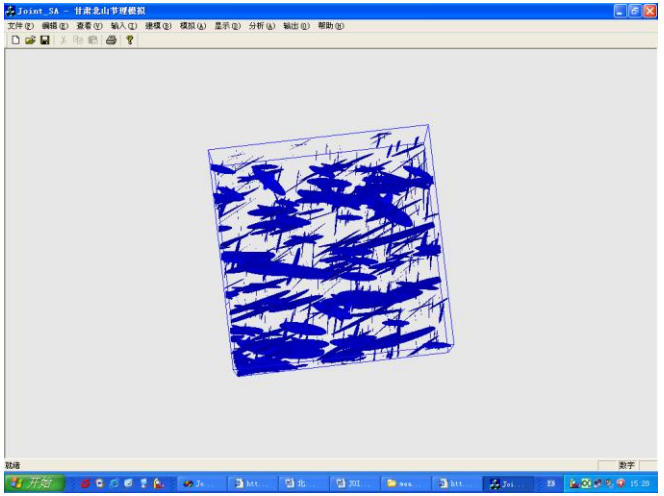

- Introduction
- Field survey and sampling
- Joint characteristics
- **Mechanical properties**
- In-situ testing results
- Conclusions

Mechanical properties of intact rock

Specimen size	Test items
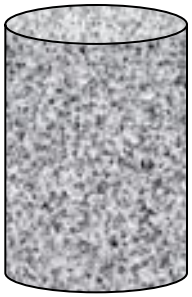 φ50×100	Water-content coefficient ;Hygroscopic coefficient; Dry density ； Acoustic wave measurement ； Uniaxial compression strength and deformation; Triaxial strength and deformation
φ60×30	Water-content coefficient ;Hygroscopic coefficient; Dry density ； Brazilian test
40×40×20	Shear strength

Specimen after tests

Uniaxial compression

Triaxial compression

Direct shear

Brazilian splitting

Uniaxial and triaxial compression tests

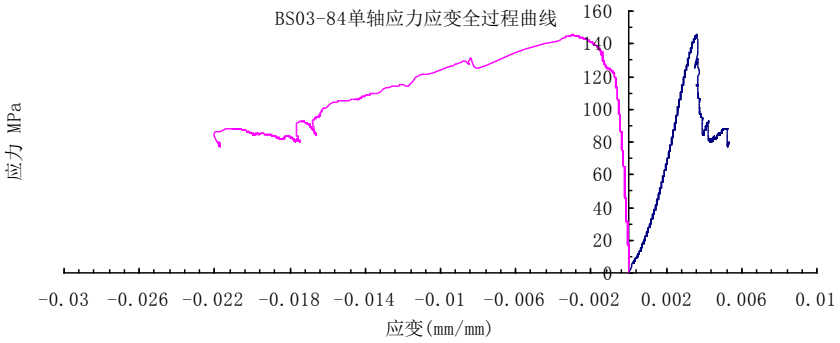

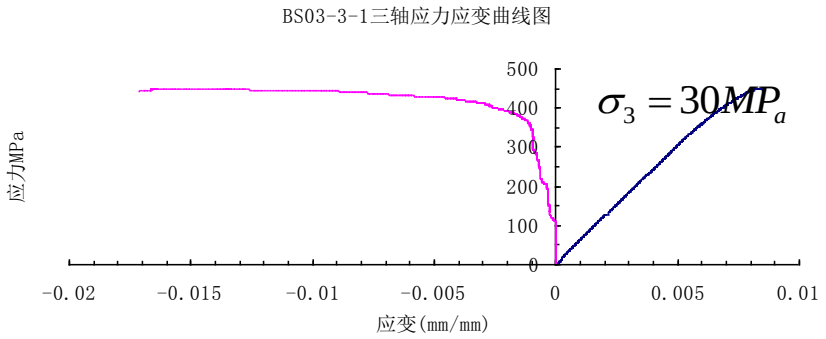

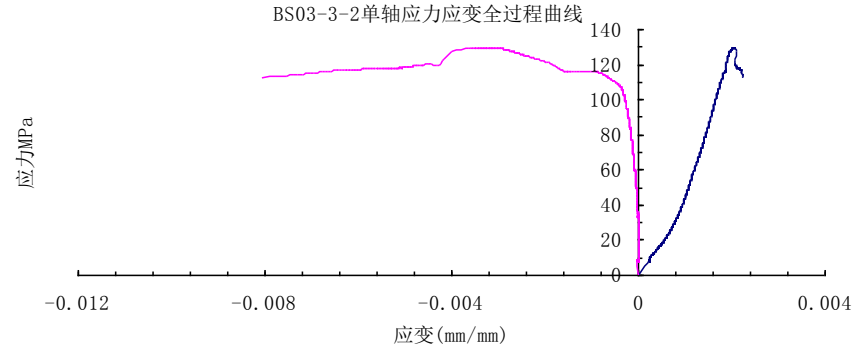

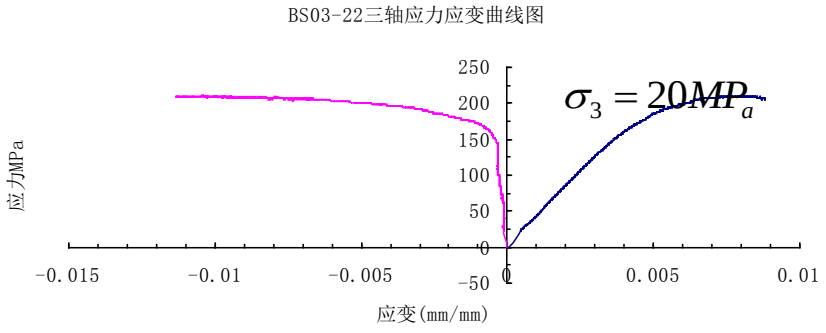

Uniaxial compression test

Triaxial compression test

Conclusions of rock mechanics characteristics

- Both rock types have high mechanical strength and high stiffness (UCS$_{max}$ up to 140Mpa).
- Monzonite granite is more homogeneous and has higher mechanical strength.
- Tonalite is inhomogeneous and its mechanical strength is enhanced with depth.
- Rock below 300m has superior homogeneity and its mechanical strength is higher.

- Introduction
- Field survey and sampling
- Joint characteristics
- Mechanical properties
- **In-situ testing results**
- Conclusions

Hydraulic Fracturing and High-pressure Injection Testing were performed in borehole BS03

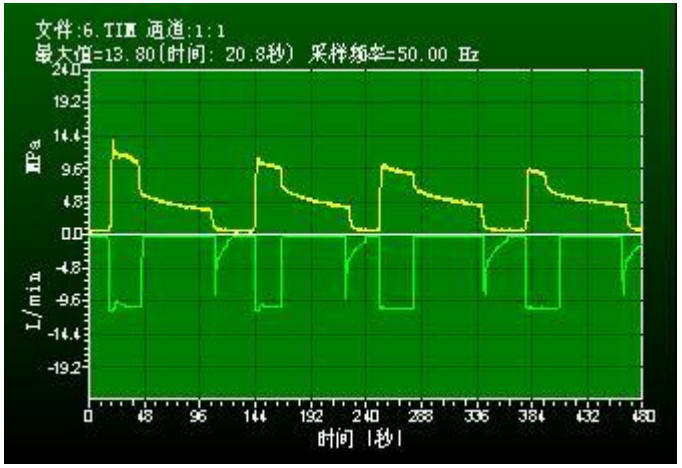

Geostress characteristic

Geostress measured by hydraulic fracture method

Hypothesis:

1.Host rock is linear, homogeneous, isotropic elastic medium.

2.Injection water flow meet with the Darcy's law in rock pore .

3. Vertical stress σ_v is one of the principal stress

Results of measurement of geostress

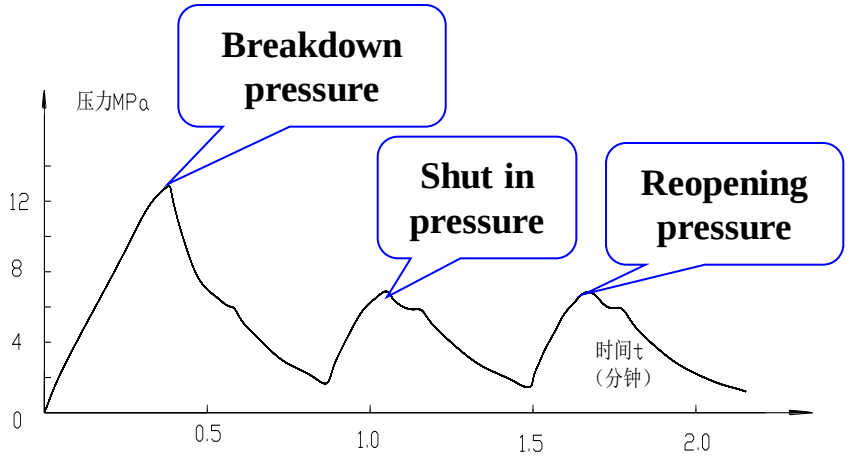

Pressure vs. time curve for depth 283.51~284.51m

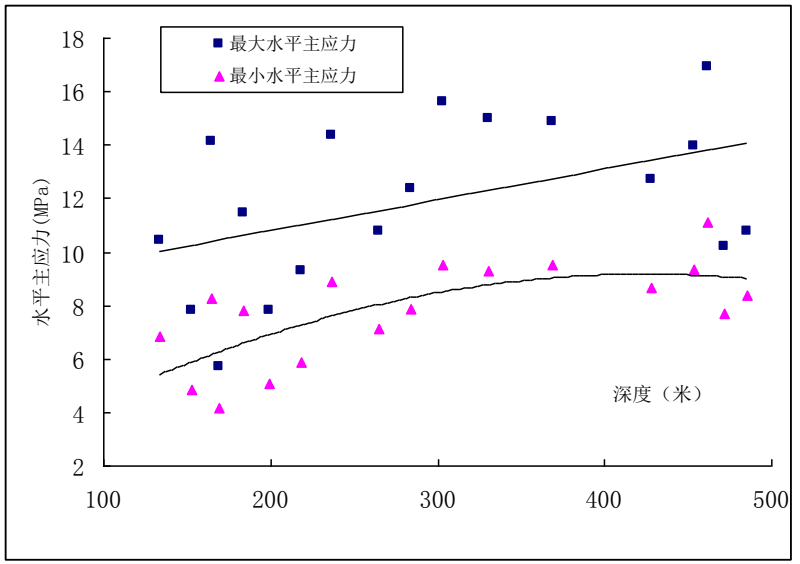

The maxim horizontal geostress is 17.52MPa. The moderate geostress range is 10MPa<σ_1<20MPa

➢**The geostress of Borehole 3 is moderate and increases with depth**

Seepage characteristic

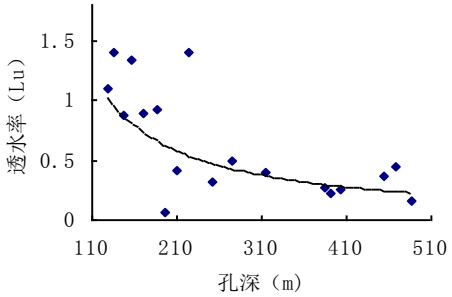

Injection rate vs. depth

Permeability coefficient of every sections can be obtained from high pressure injection tests.

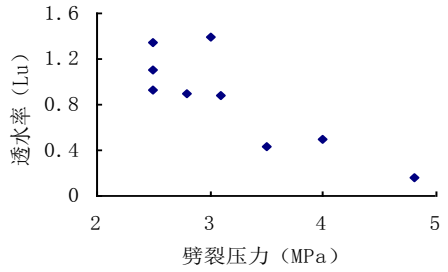

Splitting pressure vs. injection rate

The geometric mean value of permeability coefficient for the all of the testing sections can be used to describe permeability coefficient of the borehole.

$$\bar{K} = \sqrt[n]{K_1 K_2 \cdots K_n}$$

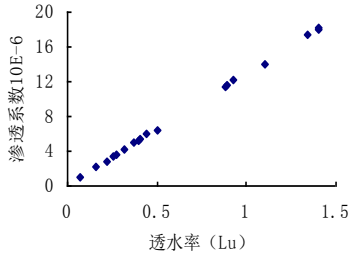

Permeability coefficient vs. Injection rate

➢**The geometric mean permeability coefficient of borehole BS03 is 4.4×10^{-6} cm/s .**

Seepage characteristic (continued)

Flow in a single fracture is the basis for the determination of the hydraulic conductivity tensor for fractured medium

Generally , in permeability domain, hydraulic gradient is not parallel to the fracture plane. But water flow velocity in fractures is related to hydraulic gradient which is parallel with fracture plane.

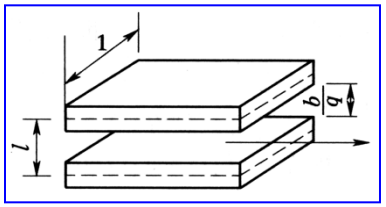

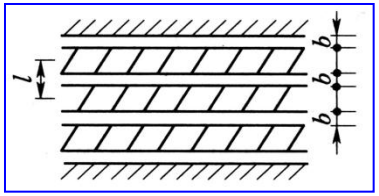

Permeability figure of hydraulic gradientparallel with fracture plane

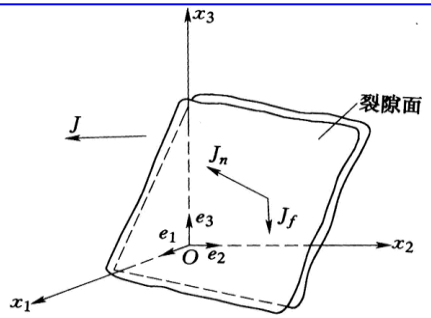

Permeability figure of hydraulic gradient not parallel with fracture plane

$$K=\sum_{i=1}^{n}K_{ei}\begin{bmatrix}1-\cos^2\beta_i\sin^2\gamma_i & -\sin\beta_i\cos\beta_i\sin^2\gamma_i & -\cos\beta_i\sin\gamma_i\cos\gamma_i\\ -\sin\beta_i\cos\beta_i\sin^2{}_i & 1-\sin^2\beta_i\sin^2\gamma_i & -\sin\beta_i\sin\gamma_i\cos\gamma_i\\ -\cos\beta_i\sin\gamma_i\cos\gamma_i & -\sin\beta_i\sin\gamma_i\cos\gamma_i & 1-\cos^2\gamma_i\end{bmatrix}$$

Rock mass characterization for the preselected Beishan area

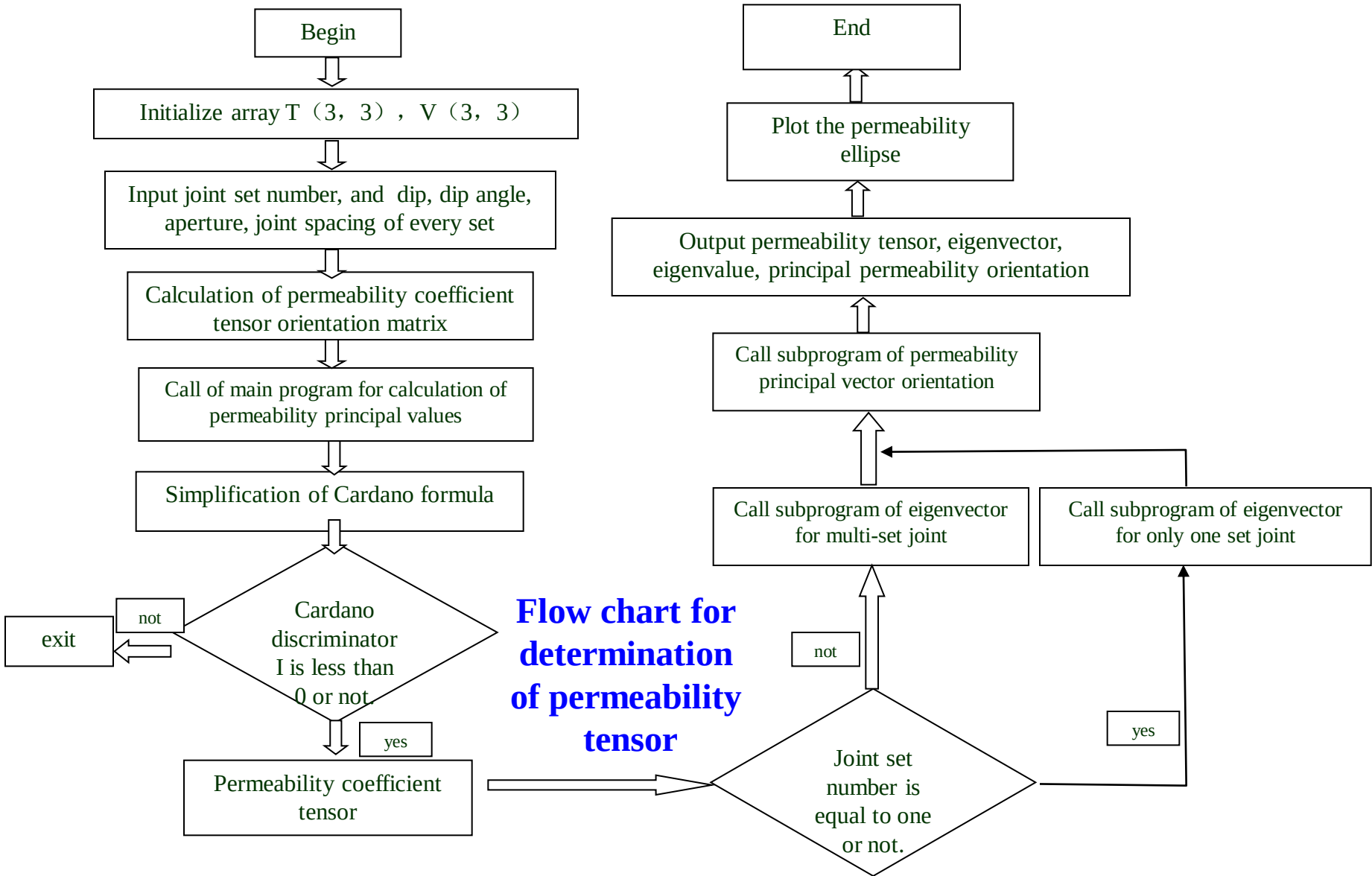

Seepage characteristic (continued)

Hydraulic parameters of 4 set joint：

1st：dip 43.19°， dip angle 70.58°， spacing 2.75m

2nd：dip 141.75°， dip angle 60.75°， spacing 5.03m

3rd：dip 223.23°， dip angle 67.05°， spacing 2.11m

4th：dip 348.03°， dip angle 68.14°， spacing 8.64m

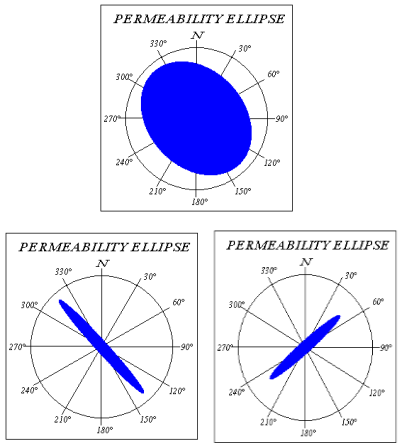

Permeability ellipse

Hydraulic conductivity tensor

$$K=\begin{bmatrix} 0.823\times10^{-5} & -0.763\times10^{-5} & 0.194\times10^{-5} \\ -0.763\times10^{-5} & 1.070\times10^{-5} & -0.016\times10^{-5} \\ 0.194\times10^{-5} & -0.016\times10^{-5} & 1.390\times10^{-5} \end{bmatrix}$$

Permeability principal value

0.157×10^{-5} 0.135×10^{-4} 0.177×10^{-4}

Permeability principal vector

$\alpha_1(-0.763,\ -0.637,\ 0.112)$

$\alpha_2(0.146,\ -0.338,\ -0.930)$

$\alpha_3(0.630,\ -0.692,\ 0.351)$

3 permeability principal orientation：

1dip 230.12°， dip angle 6.42°

2dip 336.61°， dip angle 68.36°

3dip 137.70°， dip angle 20.57°

- Introduction
- Field survey and sampling
- Joint characteristics
- Mechanical properties
- In-situ testing results
- **Conclusions**

Conclusions

- The quantitative parameters describing joint characteristics have been obtained . Rock mass of Beishan are **very slightly jointed**.

- Rock in the research area is high density, low water-content, low porosity, **low permeability**

- Rock in the research area is high mechanical strength, high stiffness (UCS_{max} up to **140 MPa** . **Very hard & brittle**.)

- The geostress of bohole BS03 is **moderate** and increases with depth. The mean permeability coefficient is only 4.4×10^{-6} cm/s .

Thanks for your attention!

Multi-scale Applications of Electrical Resistivity Tomography in the Site Characterization for HLW Disposal

Qi You ZHOU

Department of Hydrosciences, School of Earth Sciences and Engineering
Nanjing University, Nanjing 210093, China

October 15, 2012

OUTLINE

1. Introduction
2. Objectives of this study
3. Applications of ERT at sample scale in the lab
4. Applications of ERT at block scale in the lab
5. Applications of ERT at meters scale in the field
6. Applications of ERT at hundreds of meters scale in the field
7. A site characterization concept with multi-scale and multi-dimensional ERT
8. Conclusions

The difficulties we are facing in the site characterization for HLW disposal

The difficulties we are facing in the site characterization for HLW disposal

The Main Conventional Approaches:

The difficulties we are facing in the site characterization for HLW disposal

The Main Conventional Approaches:

1. Geological and geophysical prospecting and surveying from ground surface

The difficulties we are facing in the site characterization for HLW disposal

The Main Conventional Approaches:

1. Geological and geophysical prospecting and surveying from ground surface
2. Hydraulic and tracer transport tests within boreholes

The difficulties we are facing in the site characterization for HLW disposal

The Main Conventional Approaches:

1. Geological and geophysical prospecting and surveying from ground surface
2. Hydraulic and tracer transport tests within boreholes
3. Isotope analysis and inversion methods based on water and core sampling

The difficulties we are facing in the site characterization for HLW disposal

The Main Conventional Approaches:

1. Geological and geophysical prospecting and surveying from ground surface
2. Hydraulic and tracer transport tests within boreholes
3. Isotope analysis and inversion methods based on water and core sampling

The difficulties we are facing in the site characterization for HLW disposal

The Main Conventional Approaches:

1. Geological and geophysical prospecting and surveying from ground surface
2. Hydraulic and tracer transport tests within boreholes
3. Isotope analysis and inversion methods based on water and core sampling

The Difficulties:

The difficulties we are facing in the site characterization for HLW disposal

The Main Conventional Approaches:

1. Geological and geophysical prospecting and surveying from ground surface
2. Hydraulic and tracer transport tests within boreholes
3. Isotope analysis and inversion methods based on water and core sampling

The Difficulties:

1. The extremely high heterogeneity and anisotropy of the site

The difficulties we are facing in the site characterization for HLW disposal

The Main Conventional Approaches:

1. Geological and geophysical prospecting and surveying from ground surface
2. Hydraulic and tracer transport tests within boreholes
3. Isotope analysis and inversion methods based on water and core sampling

The Difficulties:

1. The extremely high heterogeneity and anisotropy of the site
2. The scale effects of parameters

The difficulties we are facing in the site characterization for HLW disposal

The Main Conventional Approaches:

1. Geological and geophysical prospecting and surveying from ground surface
2. Hydraulic and tracer transport tests within boreholes
3. Isotope analysis and inversion methods based on water and core sampling

The Difficulties:

1. The extremely high heterogeneity and anisotropy of the site
2. The scale effects of parameters
3. The data obtained at points or along lines isn't enough in describing the 3-D structure of the site

The extremely high heterogeneity and anisotropy of the site

The extremely high heterogeneity and anisotropy of the site

The extremely high heterogeneity and anisotropy of the site

The fractal structure and scale effects in dispersivity

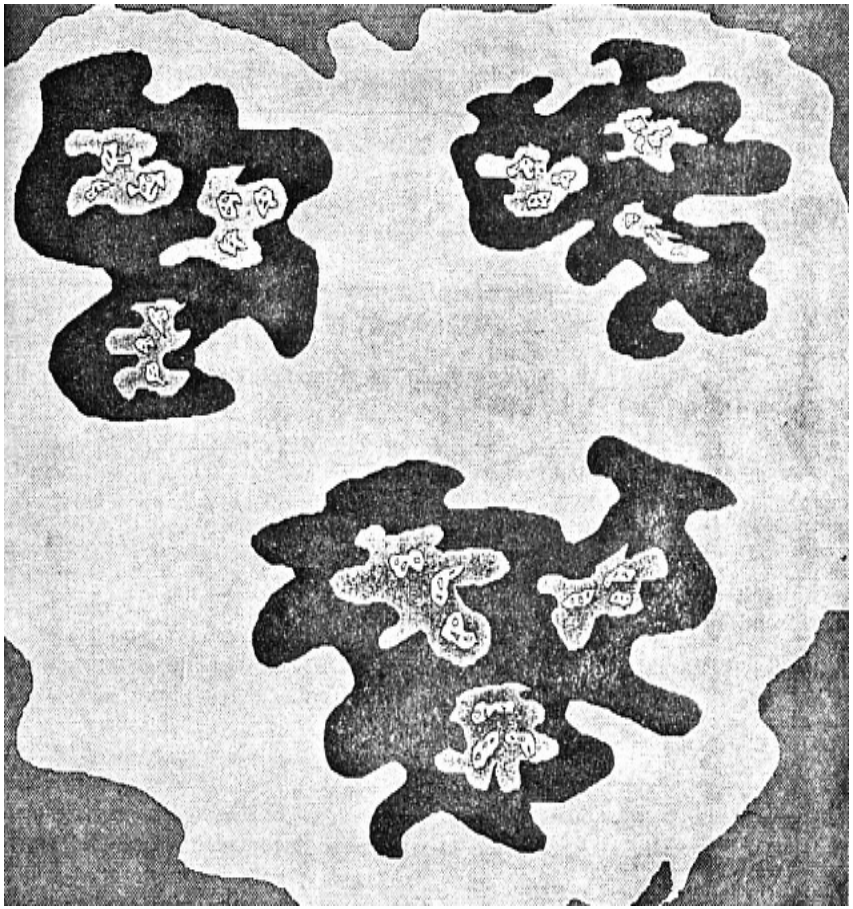

from Wheatcraft and Tyler [1988]

The fractal structure and scale effects in dispersivity

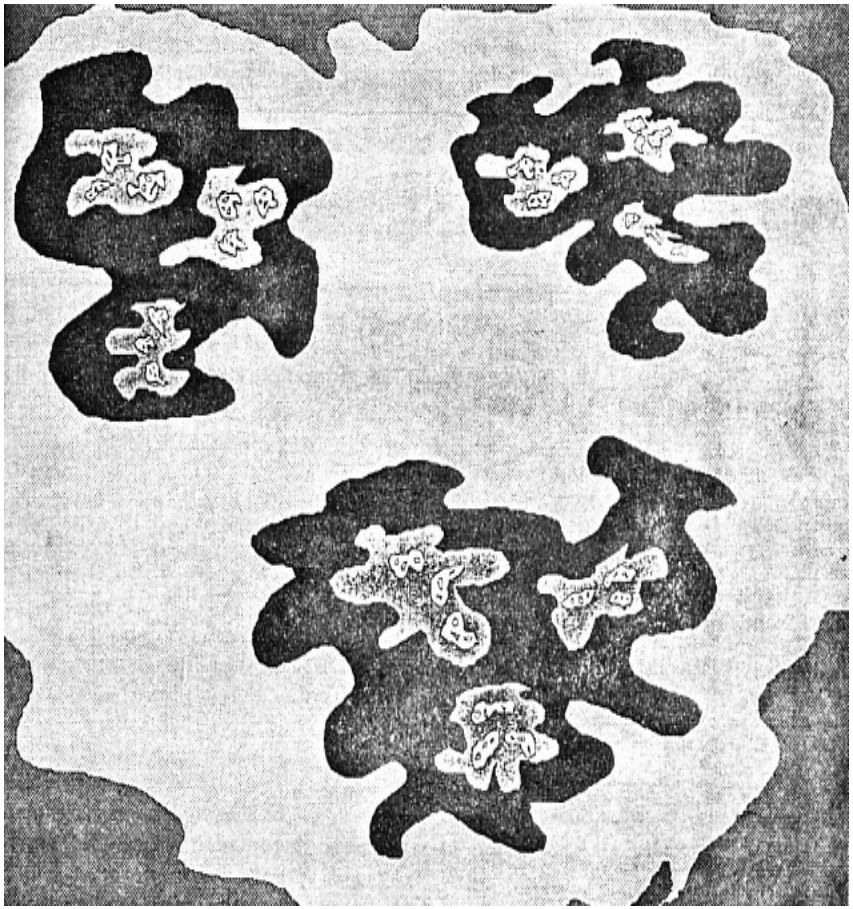

from Wheatcraft and Tyler [1988]

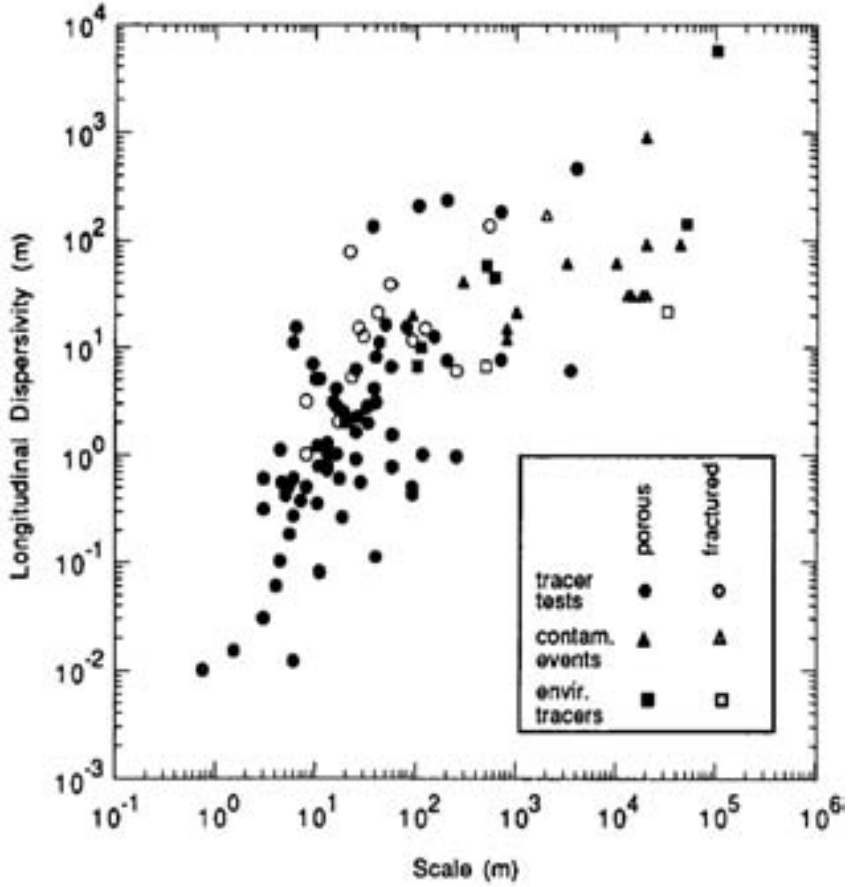

from Gelhar et al.[1992]

Currently available geophysical methods and the advantages of ERT

Currently available geophysical methods and the advantages of ERT

1. Seimic surveying
2. Gravity Surveying
3. Electromagnetic Surveying, VLF, Slingram, EH4
4. High density electrical resistivity tomography, ERT

Currently available geophysical methods and the advantages of ERT

1. Seimic surveying
2. Gravity Surveying
3. Electromagnetic Surveying, VLF, Slingram, EH4
4. High density electrical resistivity tomography, ERT

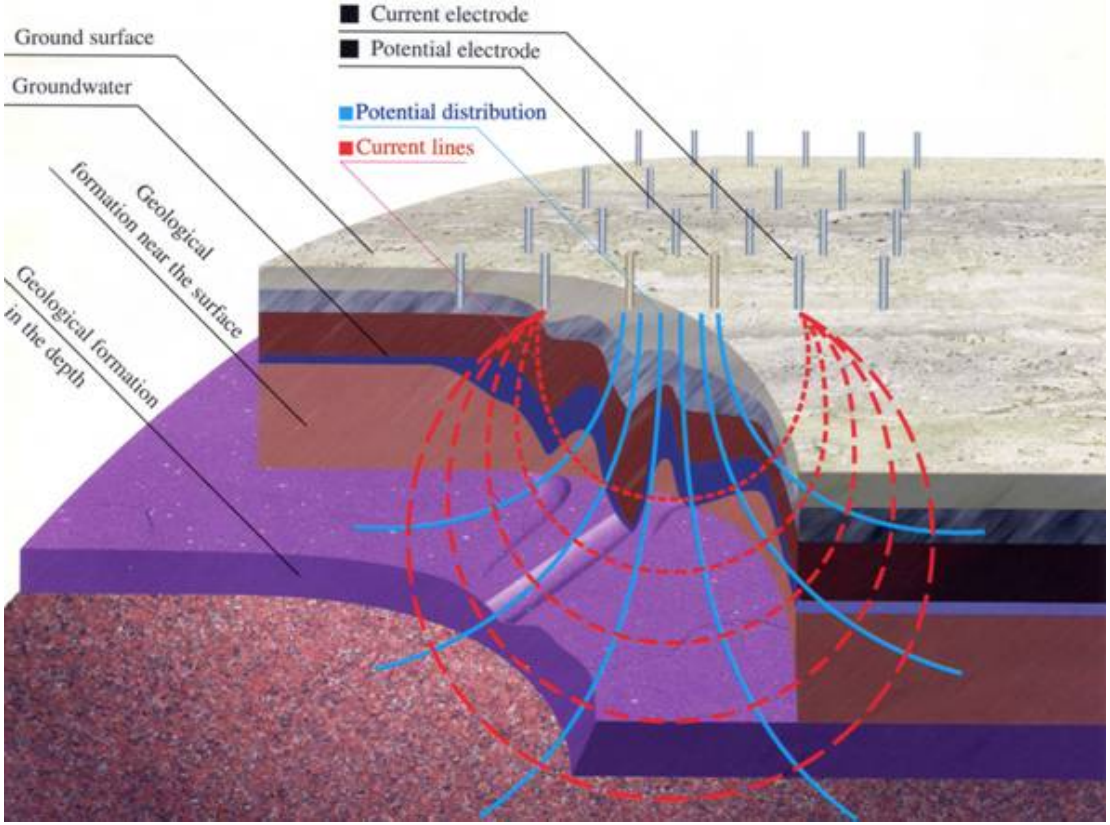

Currently available geophysical methods and the advantages of ERT

1. Seimic surveying
2. Gravity Surveying
3. Electromagnetic Surveying, VLF, Slingram, EH4
4. High density electrical resistivity tomography, ERT

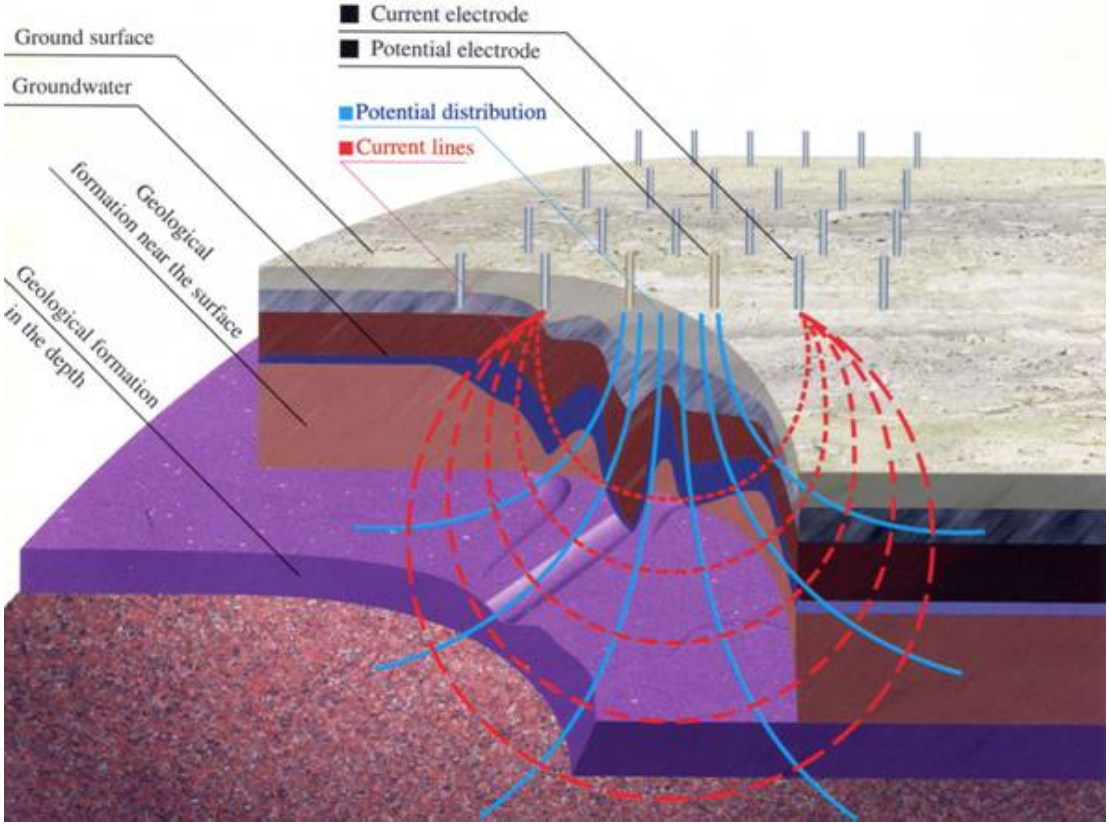

Advantages of ERT

- with robust theoretical foundation
- sensitive to water flow and solute transport
- can be used for test monitoring
- multi-scale and multi-dimensional survaying possible

Why is it possible for ERT to be used at multi-scales?

Its measurement range is determined by electrode interval, which can be easily adapted to different scales of centimeters to kilometers.

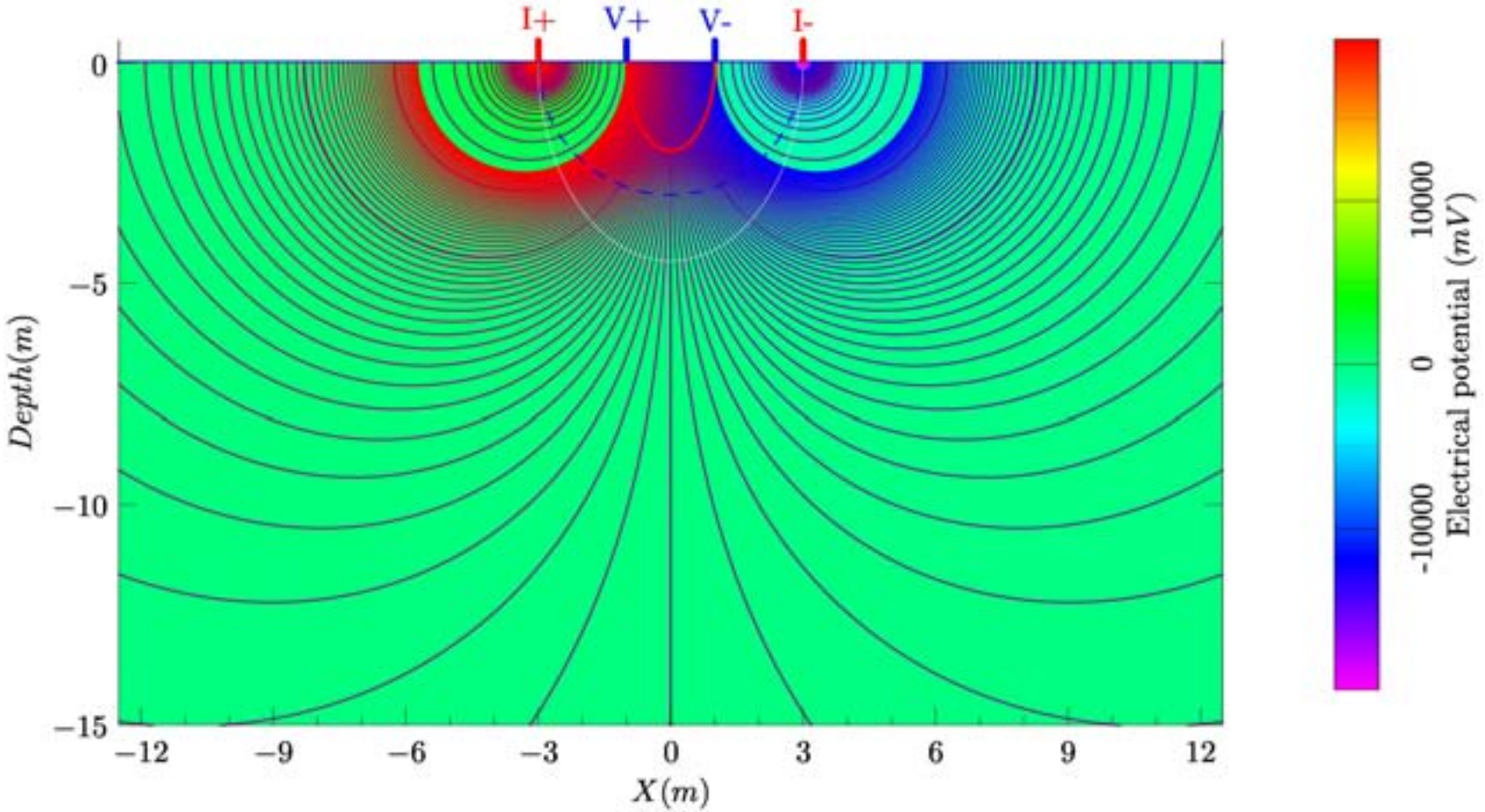

Why is it possible for ERT to be used at multi-scales?

Its measurement range is determined by electrode interval, which can be easily adapted to different scales of centimeters to kilometers.

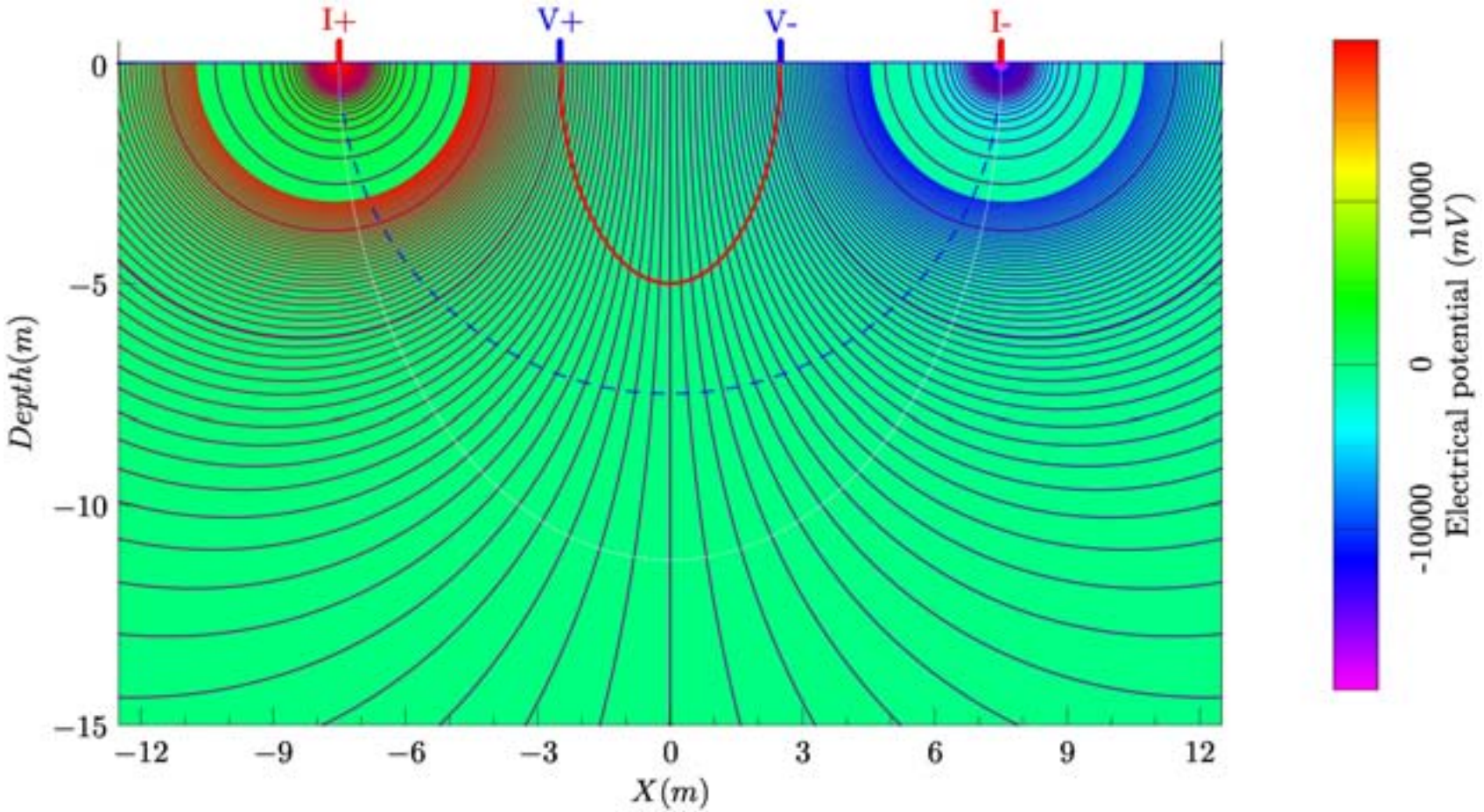

Why is it possible for ERT to be used at multi-scales?

Its measurement range is determined by electrode interval, which can be easily adapted to different scales of centimeters to kilometers.

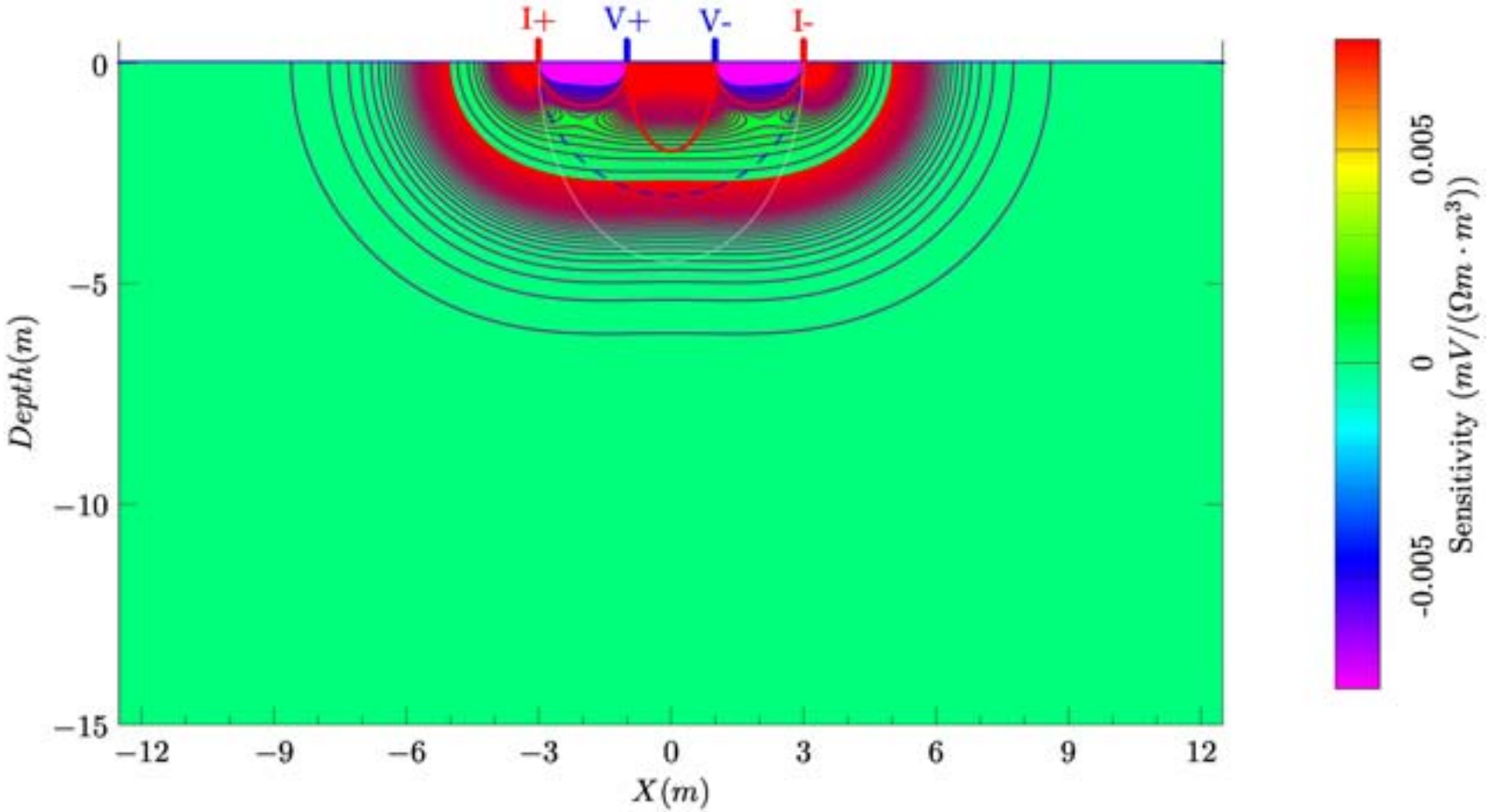

Why is it possible for ERT to be used at multi-scales?

Its measurement range is determined by electrode interval, which can be easily adapted to different scales of centimeters to kilometers.

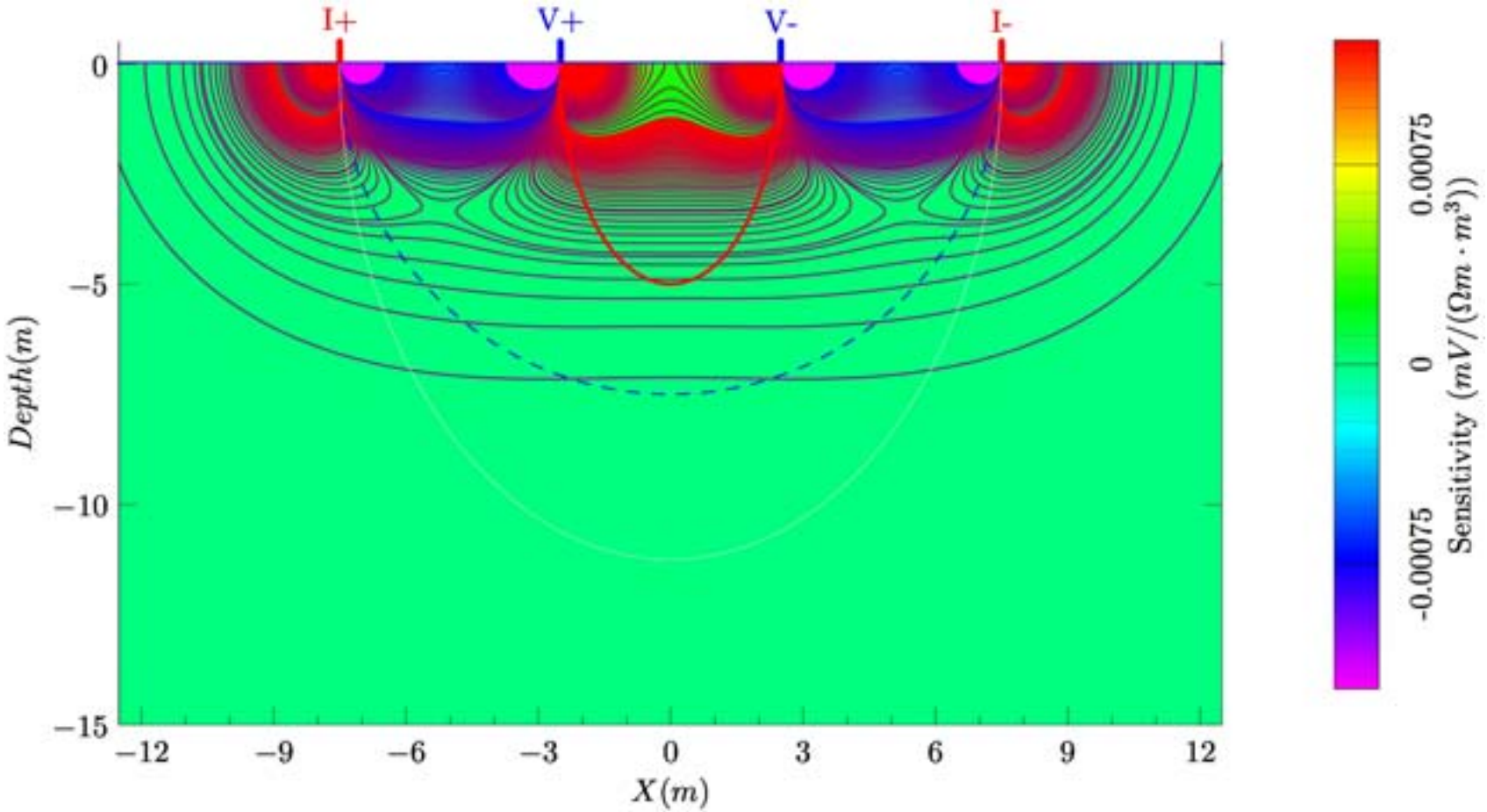

Why is it possible for ERT to be used at multi-scales?

Its measurement range is determined by electrode interval, which can be easily adapted to different scales of centimeters to kilometers.

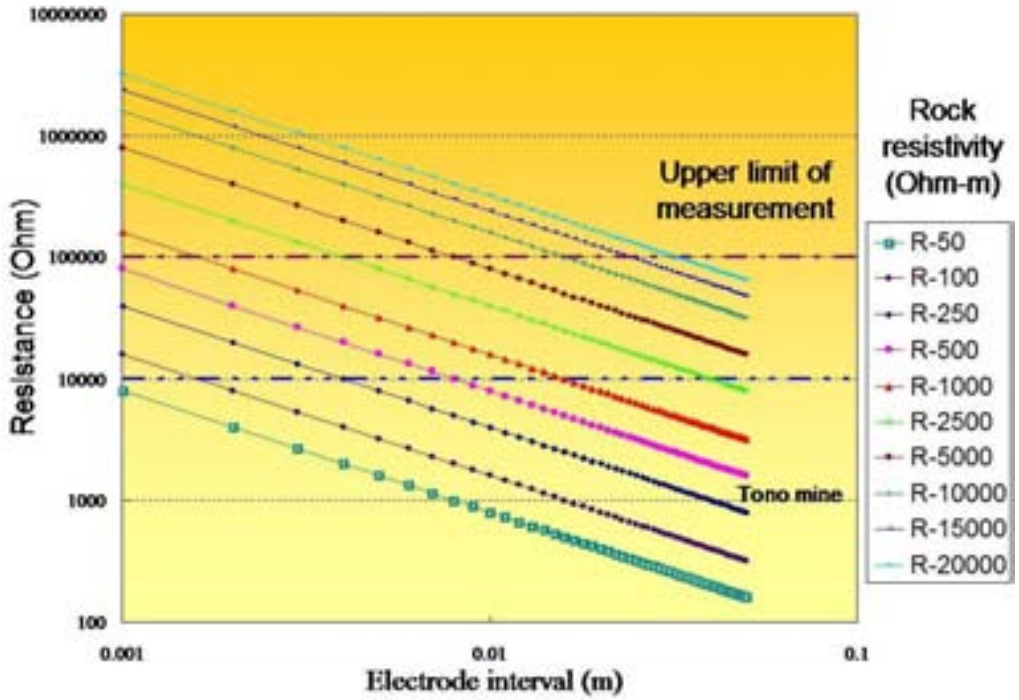

Why is it possible for ERT to be used at multi-scales?

Its measurement range is determined by electrode interval, which can be easily adapted to different scales of centimeters to kilometers.

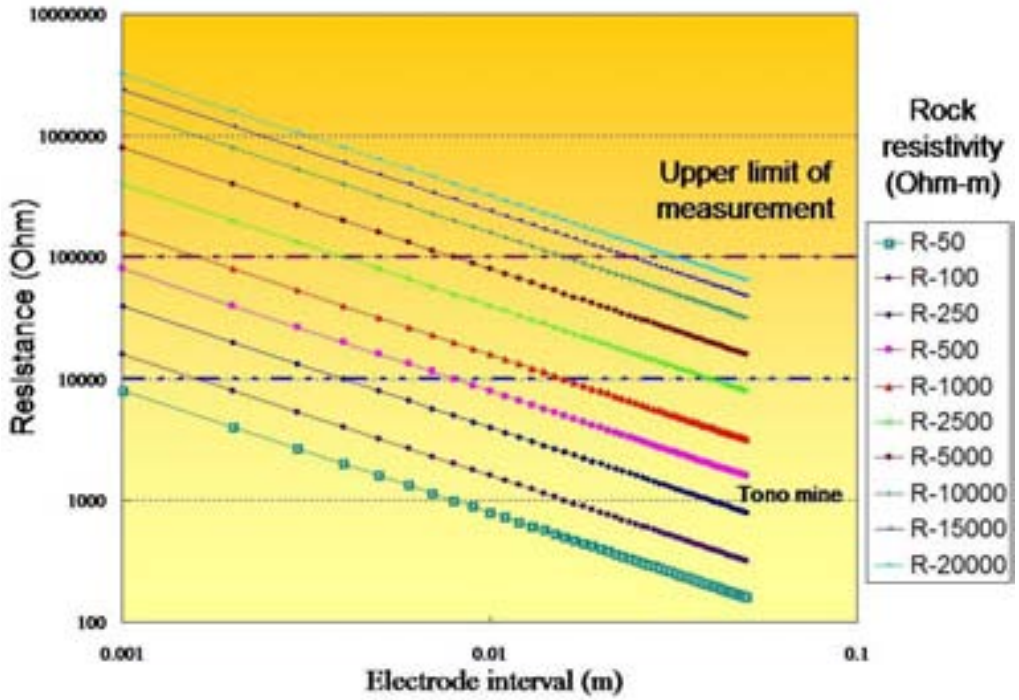

- The method may be used at sample scale in the lab to kilometers scale in the field

Why is it possible for ERT to be used at multi-scales?

Its measurement range is determined by electrode interval, which can be easily adapted to different scales of centimeters to kilometers.

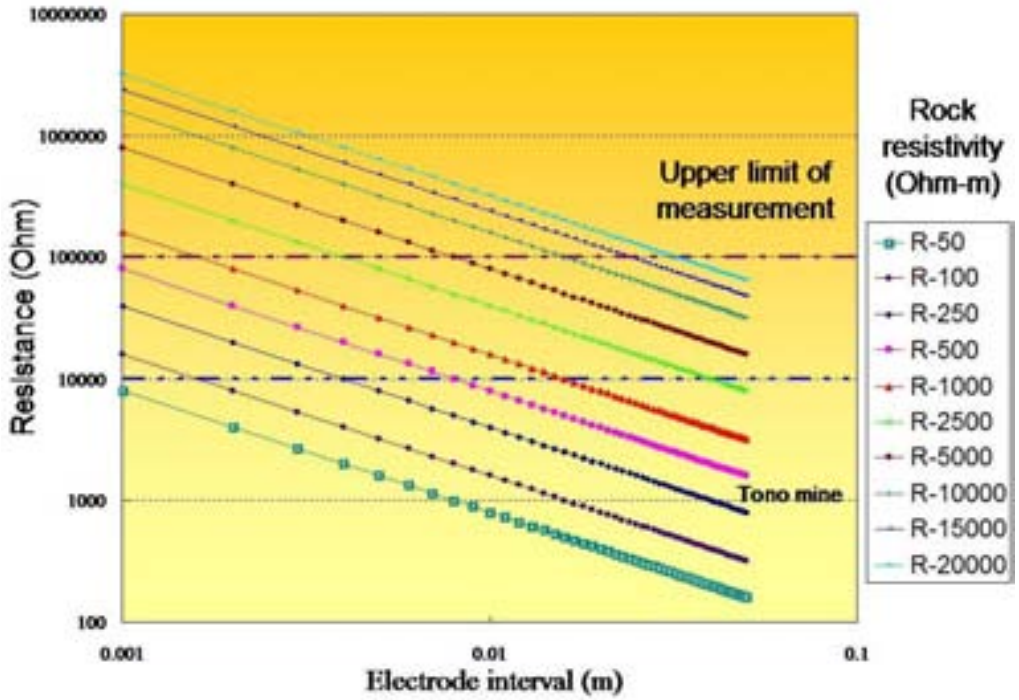

- The method may be used at sample scale in the lab to kilometers scale in the field
- Even at the same site, it may be used at different scales

Objectives of this study

By example applicatons of ERT

Objectives of this study

By example applicatons of ERT

1. at sample scale in the lab

Objectives of this study

By example applicatons of ERT

1. at sample scale in the lab
2. at block scale in the lab

Objectives of this study

By example applicatons of ERT

1. at sample scale in the lab
2. at block scale in the lab
3. at meters scale in the field

Objectives of this study

By example applicatons of ERT

1. at sample scale in the lab
2. at block scale in the lab
3. at meters scale in the field
4. at hundreds of meters scale in the field

Objectives of this study

By example applicatons of ERT

1. at sample scale in the lab
2. at block scale in the lab
3. at meters scale in the field
4. at hundreds of meters scale in the field

Objectives of this study

By example applicatons of ERT

1. at sample scale in the lab
2. at block scale in the lab
3. at meters scale in the field
4. at hundreds of meters scale in the field

To demonstrate the capabilities of ERT in the site characterization for HLW disposal at multi-scales.

Applications of ERT at sample scale in the lab

The ERT at sample scale sandstone block

- Coverage range: $10cm \times 10cm \times 2cm$
- Total electrode number: 121
- Electrode spacing: 1cm

$$\rho_a^t(x, y, z) - \rho_a^{t=0}(x, y, z)$$

The ERT at sample scale sandstone block

Coverage range:$10cm \times 10cm \times 2cm$

Total electrode number:121

Electrode spacing:1cm

$$\rho_a^t(x,y,z) - \rho_a^{t=0}(x,y,z)$$

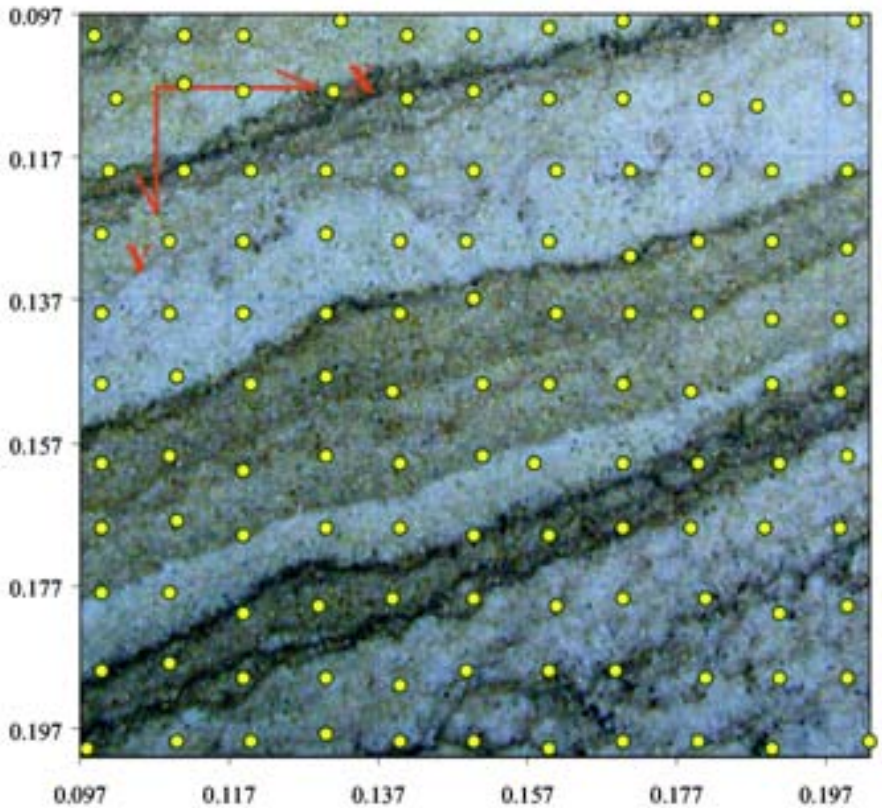

The ERT at sample scale sandstone block

Coverage range:$10cm \times 10cm \times 2cm$

Total electrode number:121

Electrode spacing:1cm

$$\rho_a^t(x,y,z) - \rho_a^{t=0}(x,y,z)$$

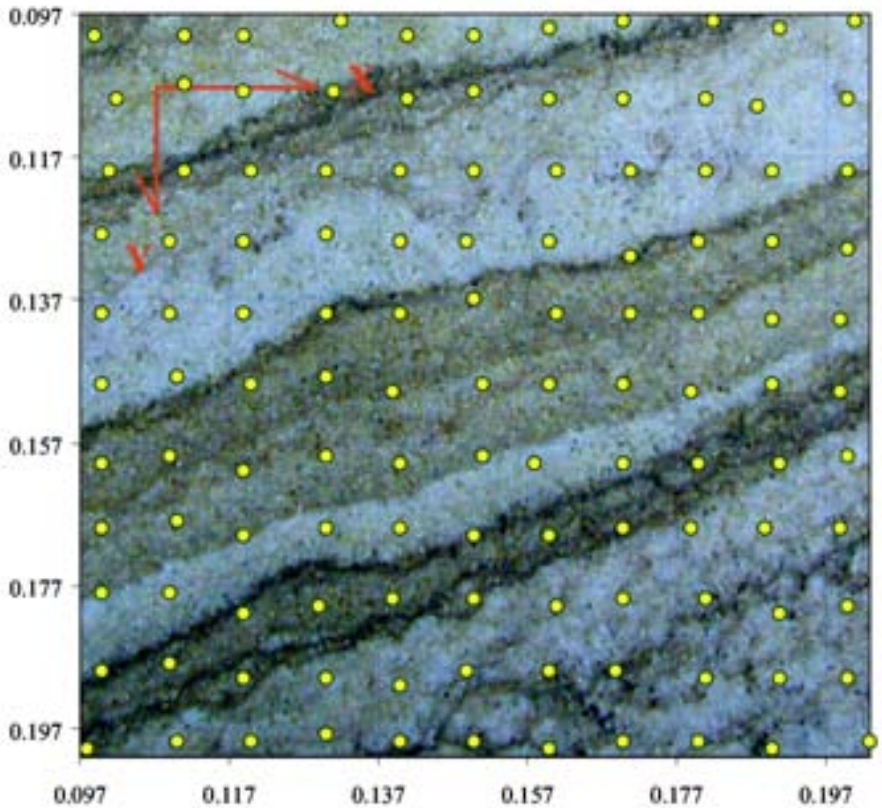

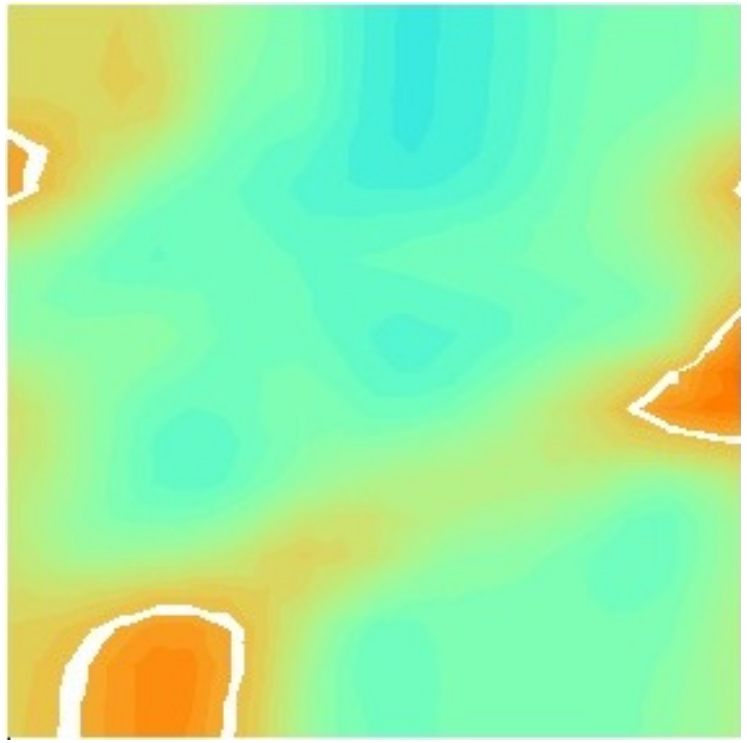

The ERT at sample scale sandstone block

Coverage range:$10cm \times 10cm \times 2cm$

Total electrode number:121

Electrode spacing:1cm

$$\rho_a^t(x,y,z) - \rho_a^{t=0}(x,y,z)$$

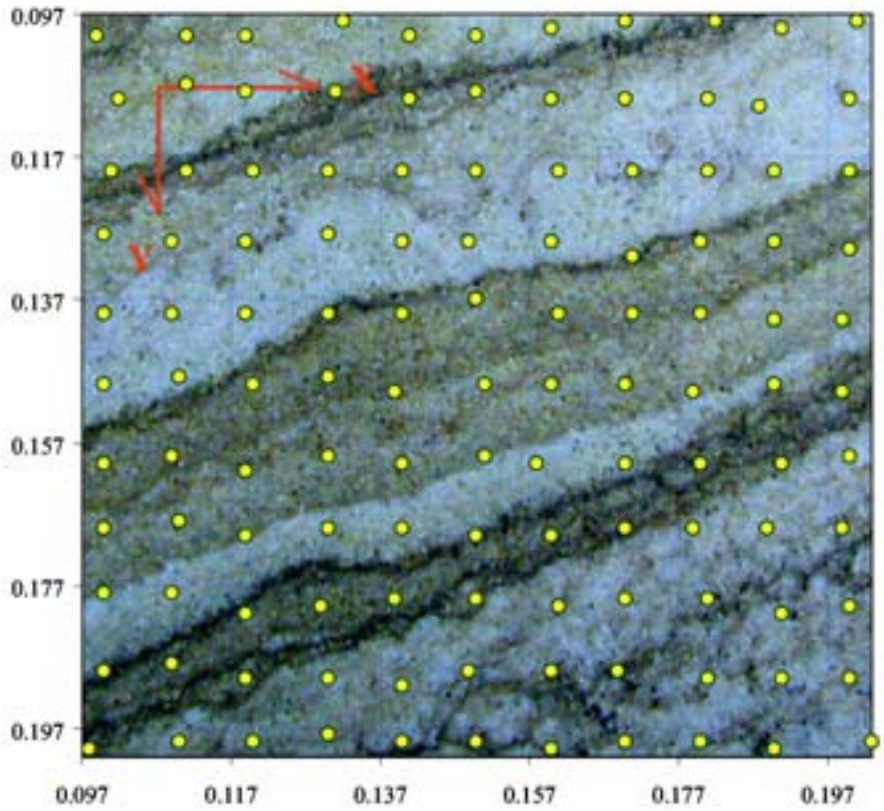

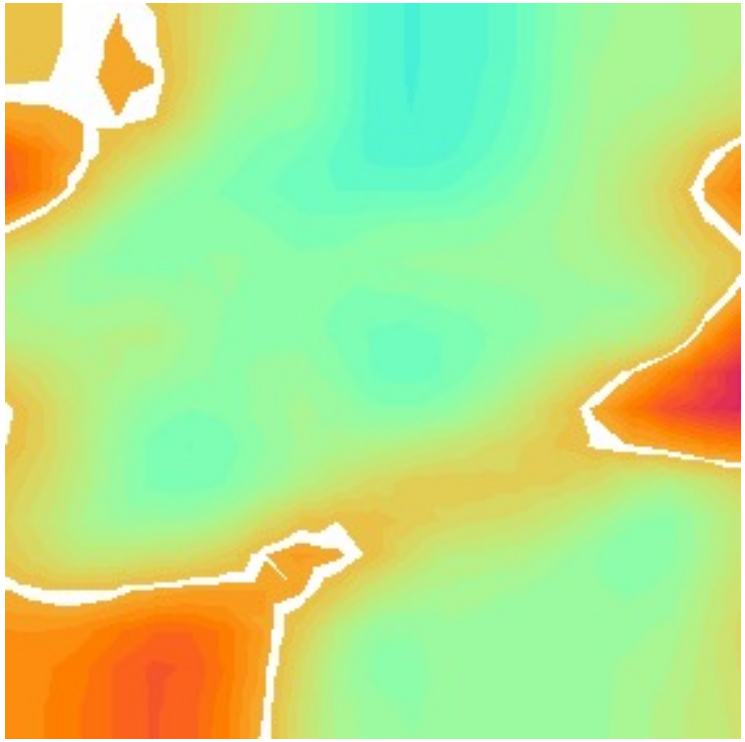

The ERT at sample scale sandstone block

Coverage range:$10cm \times 10cm \times 2cm$

Total electrode number:121

Electrode spacing:1cm

$$\rho_a^t(x,y,z) - \rho_a^{t=0}(x,y,z)$$

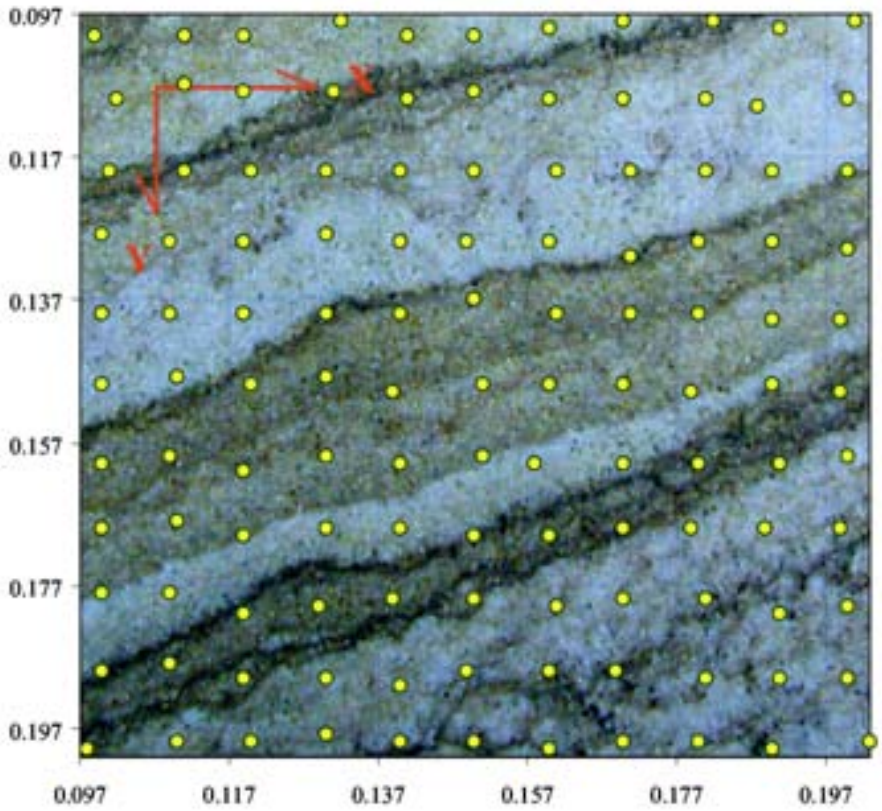

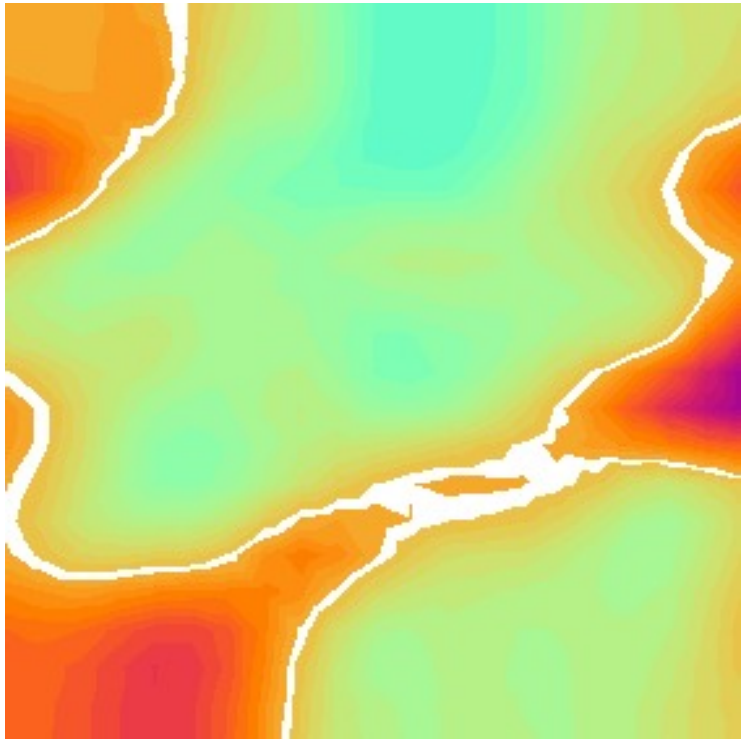

The ERT at sample scale sandstone block

Coverage range:$10cm \times 10cm \times 2cm$

Total electrode number:121

Electrode spacing:1cm

$$\rho_a^t(x,y,z) - \rho_a^{t=0}(x,y,z)$$

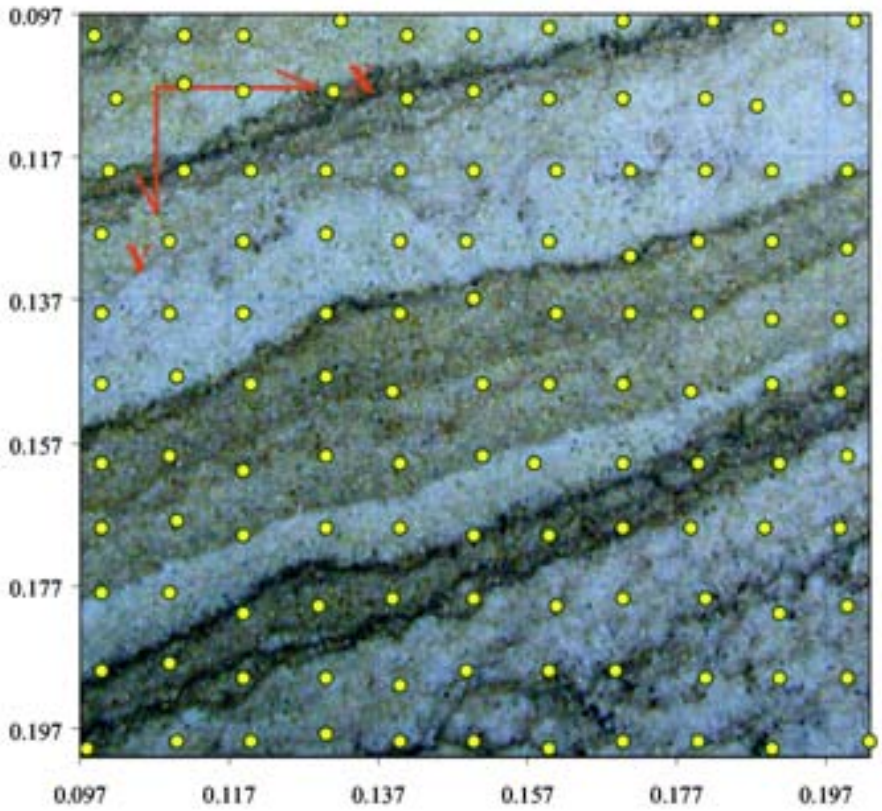

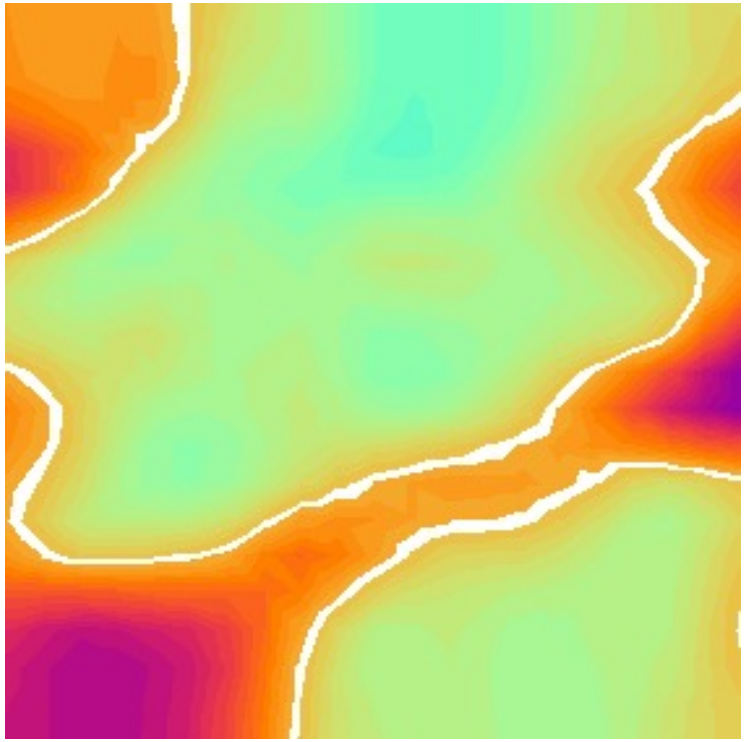

The ERT at sample scale sandstone block

Coverage range: $10cm \times 10cm \times 2cm$

Total electrode number: 121

Electrode spacing: 1cm

$$\rho_a^t(x, y, z) - \rho_a^{t=0}(x, y, z)$$

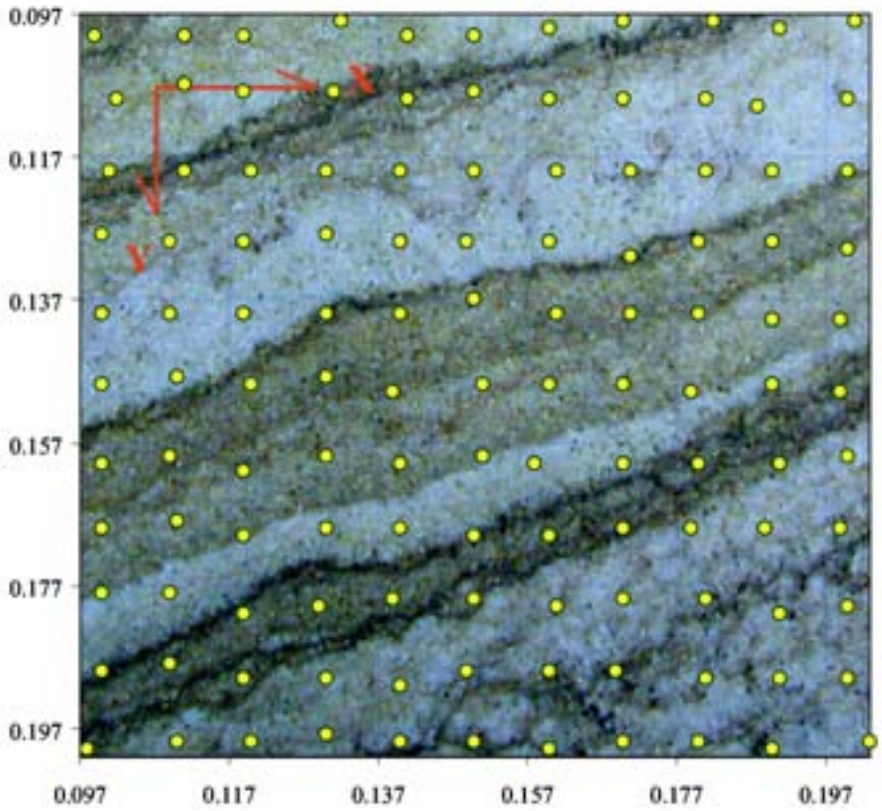

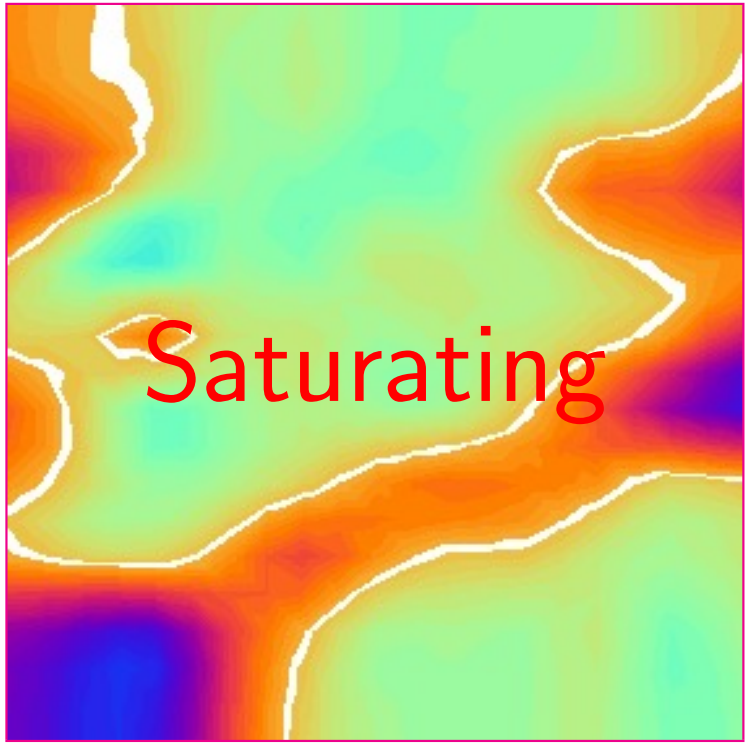

The ERT at sample scale sandstone block

Coverage range:$10cm \times 10cm \times 2cm$

Total electrode number:121

Electrode spacing:1cm

$$\rho_a^t(x,y,z) - \rho_a^{t=0}(x,y,z)$$

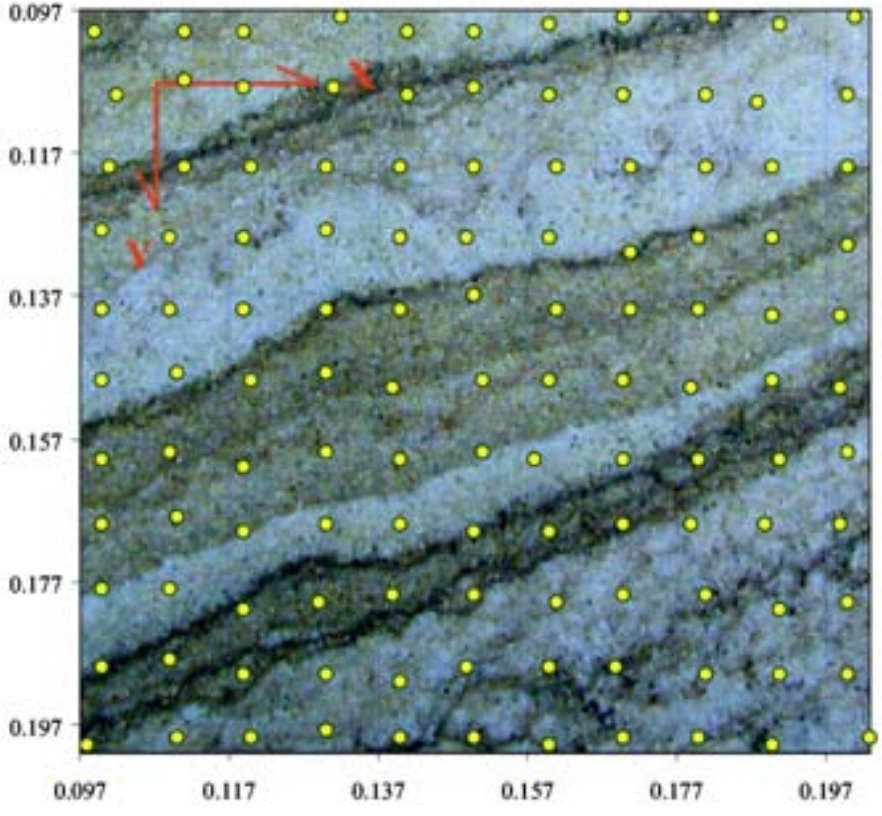

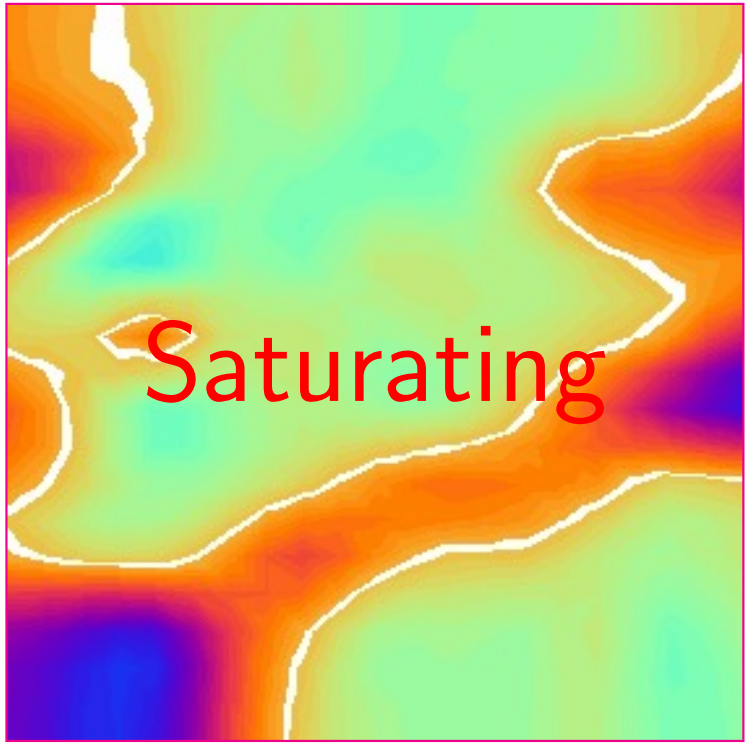

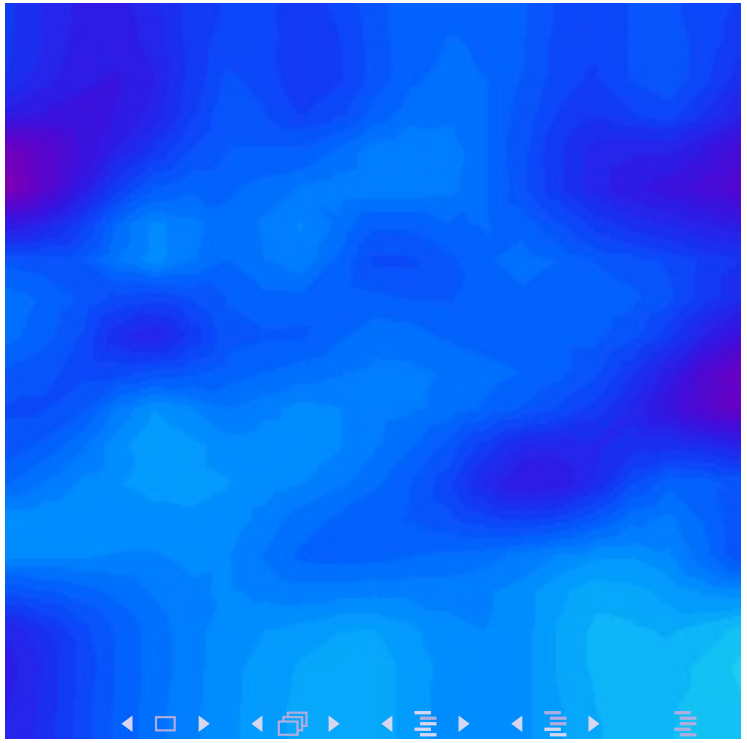

The ERT at sample scale sandstone block

Coverage range:$10cm \times 10cm \times 2cm$

Total electrode number:121

Electrode spacing:1cm

$$\rho_a^t(x,y,z) - \rho_a^{t=0}(x,y,z)$$

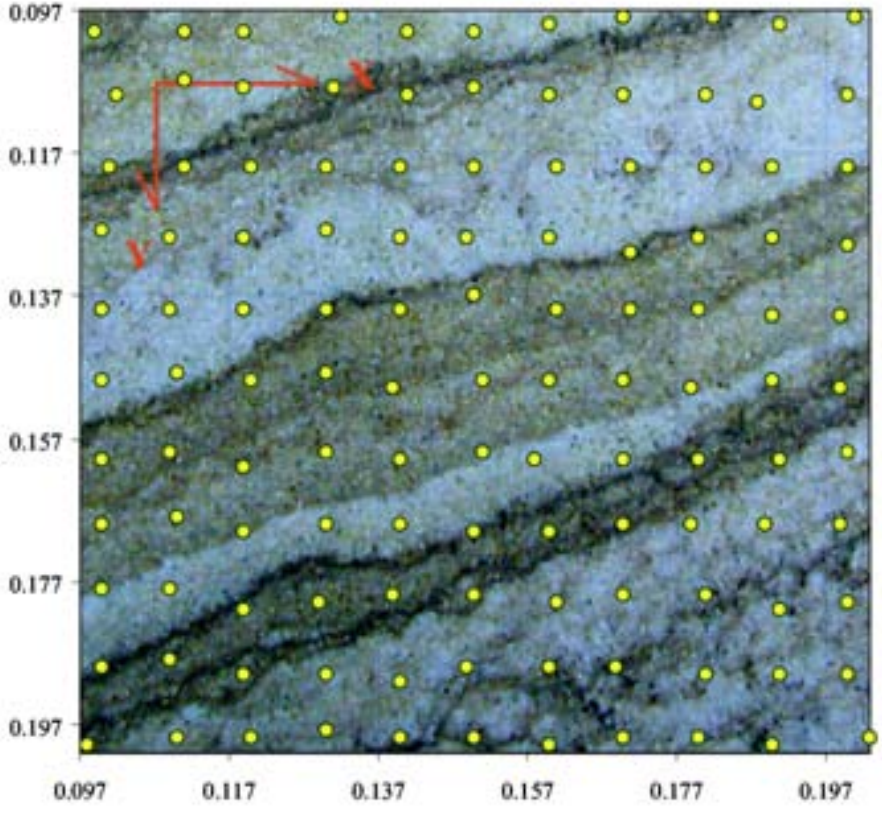

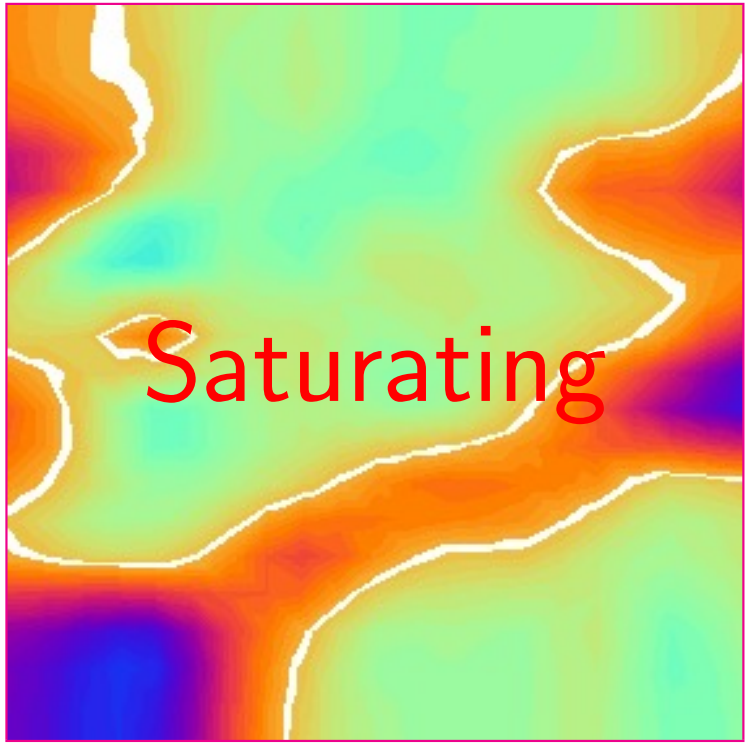

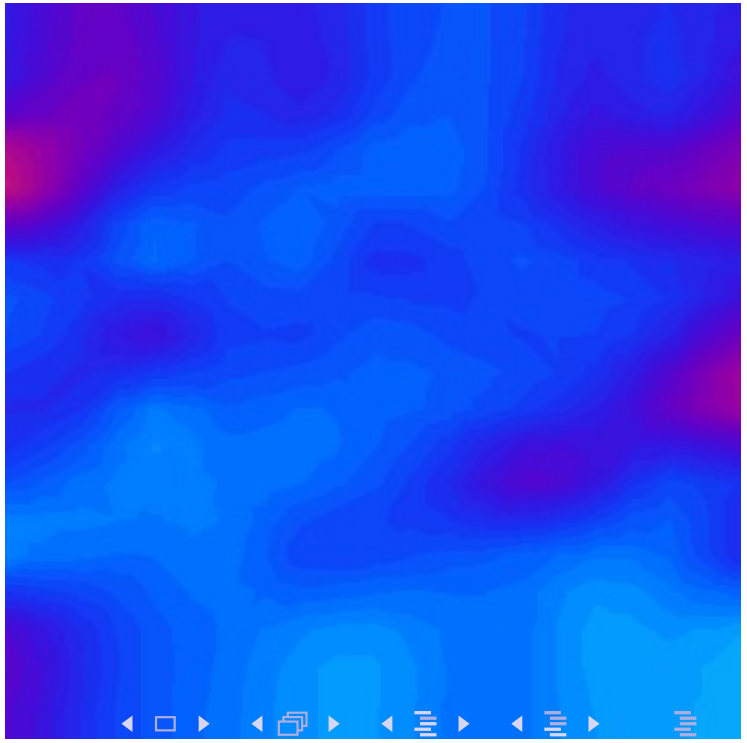

The ERT at sample scale sandstone block

Coverage range: $10cm \times 10cm \times 2cm$

Total electrode number: 121

Electrode spacing: 1cm

$$\rho_a^t(x, y, z) - \rho_a^{t=0}(x, y, z)$$

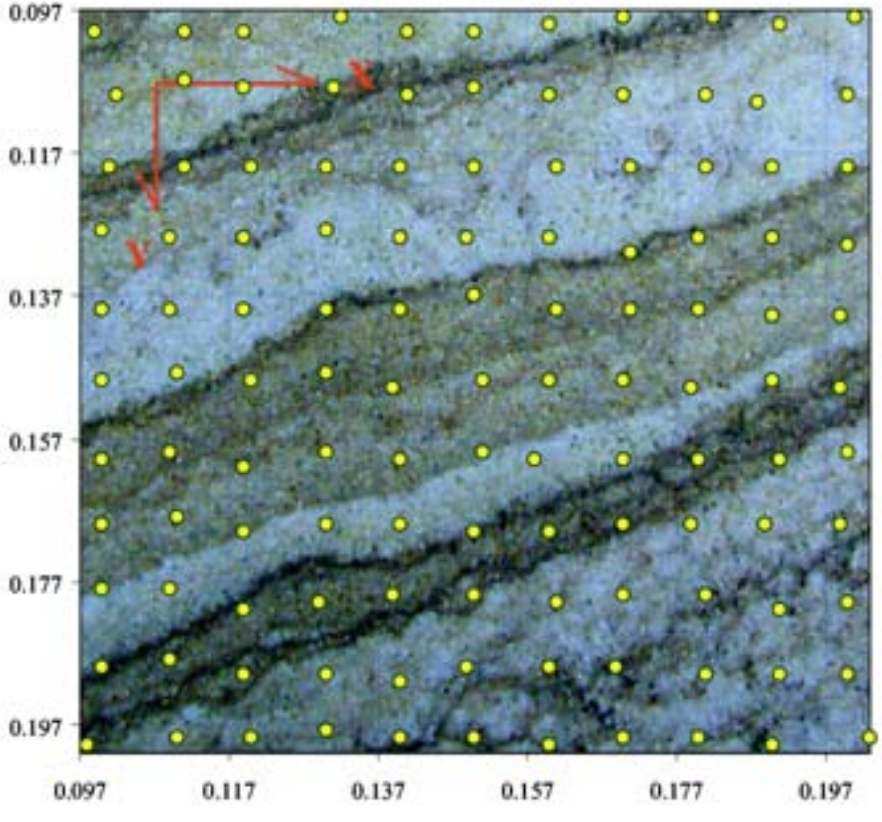

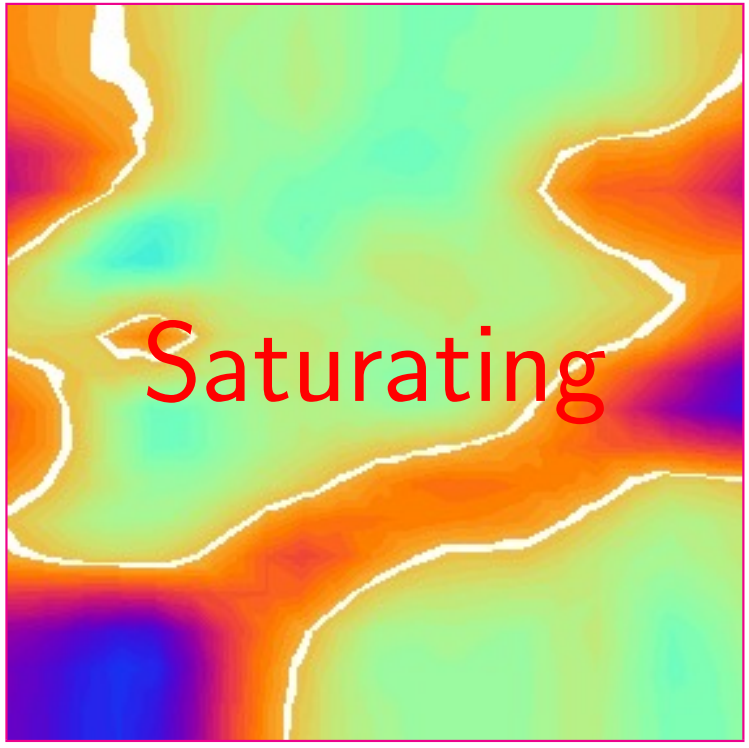

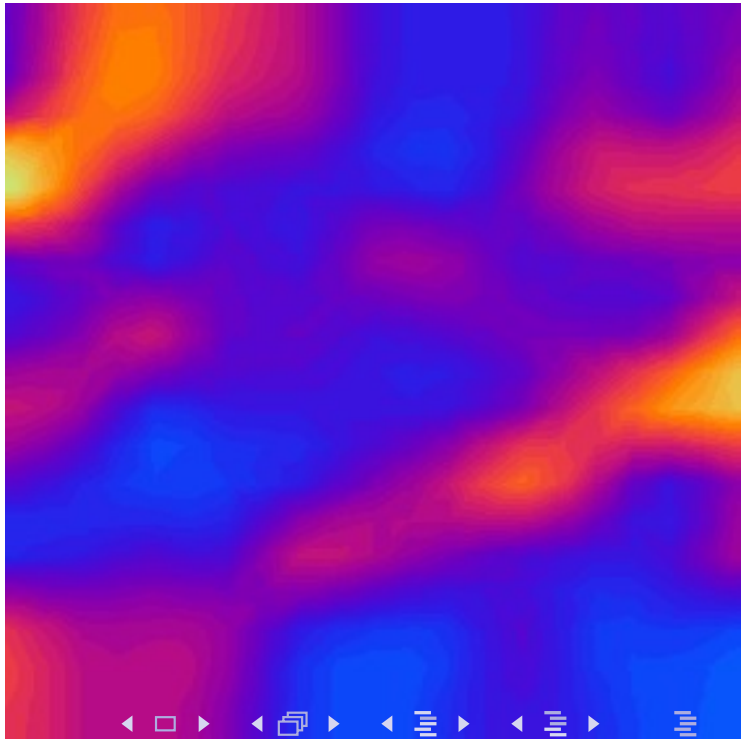

The ERT at sample scale sandstone block

Coverage range:$10cm \times 10cm \times 2cm$

Total electrode number:121

Electrode spacing:1cm

$$\rho_a^t(x,y,z) - \rho_a^{t=0}(x,y,z)$$

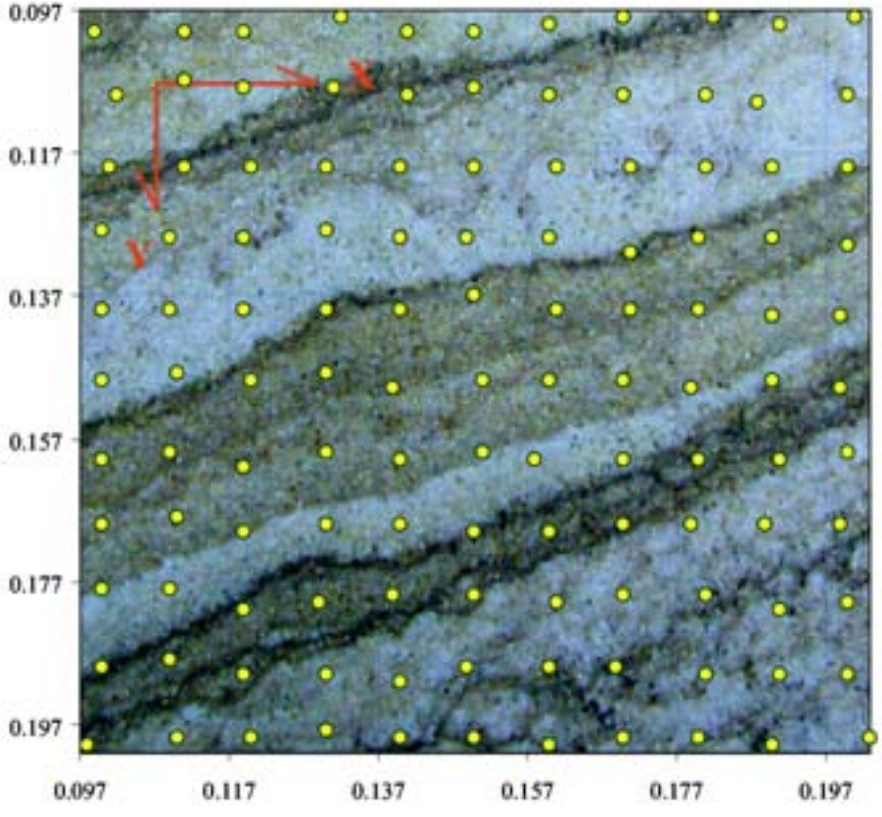

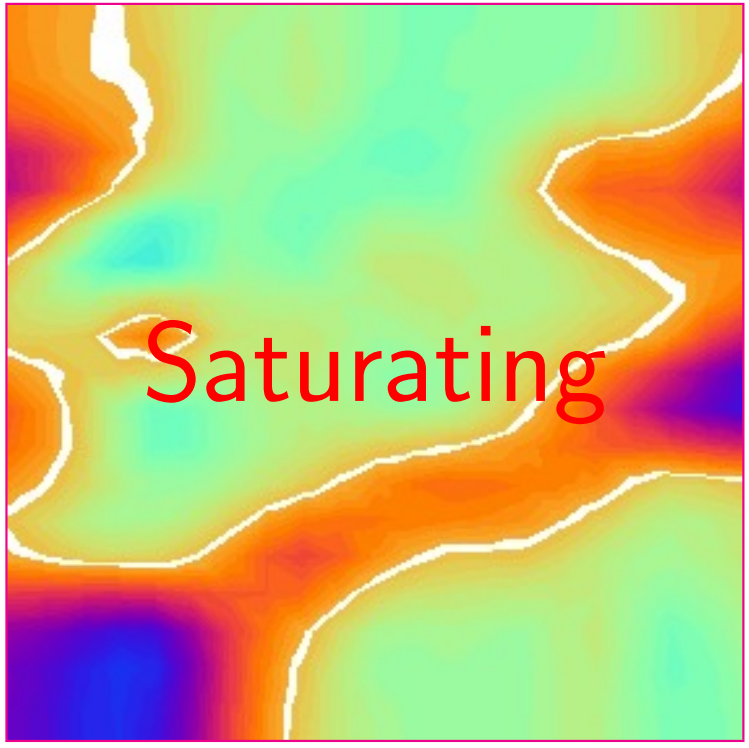

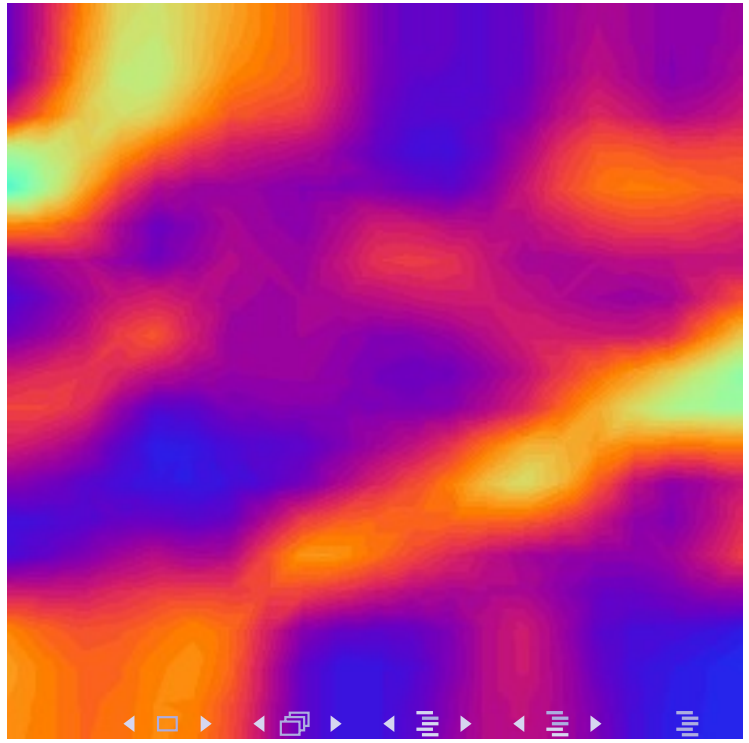

The ERT at sample scale sandstone block

Coverage range: $10cm \times 10cm \times 2cm$

Total electrode number: 121

Electrode spacing: 1cm

$$\rho_a^t(x, y, z) - \rho_a^{t=0}(x, y, z)$$

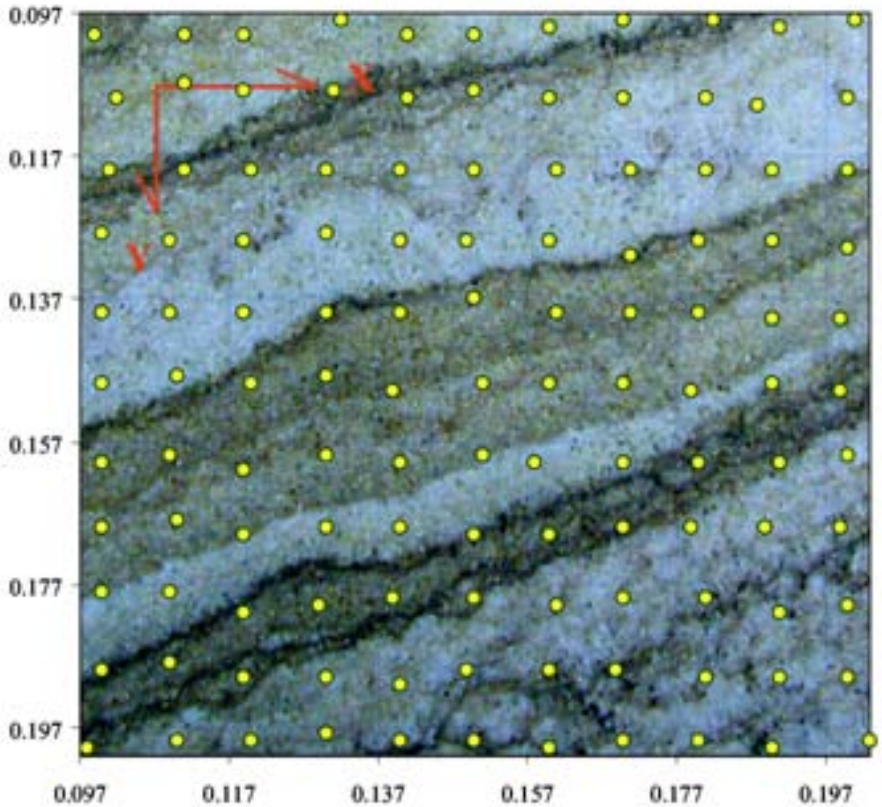

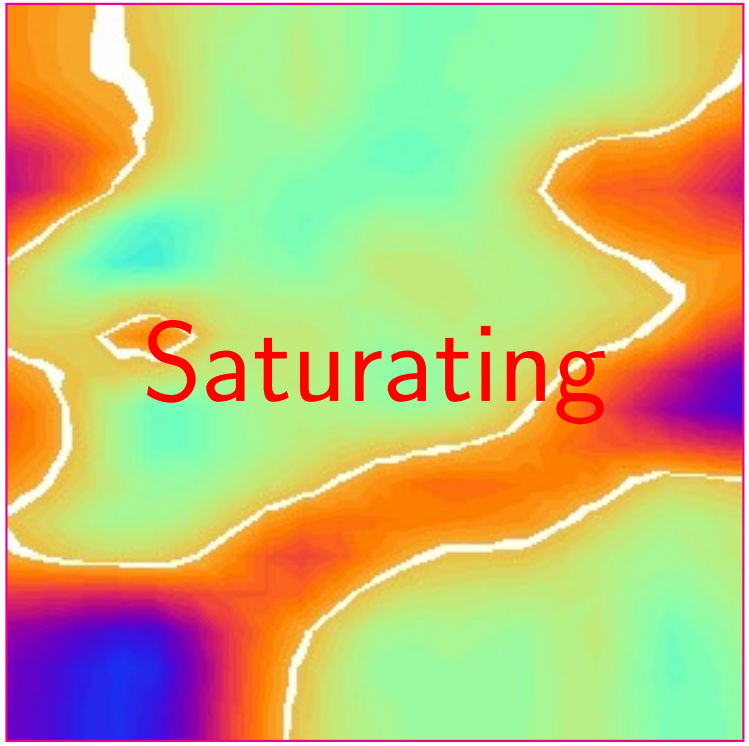

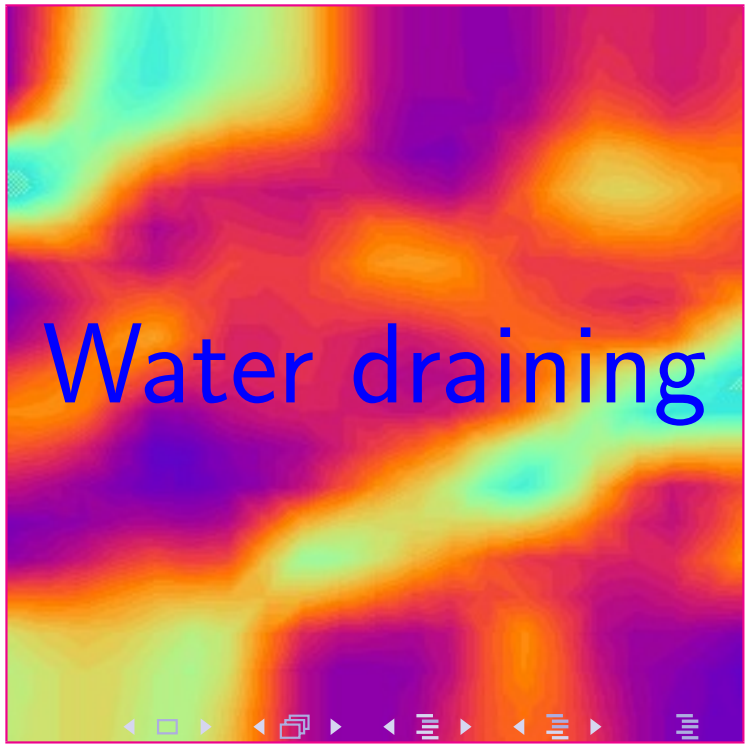

Applications of ERT at block scale in the lab

The ERT at a tuff block with fracture

Total electrode number:64

Block size:$40cm \times 40cm \times 20cm$

Electrode spacing:5cm

The ERT at a tuff block with fracture

Total electrode number:64

Block size:$40cm \times 40cm \times 20cm$

Electrode spacing:5cm

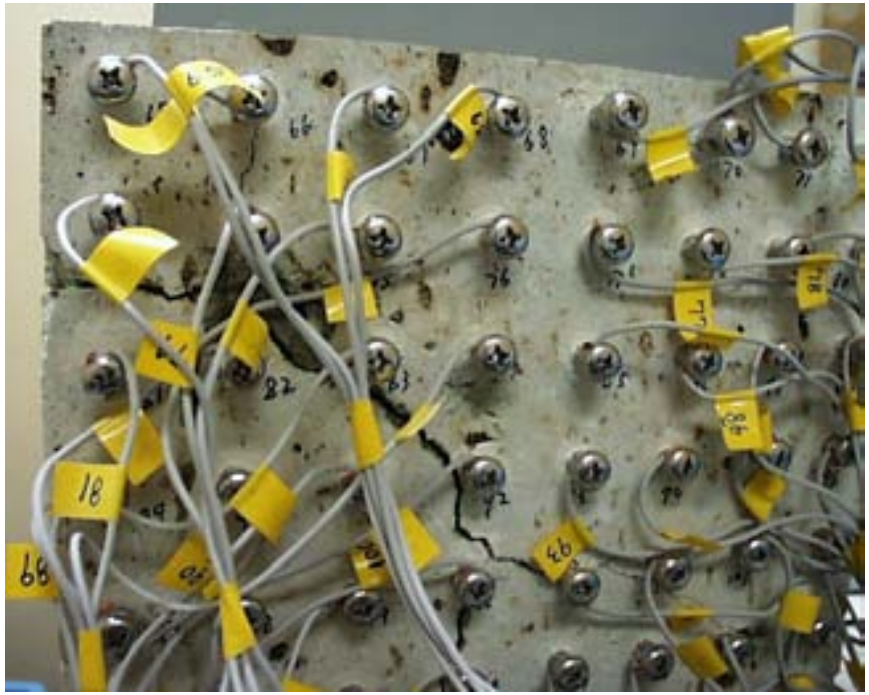

19 minutes before infiltration

The ERT at a tuff block with fracture

Total electrode number:64

Block size:$40cm \times 40cm \times 20cm$

Electrode spacing:5cm

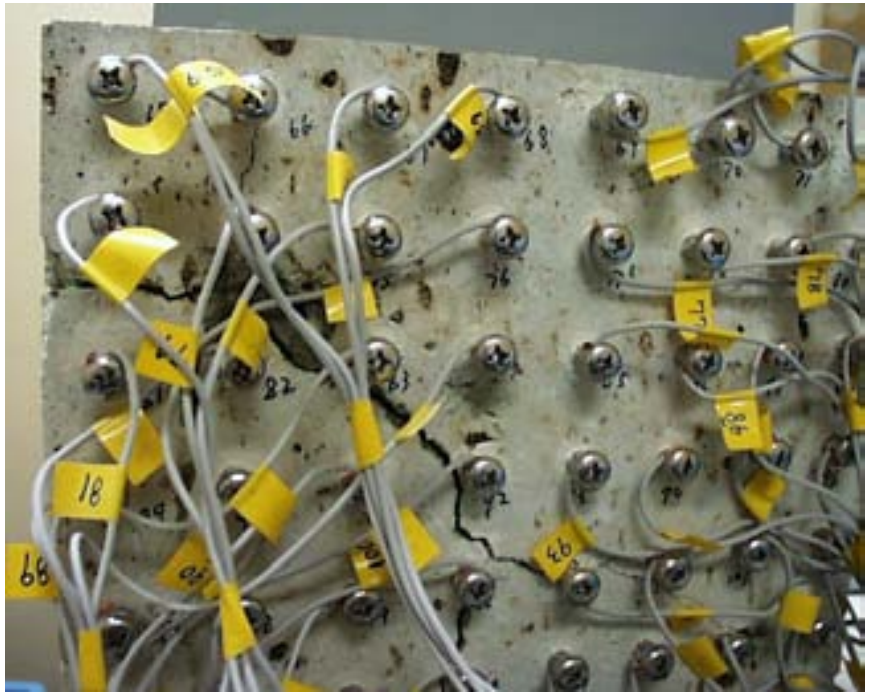

19 minutes before infiltration

At the end of the infiltration

The ERT at a tuff block with fracture

Total electrode number:64

Block size:$40cm \times 40cm \times 20cm$

Electrode spacing:5cm

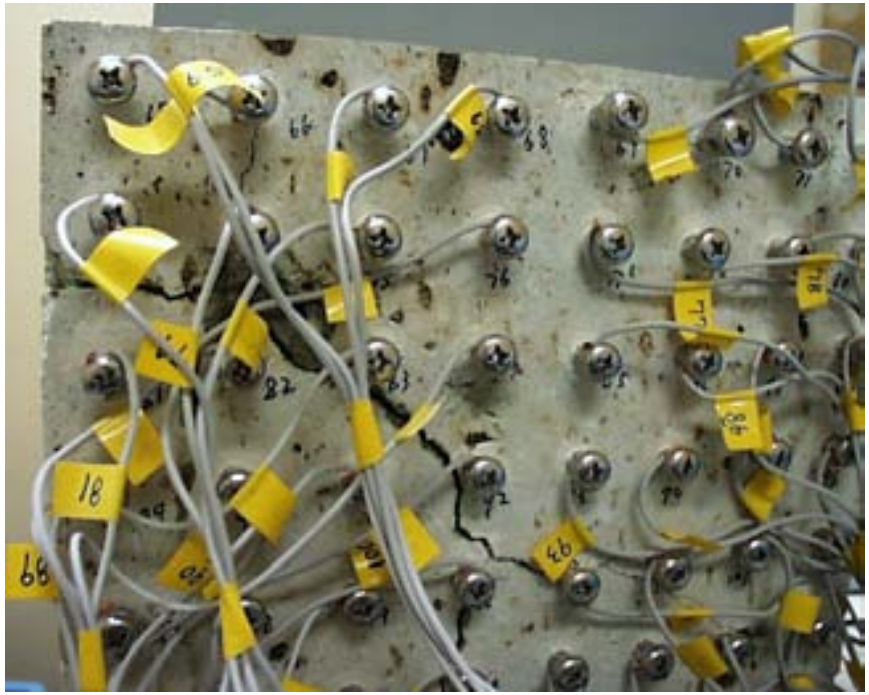

19 minutes before infiltration

At the end of the infiltration

The ERT at a tuff block with fracture

Total electrode number:64

Block size:$40cm \times 40cm \times 20cm$

Electrode spacing:5cm

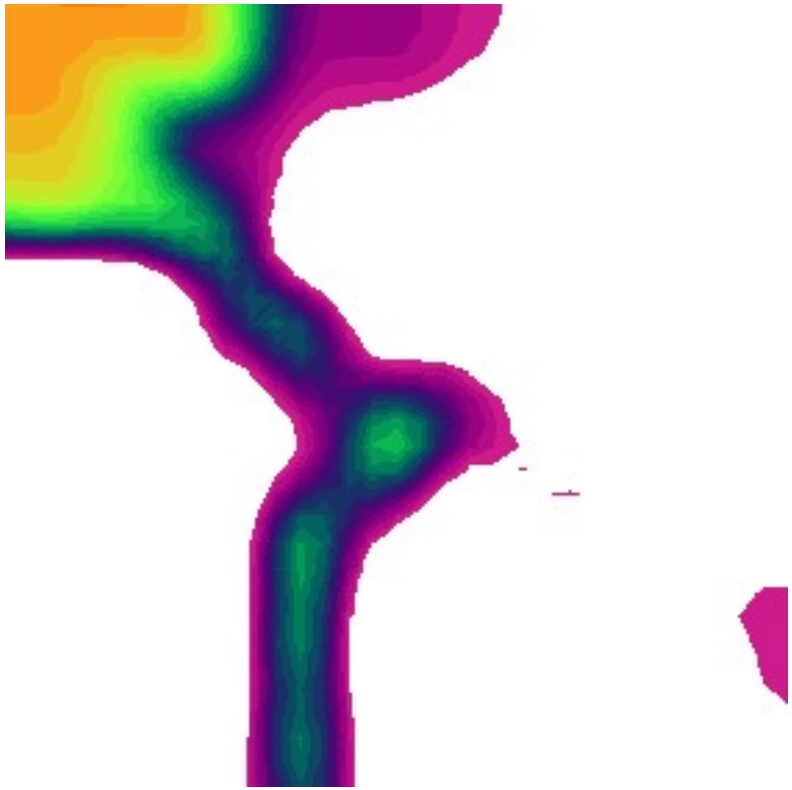

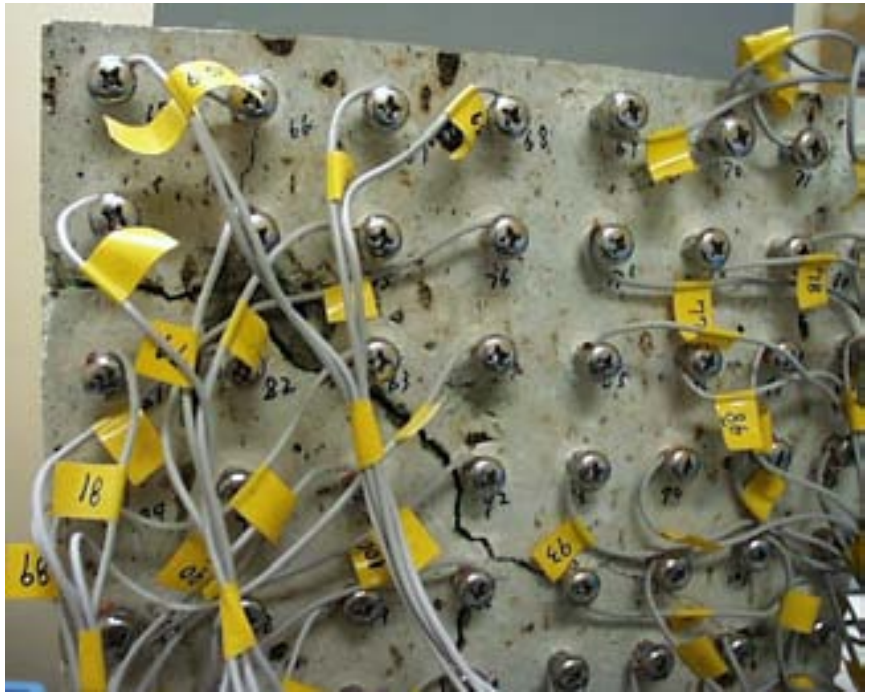

19 minutes before infiltration

At the end of the infiltration

The ERT at a tuff block with fracture

Total electrode number:64

Block size:$40cm \times 40cm \times 20cm$

Electrode spacing:5cm

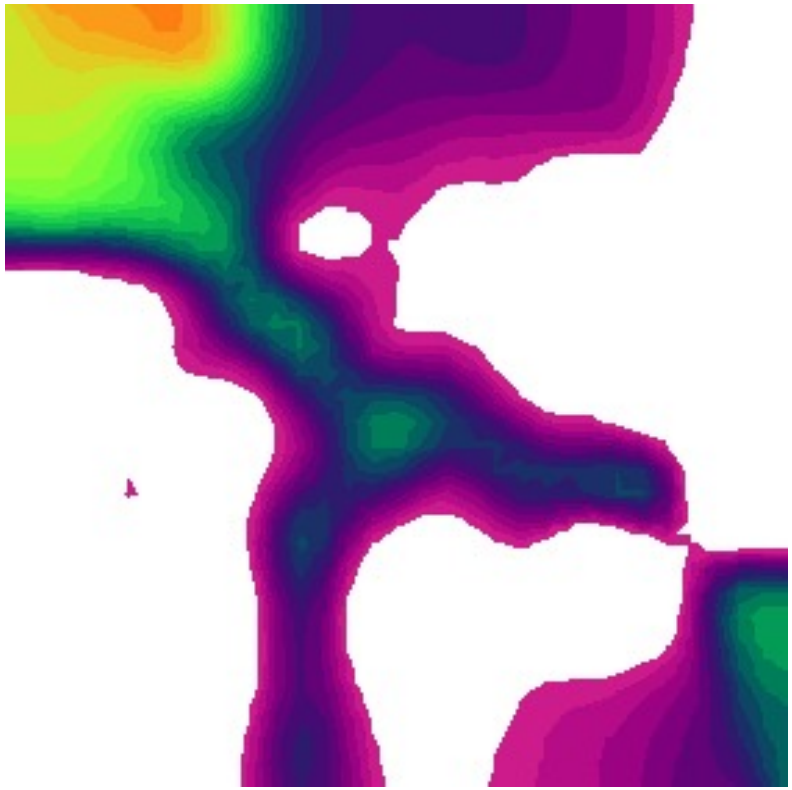

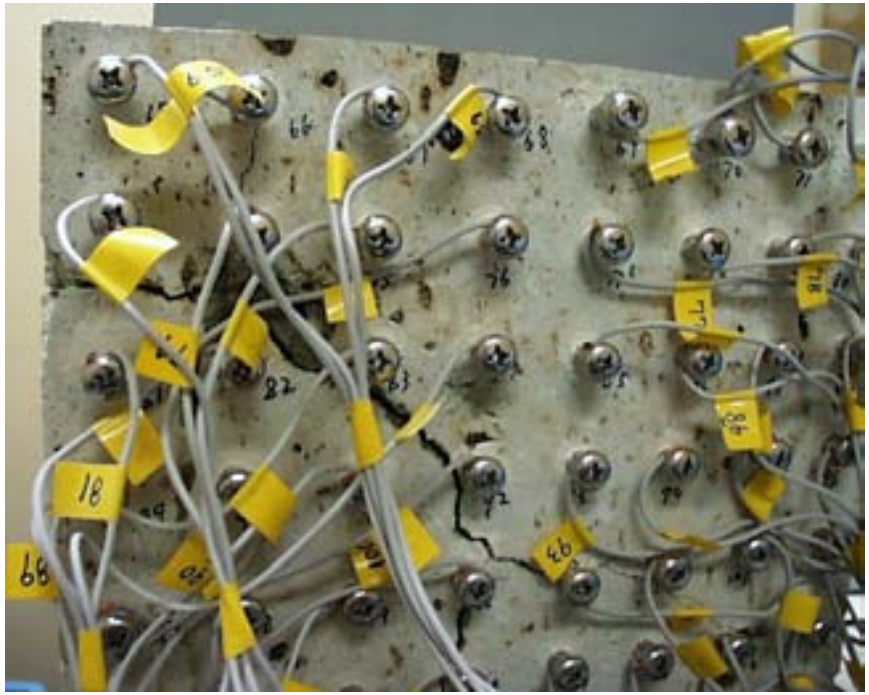

19 minutes before infiltration

At the end of the infiltration

The ERT at a tuff block with fracture

Total electrode number:64

Block size:$40cm \times 40cm \times 20cm$

Electrode spacing:5cm

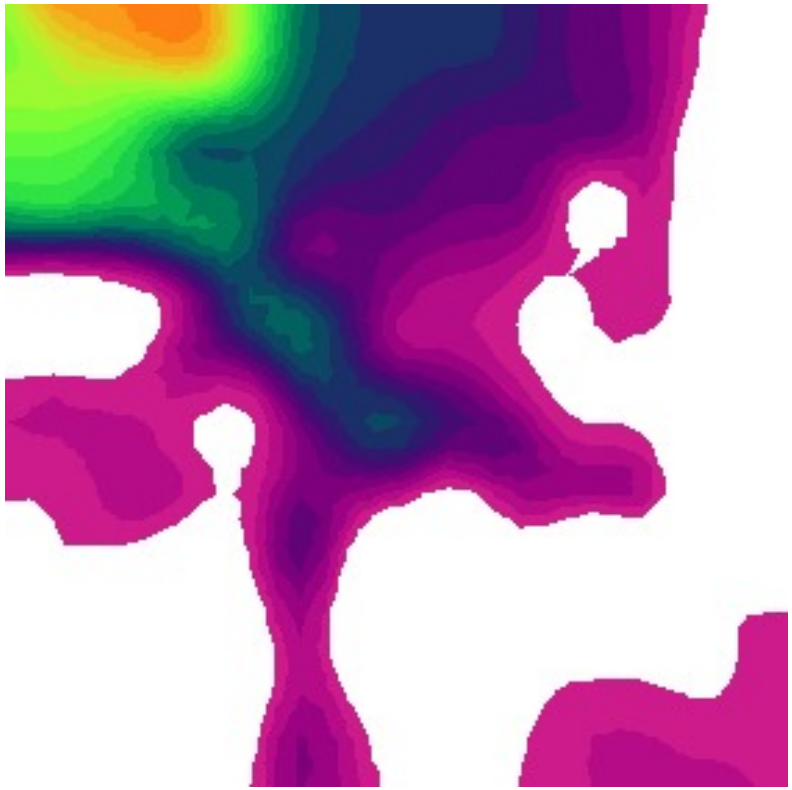

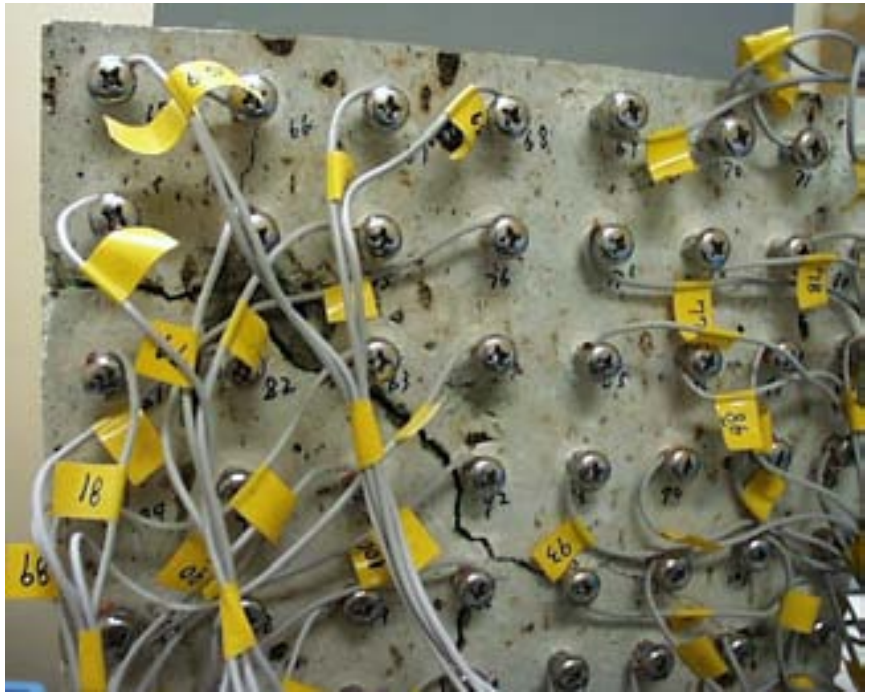

19 minutes before infiltration

At the end of the infiltration

The ERT at a tuff block with fracture

Total electrode number:64

Block size:$40cm \times 40cm \times 20cm$

Electrode spacing:5cm

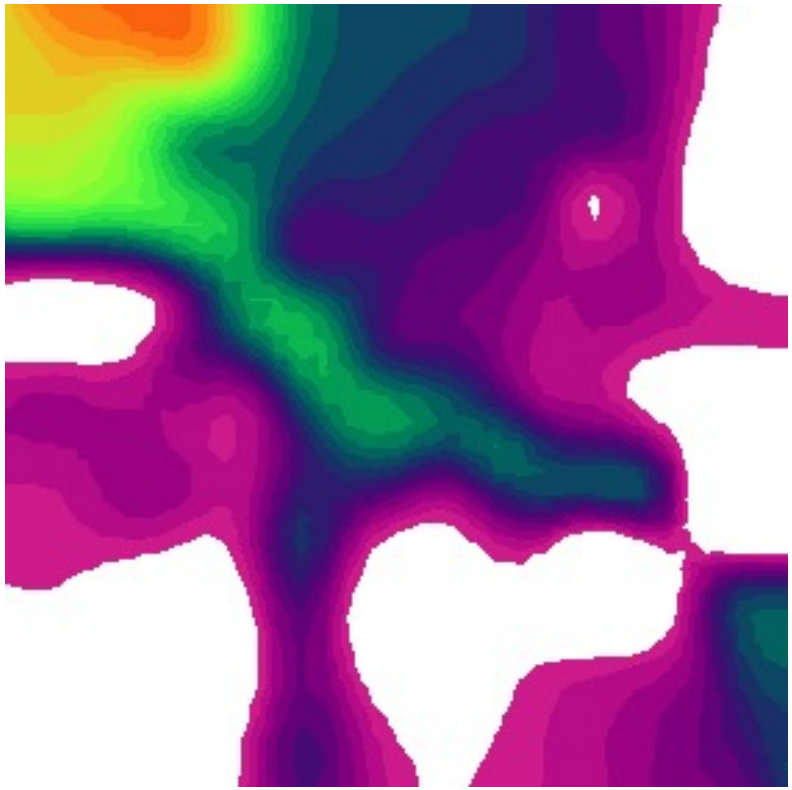

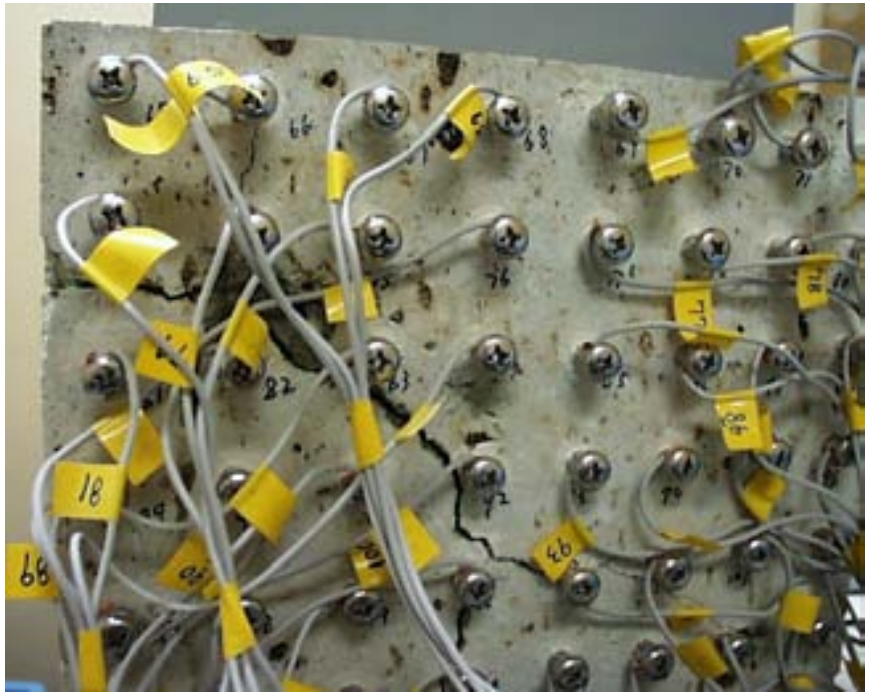

19 minutes before infiltration

At the end of the infiltration

The ERT at a tuff block with fracture

Total electrode number:64

Block size:$40cm \times 40cm \times 20cm$

Electrode spacing:5cm

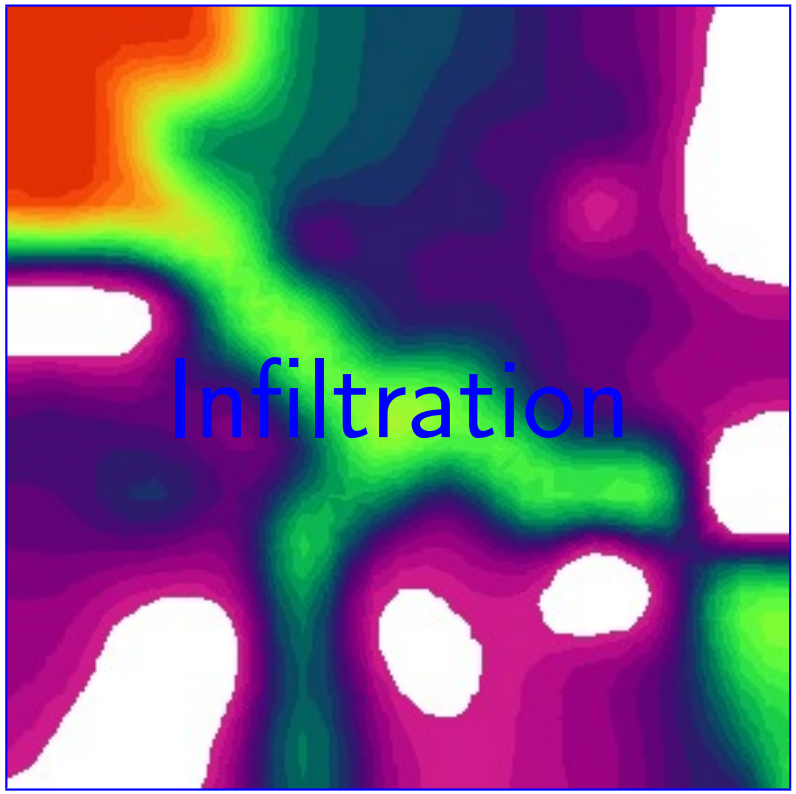

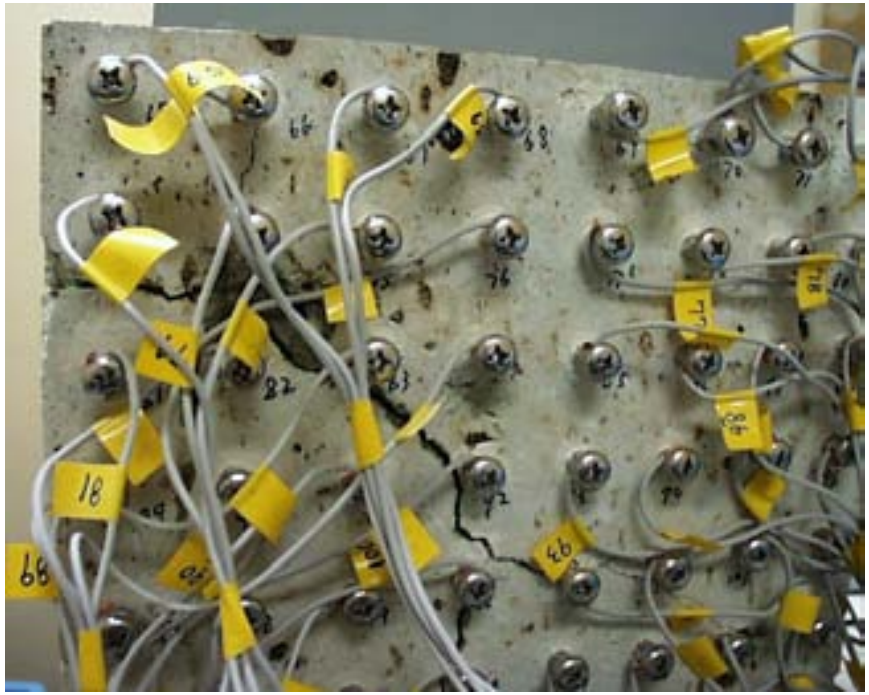

19 minutes before infiltration

At the end of the infiltration

Applications of ERT at meters scale in the field

The 3-D infiltration and ERT monitoring experiments on fractured granite rocks

Date:2009.8.13-9.13, Monitored range:3.5m×3.5m

Resistivity variations in planes during the water infiltration

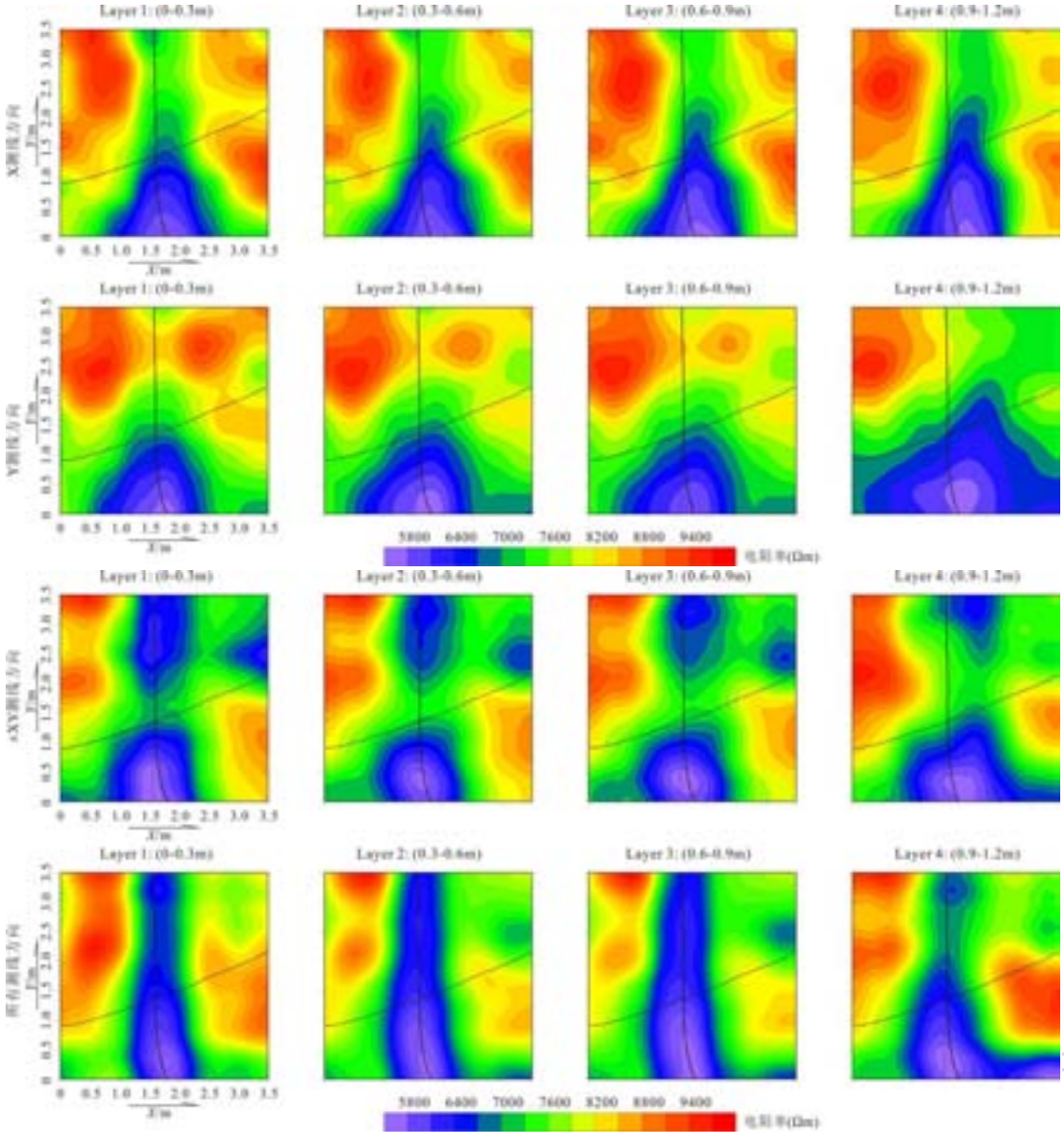

A visulization for the 3-D water flow process in fractures

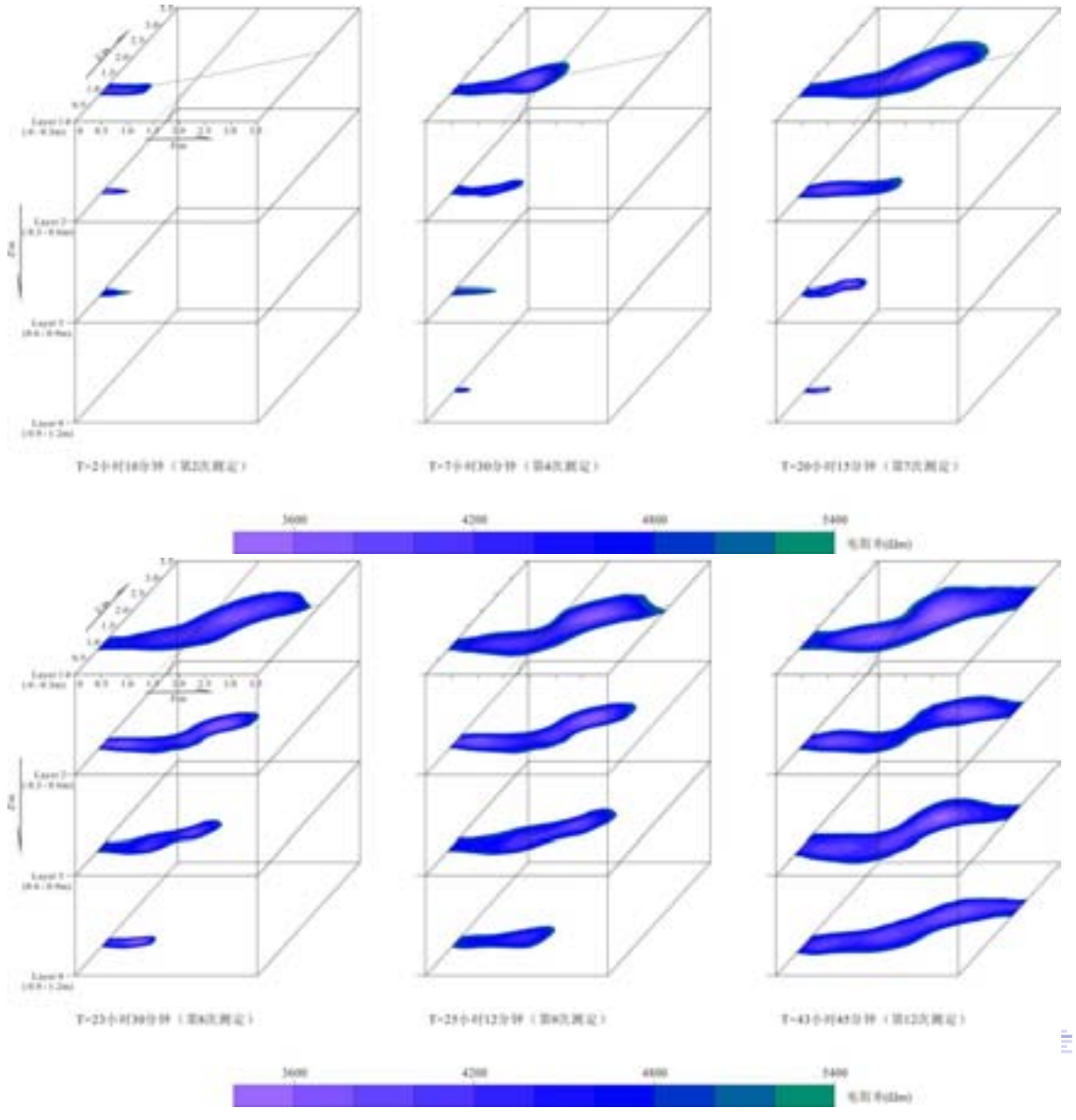

In situ infiltration and ERT monitoring experiments on low permeability granite rock

Monitored range:1.0m×1.0m

The infiltration process in planes revealed by ERT -1/2

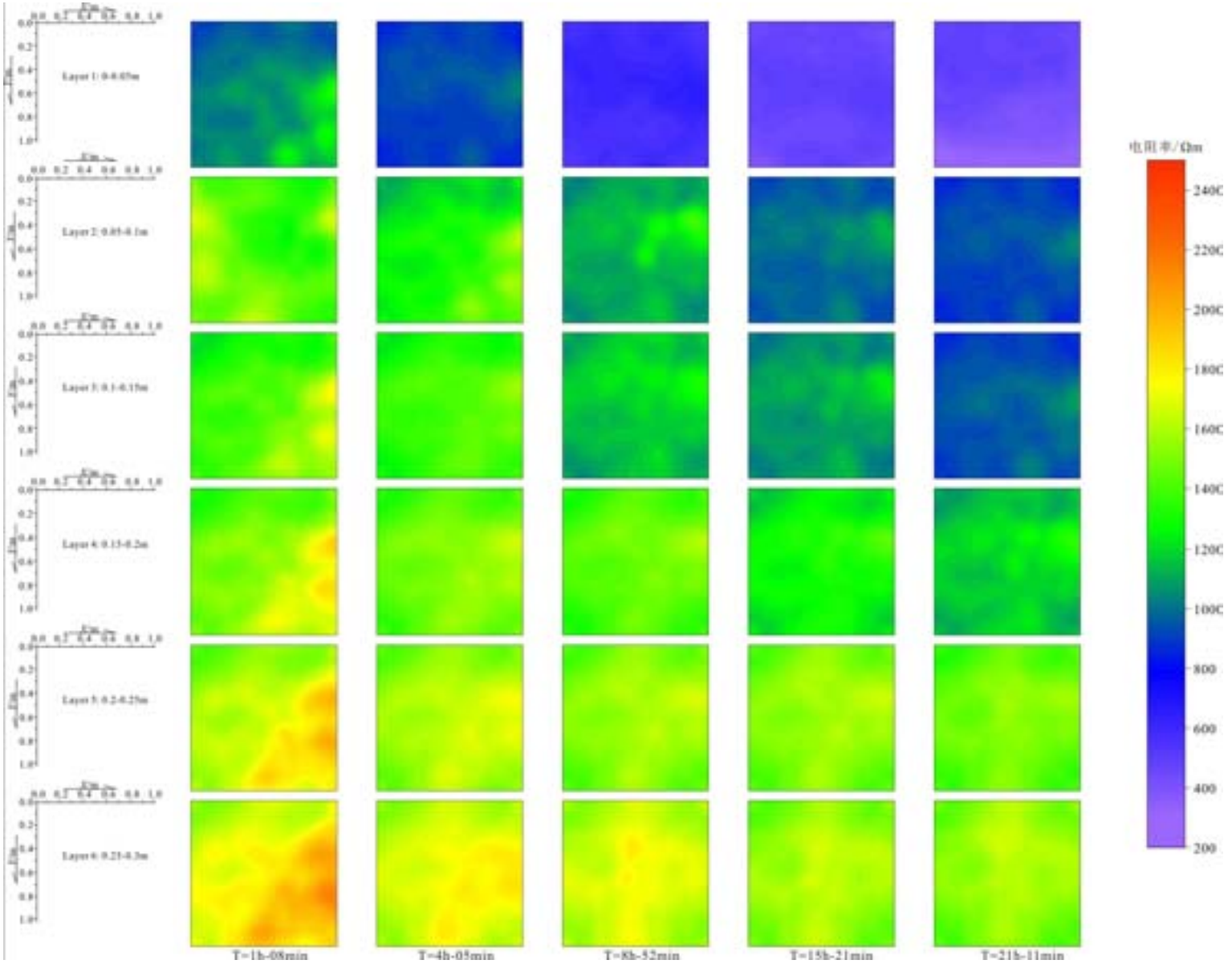

The infiltration process in planes revealed by ERT -2/2

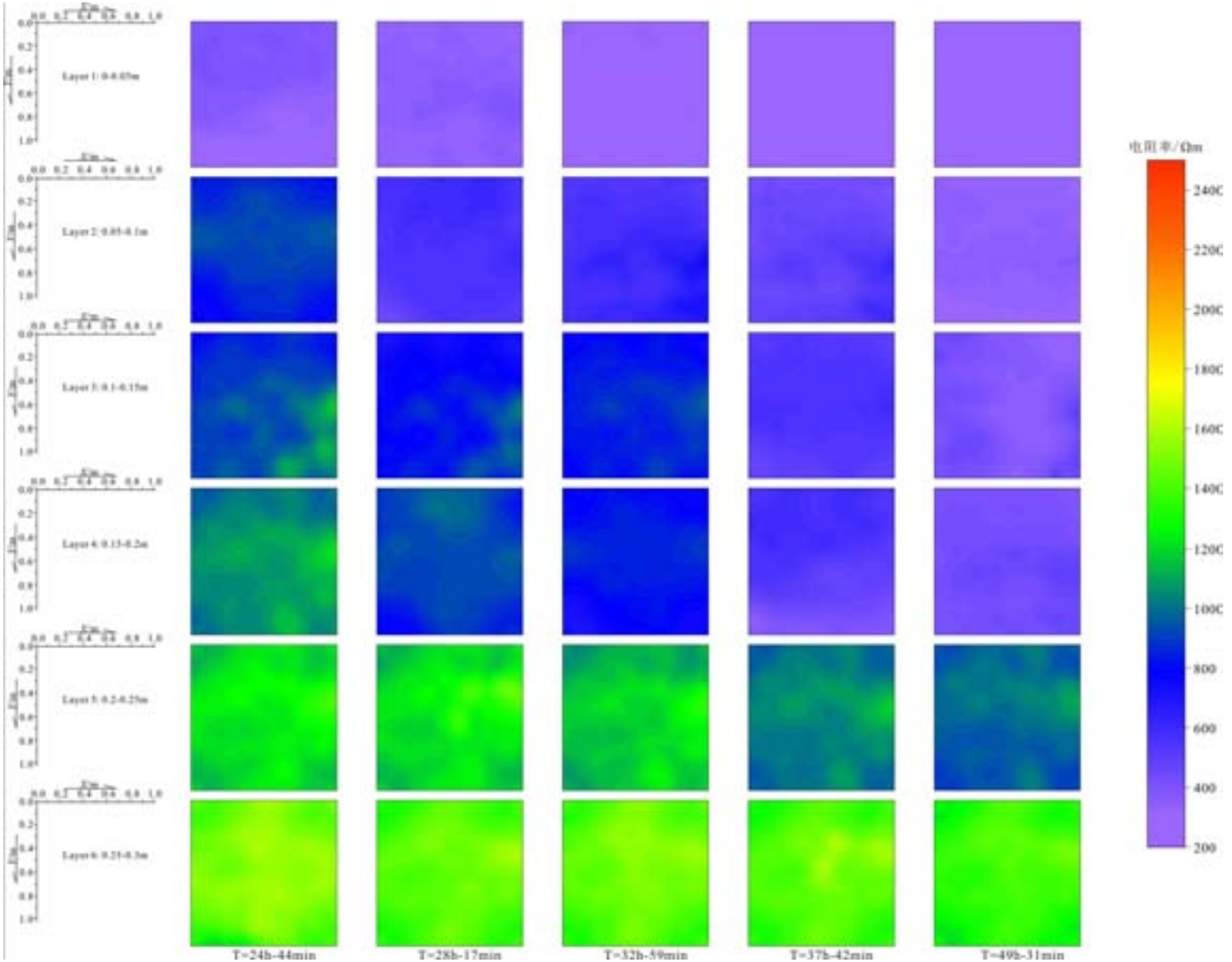

The infiltration process in sections revealed by ERT -1/2

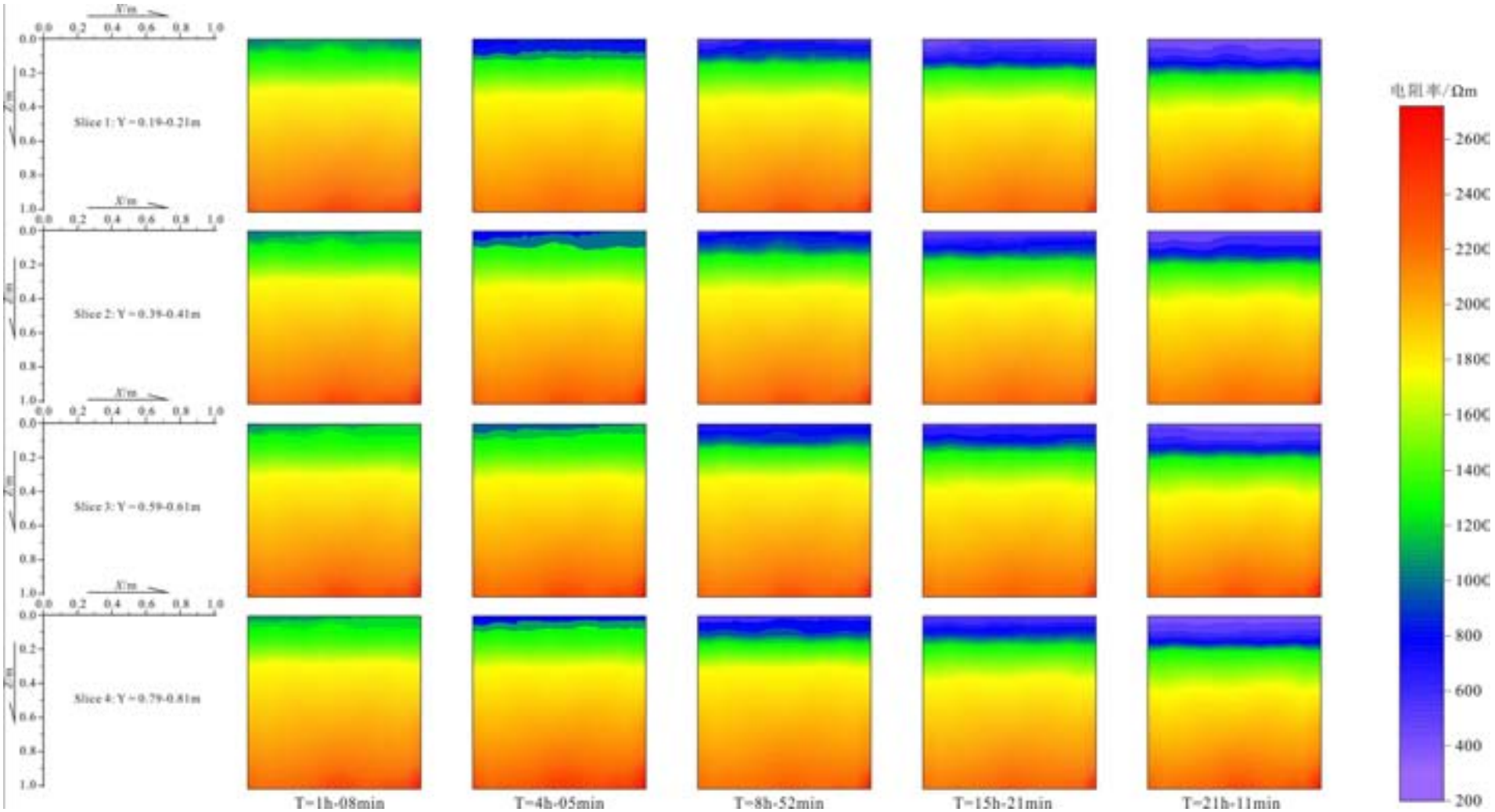

The infiltration process in sections revealed by ERT -2/2

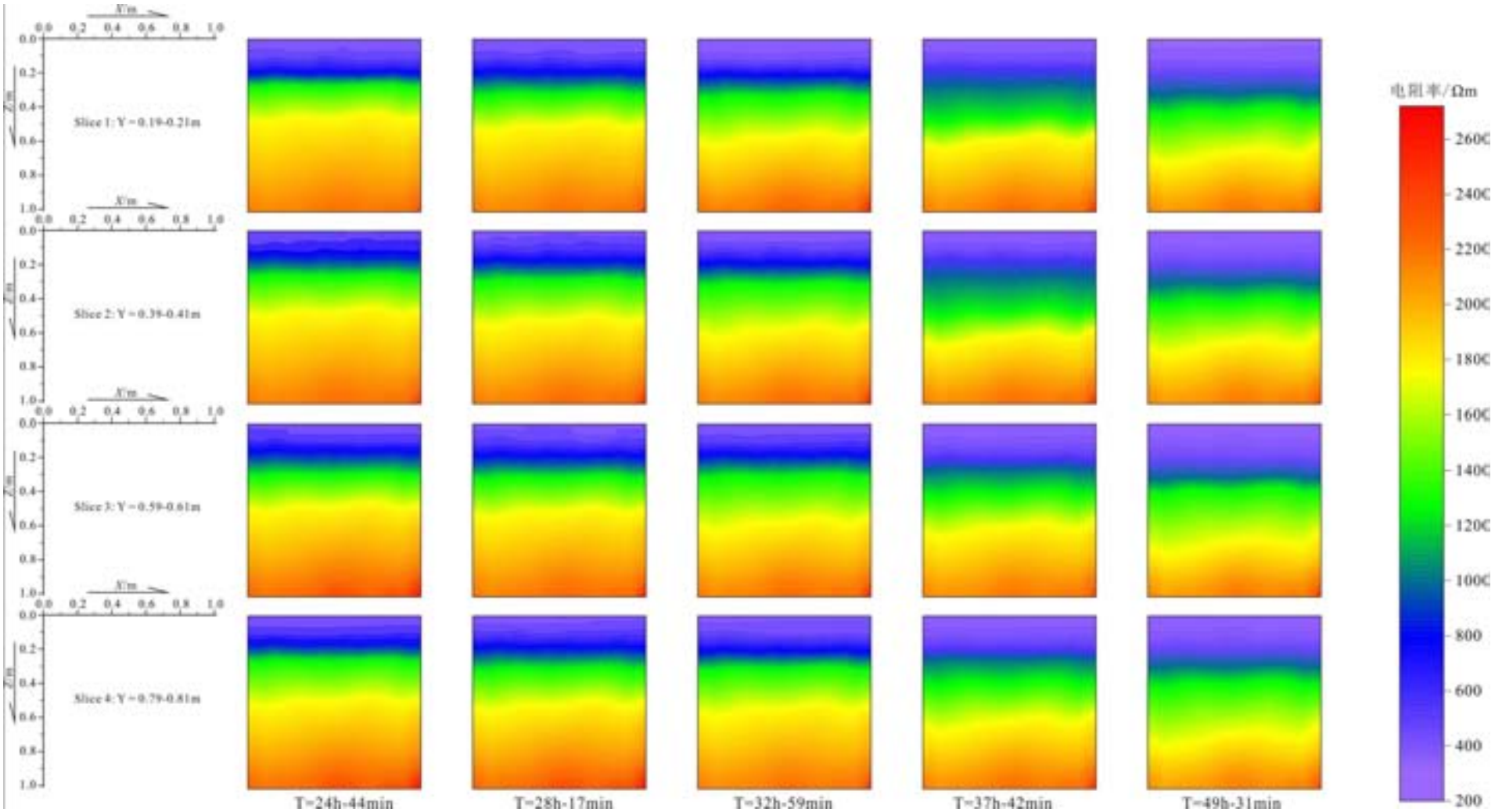

Applications of ERT at hundreds of meters scale in the field

The 2-D ERT surveying lines around borehole 5# in the field

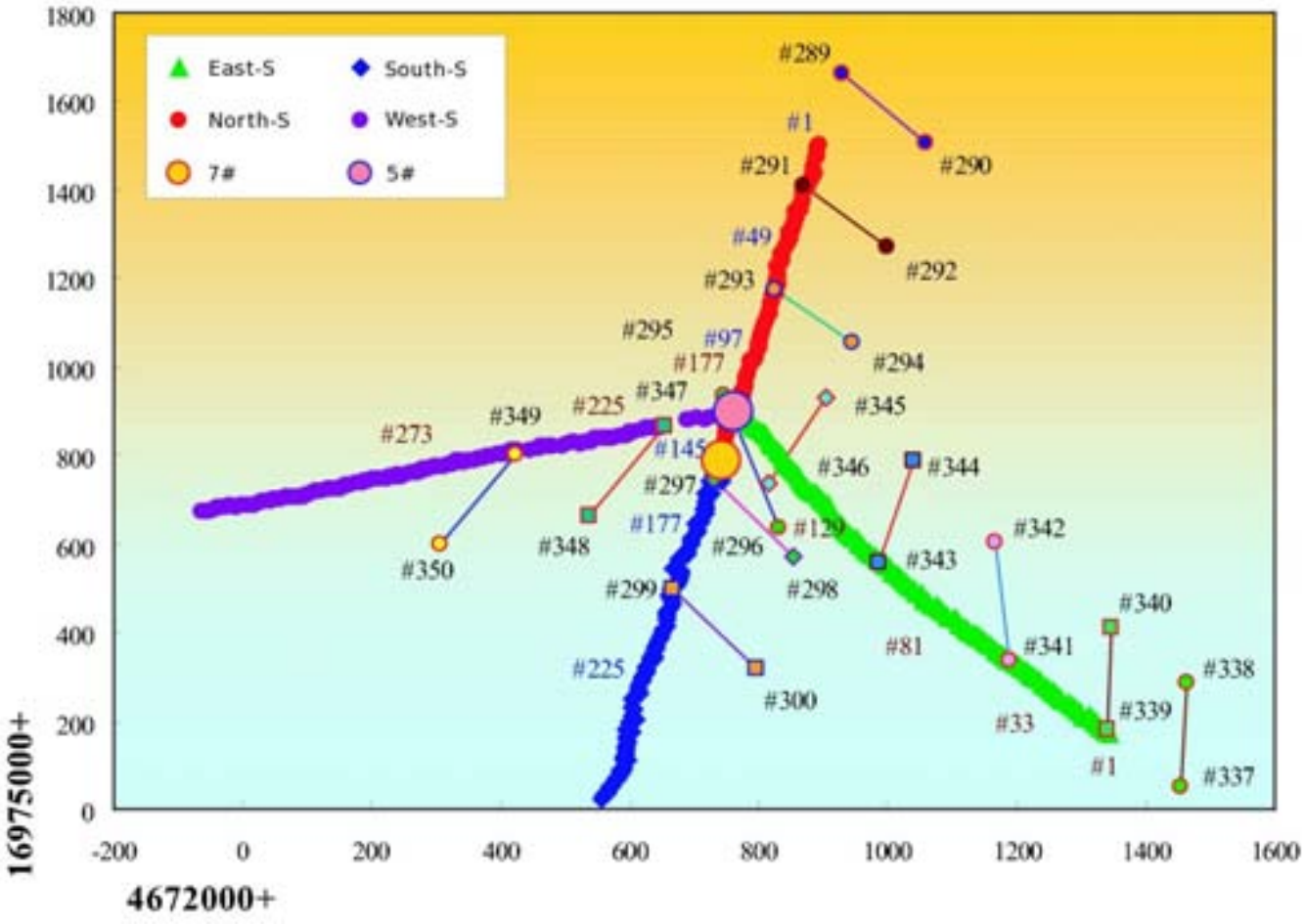

Measurement date:2008.8.13-31; Total length:3120m with south 720m, north 720m, east 880m and west 800m respectively.

The 2-D resistivity distributions obtained around borehole 5#

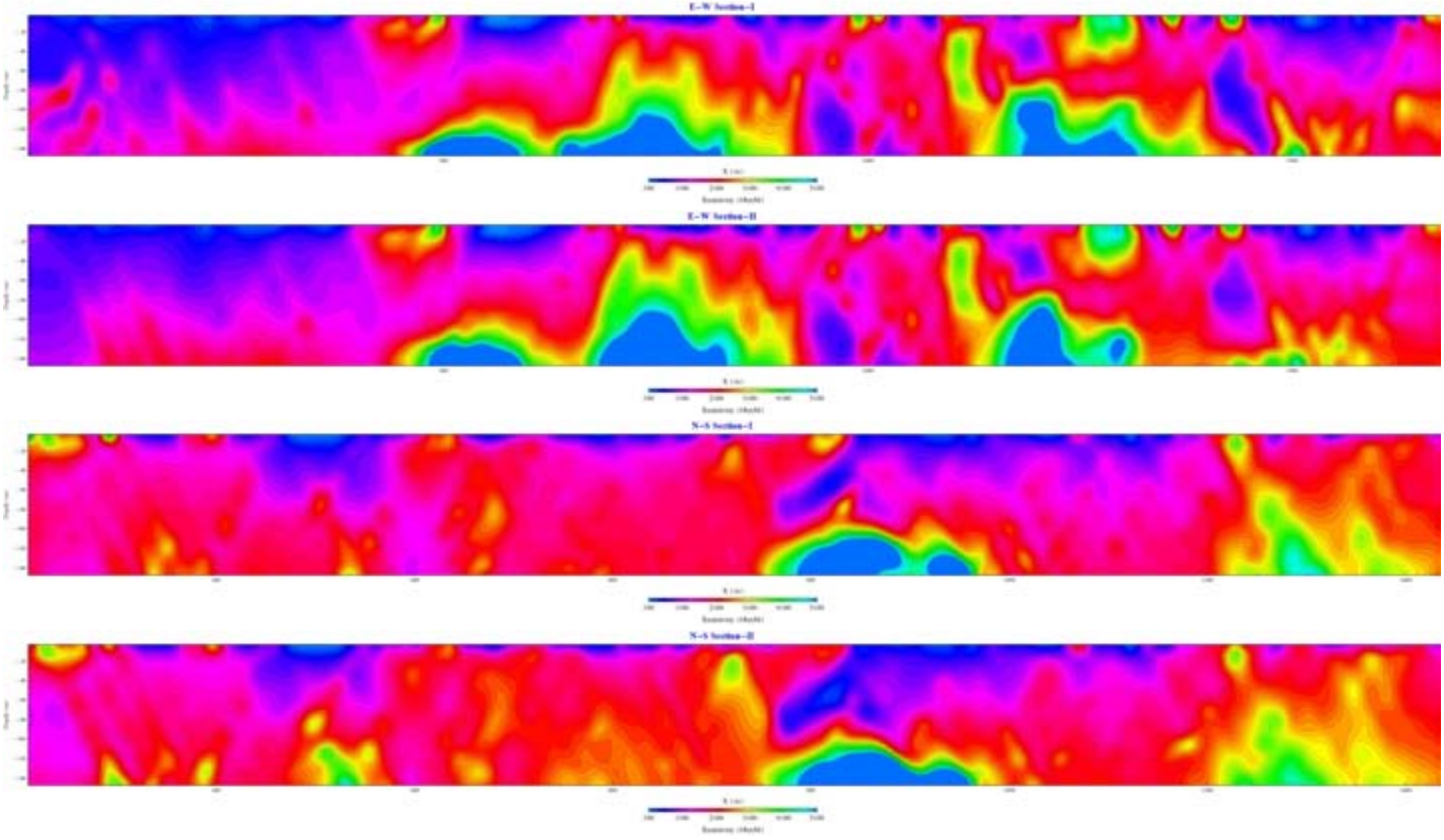

E-W(10mA),E-W(50mA),S-N(10mA),S-N(50mA), Borehole 5# is at 932m in E-W section and 620m in S-N section. Borehole 7# is at 730m in the S-N section

A comparison of the simulated 2-D ERT images with known resistivity models

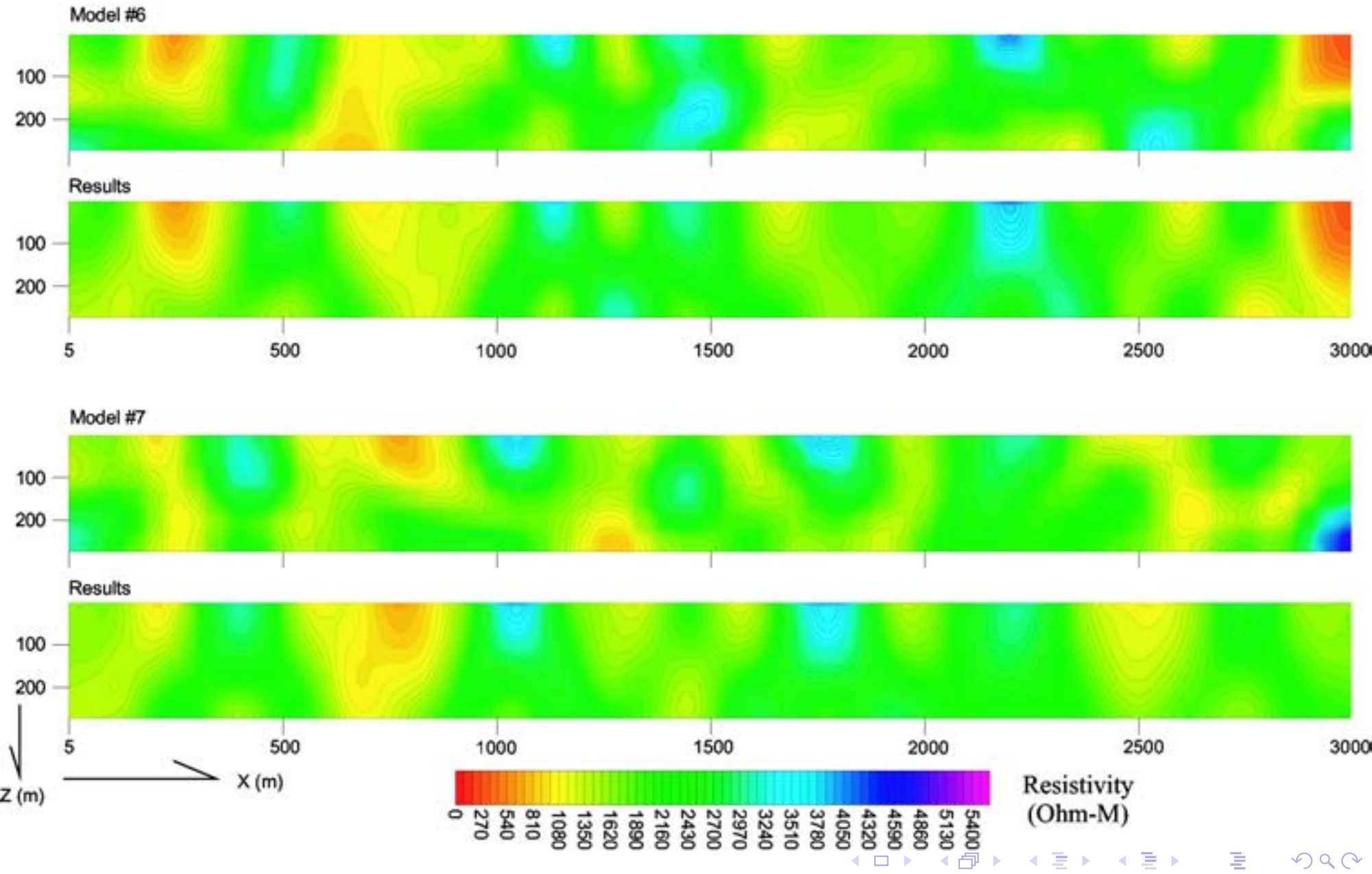

Thus constructed psuedo 3-D resistivity distribution for the site

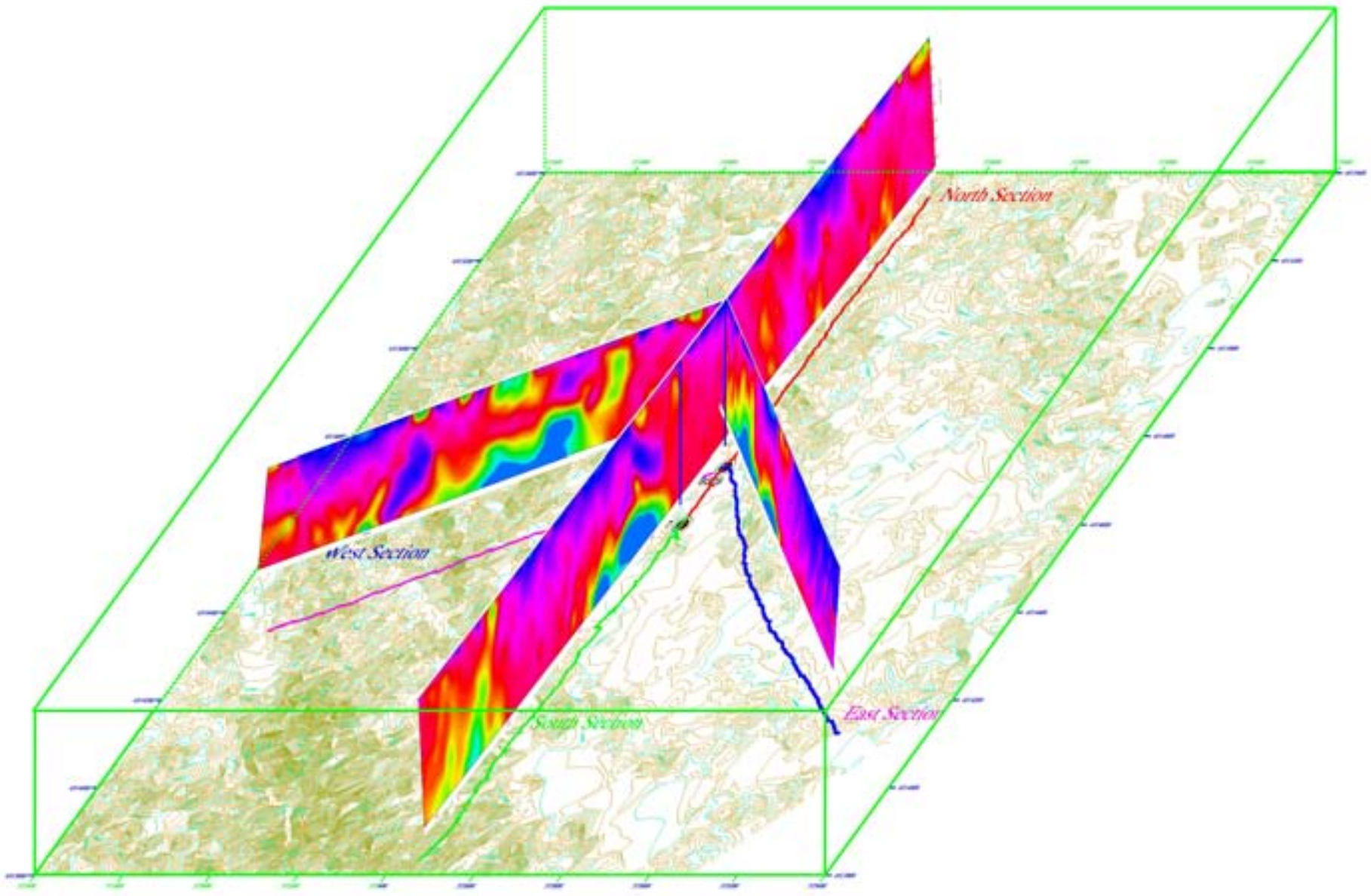

The fault interpretation in the north and south resistivity sections

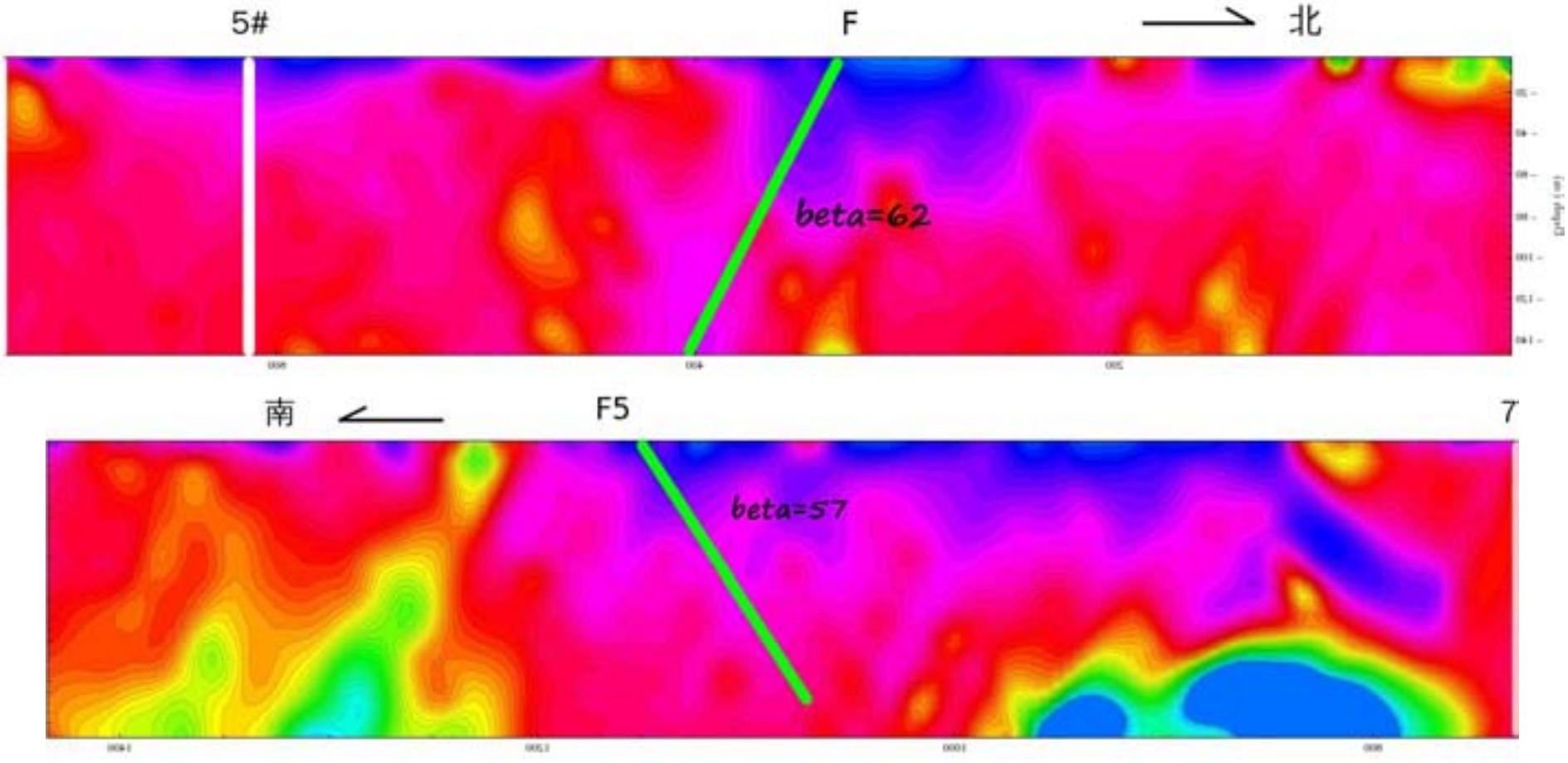

The fault interpretation in the east and west resistivity sections

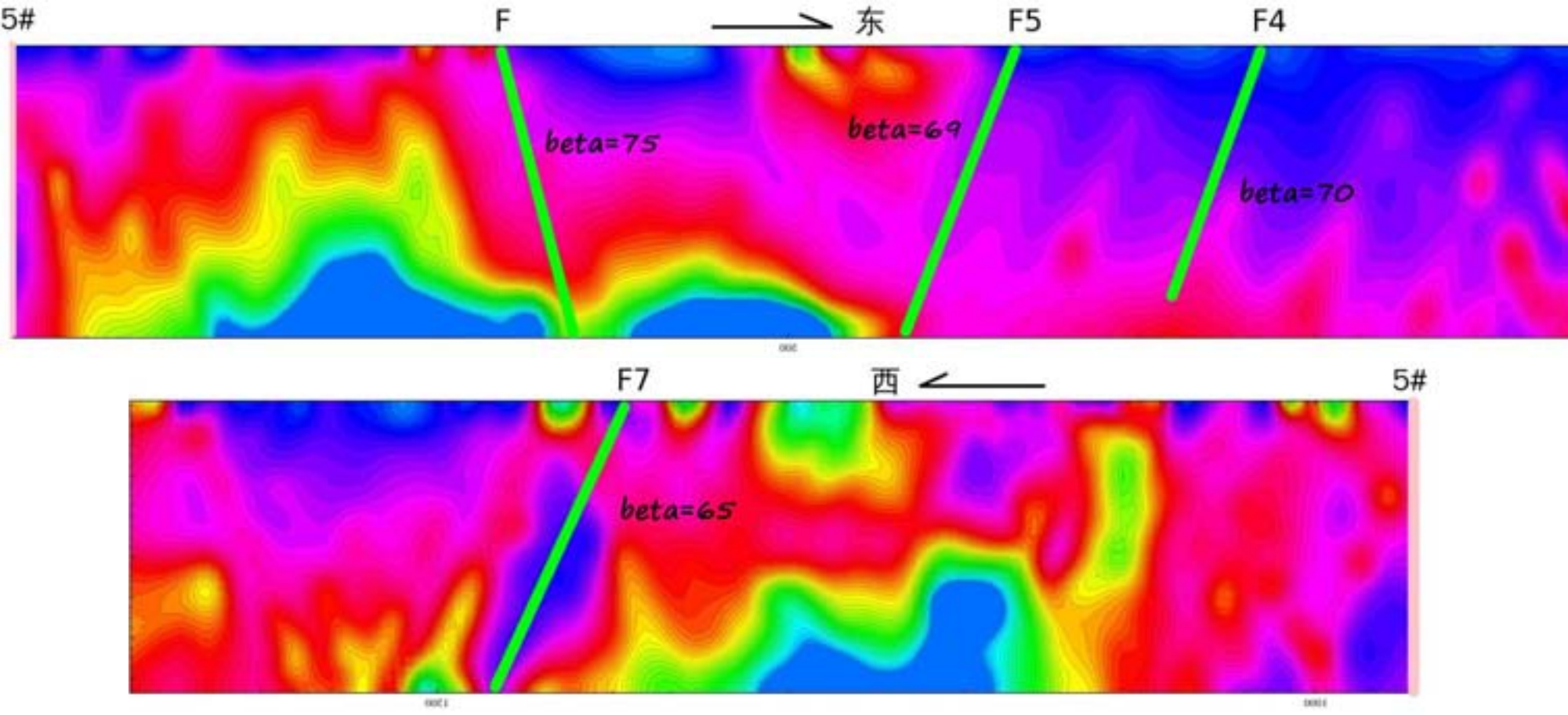

The flow system at the near surface

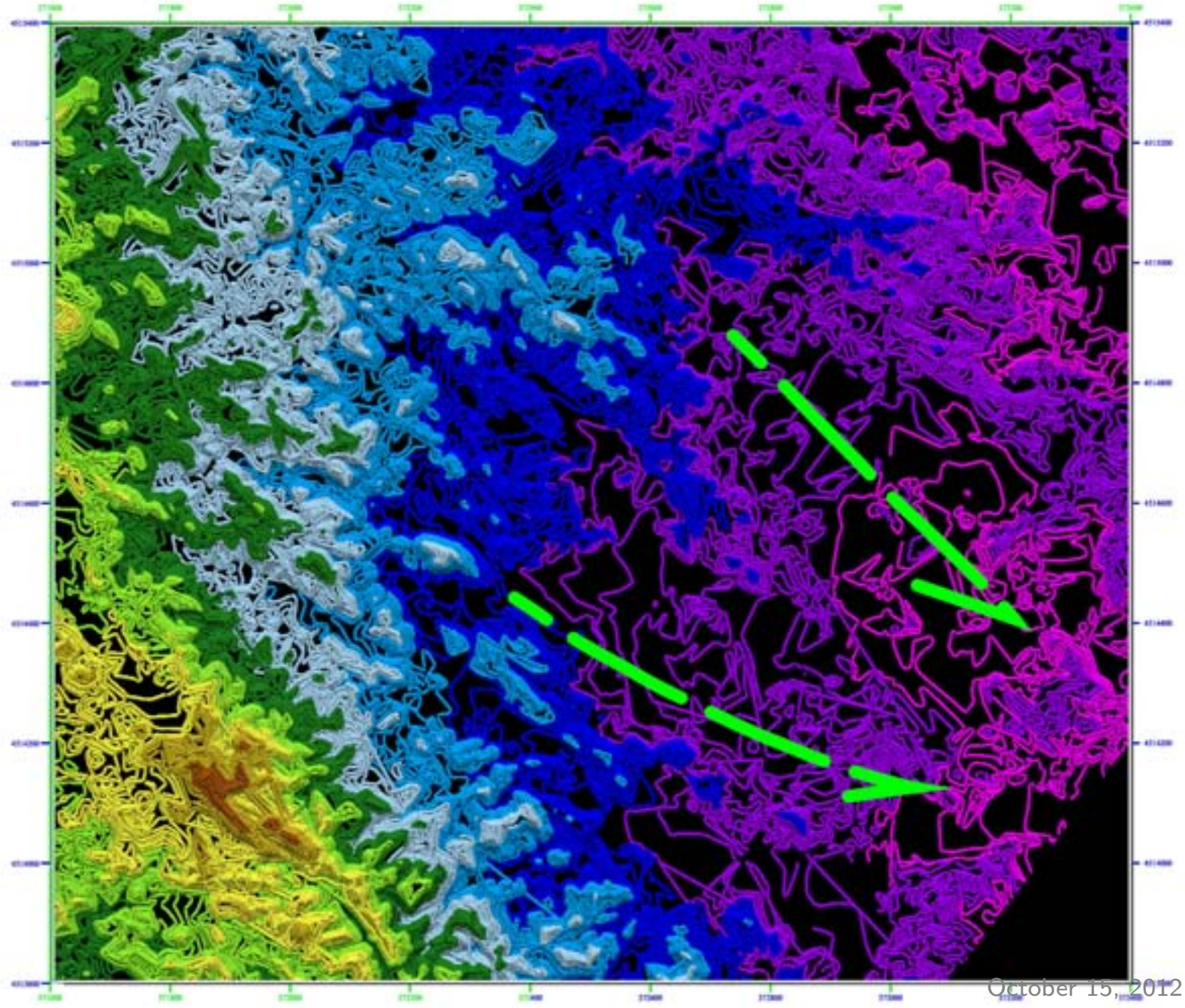

The possible flow system deep in the site

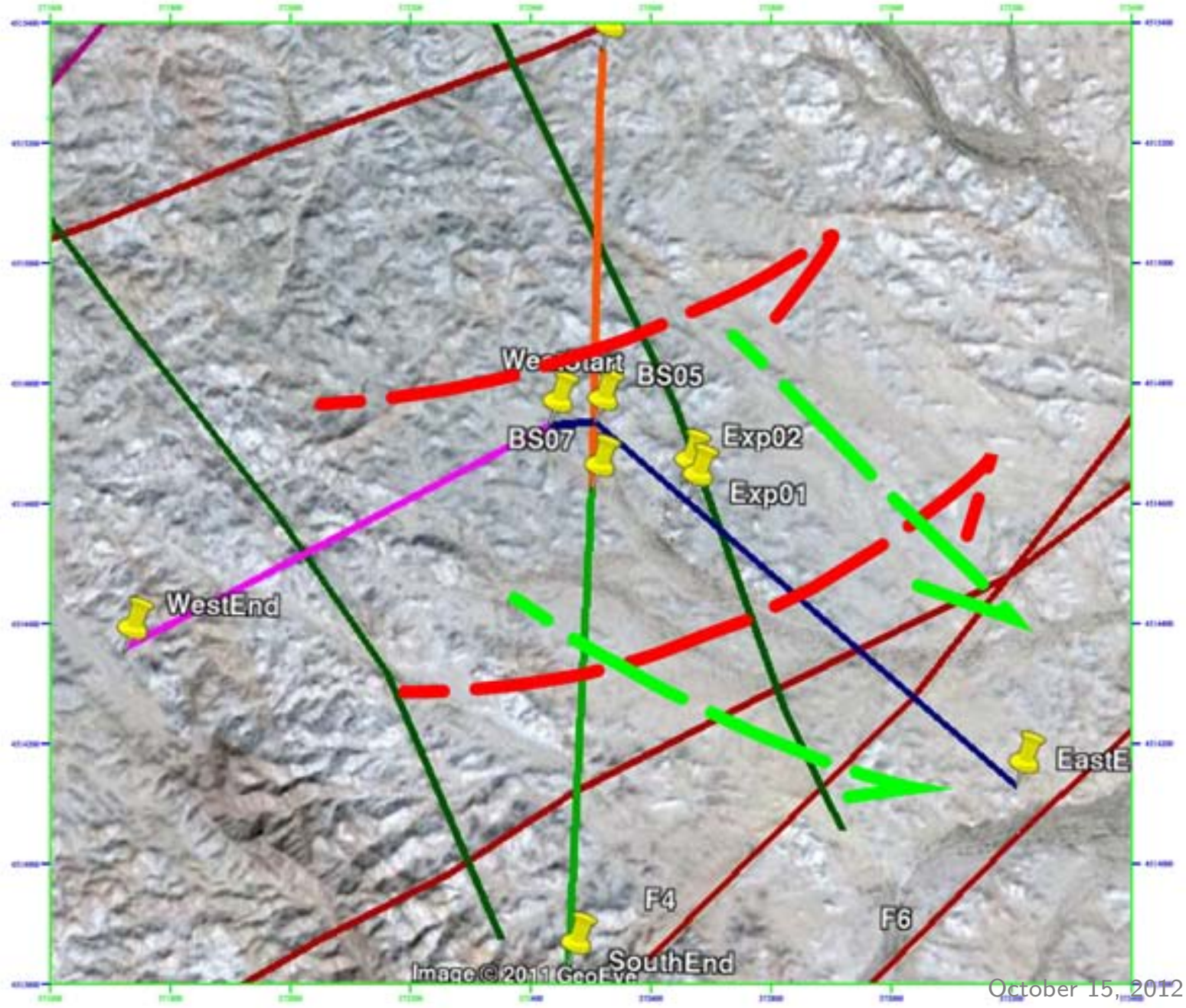

A site characterization concept based on multi-scale and multi-dimensional ERT

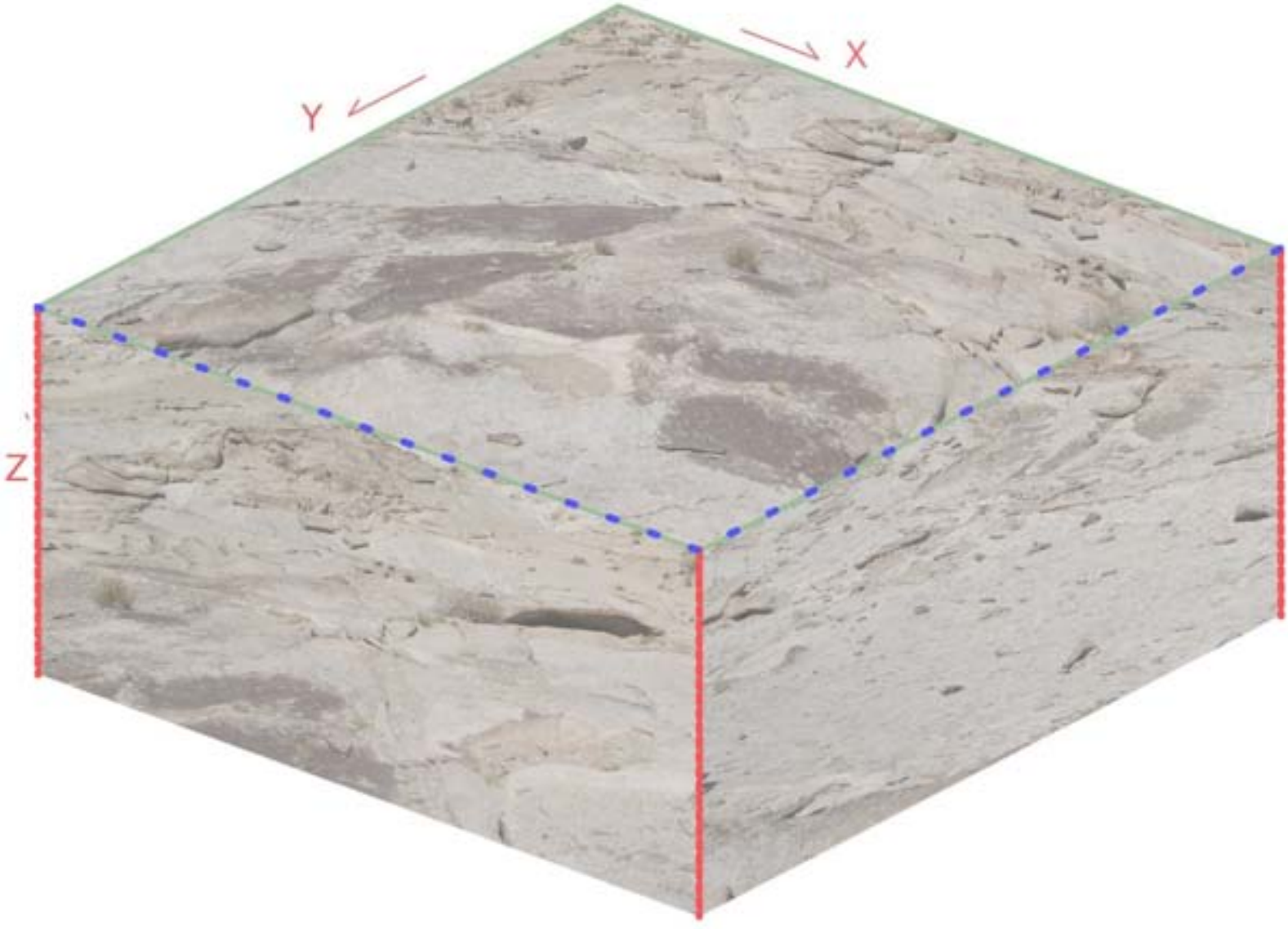

1. With electrodes at the surface and in boreholes

A site characterization concept based on multi-scale and multi-dimensional ERT

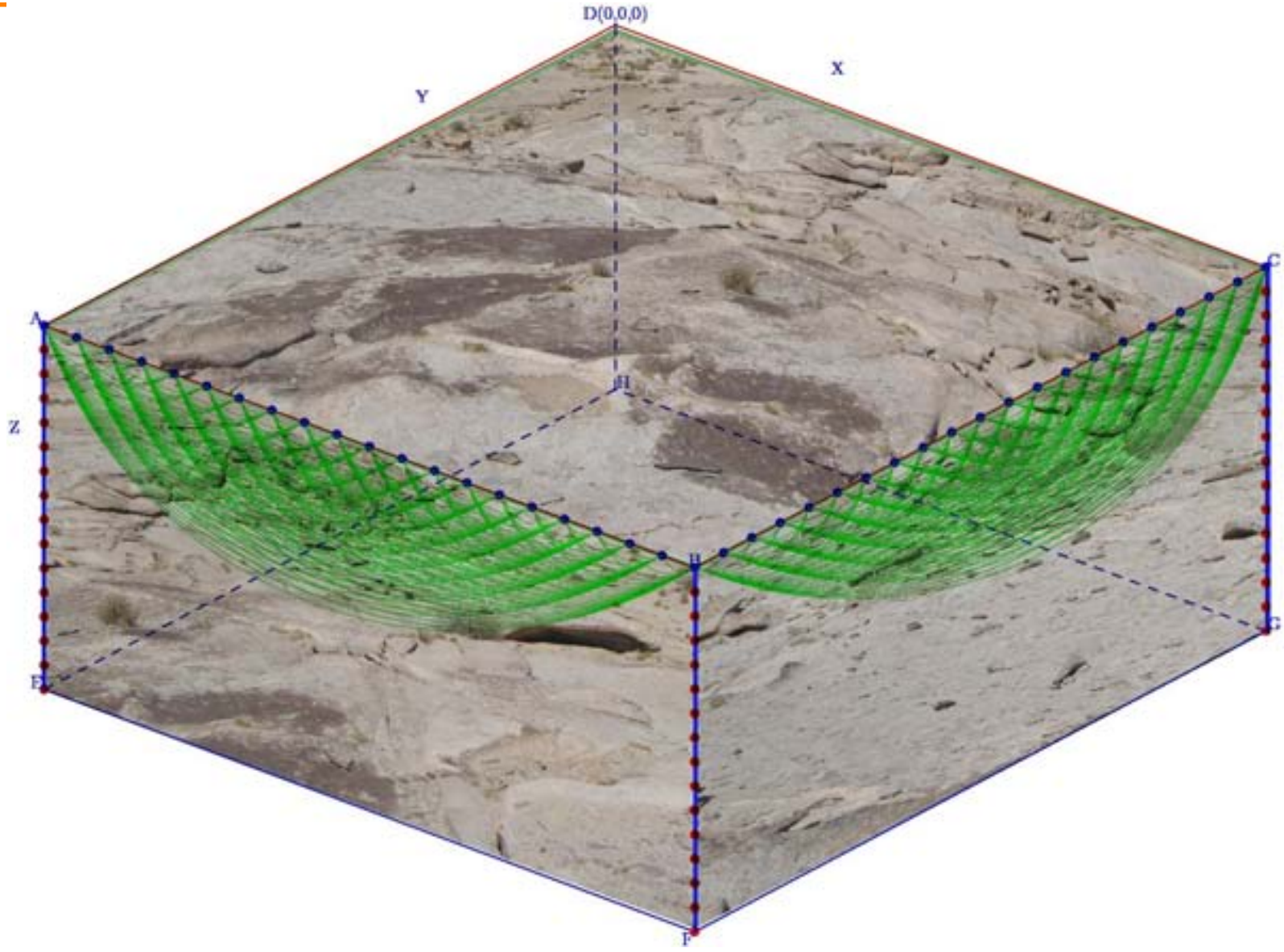

A site characterization concept based on multi-scale and multi-dimensional ERT

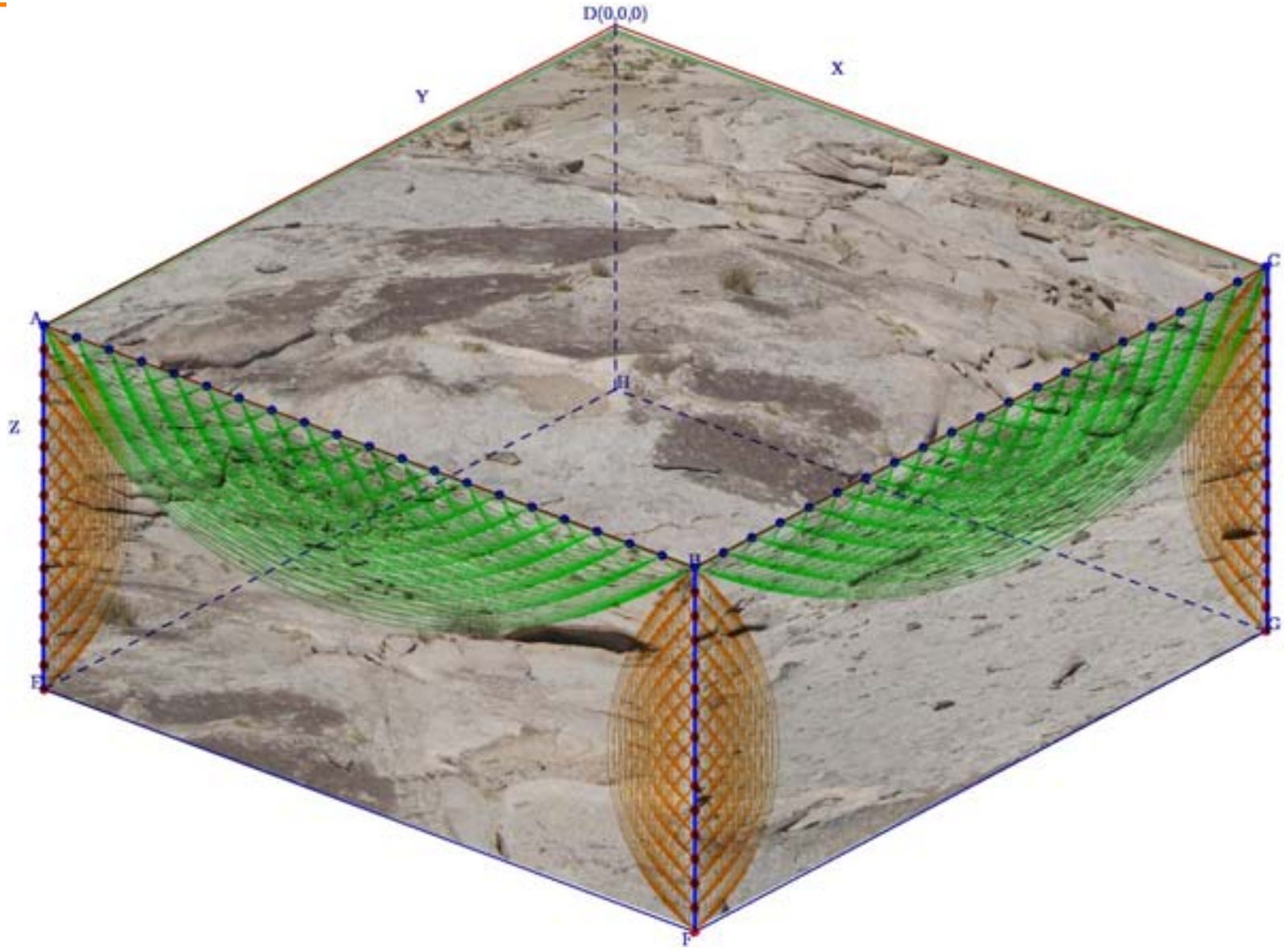

3. Deep resistivity surveying around boreholes

A site characterization concept based on multi-scale and multi-dimensional ERT

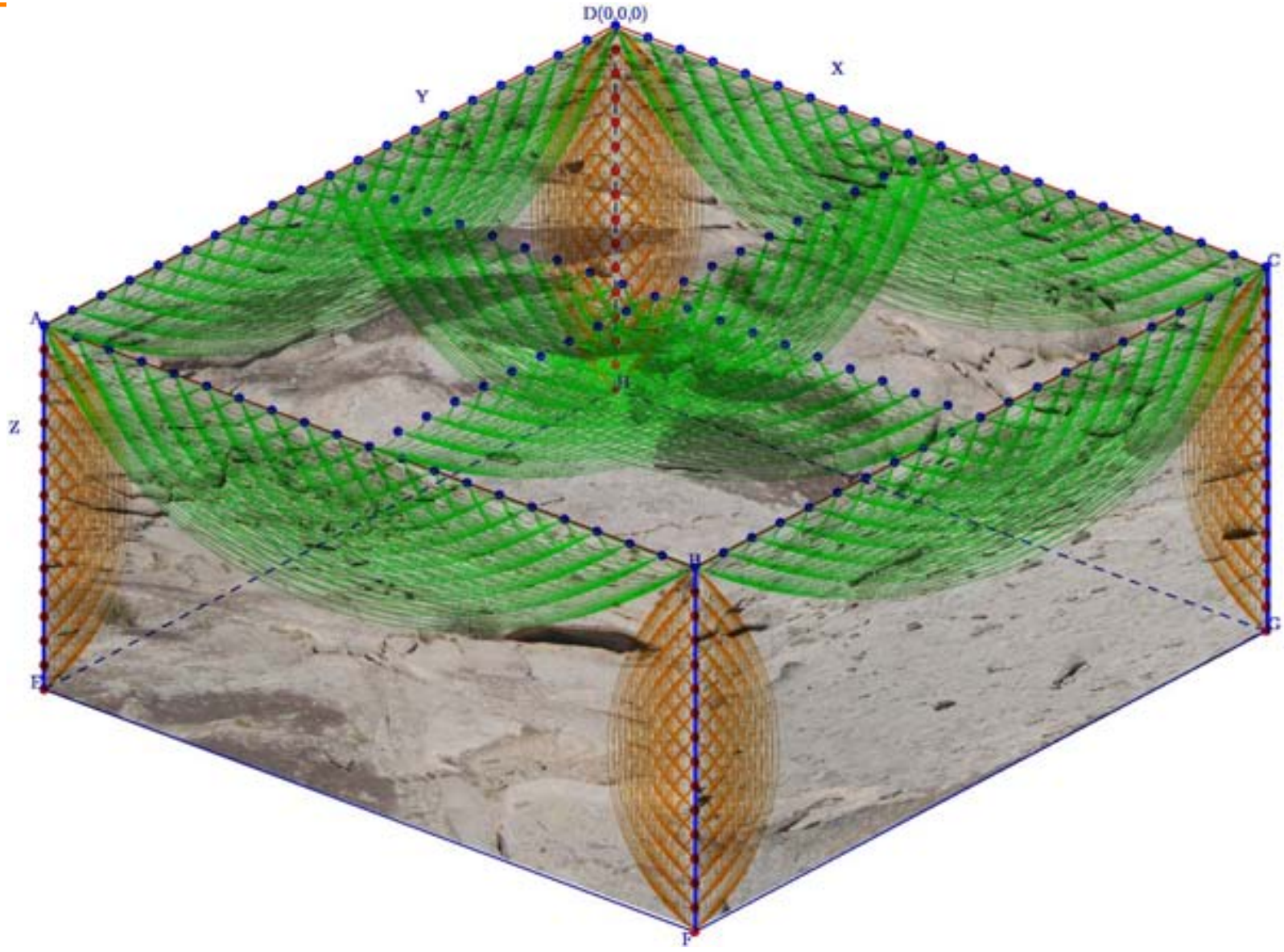

4. Characterize the site with multiple sections

A site characterization concept based on multi-scale and multi-dimensional ERT

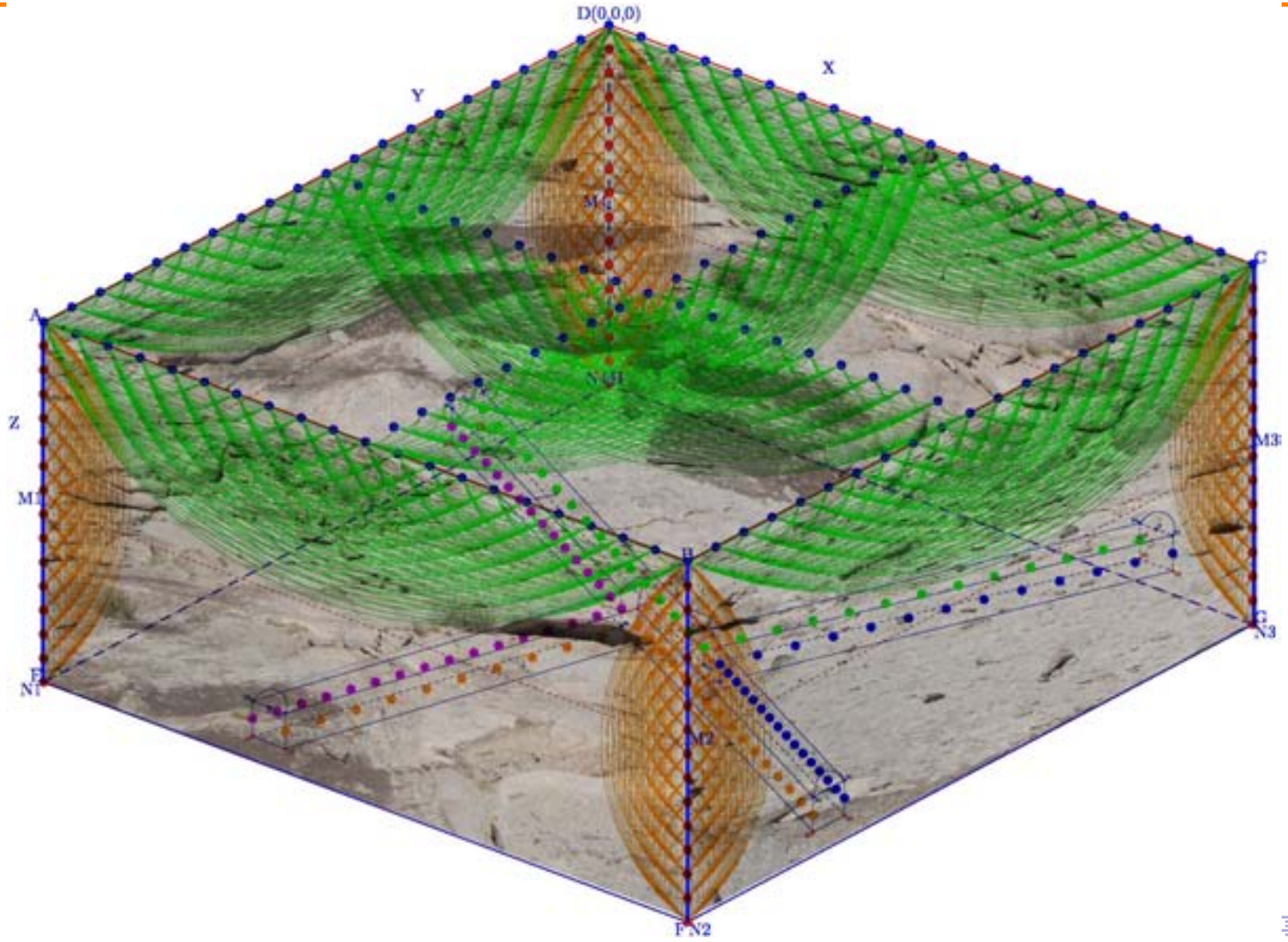

5. With electrodes installed in the tunnels

A site characterization concept based on multi-scale and multi-dimensional ERT

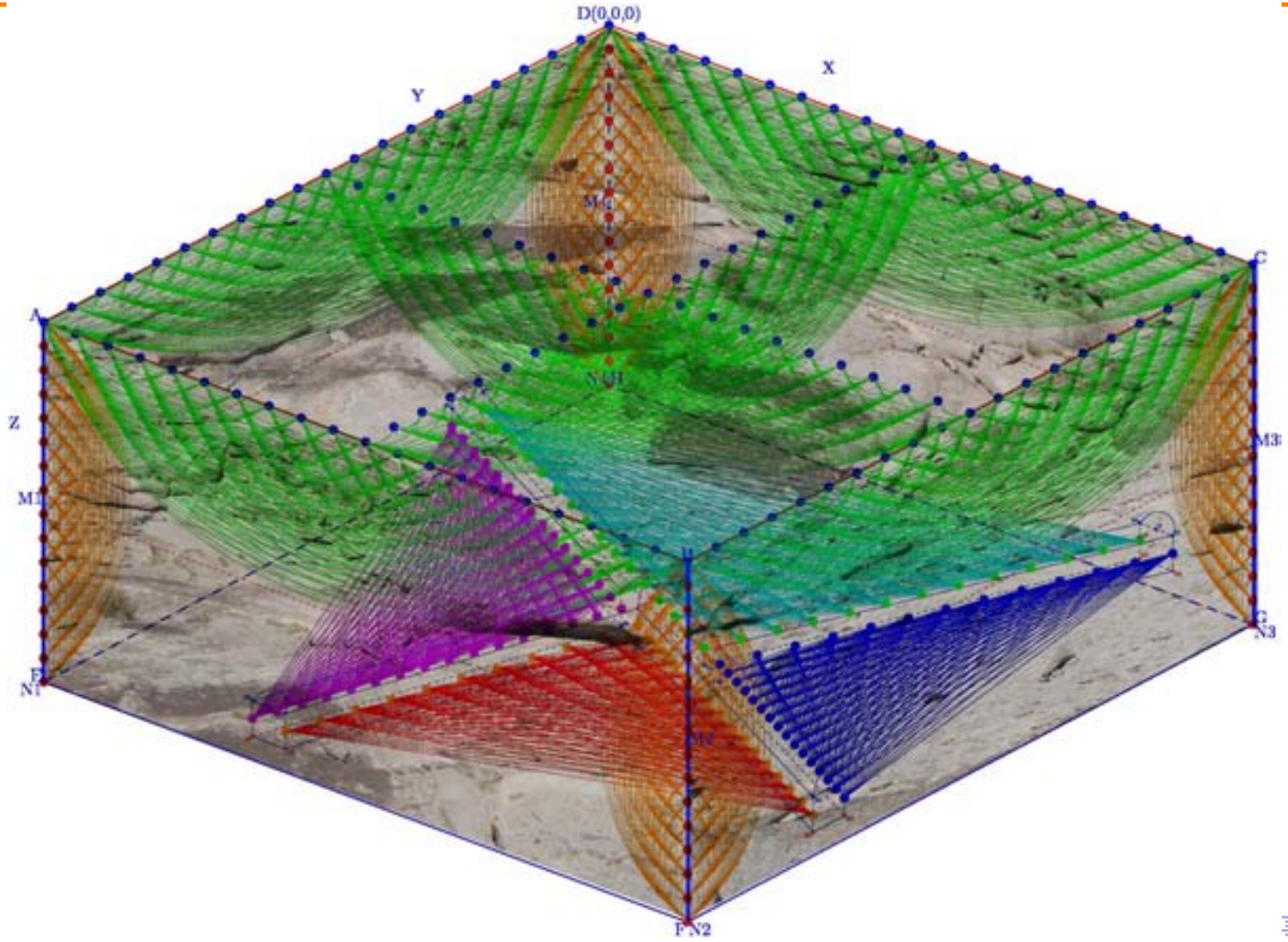

6. Resistivity surveying based on tunnel ERT

The 2D ERT measurement line from Borehole #18 to #13 conducted at Xinchang site

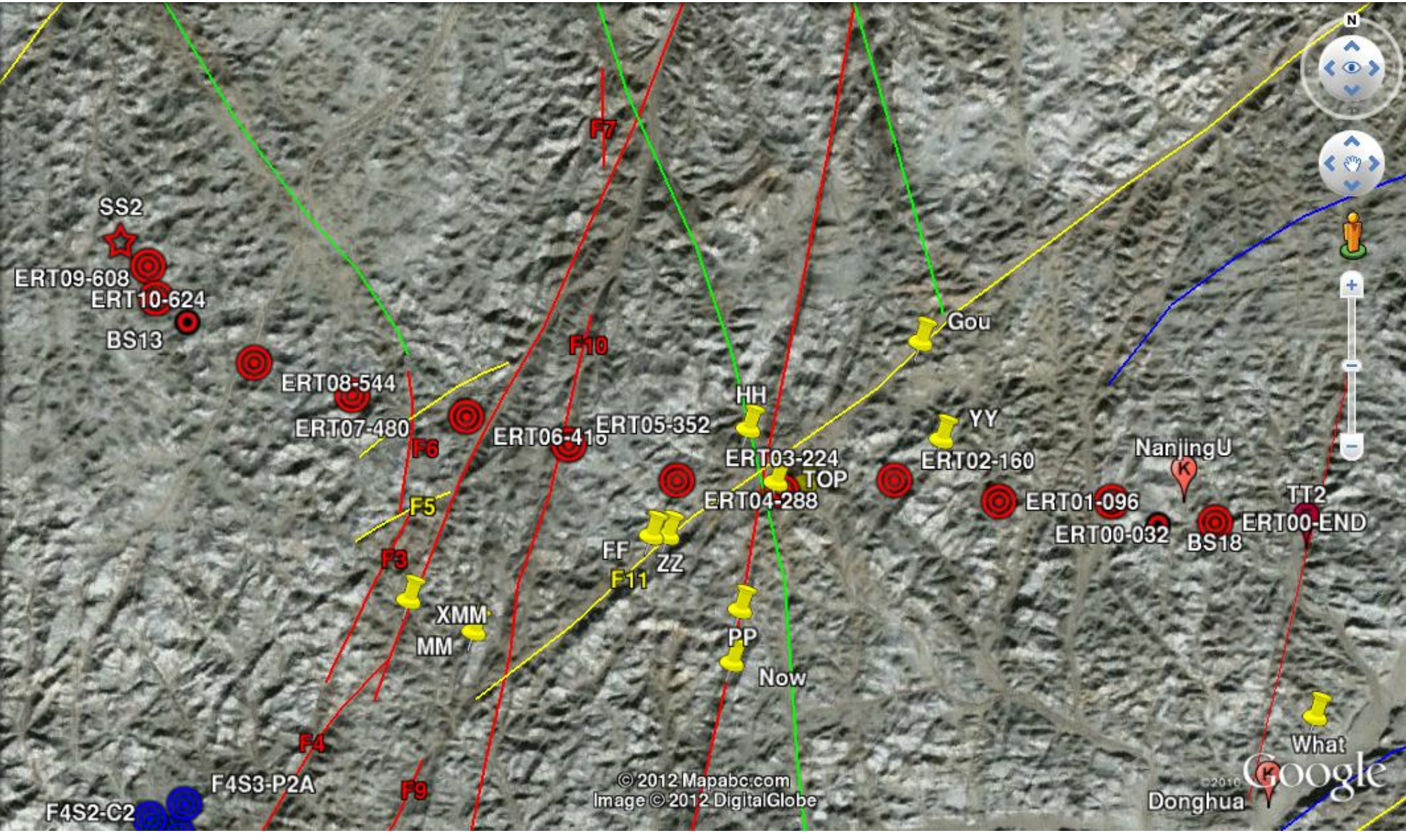

The three 2D ERT measurement sections crossing fault F4 at different positions

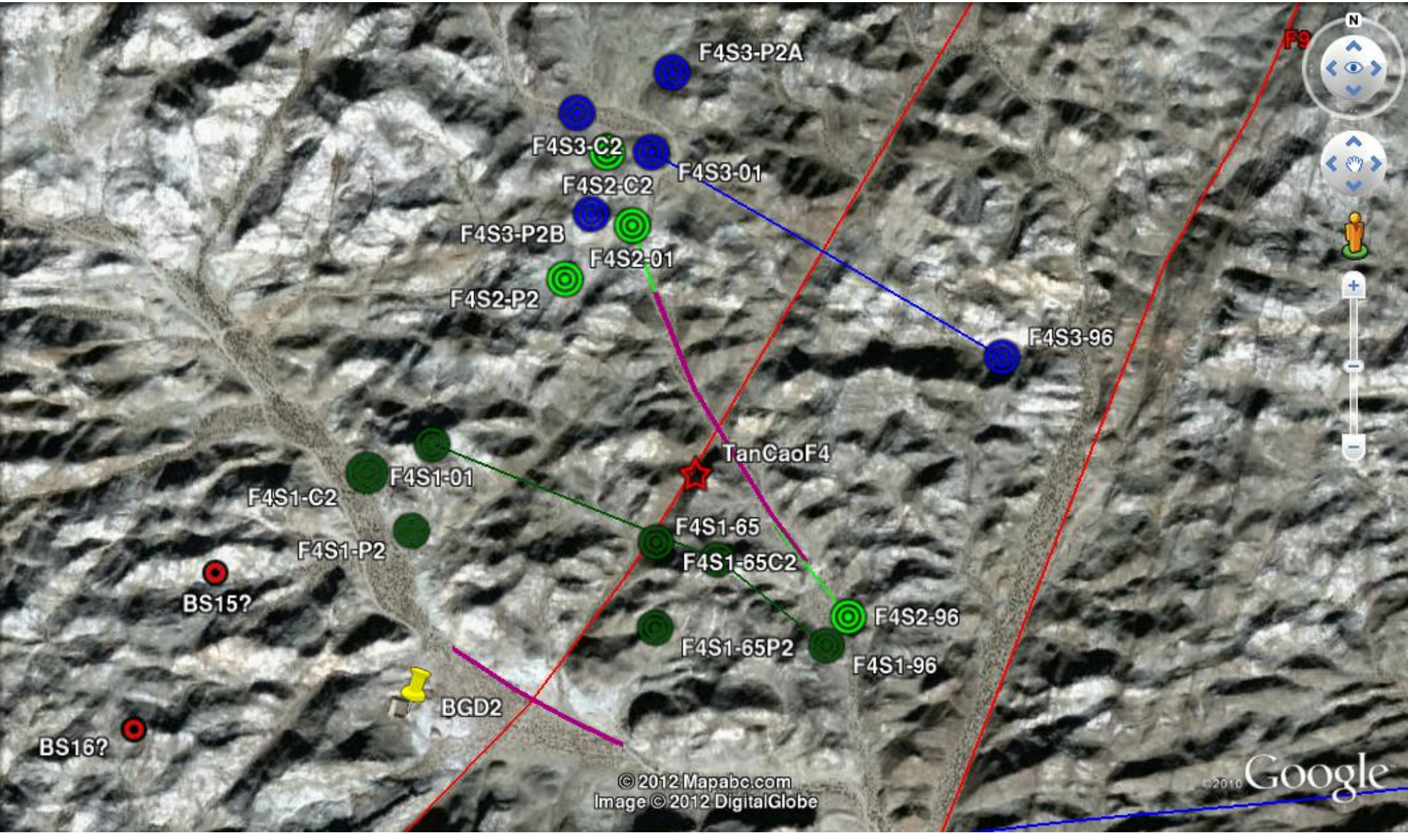

The apparent resistivity section obtained at the north side of Fault F4

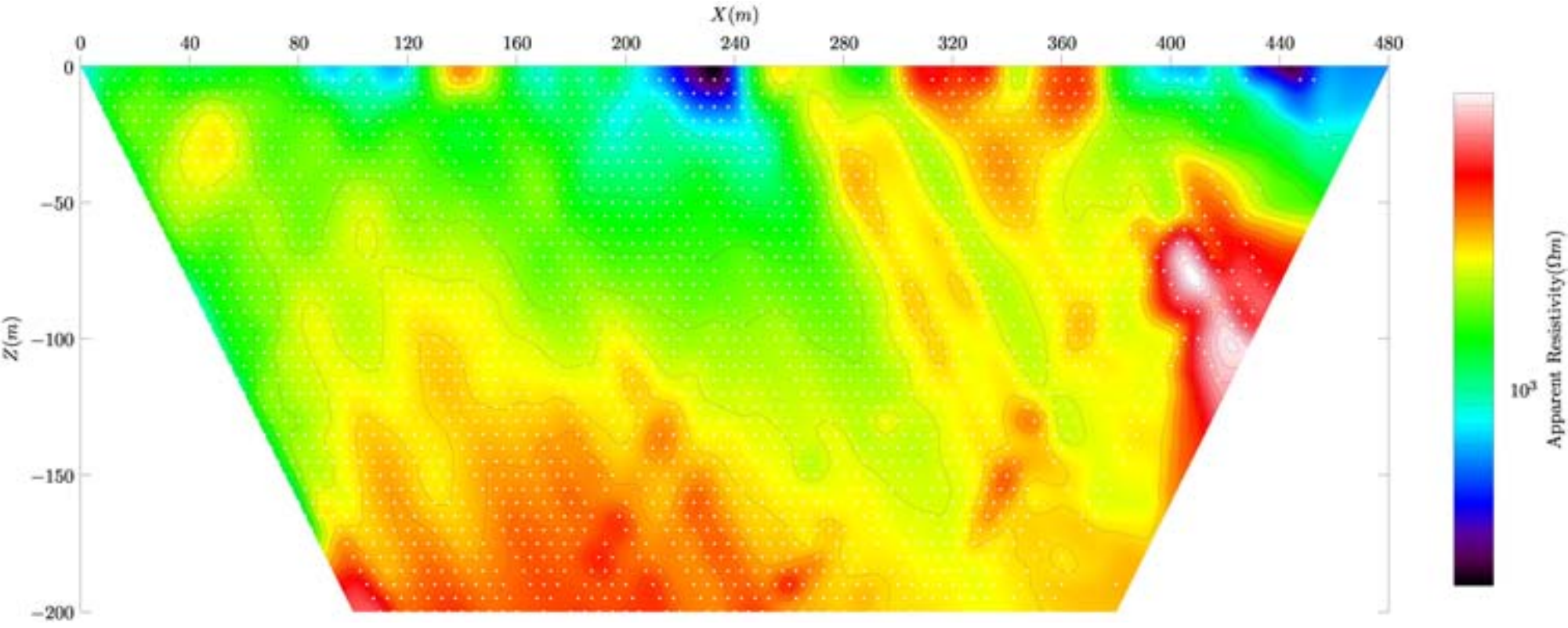

The tent setup in the Gobi field

Our ERT measurement team in the field

What did I look like when working in the field ?

Conclusions

1. In the site characterization for RWD, high density electrical resistivity tomography has great potential applications.

   It can be conducted not only in multi-scales ranging from rock samples in the lab to ground surface and boreholes in the field,

   but also in multi-dimensions at the ground surface, in the boreholes and in underground excavated cavities.

   Thus a detailed ERT surveying together with other methods may provide us with a wealth of information about the subsurface resistivity, thus help us understand the 3-D structure of the site.

Conclusions

2. A even more promising application of ERT for RWD lies in its capability and versatility of process monitoring.

   Although this usage may be limited to small spatial scales, a sequence of resistivity images at different time would help us understand the physical processes occurred and even evaluate parameters as permeability, thermal conductivity and dispersivity in multi-dimensions and multi-scales.

   This certainly would be useful in the input parameter constraint for repository security assessment.

THANKS!

NJU Campus

Characterization of fracture networks at different scales

Prof. Xiaozhao Li

Institute for Underground Space and Geo-environment,
Nanjing University

For the 2nd Chinese-German Workshop on Radioactive Waste Disposal
October 15-16, 2012,
Karlsruhe Institute of Technology (KIT), Germany

PTKA Projektträger Karlsruhe
Karlsruher Institut für Technologie

BGR Bundesanstalt für Geowissenschaften und Rohstoffe

BRIUG

OUTLINE

- Kinematic concept and fracture patterns at different scales
- Identification of permeability of fault and fracture zones
- Measurement, analysis method and non-uniform distribution of fracture trace
- Stability-controlling modes and preferential structural plane
- Simulation analysis on permeability parameters and flow path

Kinematic concept and fracture patterns at different scales

In order to build up fracture system model and identify flow pathways, a good understanding of the deformation mechanism and kinematic relations is crucial.

Kinematic concept and fracture patterns at different scales

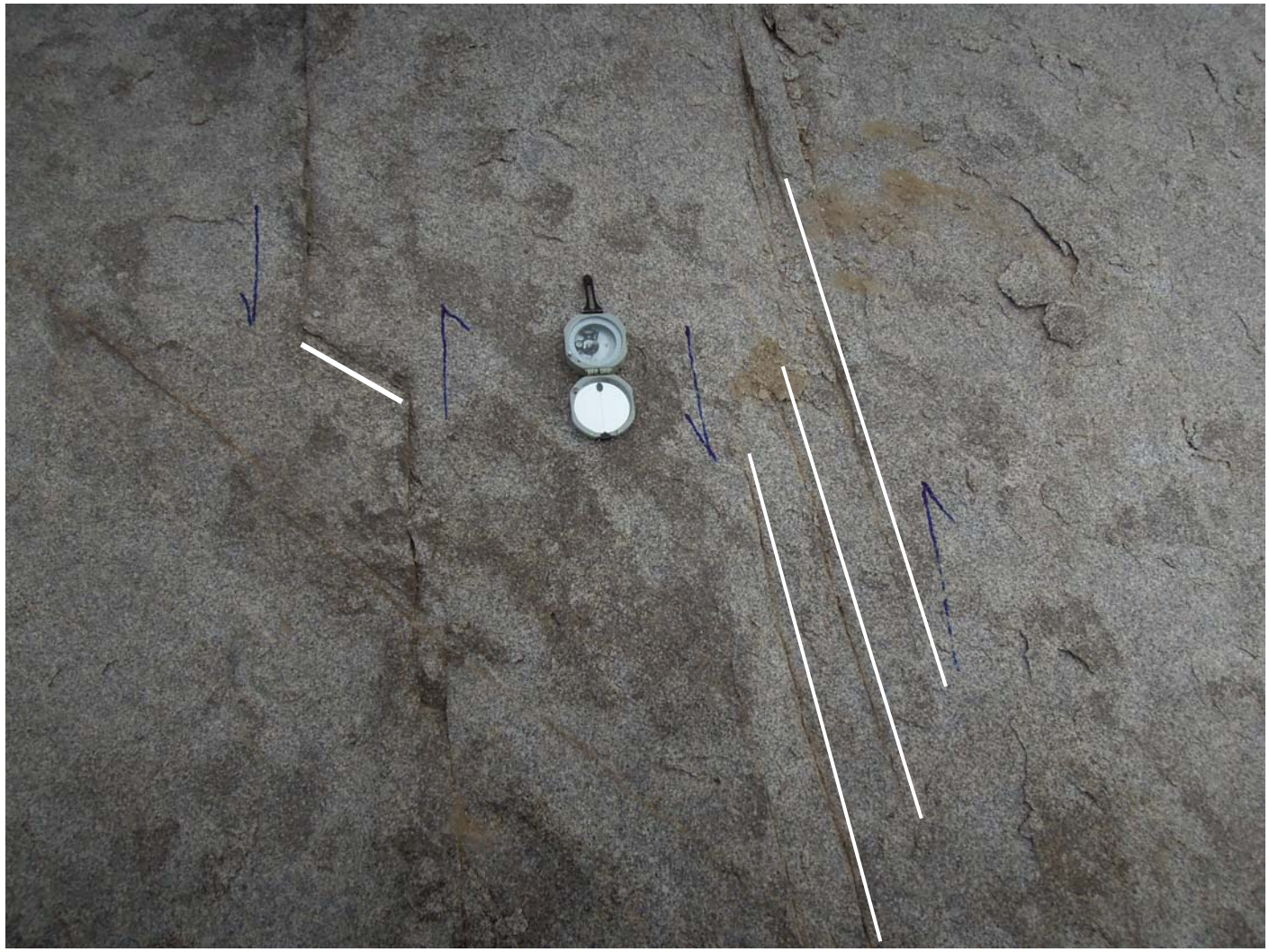

R-and T-fractures at small scale co-exist in a same location

Kinematic concept and fracture patterns at different scales

From field observation and structural analysis, we find that:

✧The low angle fractures (e.g. R-fracture in NE orientation) are more developed.

In contrast, the high angle fractures (e.g. X-fracture in NW orientation) are just in initial formation stage.

✧The low angle fractures are predominant and well developed. The developments of different type of fractures depend on stress and kinematic boundary conditions.

Kinematic concept and fracture patterns at different scales

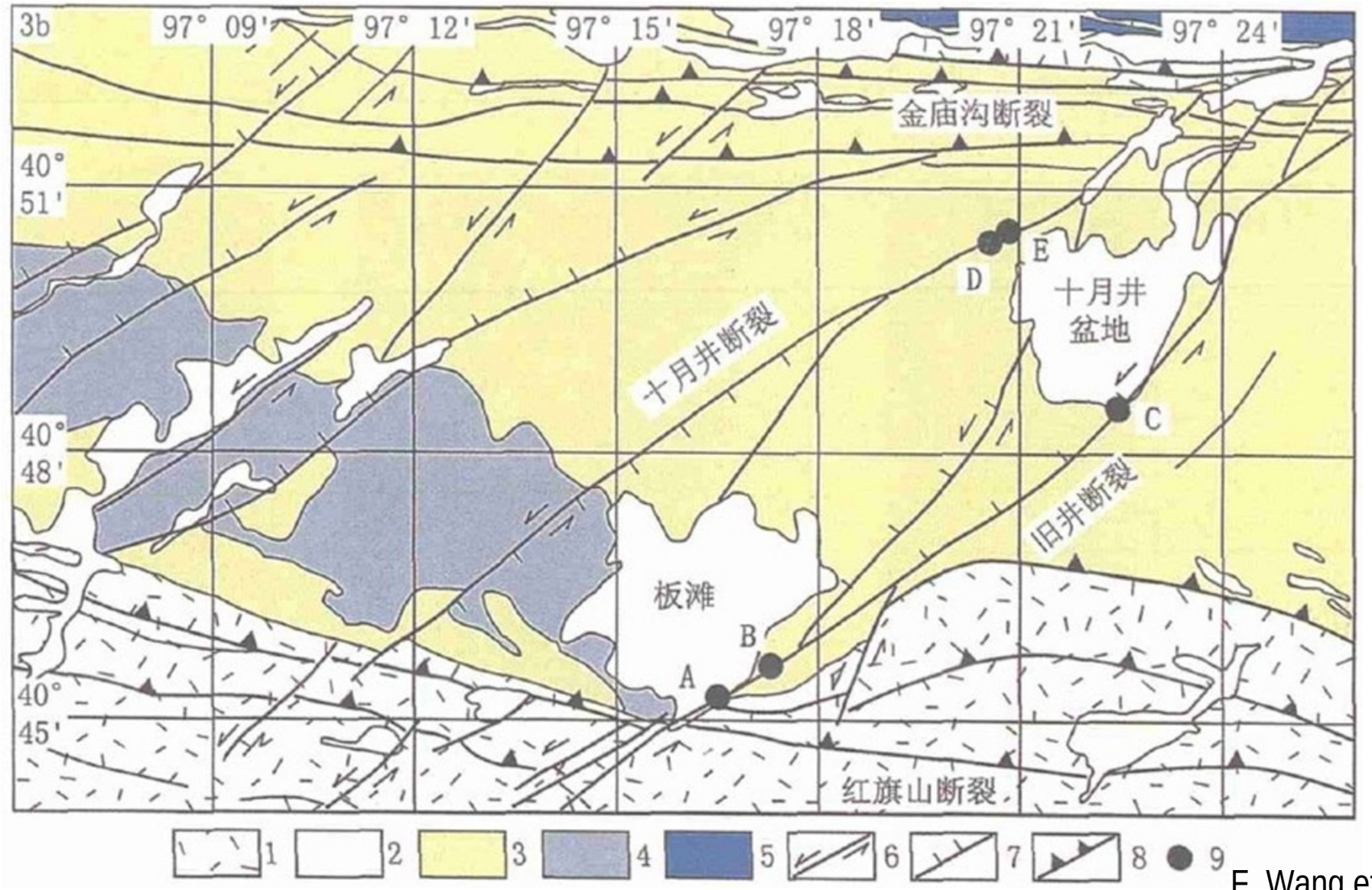

F. Wang et al, 2005

Identification of permeability of fault and fracture zones

- Internal composition and fracture architecture
- Opening and filling condition
- Stress regime

X.Z. Li, Keynote of 3rd National conf. Waste Disposal, 2010

Identification of permeability of fault and fracture zones

➢Internal composition and fracture architecture

Fault core: Both thickness and compositions of fault core are related to the length, amount slip of faults.

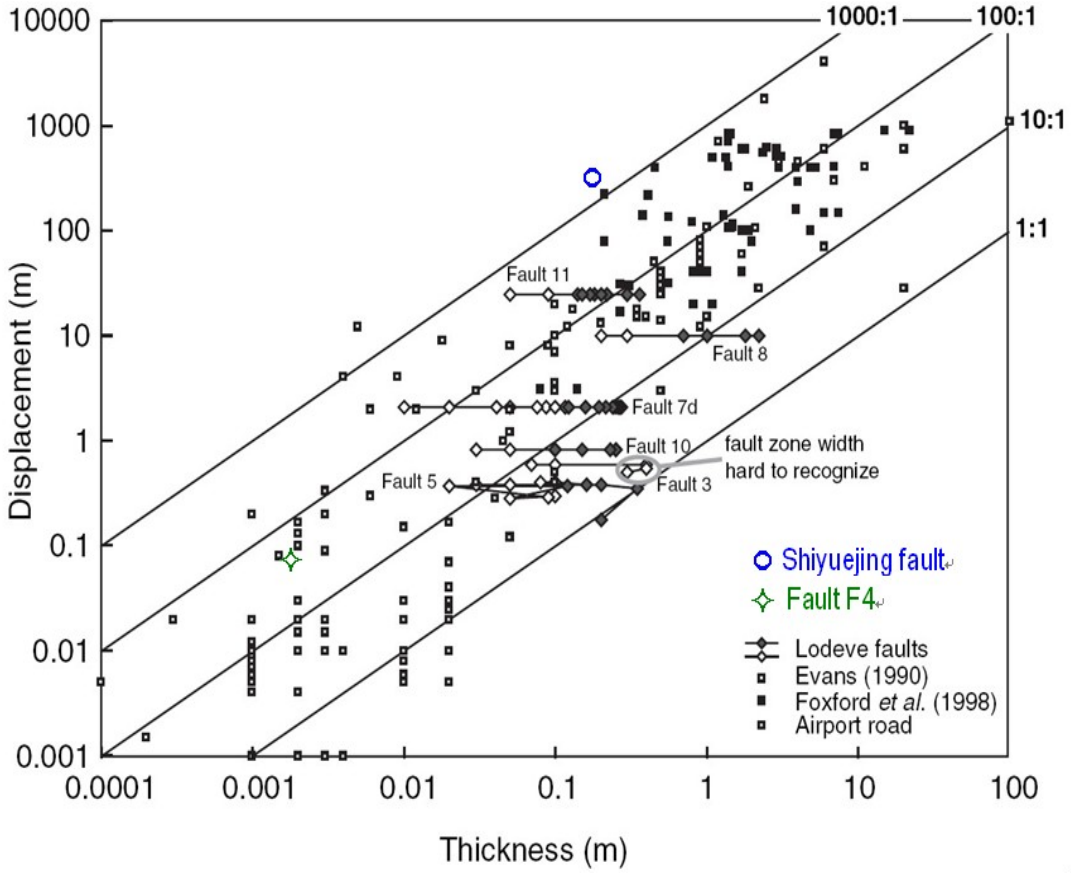

Identification of permeability of fault and fracture zones

➢Internal composition and fracture architecture

☐Shiyuejing Fault – *the main boundary of Jiujing Section*

- Left lateral tenso-slip fault
- Recent activity *(cutting relation; TL dating)*

→ A single permeable zone ?

→ Combined Conduit-Barrier (due to the clay fault gouge)

Ground water level in BS02 in the fault is 0.5m, while the level 100m away is 15.4 m, the ground water gradient reaches 15%. (by *Guo Y.H.*)

Identification of permeability of fault and fracture zones

- Internal composition and fracture architecture
  - Fracture zone near the *Shiyuejing Fault*

Dualistic model:

Fault *(Boundary)* + Stochastic joints *(inside)*?

Identification of permeability of fault and fracture zones

➢Internal composition and fracture architecture

✧Fault core of F4

The Jijicao domain boundary fault F4 belongs to the 2nd class in length. Its fault core comprises major slip surfaces, comminuted fault rocks and intensively fractured rocks. Most of the faulted rocks are made up of angular-to-subrounded survivor clasts embedded in fine grained matrix. The grayish white and brown-red bands within the comminuted fault rocks are sub-parallel to the major slip surfaces. According to the structures and compositions, five different structural domains are distinguished within the fault core.

Identification of permeability of fault and fracture zones

➢ Internal composition and fracture architecture

- The fracture patterns and densities in different fault architectural components have been identified and documented in detail.
- The intrinsic permeabilities of the fault architectural components in fault F4 were measured individually. Then permeability data can be assigned to each architectural component to simulate the detailed flow through fault zone, or to estimate the bulk hydraulic behaviour of the fault zone.

Identification of permeability of fault and fracture zones

➢Opening and sealing condition

The large fault *(regional fault):*

NE reversed fault

NW normal fault

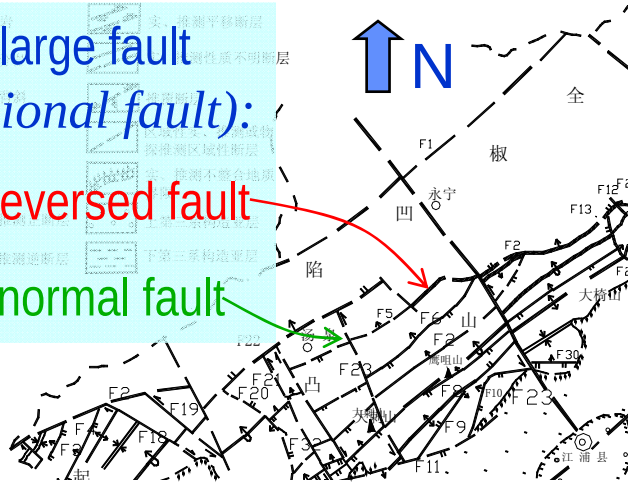

All the large faults, not only the NE-trending reversed faults, but also the NW normal faults are impermeable.

NW normal faults passed by the tunnel, impermeable

Identification of permeability of fault and fracture zones

➢Opening and sealing condition

Instead, the smaller NNW- and NWW-trending faults and fracture zones are permeable.

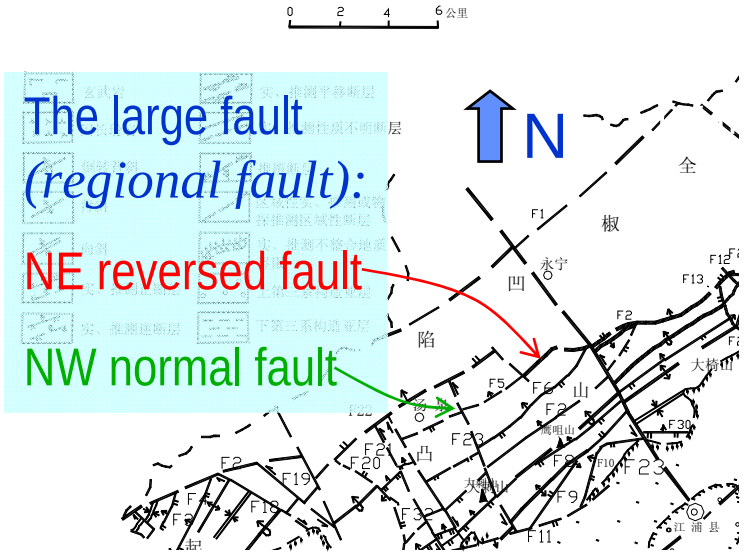

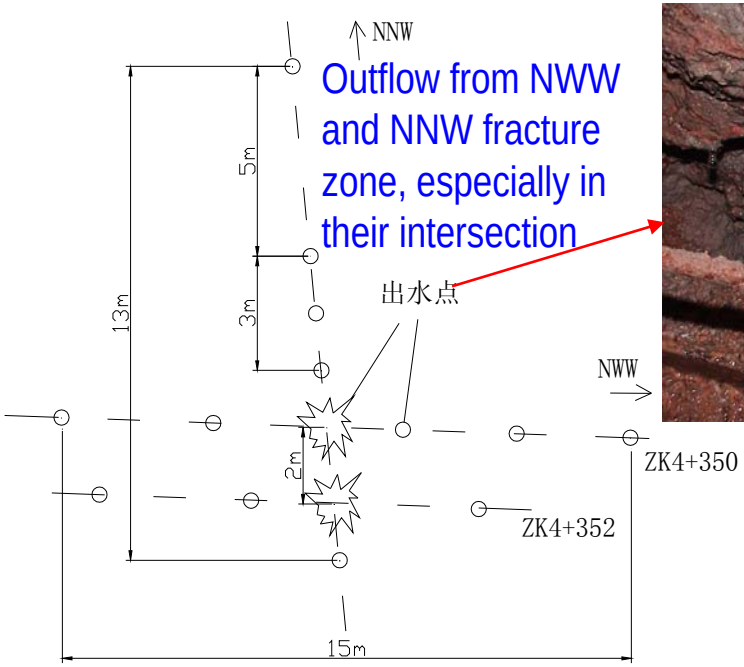

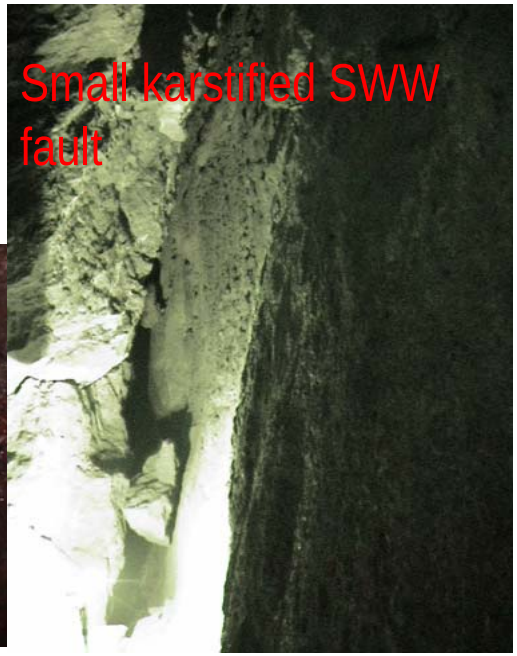

These faults and fracture zones are neotectonic structures. They are too young to be sealed.

X.Z. Li et al, China Communications press, 2006; ISGSR2007

Institute for Underground Space and Geoenvironment,
NANJING UNIVERSITY

Identification of permeability of fault and fracture zones

➢Opening and sealing condition

Determination of sealing condition is usually quite difficult. Analysis of structure evolution and identification of neotectonic structures may be helpful.

Identification of permeability of fault and fracture zones

- Stress regime - Compressive or extensional?

断层带，地层强烈挤压，不导水
Large fault, compressive, impermeable
(老山隧道)

裂隙带，张性构造应力环境，强导水带
Fracture zone, in extensional regime, high conductive corridor

Identification of permeability of fault and fracture zones

➢Stress regime - Compressive or extensional?

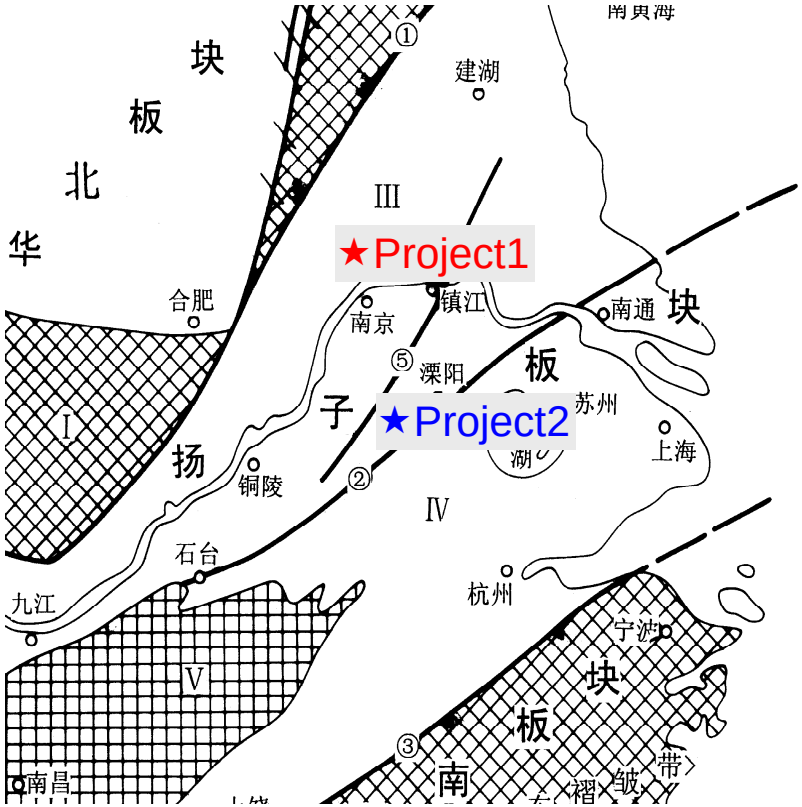

★Project1 - Laoshan highway tunnel

Inverted anticline with intensive compressive structural stress regime, inflow into tunnel is very few

★Project2 – A survey tunnel, pumped storage power station in Liyang

Maoshan - langxi thrust-nappe belt. After thrusting, the stress had been released. Inflow into tunnel like a heavy rain.

Identification of permeability of fault and fracture zones

➢ Stress regime-tectonic evolution

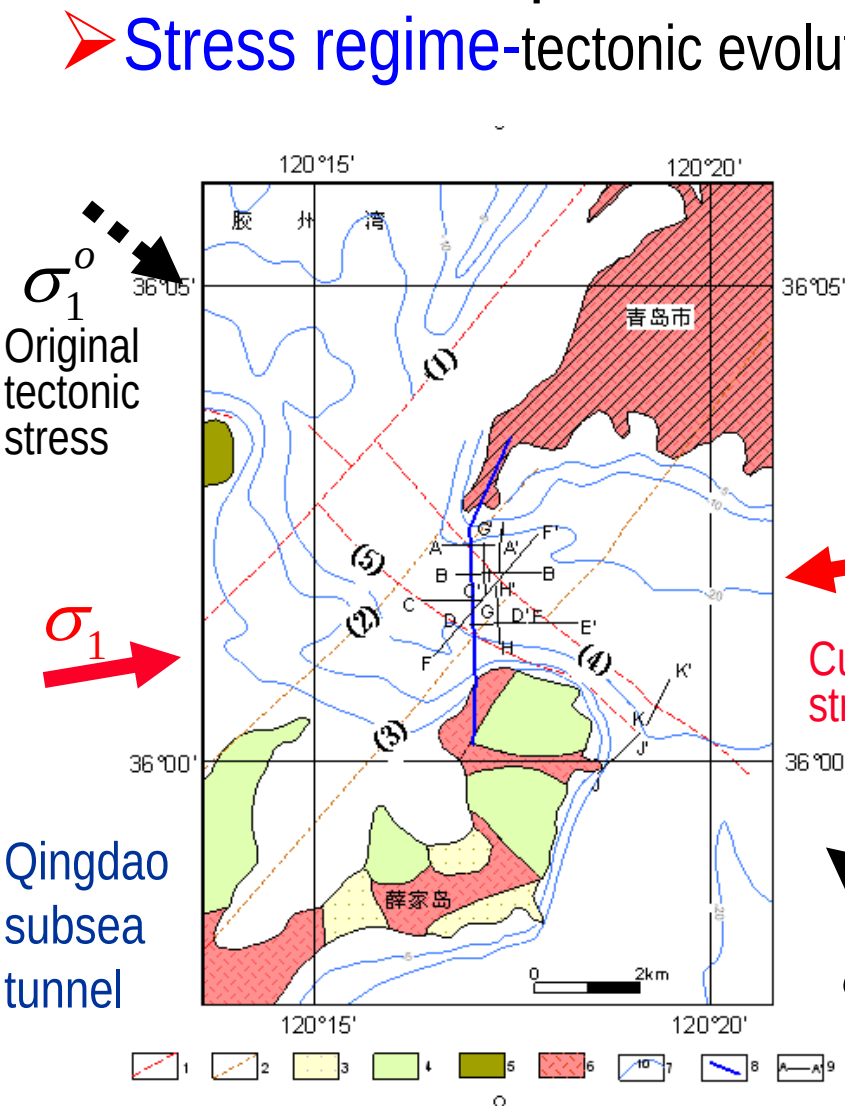

σ_1^o Original tectonic stress

σ_1

σ_1 Current stress

σ_1^o

Qingdao subsea tunnel

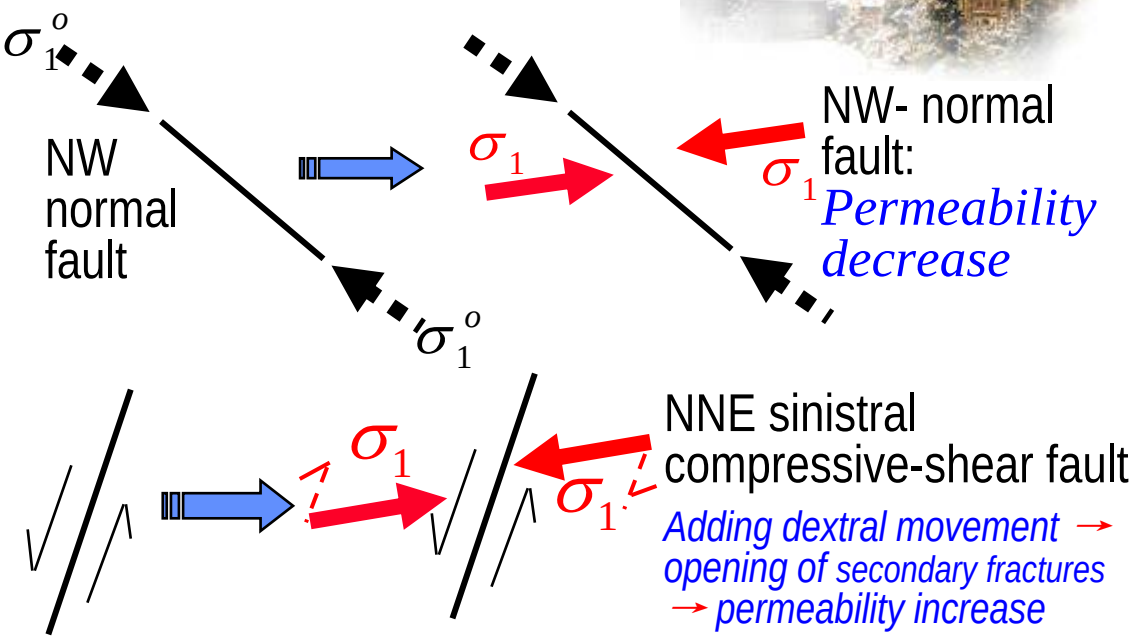

1.Conductive channel: NW fault-major fault plane; NNE fault – secondary fractures due to reverse movement

2. $K_{NW} > K_{NNE}$

MONITORING RESULTS:

1.160 l/min passed through NW fault; stable

2.40 l/min through NNE fault; unstable; Outflow varies greatly from different probing boreholes in a single working face.

Identification of permeability of fault and fracture zones

➢Stress regime

Stress regime has significant influence on the permeability of structural planes.

During tectonic evolution, especially reverse movement, the opening and permeability of fault plane and its secondary fractures will change.

Measurement, analysis method and non-uniform distribution of fracture trace

- Basic Assumption: the midpoints of trace lengths are randomly and uniformly distributed (*P.J. Pahl 1981; P. H. S. W. Kulatilake and T. H. Wu 1984;L. Zhang and H. H. Einstein 1998; M. Maul 1998; J.P. Chen 2001)*

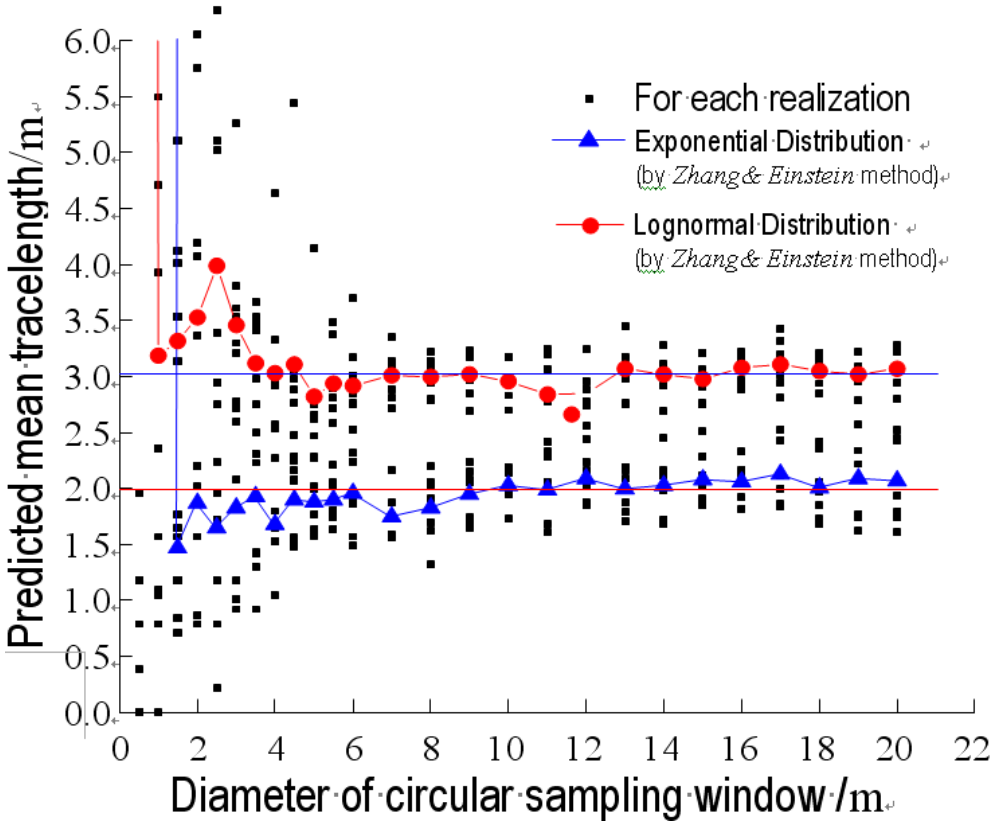

The bias in estimation of mean trace length decreases as the sampling range increases. When the range is large enough, the bias is very small.

Measurement, analysis method and non-uniform distribution of fracture trace

- The effect of non-uniformity of trace distribution on mean trace length estimation

At some locations, the bias increases, instead of decreases, when the sampling range reaches to some extent.

The non-uniformity of trace distribution may be a main reason.

→*To reduce bias in estimation, multiple windows at different locations, rather than one window, should be used.*

X.Z. Li et al. Chinese J. of Rock Mech. Eng. 2011,30(10).

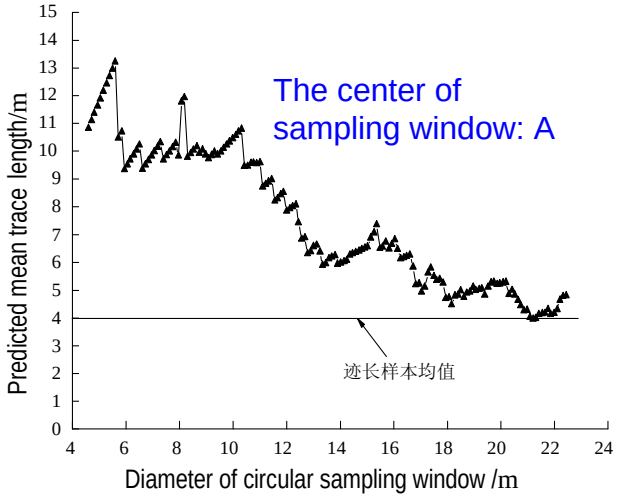

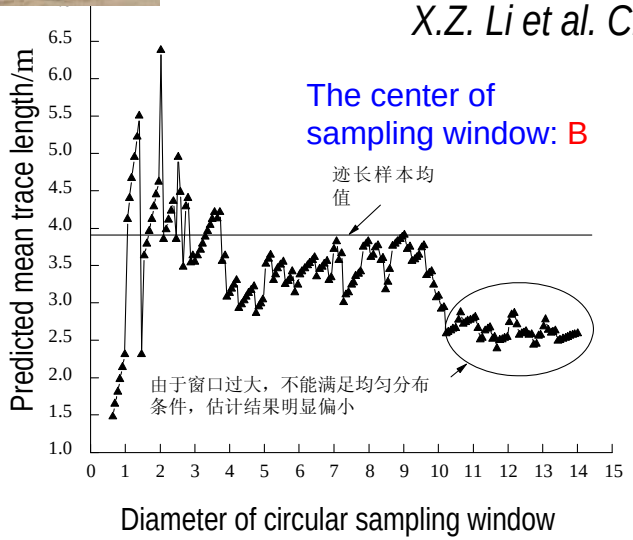

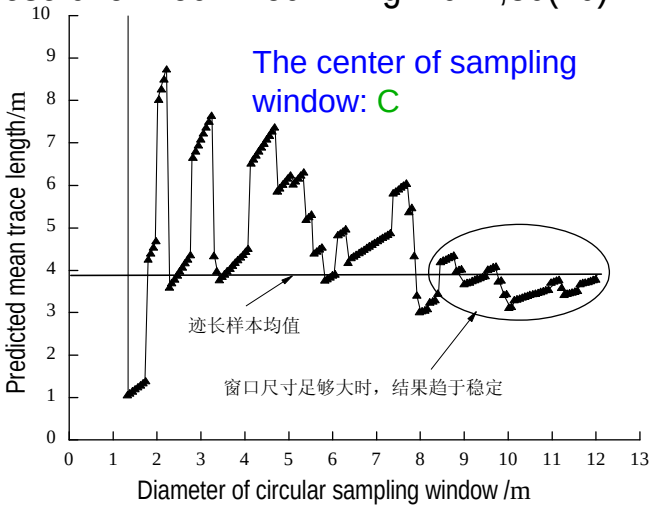

Measurement, analysis method and non-uniform distribution of fracture trace

- Basic Assumption: the midpoints of trace lengths are randomly and uniformly distributed (*P.J. Pahl 1981; P. H. S. W. Kulatilake and T. H. Wu 1984;L. Zhang and H. H. Einstein 1998; M. Maul 1998; J.P. Chen 2001)*

➢ The accurately measured distribution of fratures inside the Jijicao section

GIS-based analysis:

✧The Semivariogram & covariance of fracture area density present rhythmic variations.

✧The correlation distance in EW direction < that in NS direction.

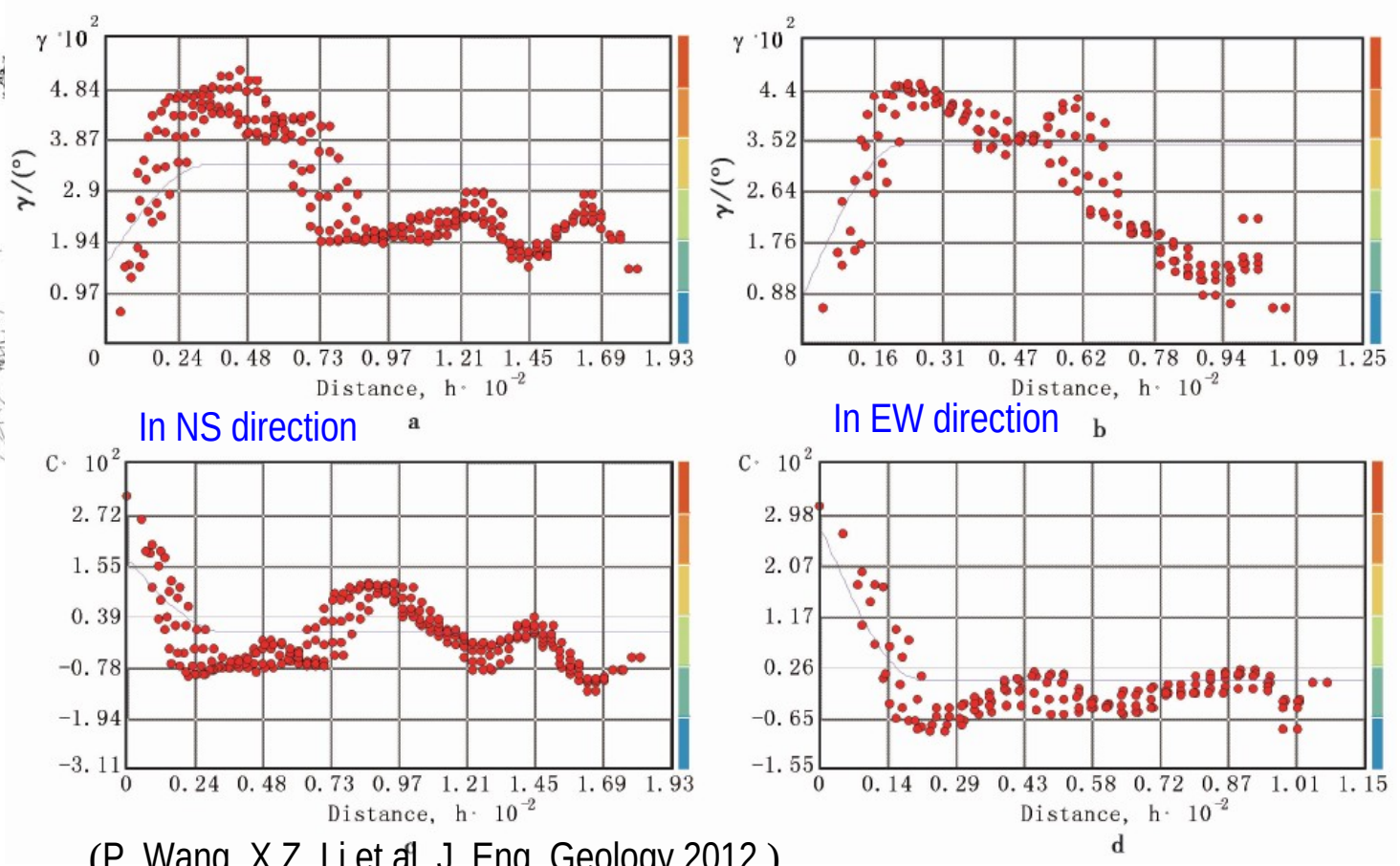

(P. Wang, X.Z. Li et al, J. Eng. Geology,2012.)

Measurement, analysis method and non-uniform distribution of fracture trace

- Structural patterns of fractures inside the sections
  - Parent-Daughter Structure

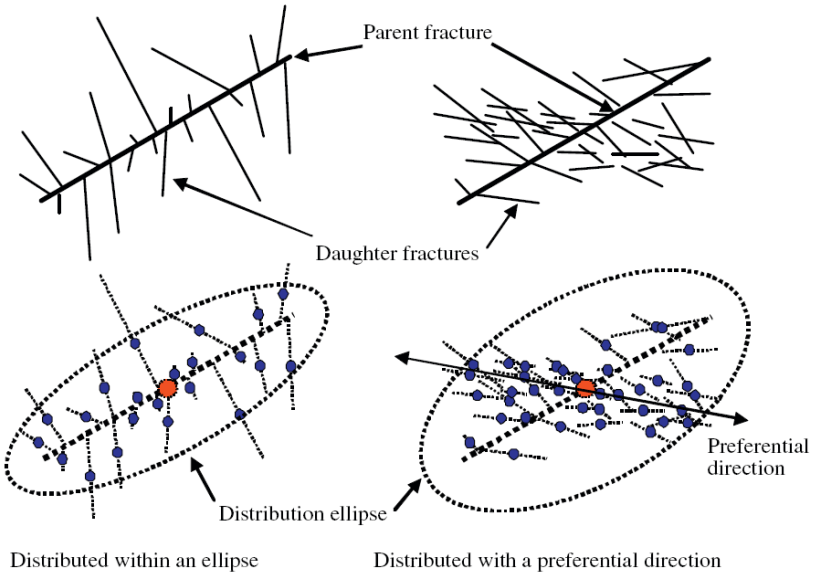

(C. Xu, P. Dowd 2010)

- Structural patterns: *even though the current simulated distributions show some preferential anisotropic directions, the structural pattern is distinct from real situation*

⇒ It is still a challenge.

- Hydrogeological significance: *although the secondary fractures are so many, the main conductive channel is the major plane.*

Measurement, analysis method and non-uniform distribution of fracture trace

- Structural patterns of fractures inside the sections
  - Conjugate shear joint sets of different periods in Beishan

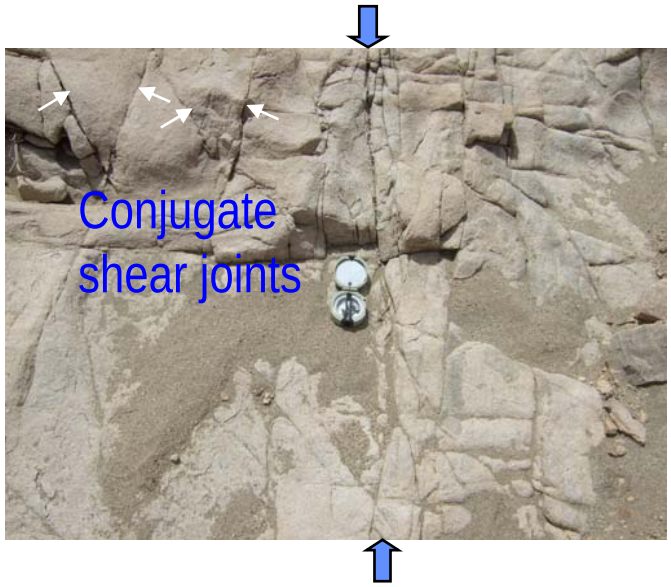

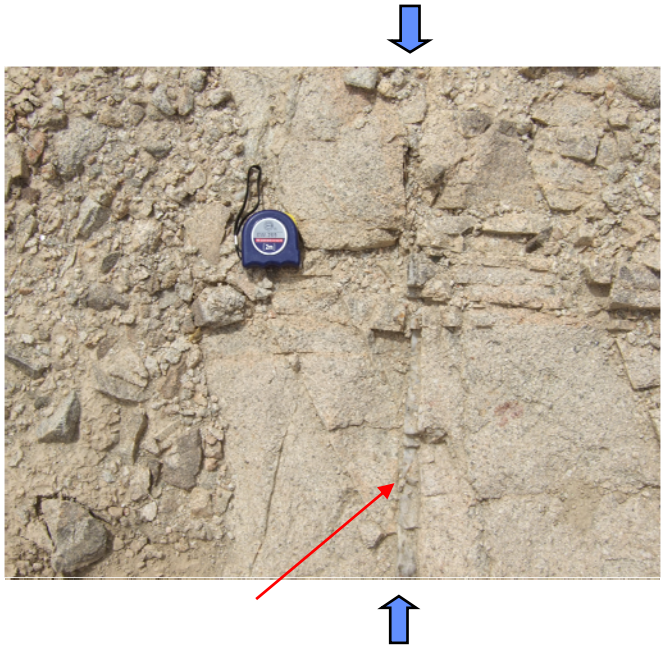

Measurement, analysis method and non-uniform distribution of fracture trace

➢Structural patterns of fractures inside the sections

❑Step Structure

–different permeability in different directions

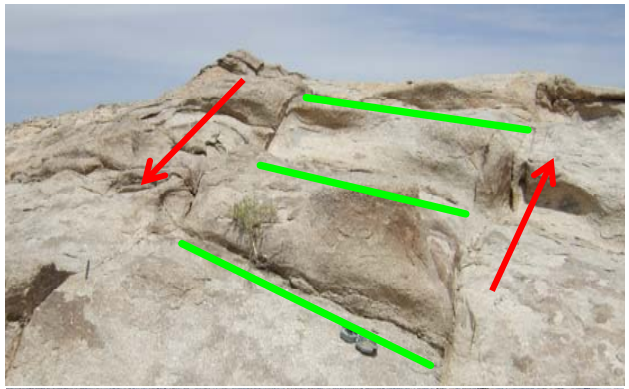

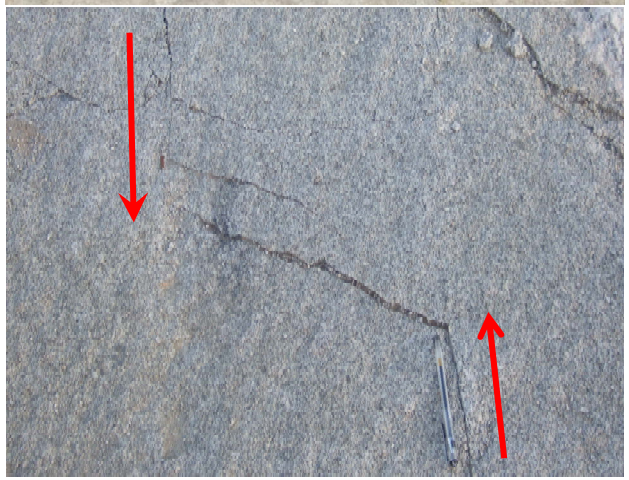

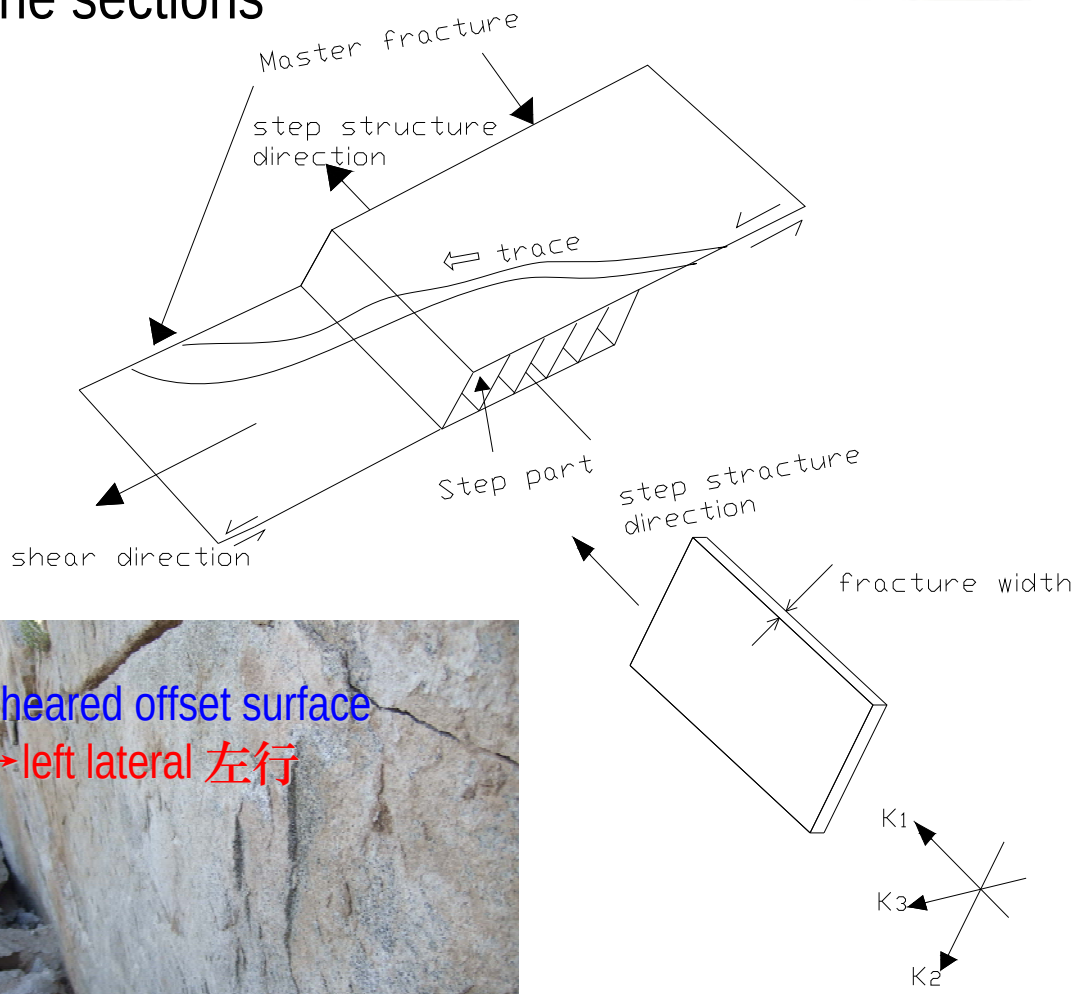

Measurement, analysis method and non-uniform distribution of fracture trace

- Structural patterns of fractures inside the sections
  - Shear fracture zone

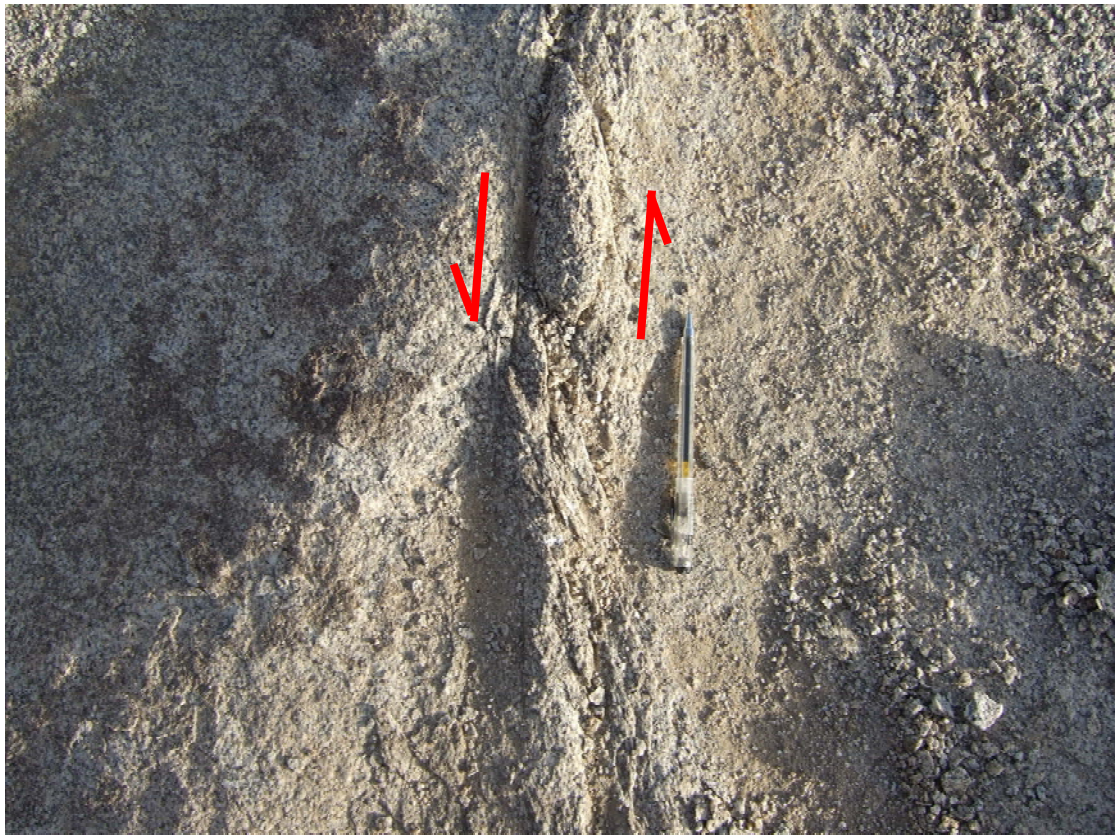

A dense tenso-shear fracture zone, formed when the major shear planes are close to each other. It forms an unified conductive channel again.

Stability-controlling modes and preferential structural plane

- Two types of stabilities and four grades of structural planes

Different grades of structural planes play different roles in stability, therefore, different evaluation methods should be taken.

Tectonic stability
- Grade I → earthquake → earthquake resistant evaluation
- Grade II → slip, creep → measures for tectonic deformation

Eng. stability
- Grade III → deformation boundary → Geo. Model for stability analysis
- Grade IV → weaken rocks → rockmass quality rating

The activity time of some faults maybe relatively new, but because of it's limited scale, don't worry too much about the induced earthquake. But it's tectonic deformation merits attention when tunnel has to pass through them.

Some structural planes may act as the deformation boundary, or controlling the failure mode, they shouldn't be dealt simply in rockmass quality evaluation.

X.Z. Li, Keynote of 3rd National conf. Waste Disposal, 2010

Stability-controlling modes and preferential structural plane

- Geometrical combination and Preferential Structural Plane

Just small joints oblique to tunnel surface – Heavily damage

Small joints oblique to the working face- rugged surface

Small joints parallel to the working face

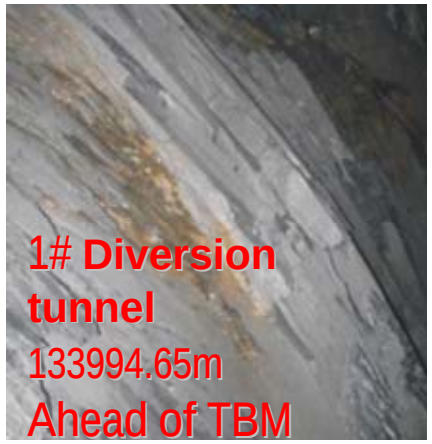

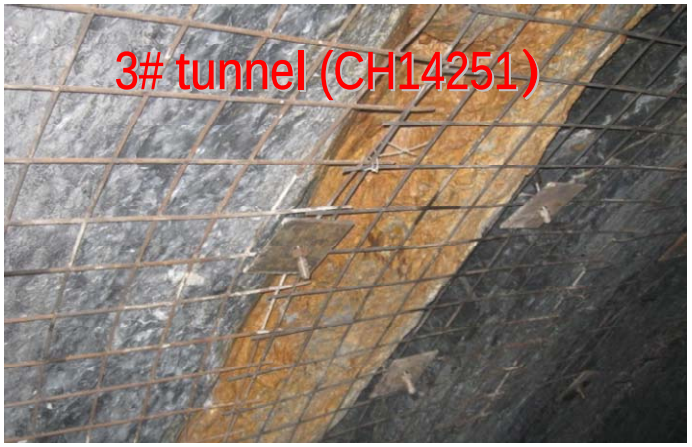

Even a fault, no obvious influence

Taken from Jinping Hydropower Station

Stability-controlling modes and preferential structural plane

- Geometrical combination and Preferential Structural Plane

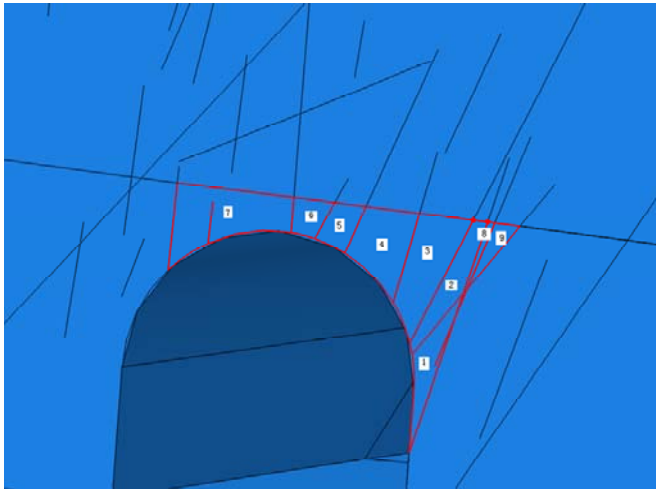

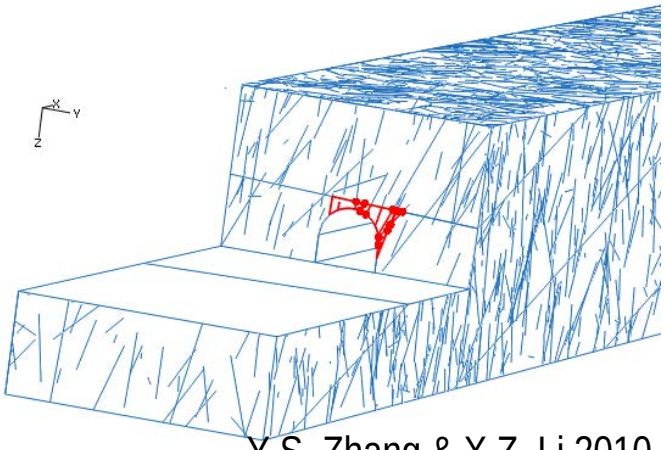

Y.S. Zhang & X.Z. Li 2010

A heavy accident in Sep, 2009:

3 deaths, 7 injuries

Due to the falling of a block formed by several steep and one gentle structural plane

Stability-controlling modes and preferential structural plane

- Geometrical combination and Preferential Structural Plane

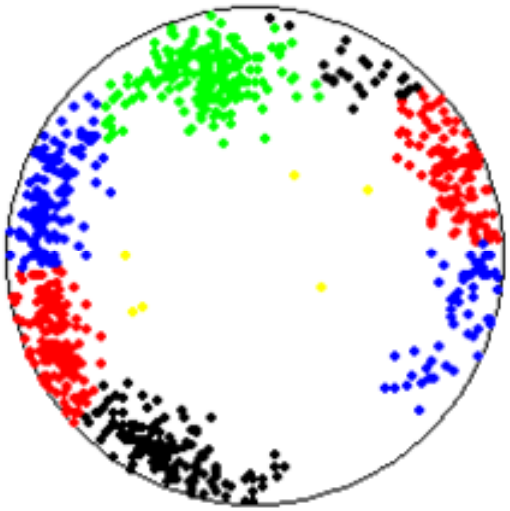

Outcrops around BS03

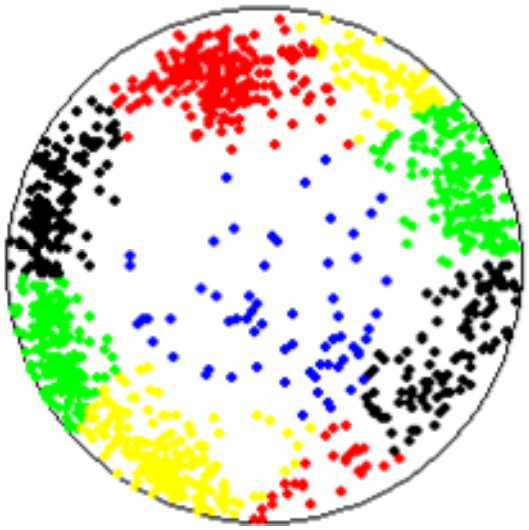

Outcrops around BS03
+ BS03 boreholes

Stability-controlling modes and preferential structural plane

- Geometrical combination and Preferential Structural Plane

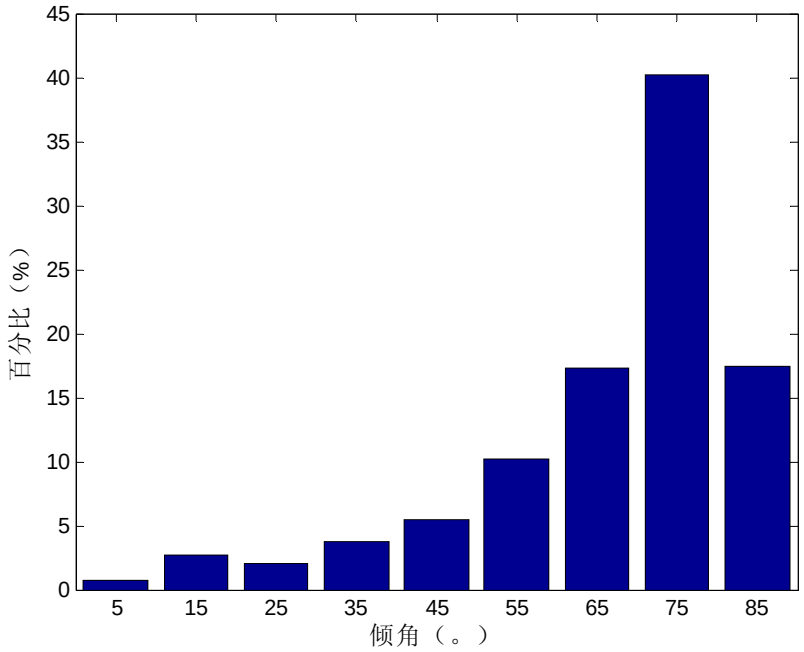

Frequency of fracture in different dip angles in BS03

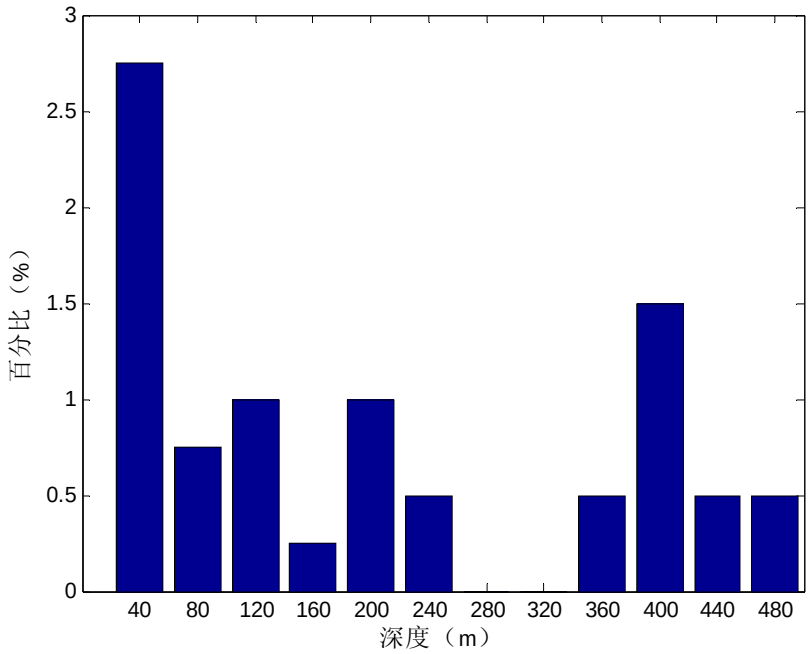

Frequency of gentle structural planes in different depth

Stability-controlling modes and preferential structural plane

- Geometrical combination and Preferential Structural Plane

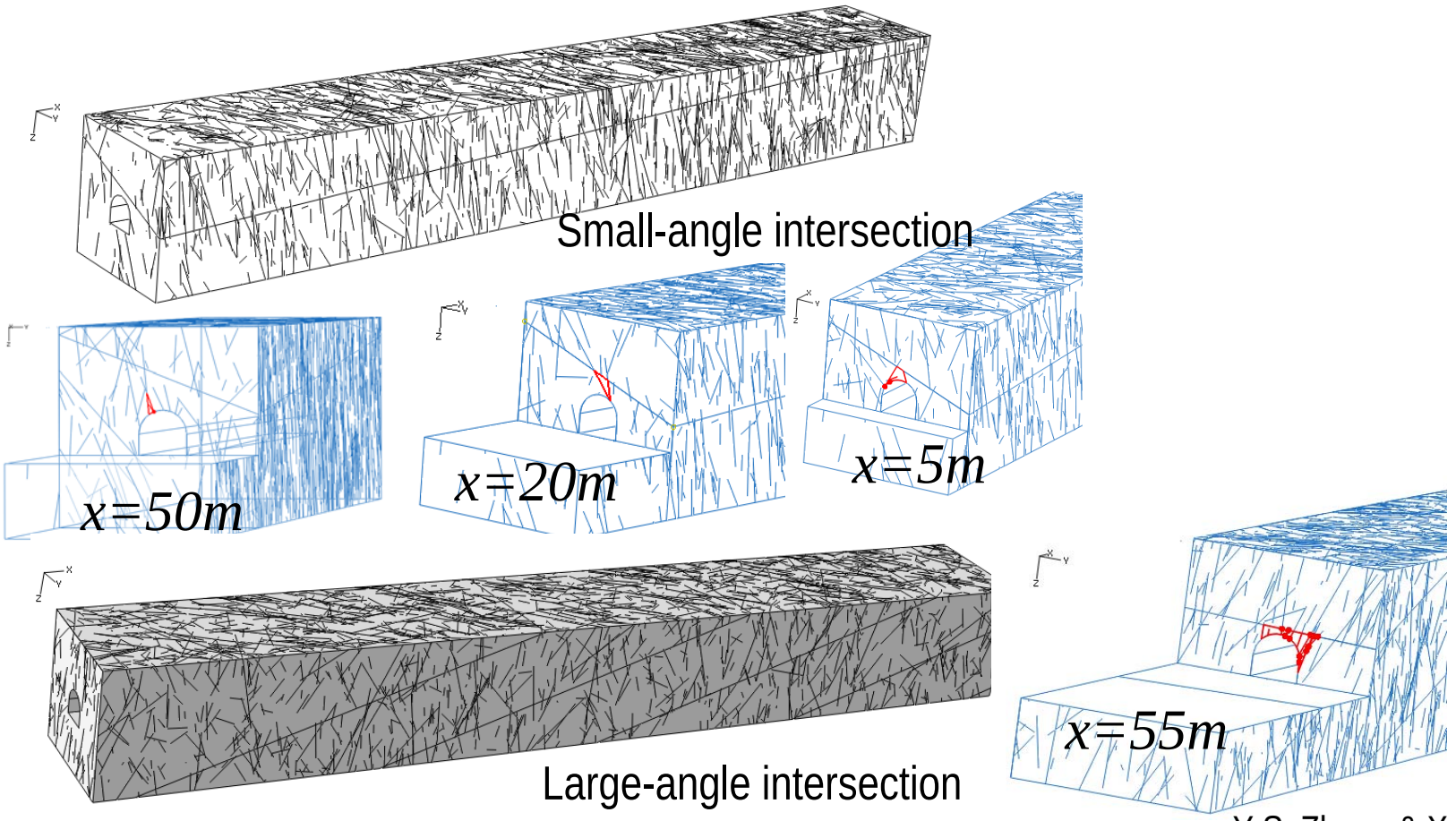

Y.S. Zhang & X.Z. Li 2010

Simulation analysis on permeability parameters and flow path

- *Back analysis of fracture transmissivity and fractured rockmass permeability*

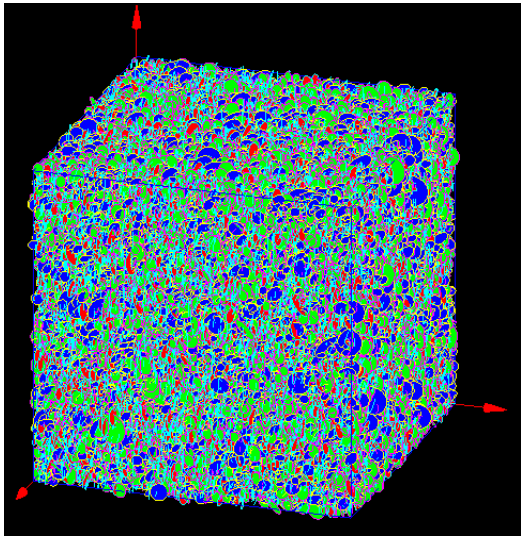

Stochastic fracture network model created on the basis of statistics of over 800 fractures around borehole BS03

+

Deterministic fractures passed by borehole observed by BT (Borehole Televiewer)

Injection water pressure P

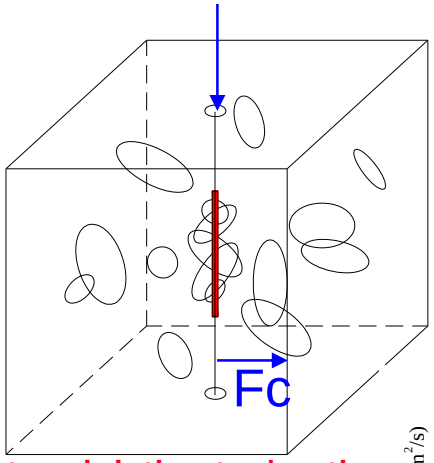

Deterministic-stochastic model

Deterministic fracture observed by BT placed in the stochastic fracture network

Giving initial transimissivity T_0, calculate the injection flow F_c

compared with observed flow in Paker Test-F_p: $F_c = F_p$?

no $T=T_1$

yes stop

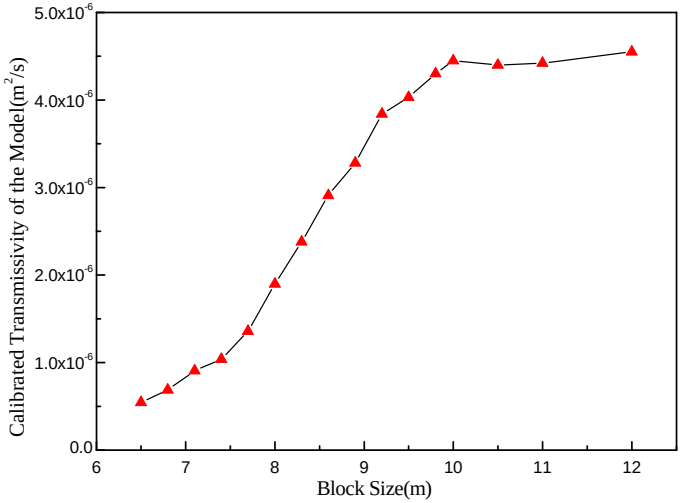

Back analysis (Wang M 2000)

Simulation analysis on permeability parameters and flow path

- *Back analysis of fracture transmissivity and fractured rockmass permeability*

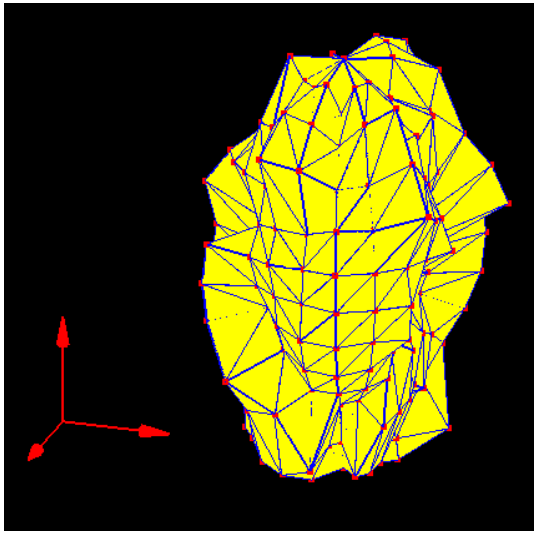

341 /21

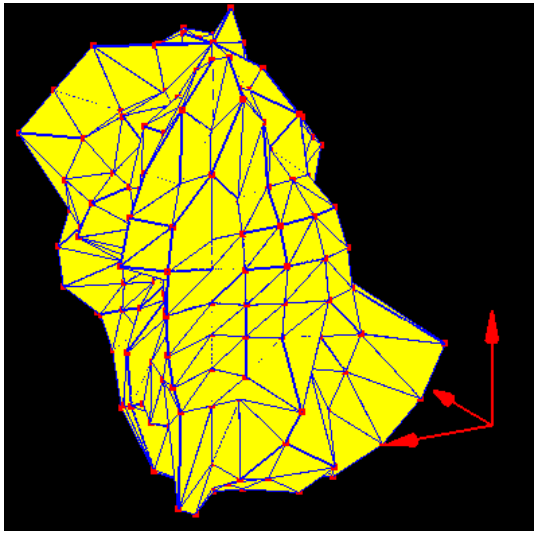

209 /19

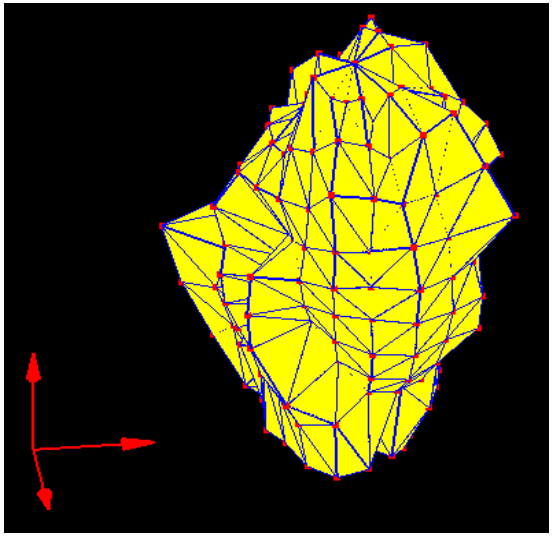

7 /31

空间方向渗透系数变化

Simulation analysis on permeability parameters and flow path

- *Back analysis of fracture transmissivity and fractured rockmass permeability*

Variation of hydraulic conductivity on vertical planes in different directions

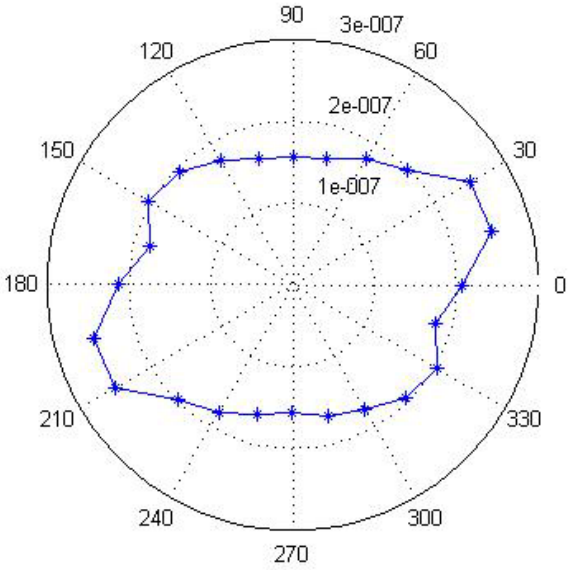

S-N

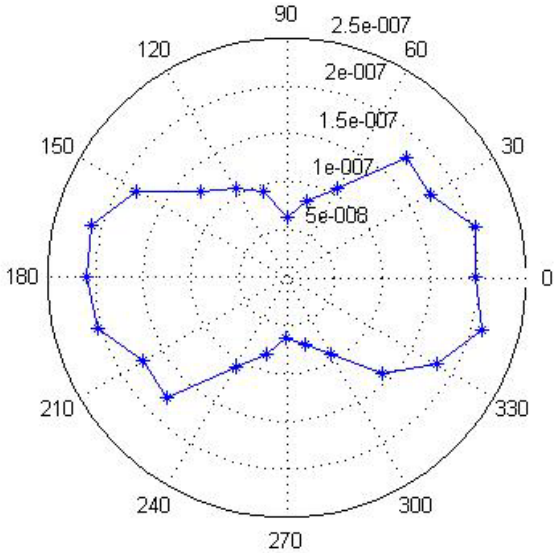

W-E

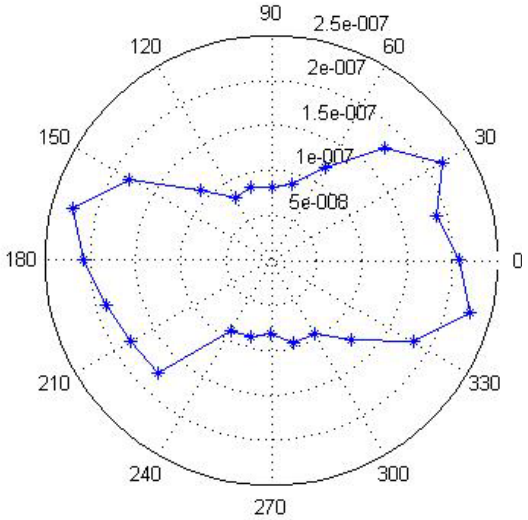

N45 E

Strike map

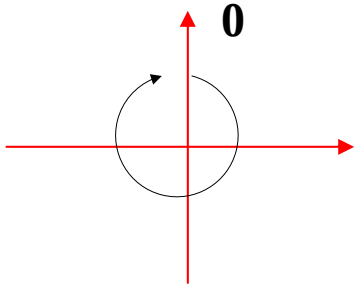

	渗透主值($\times 10^{-7}$)（m/s）	走向(°)	与水平面夹角(°)
K_1	2.08	110.3	80.0
K_2	1.71	349.6	5.1
K_3	0.47	258.9	8.6

Simulation analysis on permeability parameters and flow path

- *Back analysis of fracture transmissivity and fractured rockmass permeability*

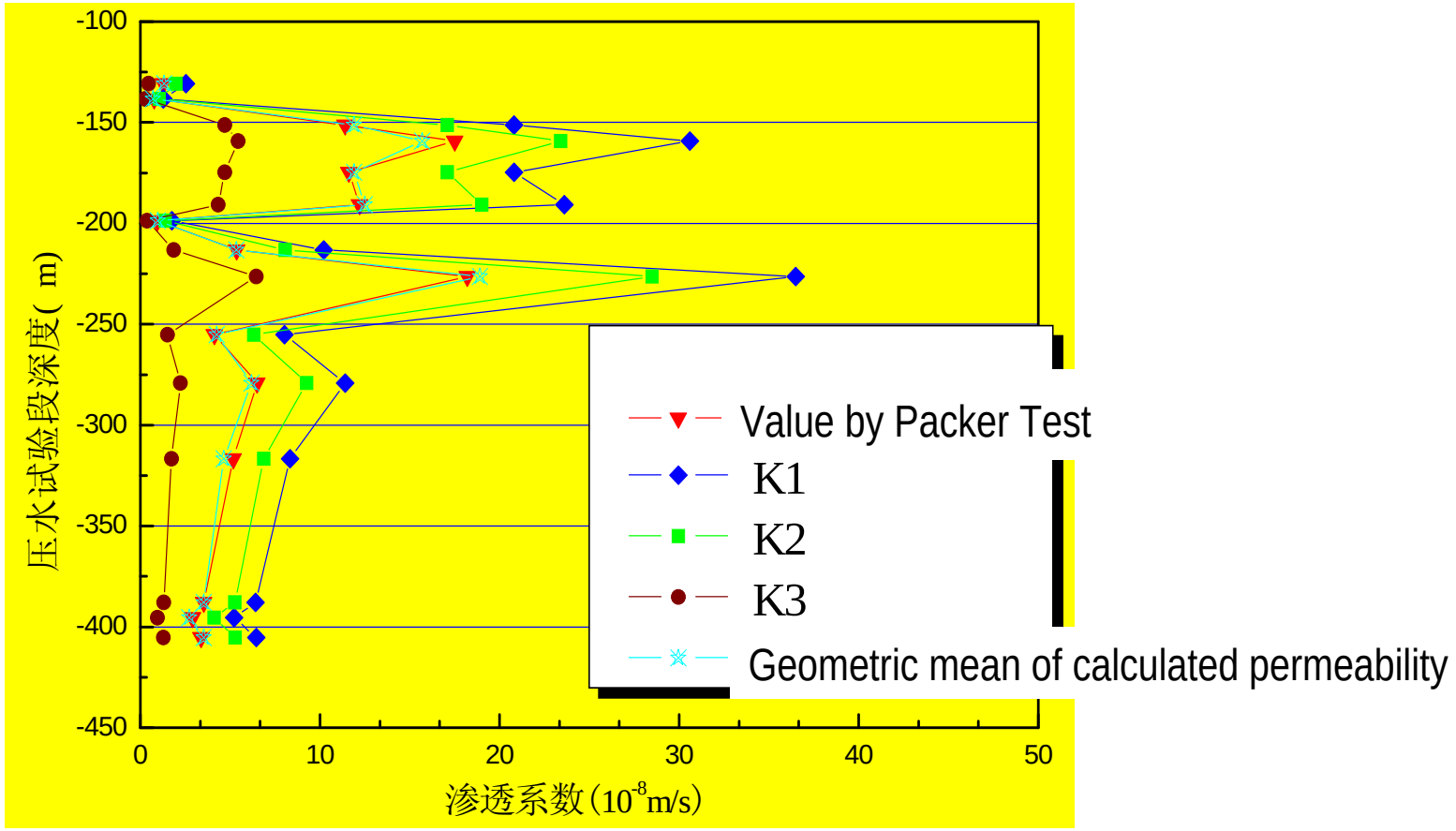

(X.Z. Li & C.L. Ji, Proc. *ICADD9 -Singapore* 2009; J. Eng. Geology,2010,18(2).)

Simulation analysis on permeability parameters and flow path

Simulation on flow path of fracture system

✧OUTCROP3826

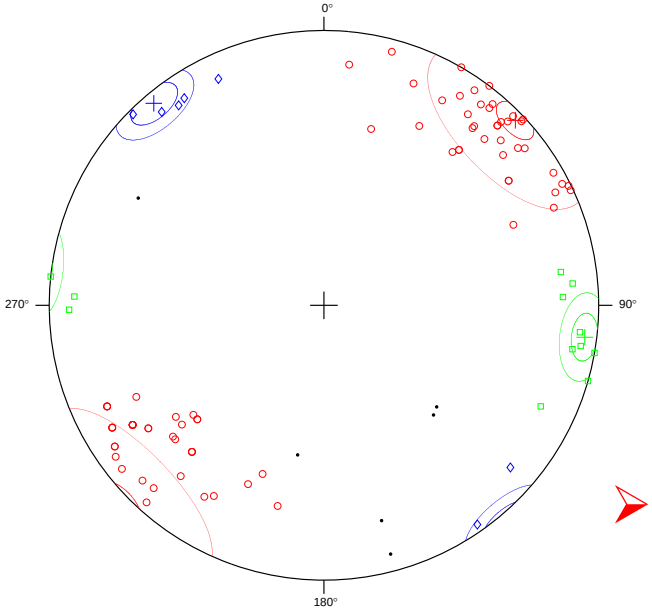

	α	ϕ	R%	k	ω	δ	Anzahl
○	226	86	85.7	13.8	22	5.1	93
□	277	85	97.2	67.3	9.7	5.2	19
◇	140	86	97	61.5	10	6	16

➢Identification of significant orientation sets

X.Z. Li & Q. Liu 2008

Simulation analysis on permeability parameters and flow path

Simulation on flow path of fracture system

➢ Trace length statistics in each set

-significant exponential-distribution

✧ OUTCROP3826

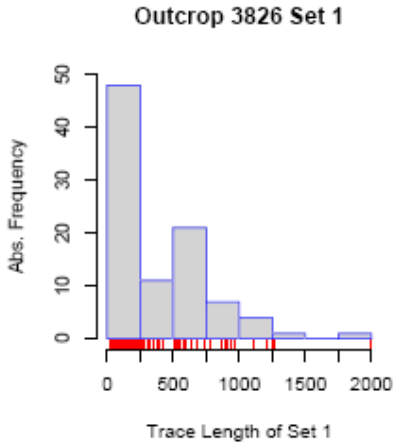

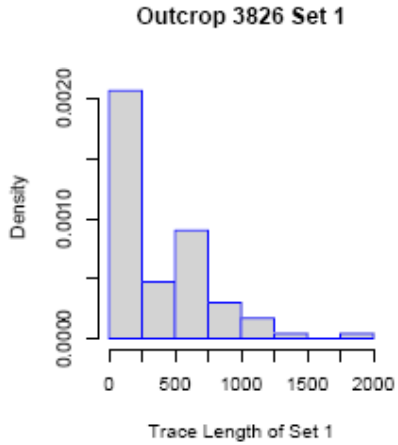

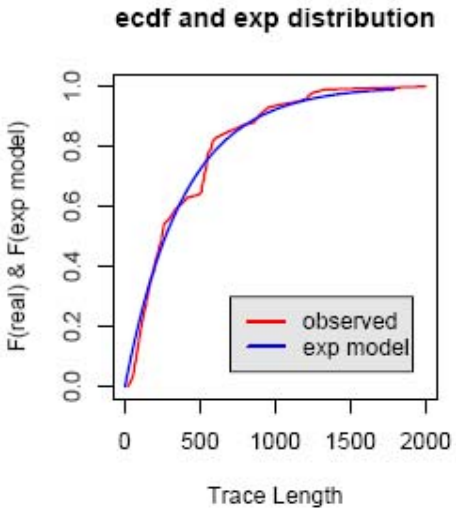

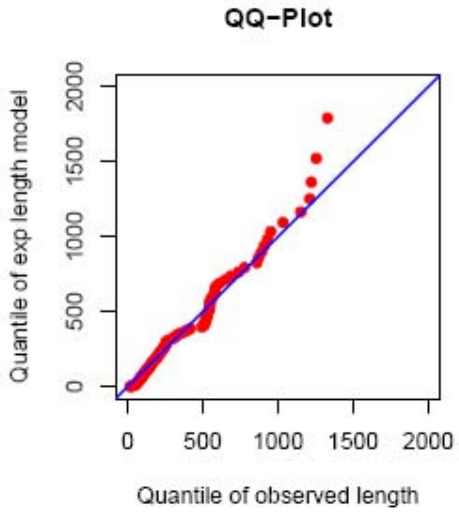

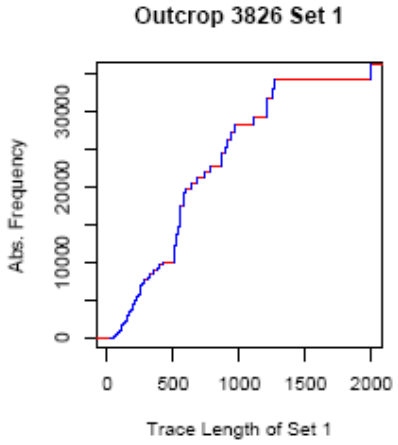

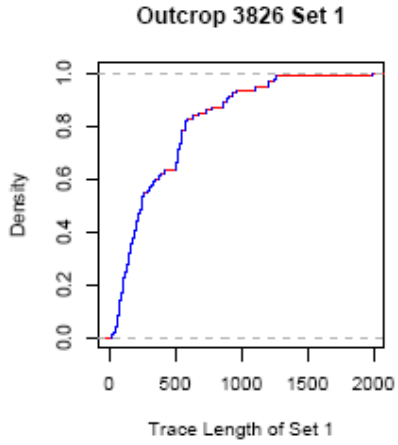

X.Z. Li & Q. Liu 2008

Simulation analysis on permeability parameters and flow path

- *Simulation on flow path of fracture system*

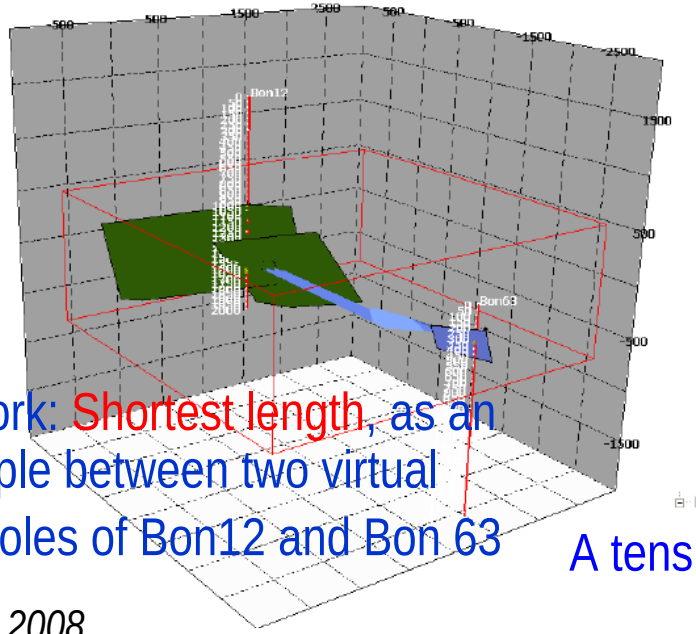

Network: Shortest length, as an example between two virtual boreholes of Bon12 and Bon 63

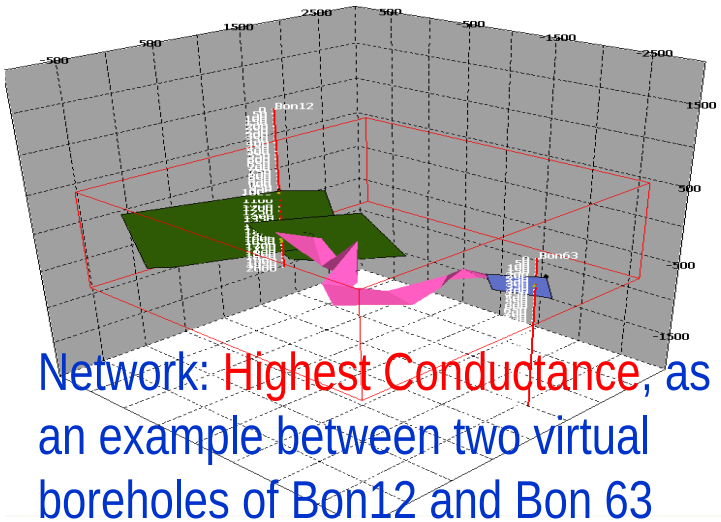

Network: Highest Conductance, as an example between two virtual boreholes of Bon12 and Bon 63

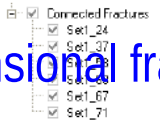

A tensional fracture with comparatively strong weathering

X.Z. Li & Q. Liu 2008

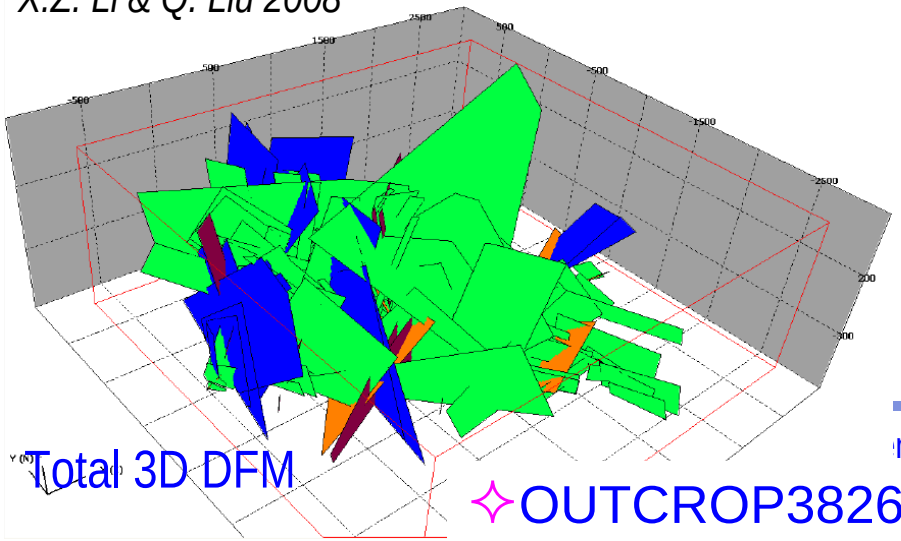

Total 3D DFM

✧OUTCROP3826

Conclusions

- In order to build up fracture system model and identify flow pathways, a good understanding of their deformation and kinematic relations is crucial. From field observation and structural analysis, we find that the low angle fractures are more developed, while the high angle fractures are just initial development stage in the study area. The developments of different type of fractures depend on stress and kinematic boundary conditions.
- The internal composition and fracture architecture, their opening and sealing condition and stress regime are three crucial factors affecting the permeability of fault zones.
- Both thickness and compositions of fault core are related to the length, amount slip of faults. The fracture patterns and densities in different fault architectural components should be identified and documented in detail.
- An understanding of tectonic evolution is helpful for the characterization of these factors. The identification of the main active periods maybe helpful for analysis of the opening and filling condition. During tectonic evolution, especially reverse movement, the opening and permeability of fault plane and its secondary plane will change.
- The GPS and GIS technique are very helpful for the measurement and analysis of fracture distribution. The non-uniformity of locations is one of the main reasons for the bias in estimation of fracture intersection situation and mean trace length. Even though the current simulated distributions show some preferential anisotropic directions, the structural pattern is distinct from real situation.

Conclusions

- Different grades of structural planes play different roles in stability, therefore, different evaluation methods should be taken.
- Due to the geometrical combination of structural planes and tunnel, there maybe preferential structural plane which controls the failure modes and probability of intersecting tunnel and forming blocks.
- Deterministic-stochastic model combining with packer test and back analysis can be used for estimation of transimissivity of fracture and spatial variation of fractured rockmass.
- On the basis of 3D fracture network simulation, the flow path with shortest length or highest conductance can be searched out. But, how to comprehensively consider the geometrical connection and the preference of geological properties in a model needs to be further studied.

Acknowledgements

The work is supported by *National Key Basic Research Program of China (973 Program)*, *National Natural Science Foundation of China* (NSFC) and *Key projects of National Foundation for Disposal of Radioactive Waste*. The field work is supported by the *Beijing Research Institute of Uranium Geology*.

Thanks a lot for your attention!

German experience and investigations in the characterisation of potential host rocks

SHAO, H. & SÖNNKE, J.

Federal Institute for Geosciences and Natural Resources (BGR)
Stilleweg 2, D-30655 Hanover, Germany

Introduction

1. Objectives of international cooperations
2. Objectives of projects in claystone
3. Examples of German projects in argillaceous rocks
4. Examples of main tasks in different host rocks
5. Results of some investigations in crystalline rocks
6. Outlook

BGR ACTIVITIES IN RADIOACTIVE WASTE DISPOSAL

- Research since more than 25 years
- Site specific investigations

Gorleben, Morsleben, Konrad

- Research and development

Host rocks,

geotechnical barriers,
scenario analyses

- International co-operation

International URLs,

bilateral agreements

Site Selection

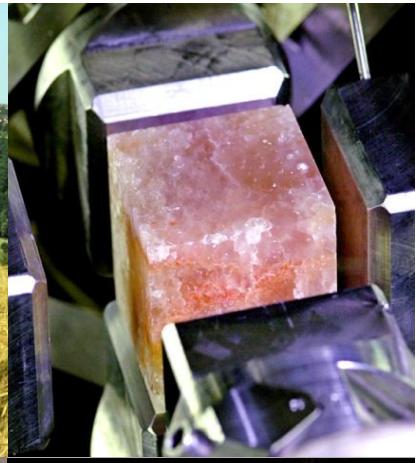

Research

Site Exploration

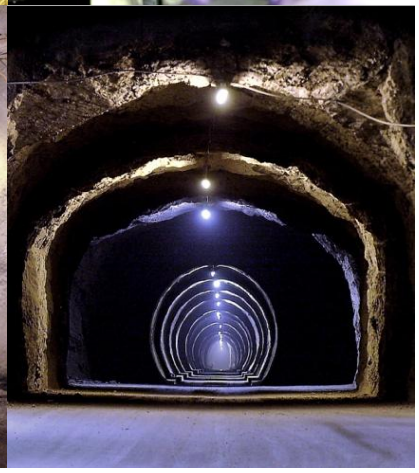

Long-Term Safety

BGR Research Programs in URL's

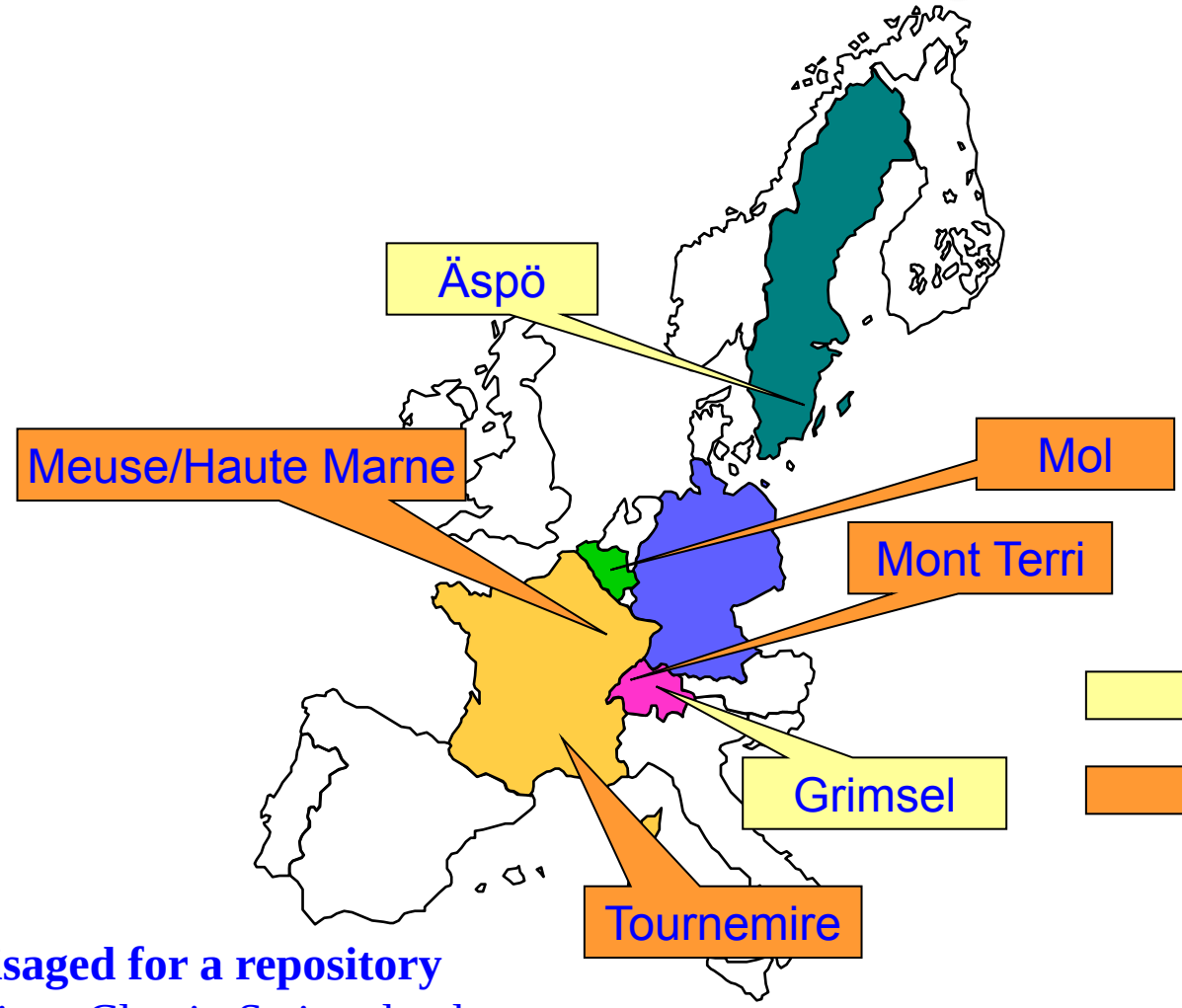

Crystalline rocks

Argillaceous rocks

Envisaged for a repository

- Opalinus Clay in Switzerland
- Callovo-Oxfordian in France
- Boom Clay in Belgium

Site characterisation

International Cooperation

Objectives:

- Information exchange on storage facilities
- Selection and characterisation methodologies for disposal sites
- Information exchange on disposal concepts
- Safety assessment of disposal facilities during the operating and post-closure phases
- Participation in experimental programmes carried out in underground laboratories or facilities
- Participation in demonstration programmes
- Characterisation of the behaviour of waste under repository conditions

Argillaceous rocks as host rock for the disposal of radioactive waste

BGR-Projects

- Konrad-Mine (D)
  - Characterisation of argillaceous rock formations in the overburden of a repository

R & D

- Tournemire (F)
- Grimsel (CH), Äspö (S)
- Mont Terri (CH)
- Bure (Meuse, Haute-Marne) (F)

Objectives of R&D in argillaceous rock formations

- Properties and effectiveness of bentonite in geotechnical barriers
- Development and tests of methods for the characterisation of argillaceous rock formations

Studies for argillaceous rock formations in Germany

- Site selection criteria
- Site characterisation
- Longterm safety analysis (incl. scenarios and FEPs) for a repository in argillaceous rocks

Project: AnSichT

Argillaceous rock formations in Germany

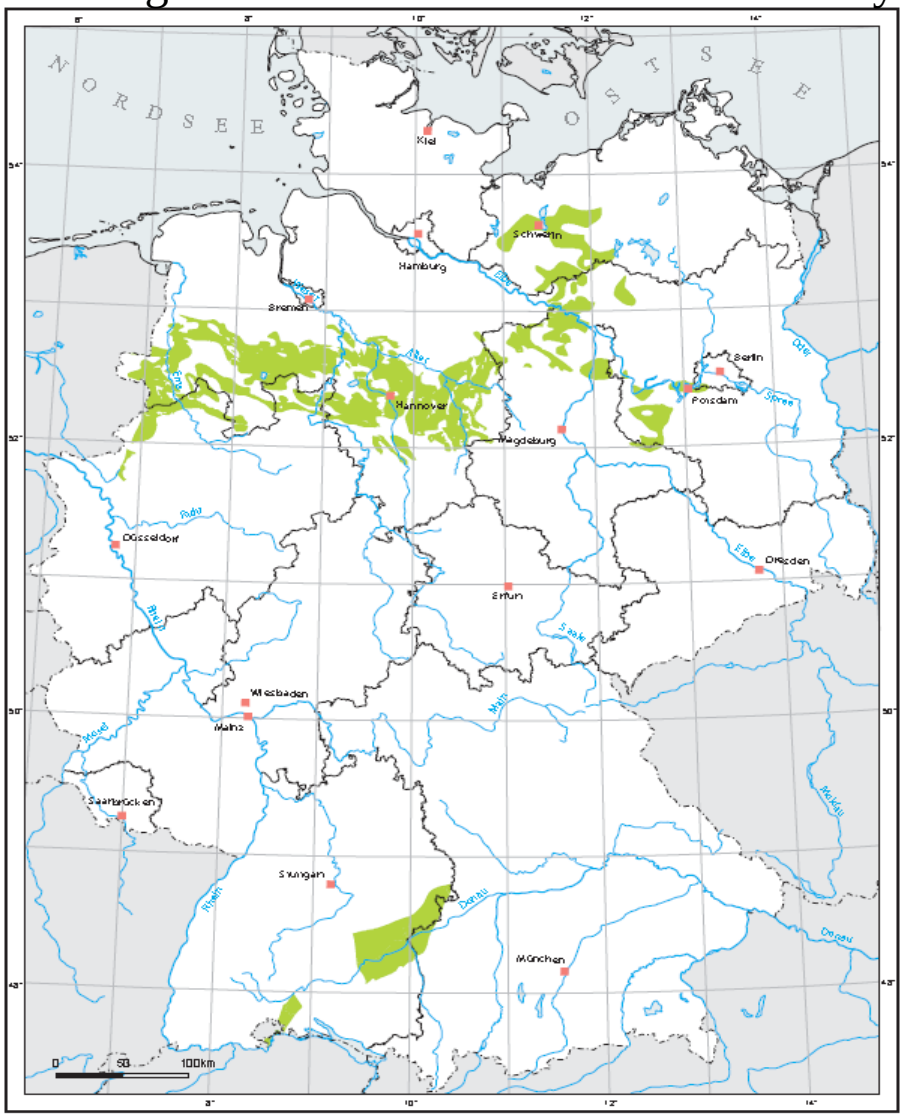

Claystone formations in Germany potentially suitable for further investigations

Stratigraphic position

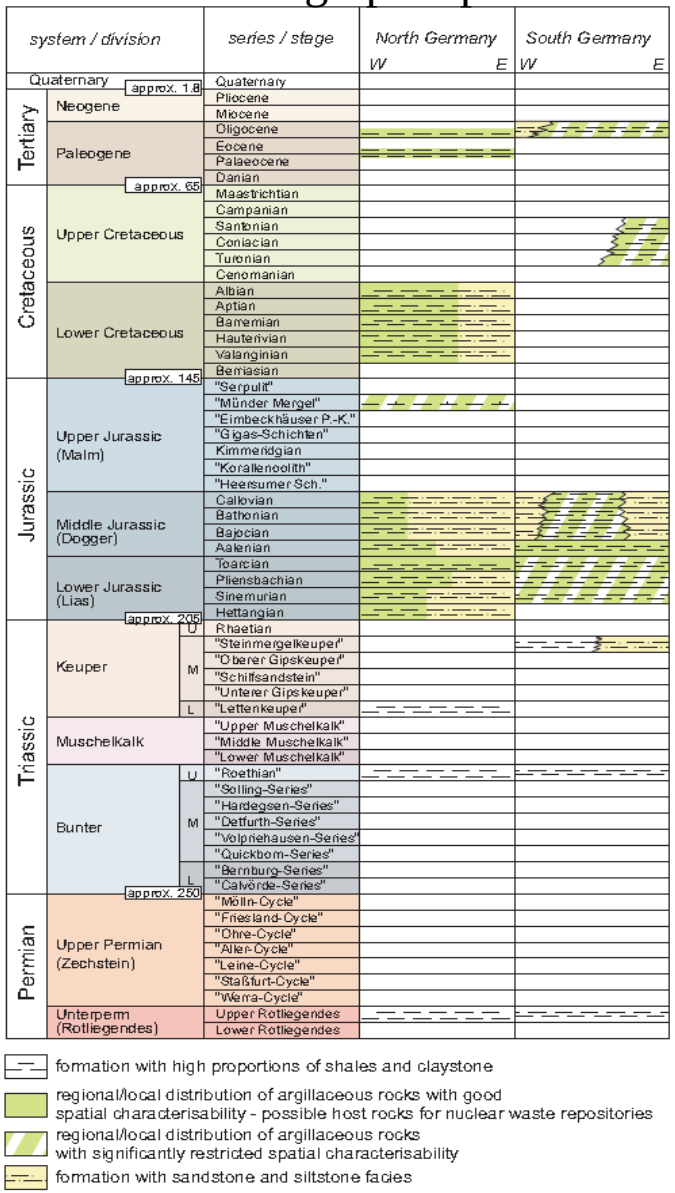

formation with high proportions of shales and claystone

regional/local distribution of argillaceous rocks with good spatial characterisability - possible host rocks for nuclear waste repositories

regional/local distribution of argillaceous rocks with significantly restricted spatial characterisability

formation with sandstone and siltstone facies

BGR Bundesanstalt für Geowissenschaften und Rohstoffe

Project: AnSichT

Methodik und **An**wendungsbezug eines **Sich**erheitsnachweiskonzeptes für ein HAW-Endlager im **T**onstein

„AnSichT“

Methodology and application of a safety case concept for a HAW-repository in argillaceous rock formations

Project: AnSichT

Objectives:

- Evaluation of the instruments for safety assessment of HAW repositories in argillaceous rock formations in Germany (North and South-Germany)
- Development of methods for the proof of the integrity of technical, geotechnical and geological barriers
- Conceptual geological model, repository and safety concepts for a model site
- Compilation of representative data
- Development of a specific FEP-catalogue for two model-sites in argillaceous rocks
- Methodology for scenario development and analysis
- Recommendation for future works

GORLEBEN Site

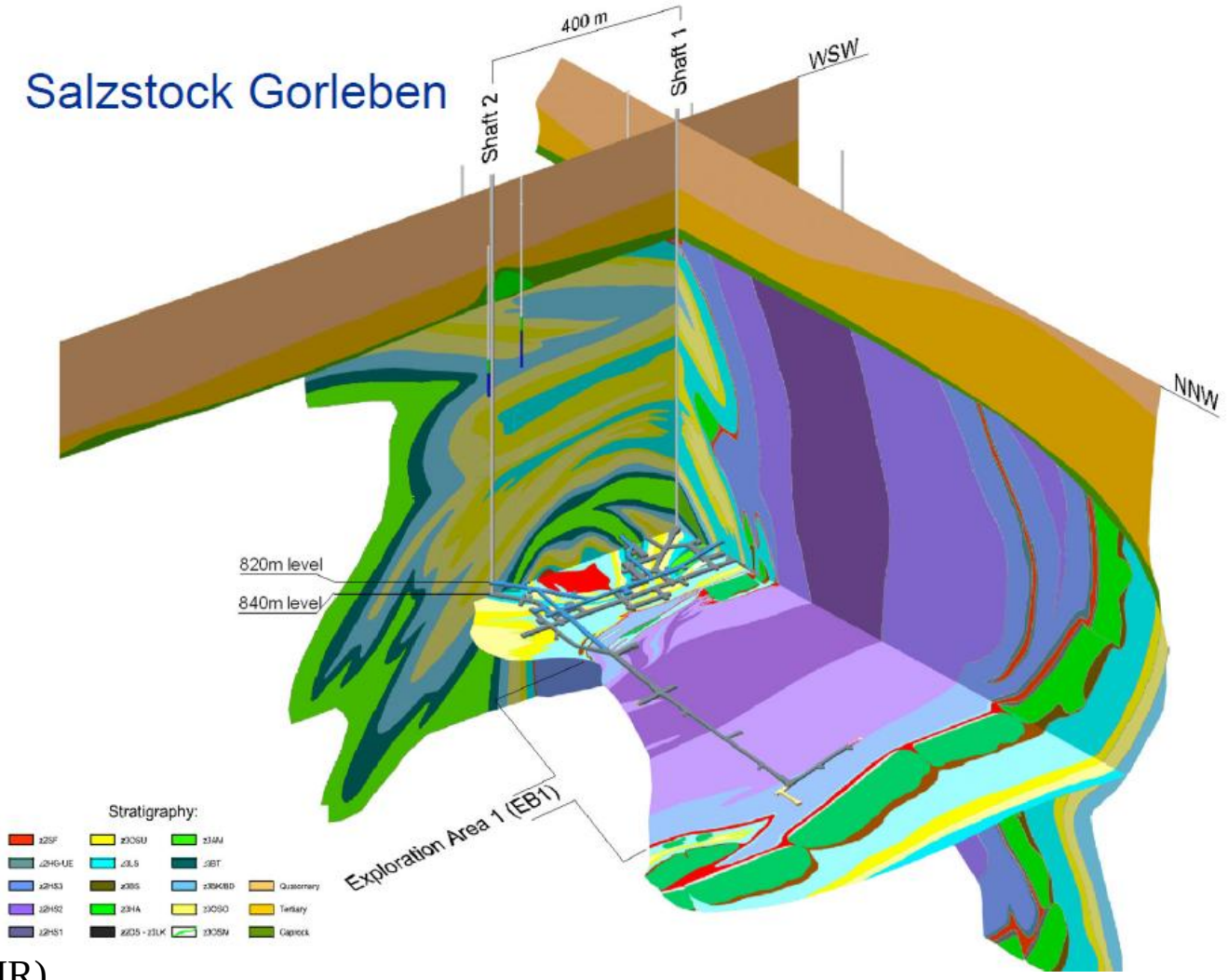

- Geological exploration
- Geotechnical investigations
  - Permeability
  - Deformation
  - Stress
- Geophysical investigation
  - Temperature
  - Ultrasonic
  - Electromagnetic Reflection (EMR)
- Current focus: hydrocarbons in salt

3D-Model

Argillaceous rock formations

Special tasks

- Transport processes & reactions
- Diffusion & retention
- Geochemistry & microbiology
- Gas migration & pore pressure
- Rock mechanics

Connected processes (THMC)

- Rock specific
- Concept specific (materials)

- Scale dependant tasks and methods (From regional to micro scale)

- Demonstration experiments

Special methods are to be developed

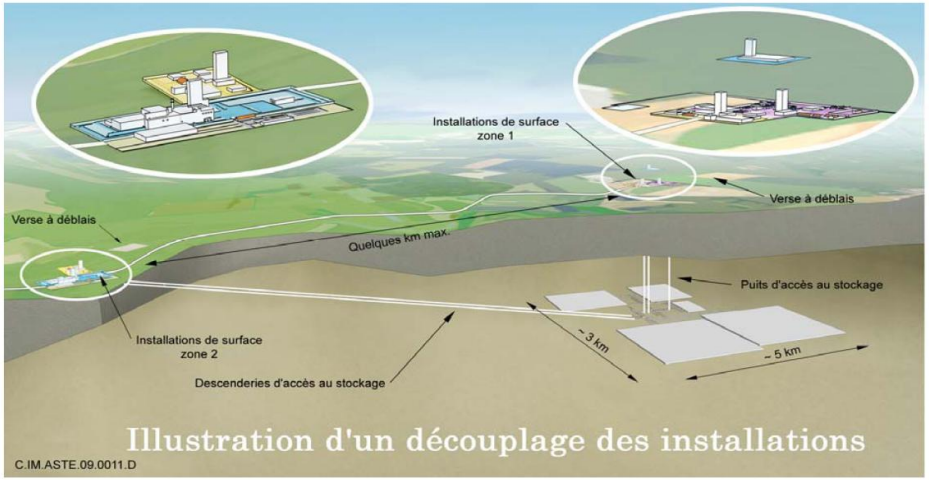

GEOLOGICAL SECTION OF PARIS BASIN

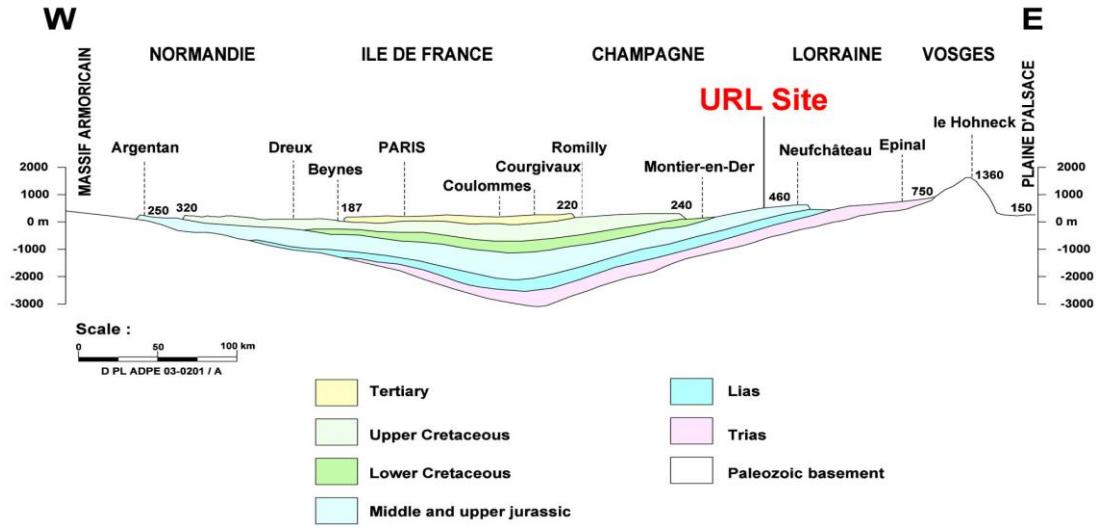

Quelle ANDRA

Granitic rocks

Main projects (Grimsel Test Site & Äspö URL)

Processes and long-term behaviour of the engineered barriers

- Full scale experiments
- Gas migration
- Sealing tests of the EB

Radionuclide transport
interactions between waste, engineered and geological barriers

Characterisation of the geological barriers

- Diffusion
- Hydrogeological, geomechanical and geological characterisation of the rock & the fracture system

Technical and operational aspects of repository constructions

Grimsel Test Site

Quelle NAGRA

Investigations in Crystalline Rock

- ***Development & Application of methods and models***

Fractured rock characterisation:

BK, GS, EFP (Grimsel Test Site)

TURE, TASK 5 (Hard Rock Laboratory Äspö)

Near-field characterisation:

ZPK, CTN (Grimsel Test Site)

TPF (Hard Rock Laboratory Äspö)

Geological and geotechnical barriers:

GMT, FEBEX, *GAST* (Grimsel Test Site)

PR, EBS, LASGIT (Hard Rock Laboratory Äspö)

Fractured Rock Characterisation

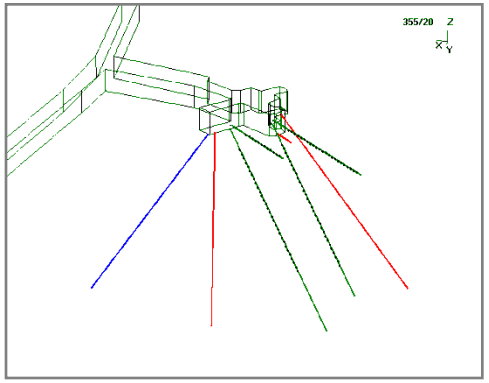

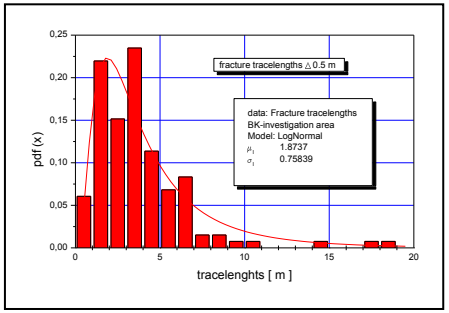

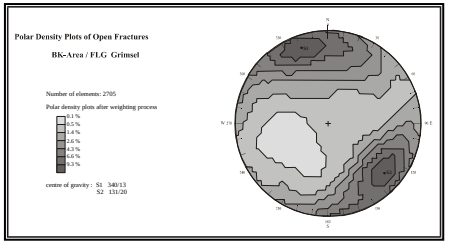

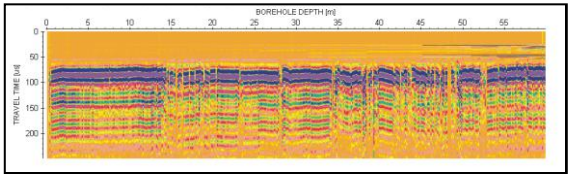

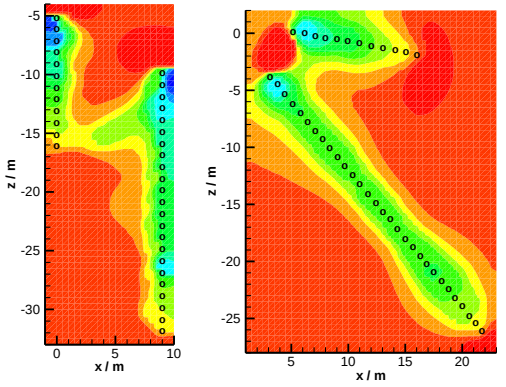

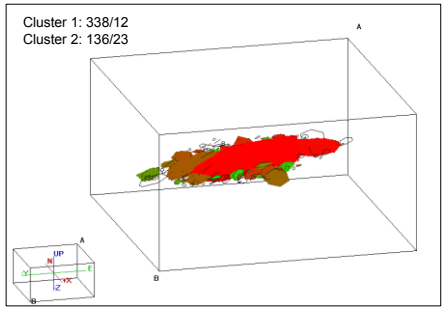

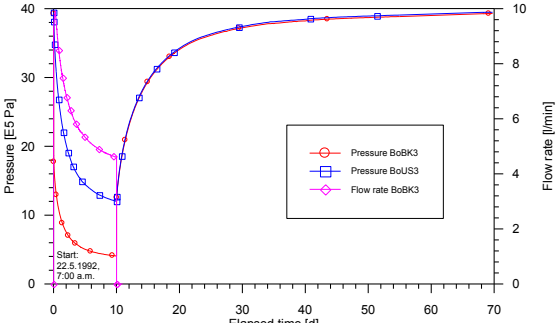

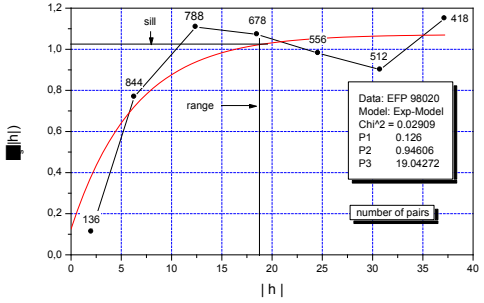

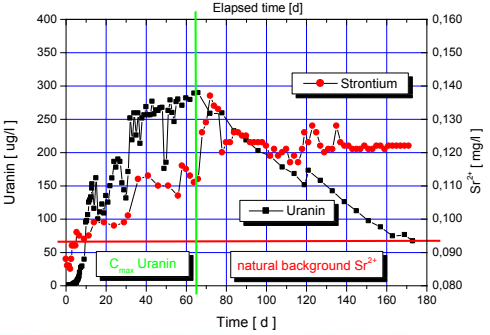

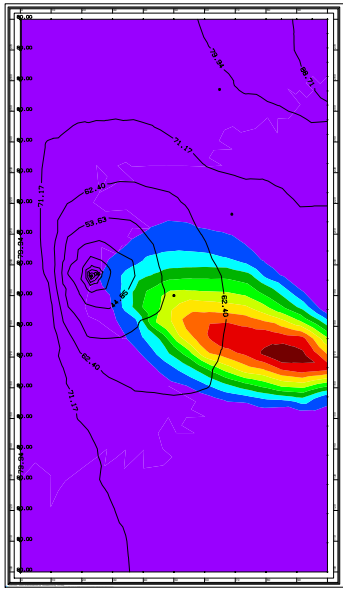

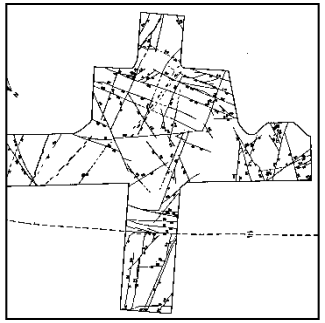

Field studies:
Geophysical &
geotechnical
Testing

Field studies:
Drilling
mapping

Desk studies:
Evaluation
Analysis

Desk studies:
Conceptualisation
Modelling
Assessment

BGR Bundesanstalt für Geowissenschaften und Rohstoffe

Small Scale Solute Transport in Fractured Rock

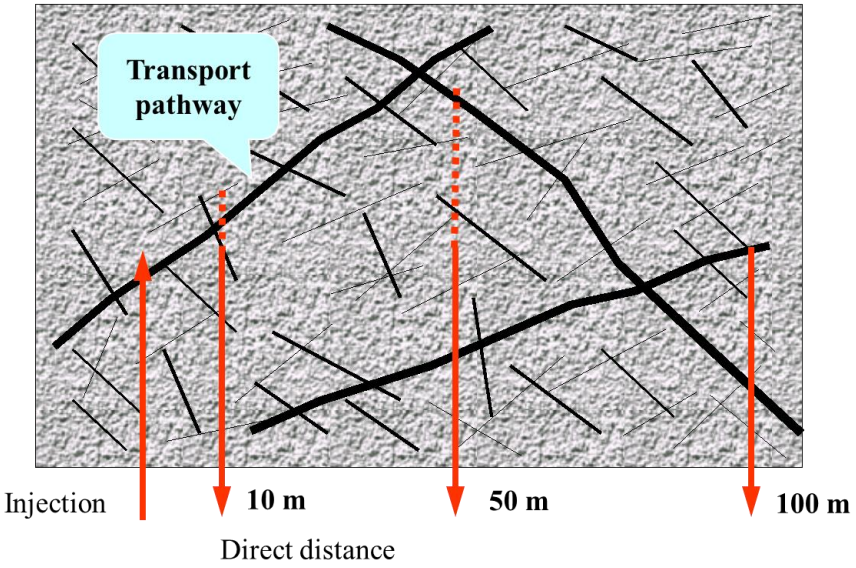

Single fracture model

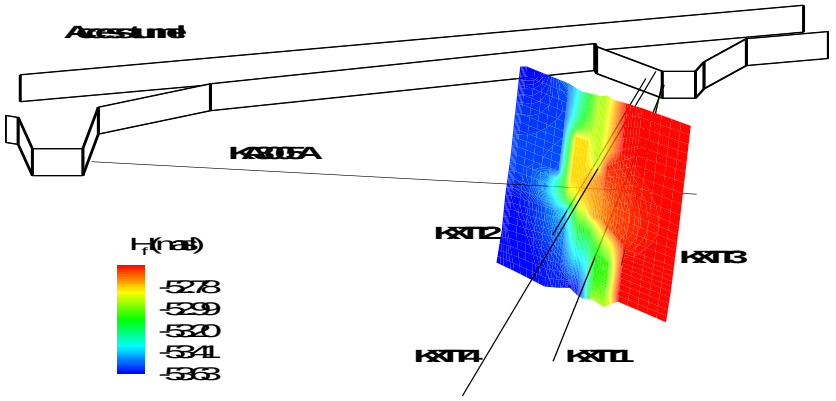

Small Scale
(< 10 m)
Single Feature Model
Flow and Advection
in Fracture

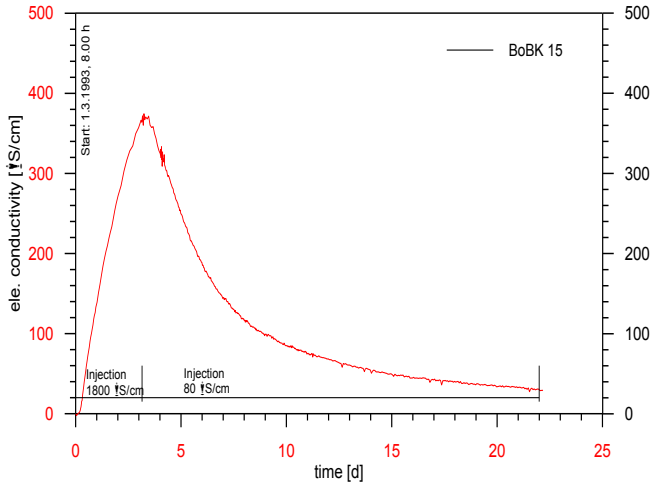

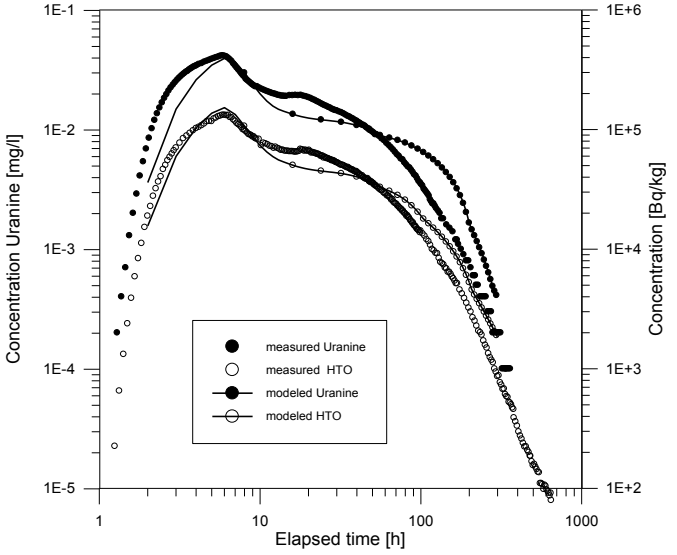

Block Scale Solute Transport in Fractured Rock

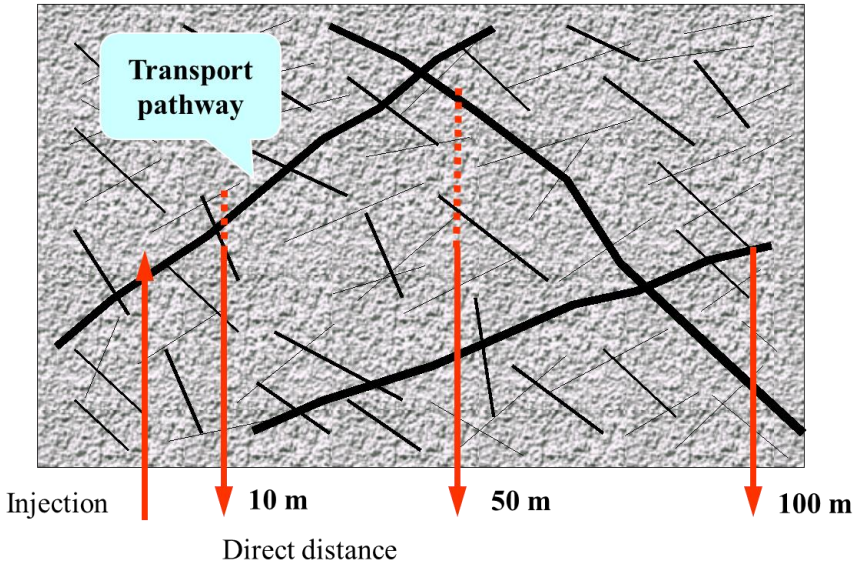

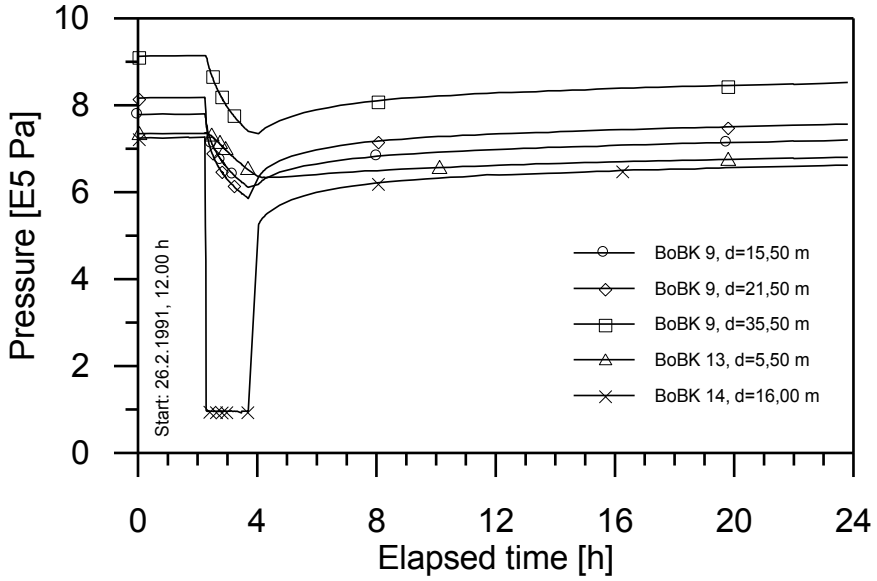

Intermediate Scale
(< 50 m)
Fracture Network Model
Flow and Advection
in Fracture System

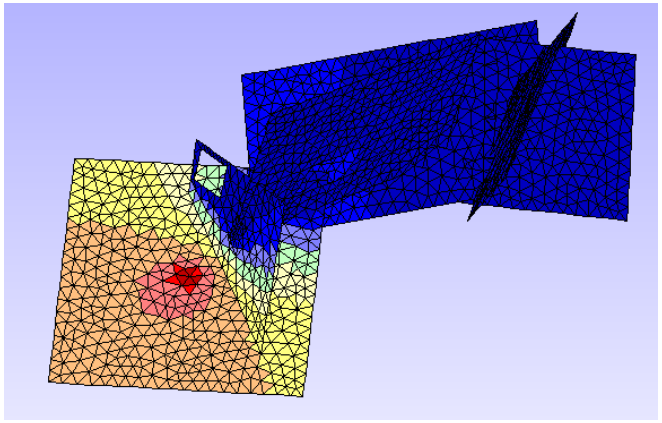

fracture network model

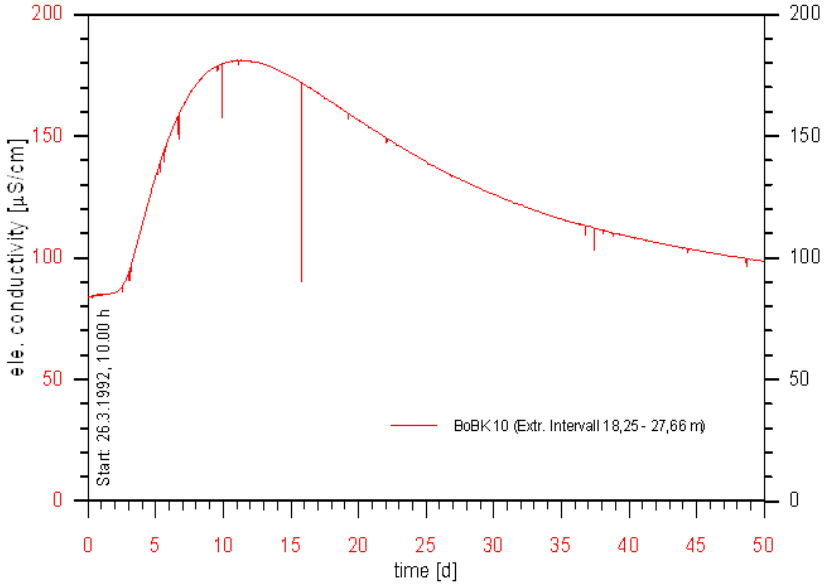

Large Scale Solute Transport in Fractured Rock

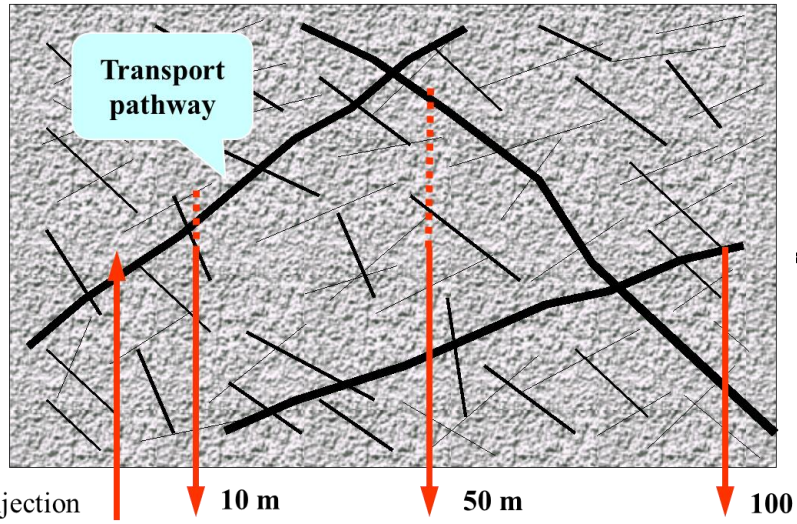

Large Scale
(> 100 m)
Coupled Fracture and Matrix model
Flow and Advection in Fracture System
Diffusion and Sorption in Matrix

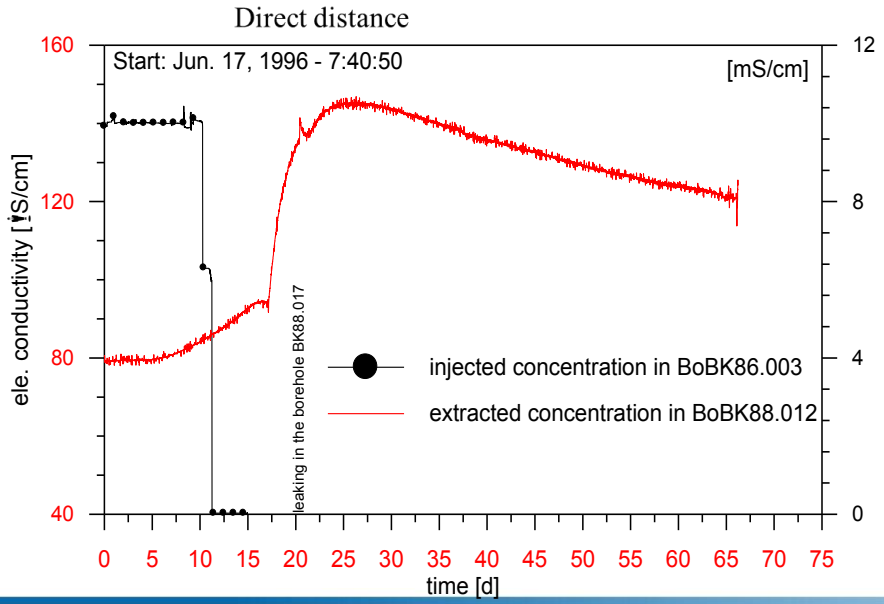

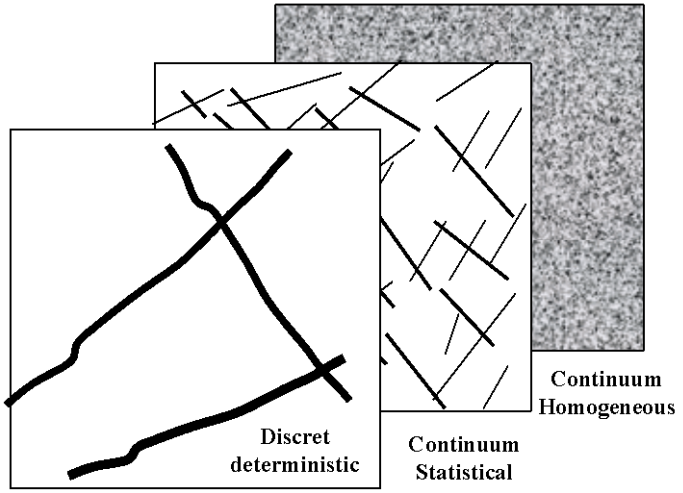

Conceptual model

Scale Dependency of Solute Transport in Fractured Rock

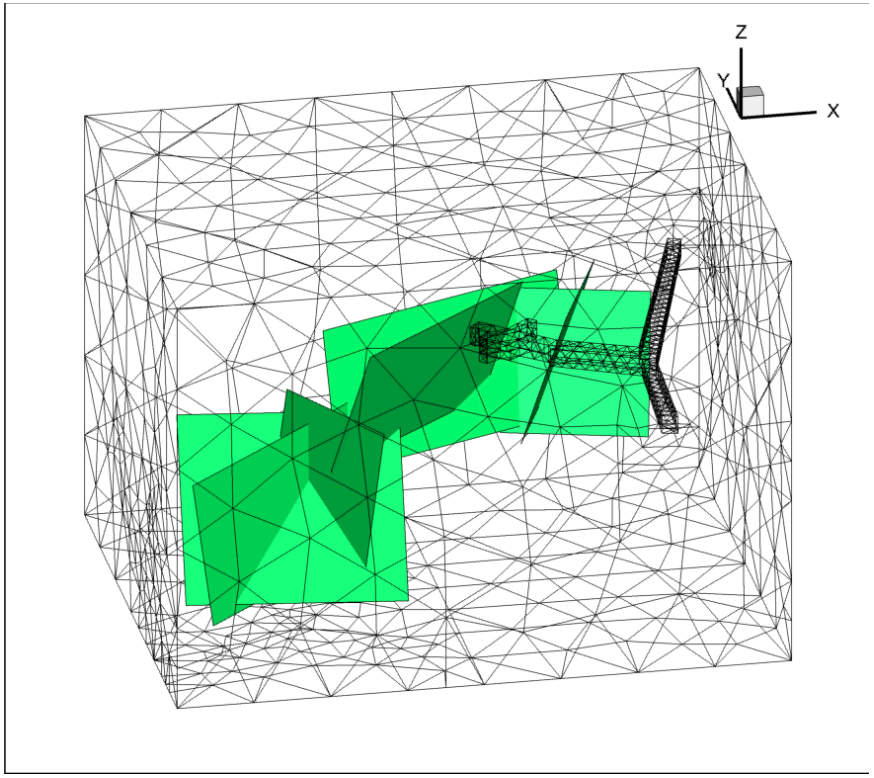

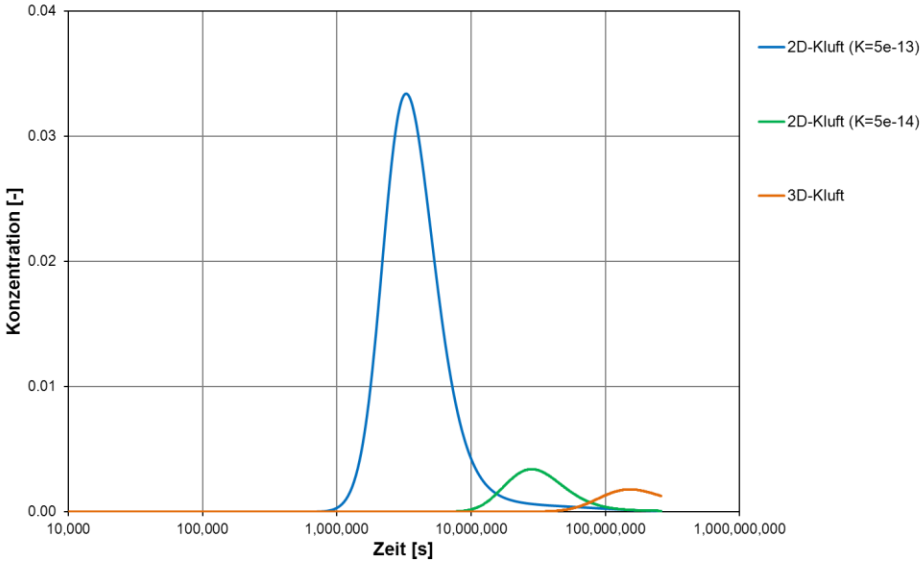

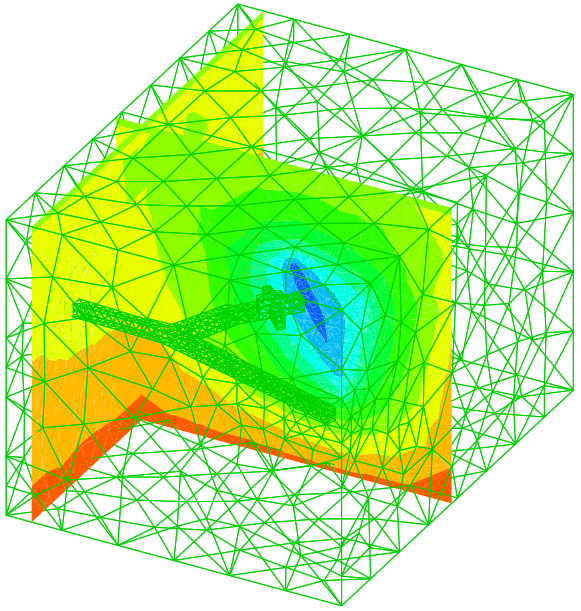

Coupled fracture and matrix model

Near-field Characterisation

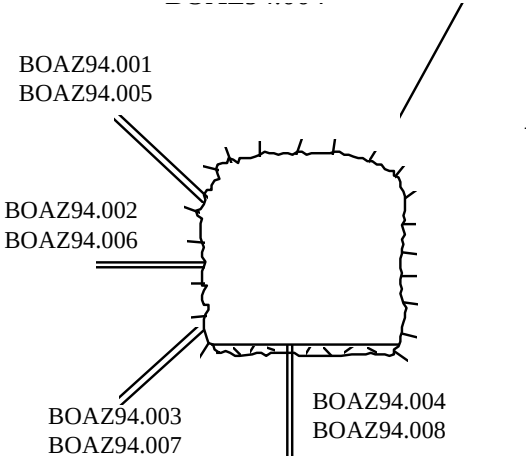

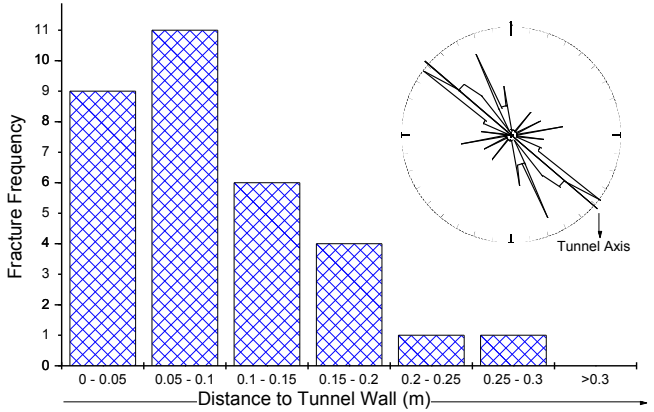

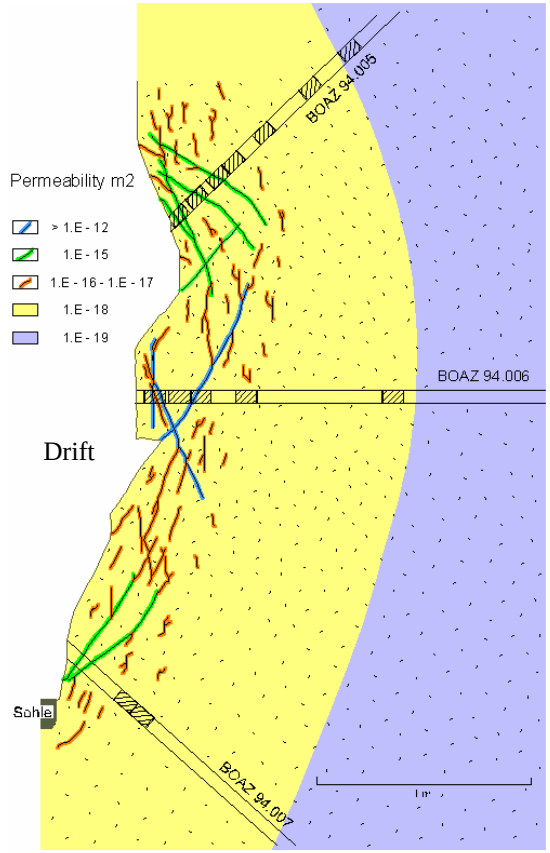

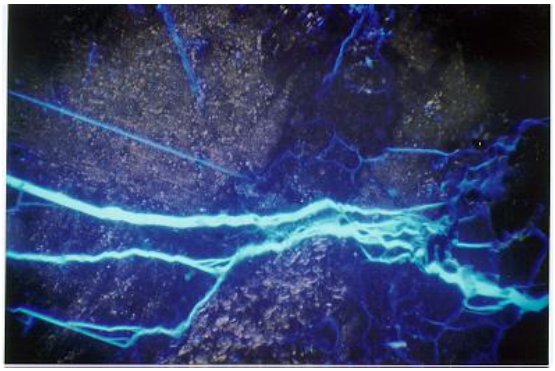

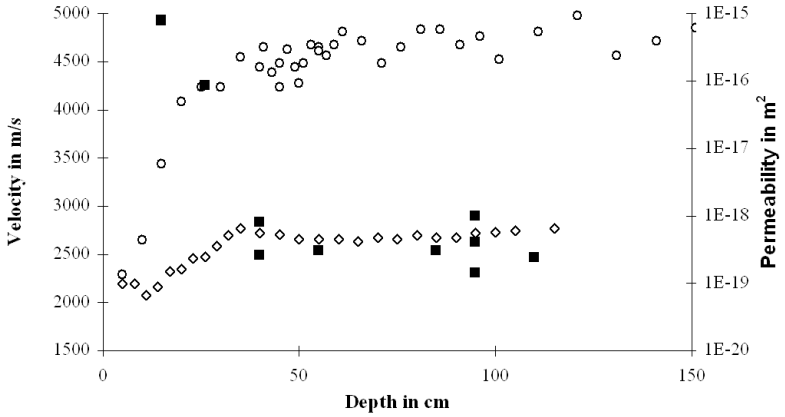

Thin section photo: micro fissure network marked with the fluoresced resin (picture 1.2 mm)

Near-field Hydraulic Properties

Grimsel (CH)

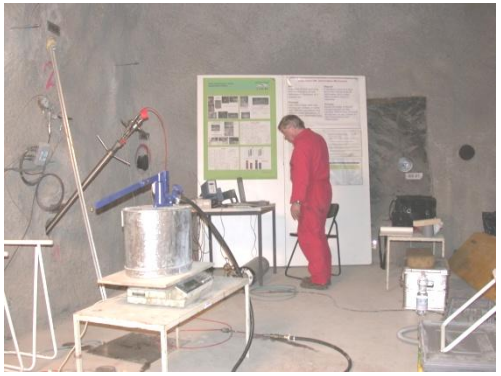

Mont Terri (CH)

since 2011 Gorleben (D)

Äspö (S)

Bure (F)

Granite:
$k < 10^{-18}$ m²
EDZ: 0.03 – 0.5 m
Fracture

Clay:
$k < 10^{-19}$ m²
EDZ: 1.0 - 2.5 m
Anisotropy

Salt rock:
$k << 10^{-20}$ m²
EDZ: k. A.

Geological and Geotechnical Barriers

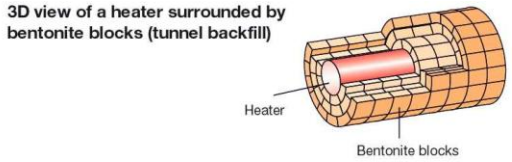

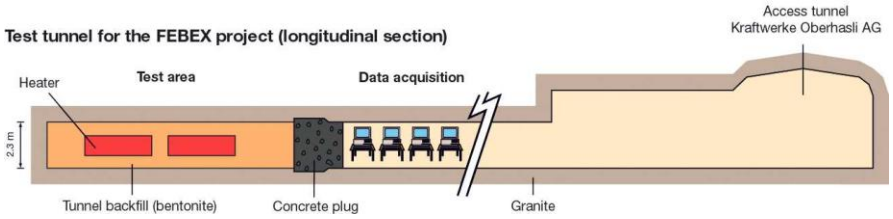

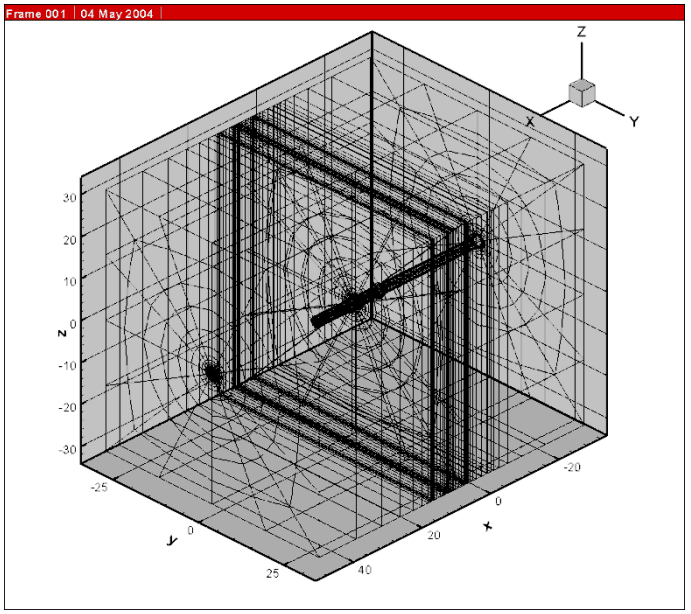

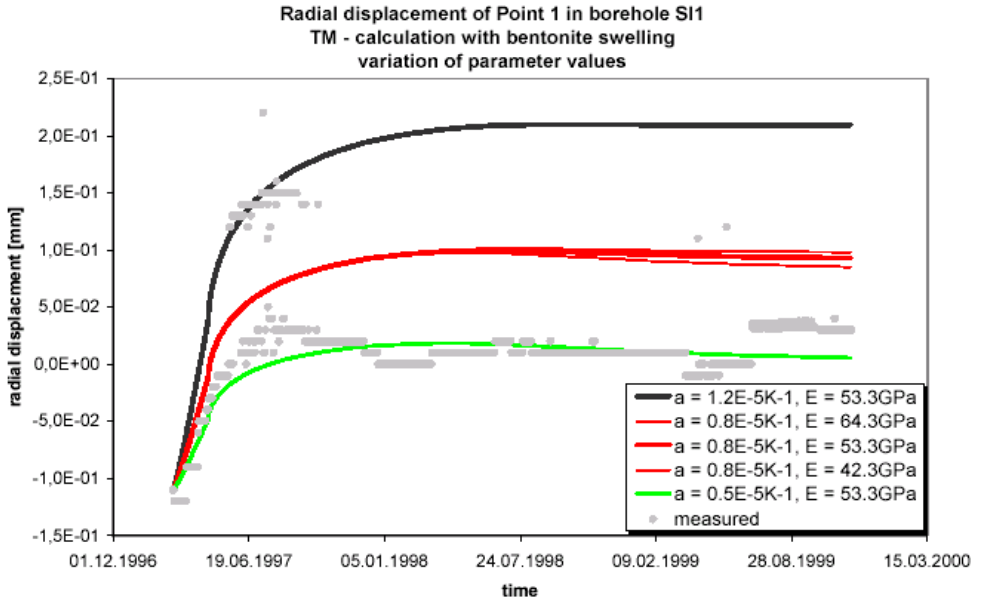

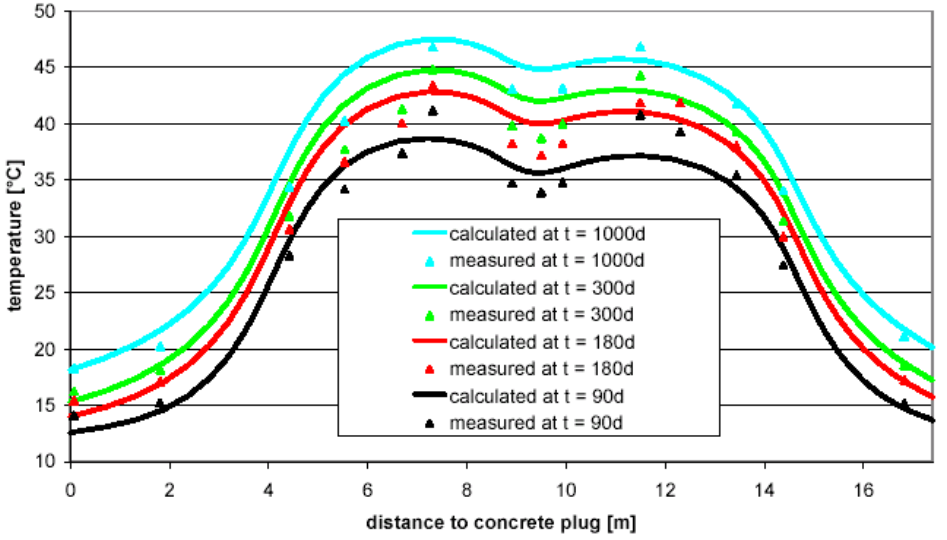

Cooperation between BGR and BRIUG

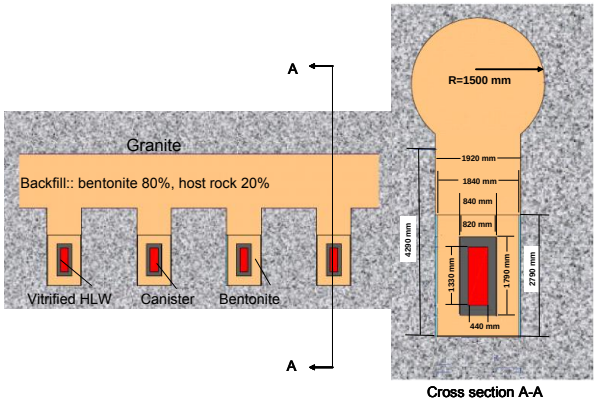

Cross section A-A

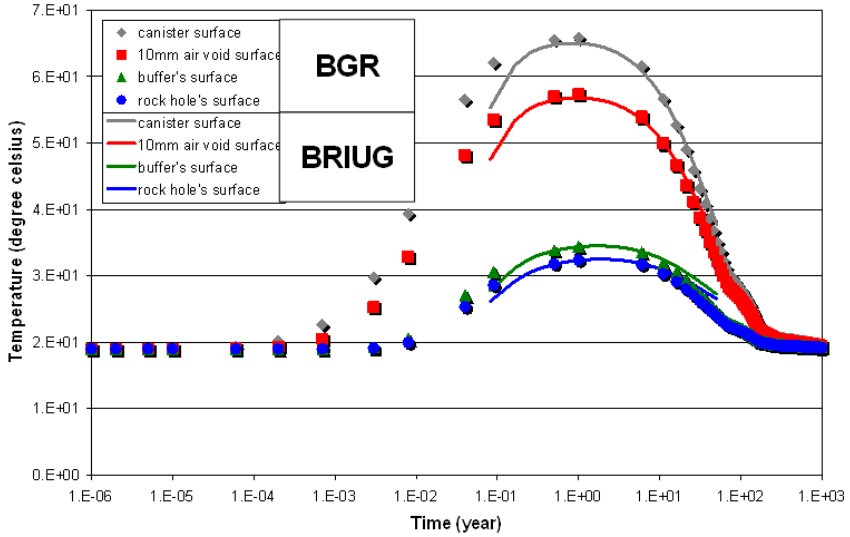

Thermal and hydraulic properties comparison GMZ Bentonite, MX-80, and FEBEX-Bentonite.

	GMZ	MX-80	FEBEX
Porosity (-)	0.4	0.39	0.41
Permeability (m²)	9e-21	4e-21	6e-21
Thermal conductivity (dry – wet) (W/mK)	0.3-1.5	0.3-1.3	0.4-1.5
Heat capacity (J/kgK)	1200	800	1600

SINOROCK2009, Hongkong

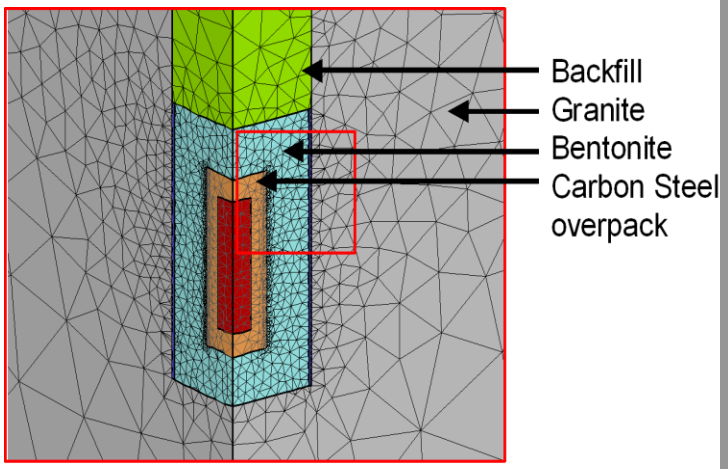

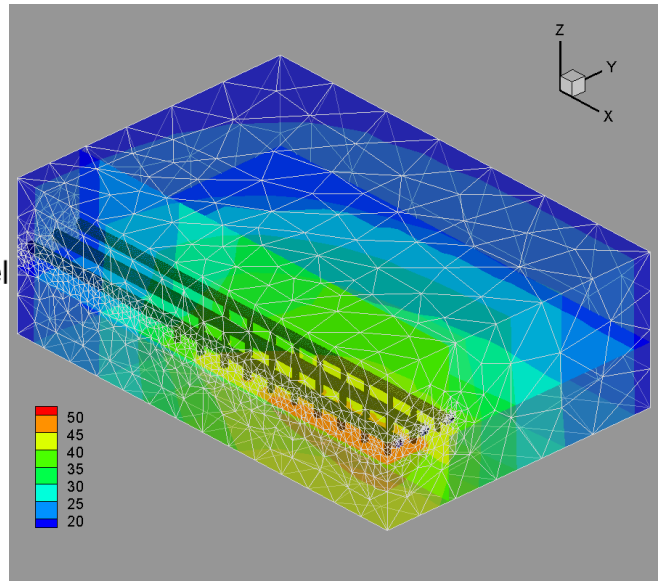

ISRM2011, Beijing

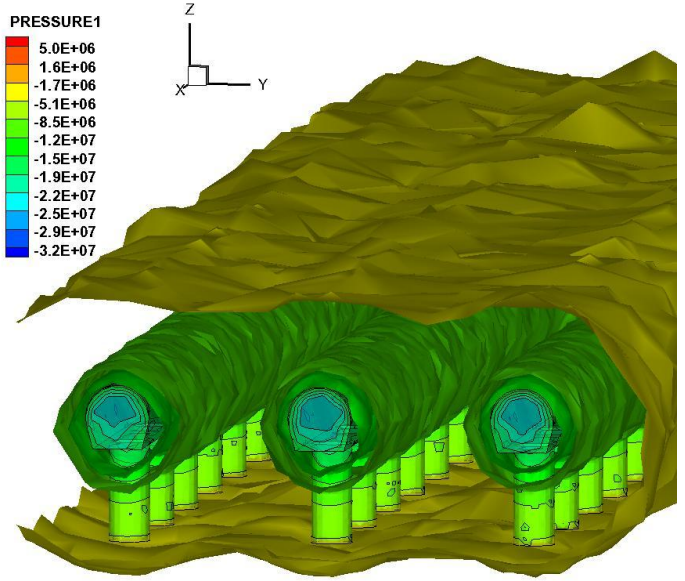

BGR Current & Future Activities

R+D	Salt	Argillaceous rock formations	Granite
Characterisation of potential host rocks	x	**X**	(X)
Geotechnical barriers, Excav. Disturbed Zone	X	X	X
Siting of potential host rocks in Germany	**X**	**X**	**X**
Safety assessment	**X**	**X**	(x)

Thank you for your attention!

Radionuclide transport in crystalline formations: laboratory and field experiments

Thorsten Schäfer

INSTITUTE FOR NUCLEAR WASTE DISPOSAL (INE)

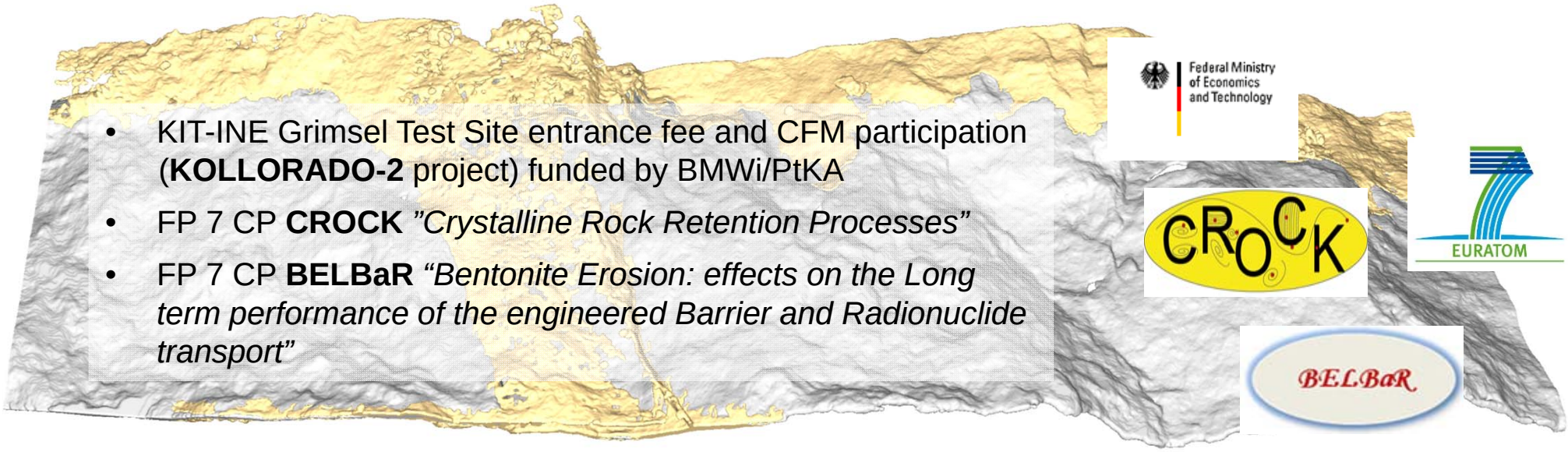

- KIT-INE Grimsel Test Site entrance fee and CFM participation (**KOLLORADO-2** project) funded by BMWi/PtKA
- FP 7 CP **CROCK** *"Crystalline Rock Retention Processes"*
- FP 7 CP **BELBaR** *"Bentonite Erosion: effects on the Long term performance of the engineered Barrier and Radionuclide transport"*

Acknowledgement (CFM Partners)

Min-Hoon Baik *Korea Atomic Energy Research Institute (KAERI)*

Kazuki Iijima *Japan Atomic Energy Agency (JAEA)*

Kotaro Nakata *Central Research Institute of Electric Power Industry (CRIEPI)*

Undaria Yamada
Masaya Suzuki *National Institute of Advanced Industrial Science and Technology*

Ursula Alonso
Tiziana Missana *The Centre for Energy-Related, Environmental &Technological Research*

Susanna Wold
Vladimir Cvetkovic *Royal institute of Technology , representative for SKB*

Pirrko Hölttä
Kari Koskinen *University of Helsinki, POSIVA*

Paul Reimus Los Alamos National Laboratory (LANL)

Bill Lanyon *Fracture-Systems Ltd.*

Thomas Trick,
Karam Kontar *SOLEXPERTS AG, Swiss precision monitoring*

Ingo Blechschmidt
Andrew Martin *NAGRA*

Claude Degueldre *PSI, Laboratory for Waste Management (LES)*

Ulrich Noseck, Judith Flügge *Gesellschaft für Anlagen- und Reaktorsicherheit (GRS) mbH*

T. Schäfer, F. Huber , C. Walther, M. Lagos, G. Darbha, S. Büchner, W. Hauser , M. Bouby, P. Höss, A. Pudewills, Horst Geckeis

Karlsruhe Institute of Technology (KIT)
Institute for Nuclear Waste Disposal (INE)

Outline

- INTRODUCTION
  - Conceptual Approach
  - Normal evolution Scenario (KBS-3 concept)
  - **C**olloid **R**adionuclide **R**etardation & **C**olloid **F**ormation & **M**igration projects
- RESULTS & DISCUSSION
  - Bentonite Erosion / Colloid Formation (Laboratory studies)
  - Colloid associated radionuclide transport
    - Hydraulics at Grimsel Test Site
    - Migration Experiments
    - Comparison of Laboratory and Field data
- SUMMARY & FUTURE ACTIVITIES

Conceptual Approach

- Research is dedicated to study
  - **Colloid formation/bentonite erosion**
  - **Groundwater/porewater mixing zone**
  - **Colloid migration (filtration)**
  - **Colloid associated RN transport**

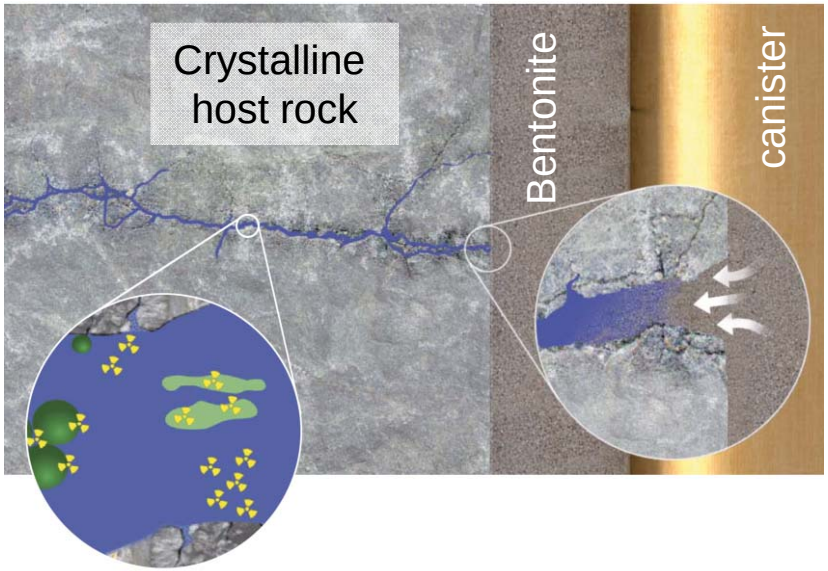

Laboratory Studies	Field Experiments	Modelling Studies
Colloid-RN interaction	*In situ* test: formation & migration	Solute, colloid and associated RN transport
Colloid Generation	Migration: colloids, homologues, RN tracers	Colloid generation
Field test analysis		

Expected Outputs

- **Significant increase in process understanding related to colloid formation at the bentonite/ host rock interface**
- **Provide PA relevant information on the colloid influence on RN migration/ retardation**
- **Gain experience in long term monitoring for repository surveillance.**

Normal evolution scenario for Sweden's KBS-3 repository

- Dilute water intrusion from melt waters during the glaciation stage will impact groundwater compositions at repository depth.

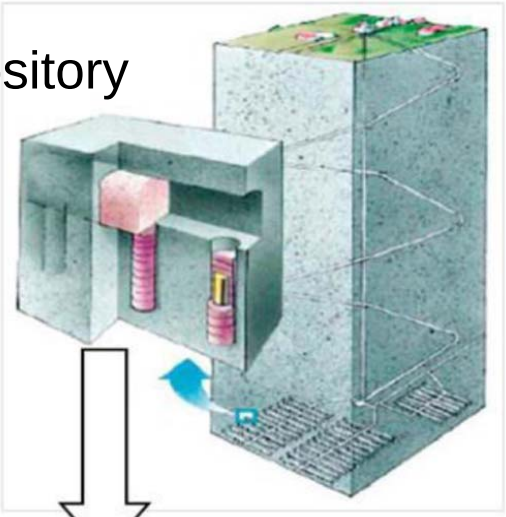

SKB report TR-06-09

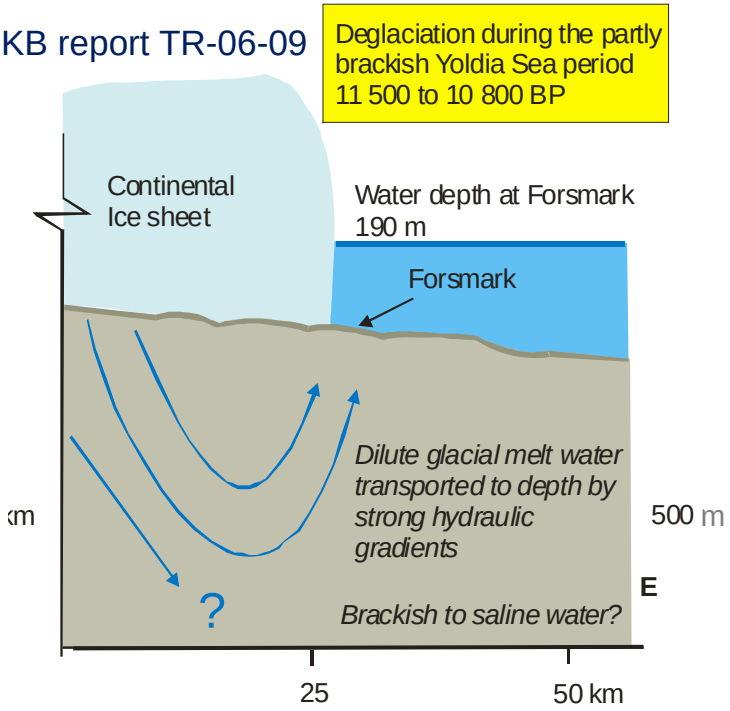

SSM report 2011:08

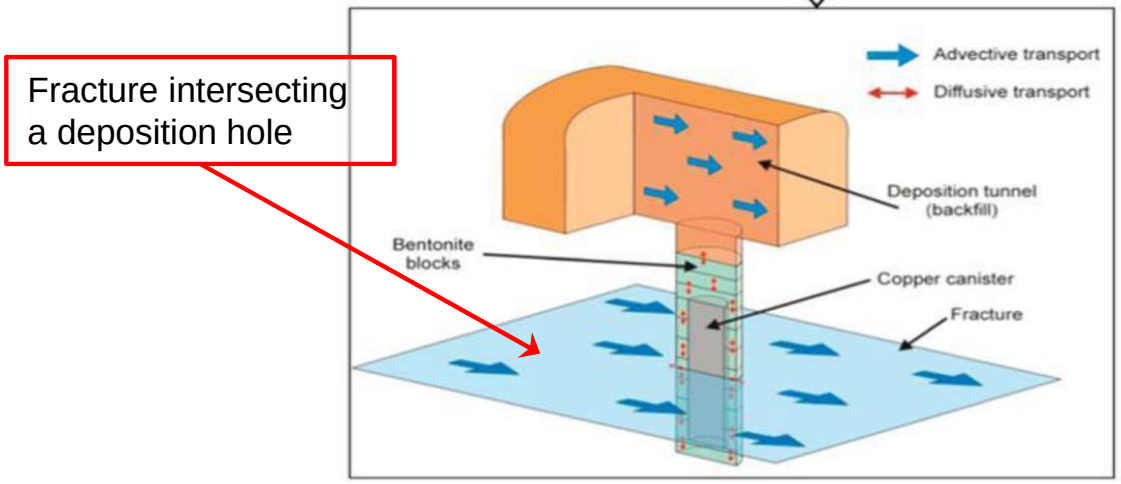

- **Buffer erosion part of the normal evolution scenario (SKB report TR-06-09)**
- **Calculations of buffer material losses could lead to advective flow conditions in some deposition holes.**
- **By regression fit to erosion rate calculations 50 deposition holes will see advective conditions by 1 million year (SSM report 2011:8)**

Where do we find glacial melt water conditions? Grimsel Test Site (GTS)

	GTS groundwater Na-Ca-HCO_3 type
Pressure (bar)	1.4 – 33
pH	9.6 ± 0.2
Ionic strength (mol/L)	0.0012
E_H *(mV)*	≤ -200
(Na^+, K^+, Rb^+, Cs^+)	0.7 mmol/L
$\Sigma(Ca^{2+},Mg^{2+},Sr^{2+})$	0.14 mmol/L
Fe_{ToT} *(µmol/L)*	0.003[+]
Total cell number (cells/mL)	4.0 ± 0.4·10[3*]
DOC (mg/L)	0.4 – 1.4

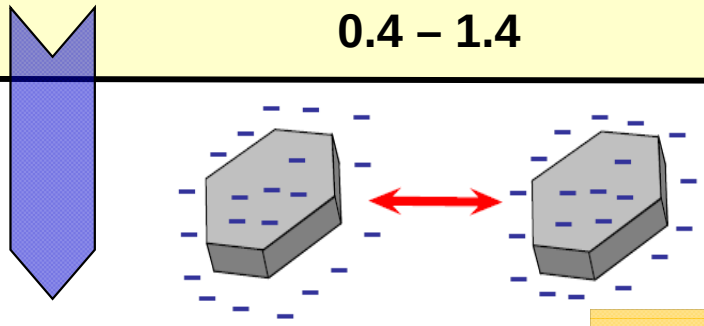

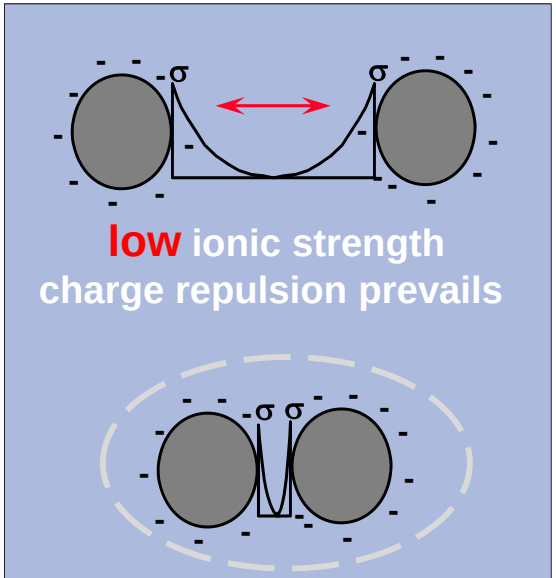

Glacial melt water

GTS ideal site to investigate experimentally effects of glacial melt water on buffer integrity & colloidal transport

[+]Frick et al. (1992); * Gillow et al. (1999)

Interaction of strongly sorbing radionuclides with colloids in low mineralized groundwaters

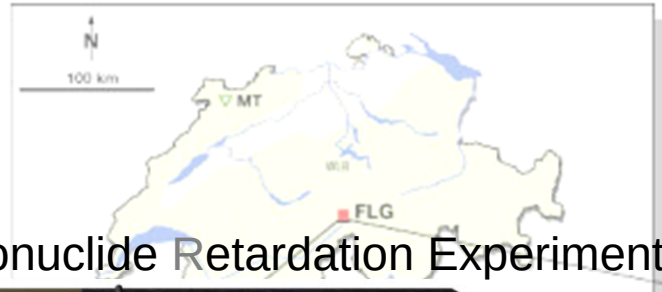

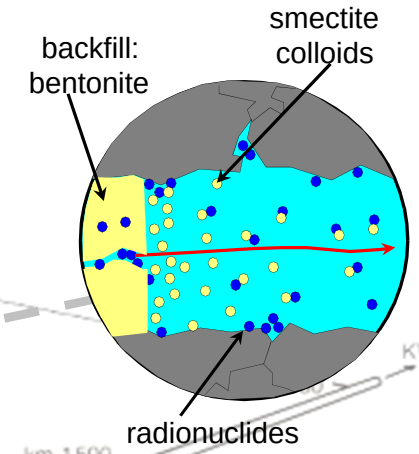

The Colloid & Radionuclide Retardation Experiment

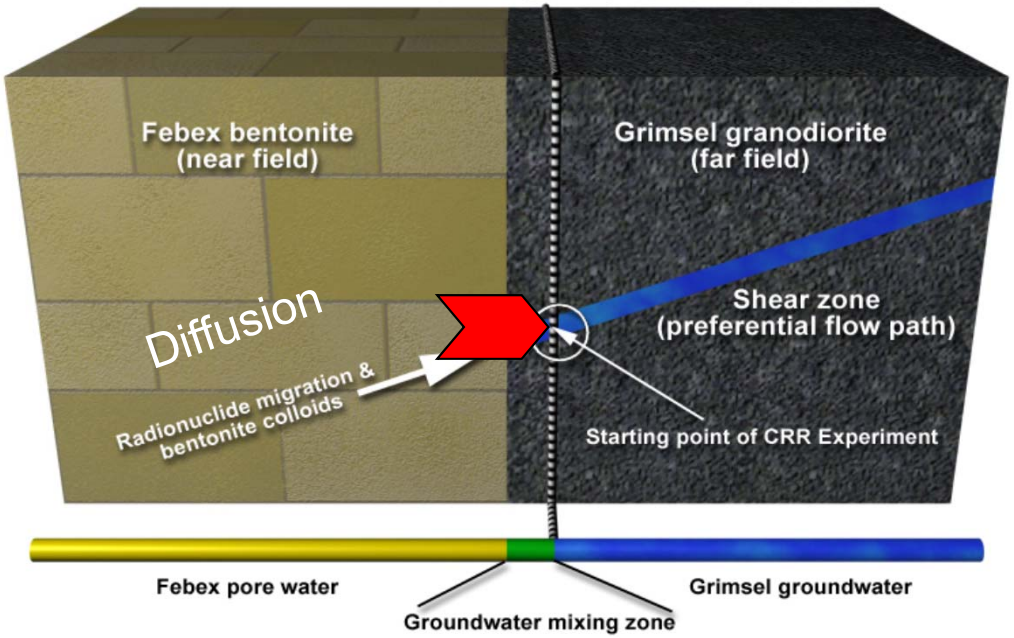

Geckeis et al.,*Radiochim. Acta* 2004, 92, 765-774.
Möri et al., *Colloids and Surfaces A* 2003, 217(1-3), 33-47.
Schäfer et al., *Radiochim. Acta* 2004, 92, 731-737.
Kretzschmar & Schäfer, 2005, *Elements*, 1(4): 205-210.

Project duration: 1997-2004

Colloid Formation and Migration

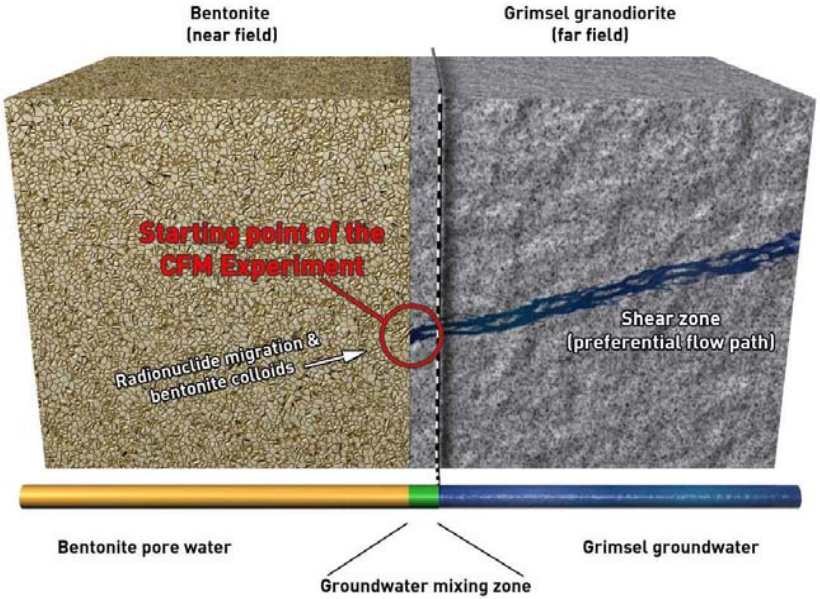

Project duration: 2004-2015

Outline

- INTRODUCTION
  - Conceptual Approach
  - Normal evolution Scenario (KBS-3 concept)
  - **C**olloid **R**adionuclide **R**etardation & **C**olloid **F**ormation & **M**igration projects
- RESULTS & DISCUSSION
  - Bentonite Erosion / Colloid Formation (Laboratory studies)
  - Colloid associated radionuclide transport
    - Hydraulics at Grimsel Test Site
    - Migration Experiments
    - Comparison of Laboratory and Field data
- SUMMARY & FUTURE ACTIVITIES

Colloid Formation/ Bentonite erosion (Mock-up)

Compacted Febex bentonite ring provided by CIEMAT

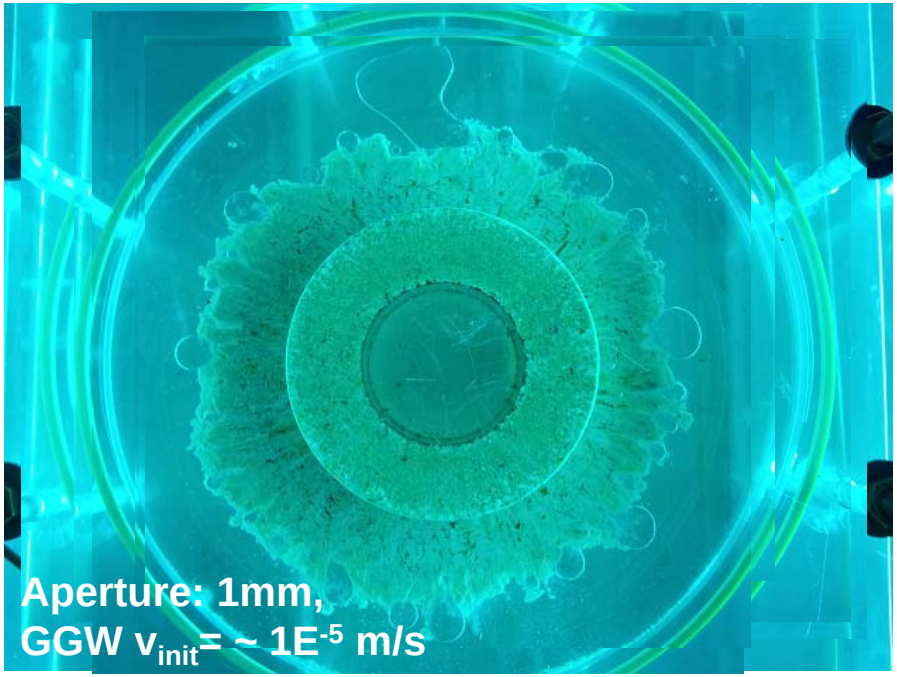

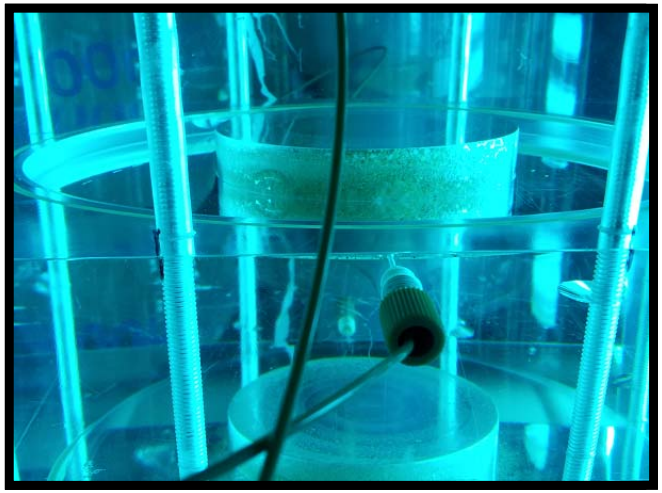

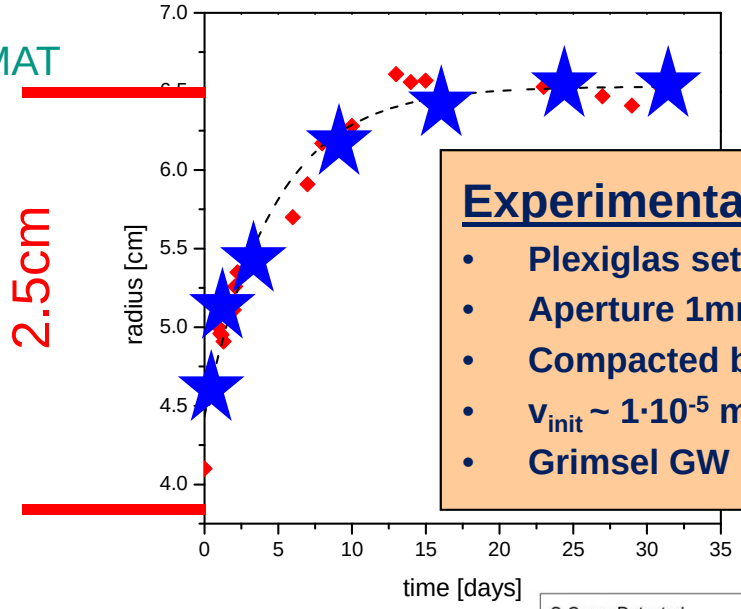

Experimental details:

- Plexiglas set-up
- Aperture 1mm
- Compacted bentonite 1650 kg/m^3
- v_{init} ~ 1·10^{-5} m/sec
- Grimsel GW

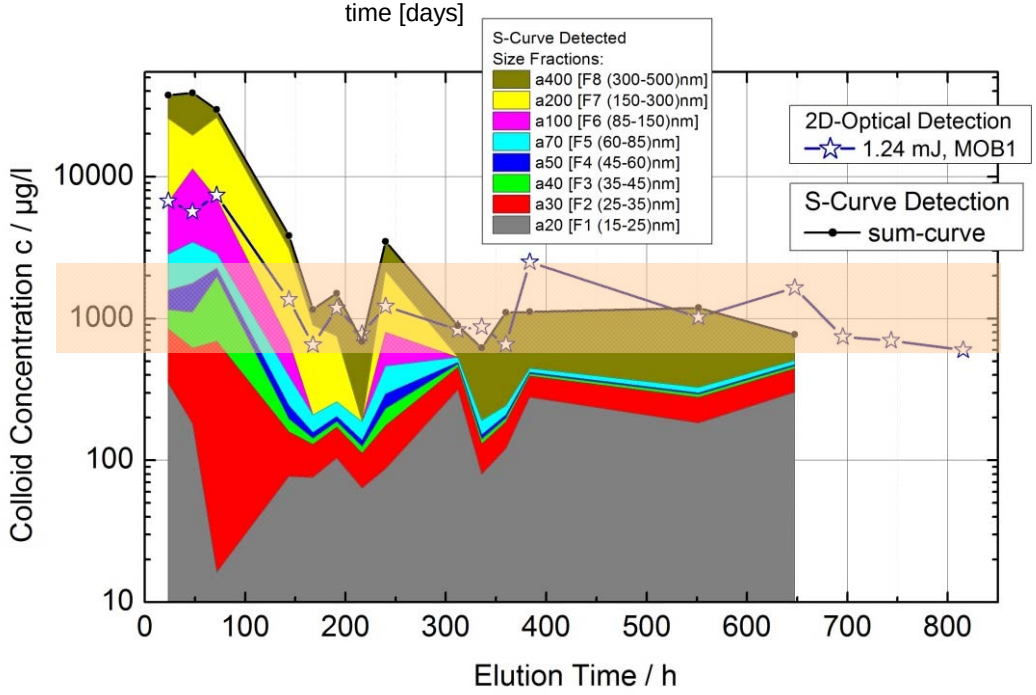

Colloid Formation/ Bentonite erosion (Mock-up)

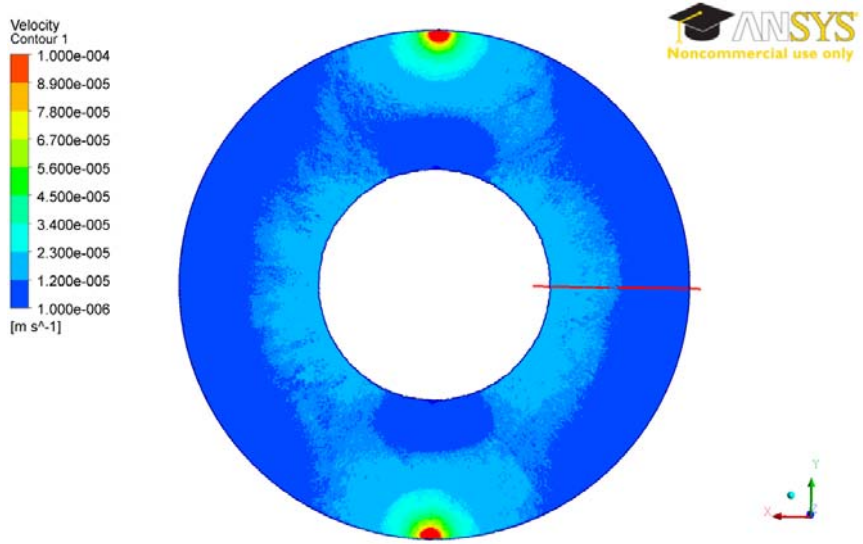

End of Experiment

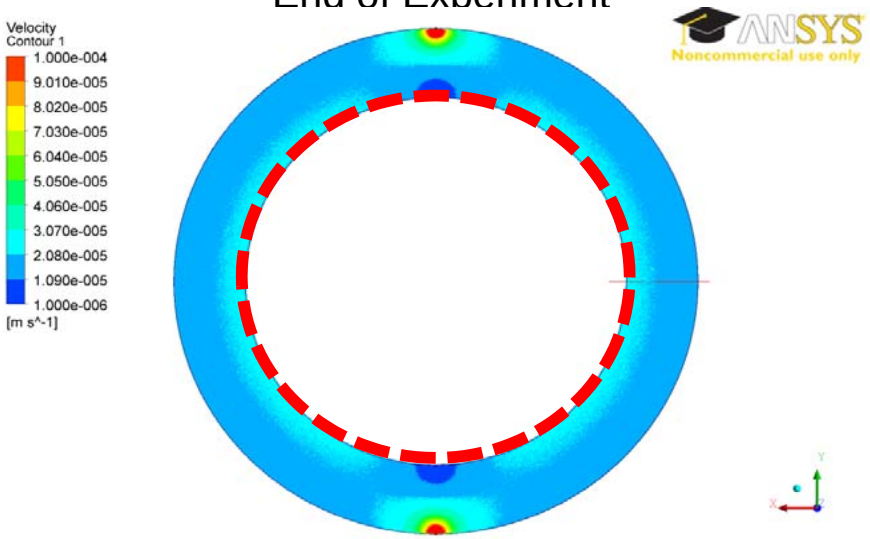

SKB TR-10-64 (Bentonite erosion model)

- Fracture aperture (*2b*) 1mm
- Water velocity (*v*) varied
- Cylindrical deposition borehole (Ø 1.75m)

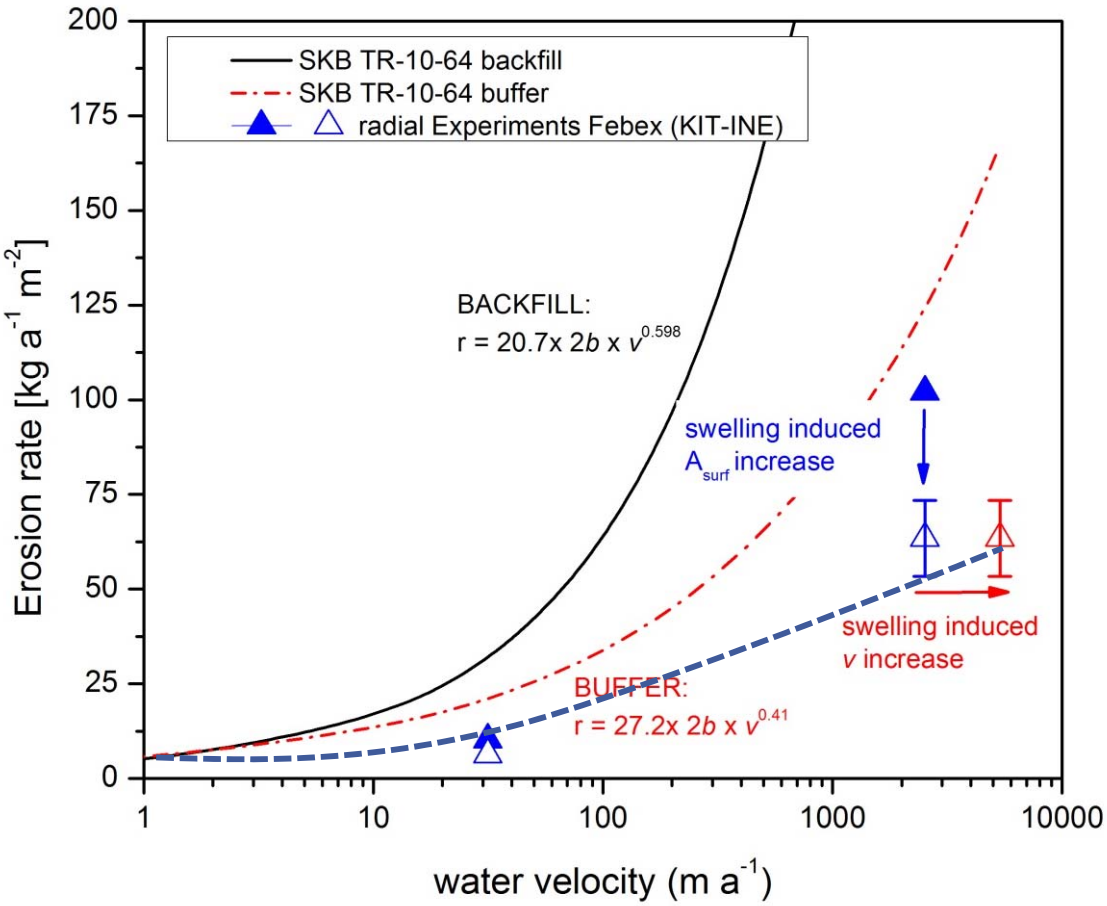

Migration (MI) shear zone (GTS, Switzerland)

(1730 m a.s.l., depth 450 m)

(1) Grimsel Test Site, (2) Rätherichsbodensee,
(3) Grimselsee and (4) Juchlistock.

- ✓ A zone with many discontinuities
- ✓ Signs of ductile and brittle deformation
- ✓ Some water inflow into the tunnel
- ✓ Core sample for lab experiments

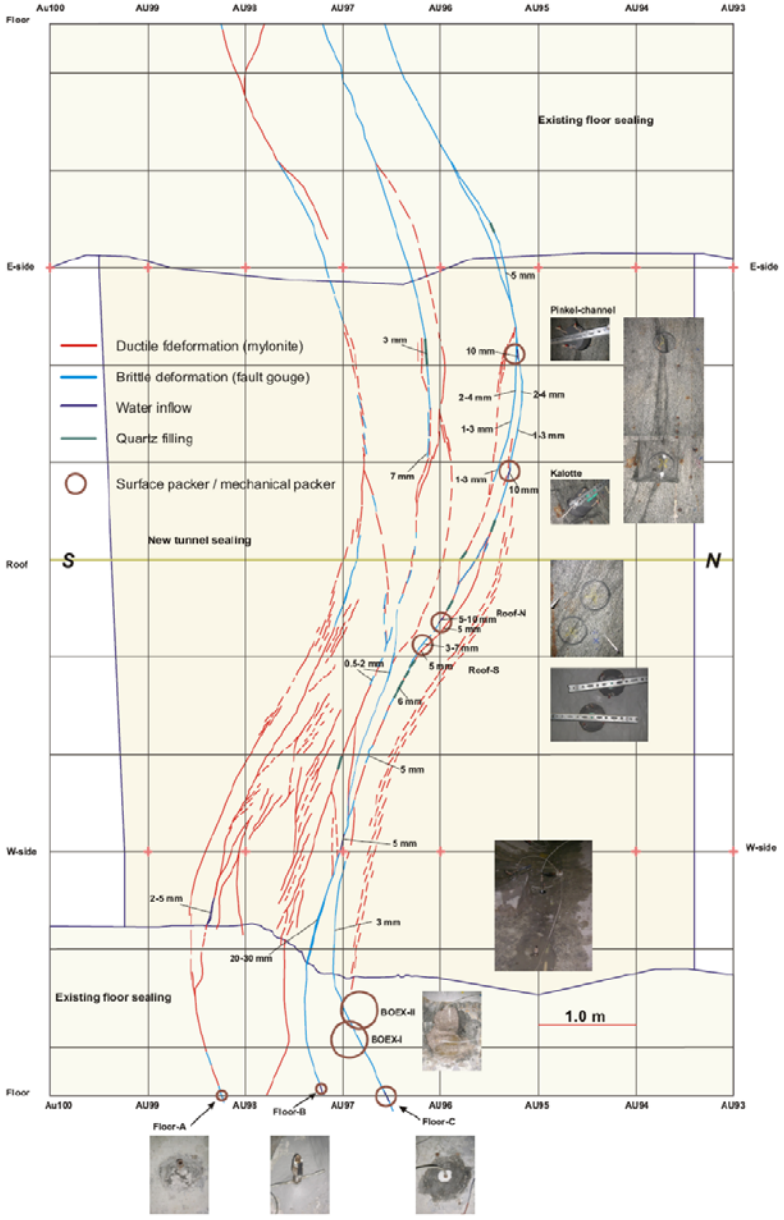

Micro-scale CFD on real fracture geometries

Schäfer et al. (2012) *Appl. Geochem.* 27(2), 390.; Huber et al. (2012) *J. Contam. Hydrol. 133, 40-52.*

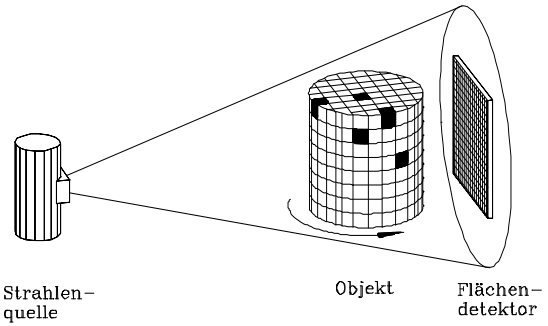

- Procon X-Ray Alpha 160 kV max. Flat panel-detector, max. 2048 x 2048 px, max. resolution ~ 1 µm / px.
- µCT @ BAM (Berlin) core scanned with 900 projections over 360° rotation of the sample at 220 kV voxel resolution 80 µm

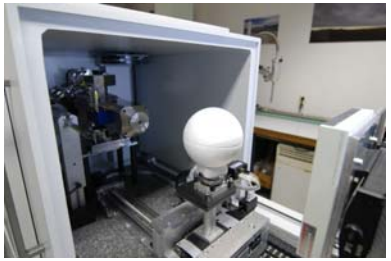

Methological approach

µXCT

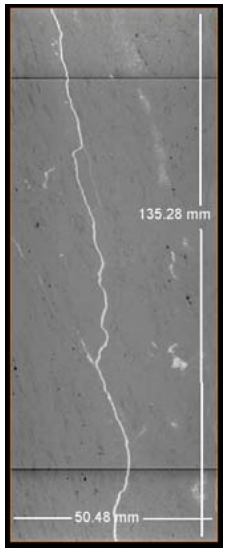

Geometry reconstruction

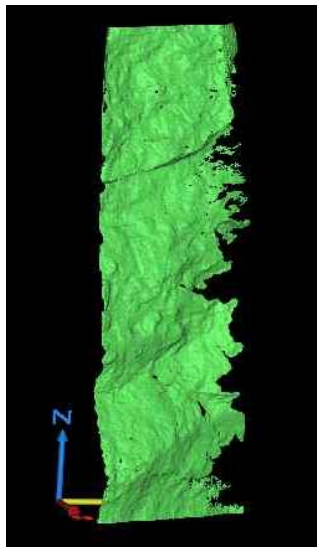

Preprocessing

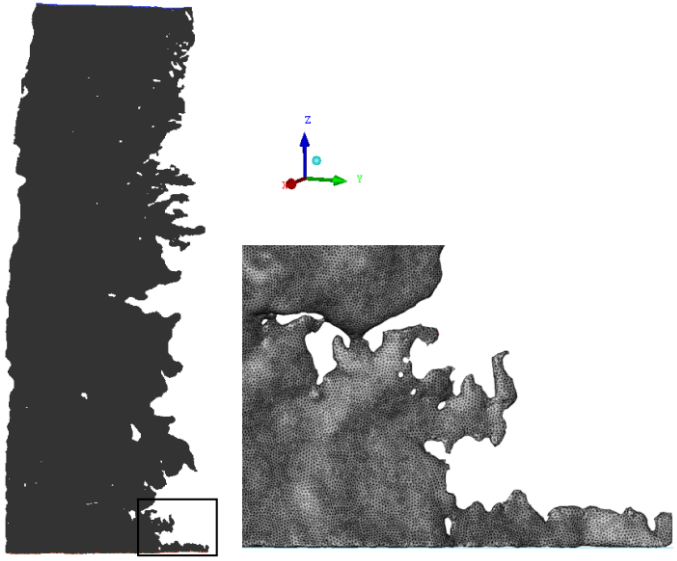

Postprocessing

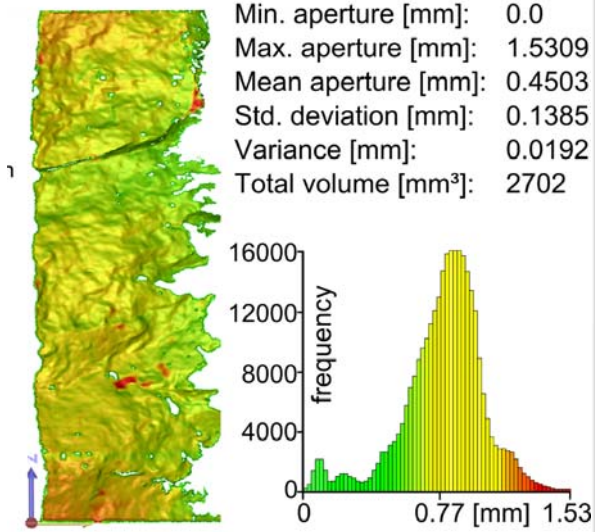

Full 3D computational fluid dynamic (CFD)

Schäfer et al. (2012) *Appl. Geochem.* 27(2), 390.; Huber et al. (2012) *J. Contam. Hydrol. 133, 40-52.*

Velocity distribution

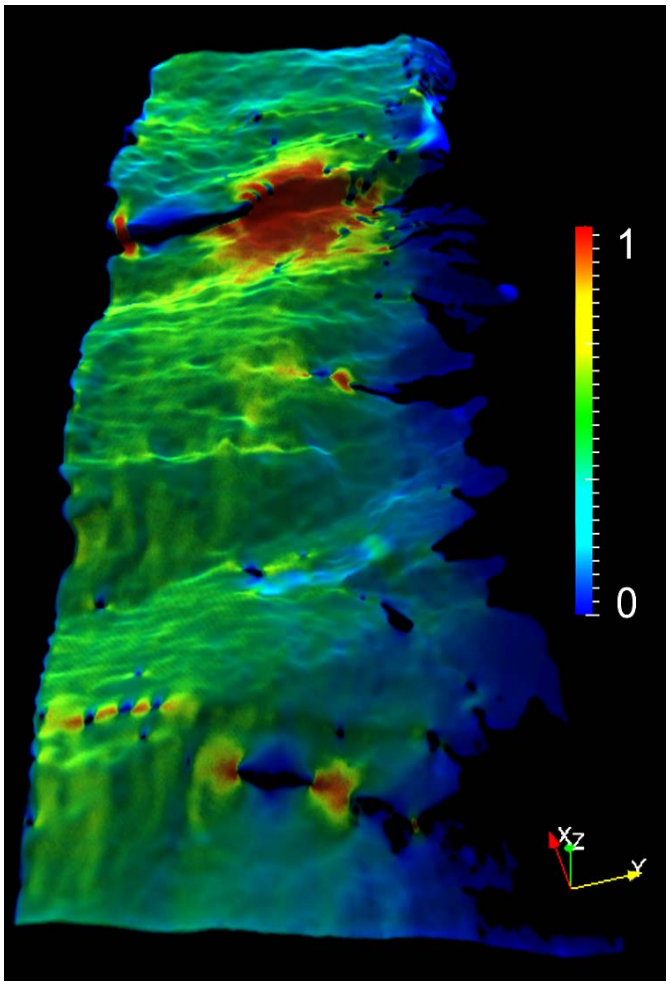

Particle Tracing

Full 3D model ~ 10.5 Mio elements

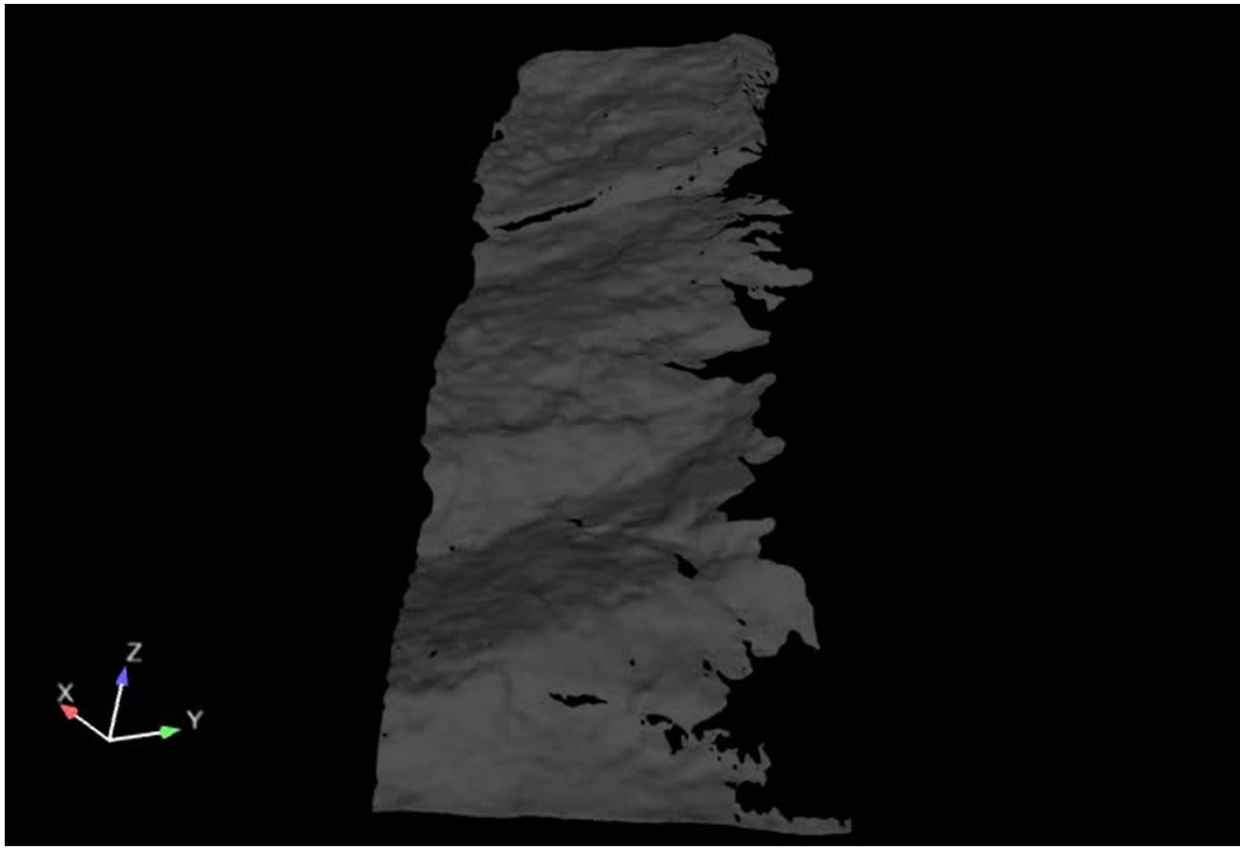

Wedge shaped fracture geometry

Pressure inlet and outlet (pressure = 0); Step input (C = 1 for t > 0)

Colloid associated RN transport

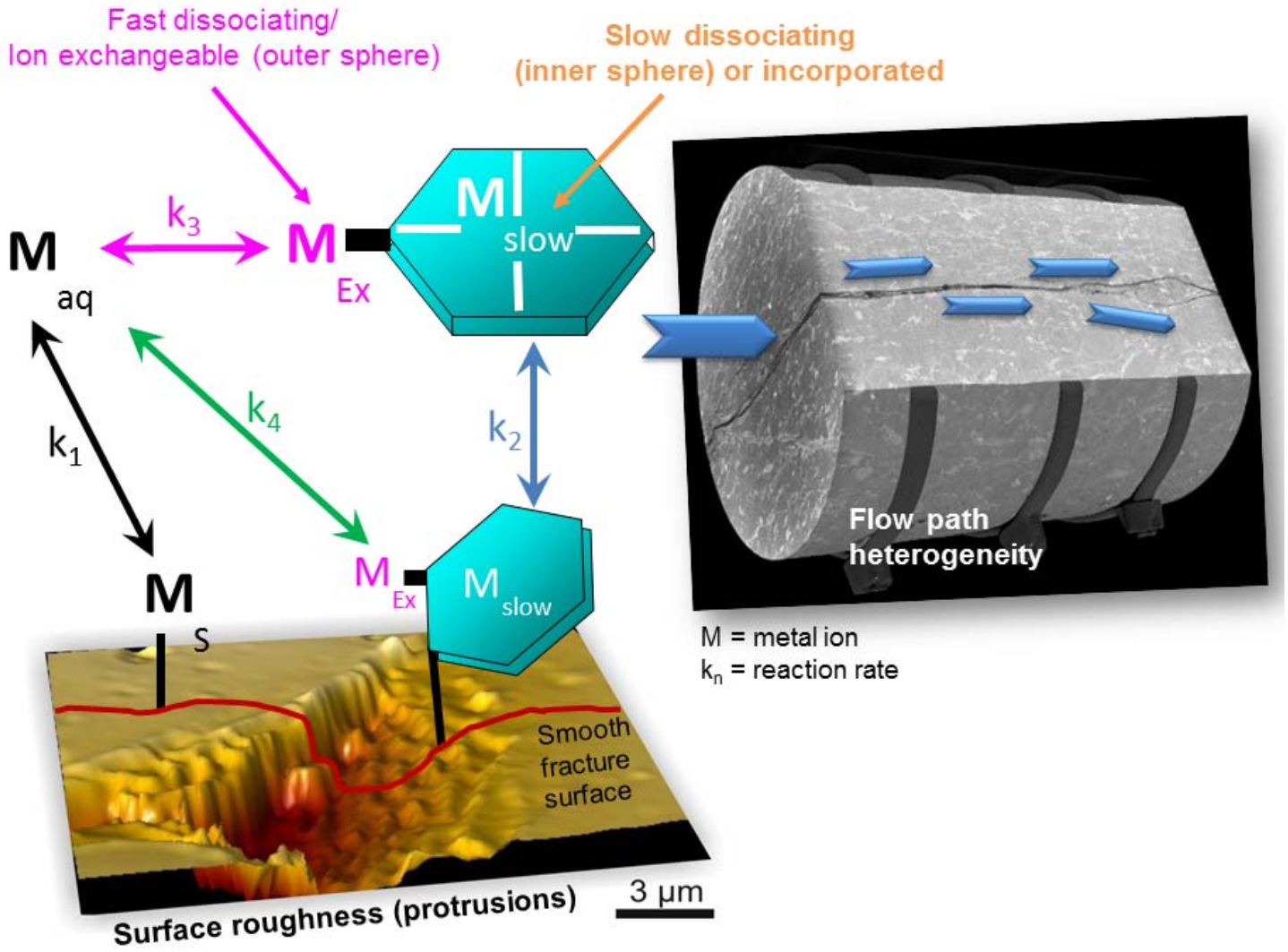

What did we know after CRR at the start of CFM?

Geckeis et al. (2004) *Radiochim. Acta 92, 765;* Möri et al. (2003) *Colloids Surf. A 217, 33;* Schäfer et al. (2004) *Radiochim. Acta 2004, 92, 731.*

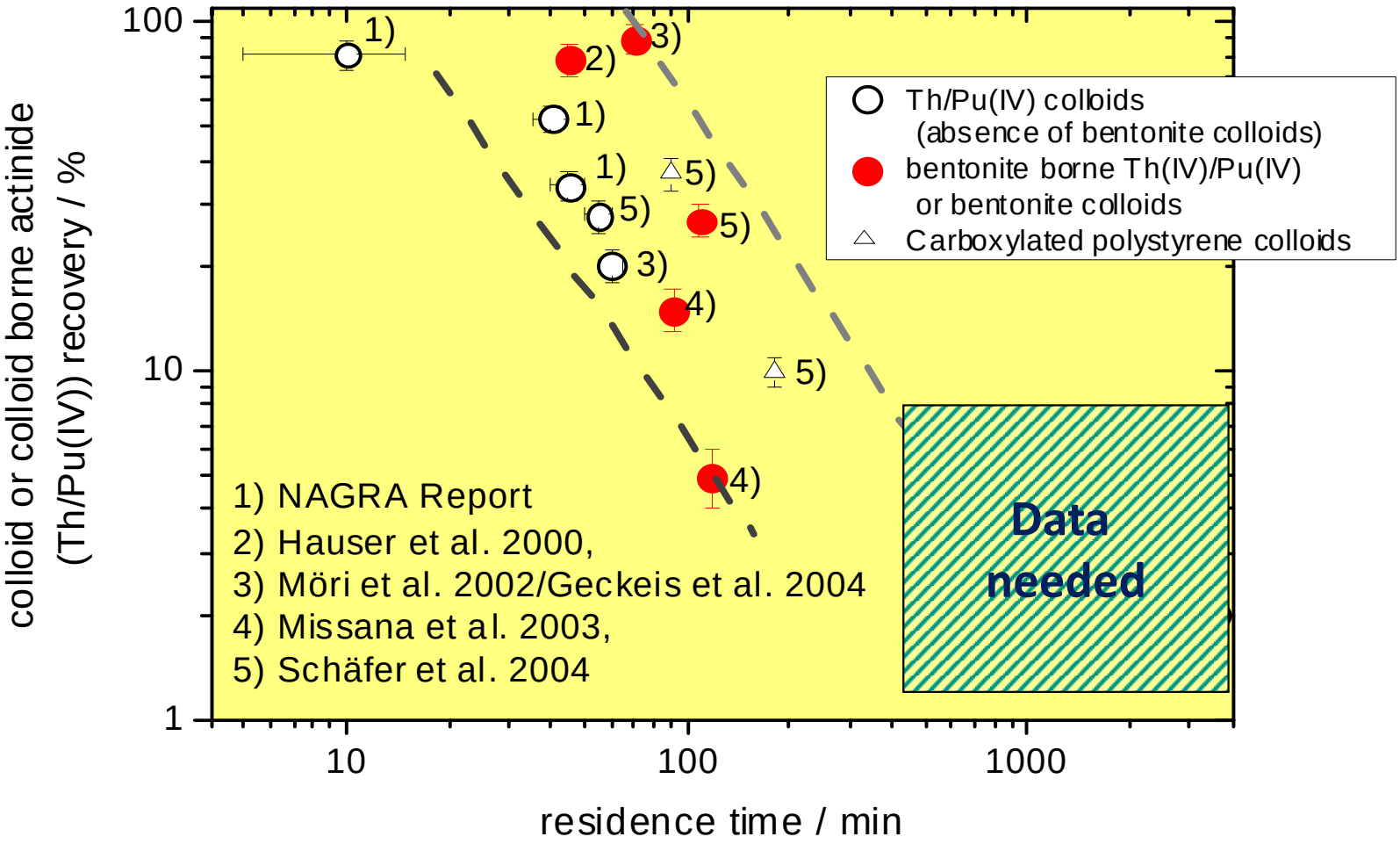

Tunnel sealing system and flow control

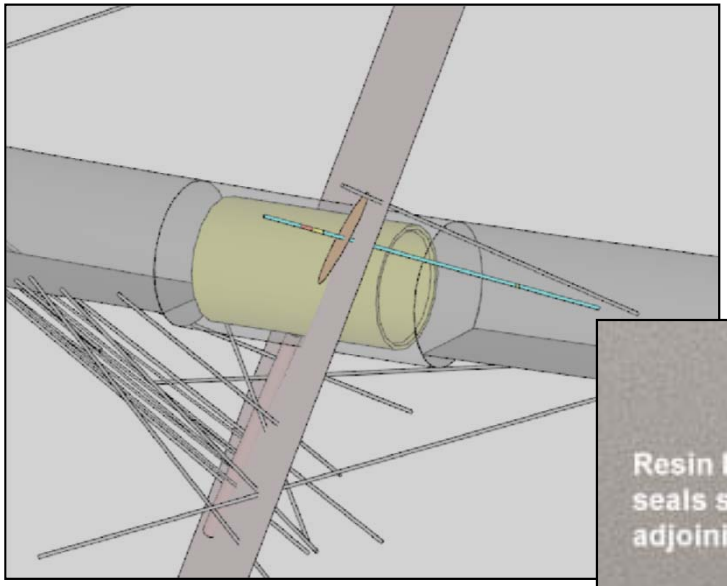

- Schematic of the site of the CFM in-situ experiment
- Schematic of the "*megapacker*" with its key elements and functionalities

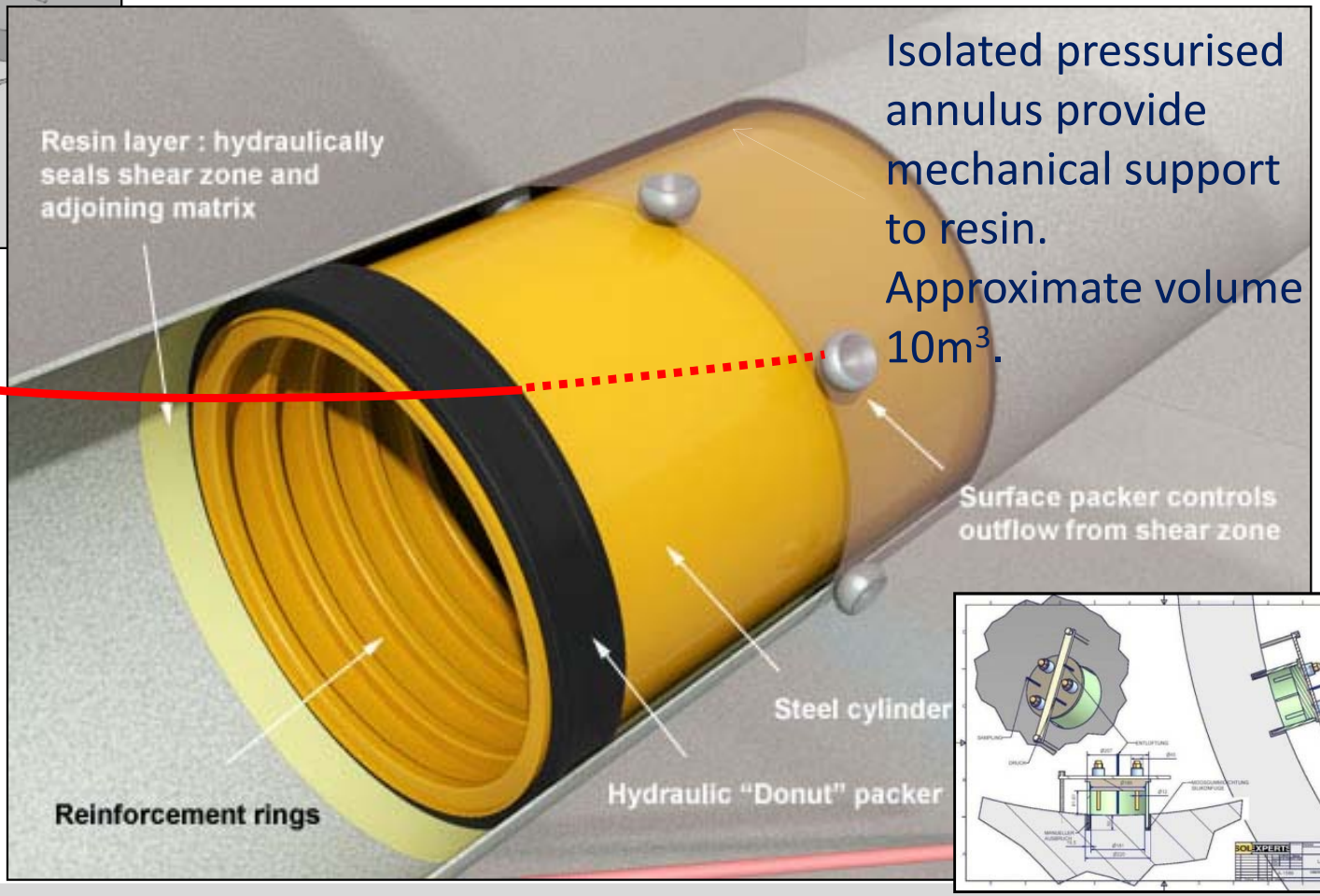

Extraction flow control and analysis

Hydraulic conditions established

- **Hydraulics of shear zone controlled by outflow from “Pinkel” surface packer.**
- **Under constant flow conditions:**
  - Head varies by ~1m over year due to influence of lake levels
  - Head difference/gradient is very stable <10mm
  - Gradient ~60mm/6m ~1%
- **Unique opportunity to study flow and transport at near repository conditions**

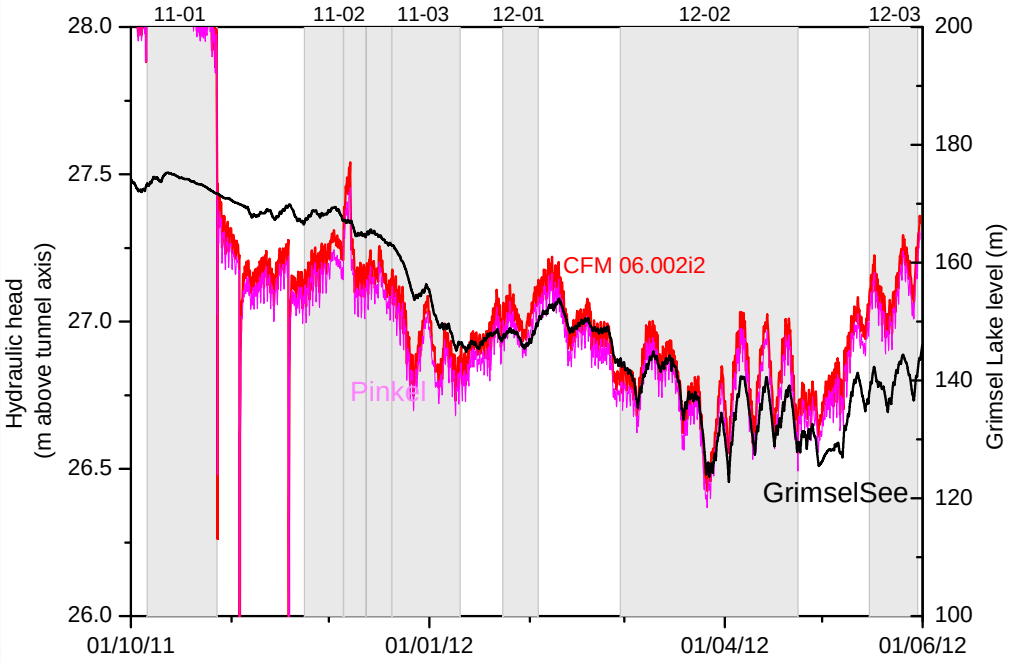

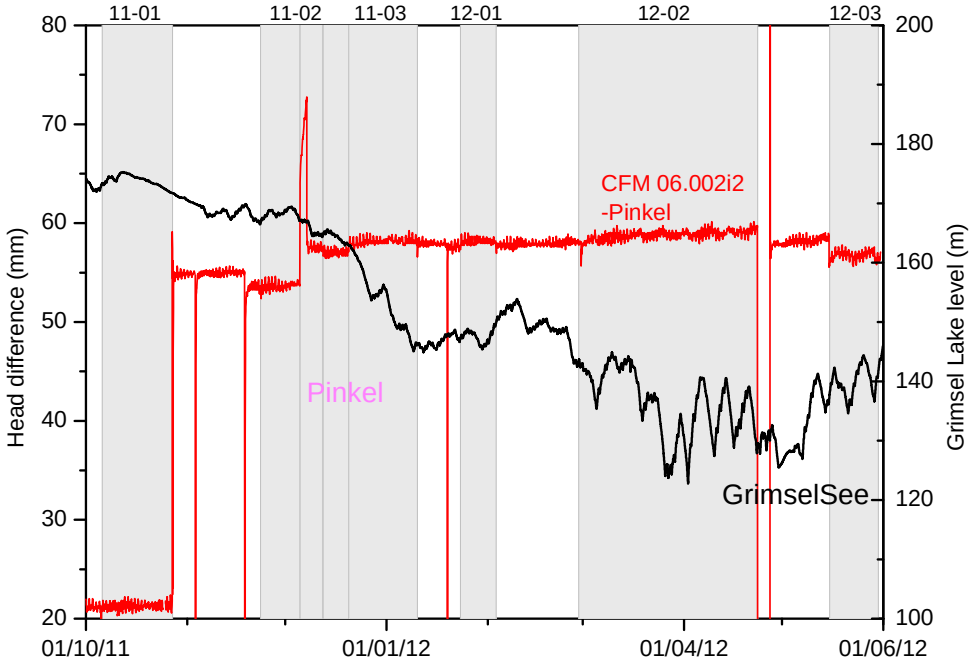

CFM project: Tracer Test Runs

- With different combinations of **homologues** or **RN's**, colloids and conservative tracers
- Injection into the MI shear zone in borehole CFM 06.002-i2 and extraction at the Pinkel surface packer

Run 08-01: direct tracer injection with 10 mL·min^{-1}; extraction flowrate 160 mL·min^{-1} (CRR configuration)

Run 10-01: tracer recirculation and 50 mL·min^{-1} extraction flowrate.

Run 10-03: tracer recirculation and 10 mL·min^{-1} extraction flowrate.

Run 12-02: tracer recirculation and 25 mL·min^{-1} extraction flowrate, slight injection with 0.33 mL·min^{-1}

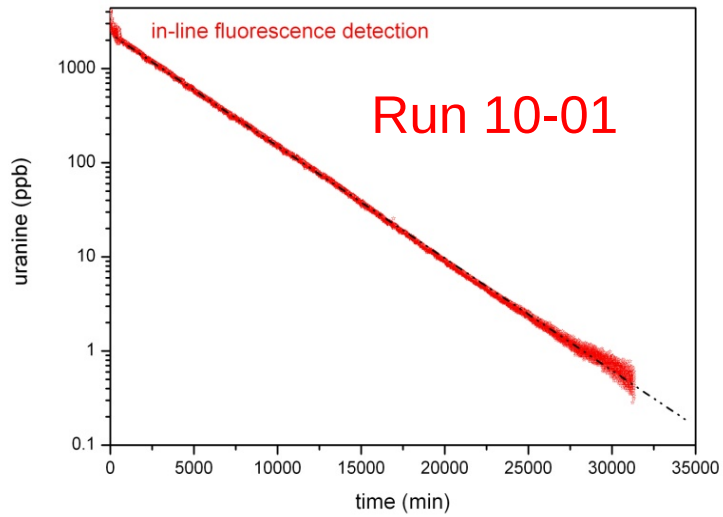

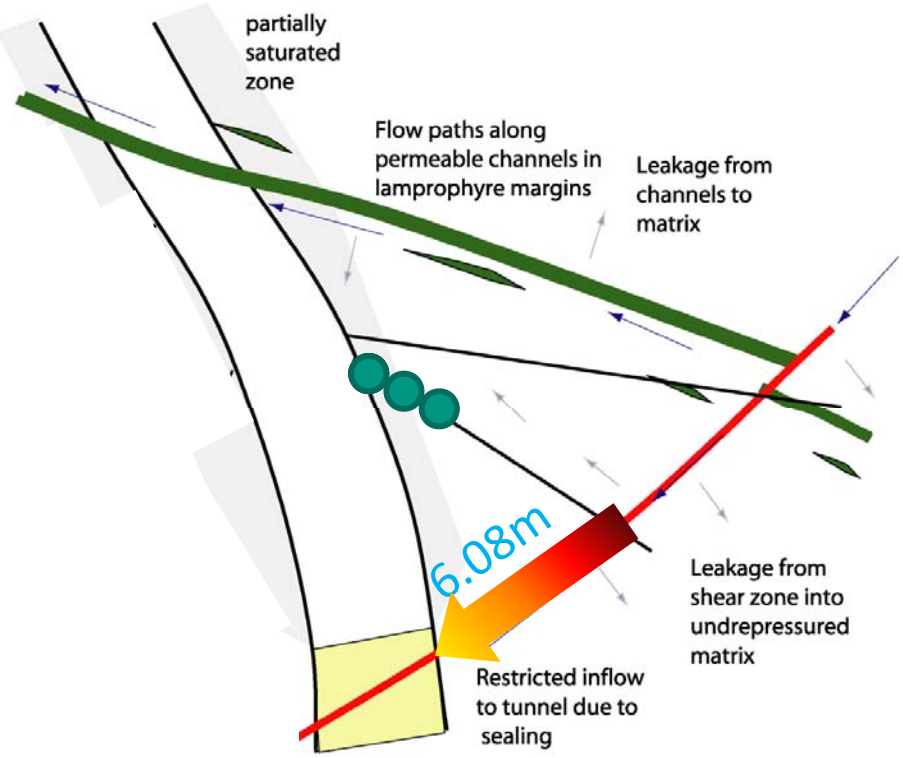

Injection Radionuclide cocktail: Run 12-02

- **Bentonite concentration:**
  - Total: 101.4 ± 2.5 mg/L
  - 8.9 ± 0.4 mg/L Ni-montmorillonite, rest Febex derived colloids
- **Conservative tracer Amino-G:**
  - 1646± 8 ppb
- **ICP-MS & gamma- spectrometry data**
- **Colloid association:**
  - Na-22: 0-3%, Cs-137: 97%, Ba-133: 24-34%
  - Am(III):100%, Th(IV):95-97%, Pu(IV):100%, Np(V):0%

Isotope	Half life	Reference date	Reference hour	Max. Activity based on license*	Total activity in emitter
Na-22	2.602 a	22.2.2012	12:00h	2.0 MBq	**1.17 MBq**
Ba-133	10.51 a	22.2.2012	12:00h	2.52 MBq	**1.97 MBq**
Cs-137	30.0 a	22.2.2012	12:00h	900 kBq	**785 kBq**
Th-232	1.41E10 a	22.2.2012	12:00h	8.5 mBq	**8 mBq**
Np-237	2.14E6 a	22.2.2012	12:00h	130 Bq	**119 Bq**
Am-243	7380 a	22.2.2012	12:00h	360 Bq	**290 Bq**
Pu-242	3.76E5 a	22.2.2012	12:00h	200 Bq	**190 Bq**

* BAG Bewilligungs-Nr. AG-1510.01.001

Breakthrough curves: Run 12-02

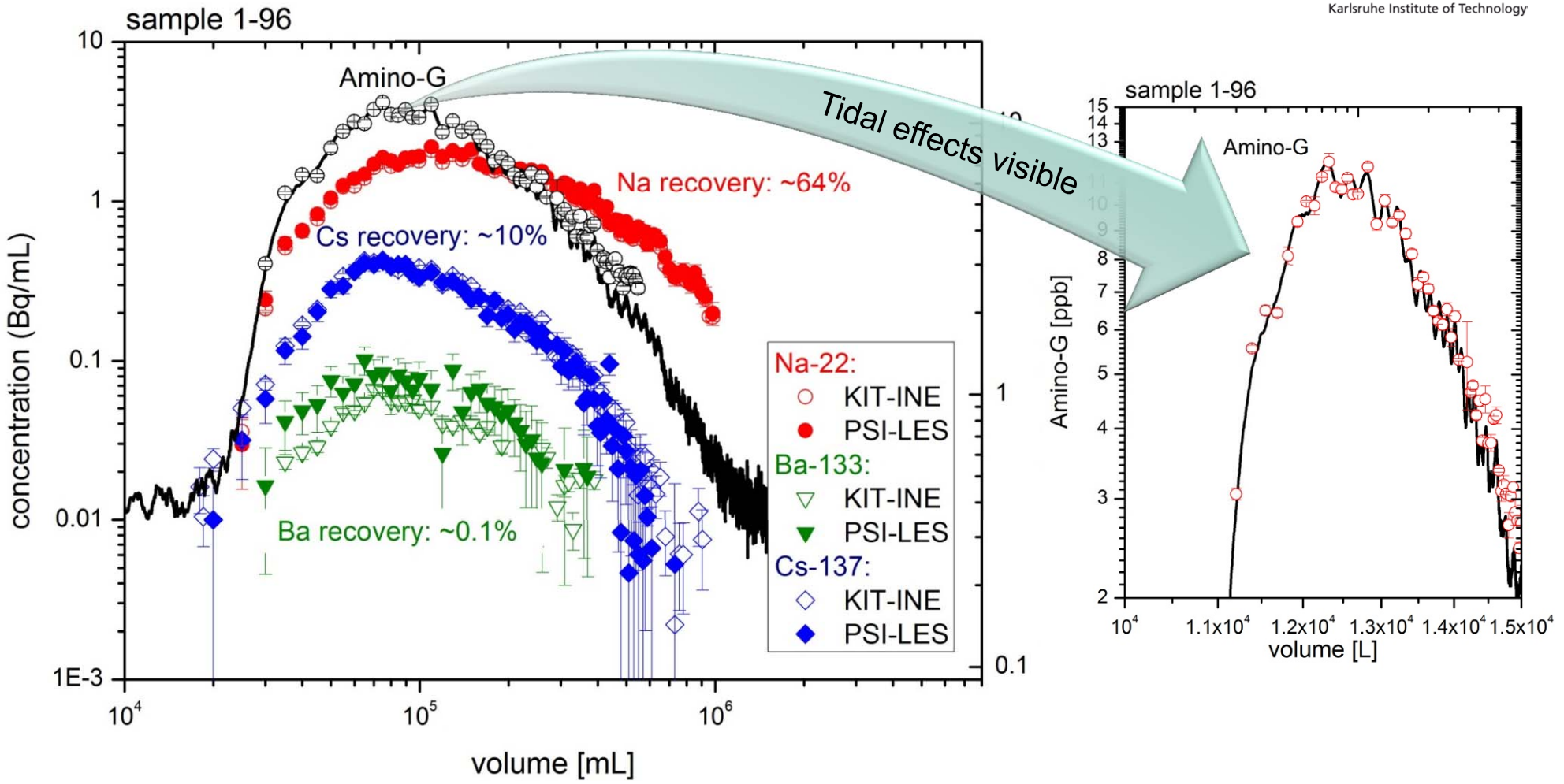

- ✓ Quantitative conservative tracer recovery (Amino-G)
- ✓ Dilution factor: **~137**
- ✓ Very good match between PSI-LES and KIT-INE data for gamma spectrometry

HR-ICP-MS results: Run 12-02 (first results)

^{242}Pu:

Recovery: ~124ng

Injected: 1266ng

=> ~10% recovery

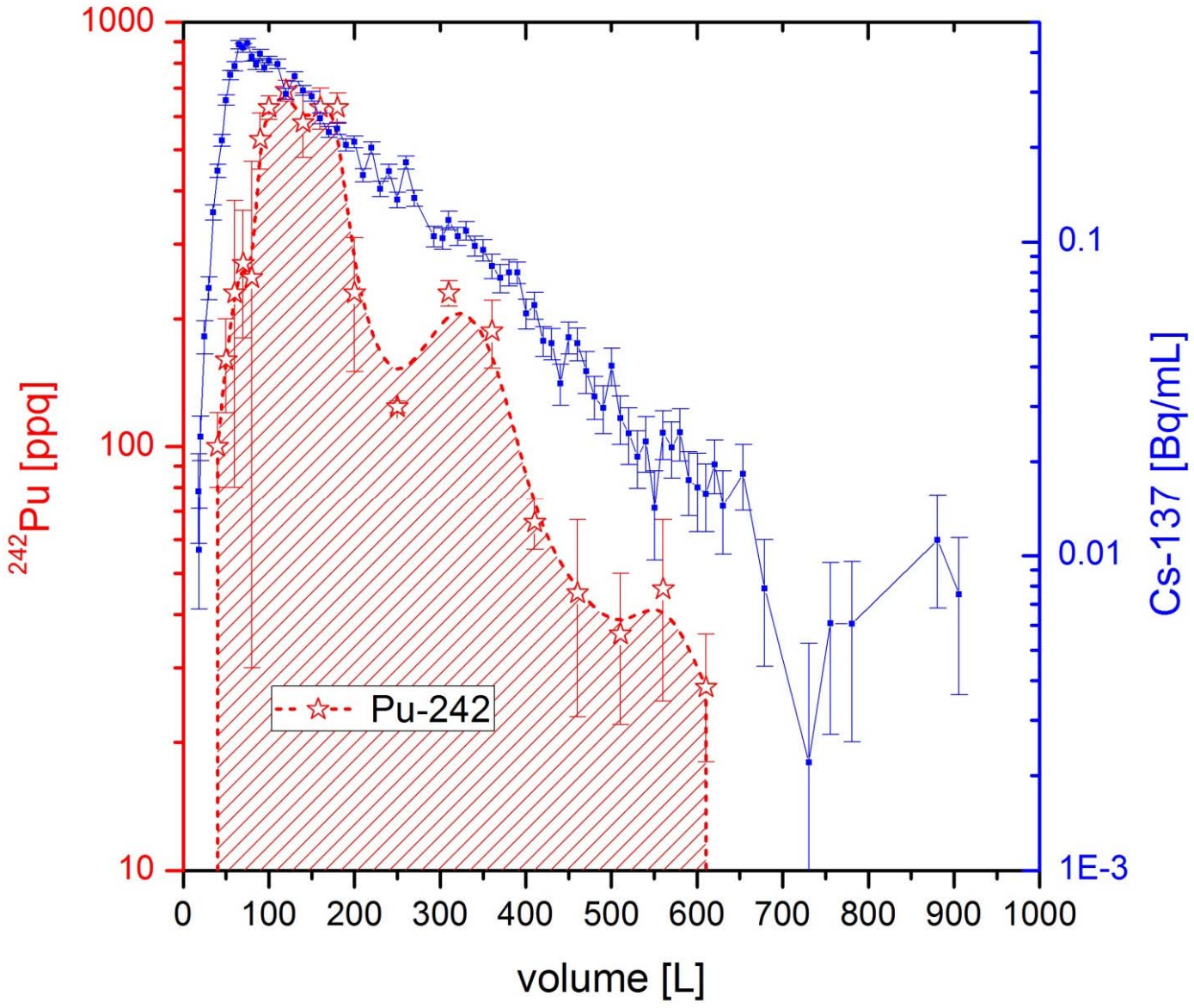

Units to deal with:

- **Mass units:**

  dilution:

- (milligram) mg/L or 1000 mg/m^3 or ppm (1 parts per million, 1/1000g per 1000g solution = 1/1,000,000) 10^{-6}
- (microgram) µg/L or 1mg/m^3 or ppb (1 parts per billion, = 1/1,000,000,000) 10^{-9}
- (nanogram) ng/L or 1µg/m^3 or ppt (1 parts per trillion = 1/1,000,000,000,000) 10^{-12}
- (picogram) pg/L or ppq (1 part per quadrillion = 1/1,000,000,000,000,000) 10^{-15}

What does ppq mean in reality?

⇒ **1ppq means 10 Swiss sugar cube (~4.4g each) homogeneously diluted in the volume of Lake Constance ~44g/48km³.**

On-site in-line LIBD measurements

- The INE mobile LIBD system (MOB2)

Laser-induced
Breakdown Detection (LIBD)

Single solid particles are ionized
in the focus of a laser beam;
Breakdown plasma formation;
Breakdown probability ~ f(N, d)
Laser energy dependency ~ f(d)

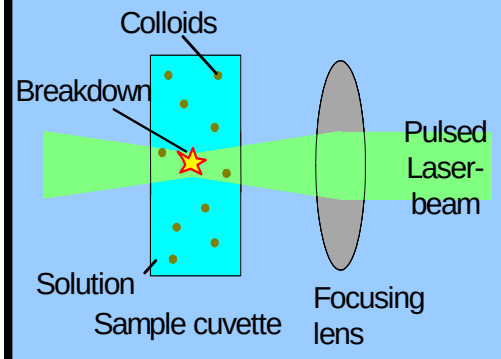

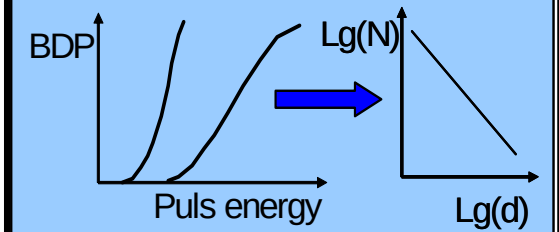

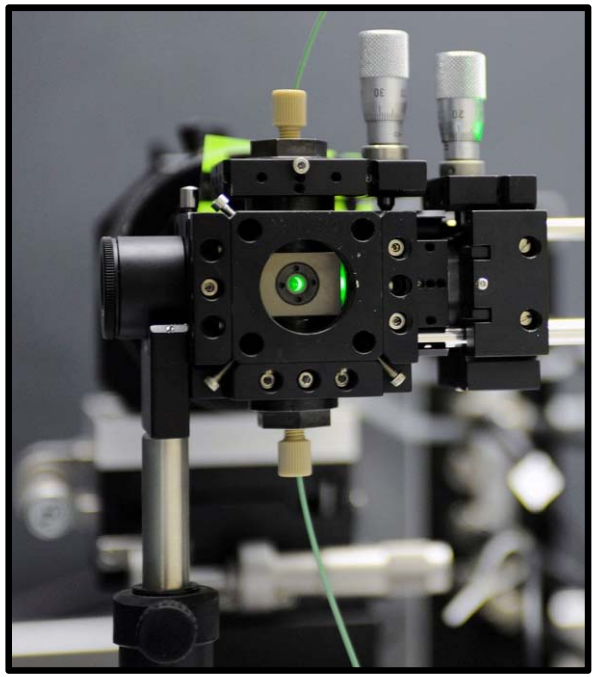

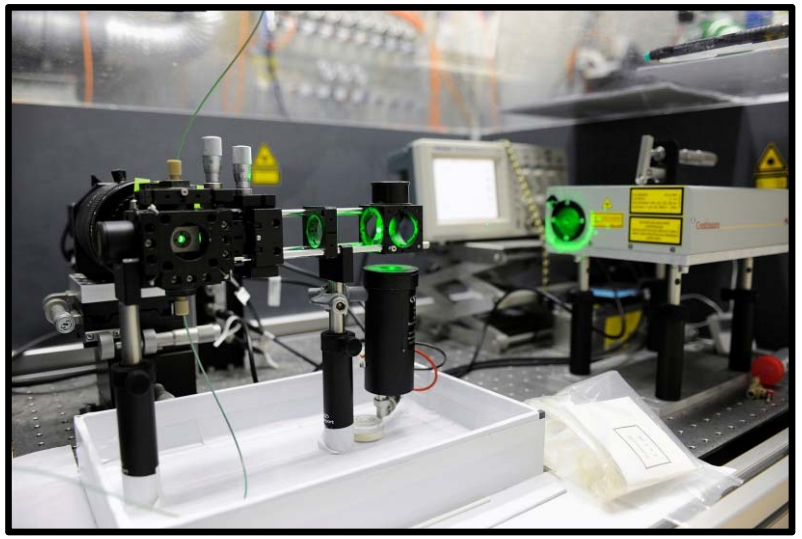

Colloid detection sites

INE (laboratory)

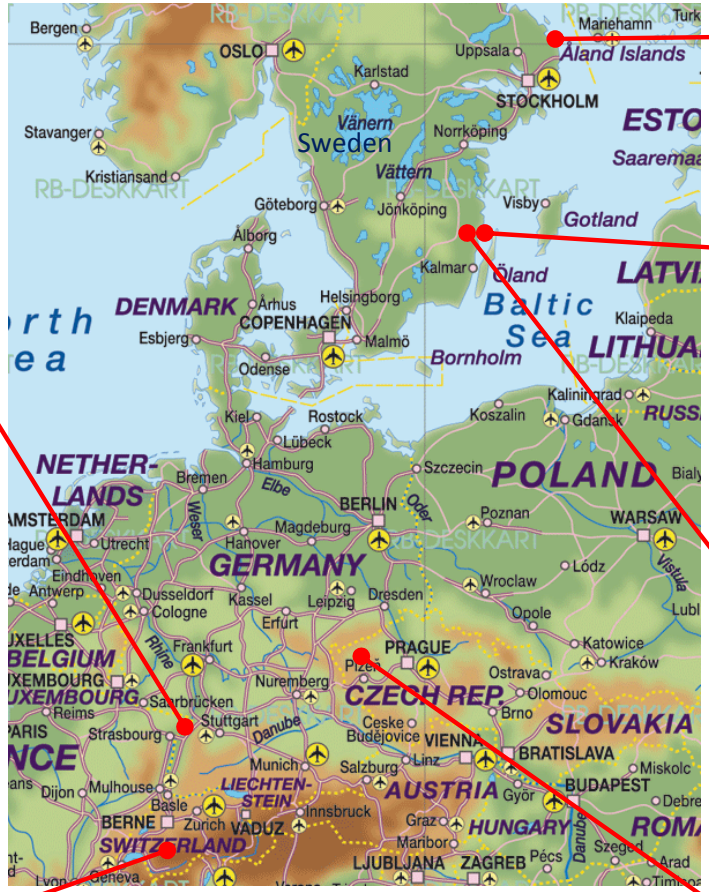

Forsmark (sampling cylinder)

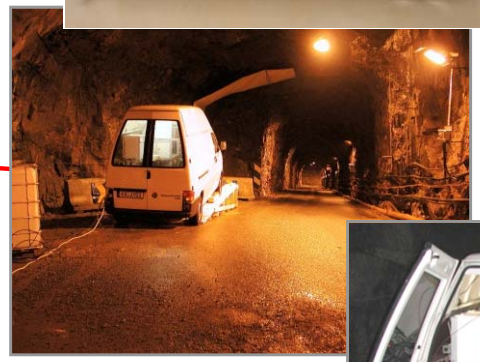

Äspö Underground Laboratory (in-situ)

SKB
Svensk Kärnbränslehantering AB

Laxemar (sampling cylinder)

Grimsel Test Site (in-situ)

nagra

Ruprechtov (remote operated sampling cylinder)

ÚJV
SÚRAO
GRS
Gesellschaft für Anlagen- und Reaktorsicherheit (GRS) mbH

On-site in-line LIBD measurements

- Colloid mass recovery
  - Mobile LIBD (MOB2)

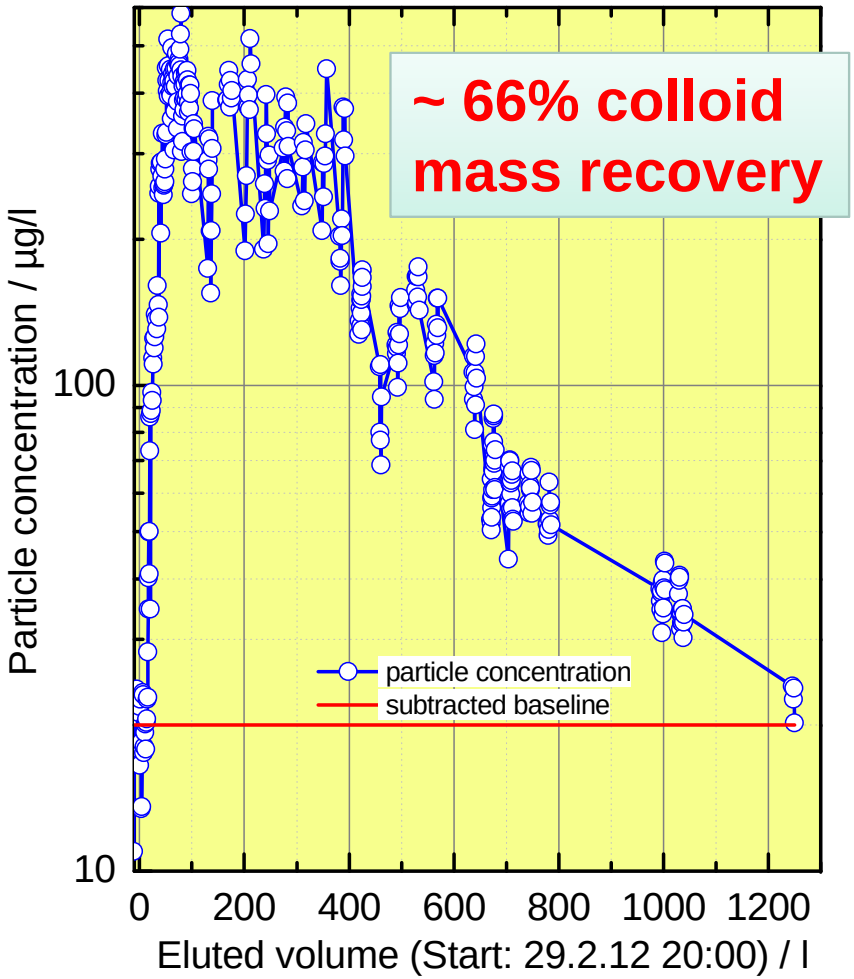

- Average colloid diameter

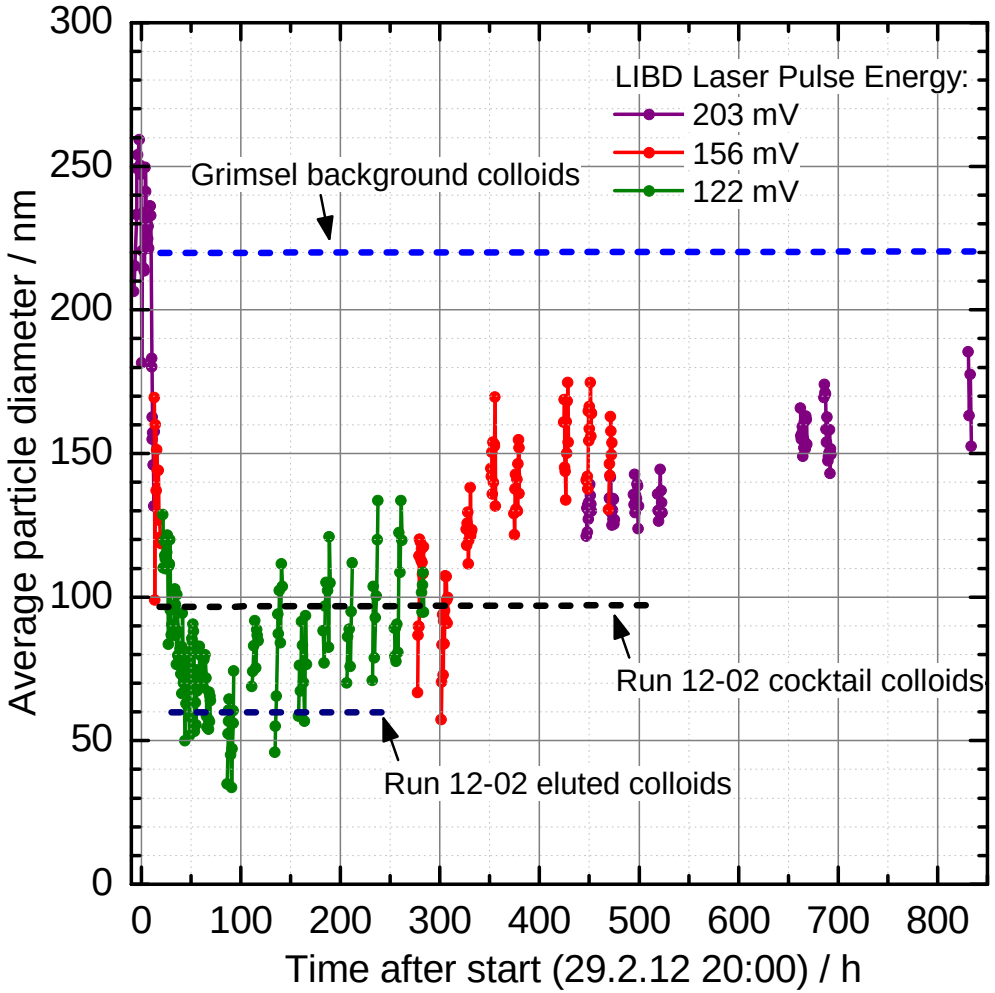

Synopsis of migration experiments

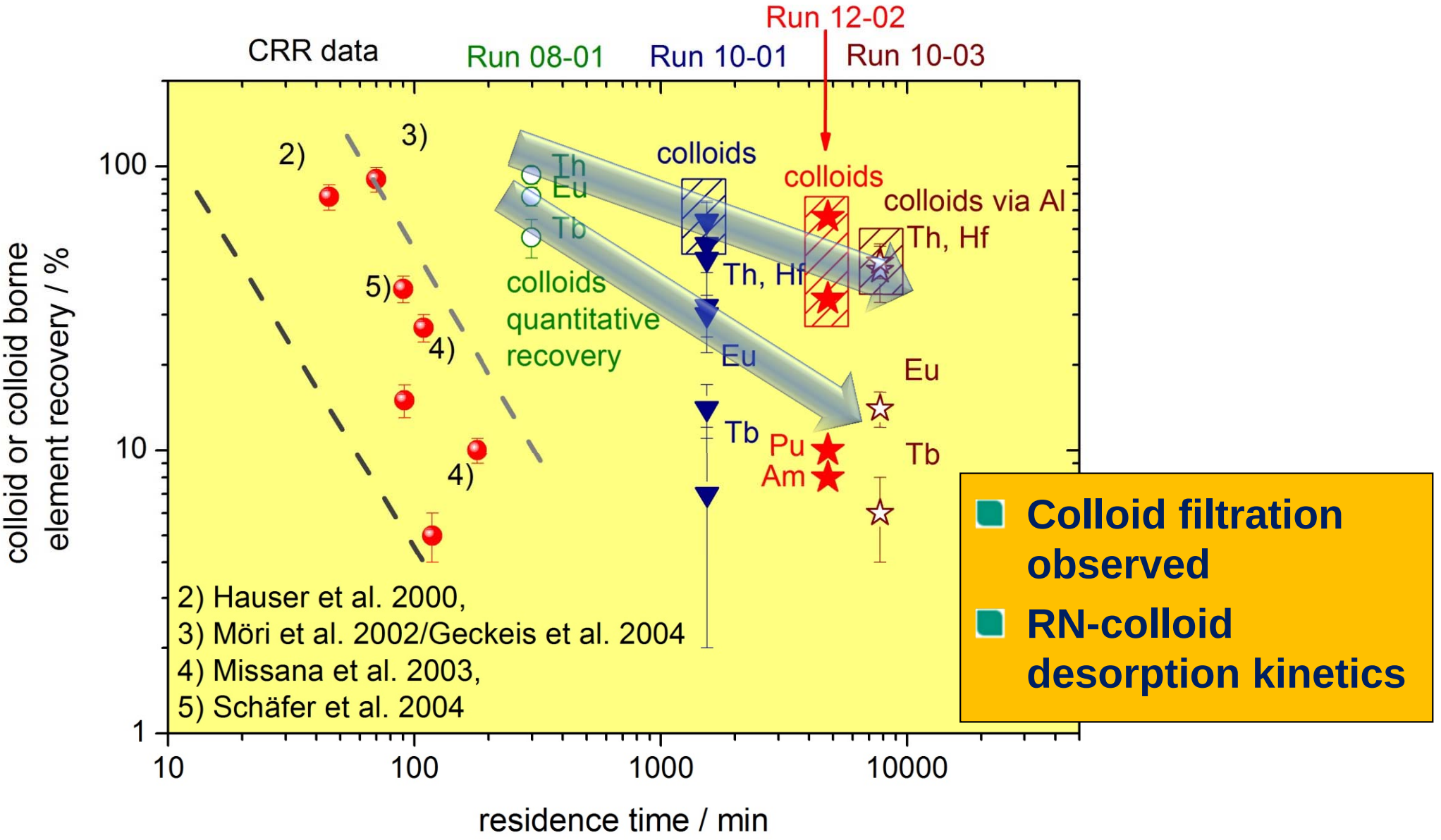

- **Colloid filtration observed**
- **RN-colloid desorption kinetics**

Does the field migration data fit to laboratory desorption experiments?

Huber et al. (2011) *Appl. Geochem.* 26, 2226-2237.

From binary system data
(Note: No colloid – FFM interaction)

$$R_{d,tot} = \frac{K_{d,FFM}}{1 + C_C \cdot K_{d,coll}}$$

*Binary data from NTB 03-02

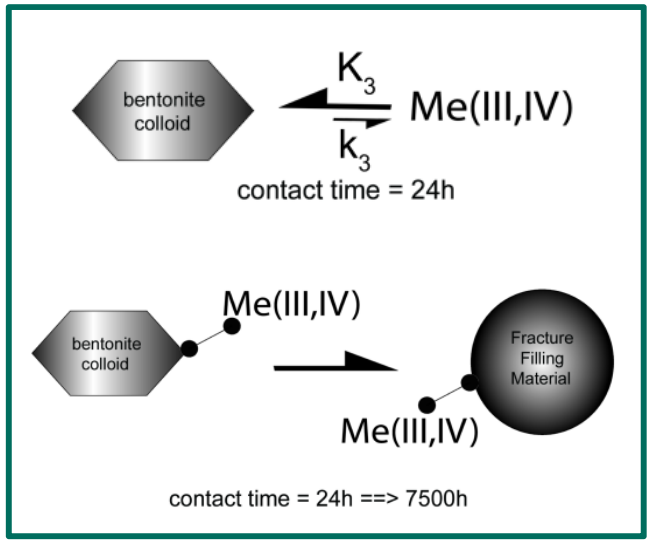

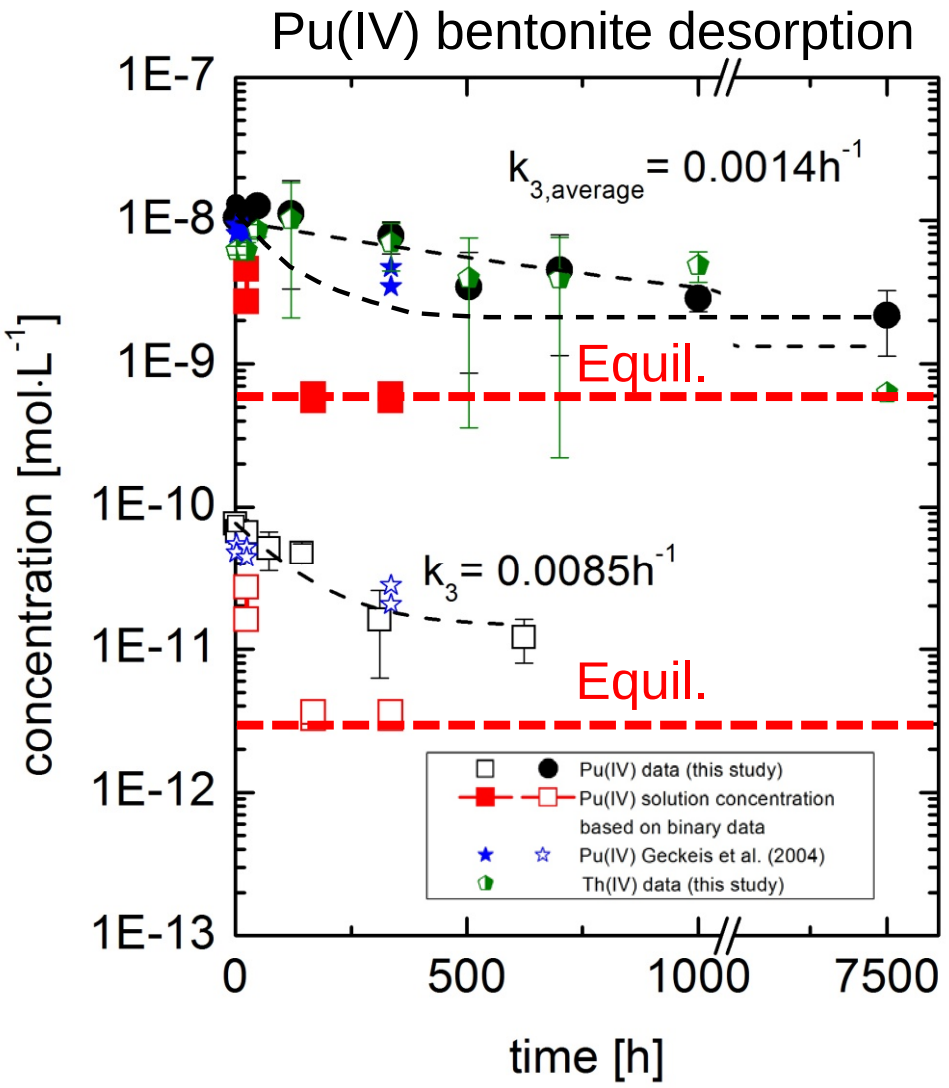

Modelling of tracer tests: Comparison RN reversibility

- Modelling of tracer migration tests
  - **GRS, KIT, LANL, Nagra, SKB/KTH**
- Homologue tracer tests 08-01,10-01,10-03 + conservative tracer tests
- **Model showing consistency in homologue sorption/ desorption and colloid filtration parameters between laboratory and in situ data.**

Laboratory experiment derived desorption rate

	Pu(IV)/Th(IV)	Am(III)
k_3 „high C“	0.0014hr^{-1}	0.0037hr^{-1}
k_3, „low C“	0.0085hr^{-1}	0.009hr^{-1}

RELAP-Model Test 10-03

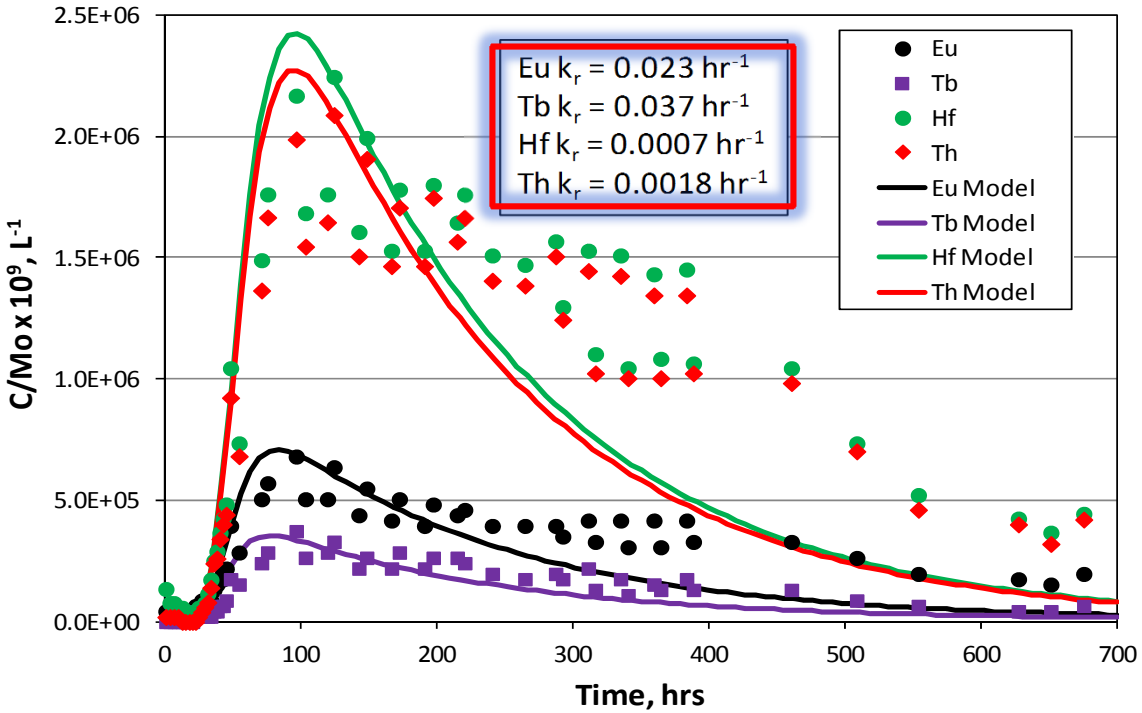

Conclusions (1/2)

- Control of the hydraulic system has allowed further decrease in gradients and consequent increase in travel time. The megapacker sealing system works well and is ready for the long-term in-situ experiment!
- Flow velocity and gradient in shear zone more relevant to post-closure situation: 1% gradient and ~10^{-5} m/s while maintaining high recovery.
- Reduction in hydraulic gradients has resulted in
  - Detection of influence of distant boundary conditions
  - Identification of cyclic flow and transport processes in shear zone
  - A conservative tracer has always to be added!
- In situ colloid/homologue tracer tests demonstrate:
  - Radionuclide/homologue colloid associated transport over increasing residence time detectable.
  - Colloid mobility highly sensitive to fracture geometry (flow path) and fracture surface roughness.
  - Radionuclide/Homologue recovery is in-line with batch data on bentonite sorption/reversibility studies.

Conclusions (2/2)

- **URL activities on radionuclide migration** (matrix diffusion & colloid migration) constitute an **up-scaling of laboratory experiments** and is an important part of the **confidence building and uncertainty reduction**.
- **Testing and development of conceptual and numerical models** of processes potentially relevant to radionuclide transport through rock.
- **Experiments related to long-term processes**, post-operational phases, e.g. bentonite buffer/backfill stability are necessary to obtain **mechanistic understanding of empirical correlations currently used in conceptual models under realistic conditions**.
- **Instrumentation experience** gained under real-site conditions especially on the **reliability of long-term monitoring** systems will **foster technical innovation and will therefore improve monitoring**.

thank you for your attention

2nd Chinese-German Workshop on Radioactive Waste Disposal
Karlsruhe, October 15-16, 2012

A fractional derivative approach to creep of salt rock

H. W. Zhou et al

State Key Laboratory of Coal Resources and Safe Mining
China University of Mining and Technology (Beijing)
Email: zhw@cumtb.edu.cn

Contents

1. Motivation

2. Fractional derivative approach: constant-viscosity

3. Laboratory experiments of salt rock creep

4. Fractional derivative approach: variable-viscosity

5. Conclusions

6. Furthermore works

1. Motivation: engineering background

Oil & gas storage

Nuclear waste disposal

CO_2 emission

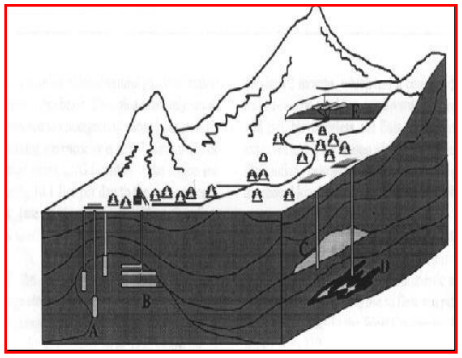

- Low permeability
- Low porosity
- Good performance in mechanics

Salt rock: An ideal medium for the underground energy storage, for disposal of CO2 and high-level radioactive

1. Motivation: problem

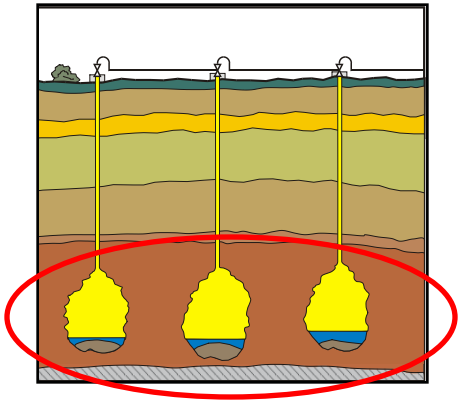

Decrease of effective storage volume

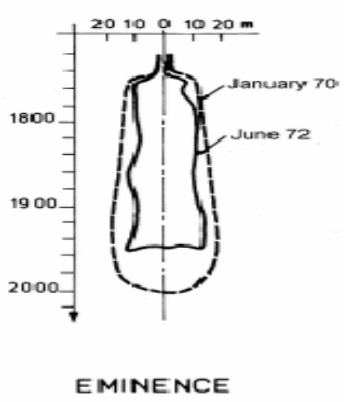

Eminence in USA

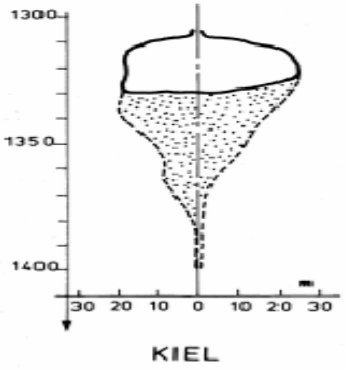

Kiel in Germany

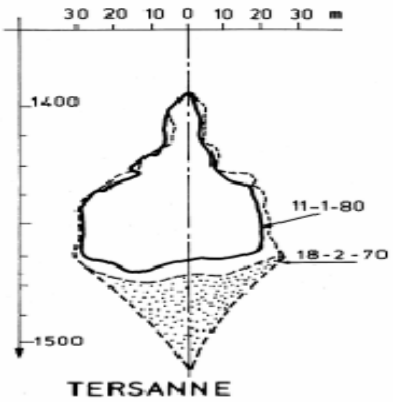

Tersanne in France

(Berest and Brouard, 2003)

Reason

- Variation of the internal pressures
- Time-dependent behavior of salt rock

How we predict the large deformation of salt rock in a long term service: Time-dependent behavior of salt rock?

1. Motivation: experimental study

Laboratory experiment of salt rock creep

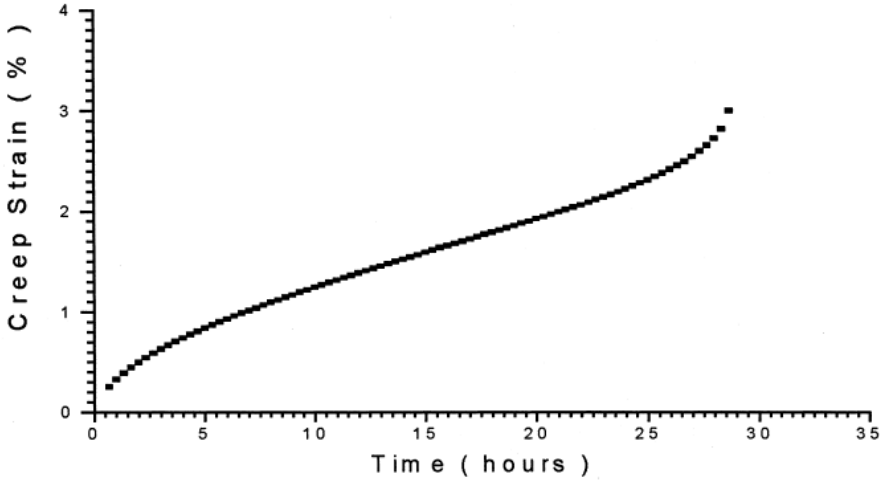

(Yang et al, 1999)

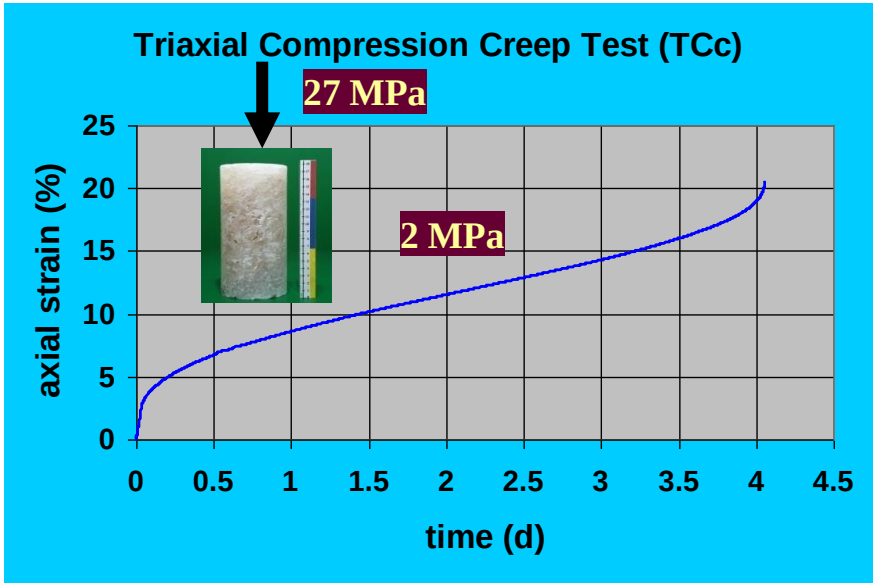

(Hou et al, 2004)

How we get a modeling?

1. Motivation: modeling

- Empirical models: fewer parameters but long experimental time.
- Component models: the advantage of flexible description of different creep deformations and the disadvantage of a mathematical complexity of a creep constitutive equation, such as Maxwell, Kelvin, Bingham, …
- Mechanism-based creep constitutive models: cracking and damage growth at the micro-scale

such as Urai, Chris Spiers, Hendrik, Zwart, Lister. Nature 324, 1986

1. Motivation: modeling

Change our channel:

the application of fractional calculus to viscoelastic and viscoplastic relations?

Component models + Fractional derivative

→ Fractional derivative approach: constant-viscosity

Creep damage + Fractional derivative

→ Fractional derivative approach: variable-viscosity

1. Introduction: meaning of derivative

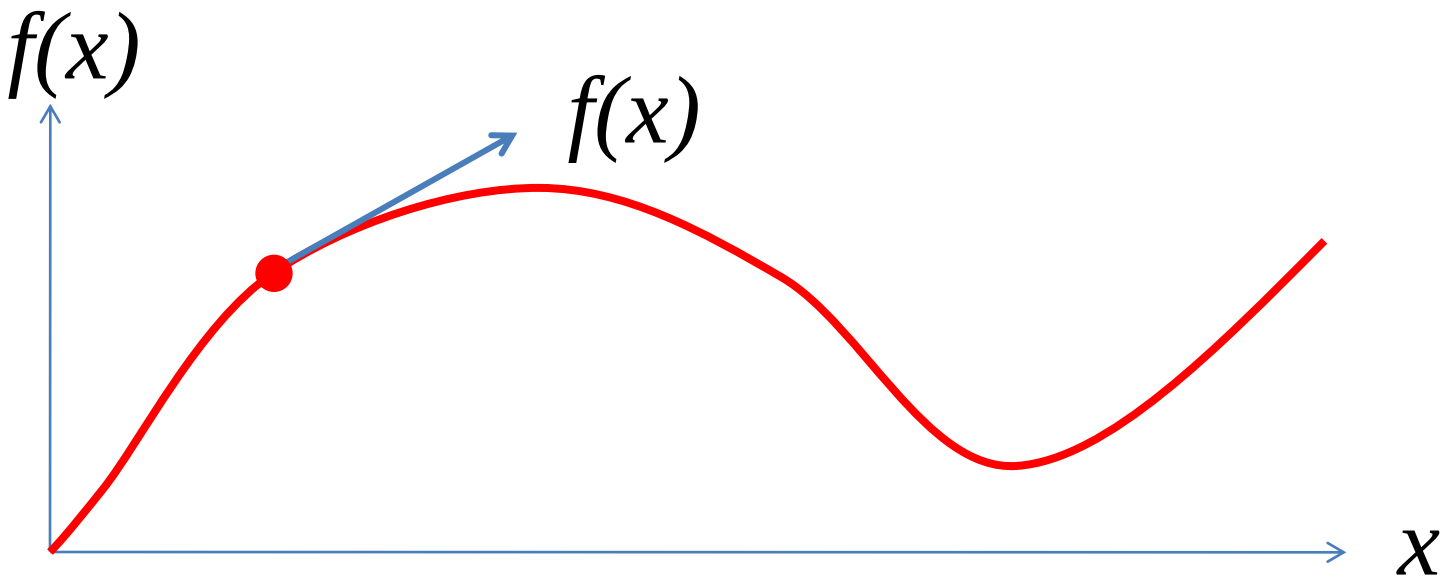

The first order integer derivative with respect to x

$$f'(x) = \frac{df(x)}{dx}$$

may be tangent direction geometrically

or speed physically

What if the order will be 1/2 ?

1. Motivation: beginning of fractional derivative

Inventor of derivative and integration

①

②

Introducer of derivative and integration

Leibniz (1646-1716)

L'Hospital (1661-1704)

Nova Methodus pro Maximis et Minimis (1684)

L'analyse des infiniment petits pour l'intelligence des lignes courbes (1696)

① *What if the order will be 1/2* ?

② *It will lead to a paradox, from which one day useful consequences will be drawn (*September 30th, 1695*)*

Can the meaning of derivatives with integer order be generalized to derivatives with non-integer orders?

1. Motivation: remarkable contributions

Euler
1707-1783

Laplace
1749-1827

Fourier
1768-1830

Abel
1802-1829

Liouville
1809-1882

Riemann
1826-1866

$$\frac{\mathrm{d}^{\frac{1}{2}} f(t)}{\mathrm{d}t^{\frac{1}{2}}} = \frac{1}{\sqrt{\pi}} \frac{\mathrm{d}}{\mathrm{d}t} \int_0^t \frac{f(\tau)}{(t-\tau)^{\frac{1}{2}}} \mathrm{d}\tau \qquad f(t)=t \Longrightarrow \frac{\mathrm{d}^{\frac{1}{2}} t}{\mathrm{d}t^{\frac{1}{2}}} = \frac{2}{\sqrt{\pi}} t^{1/2}$$

which definition of a ½-order was introduced by Laplace in 1812.

1. Motivation: Abel's contributions

The first use of fractional operation was given by Abel in 1823.

Niels Henrik Abel
(1802–1829)

In 1823, Abel wrote a paper in French. It was "a general representation of the possibility to integrate all differential formulas" (Norwegian: en alminnelig Fremstilling af Muligheten at integrere alle mulige Differential-Formler). Because of it, Abel's work was regarded as the first use of fractional calculus.

1. Motivation: recent publications

G. W. Scott Blair. The role of psychophysics in rheology. Journal of Colloid Science, 1947, Vol.2, pp.21-32

$$\sigma = G\lambda^{\xi} \frac{\mathrm{d}^{\xi}\varepsilon}{\mathrm{d}t^{\xi}}, \quad (0 \le \xi \le 1)$$

1000 papers (more or less) in journal and proceedings per year.

Herrmann, R. Fractional Calculus: An Introduction for Physicists (2011)
Ortigueira, M.D. Fractional Calculus for Scientists and Engineers (2011)
Mainardi, F. Fractional Calculus and Waves in Linear Viscoelasticity (2010)
Podlubny, I. Fractional Differential Equations (1999)

2. Fractional derivative approach: the Able dashpot

Abel dashpot

The constitutive relation: $\sigma(t) = \eta^{\gamma} D^{\gamma}\left[\varepsilon(t)\right] \quad (0 \le \gamma \le 1)$

Special cases:

① $\gamma = 0 \longrightarrow \sigma(t) = C$ Hooke body, an ideal solid.

② $\gamma = 1 \longrightarrow \sigma(t) = \eta\varepsilon'(t)$ Newtonian body, an ideal fluid.

The Abel dashpot describe a material between an ideal solid and an ideal fluid.

2. Fractional derivative approach: the Able dashpot

Let $\sigma(t) = \sigma = \text{const}$, then $\varepsilon(t) = \dfrac{\sigma}{\eta} \dfrac{t^{\gamma}}{\Gamma(1+\gamma)}, (0 \le \gamma \le 1).$

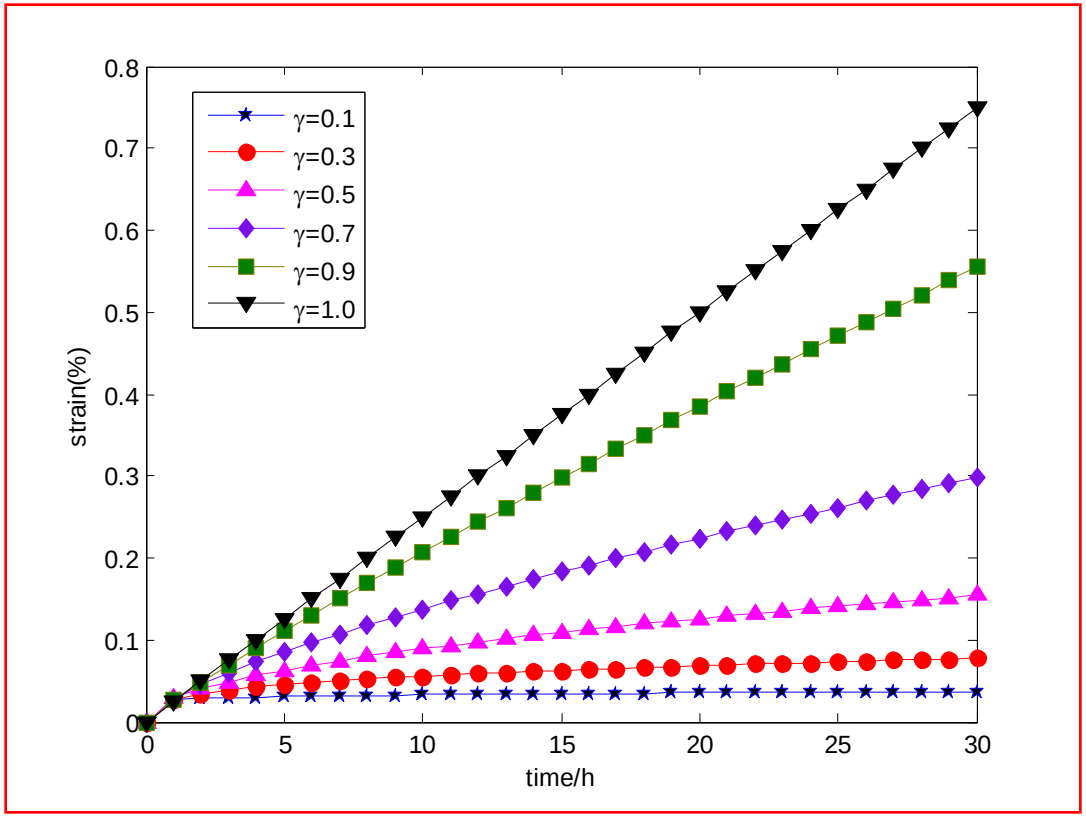

$\sigma = 20Mpa \quad \eta = 0.8Gpa \cdot h$

2. Fractional derivative approach: a new model

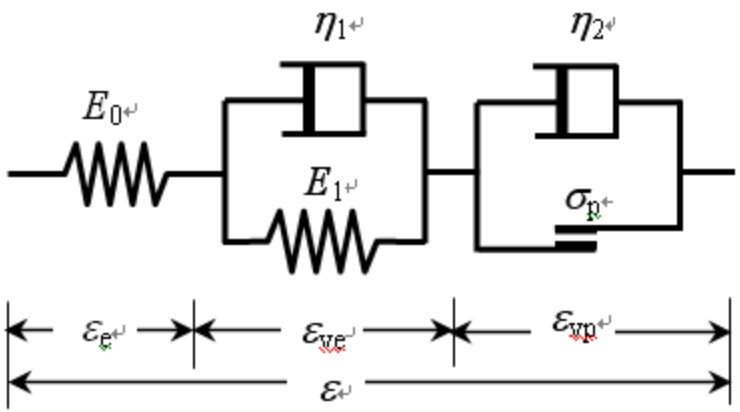

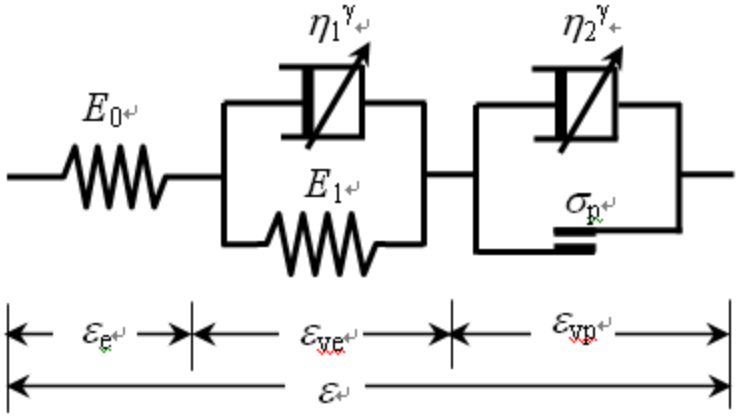

(a) Nishihara model

(b) Fractional derivative model

$$\varepsilon(t)=\begin{cases}\dfrac{\sigma}{E_0}+\dfrac{\sigma}{E_1}\left(1-e^{-\frac{E_1}{\eta_1}t}\right), & \sigma<\sigma_s\\ \dfrac{\sigma}{E_0}+\dfrac{\sigma}{E_1}\left(1-e^{-\frac{E_1}{\eta_1}t}\right)+\dfrac{\sigma-\sigma_s}{\eta_2}t, & \sigma\geq\sigma_s\end{cases}$$

$$\varepsilon(t)=\begin{cases}\dfrac{\sigma}{E_0}+\dfrac{\sigma}{\eta_1^{\gamma}}\displaystyle\sum_{k=0}^{\infty}\frac{\left(-\frac{E_1}{\eta_1^{\gamma}}\right)^k t^{r(1+k)}}{\gamma(1+k)\Gamma\left[(1+k)\gamma\right]} & (\sigma<\sigma_s)\\ \dfrac{\sigma}{E_0}+\dfrac{\sigma}{\eta_1^{\gamma}}\displaystyle\sum_{k=0}^{\infty}\frac{\left(-\frac{E_1}{\eta_1^{\gamma}}\right)^k t^{\gamma(1+k)}}{\gamma(1+k)\Gamma\left[(1+k)\gamma\right]}+\dfrac{\sigma-\sigma_s}{\eta_2^{\gamma}}\dfrac{t^{\gamma}}{\Gamma(1+\gamma)} & (\sigma\geq\sigma_s)\end{cases}$$

2. Fractional derivative approach: parameter determination

Least-square analysis

Using the experimental data of time-dependent deformation of salt rock under uniaxial compression (Hou, 1997), we determine the parameters of the fractional model data.

$$\varepsilon(t)=\frac{\sigma}{E_0}+\frac{\sigma}{E_1}-\frac{\sigma}{E_1}E_\gamma\left(-\frac{E_1}{\eta_1^{\gamma}}t^{\gamma}\right)+\frac{\sigma-\sigma_s}{\eta_2^{\gamma}}\frac{t^{\gamma}}{\Gamma(1+\gamma)}$$

Mittag-Leffler function: $E_\gamma(x)=\sum_{n=0}^{\infty}\frac{x^n}{\Gamma(1+\gamma n)}$

$E_0, E_1, \eta_1^{\gamma}, \eta_2^{\gamma}, \gamma$ can be determined by a least-squares function, *i.e.*,

$$\varepsilon_{LS}(E_0, E_1, \eta_1^{\gamma}, \eta_2^{\gamma}, \gamma)=\sum_{i=1}^{N}\{\varepsilon_i-\varepsilon(t_i)\}^2$$

2. Fractional derivative approach: parameter determination

The fractional model adequately represents the time-dependent deformation of salt rock.

Parameters determined by fitting analysis

E_0 (Gpa)	E_1 (Gpa)	η_1^γ (Gpa·h$^\gamma$)	η_2^γ (Gpa·h$^\gamma$)	γ	Least-squares error
22.98	9.88	1.23	13.76	0.31	4.31×10^{-5}

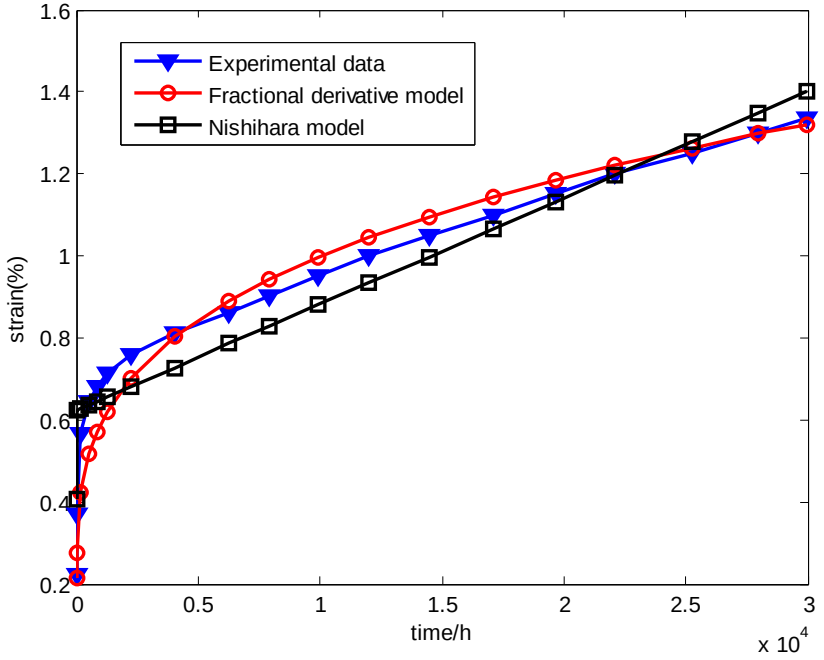

Laboratory experimental conditions of salt rock: uniaxial load: 14.1Mpa, temperature: room, period: 1256 days (Hou, 1997)

2. Fractional derivative approach: sensitivity study

- *Effect of the fractional derivative order*

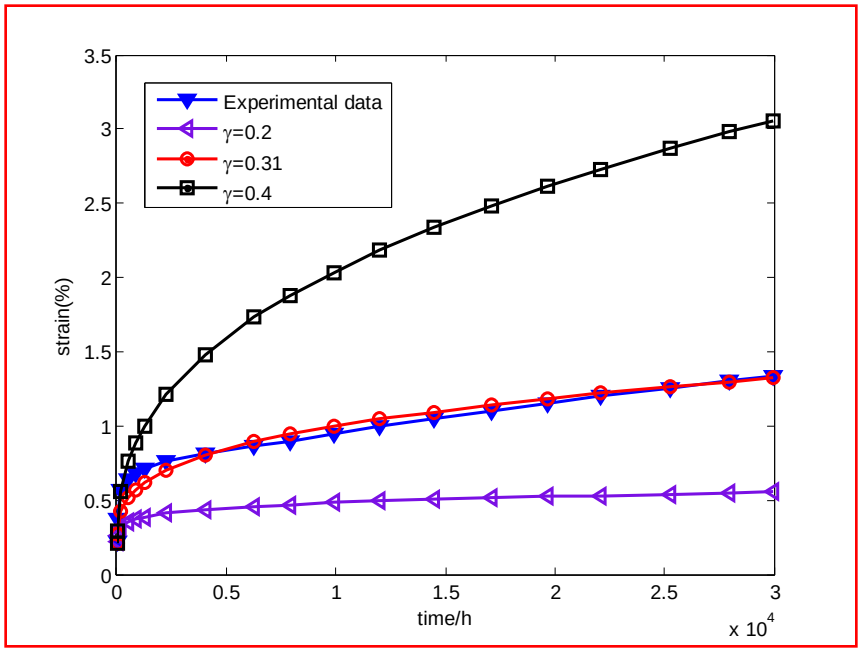

$\sigma \geq \sigma_s \quad \sigma = 14.1Mpa, \sigma_s = 8.46Mpa, E_0 = 22.98Gpa$

$\eta_1^\gamma = 1.23Gpa \bullet h^\gamma, E_1 = 9.88Gpa, \eta_2^\gamma = 13.76$

The higher the fractional derivative order, the higher the creep strain.

- *Effect of the stress level*

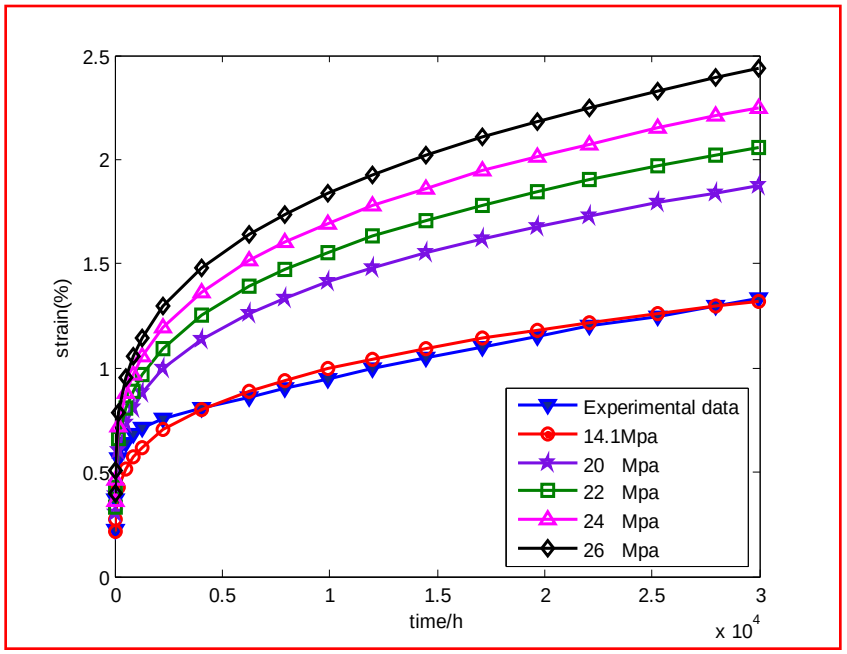

$\sigma_s = 8.46Mpa, E_0 = 22.98Gpa, E_1 = 9.88Gpa$

$\eta_1^\gamma = 1.23Gpa \bullet h^\gamma, \eta_2^\gamma = 13.76, \gamma = 0.31$

The higher the stress level, the higher the creep strain.

2. Fractional derivative approach: a special case

- *Discussion: fractional Nishihara model in the case of* $\gamma = 1$

$$\varepsilon(t) = \begin{cases} \dfrac{\sigma}{E_0} + \dfrac{\sigma}{E_1}\displaystyle\sum_{k=1}^{\infty} \dfrac{(-1)^{k+1}\left(\dfrac{E_1}{\eta_1}t\right)^k}{k!}, & \sigma < \sigma_s \\ \dfrac{\sigma}{E_0} + \dfrac{\sigma}{E_1}\displaystyle\sum_{k=1}^{\infty} \dfrac{(-1)^{k+1}\left(\dfrac{E_1}{\eta_1}t\right)^k}{k!} + \dfrac{\sigma-\sigma_s}{\eta_2}t, & \sigma \geq \sigma_s \end{cases} \xrightarrow{\gamma = 1} \varepsilon(t) = \begin{cases} \dfrac{\sigma}{E_0} + \dfrac{\sigma}{E_1}\left(1 - e^{-\frac{E_1}{\eta_1}t}\right), & \sigma < \sigma_s \\ \dfrac{\sigma}{E_0} + \dfrac{\sigma}{E_1}\left(1 - e^{-\frac{E_1}{\eta_1}t}\right) + \dfrac{\sigma-\sigma_s}{\eta_2}t, & \sigma \geq \sigma_s \end{cases}$$

Fractional derivative model

Nishihara model

Nishihara model is a special case of the fractional model.

International Journal of Rock Mechanics & Mining Sciences 48 (2011) 116–121

Contents lists available at ScienceDirect

International Journal of
Rock Mechanics & Mining Sciences

journal homepage: www.elsevier.com/locate/ijrmms

A creep constitutive model for salt rock based on fractional derivatives

H.W. Zhou*, C.P. Wang, B.B. Han, Z.Q. Duan

State Key Laboratory of Coal Resources and Safe Mining, China University of Mining and Technology, Beijing 100083, China

ARTICLE INFO

Article history:
Received 1 February 2010
Received in revised form
12 July 2010
Accepted 17 November 2010

Keywords:
Salt rock
Creep constitutive model
Time-based fractional derivative
Nishihara model
Parameter fit analysis

ABSTRACT

By replacing a Newtonian dashpot in the classical Nishihara model with the fractional derivative Abel dashpot, a new creep constitutive model is proposed on the basis of time-based fractional derivative. The analytic solution for the fractional derivative time-dependent constitutive model is given. The parameters of the fractional derivative model and the Nishihara model are determined by fitting to existing experimental results of time-dependent deformation of salt rock. The results estimated by the fractional derivative model proposed in the paper are in better agreement with the experimental data than the results estimated by the Nishihara model. A sensitivity study for the analytic solution of the time-based fractional derivative model is carried out, showing the effects of fractional derivative order and stress level on creep strain of salt rock. It is shown that the time-based fractional derivative model can be simplified to the Nishihara model for the special case of fractional derivative order equal to 1.0.

© 2010 Elsevier Ltd. All rights reserved.

H. W. Zhou, C. P. Wang, B. B. Han, Z. Q. Duan. *International Journal of Rock Mechanics and Mining Sciences*, 2011, 48(1), 116-121

3. Laboratory experiments of salt rock creep: sampling

Chuwang Well No. 1 at depth of 1982 m from ground surface, Jianghan Oilfield, Hubei Province, Central China

Sample No.	Weight/g	Diameter/mm	Height/mm
RS01a	1430.35	75.01	150.14
RS02a	1473.83	75.03	149.98
RS05a	1447.25	75.22	150.22

3. Laboratory experiments of salt rock creep: setup

(at Sichuan University, Chengdu, China)

- Uniaxial loading: stress level at 4Mpa, 6Mpa, 8Mpa …
- Measurement of axial displacement: displacement sensor

3. Laboratory experiments of salt rock creep

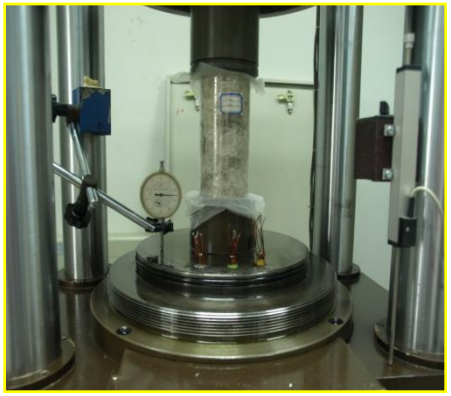

RS01a (140 days)

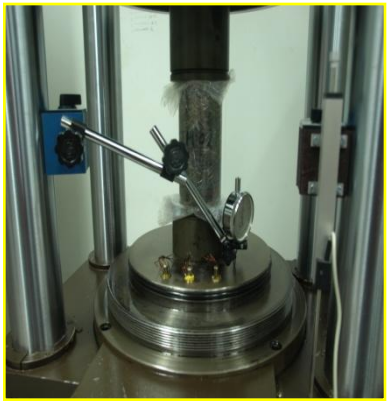

RS02a (157 days)

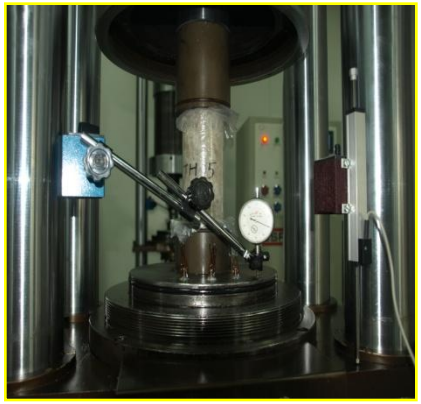

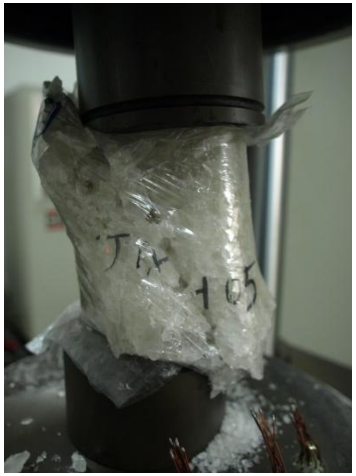

RS05a (136 days)

3. Laboratory experiments of salt rock creep

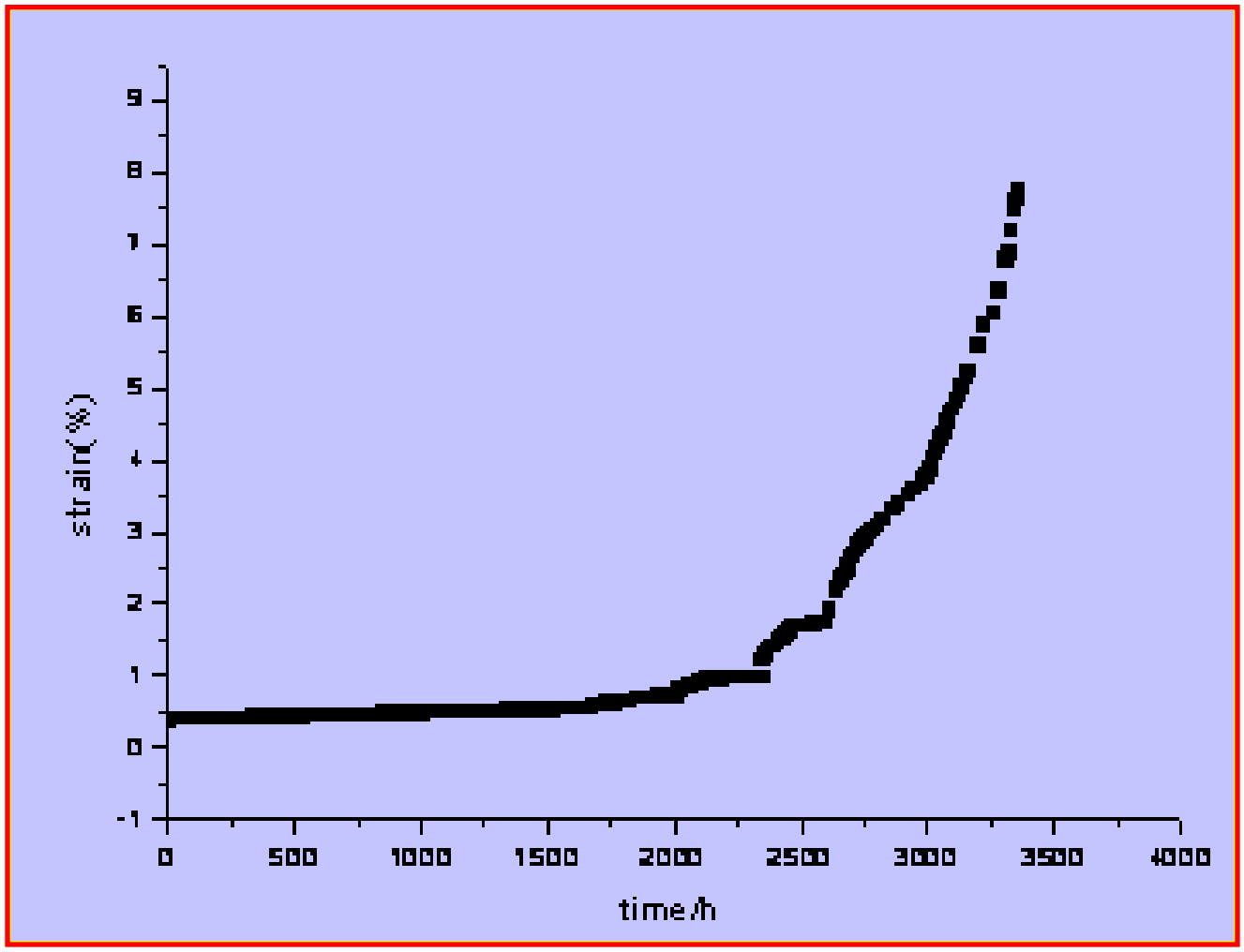

RS05a (136 days)

3. Laboratory experiments of salt rock creep: CT setup

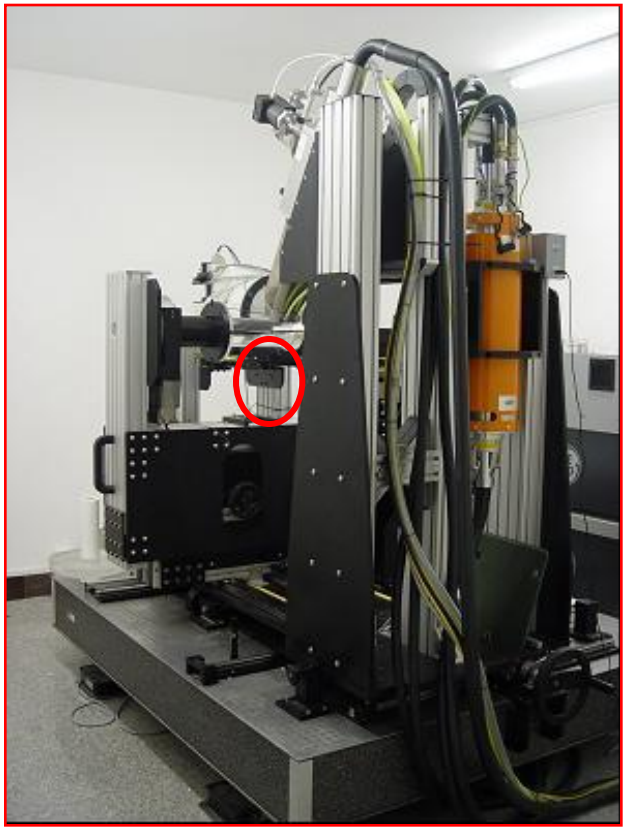

CT setup at CUMTB

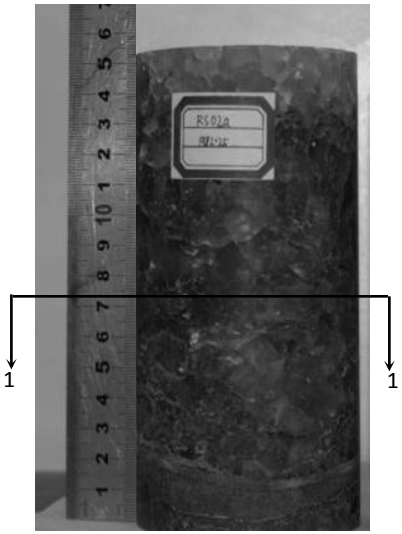

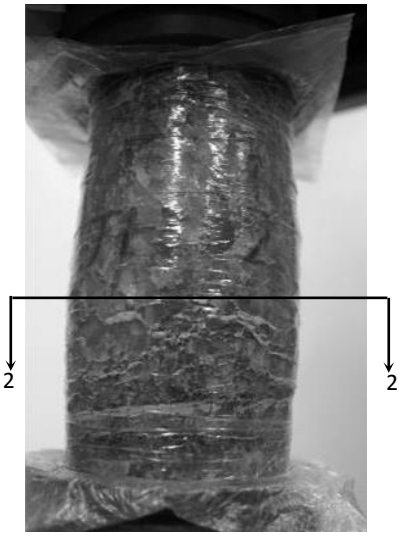

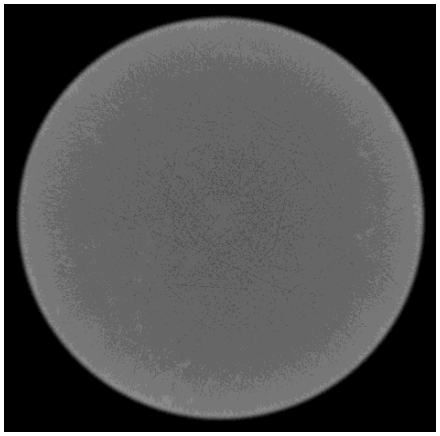

Before

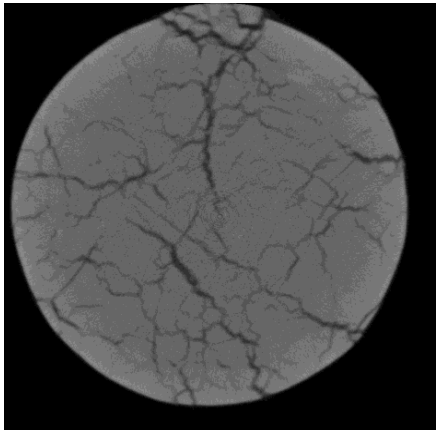

After

4. Fractional derivative approach: variable-viscosity

Before

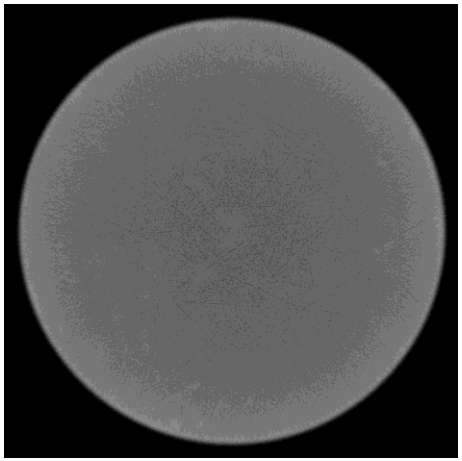

After

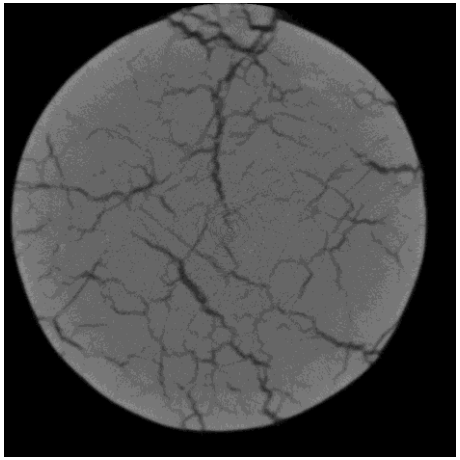

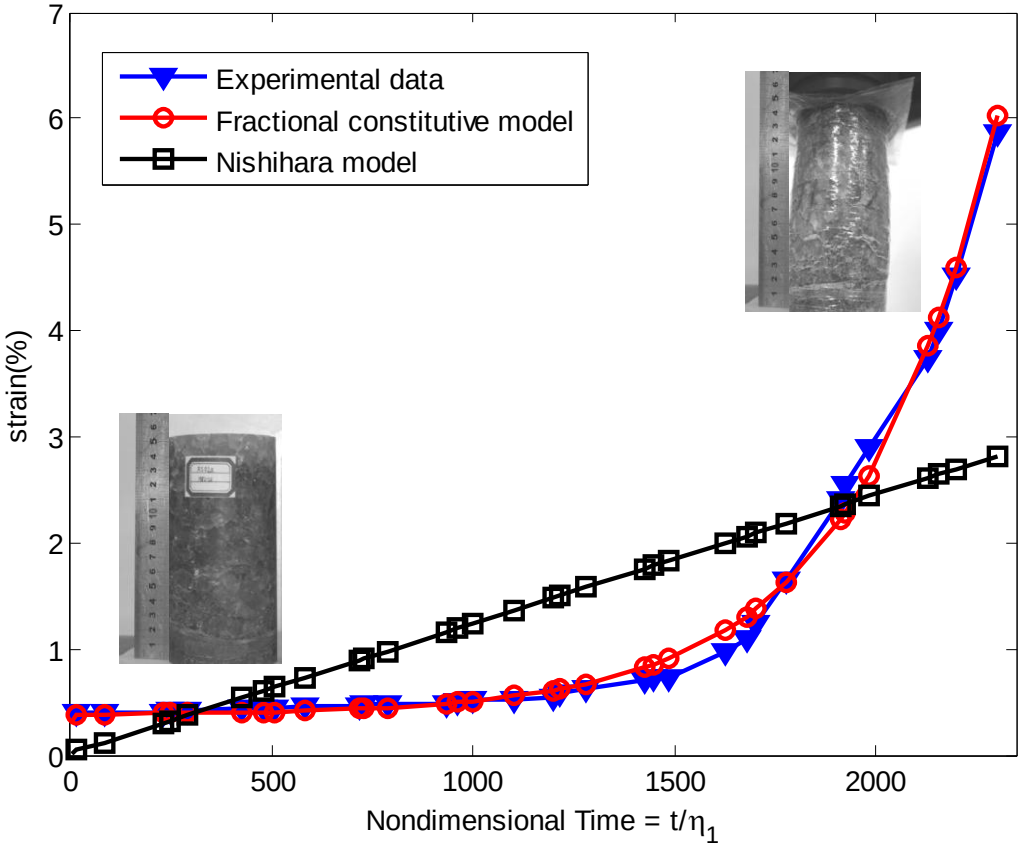

Experimental conditions: uniaxial load-18MPa, temperature-22℃, and period-140 days

4. Fractional derivative approach: variable-viscosity

Before

After

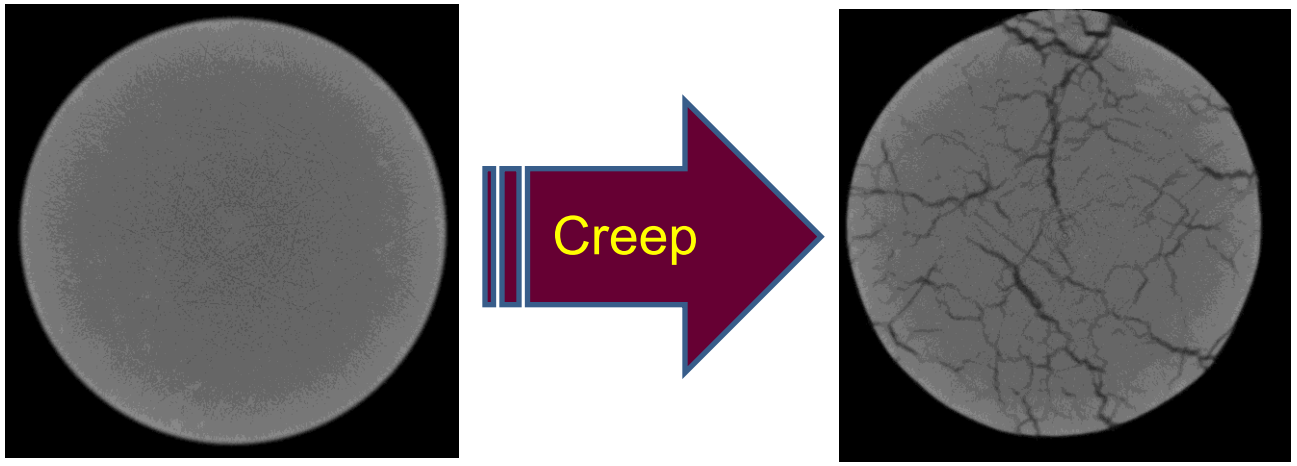

Constant -viscosity

$$\sigma(t) = \eta^{\beta} D_t^{\beta}\left[\varepsilon(t)\right]$$

Variable-viscosity

$$\sigma(t) = \eta^{\beta'} D_t^{\beta}\left[\varepsilon(t)\right]$$

$$\eta^{\beta'} = (1-d)\cdot\eta^{\beta}$$

(after Urai, Spiers, Hendrik, Zwart, Lister. Nature 324, 1986)

d is the damage variable $0 \le d < 1$

4. Fractional derivative approach: variable-viscosity

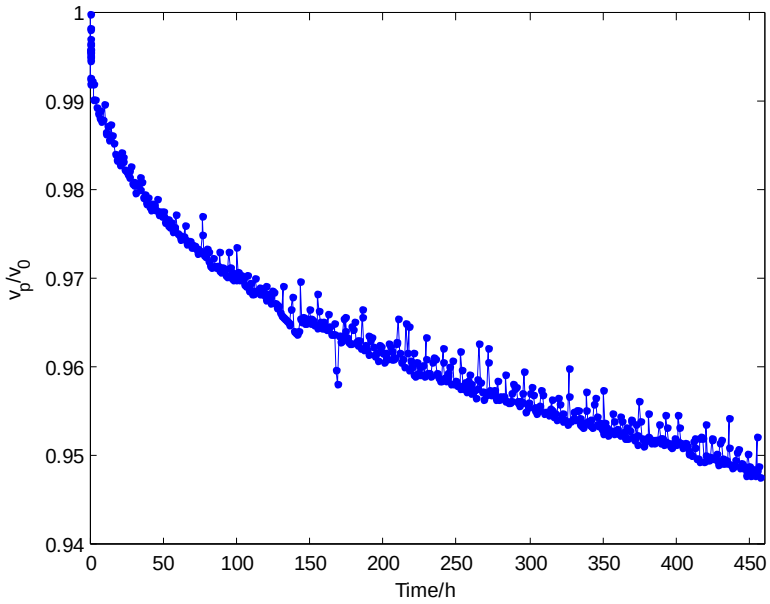

The ultrasonic wave speed of salt rock during creep test

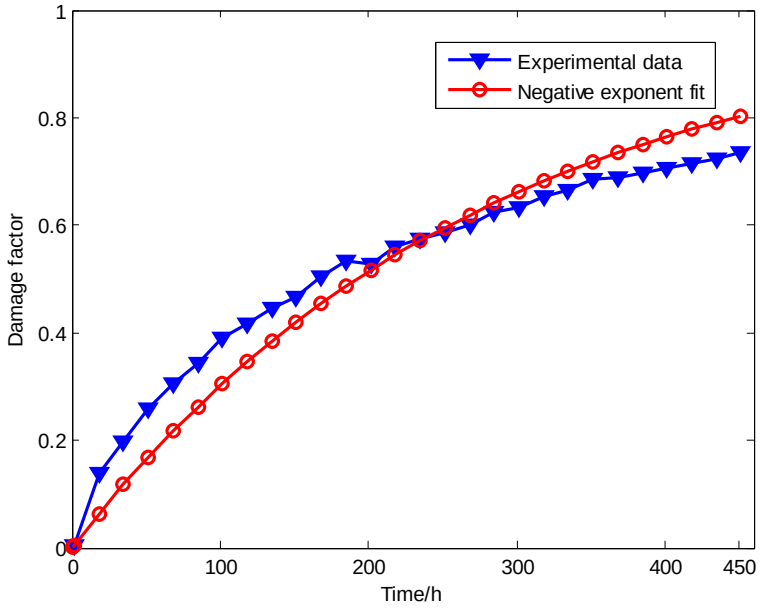

Increase of damage variable with time

(Hou et al 2003) $$d = 1 - \frac{1}{1+\varepsilon_v}\frac{v_p}{v_0}$$

$$d = 1 - e^{-\alpha t}$$

$$\eta^{\beta'} = (1-d)\cdot\eta^{\beta} \Rightarrow \sigma(t) = (\eta^{\beta} e^{-\alpha t}) D_t^{\beta}[\varepsilon(t)] \quad (0 \le \beta \le 1)$$

4. Fractional derivative approach: variable-viscosity

$$\sigma(t) = (\eta^{\beta} e^{-\alpha t}) D_t^{\beta}[\varepsilon(t)] \quad (0 \le \beta \le 1)$$

$$\varepsilon(t) = \frac{\sigma}{\eta^{\beta}} t^{\beta} \sum_{k=0}^{\infty} \frac{(\alpha t)^k}{\Gamma(k+1+\beta)}$$

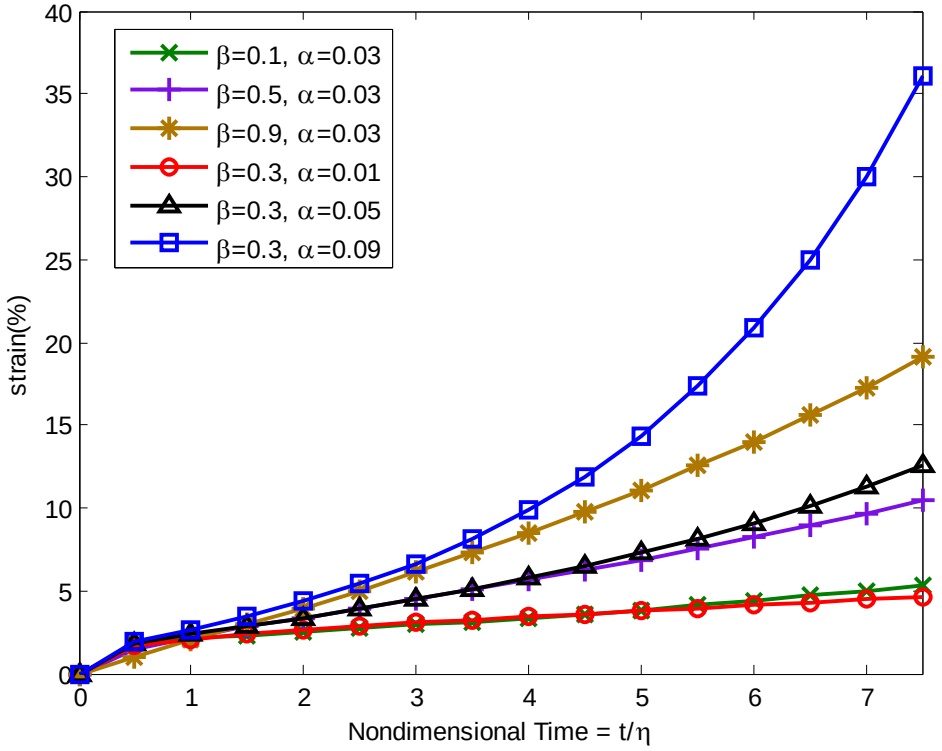

Creep strain described by the variable-viscosity Abel dashpot

4. Fractional derivative approach: variable-viscosity

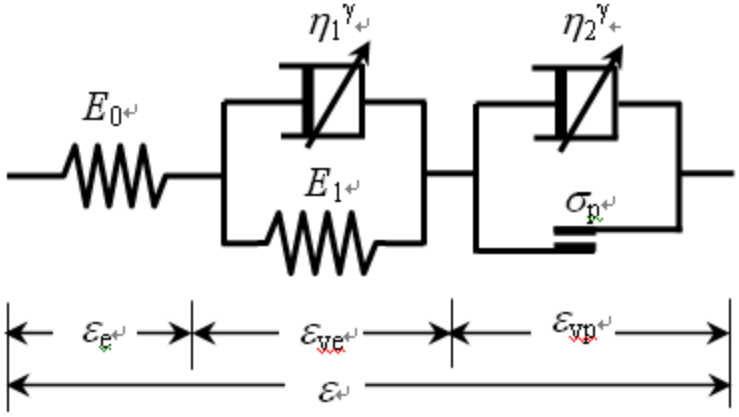

The variable-viscosity fractional derivative model

$$\varepsilon(t)=\frac{\sigma}{E_0}+\frac{\sigma}{\eta_1^\beta}\sum_{k=0}^{\infty}\frac{\left(-\frac{E_1}{\eta_1^\beta}\right)^k t^{\beta(1+k)}}{\beta(1+k)\Gamma[(1+k)\beta]}+\frac{\sigma-\sigma_s}{\eta_2^\beta}t^\beta\sum_{k=0}^{\infty}\frac{(\alpha t)^k}{\Gamma(k+1+\beta)} \qquad (\sigma\geq\sigma_s)$$

$$\varepsilon(t)=\frac{\sigma}{E_0}+\frac{\sigma}{E_1}-\frac{\sigma}{E_1}E_{\beta,1}[-E_1(\frac{t}{\eta_1})^\beta]+(\sigma-\sigma_s)(\frac{t}{\eta_2})^\beta E_{1,1+\beta}(\alpha t)$$

4. Fractional derivative approach: variable-viscosity

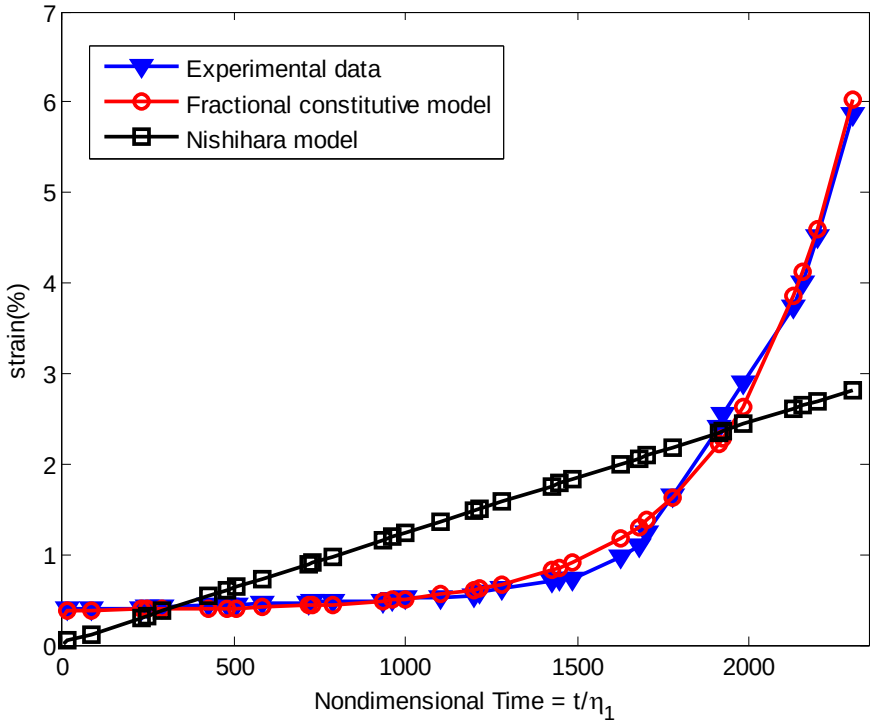

	E_0 (GPa)	E_1 (GPa)	η_1^β (GPa·h$^\beta$)	η_2^β(GPa·h$^\beta$)	β	α(h^{-1})	LSF errors
Fractional derivative model	5.73	27.59	1.40	178.63	0.3	0.0021	4.2×10^{-5}

4. Fractional derivative approach: variable-viscosity

- Sensitivity of the creep strain to the stress level

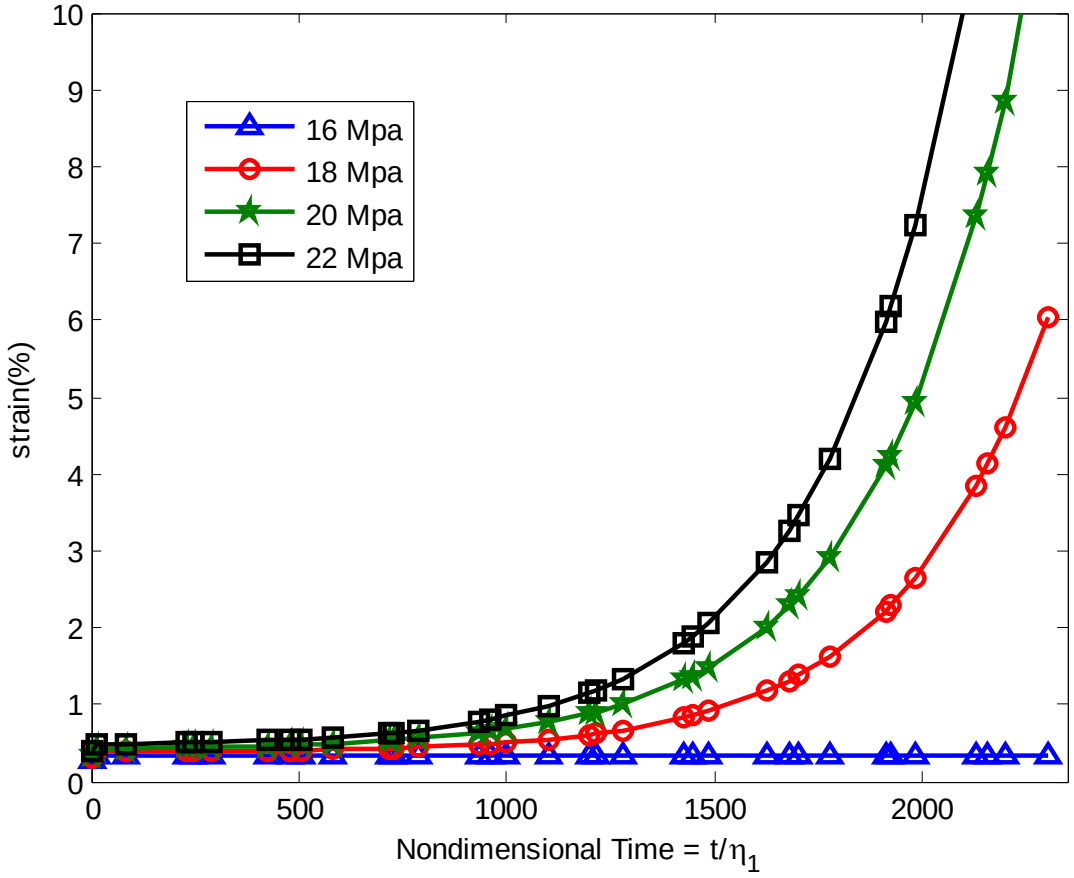

Fig. 6 Sensitivity of the creep strain to the stress level σ ($\sigma_s = 16$ MPa, $E_0 = 5.37$ GPa, $E_1 = 27.59$ GPa, $\eta_1^{\beta} = 1.4\ \mathrm{GPa\,h}^{\beta}$, $\eta_2^{\beta} = 178.63\ \mathrm{GPa\,h}^{\beta}$, $\beta = 0.3$ and $\alpha = 0.0021\ \mathrm{h}^{-1}$)

4. Fractional derivative approach: variable-viscosity

- Sensitivity of the creep strain to the fractional derivative order

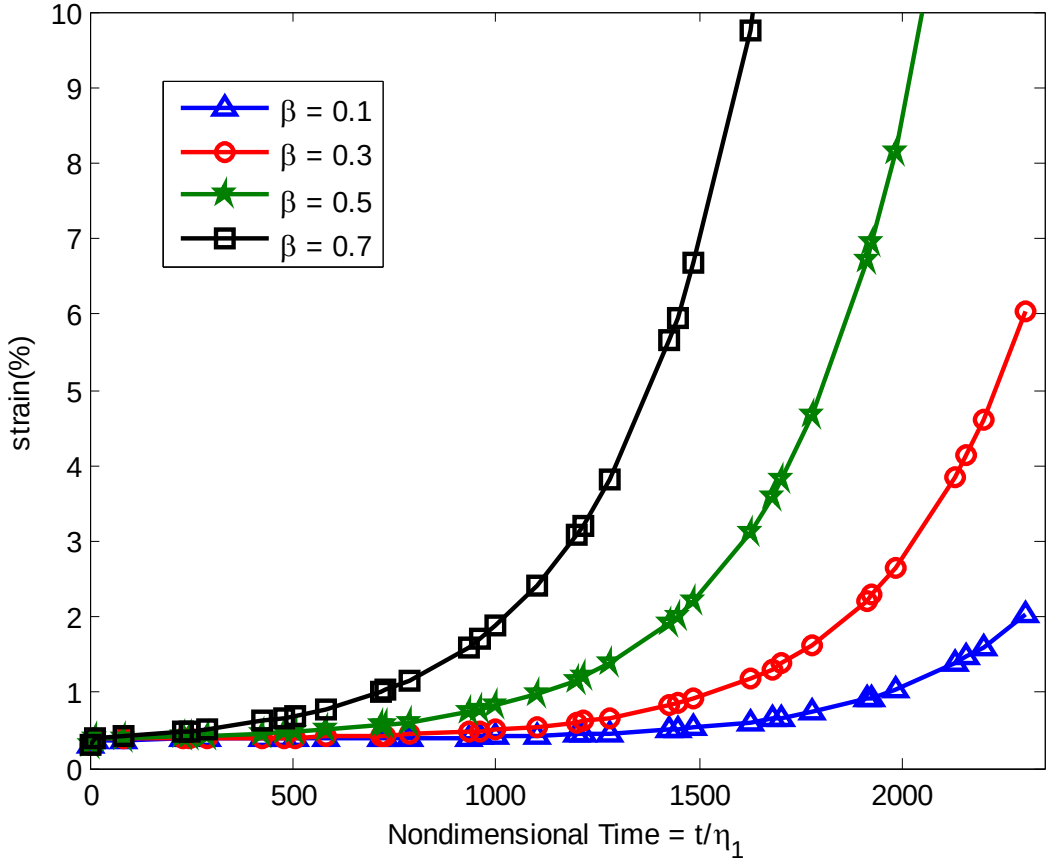

Fig. 7 Sensitivity of the creep strain to the fractional derivative order β ($\sigma_s = 16$ MPa, $E_0 = 5.37$ GPa, $E_1 = 27.59$ GPa, $\eta_1^{\beta} = 1.4\ \text{GPa}\,\text{h}^{\beta}$, $\eta_2^{\beta} = 178.63\ \text{GPa}\,\text{h}^{\beta}$, $\sigma = 18$ MPa, $\alpha = 0.0021\ \text{h}^{-1}$)

4. Fractional derivative approach: variable-viscosity

- Sensitivity of the creep strain to the parameter α

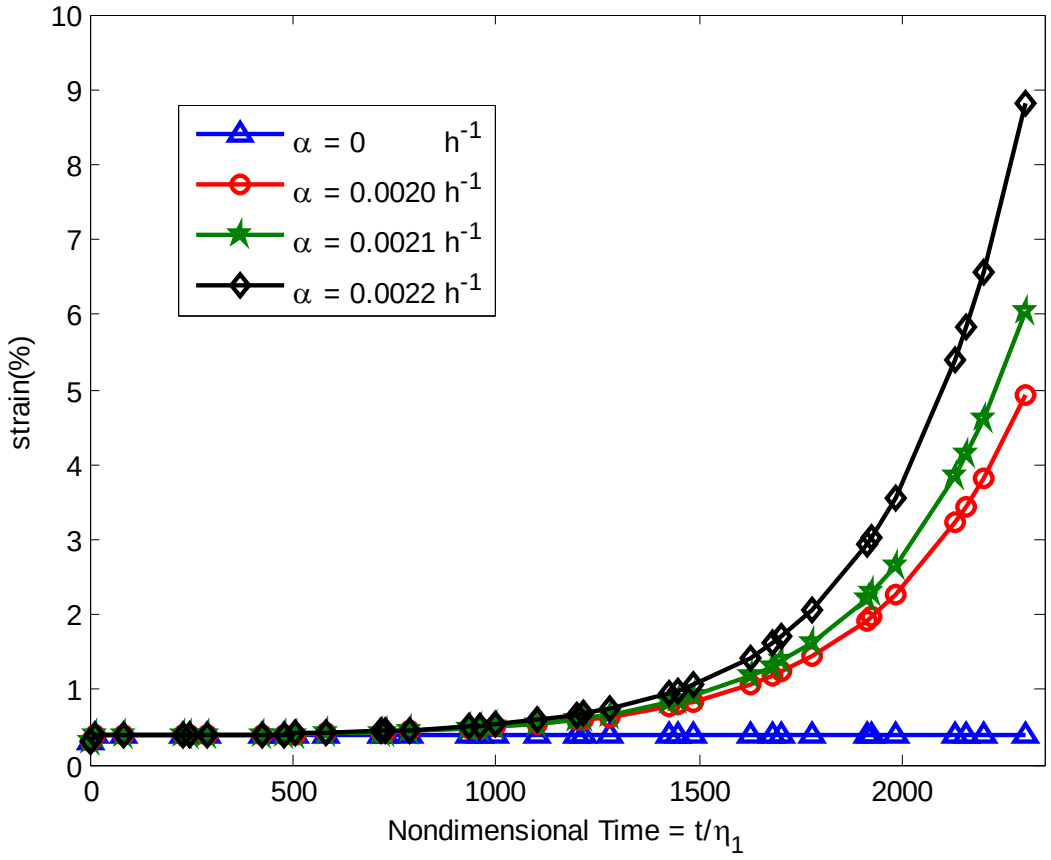

Fig. 8 Sensitivity of the creep strain to the exponent α ($\sigma_s = 16$ MPa, $E_0 = 5.37$ GPa, $E_1 = 27.59$ GPa, $\eta_1^{\beta} = 1.4\ \text{GPa}\,\text{h}^{\beta}$, $\eta_2^{\beta} = 178.63\ \text{GPa}\,\text{h}^{\beta}$, $\sigma = 18$ MPa, $\beta = 0.3$)

Mech Time-Depend Mater
DOI 10.1007/s11043-012-9193-x

A fractional derivative approach to full creep regions in salt rock

H.W. Zhou · C.P. Wang · L. Mishnaevsky Jr. · Z.Q. Duan · J.Y. Ding

Received: 4 July 2012 / Accepted: 11 September 2012
© Springer Science+Business Media Dordrecht 2012

Abstract Based on the definition of the constant-viscosity Abel dashpot, a new creep element, referred to as the variable-viscosity Abel dashpot, is proposed to characterize damage growth in salt rock samples during creep tests. Ultrasonic testing is employed to determine a formula of the variable viscosity coefficient, indicating that the change of the variable viscosity coefficient with the time meets a negative exponent law. In addition, by replacing the Newtonian dashpot in the classical Nishihara model with the variable-viscosity Abel dashpot, a damage-mechanism-based creep constitutive model is proposed on the basis of time-based fractional derivative. The analytic solution for the fractional-derivative creep constitutive model is presented. The parameters of the fractional derivative creep model are determined by the Levenberg–Marquardt method on the basis of the experimental results of creep tests on salt rock. Furthermore, a sensitivity study is carried out, showing the effects of stress level, fractional derivative order and viscosity coefficient exponent on creep strain of salt rock. It is indicated that the fractional derivative creep model proposed in the paper provides a precise description of full creep regions in salt rock, i.e., the transient creep region (the primary region), the steady-state creep region (the secondary region) and the accelerated creep region (the tertiary region).

Keywords Salt rock · Abel dashpot · Variable viscosity coefficient · Fractional derivative · Creep constitutive model

H. W. Zhou, C. P. Wang, L. Mishnaevsky Jr., Z. Q. Duan, J. Y. Ding. *Mechanics of Time-Dependent Materials*, in press, published online Sep 28, 2012

5. Conclusion remarks

- The variable viscosity Abel dashpot, characterized by damage growth of salt rocks during the creep tests, is available in description of the non-steady creep process or the accelerated creep region.

- The new fractional derivative creep model proposed in the paper is capable of giving a precise approach to full creep regions in salt rock.

6. Furthermore works

- Further research on the physical meaning of the derivative order is important and necessary.
- Application of fractional derivative model to numerical simulation of creep deformation of salt cavities is still a big task.

Thank you for your attention

H. W. Zhou

State Key Laboratory of Coal Resources and Safe Mining

China University of Mining and Technology (Beijing)

Email: zhw@cumtb.edu.cn

TU Clausthal

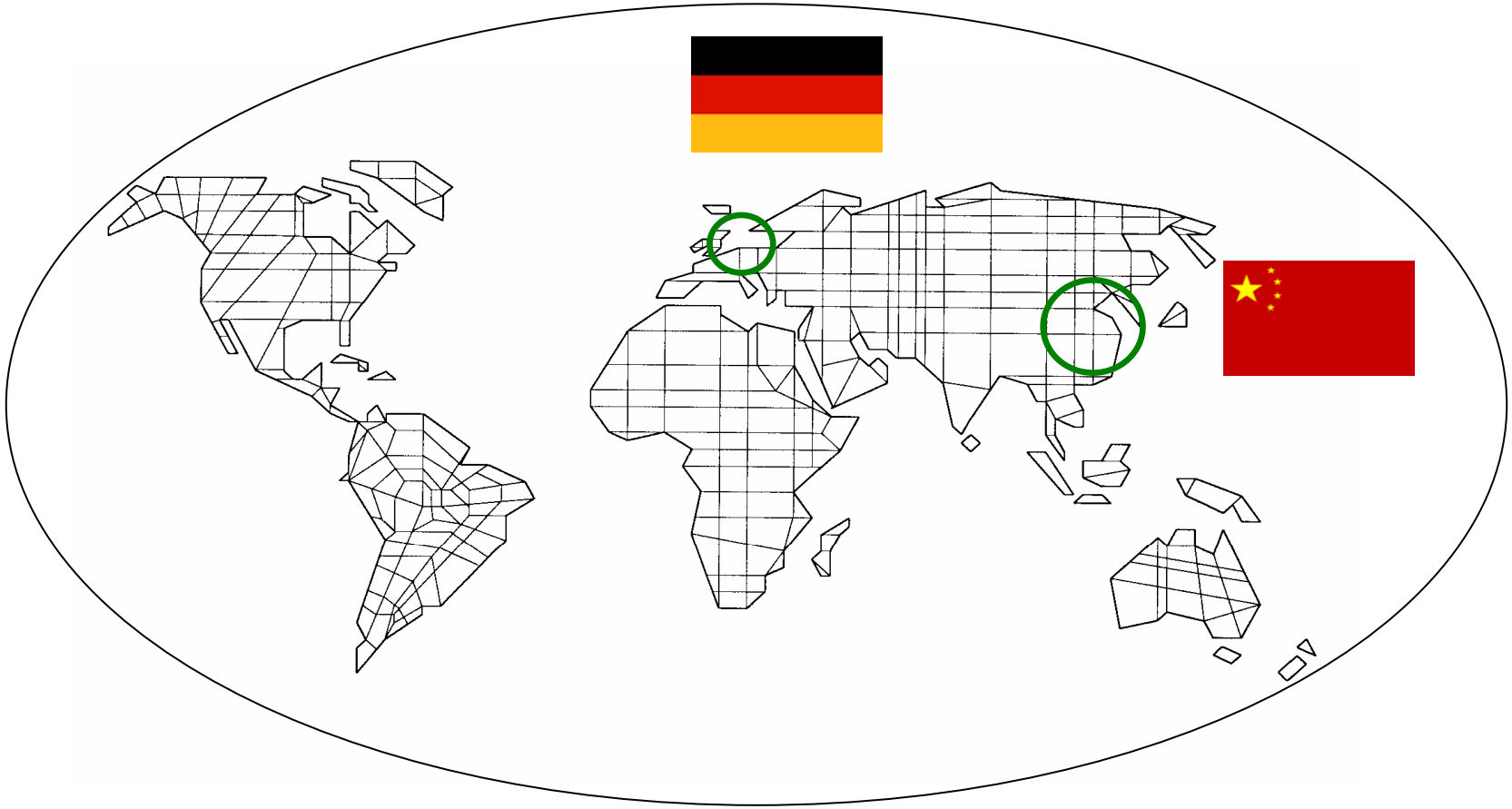

2nd Chinese-German Workshop on Radioactive Waste Disposal

Oct. 15 – 16, 2012 Karlsruhe, Germany

TU Clausthal

Basic Principles of Waste Disposal in Rock Salt Mass

- Some Selected Remarks

Univ. Prof. Dr.-Ing. habil K.-H. Lux

Clausthal University of Technology

Overview

1. Underground Waste Disposal in Germany
2. Specialized Safety Analysis as well as Safety Criteria with Respect to Rock Salt
3. Contributions of Department of Waste Disposal and Geomechanics to Safety Analysis
4. Some Concluding Remarks

Overview

1. Underground Waste Disposal in Germany
2. Specialized Safety Analysis as well as Safety Criteria with Respect to Rock Salt
3. Contributions of Department of Waste Disposal and Geomechanics to Safety Analysis
4. Some Concluding Remarks

Chemotoxic Waste

Hazardous Waste

Underground waste Disposal

⇓ ⇓

Waste Isolation from Biosphere

Waste Utilisation for Backfilling

Radioactive Waste

Underground waste Disposal

⇓

Waste Isolation from Biosphere

! Long Term Protection of Environment against Remigration of Waste !

Activities for Underground Rad-Waste Disposal in the World

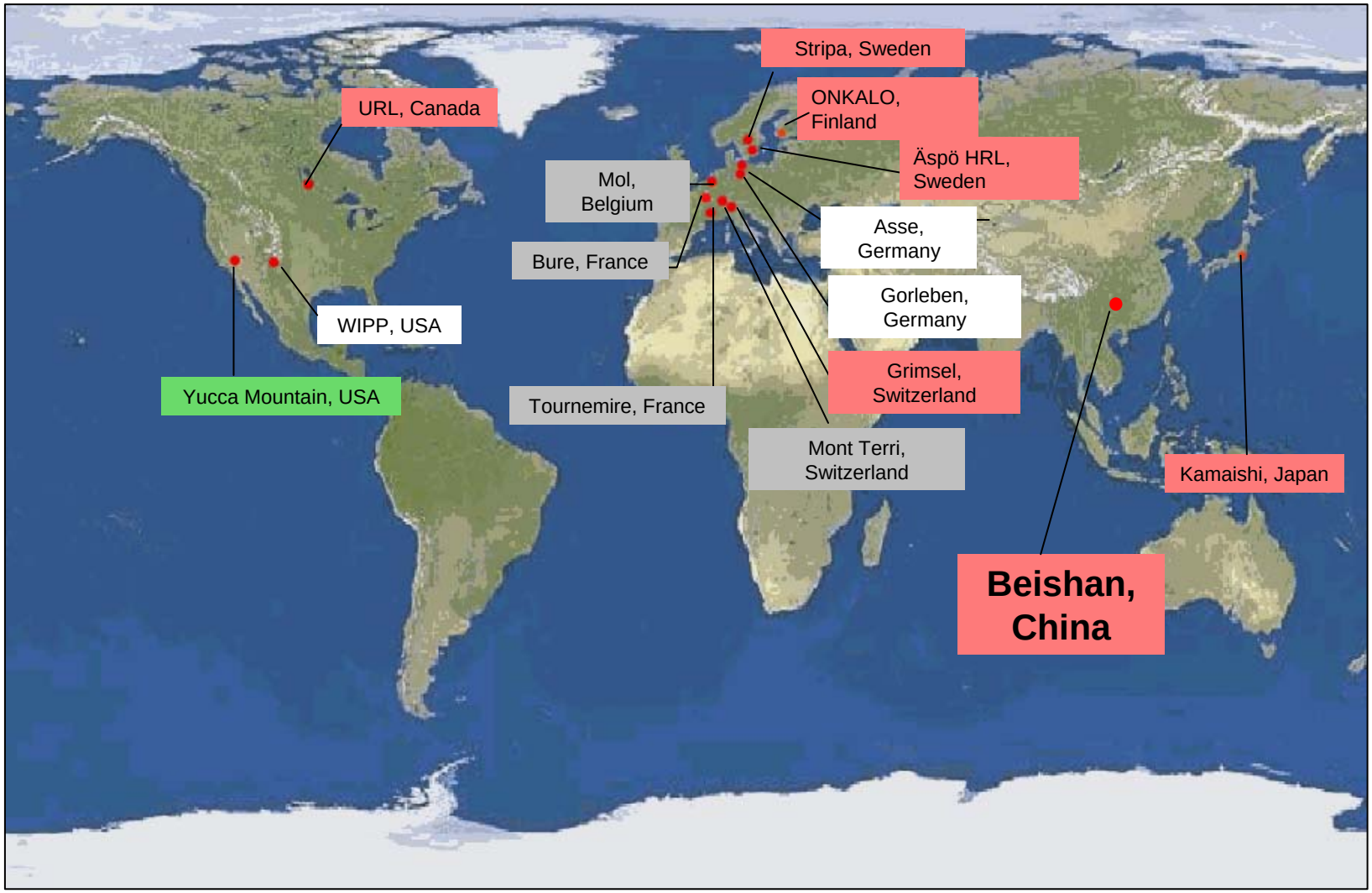

Underground Waste Disposal in Germany – Chemotoxic-Waste

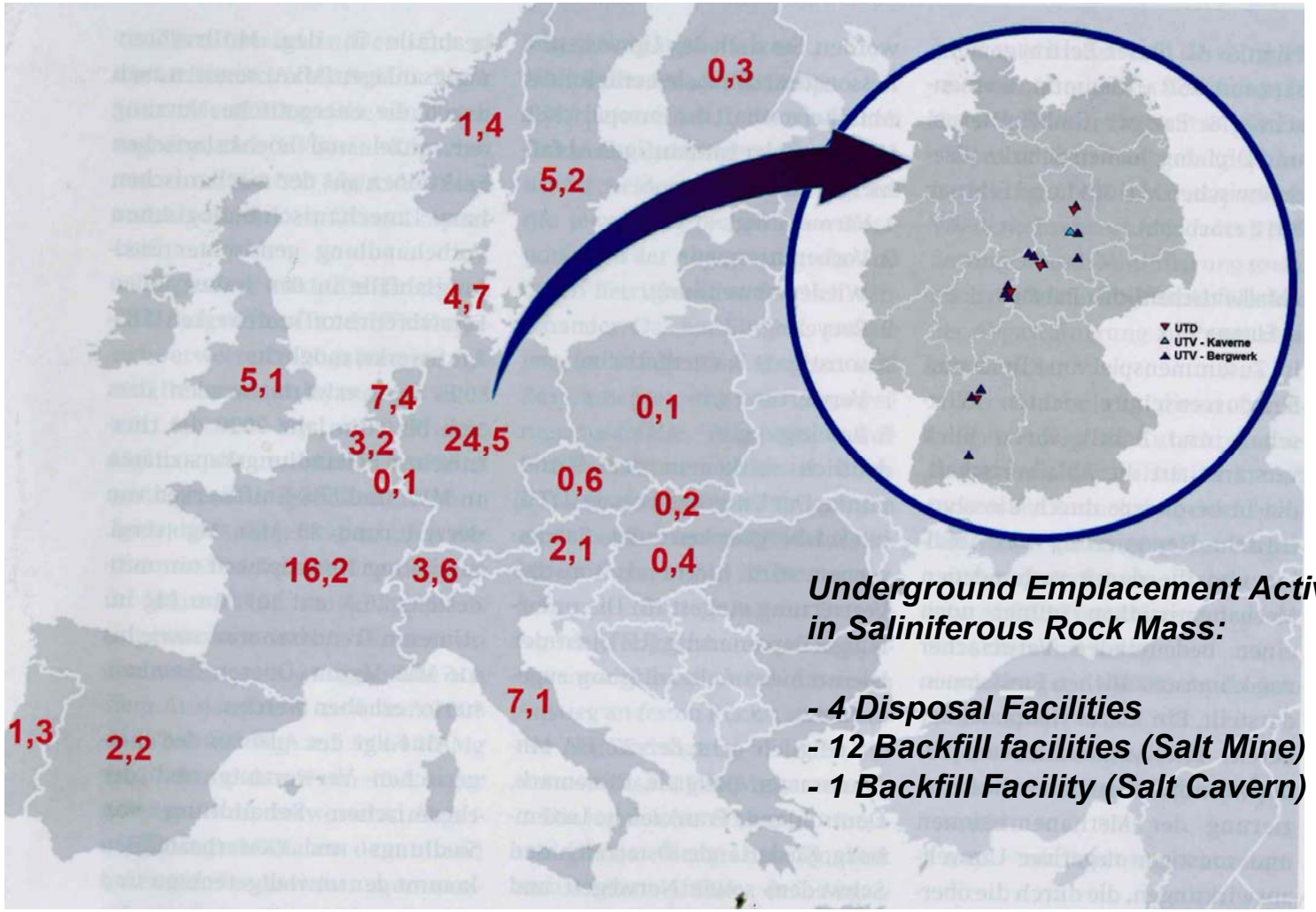

Thermal plants (WTE plants and RDF power plants) in European States by capacity in Mio t

Current Status of Site Activities:

- Morsleben (rock salt)
  - ∗ *to be closed*
- Asse (rock salt)
  - ∗ *waste recovery under investigation*
- Konrad (claystone)
  - ∗ *operation prepared*
- Gorleben (rock salt)
  - ∗ *exploration at low intensity*
  - ∗ *preliminary safety assessment*

Legal Activities:

Guidelines BMU (2010) → Heat Producing High Active Waste

Federal Government Law (?) → New Site Identification and Site Characterisation Procedure (including / excluding Gorleben site ?) ⇒ precondition: no preselected host rock mass type

Identified Geotectonic Systems for Underground Waste Disposal

Future ***Past, Presence***

? ? ?

Crystalline Formations (granite)

Sedimentary Formations (claystone, clay)

Evaporitic Formations (rock salt)

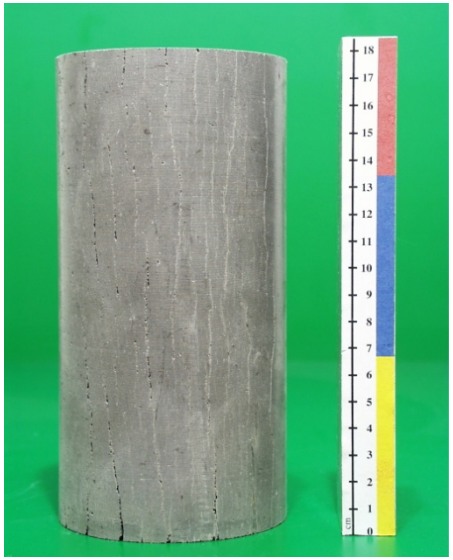

Saliniferous Structures – Bedded Salt

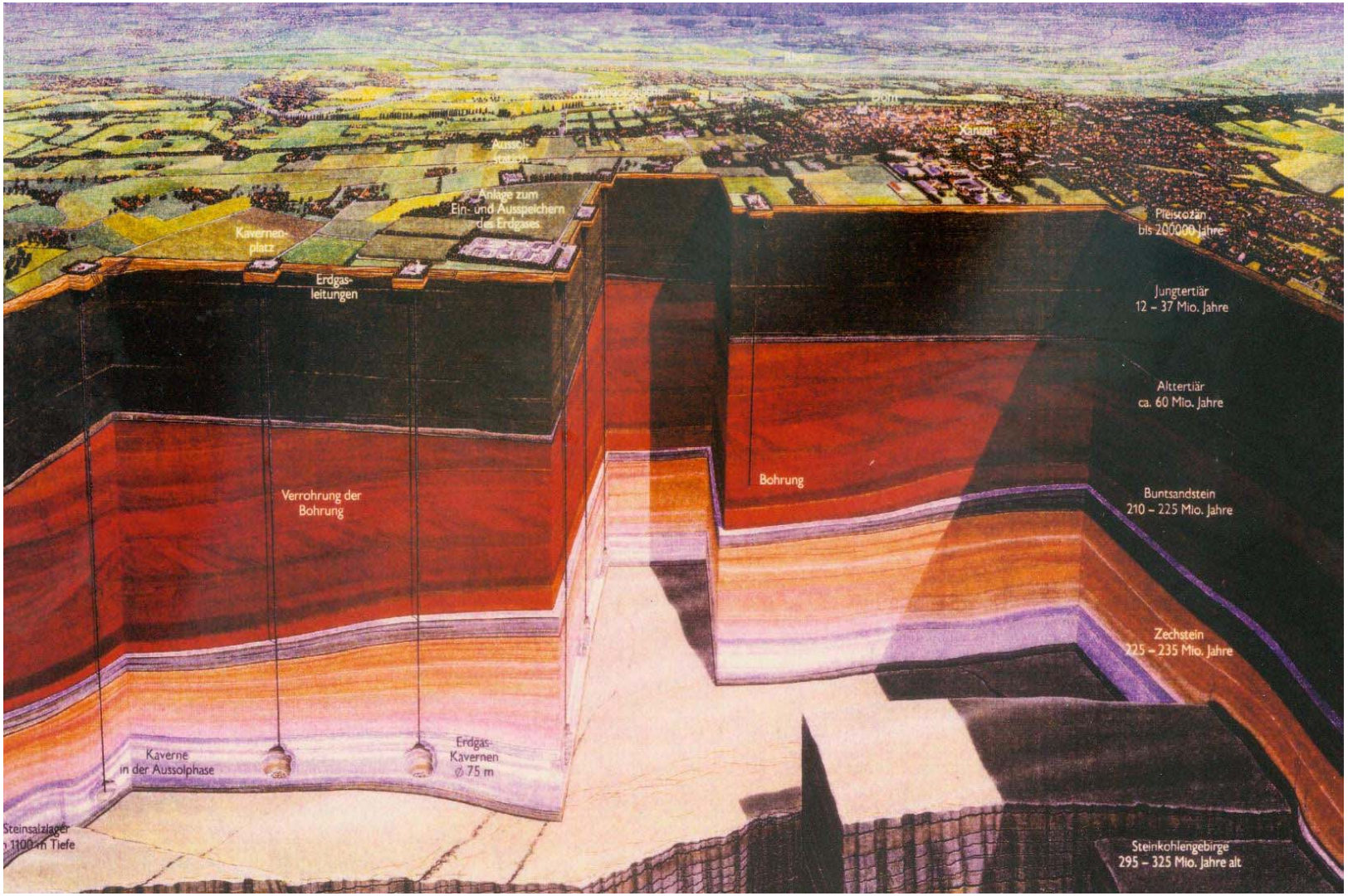

Basic Principles for Radwaste Disposal:

- national disposal
- protection of human beings and the environment against radiation
- protection of human beings against chemotoxic harmful substances
- disposal in deep underground formations
- complete isolation of waste in rock mass (CC)
- multibarrier system against release of hazardous substances back to biosphere
- time of prognosis > 1 Mio. years
- no design for retrival of waste after end of disposal operation and sealing
- maintenance-free disposal → after repository closure no monitoring as well as no repair work

➔ ***Final disposal – basic objectives:***

safe, without time limit, maintenance-free

as well as

accepted by public

How may it work?

Overview

1. Underground Waste Disposal in Germany
2. Specialized Safety Analysis as well as Safety Criteria with Respect to Rock Salt
3. Contributions of Department of Waste Disposal and Geomechanics to Safety Analysis
4. Some Concluding Remarks

Basic Demand:

Protection of the Environment Against → ***Hazardous Waste (acc. to Waste Law)***

→ ***Radioactive Waste (acc. to Atomic Law)***

→ ***Mining Waste (acc. to Mining Law)***

Resulting from Human Activities

Basic Safety Principle:

- Isolation of Hazardous Waste from Biosphere – CC

Additional Demands:

- long term (> 1 Mio years, permanent)
- safe
- maintenance-free
- no necessity regarding retrievability after abandonment

Basic Public Principle:

May be Necessary but … NIMBY ⇒

General Demand with Respect to Underground Waste Disposal ⇒

Principally No Return of Hazardous Particles to Biosphere

Additional Specified Demands ⇒

- long term / permanent
- safe
- maintenance-free
- no necessity regarding retrievability after abandonment

Current Procedure:

Documentation of Isolation of Waste from Biosphere in Deep Underground Rock Mass Formations

- *Safety well documented acc. to International State of the Art*

\+ ***Participation of Public in Process***

Detailed Procedure of Realisation ⇒

(1) Development of Excellent Knowledge

(2) Selection of a Basically Suitable Site based on *Preliminary Prognostic Safety* Analysis as well as on *Public Participation*

(3) Site-Specific Repository Design

(4) *First Prognostic Safety Analysis* / Licencing Procedure, *Public Participation*

(5) Extensive Monitoring during Construction and Operation

(6) *Updated Prognostic Safety Analysis,* during Operation, *Public Participation*

(7) *Final Prognostic Safety Analysis* before Closure, *Public Participation*

(8) Closure of Repository

(1/1) Legal Demand: Isolation of Chemotoxic Waste in Rock Salt Formations

(1/2) Legal Demand: Isolation of Radioactive Waste in Suitable Underground Formations

- long term – safe - no necessarity retrievablity after abandonment - maintenance-free

(2) Engineering Realisation ⇒ Creation of a ***Multibarrier System*** against Radionuclide / Toxic Waste Mobilisation / Migration

consisting of ⇒

Geologic Barrier(s) ***Geotechnical Barrier(s)*** ***Technical Barrier(s)***

Barrier = physical element of repository preventing hazardous / radioactive waste mobilization / migration

during construction, operation, as well as in the long term

after closure during long term

during operation (repository in rock salt mass)

Underground Waste Repositories:

Where to dispose off? How to dispose off? Who is responsible? When should final disposal takes place?

THMC – Analysis of Physicochemical Processes in Near Field

$$\mathbf{M \rightarrow \tilde{M}/T \rightarrow \tilde{T}/H \rightarrow \tilde{H}/C \rightarrow \tilde{C}}$$

Construction – Operation – Closure

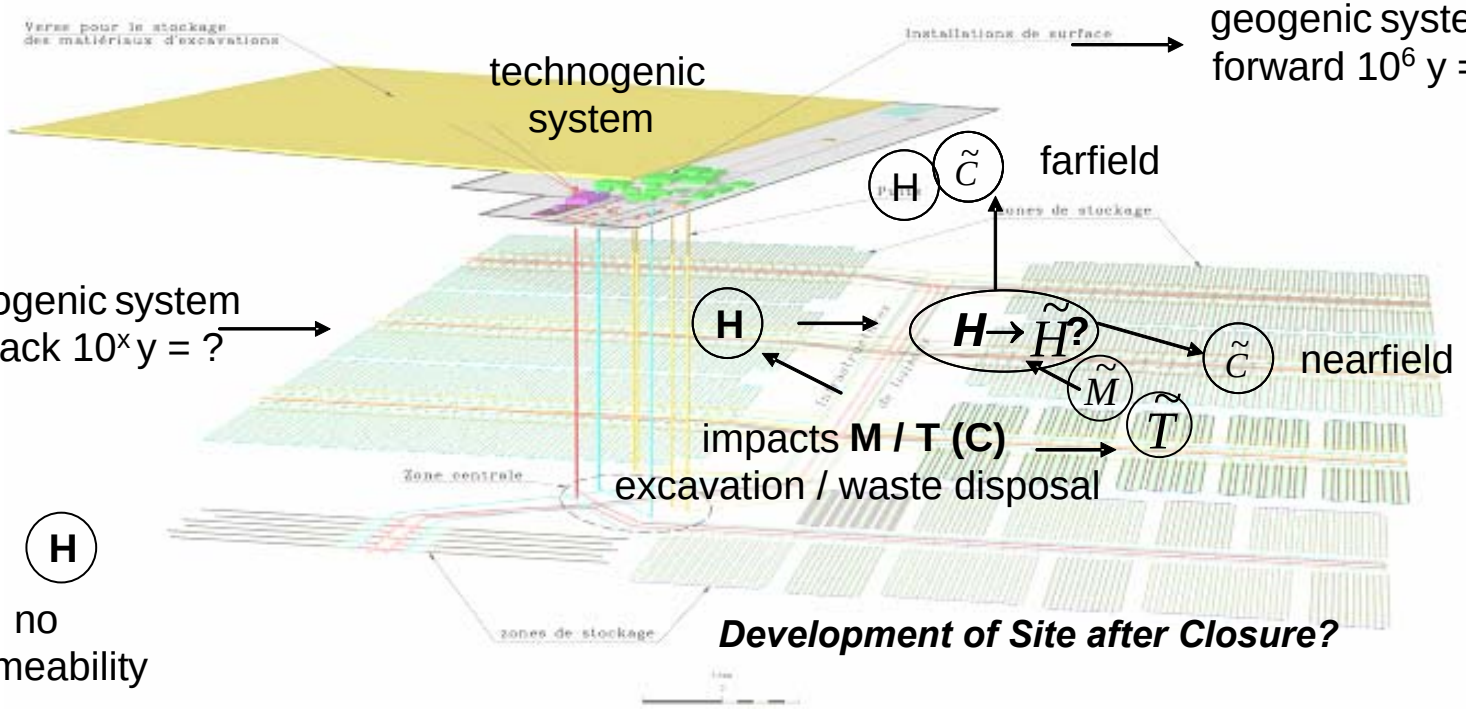

Probability of Occurrence of Possible Future Developments of Site

- *developments with high probability* $\Rightarrow$ **complete isolation!**
- *developments with low probability* $\Rightarrow$ **admissible release! (=safe isolation)**

Rock Mass Properties Must be Related to Safety Principles – ***Why Rock Salt Mass?***

⇓

Basic Rock salt mass properties with Respect to Waste Disposal:

- excellent hydraulic properties (impermeable = tight → no natural pathways for fluids)
- good mechanical properties regarding strength (no destrengtening joint system, sufficient load bearing capacity)
- good mechanical properties regarding deformability (ductile behaviour, plastic-viscous / creep → reclosure of underground holes)
- good thermal properties (→ relativ high heat conductivity)
- good mechanical properties regarding fissure closure (→ self-sealing / self-healing)

but:

- worse geochemical properties regarding sorption (less / no sorption capacity)
- worse geochemical properties regarding rock material stability (→ soluble in fresh water)

⇒ **Documentation of *Geochemical Stability of Site Specific Saliniferous Rock Mass System Obligatorily Necessary! (in past and presence as well as in future including waste disposal impacts)***

Geological Barrier(s) in Saliniferous Geosystems

Alternative Thesis:

- just one intact geologic barrier necessary ⇒
  rock salt mass
- two intact geologic barriers necessary ⇒
  rock salt mass (main barrier)

  +

  non rock salt formation (to protect rock salt formation against groundwater access and to realize some sorption capacity at site as well as to give some kind of redundancy and diversity)

?

General Properties / Criteria

(a) before repository construction

→ impermeable rock salt mass (tight crystalline fabric as well as no naturally induced pathways for fluid flow)

⇒ ***Documentation of Existing Geological Barrier Integry (site selection process)***

(b) after repository construction and disposal of waste in the long term

→ impermeable rock salt mass too (no technically induced pathways during construction, operation, abandonment)

⇒ ***Documentation of (absolute or sufficient?) Preservation of Pre-Existing Geological Barrier Integrity (during Exploration, Construction, Operation and Abandonment Phase as well as in the Long Term)***

BMU – Guidelines (2010) ⇒

Basic Criteria with Respect to Guarantee Long Term Safety

(1) Appropiate Site with Intact Geologic Barrier System →

(2) Maintenance of Naturally Existing Geologic Barrier Integrity

(2/1) - mechanical integrity:

no damage

(2/2) - hydraulical integrity:

no fluid infiltration

(2/3) - chemical integry:

limited temperature change

Identifying as well as Determining

Isolating Rock Mass Area Around Repository

acc. to AKEnd (2002)

best available location that can be identified in Germany´s underground fulfilling pre-given site-selection criteria

documentation of maintenance *of pre-existing barrier integrity* or just documentation of *sufficient barrier integrity* ?

→ *some local / zonal loss of barrier integrity perhaps only temporarily may be tolerable if guarenteeing long term safety of re-pository at any time*

How to Demonstrate Safety at Repository Site for the (Unknown) Long Term Development (> 1 Mio Years ?)

Fundamentals:

(1) Reliable geoscientific understanding of geotectonic development of the site in the past (> 10 Mio years)

(2) Geoscientific based extrapolation of geotectonical possible developments of the site with high or less degree of probability of occurence in the future considering all possible impacts and processes (time scale > 1 Mio years) – *acc. to State of the Art*

⇓

(3) – (6) Related Geotechnical Activities

Precondition:

(3) Good and complete understanding of site-specific T-H-M-C-B-(Tr) processes relevant to selected site with respect to site-specific conditions taking into account

⇒

- ***rock mass system***
- ***mine system (shafts, drifts, chambers)***
- ***disposed off waste properties***
- ***sealing system***

How to Demonstrate Safety at Site for the (Unknown) Long Term Development (> 1 Mio Years ?)

(4) ***Physicochemical Modelling*** of relevant processes and their interaction (T-H-M-C)

(5) ***Numerical Simulation*** of possible disposal system developments considering

- site developments with high degree of probability to occur in order to demonstrate ***complete isolation of waste (!)***
- site developments with low degree of probability to occur

in order to analyse

possible mobilisation / migration of waste towards biosphere

Complete isolation (!)

ETI → safe isolation (!)

ETI → unsafe disposal (!)

(6) ***Proof of safety*** for numerically determined results

- proof of complete isolation of waste (criteria? necessary safety margins?)
- proof of limited as well as tolerable release of harmful particles with respect to waste

specific environmental protection criteria → chemotoxic waste – (deep) groundwater

→ radiotoxic waste - biosphere

including Sensitivity Analysis

How to Demonstrate Safety at Site for the (Unknown) Long Term Development (> 1 Mio Years ?)

Key Elements for Safety Analysis

- ***Documentation of Isolation***
- ***Analysis of Mobilisation / ETI***

$\Rightarrow$ T

M

H

C

processes - individual as well as
- coupled (one side / two sides - if necessary with respect to safety aspects)

- ***Identifikation***
- ***Understanding***
- ***Modelling (Formula)***
- ***Characterisation (Site-Specific)***

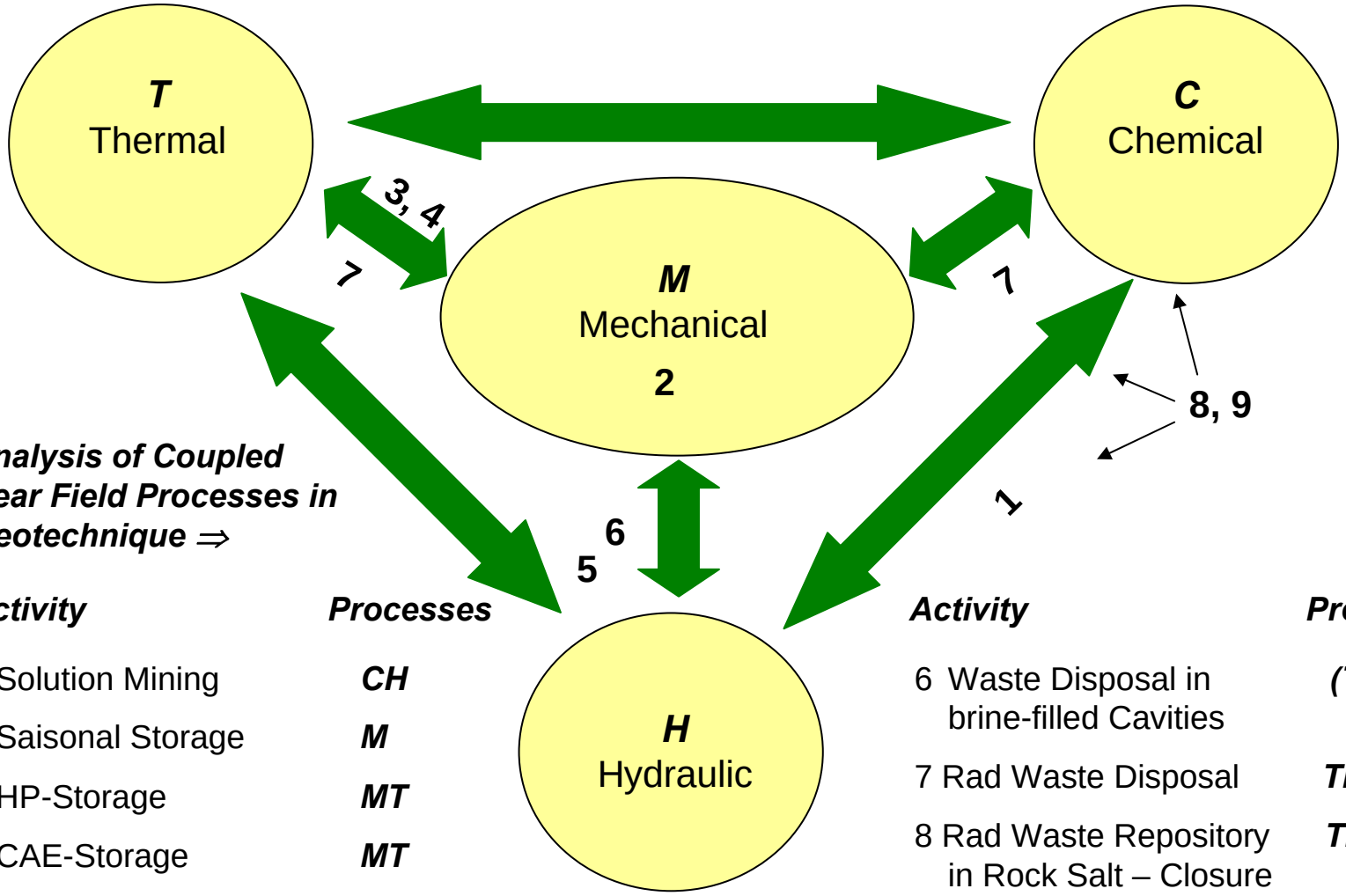

Analysis of Coupled Near Field Processes in Geotechnique ⇒

Activity	*Processes*
1 Solution Mining	***CH***
2 Saisonal Storage	***M***
3 HP-Storage	***MT***
4 CAE-Storage	***MT***
5 Cavern Abandonment	***MH (T)***

Activity	*Processes*
6 Waste Disposal in brine-filled Cavities	***(T)HM***
7 Rad Waste Disposal	***TM / THC***
8 Rad Waste Repository in Rock Salt – Closure	***THM / THC***
9 Rad Waste Repository in Rock Salt – Accident	***THM-C***

Overview

1. Underground Waste Disposal in Germany
2. Specialized Safety Analysis as well as Safety Criteria with Respect to Rock Salt
3. Contributions of Department of Waste Disposal and Geomechanics to Safety Analysis
4. Some Concluding Remarks

(1/1) Laboratory Investigations

Rock Mechanical Lab of TUC

- ***strength properties***
- ***deformation properties (elastic-viscous behaviour)***
- ***damage properties***
- ***healing properties***
- ***hydraulic properties (1-/2-phase flow)***
- ***infiltration properties***

with respect to

- ***rock materials***
- ***backfill materials***
- ***geotectonic barrier materials***
- ***waste materials***

(1/1) Strength Properties as well as Damage Properties

$$D = 1 - \frac{1}{1-\varepsilon_{vol}} \cdot \left(\frac{v_p}{v_{p0}} \right)^2$$

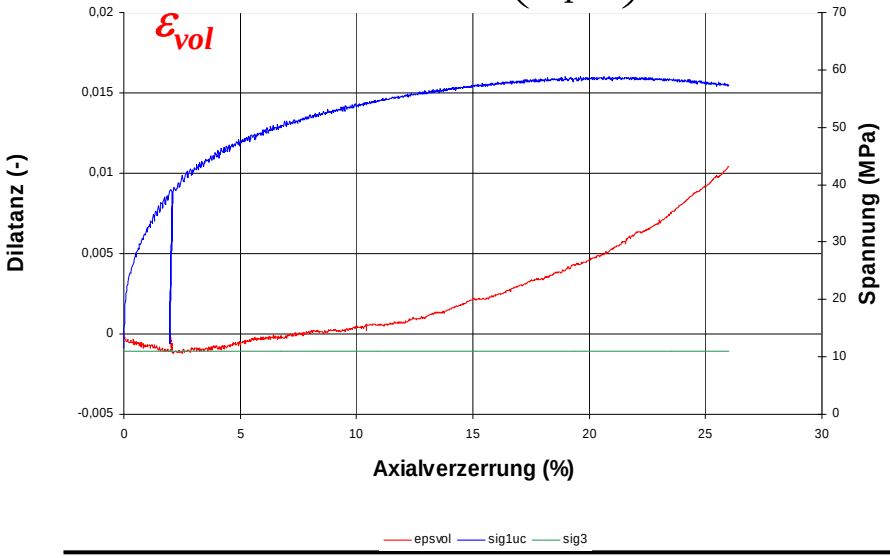

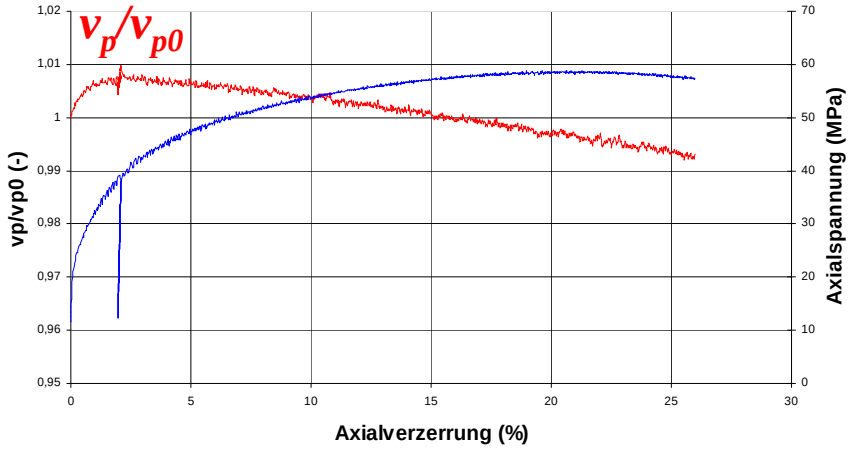

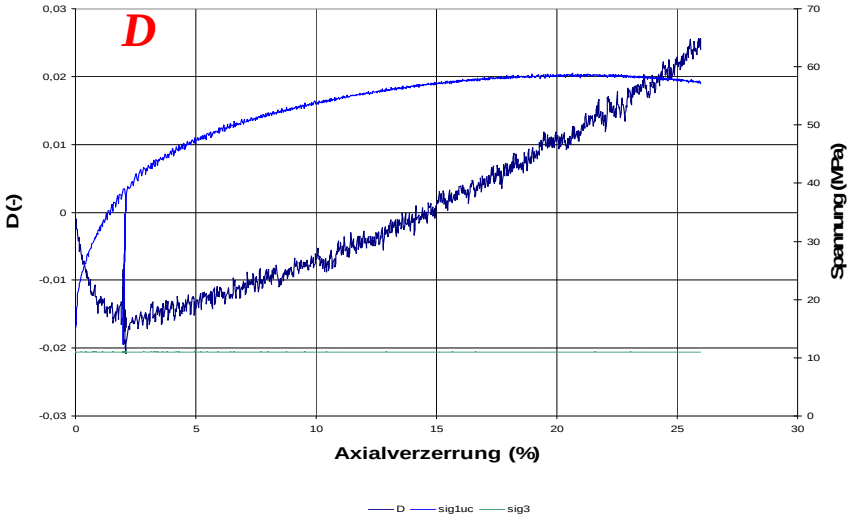

(1/2) Deformation / Creep Properties as well as damage properties

Creep Phases: (I) Transient Creep, (II) Stationary Creep, (III) Accelerated Creep, (IV) Creep Failure

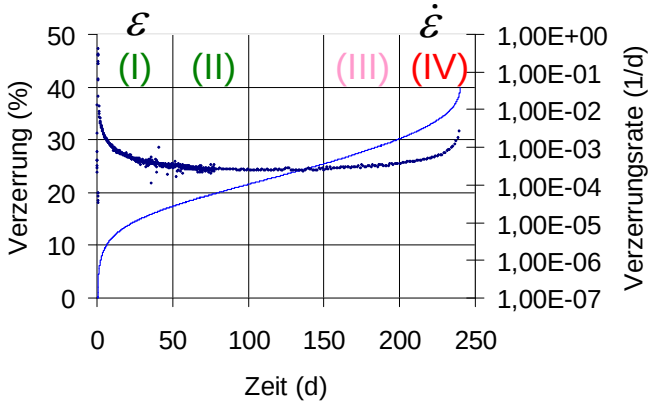

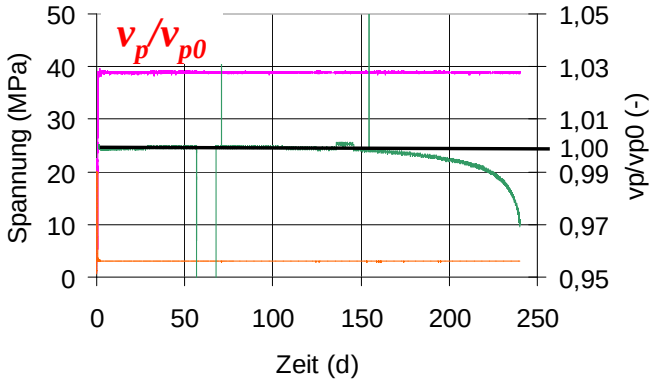

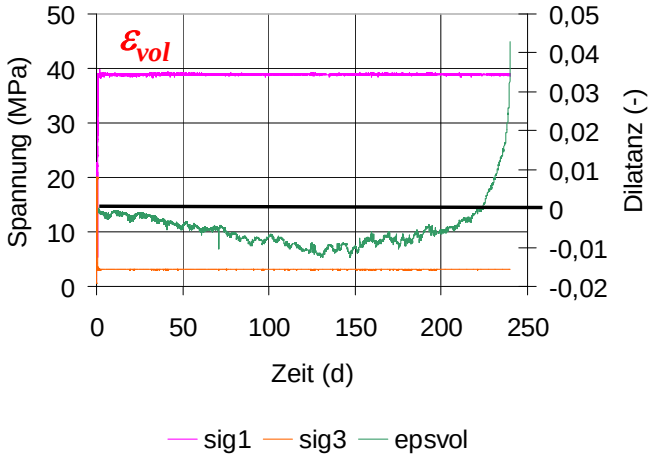

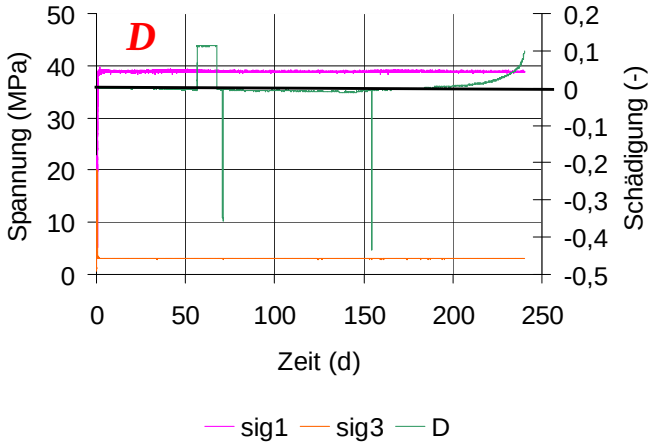

Lab Investigations → Physical Modelling

(1/3) Deformation / Creep Properties – Recreation of Damage / Healing

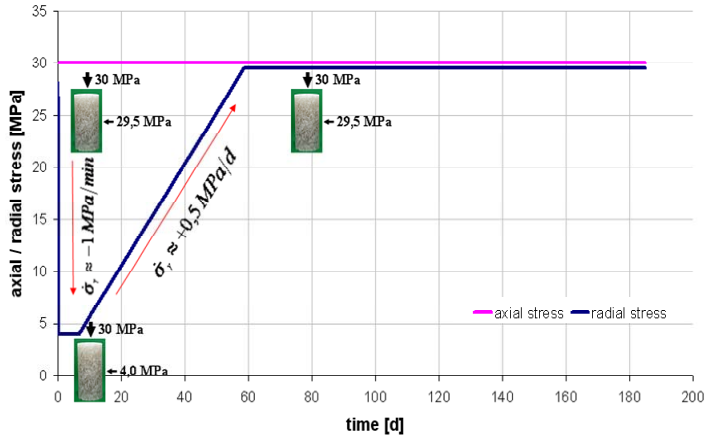

Back-formation of Damage

$$\dot{\varepsilon}_{ij}^{h} = -\varepsilon_{vol} \cdot \left(\frac{1}{fc1} \cdot \dot{F}^{h} + \frac{I_1}{fs1} + \frac{1}{fh} \right) \cdot \frac{\partial Q^{h}}{\partial \sigma_{ij}}$$

$$\dot{D} = -D \cdot \left(\frac{\dot{F}^{h}}{fc1 \cdot fc2} + \frac{I_1}{fs1 \cdot fs2} + \frac{1}{fh} \right)$$

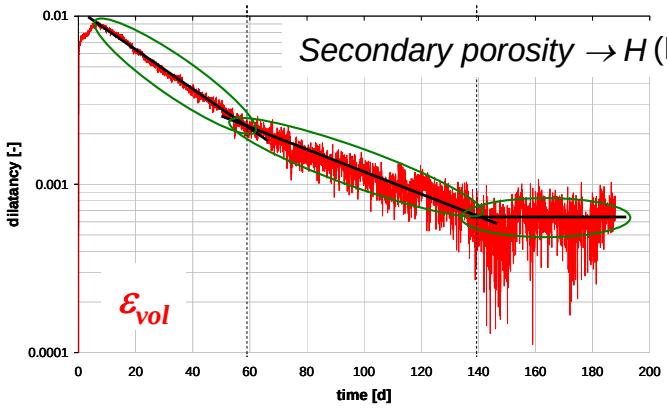

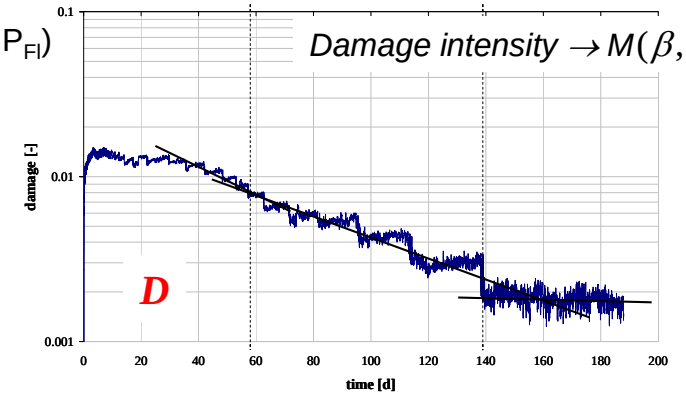

(1/4) Infiltration Properties

Lab test experience

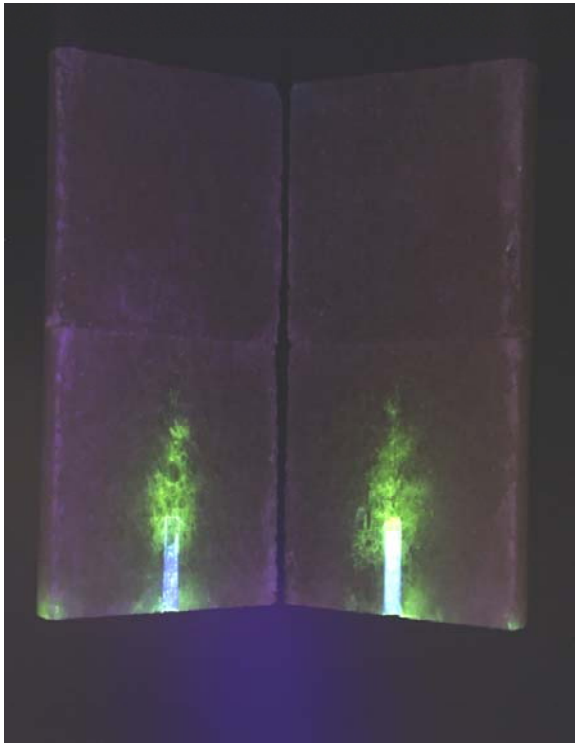

Salt rock sample with infiltration of liquid

$$-\bar{v}_{\inf} = a \cdot \exp\left(b \cdot \Delta p_{Fl}\right)$$

$$-\Delta p_{Fl} \uparrow = \beta \cdot \Delta K$$

$$-\Delta p_{Fl} \downarrow = \beta \cdot \Delta \phi^{s}$$

Flow related to Darcy

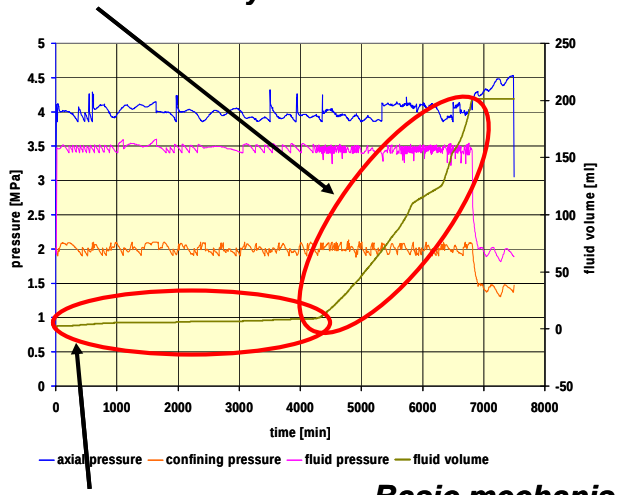

Infiltration phase

Basic mechanisms

Physical Model

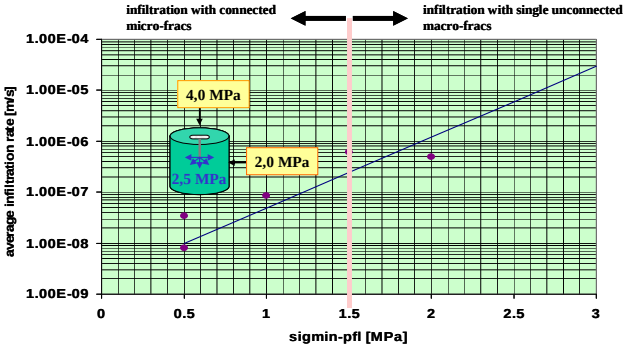

pressure-dependent representation of the average rate of infiltration $v_{\inf}$

(2) Physical Modelling Development of Constitutive Model Lux/Wolters
(2/1) Creep Process without Damage

$$\varepsilon_{ij} = \varepsilon_{ij}^{e} + \varepsilon_{ij}^{ie}$$

$$\varepsilon_{ij}^{ie} = \varepsilon_{ij}^{vp}$$

modLubby2: $\sigma \rightarrow \sigma/(1-D)$, mod$\bar{G}_k$, mod$\bar{\eta}_m$

$$\varepsilon_{ij}^{vp} = \frac{3}{2} \cdot \left[\frac{1}{\bar{\eta}_k(\sigma)} \cdot \left\{ 1 - \frac{\varepsilon^{tr} \cdot \bar{G}_k(\sigma)(1-D)}{\sigma_v} \right\} + \frac{1}{\bar{\eta}_m(\sigma,T)} \right] \cdot \frac{s_{ij}}{(1-D)}$$

$$D = 1 - \frac{1}{1-\varepsilon_{vol}} \cdot \left(\frac{v_p}{v_{p0}} \right)^2$$

$D = 0$ *if no damage*

$\Rightarrow$

modLubby2 without damage

$$\varepsilon_{ij}^{vp} = \frac{3}{2} \cdot \left[\frac{1}{\bar{\eta}_k} \cdot \left(1 - \frac{\varepsilon_{tr}}{\varepsilon_{tr\max}} \right) + \frac{1}{\bar{\eta}_m} \right] \cdot s_{ij}$$

$$\varepsilon_{tr\max} = \frac{1}{\bar{G}_k} \cdot \sigma_v$$

$$\bar{\eta}_k(\sigma) = \bar{\eta}_k^{*} \cdot \exp(k_2 \cdot \sigma_v)$$

$$\bar{G}_k(\sigma) = \bar{G}_k^{*} \cdot \exp(k_1 \cdot \sigma_v) \cdot \left(\frac{\sigma_v}{\sigma^{*}} \right)^{b}$$

$$\bar{\eta}_m(\sigma,T) = \bar{\eta}_m^{**} \cdot \exp(m \cdot \sigma_v) \cdot \exp(l \cdot T) \cdot \left(\frac{\sigma_v}{\sigma^{*}} \right)^{a}$$

(2) Physical Modelling Development of Constitutive Model Lux/Wolters
(2/2) Creep Process with Damage

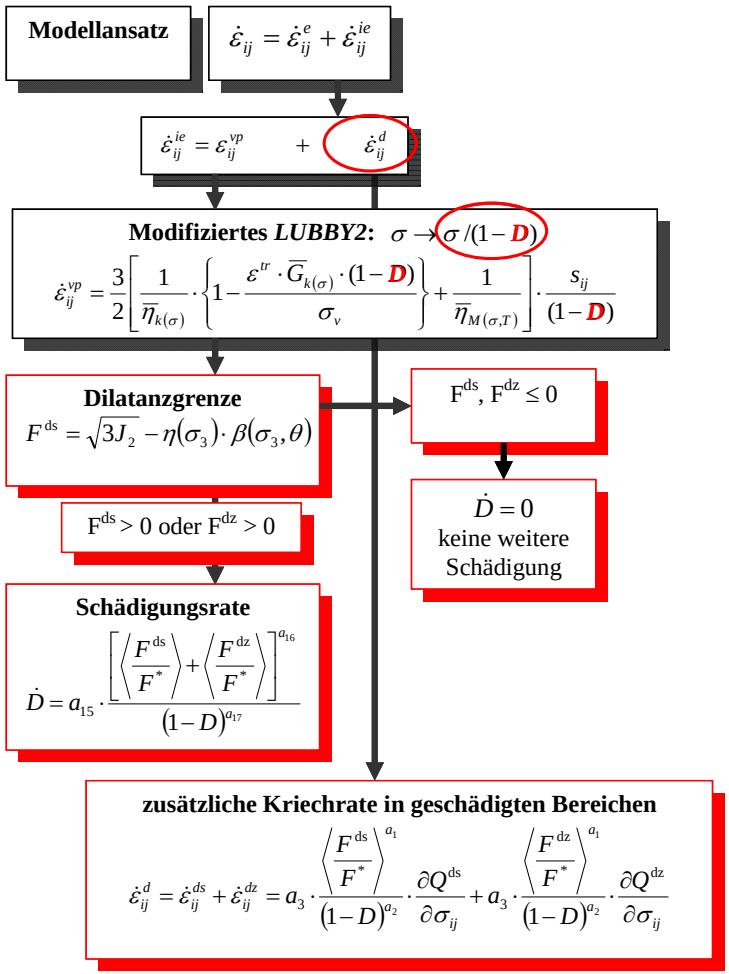

Damage of Rock Fabric

micro-/macrofissurisation
→ dilatancy / destrengthening
→ damage

Damage Intensity Factor:

$$D = 1 - \frac{1}{1-\varepsilon_{vol}}\cdot\left(\frac{v_p}{v_{p0}}\right)^2$$

$$D \approx \left|\varepsilon_{vol}\right|$$

Implementation of Damage D as well as Damage-induced Creep in the Constitutive Model LUBBY2

(2) Physical Modelling Development of Constitutive Model Lux/Wolters
(2/3) Creep Process with Damage and Recreation of Damage (Healing)

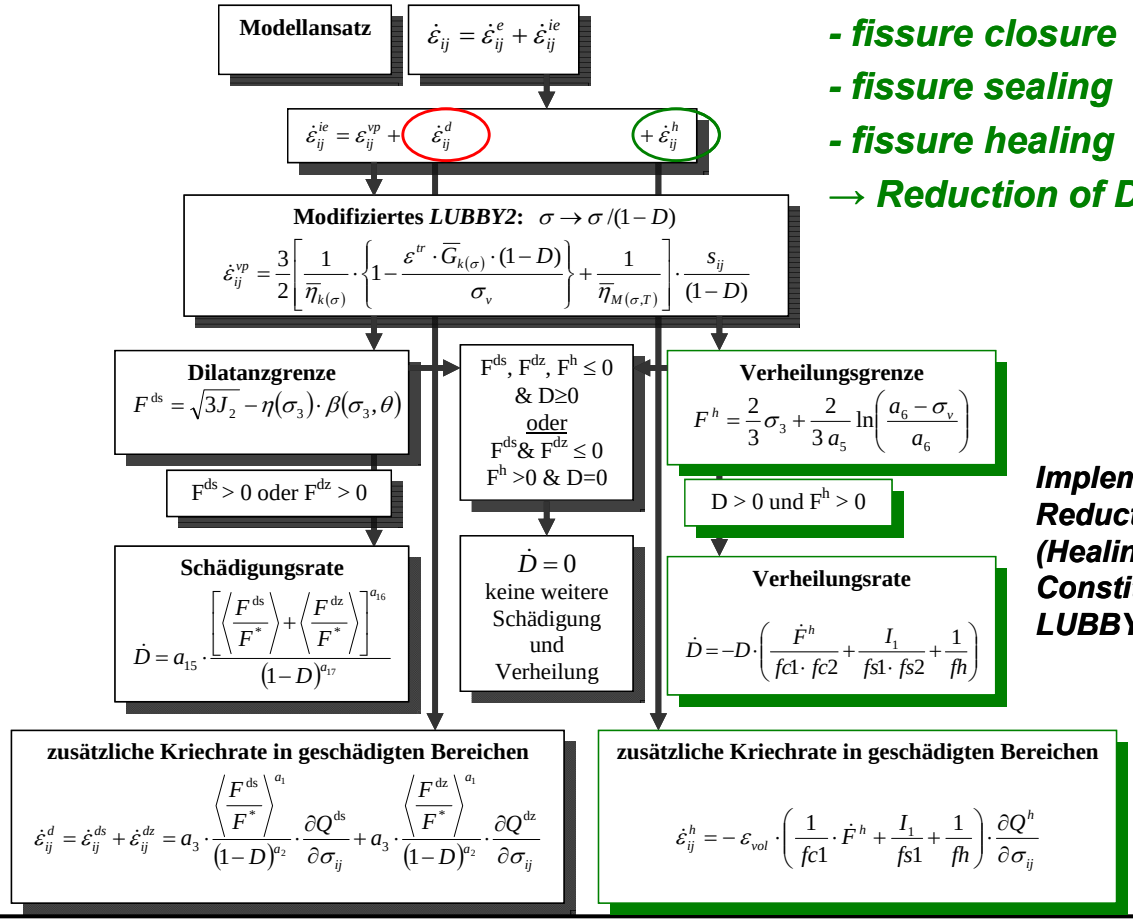

Recreation of Rock Fabric Quality
- fissure closure
- fissure sealing
- fissure healing
→ Reduction of Damage (Healing)

Implementation of Reduction of Damage (Healing) in the Constitutive Model LUBBY2

(2) Physical Modelling Development of Constitutive Model Lux/Wolters
(2/4) Mechanical Processes coupled with Hydraulic Processes

General Demands

- Mechanical Stability
- Tightness
- Acceptable surface subsidence
- Environmental safe abandonment

Salt Cavern – Rock Mass Behaviour after Abandonment

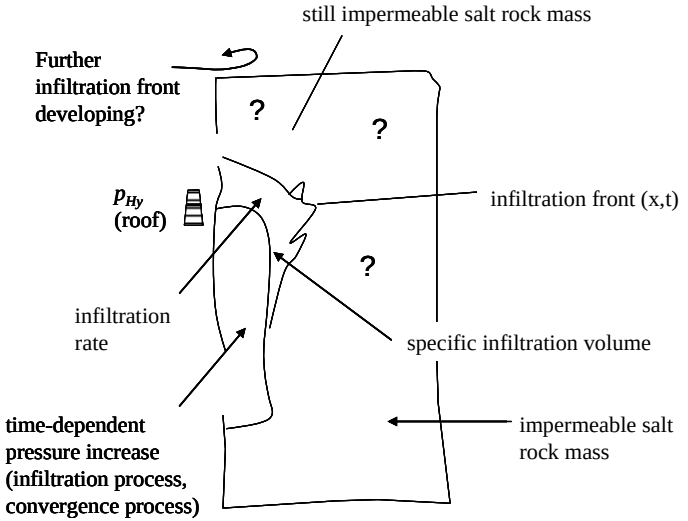

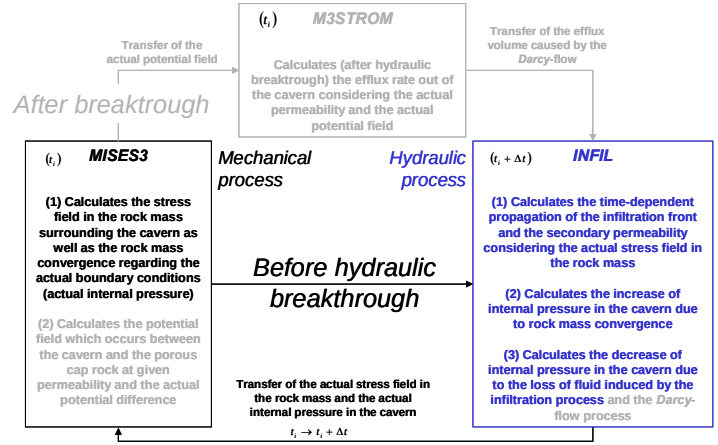

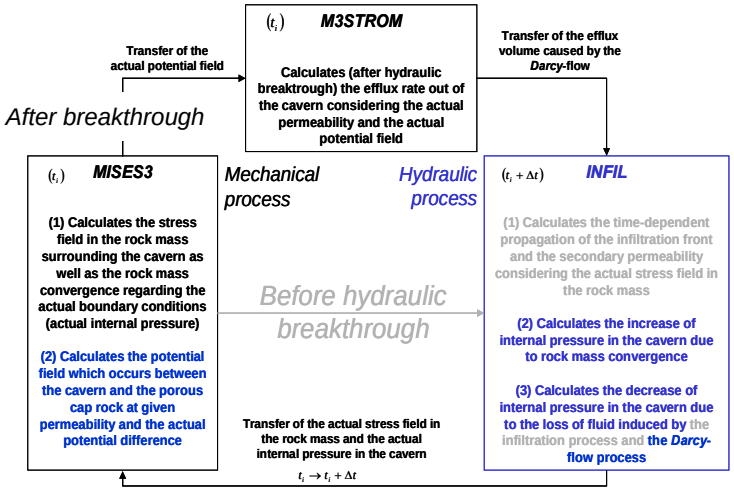

(3) Numerical Simulations – Validation / Prognosis
(3/1) Morsleben Repository – Abandonment / Barrier Integrity

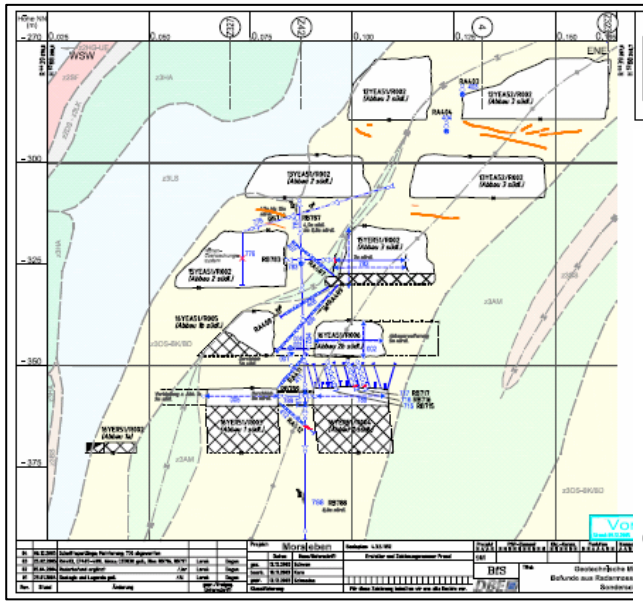

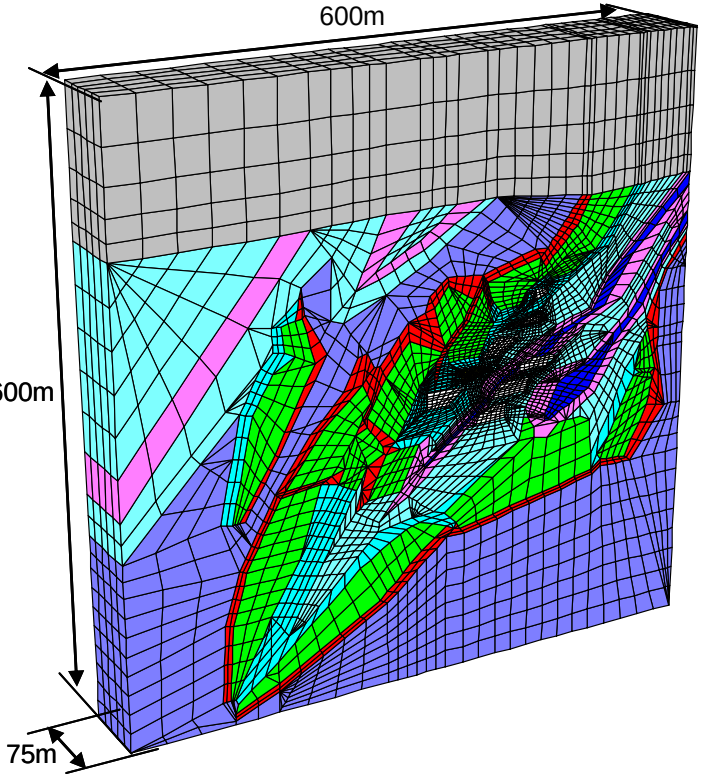

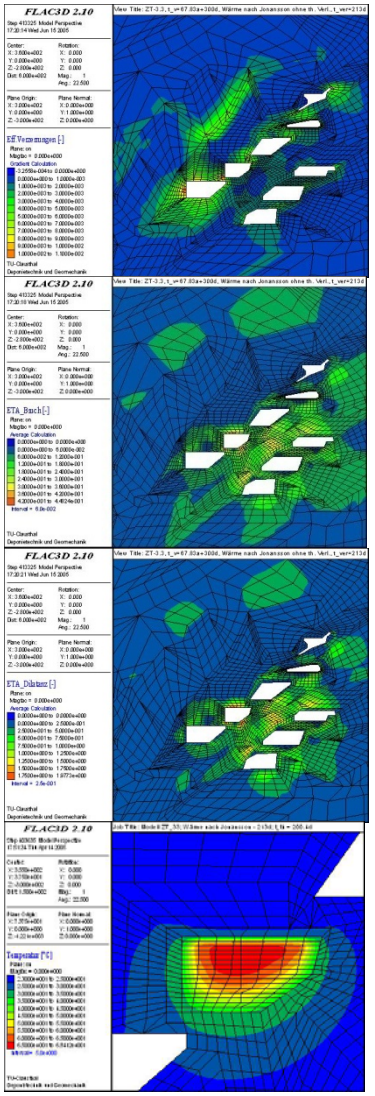

(3) Numerical Simulations – Validation / Prognosis
(3/2a) Asse Repository – Mine Behaviour / Dry Conditions

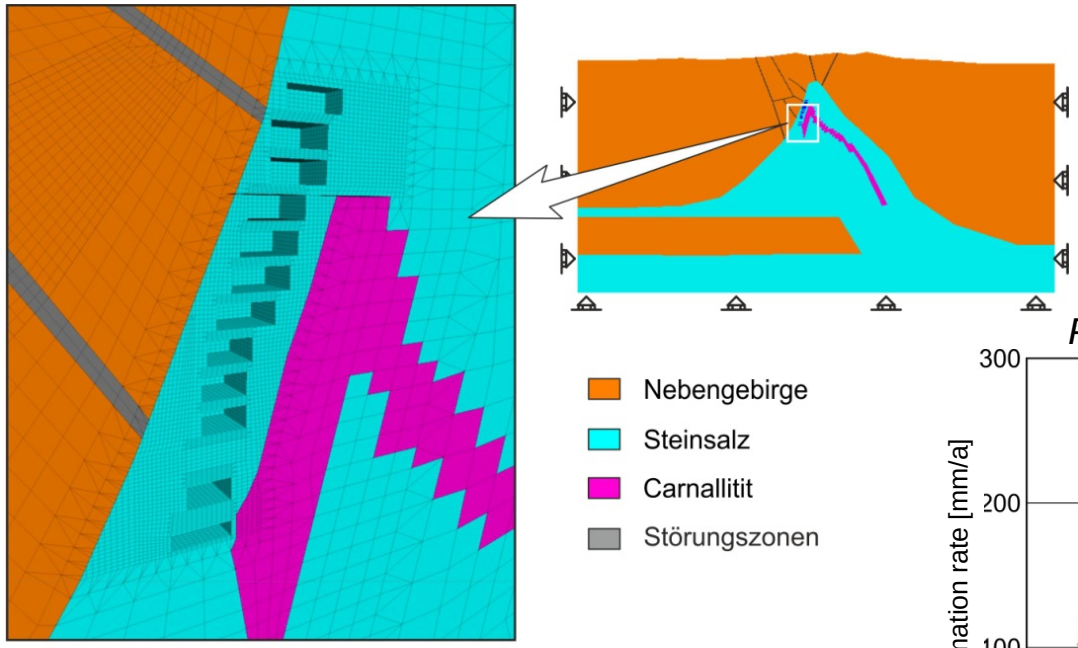

Projekt: ASSE II Zonen: ***62.099***
Modell: BM Asse V2/3D Abmessungen: 5.000 x 36 x 2.525 m

Pillar Deformation Rate in Dependence of Time

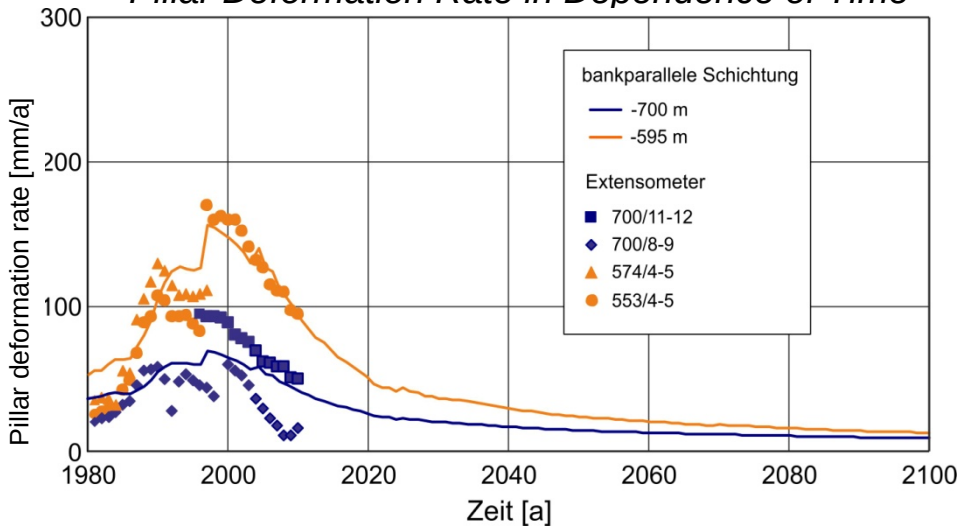

Validation *Prognosis →*

(3) Numerical Simulations – Validation / Prognosis
(3/2b) Asse Repository – Mine Behaviour / Wet Conditions

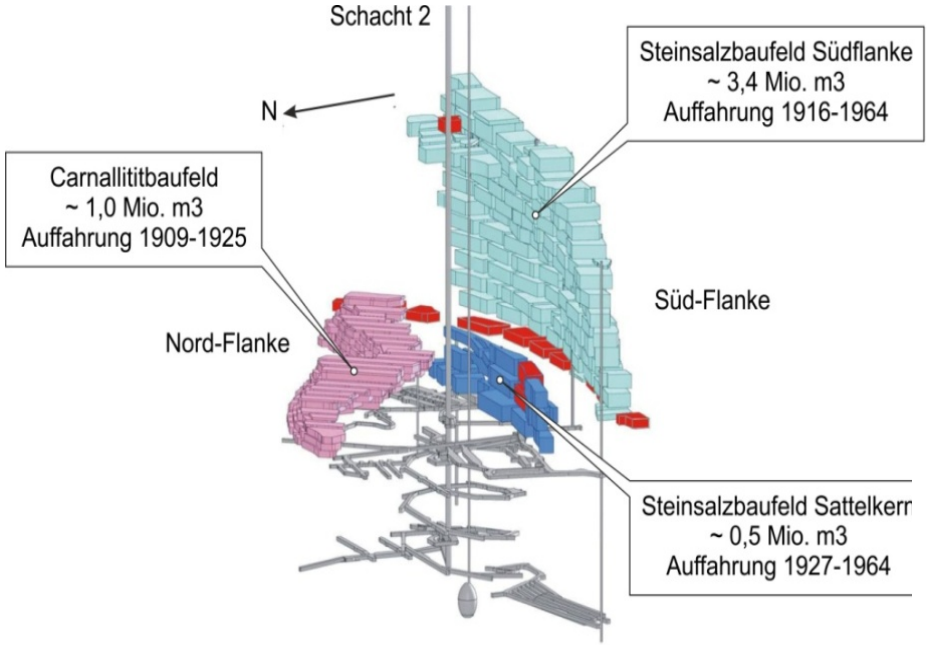

Estimation of Efflux Rate of Brine after Flooding due to Convergence as well as Gas Generation Rate

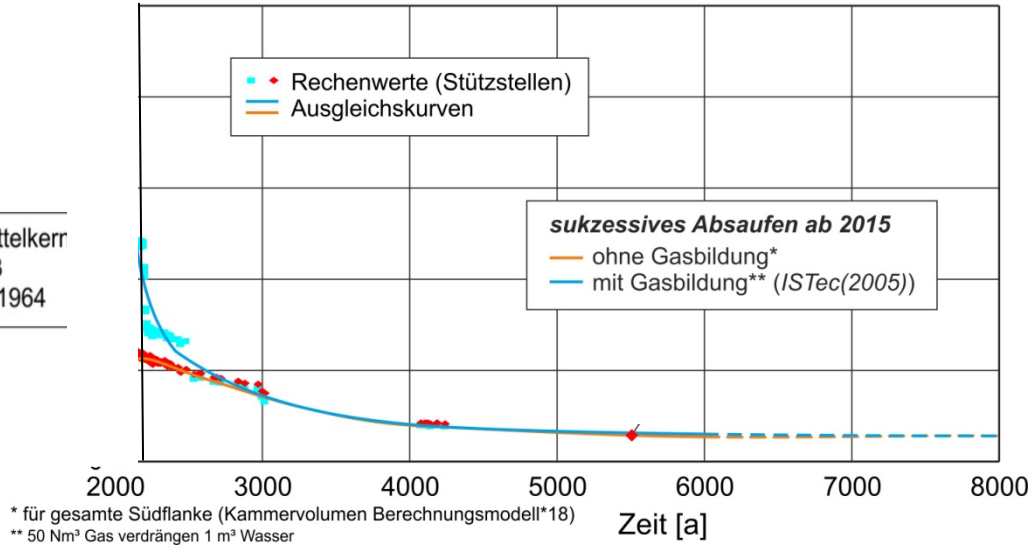

(3) Numerical Simulations – Validation / Prognosis
(3/3) Infiltration Process with Respect to Convergence and Gas Generation

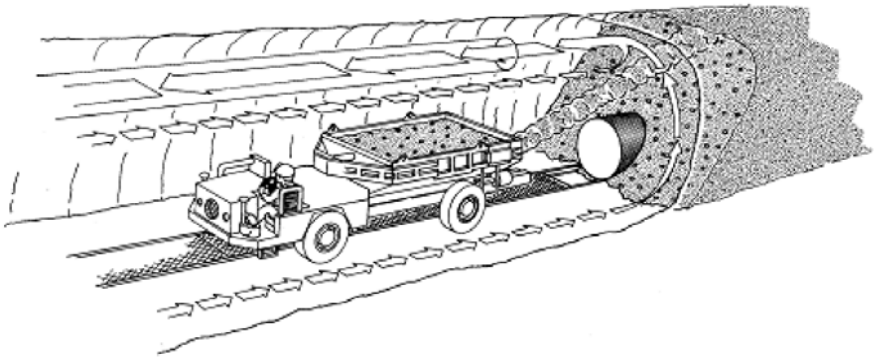

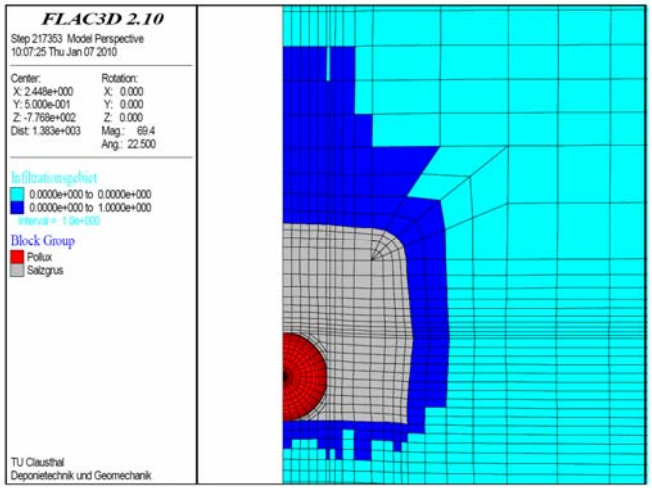

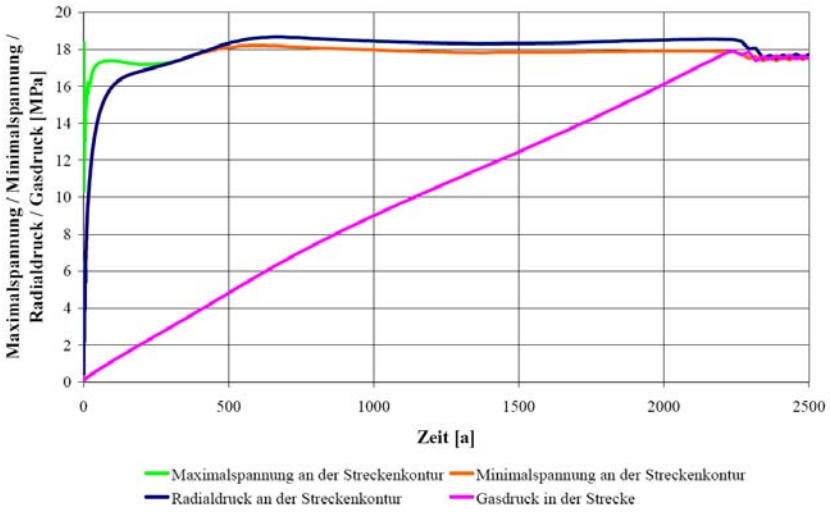

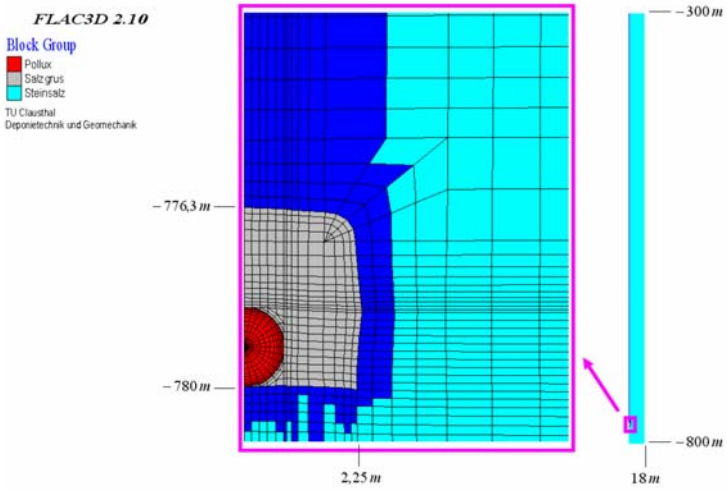

(3) Numerical Simulations – Validation / Prognosis *Static Stability ?*

(3/4a) Geotecnical Barriers – Analysis of Drift Sealing System *Functionability ?*

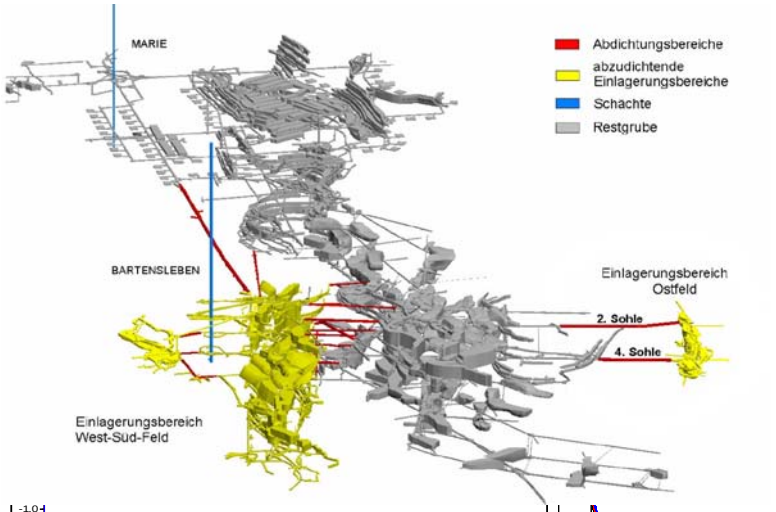

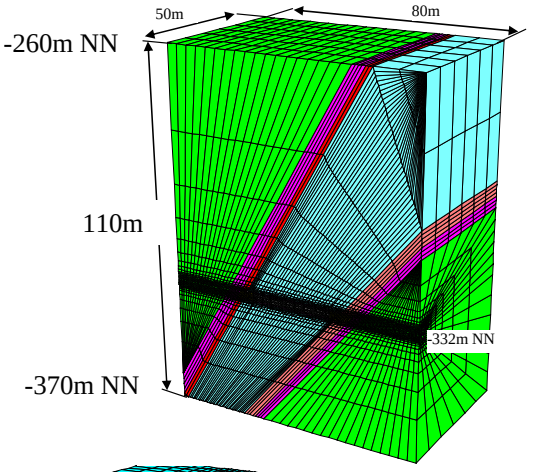

Pressure Build-up in Contract Zone

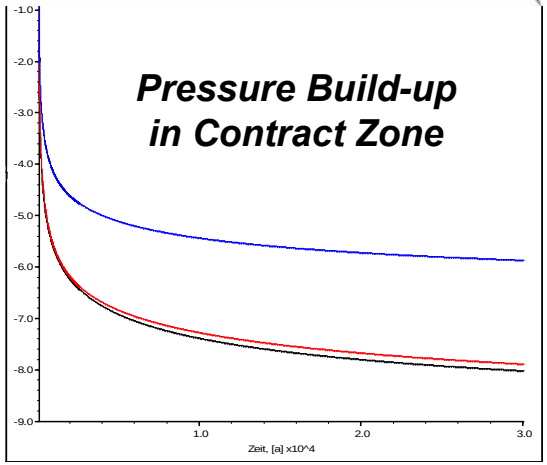

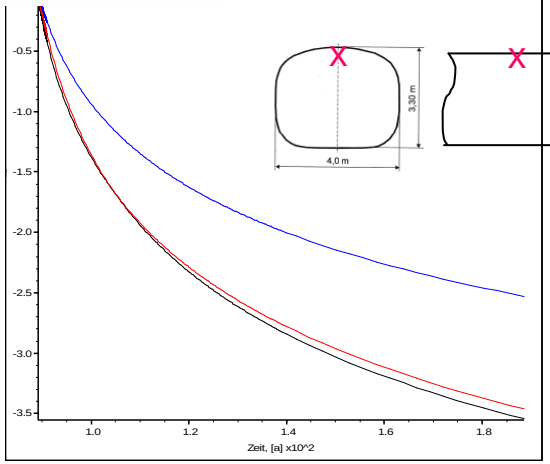

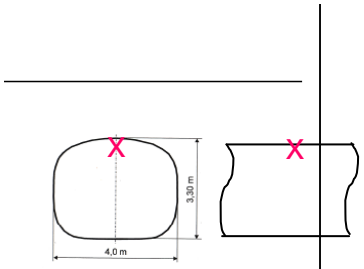

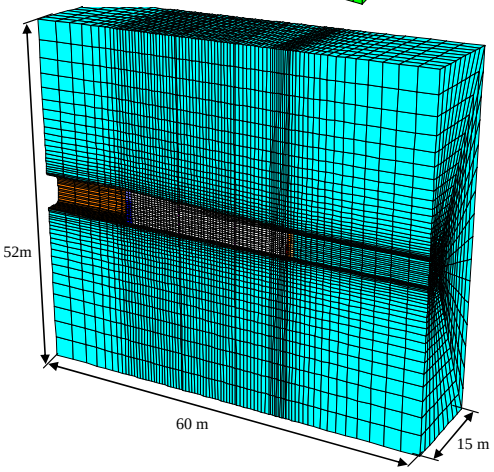

(3) Numerical Simulations – Validation / Prognosis Static Stability ?

(3/4b) Geotecnical Barriers – Analysis of Shaft Sealing System *Functionability ?*

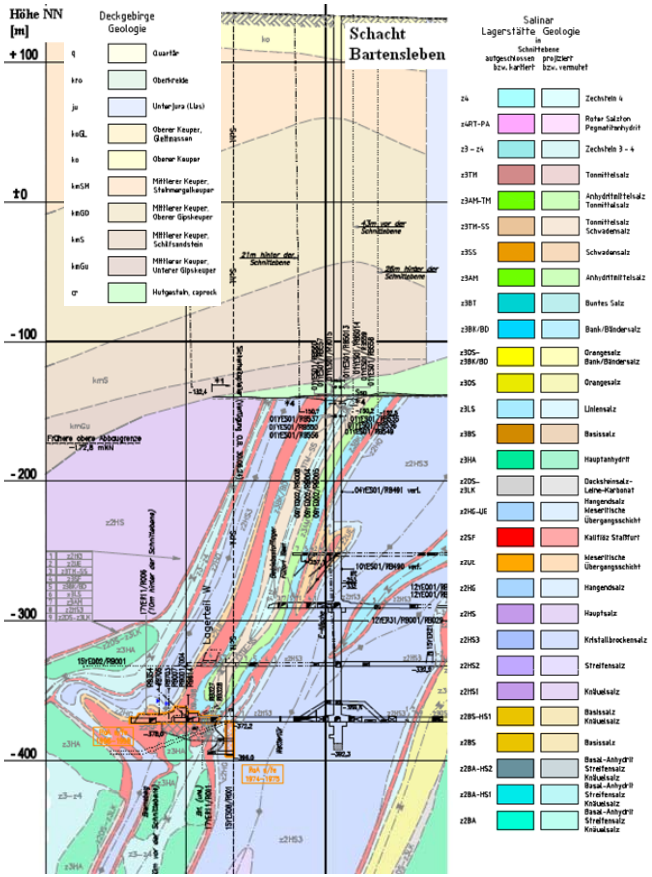

Pore-Pressure in EDZ

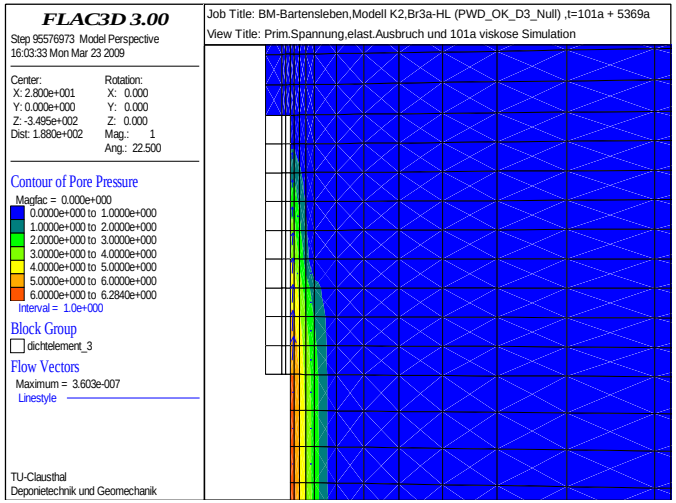

Efflux-Rate through EDZ

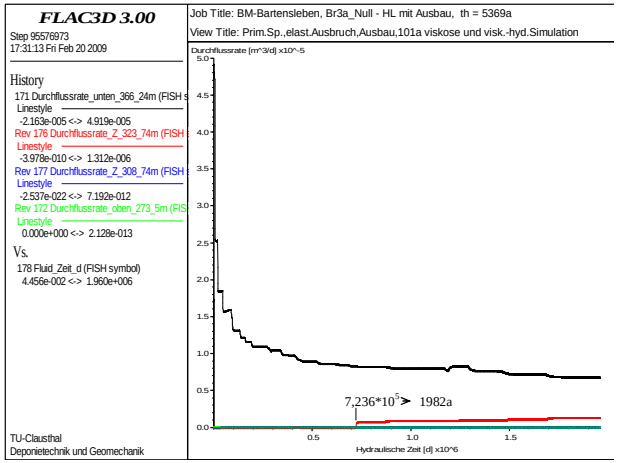

Overview

1. Underground Waste Disposal in Germany
2. Specialized Safety Analysis as well as Safety Criteria with Respect to Rock Salt
3. Contributions of Department of Waste Disposal and Geomechanics to Safety Analysis
4. Some Concluding Remarks

What do we have to do?

The human has three ways of acting wisely:

first through contemplation

– this is the noblest

second by mimicking

– this is the easiest

third by experience

– this is the bitter

Konfuzius

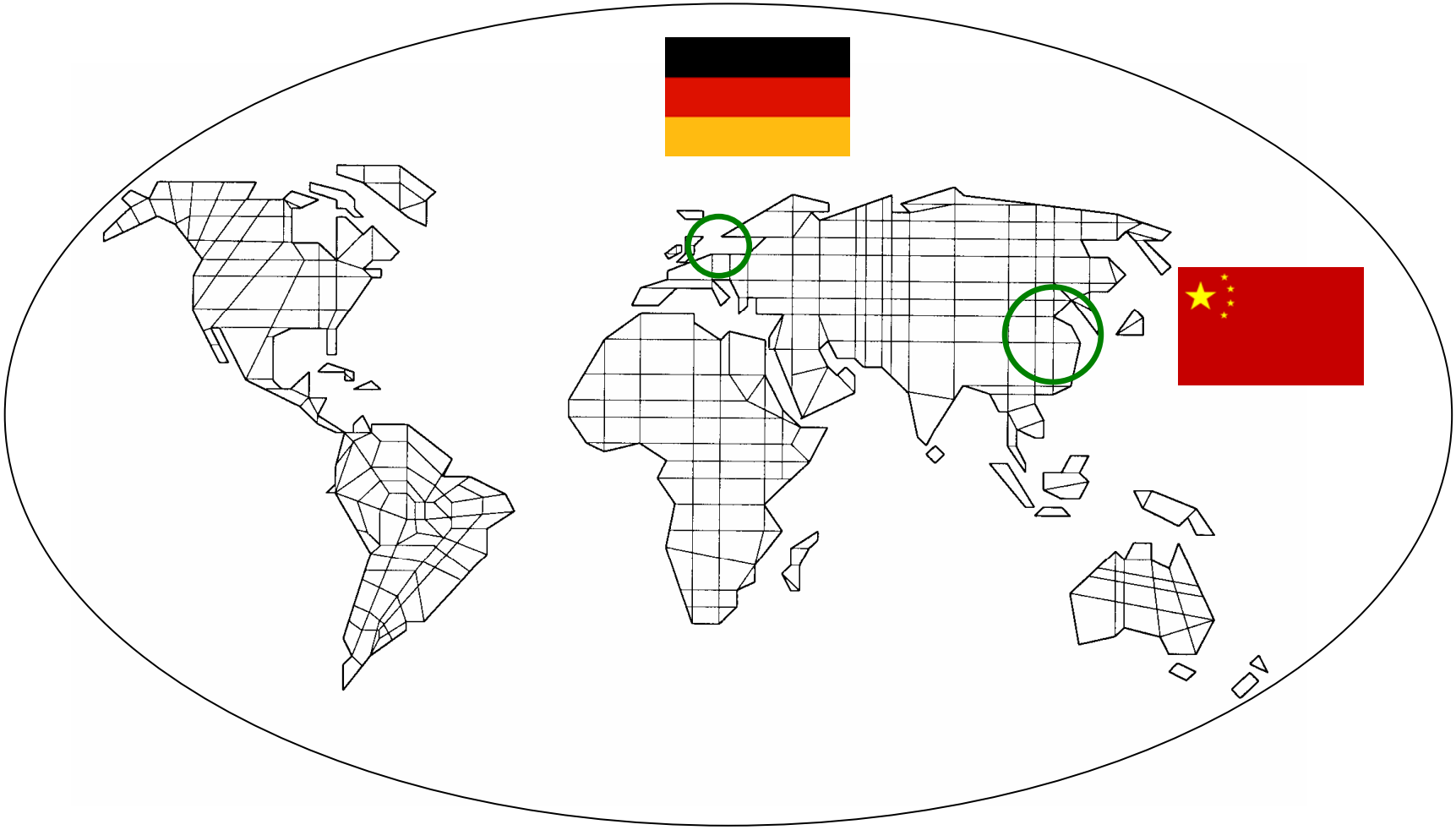

Thanks for your Attention

Tuesday, October 16, 2012

TOPIC: TECHNICAL / GEOTECHNICAL BARRIERS

東華理工大學
EAST CHINA INSTITUTE OF TECHNOLOGY

THMC Testing of Three bentonites of Potential Use for HLW Repository

Liu Xiaodong

East China Institute of Technology

10/15/2012

1 Test samples

Sample A : GMZ (Na-bentonite from Gaomiaozi deposit, China)
initial water content: 5% ±

Sample B: MX-80 (virgin MX-80 Na-bentonite, USA)
initial water content: 6% ±

Sample C: FIM (virgin Friedland Ton bentonite, German)
initial water content: 2% ±

EAST CHINA INSTITUTE OF TECHNOLOGY
東華理工大學

2 THMC testing design and the installations

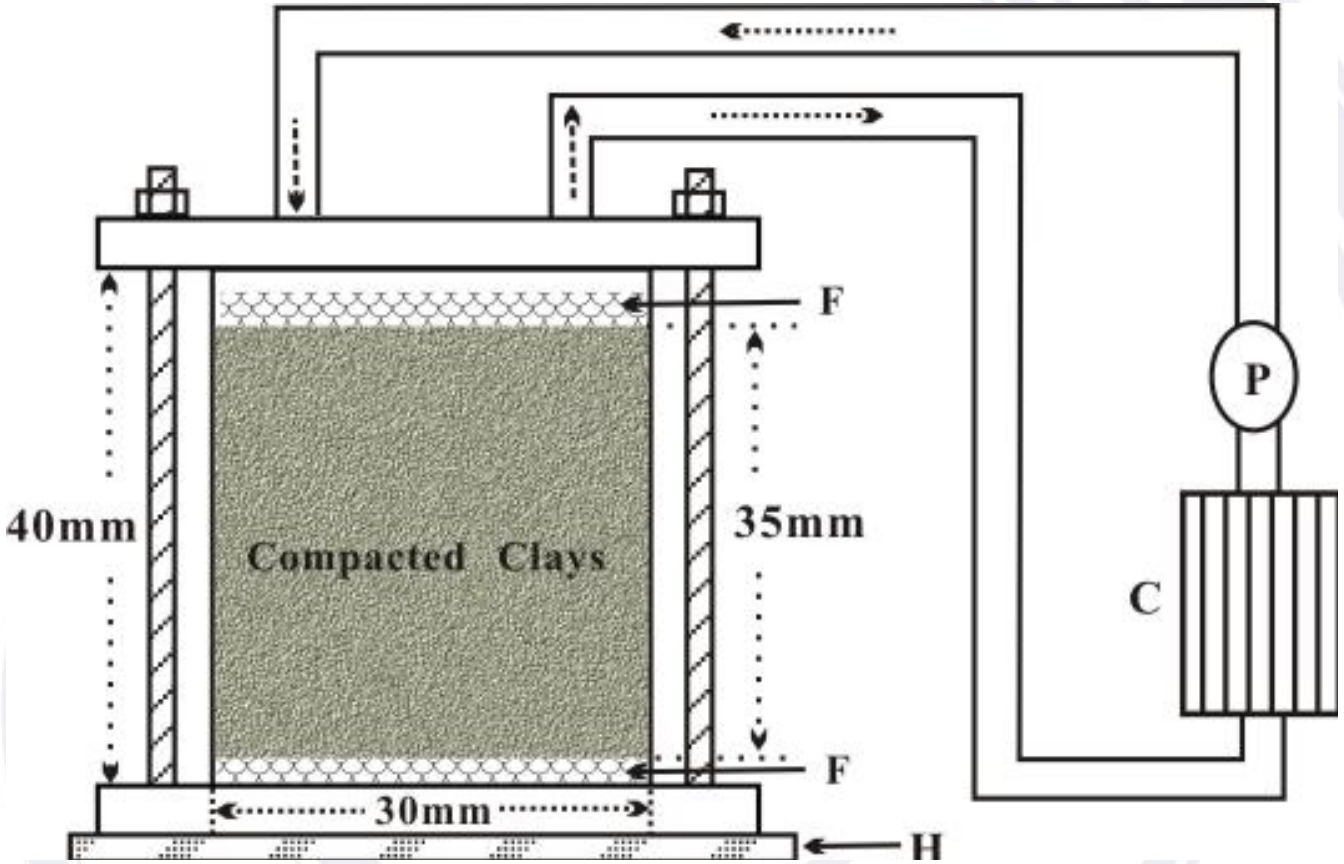

C: cooling pipes; H: heater with the temperature from 90℃ to 95℃;
F: sintered filter; P: pump for the circulation of 3.5% $CaCl_2$ solution

EAST CHINA INSTITUTE OF TECHNOLOGY
東華理工大學

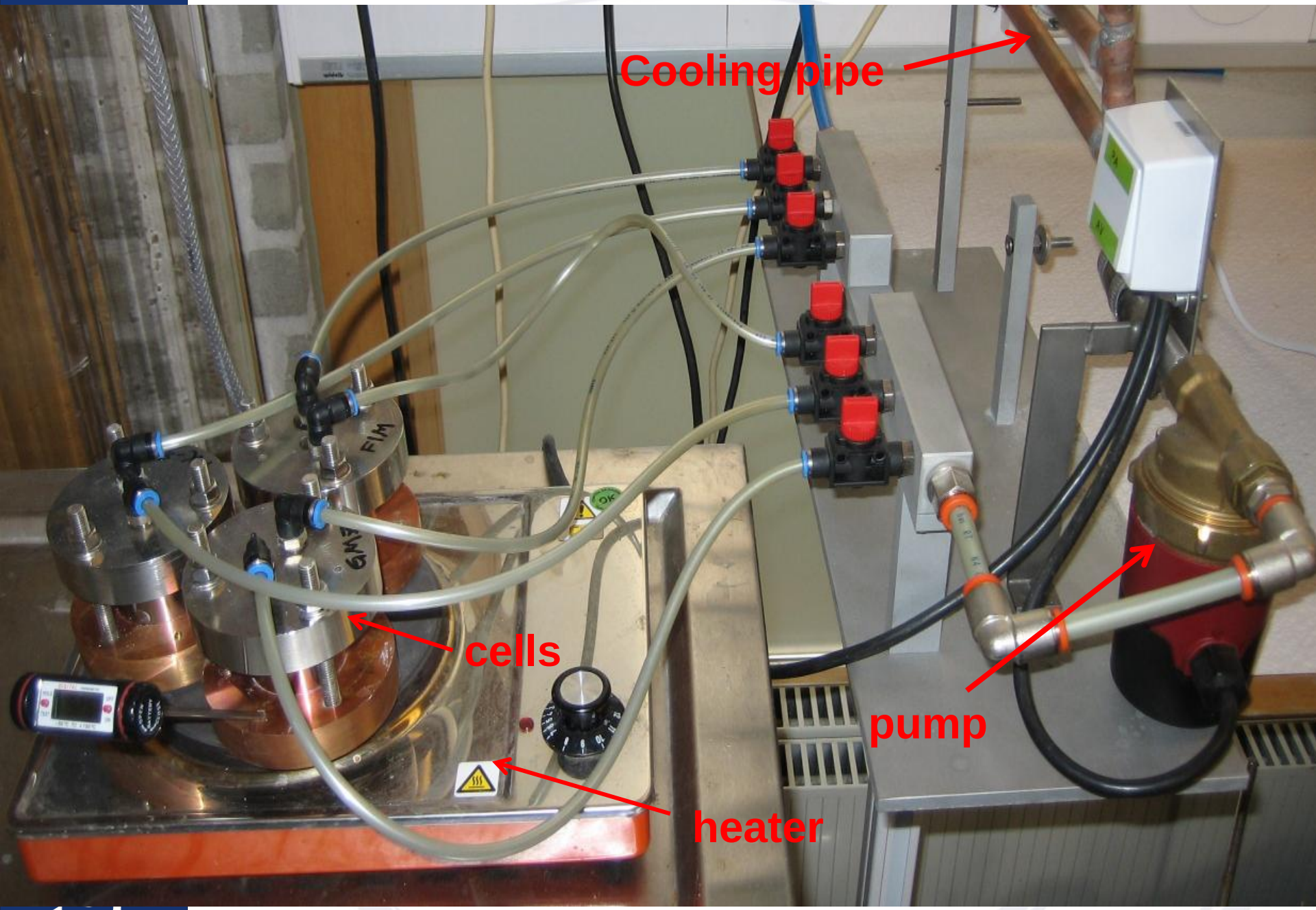
Cooling pipe
cells
pump
heater

EAST CHINA INSTITUTE OF TECHNOLOGY

東華理工大學

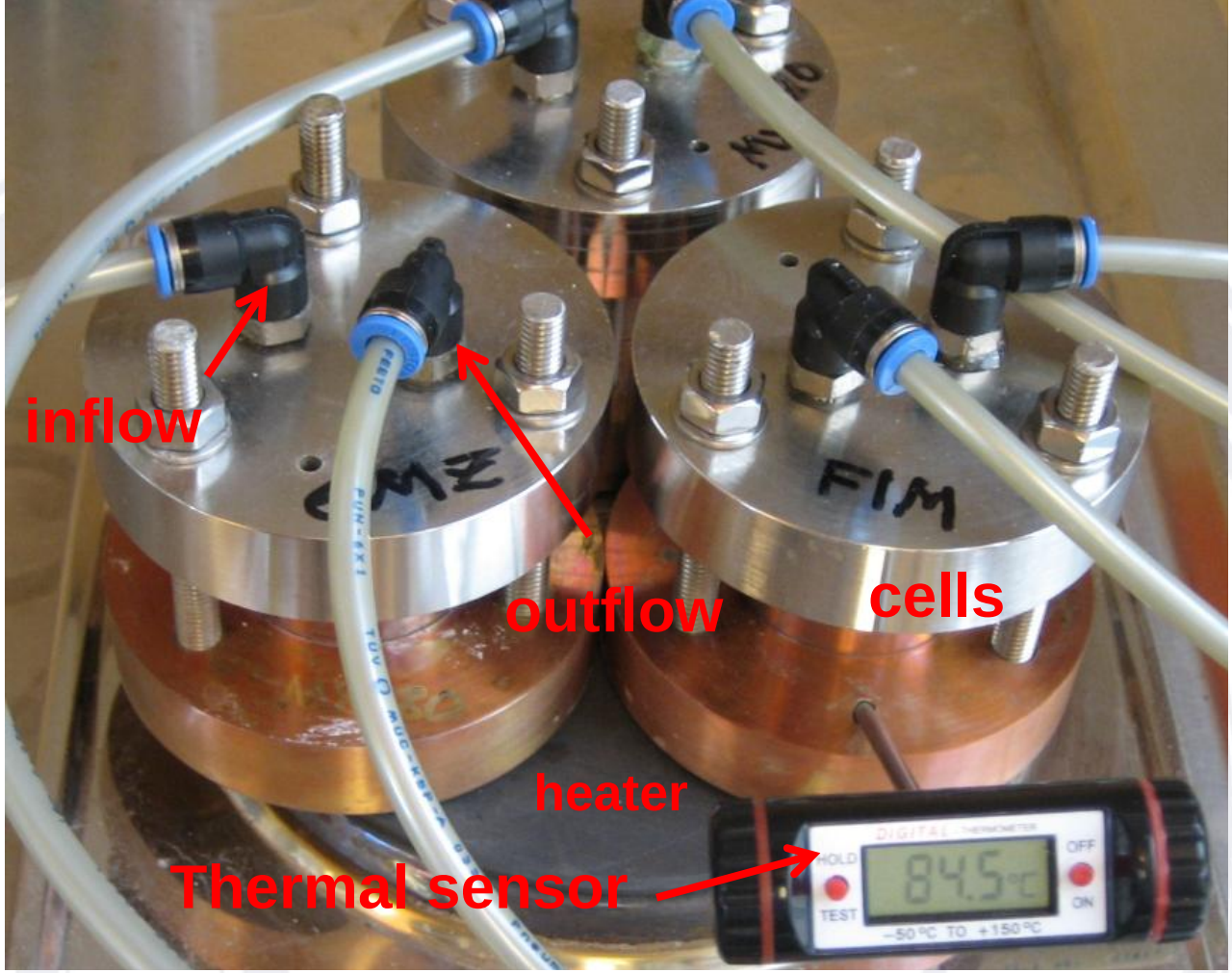

Cells: **stainless cell 40mm high with the diameter of 30 mm stainless cell was connected with the copper bottom.**

Heater: **the temperature can be adjust in 2℃.**

Thermal Sensor: **digital thermal sensor with the measurement range of －50℃ to 150℃.**

東華理工大學
EAST CHINA INSTITUTE OF TECHNOLOGY

Circulation Solution:

3.5%$CaCl_2$ (stimulate the under ground water)

Duration of the test:

continuously running in 3 weeks

Thermal gradient:

about 10°C per cm in the cells and a maximum temperature of 95°C at the bottom of the cells

Analyses specimens:

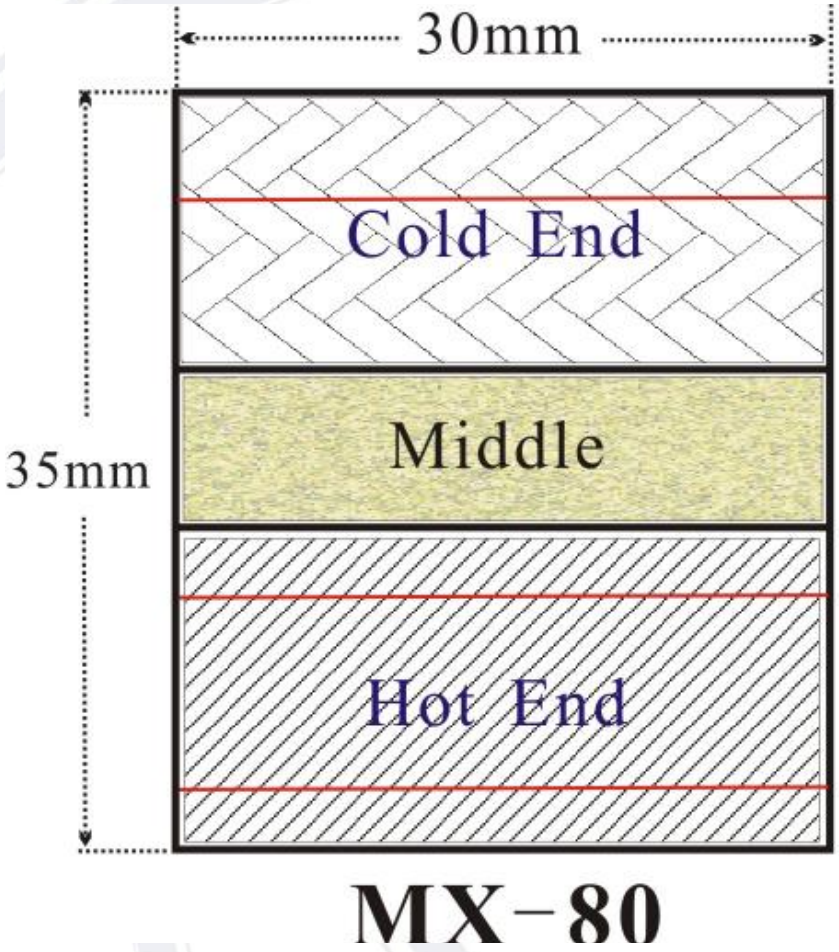

Sampling for microstructure analyses - " cold end"

Sampling for microstructure analyses

Sampling for microstructure analyses - "hot end"

At the end of the thermal/ hydrothermal treatment, the compacted bentonite in the cell will be cut into three parts for chemical, microstructure analyses etc.

EAST CHINA INSTITUTE OF TECHNOLOGY
東華理工大學

東華理工大學
EAST CHINA INSTITUTE OF TECHNOLOGY

Purpose of the test:

To reveal the possible changes of The three bentonites in hydraulic conductivity, expandability, compressibility, microstructural constitution, and mineralogical Compositions.

EAST CHINA INSTITUTE OF TECHNOLOGY
東華理工大學

3 Results of the test

3.1 Chemical changes

Chemical analysis of bentonite individual particles from the cold and hot ends, and the virgin samples were performed by use of EPMA techniques.

EAST CHINA INSTITUTE OF TECHNOLOGY

東華理工大學

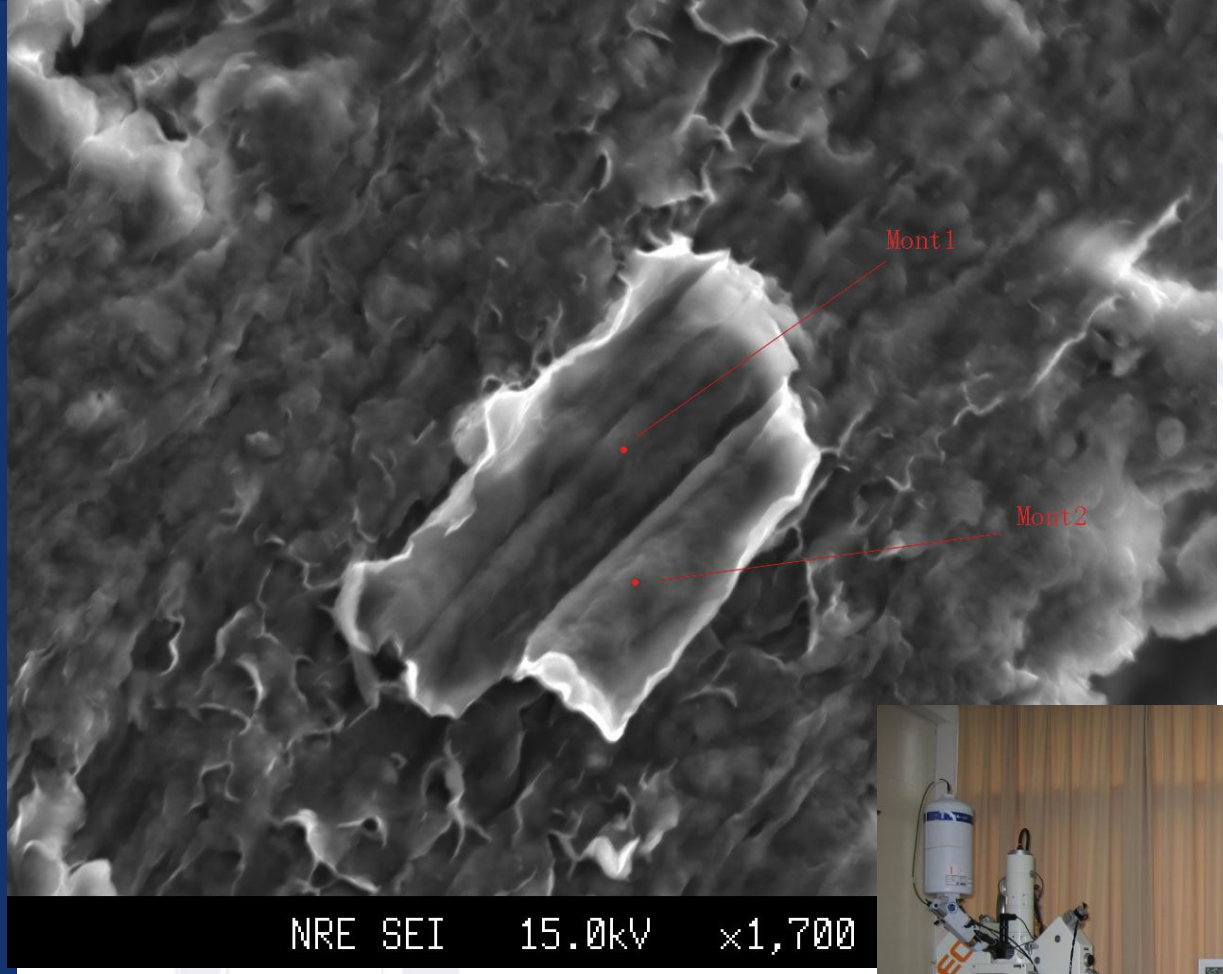

Analyses of individual particles of smectite by JXA-8100 EPMA at at Key Laboratory of Nuclear Resources and Environment of MIE, ECIT.

Sample	SiO_2	Al_2O_3	Fe_2O_3 (FeO)	CaO	MgO	K_2O	Na_2O	MnO	TiO_2	Total
GMZ "cold-end"	71.16	15.63	2.18	2.35	4.10	0.18	0.91	0.01	0.06	97.18
GMZ "hot-end"	68.44	19.58	1.90	1.97	4.80	0.10	1.03	0.05	0.00	98.37
GMZ "virgin"	**68.40**	**21.13**	**1.41**	**0.54**	**4.97**	**0.02**	**1.01**	**0.01**	**0.02**	**97.40**
MX-80 "cold-end"	63.58	21.75	3.29	1.31	2.57	0.05	0.66	0.02	0.14	94.15
MX-80 "hot-end"	60.63	20.09	2.77	0.89	3.53	0.06	0.77	0.03	0.10	90.76
MX-80 "virgin"	**61.69**	**22.36**	**3.50**	**0.31**	**2.29**	**0.20**	**0.68**	**0.02**	**0.10**	**91.14**
FIM "cold-end"	57.18	27.12	6.56	0.60	2.30	3.87	0.46	0.01	0.14	98.55
FIM "hot-end"	58.70	26.98	4.71	0.75	1.88	2.43	0.53	0.01	0.31	97.33
FIM "virgin"	**57.59**	**27.89**	**4.76**	**0.16**	**2.25**	**2.86**	**0.40**	**0.01**	**0.28**	**96.20**

Chemical Composition of the clay samples by EPMA Analyses (weight %)

EAST CHINA INSTITUTE OF TECHNOLOGY
東華理工大學

- SiO_2 increased at the cold and hot ends of GMZ and at the cold end of MX-80
- CaO increased significantly in the cold ends (due to the circulation of 3.5% $CaCl_2$ solution at the cold end of the cells)
- Na_2O increased in the hot ends of the samples by migration of Na from the colder clay where Ca^{2+} replaced of Na^{+} as adsorbed cation.
- **Fe** accumulated in the cold parts of all the clays.

3.2 Minerals and microstructure changes

X-ray diffraction, infrared spectroscopy (FTIR spectroscopy) analyses and the SEM imaging indicated the changes in microstructure and in mineral compositions of the three bentonites.

- GMZ

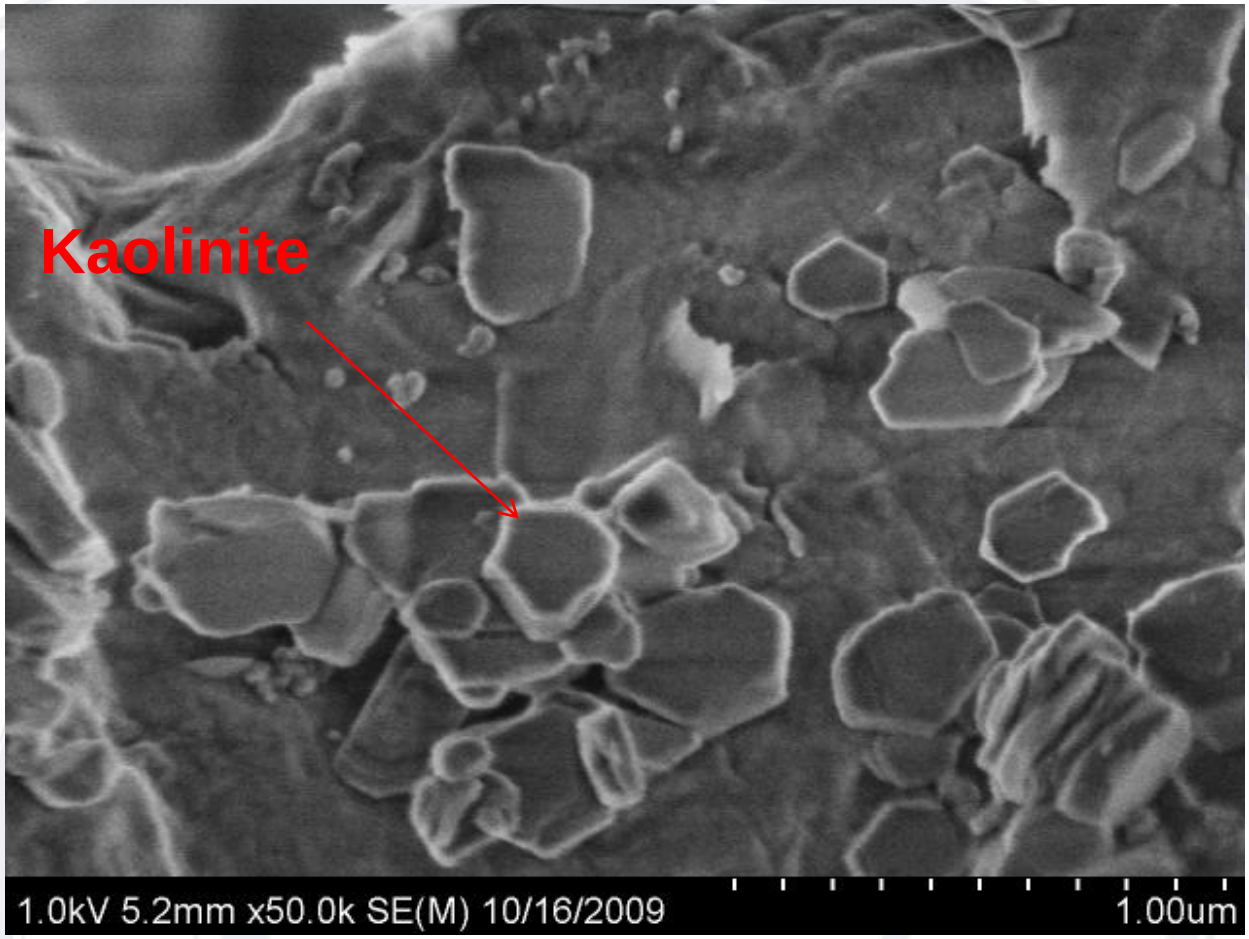

***neoformed kaolinite with well-pronounced 001 reflection occurred in the interlamellar space of montmorillonite in the hot-end specimen of GMZ**

*** presence of neoformed illite**

EAST CHINA INSTITUTE OF TECHNOLOGY
東華理工大學

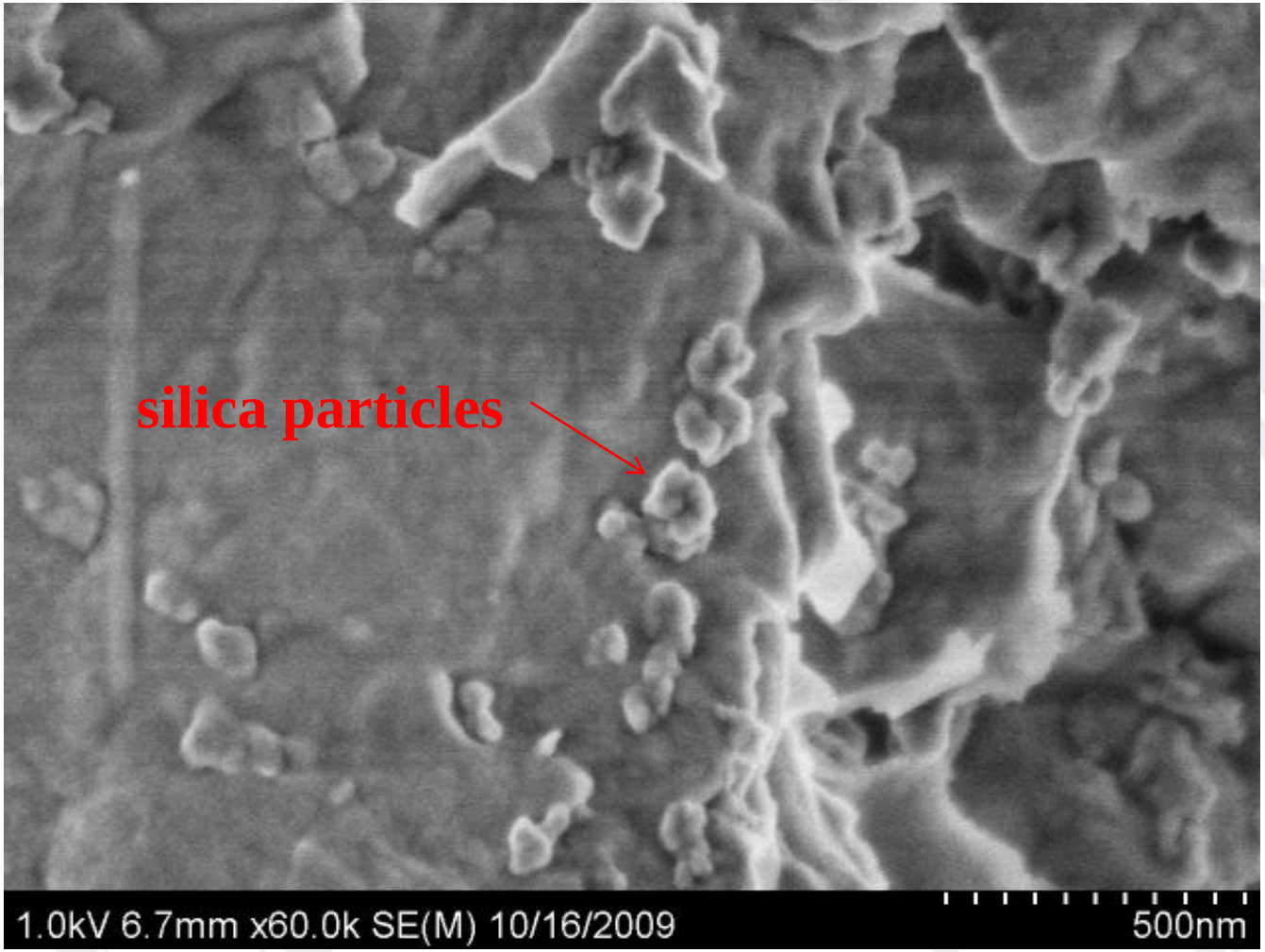

fine silica particles precipitated on smectite (montmorillonite) of GMZ,
corresponding to the SiO_2 increase by chemical analyses

EAST CHINA INSTITUTE OF TECHNOLOGY
東華理工大學

EAST CHINA INSTITUTE OF TECHNOLOGY
東華理工大學

- MX-80

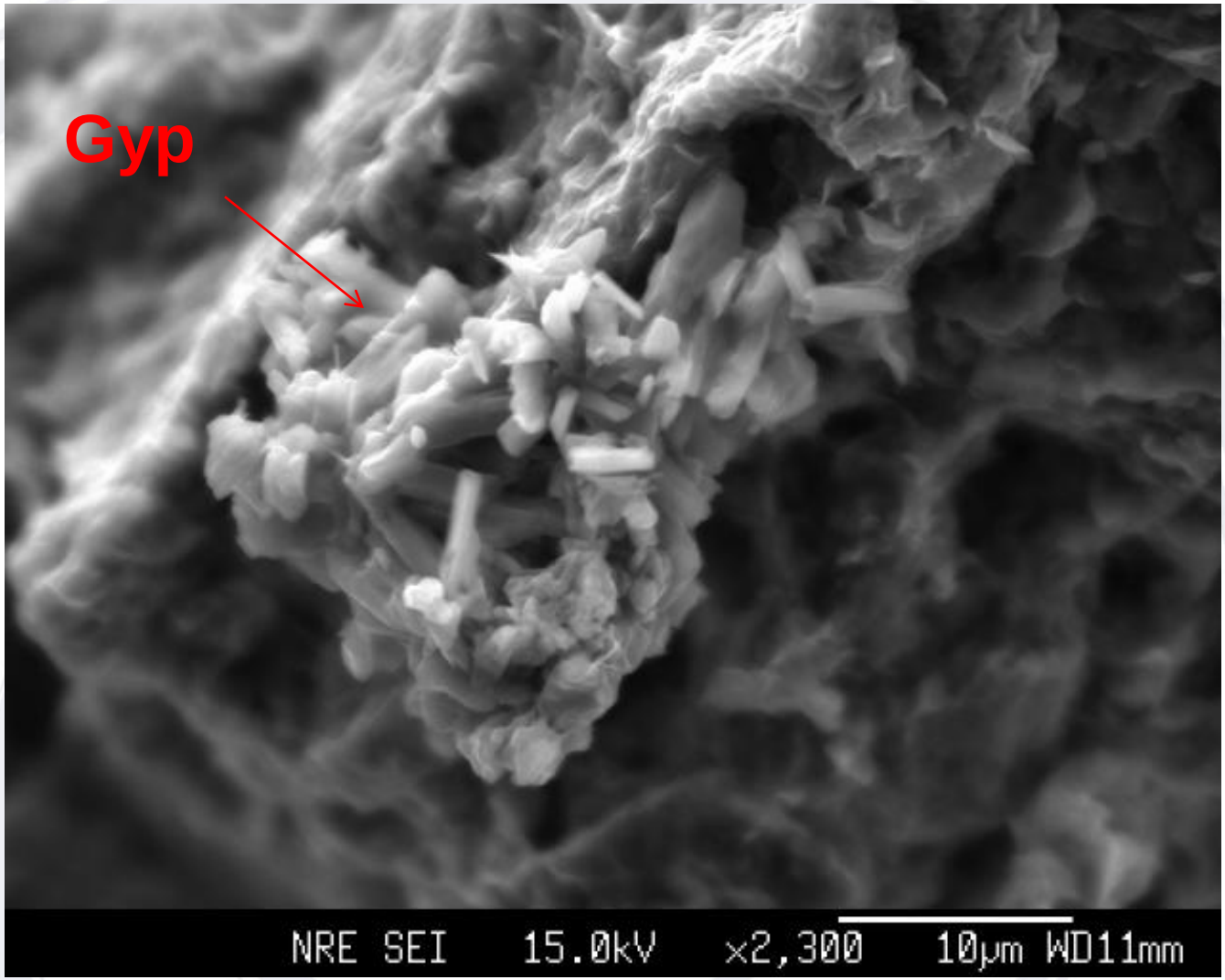

Neoformed aggregated gypsum (Gyp) crystals precipitated In the void between of montmorillonite particles

-FIM

- formation of gypsum was indicated by XRD analyses
- Precipitation of silica was documented by FTIR spectroscopy

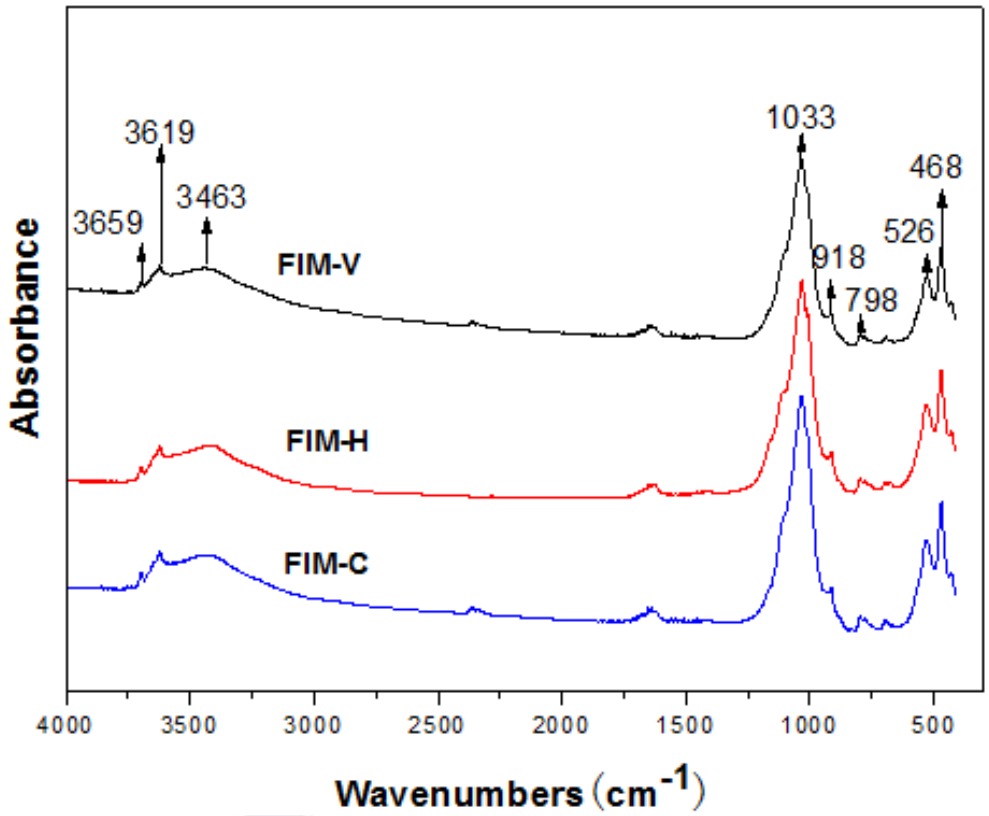

V = “virgin” material;
H = “hot-end” specimen
C = “cold-end” specimen

EAST CHINA INSTITUTE OF TECHNOLOGY
東華理工大學

3.3 Physical properties changes

3.3.1 Hydraulic conductivity and swelling pressure

Property	GMZ		MX-80		FIM	
	"hot-end"	"cold-end"	"hot-end"	"cold-end"	"hot-end"	"cold-end"
ρ/ρ_d (kg/m^3)	1871/1232	1788/1233	1951/1375	1844/1310	1958/1412	1875/1392
K(m/s)	2.6E-11	2.8E-11	1.2E-11	2.0E-11	1.8E-11	4.0E-11
p_s (MPa)	0.11	0.53	0.13	1.14	0.43	0.28

hydraulic conductivity and swelling pressure for the hot and cold end specimens for their respective densities after saturation and percolation with 3.5 % $CaCl_2$ solution for 14 days.

- **The hot samples are denser than the "cold" ones**
- **Significant changes in swelling pressure of hot end samples of GMZ and MX-80**

EAST CHINA INSTITUTE OF TECHNOLOGY 東華理工大學

3.3.2. Stress-strain behaviour

Uniaxial loading tests were made of the “hot-end” specimens and of the “virgin” clays with approximately the same density as the “hot-end” specimens.

Test sample

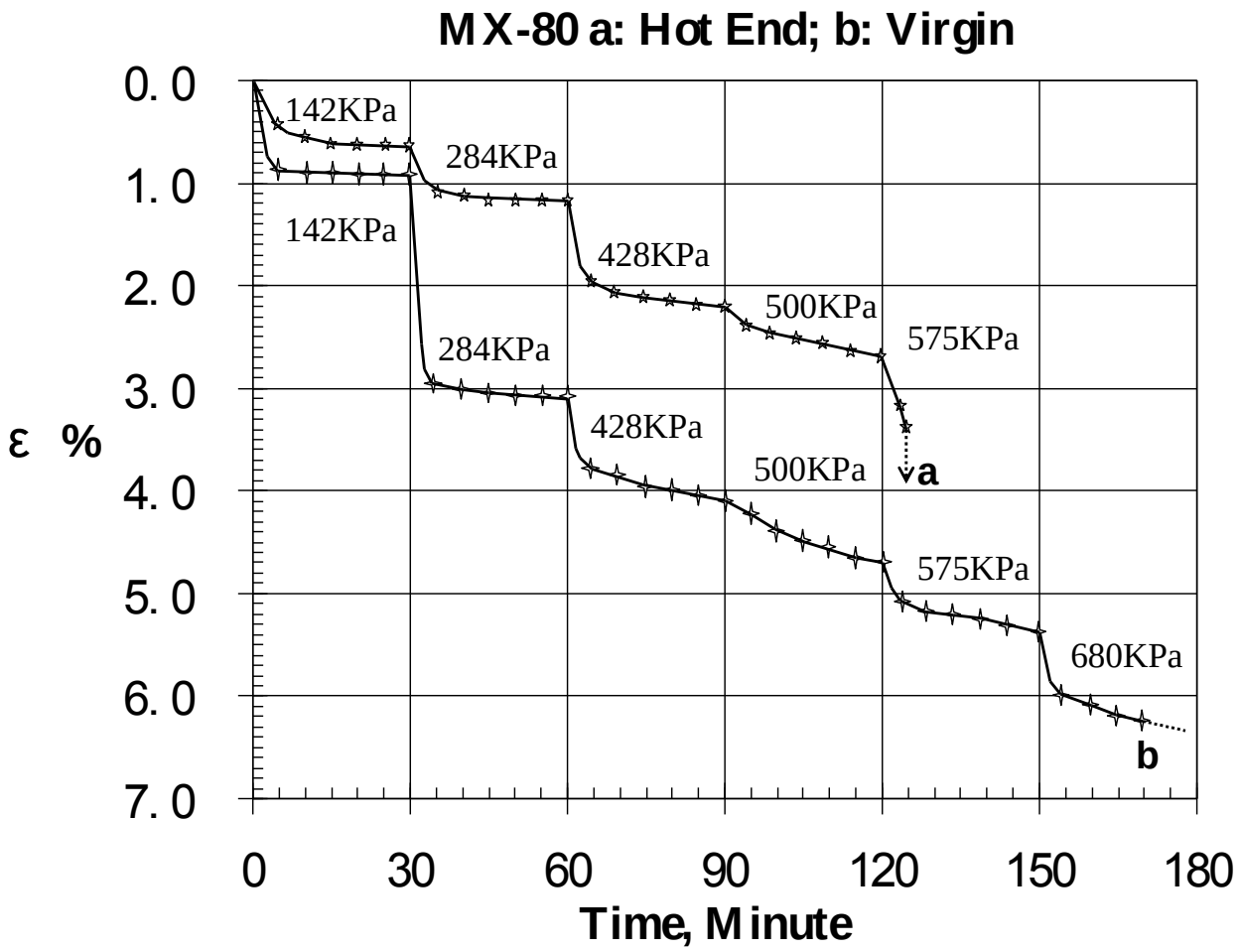

the "hot-end" specimens appear stiffer than the virgin clay samples and exhibited brittle behaviour at failure

4 Discussion

4.1 Mineralogical changes

Gypsum formed in all three bentonite specimens, kaolinite only appeared in GMZ.

But mineralogical changes were small or moderate in “hot-end” specimens in contract to the virgin samples.

EAST CHINA INSTITUTE OF TECHNOLOGY
東華理工大學

4.2 Physical properties

The hot-end specimens of all three bentonites become significantly stiffer and more brittle than those of the virgin clays while the compressive strength had dropped. The loss in strength is believed to be related to fissures that did not self-heal.

EAST CHINA INSTITUTE OF TECHNOLOGY
東華理工大學

The drop in swelling pressure of the hot-end specimens can be explained by the precipitation of siliceous components and illite that might welded the montmorillonite lamellae.

EAST CHINA INSTITUTE OF TECHNOLOGY

東華理工大學

Published paper:

Liu Xiaodong, Richard Prikryl and Roland Pusch

Applied Clay Science

Vol. 52, 419-427

EAST CHINA INSTITUTE OF TECHNOLOGY 東華理工大學

Acknowledgements

Experimental hydrothermal treatment, hydraulic conductivity, swelling pressure and uniaxial loading tests for three bentonites were conducted in Lund under the kind guidance of Prof. Roland Pusch.

東華理工大學
EAST CHINA INSTITUTE OF TECHNOLOGY

Thank you!

Experimental investigations on the thermo-hydraulic behaviour of GMZ01 bentonite

Weimin YE

Tongji University

2012. KIT/ Germany

Acknowledgements

Yu C., 2006; Qian L.X, 2007; Niu W.J., 2008; Wan M., 2010; Pan H., 2010; Wang Q. _

The authors are grateful to the National Natural Science Foundation of China (Projects No. 41030748) and China Atomic Energy Authority (Project [2007]831) .

Outline

1 Introduction

2 GMZ bentonite

3 Temperature effects on hydraulic conductivities

3.1 Saturated hydraulic conductivity

3.2 Unsaturated hydraulic conductivity

4 Conclusion

1 Introduction (Multi-barrier)

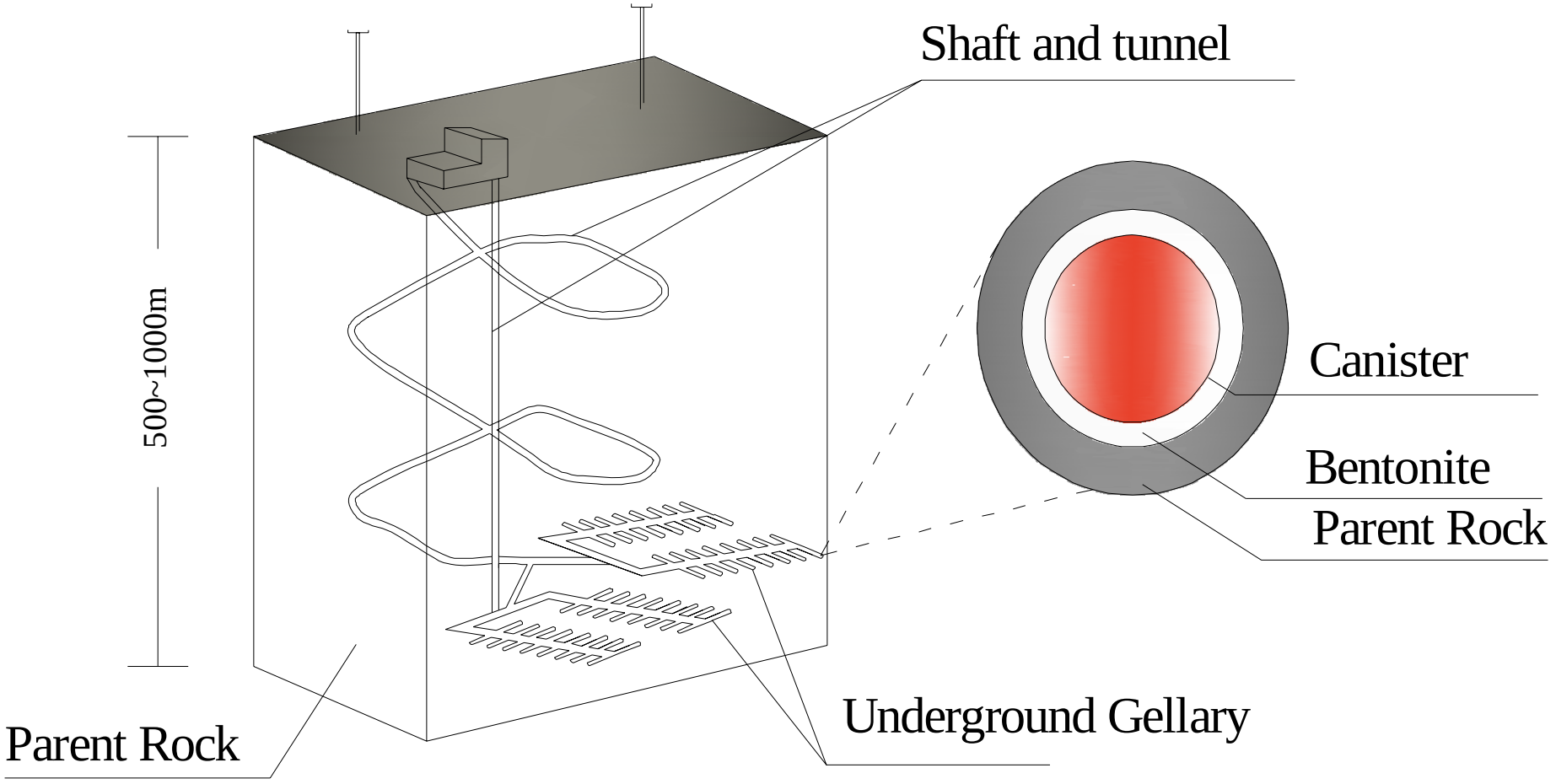

Outline

1 Introduction

2 GMZ bentonite

3 Temperature effects on hydraulic conductivities

3.1 Saturated hydraulic conductivity

3.2 Unsaturated hydraulic conductivity

4 Conclusion

2 GMZ bentonite

Xinghe county, the Inner Mongolia Autonomous Region with a distribution of 72 km^2.

Deposit >160 (120) million t

(Wen Zhijian,2005)

2 GMZ bentonite

Mineralogical composition of some bentonite (wt %)

Sample	Montmorillonite	Quartz	Cristobalite	Feldspar	Plagioclase	Kaolinite	Chalcedony
GMZ	75.4	11.7	7.3	4.3	--	0.8	
FEBEX	92 ± 3	2 ± 1		--	2 ± 1	--	
MX-80	65-82	4-12		5-8	8.2 ± 2.7	--	
Kunigel-V1	47	0.6		--	4	--	37

From: Ye et al., 2010. Engineering Geology. Vol 116(1-2):12-20.

2 GMZ bentonite

Mineralogical composition of some bentonite (wt %)

Clay	Montmorillonite	Quartz	Cristobalite	Feldspar	Plagioclase	Kaolinite	Chalcedony
GMZ	75.4	11.7	7.3	4.3	--	0.8	
FEBEX	92 ± 3	2 ± 1		--	2 ± 1	--	
MX-80	65-82	4-12		5-8	8.2 ± 2.7	--	
Kunigel-V1	47	0.6		--	4	--	37

From: Ye et al., 2010. Engineering Geology. Vol 116(1-2):12-20.

2 GMZ bentonite

Cation Exchange Capacity of some bentonite

Clay	CEC (meq/100 g)	Exchangeable cation (meq/100 g)			
		E(K+)	E(Na^+)	E(1/2Ca^{2+})	E(1/2Mg^{2+})
GMZ	77.30	2.51	43.36	29.14	12.33
FEBEX	111 ± 9	22.2 ± 1.8	25.53±2.07	42.18±3.42	31.08±2.52
MX-80	78.7 ± 4.8	1.3 ± 0.2	66.8 ± 4	6.6±0.33	4±0.3
Kunigel-V1	73.2	0.9	40.5	28.7	3.0

From: Ye et al., 2010. Engineering Geology. Vol 116(1-2):12-20.

2 GMZ bentonite

Main physical properties of some bentonite

Clay	Gs	w_L(%)	w_P(%)	Ip	S (m^2/g)
GMZ	2.66	313	38	275	570
FEBEX	2.7	102 ± 4	53±3	42±7	725
MX-80	2.76	520	42	478	562
Kunigel-V1	2.79	415	32	383	687

First choice in China (Ye et al, 2010)

From: Ye et al., 2010. Engineering Geology. Vol 116(1-2):12-20.

Outline

1 Introduction

2 GMZ bentonite

3 Temperature effects on hydraulic conductivities

3.1 Saturated hydraulic conductivity

3.2 Unsaturated hydraulic conductivity

4 Conclusion

3.1.1 Saturated hydraulic conductivity Apparatus

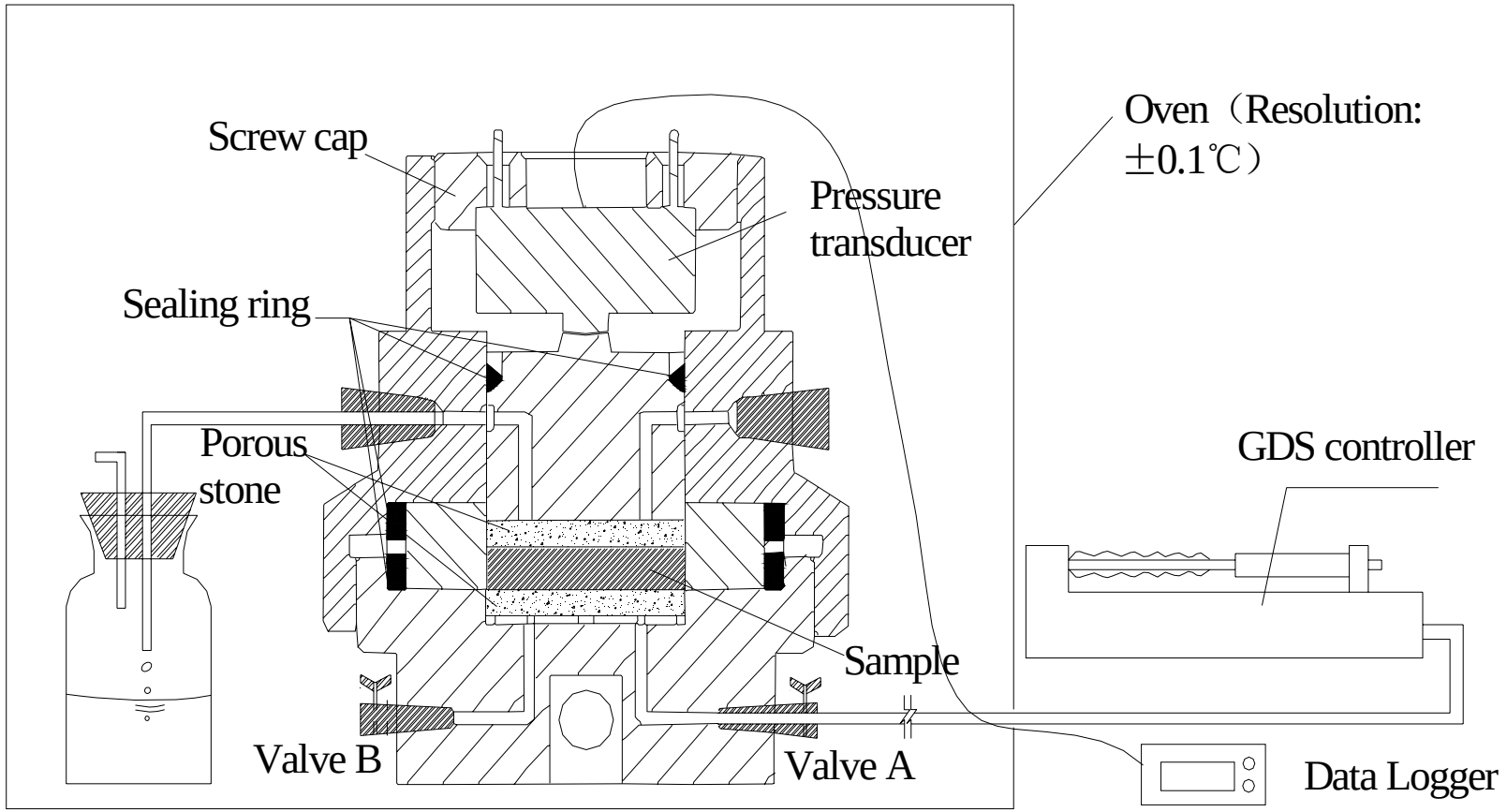

a cylindrical specimen with a height of 10 mm, diameter of 50 mm

3.1.2 Test procedures

- GMZ01 bentonite with an initial water content of 10.6%
- cylindrical specimens were compacted to dry density of 1.70 Mg/m^3 for swelling pressure tests at temperatures
- after swelling pressure test at 40 ^{0}C, saturated permeability tests at temperature path 50→60→50 →20 ^{0}C were conducted

3.1.3 Results and discussion

1) Temperature influence on swelling pressure

FEBEX bentonite (Villar，2008)

Cui et al. (2002) and Tang et al. (2008)

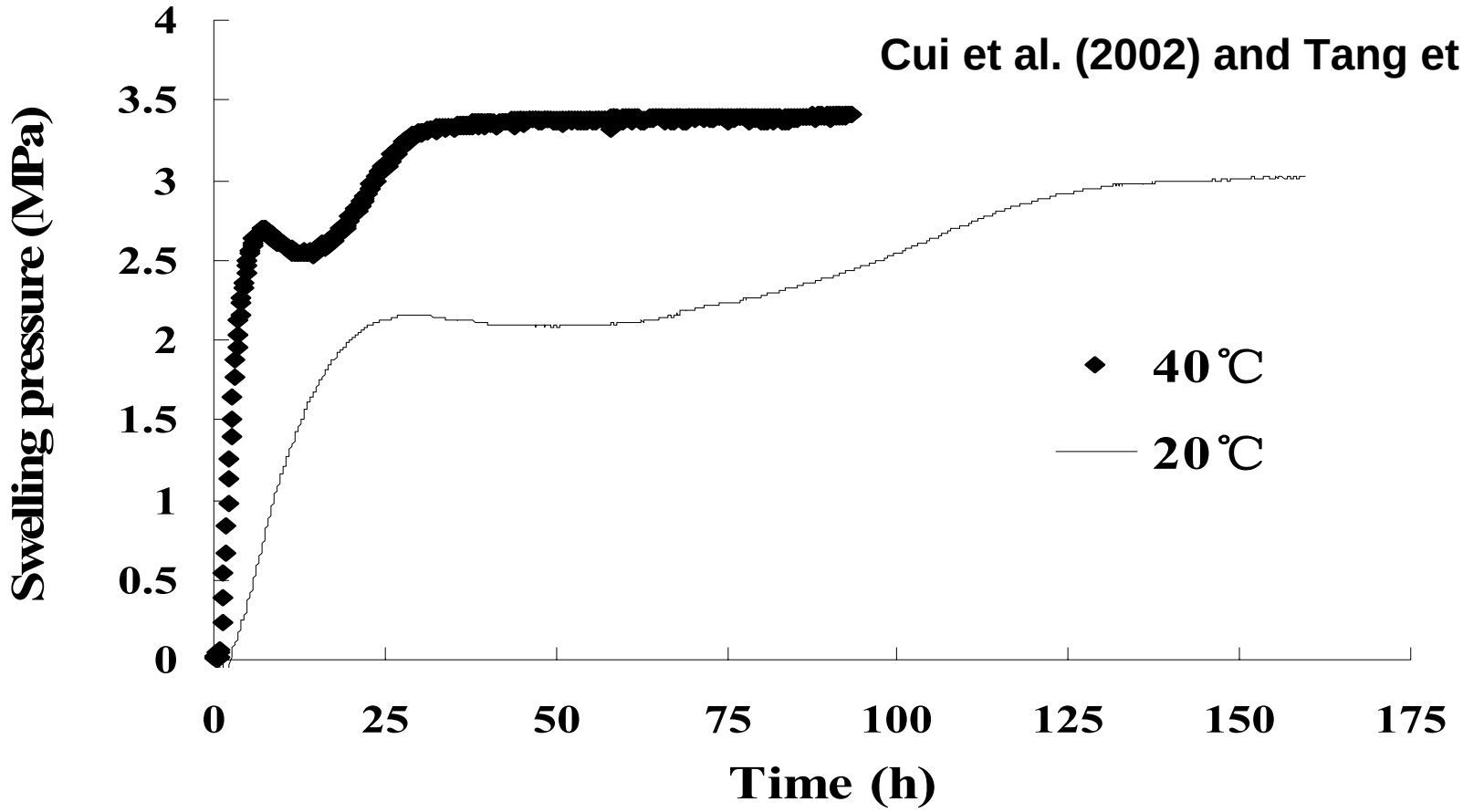

Evolution of swelling pressure with time at different temperatures

2) Temperature influences on saturated hydraulic conductivity

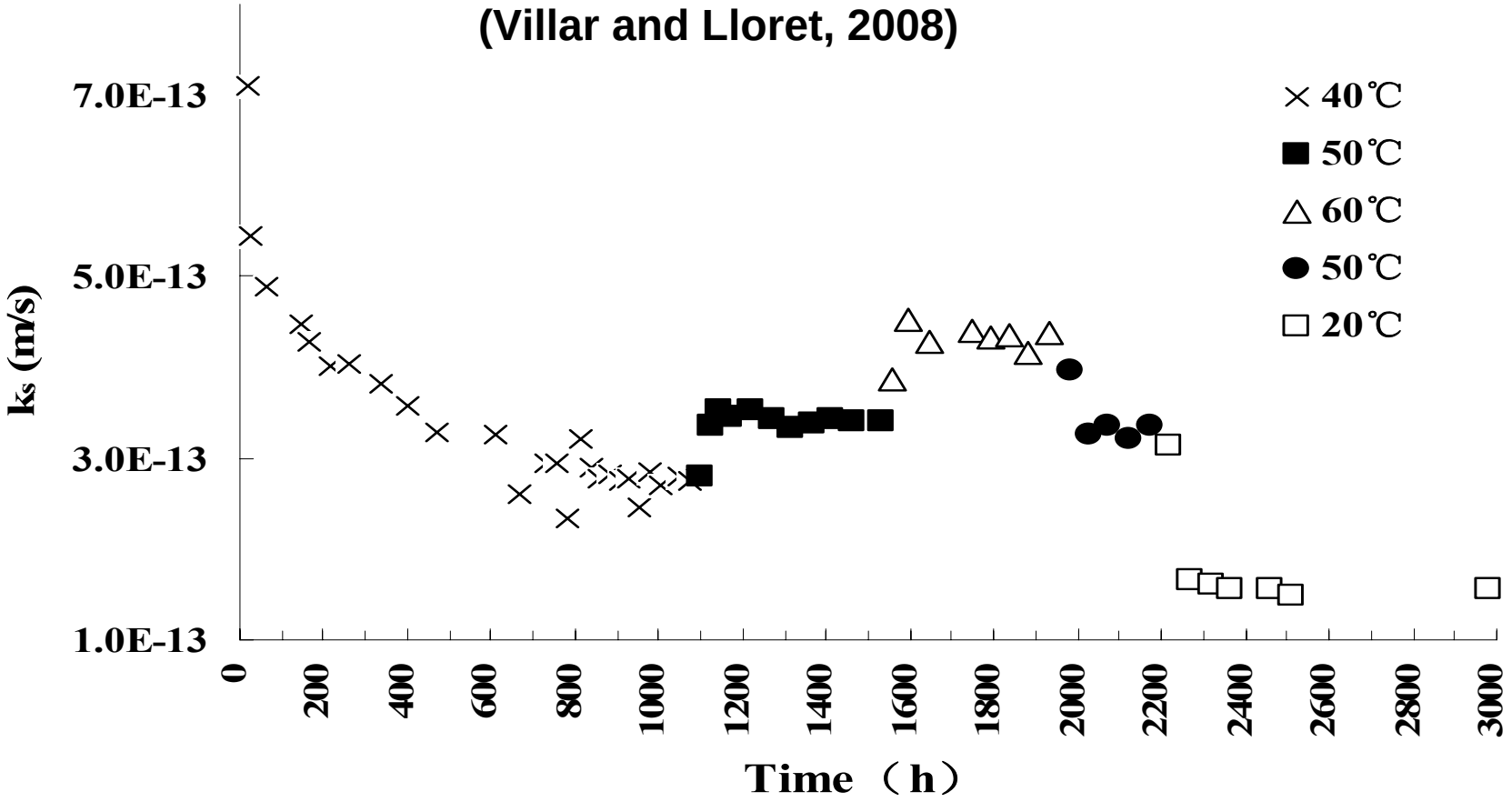

Evolution of hydraulic conductivity with time of GMZ01 bentonite

3) A hydraulic conductivity model considering temperature effects

- the influences of temperature mainly depends on the influences of temperature on η (Philip, 1963; Hopmans, 1986).

$$k_s = k_{in}\rho_w g / \eta(T)$$

where k_{in} is intrinsic hydraulic conductivity, ρ_w water density, g acceleration of gravity and $\eta(T)$ water viscosity as a function of temperature.

3) A hydraulic conductivity model considering temperature effects

- **the influences of temperature mainly depends on the influences of temperature on η (Philip, 1963; Hopmans, 1986).**

$$k_s = k_{in}\rho_w g / \eta(T)$$

- **where k_{in} is intrinsic hydraulic conductivity, ρ_w water density, g acceleration of gravity and η(T) water viscosity as a function of temperature.**

3) A hydraulic conductivity model considering temperature effects

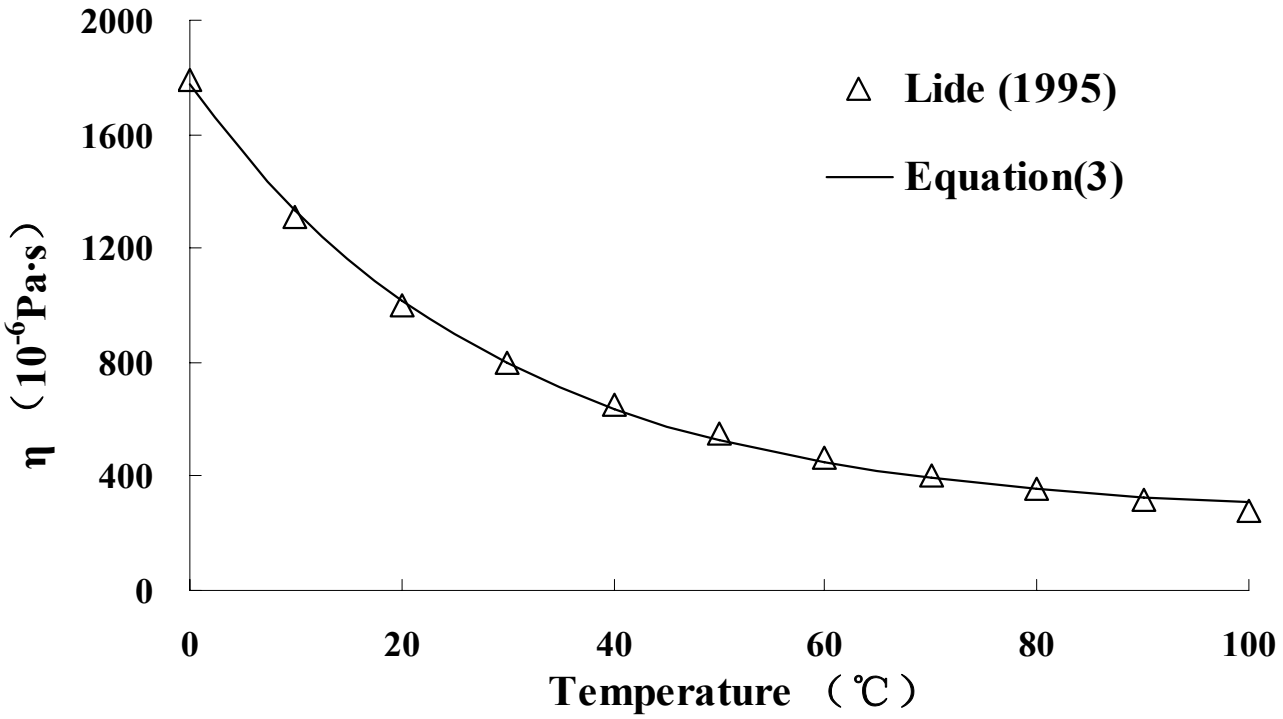

Water kinematic viscosity versus temperature

$$\eta(T) = 0.0002601 + 0.001517 \exp\left[-0.034688 \times (T - 273)\right]$$

3) A hydraulic conductivity model considering temperature effects

$$k_s = \frac{1.58\times10^{-20}\,\rho_w g}{0.0002601 + 0.001517\exp\left[-0.034688\times\left(\mathrm{T}-273\right)\right]}$$

3) A hydraulic conductivity model considering temperature effects

$$k_s = \frac{1.58\times10^{-20}\,\rho_w g}{0.0002601 + 0.001517\exp\left[-0.034688\times(T-273)\right]}$$

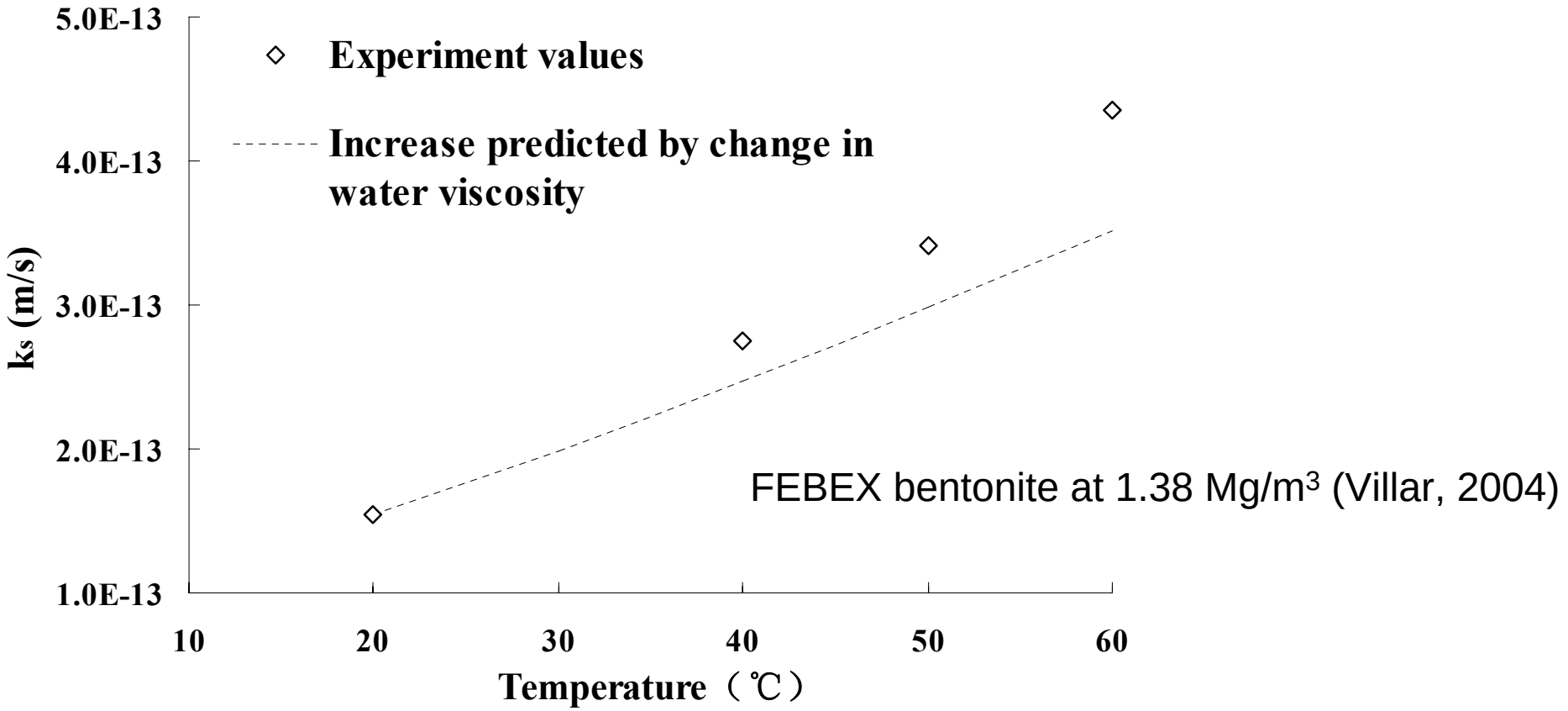

FEBEX bentonite at 1.38 Mg/m^3 (Villar, 2004)

3) A hydraulic conductivity model considering temperature effects

$$k_s = k_{in}\rho_w g / \eta(T)$$

- **Temperature effects on the intrinsic hydraulic conductivity should be considered**

  - **Under confined conditions, the microstructure of the saturated GMZ01 bentonite changes little with temperature (Wan, 2010)**

- **Heating may cause movement of high-density adsorbed water to large pores where it becomes free water (Villar, 2004)**

3) A hydraulic conductivity model considering temperature effects

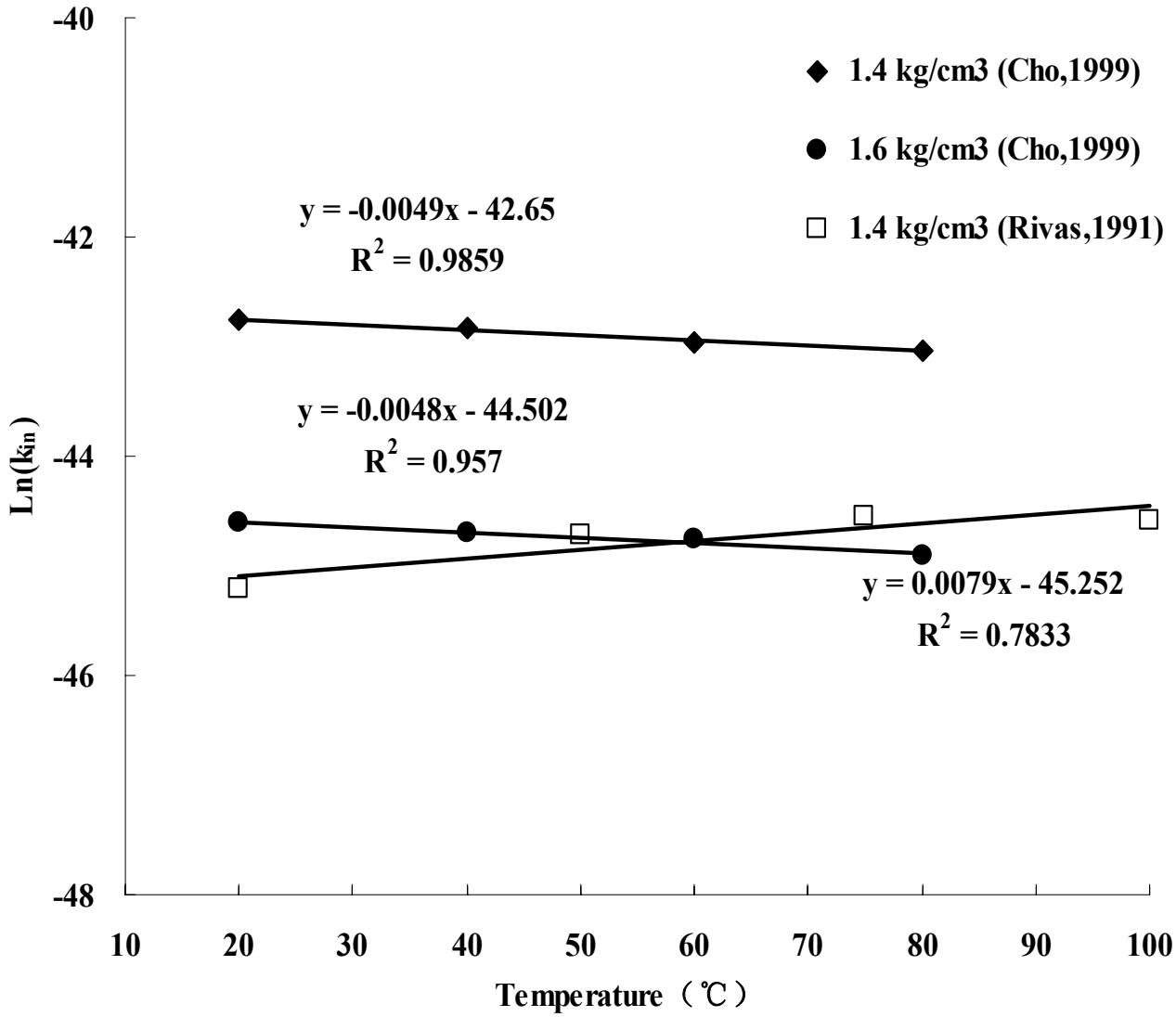

3) A hydraulic conductivity model considering temperature effects

- **Villar (2001) proposed a relationship:**

$$k_{in} = \exp(-52.94 + 7.6e)$$

$$k_{in} = \exp(\alpha + \beta \times (T - 273))$$

$$k_s = \frac{k_{in}(T)\rho_w g}{\eta(T)} = \frac{\exp(\alpha + \beta \times (T - 273))\rho_w g}{0.0002601 + 0.001517 \exp\left[-0.034688 \times (T - 273)\right]}$$

3) A hydraulic conductivity model considering temperature effects

With the saturated hydraulic conductivity values measured at 20 and 40^{0}C, α = - 45.703 and β = 0.0054.

$$k_s = \frac{k_{in}(T)\rho_w g}{\eta(T)} = \frac{\exp(-45.703 + 0.0054 \times (T - 273))\rho_w g}{0.0002601 + 0.001517 \exp\left[-0.034688 \times (T - 273)\right]}$$

With this equation, the values at 50 and 60^{0}C can be calculated.

3) A hydraulic conductivity model considering temperature effects

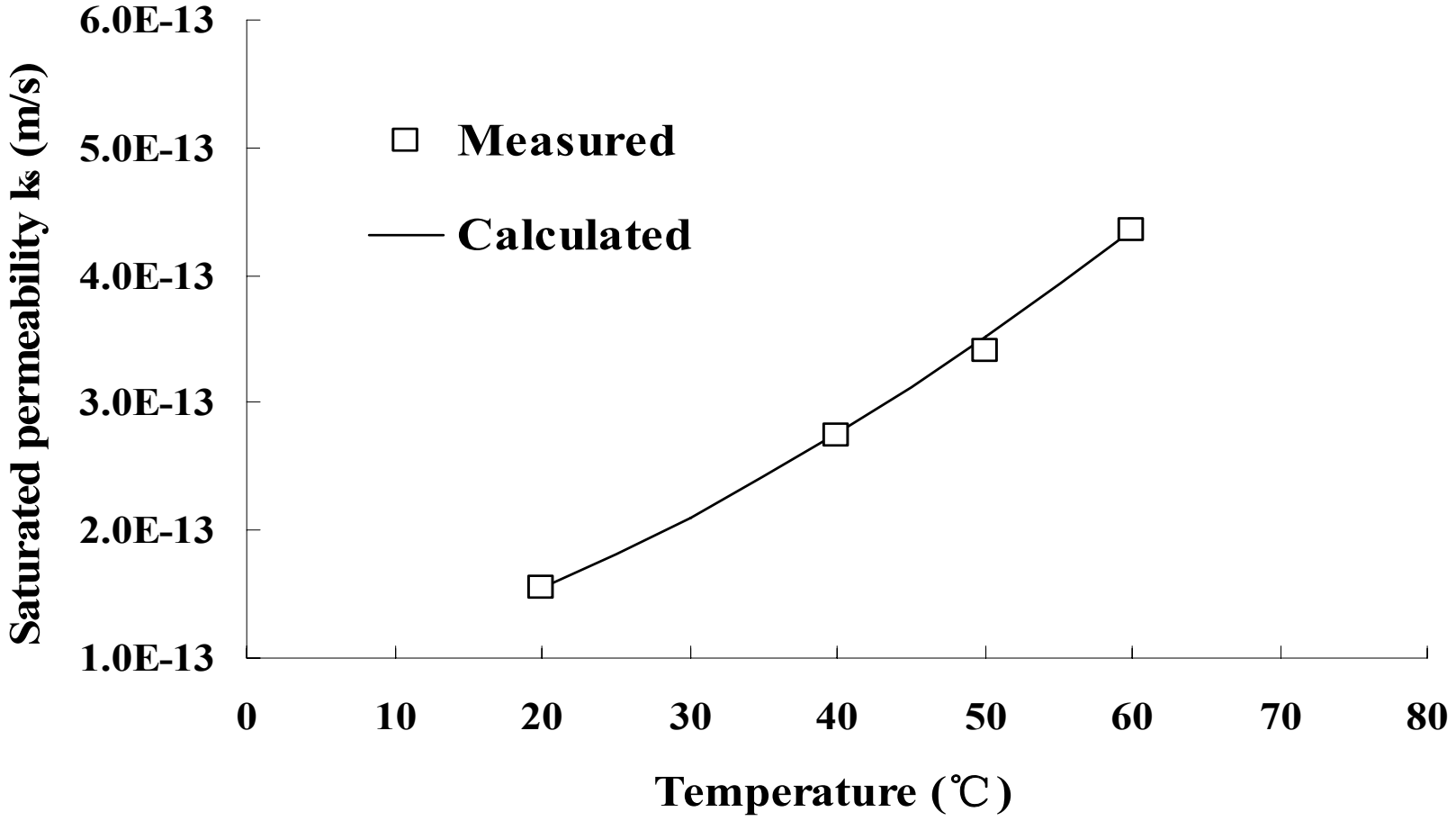

W Ye, M. Wan, B. Chen et al. Environmental Earth Sciences. 2012.

Outline

1 Introduction

2 GMZ bentonite

3 Temperature effects on hydraulic conductivities

3.1 Saturated hydraulic conductivity

3.2 Unsaturated hydraulic conductivity

4 Conclusion

3.2 Unsaturated hydraulic conductivity

- **The instantaneous profile method (Ye et al., 2009) was adopted in this study.**

- **Tests at 40 and 60 ^{0}C were performed and results were analyzed with results at 20 ^{0}C***

- **Determination of WRCs at various temperatures**

* Ye et al. An experimental study of the water transfer through confined compacted GMZ bentonite. Engineering Geology. 2009, v 108, n 3-4, p 169-176.

3.2.1 Determination SWRCs at various temperatures

For high suctions:

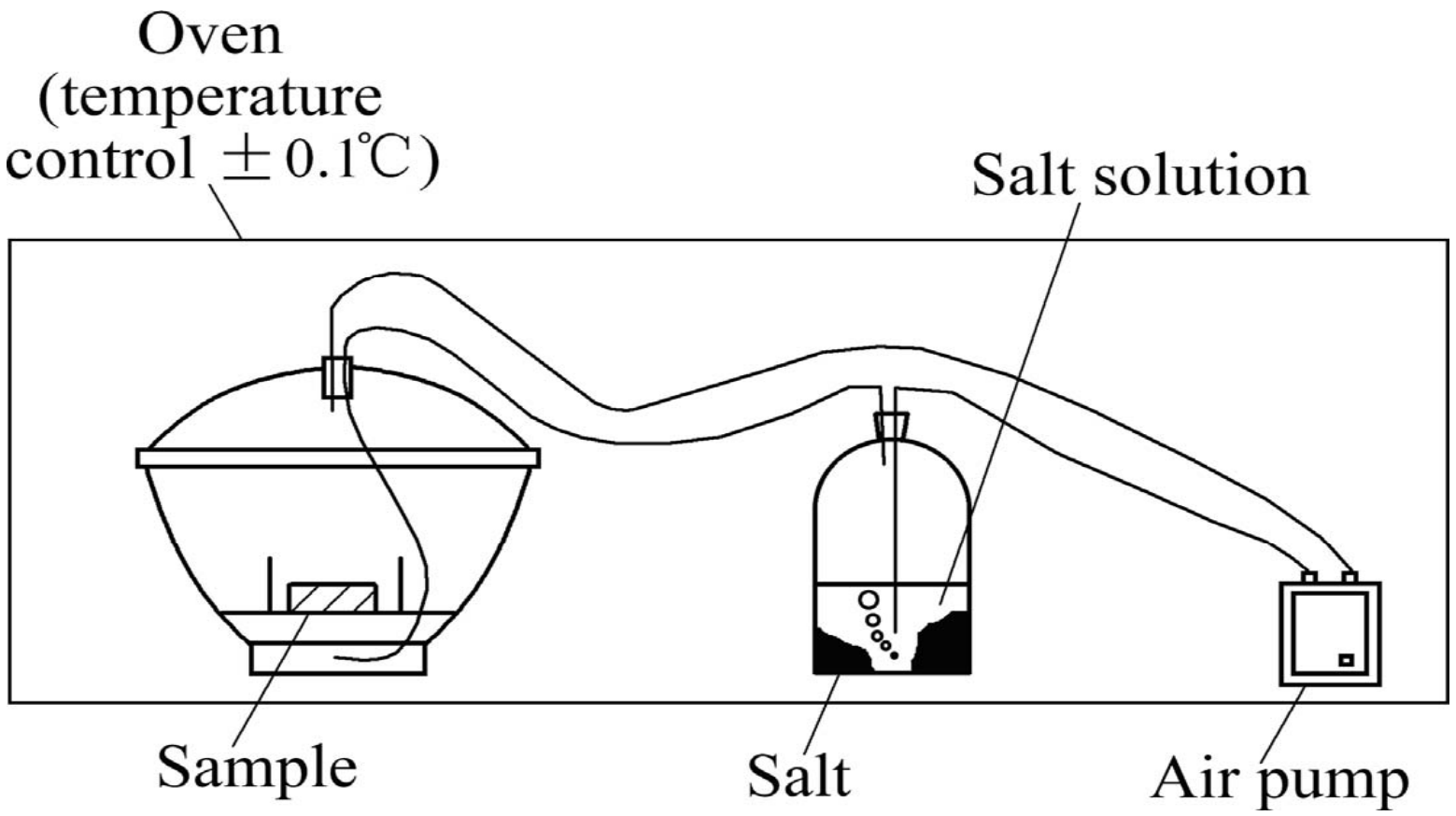

Solutions and corresponding suctions /MPa（Tang et al, 2005）

	20℃	40℃	80℃
$LiCl_2$	309		
$MgCl_2$	150	155	181
K_2CO_3	113	117	139.8
$Mg(NO_3)_2$	82	98	
$NaNO_2$	57		
NaCl	38	38.8	39.7
$(NH_4)_2SO_4$	24.9	30.8	
KCl	21	26.8	31.8
$ZnSO_4$	12.6		
KNO_3	9		
K_2SO_4	4.2	5.1	5.8

3.2.1 Determination SWRCs at various temperatures

For low suctions:

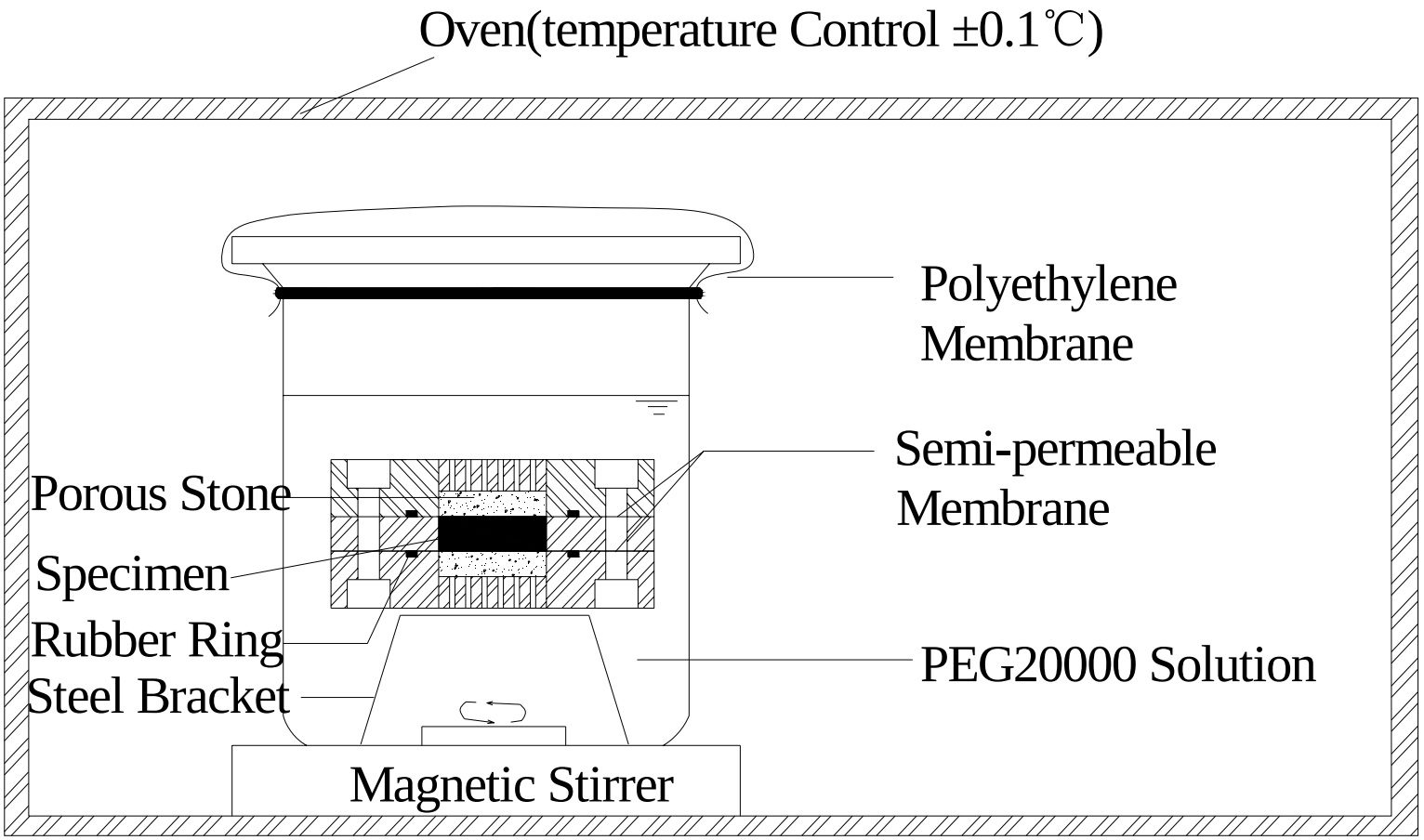

Constraint conditions and temperature control

Digital oven

unconfined

confined

20, 40 and 80 ℃ were selected

Hysteresis behaviors of unconfined compacted GMZ01 bentonite following different dry/wet path at 40° C

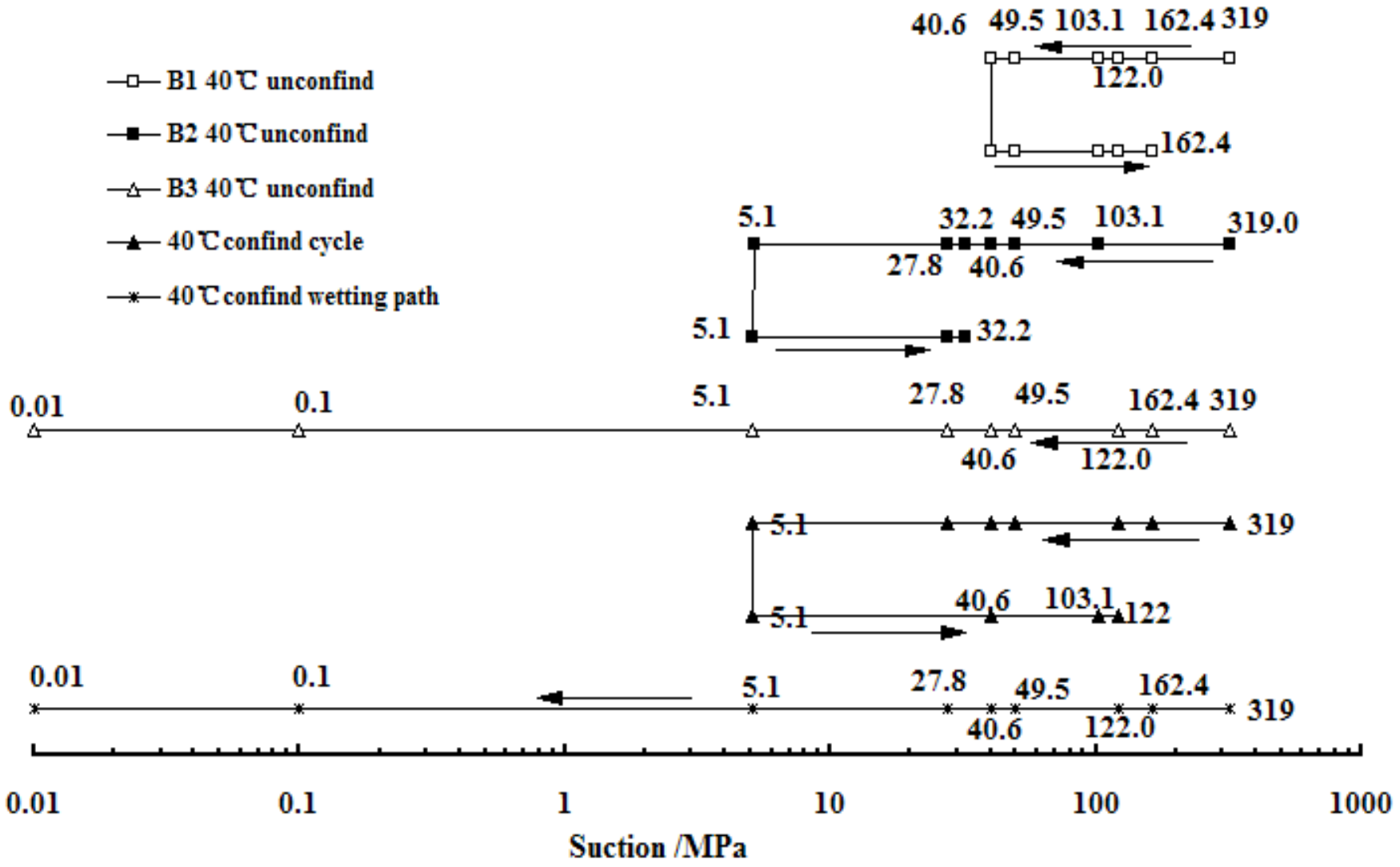

Water Retention Curve of GMZ01 Bentonite

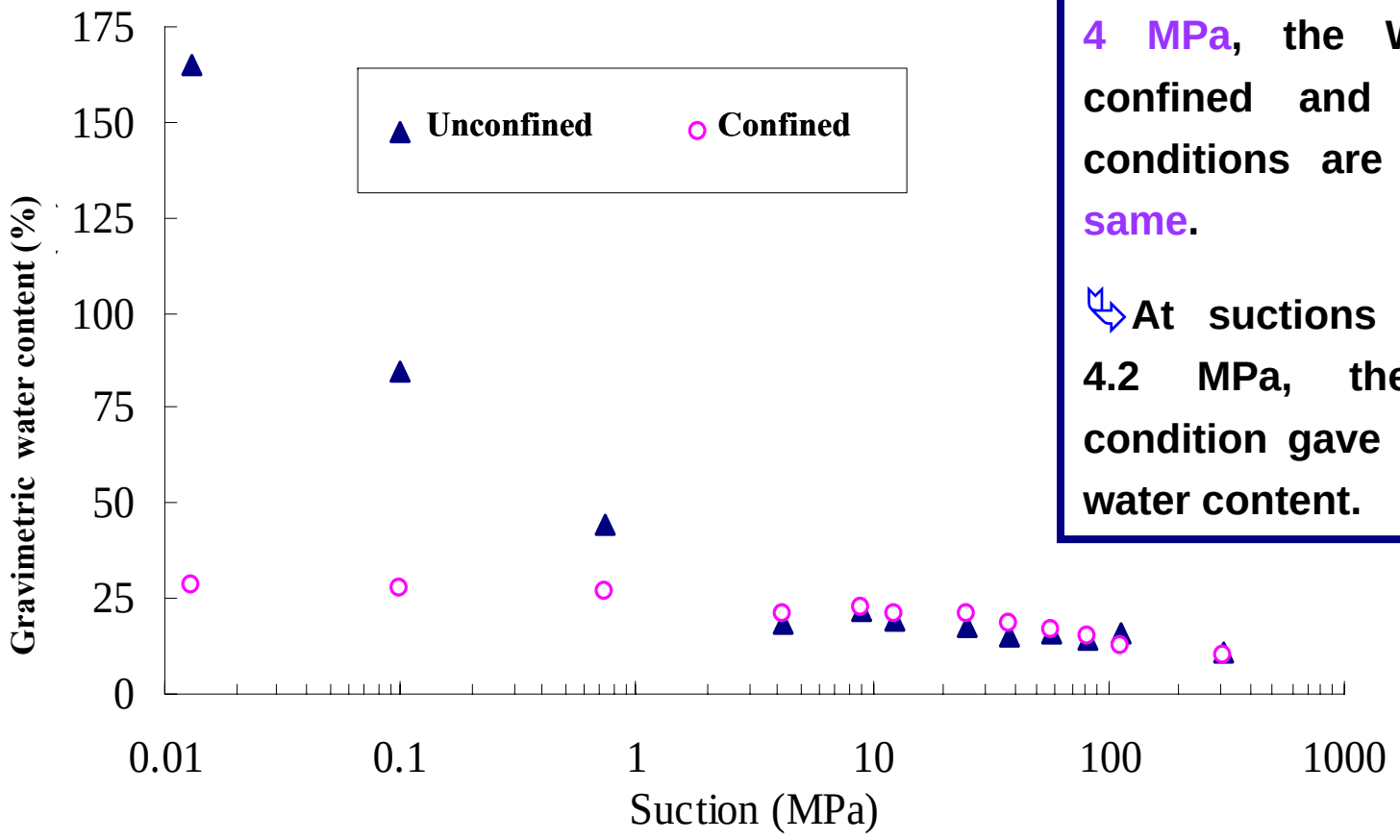

- At suctions higher than 4 MPa, the WRC under confined and unconfined conditions are almost the same.
- At suctions lower than 4.2 MPa, the confined condition gave much lower water content.

Water Retention Curves at 20℃ (Chen et al, 2006)

Hysteresis behavior of GMZ01 Bentonite (40^0C)

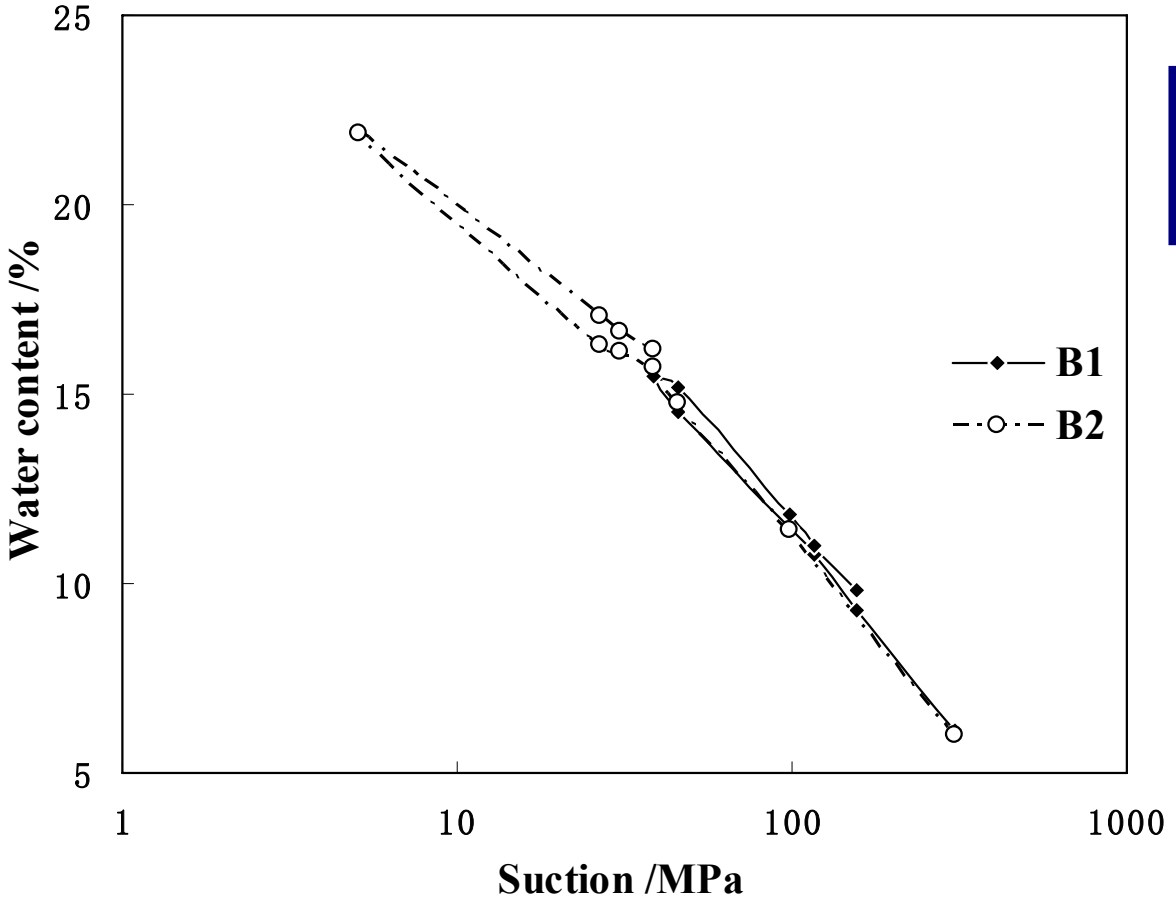

Hysteresis becomes larger in low suctions

Hysteresis behavior of GMZ Bentonite

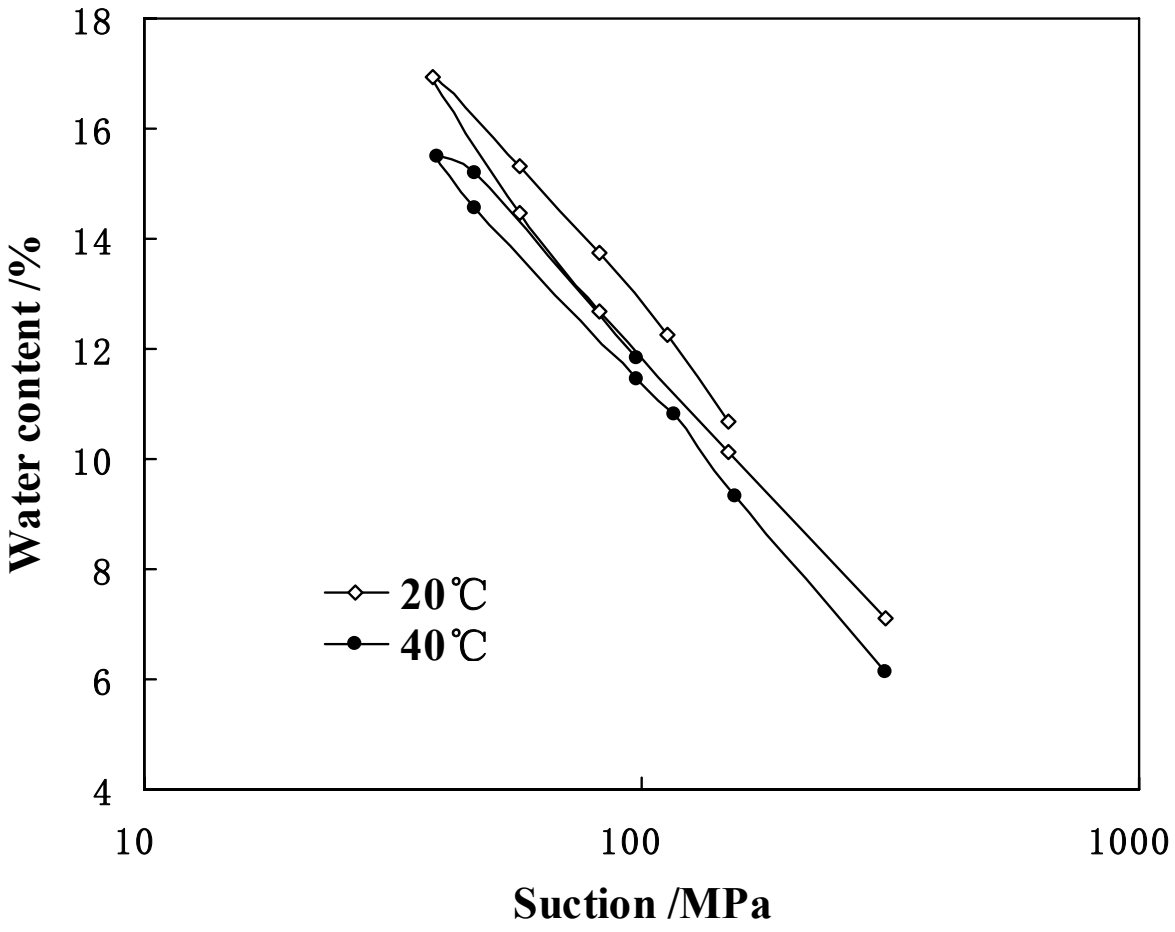

- Hysteresis loop of SWRC at 20^{0}C is larger than that at 40^{0}C.
- Hysteresis deviates as temperature rises.

Ye et al, J of Central South University of Tech., 2009, Vol. 16(1): 143-148

3.2.1 Determination SWRCs at various temperatures

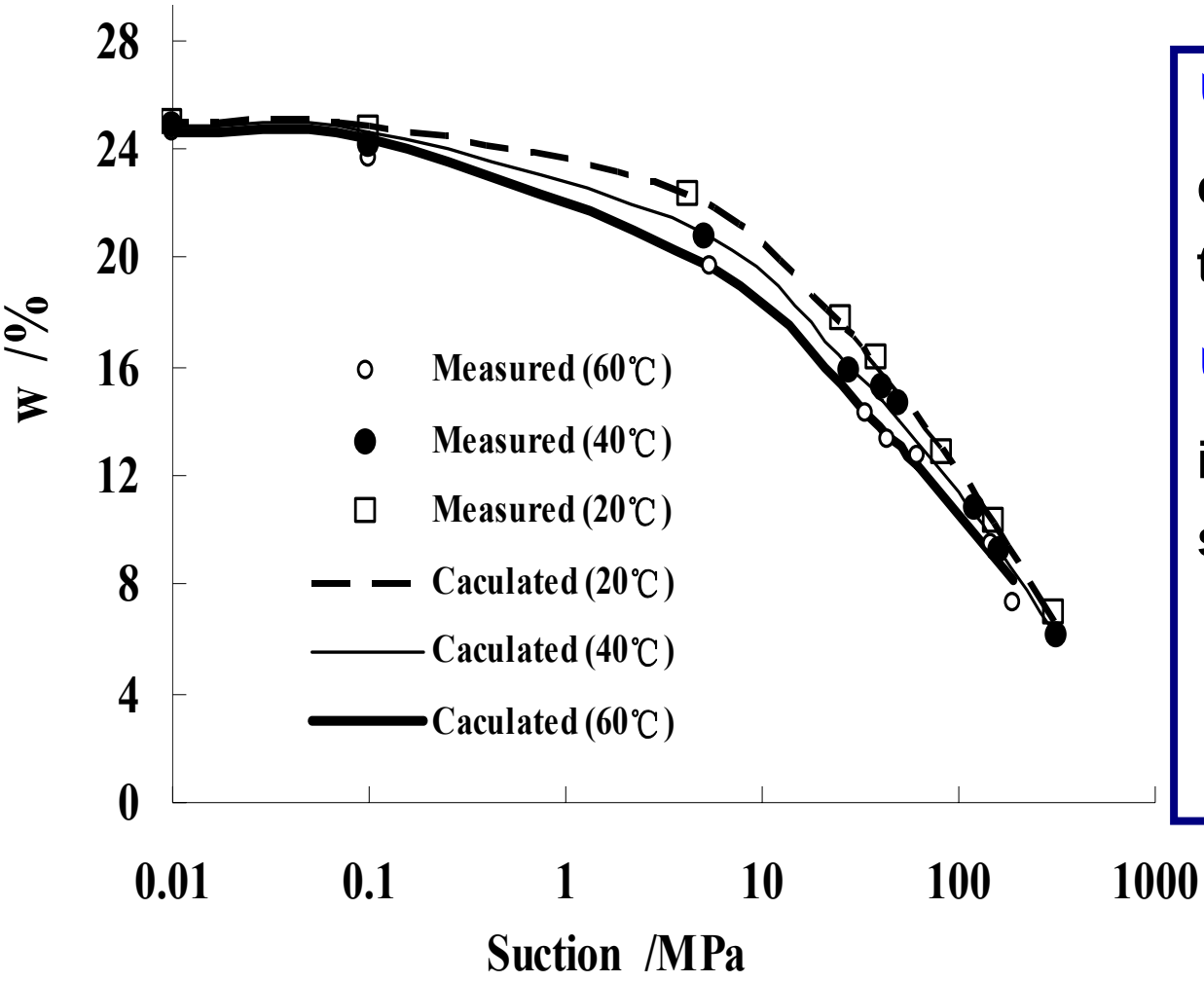

- Water retention capacity decreases as temperature rises.
- Temperature influence depends on suction

3.2.2 Infiltration tests at various temperatures

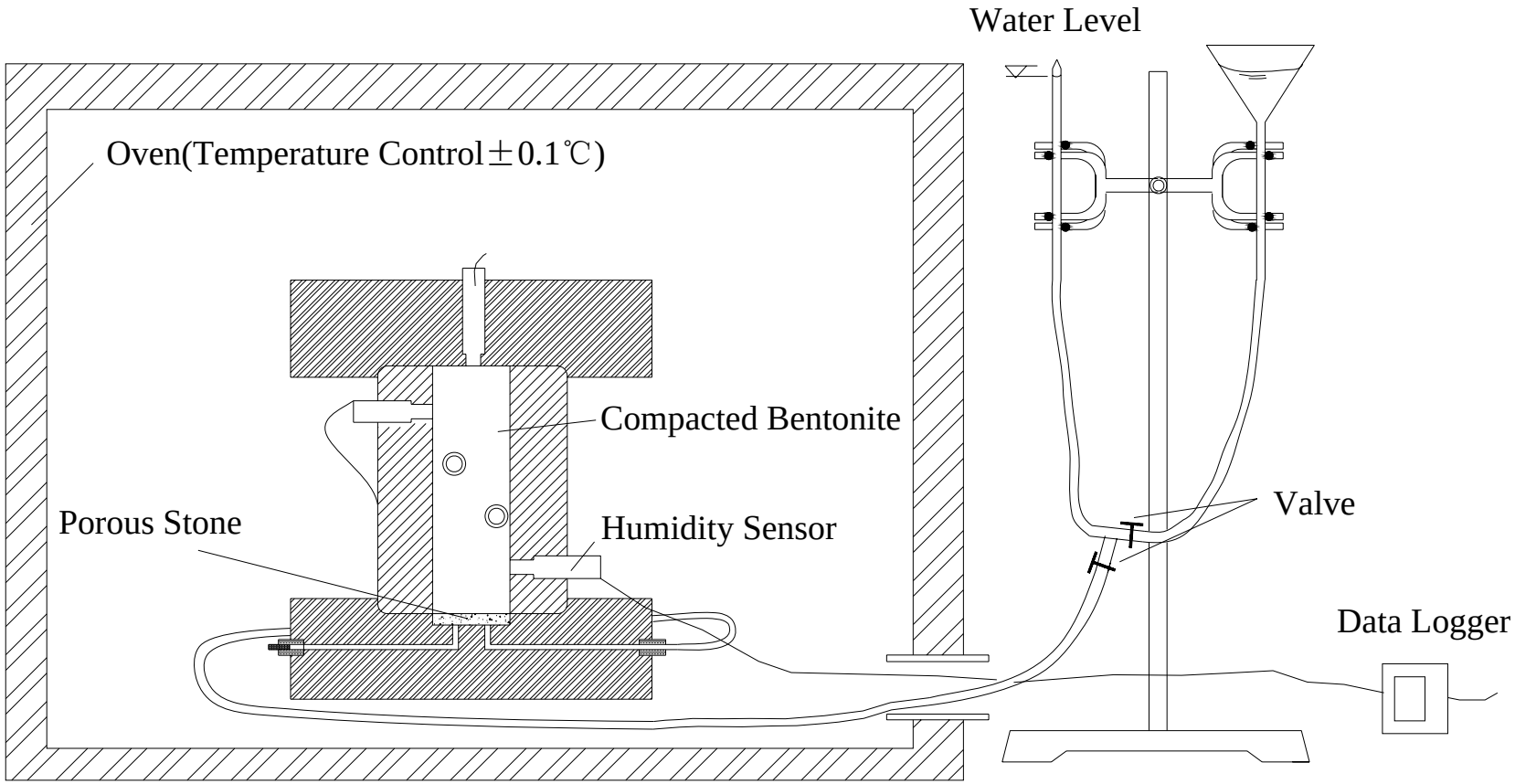

Schematic layout of the temperature controlled infiltration test

3.2.2 Infiltration tests at various temperatures

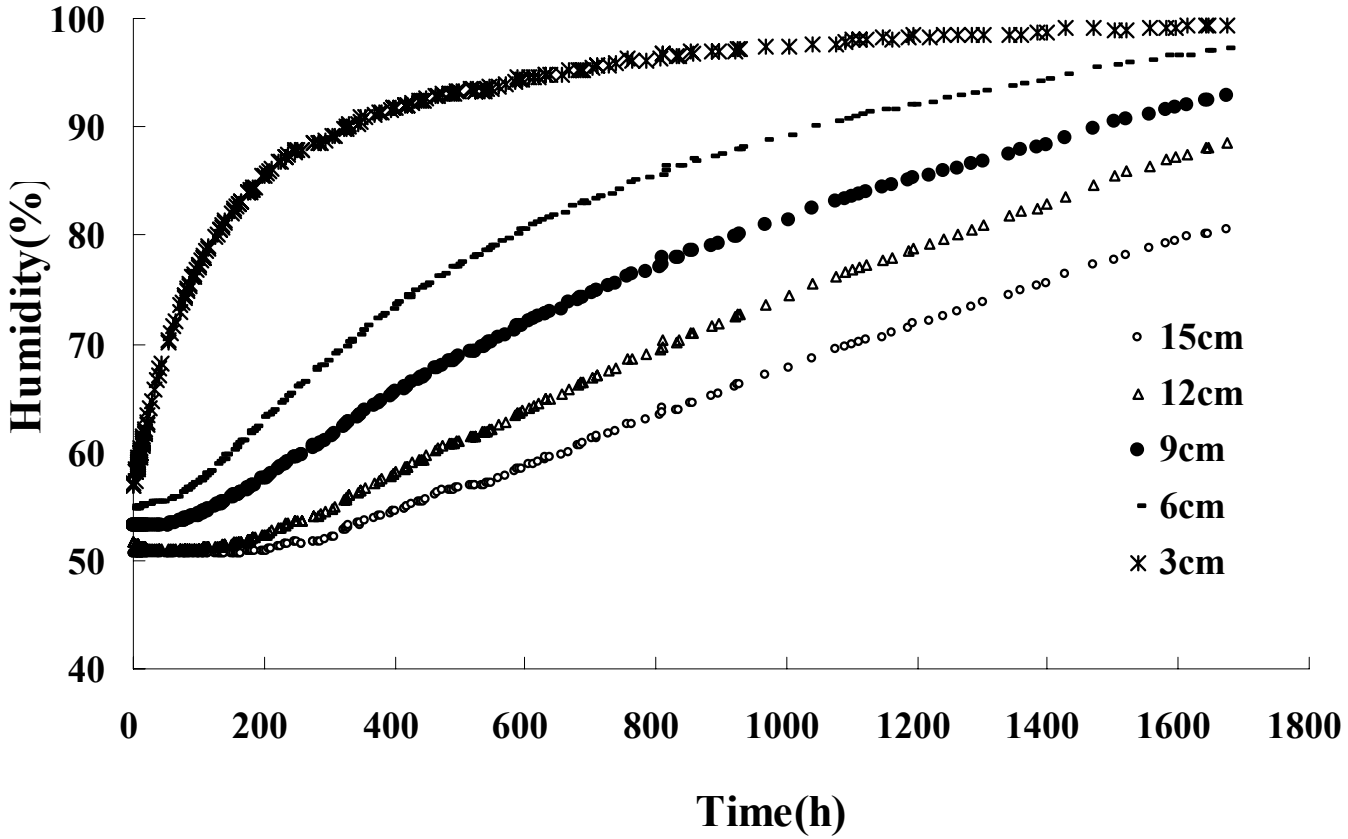

Evolution of the relative humidity of confined GMZ01 with time at 40^0C

3.2.2 Infiltration tests at various temperatures

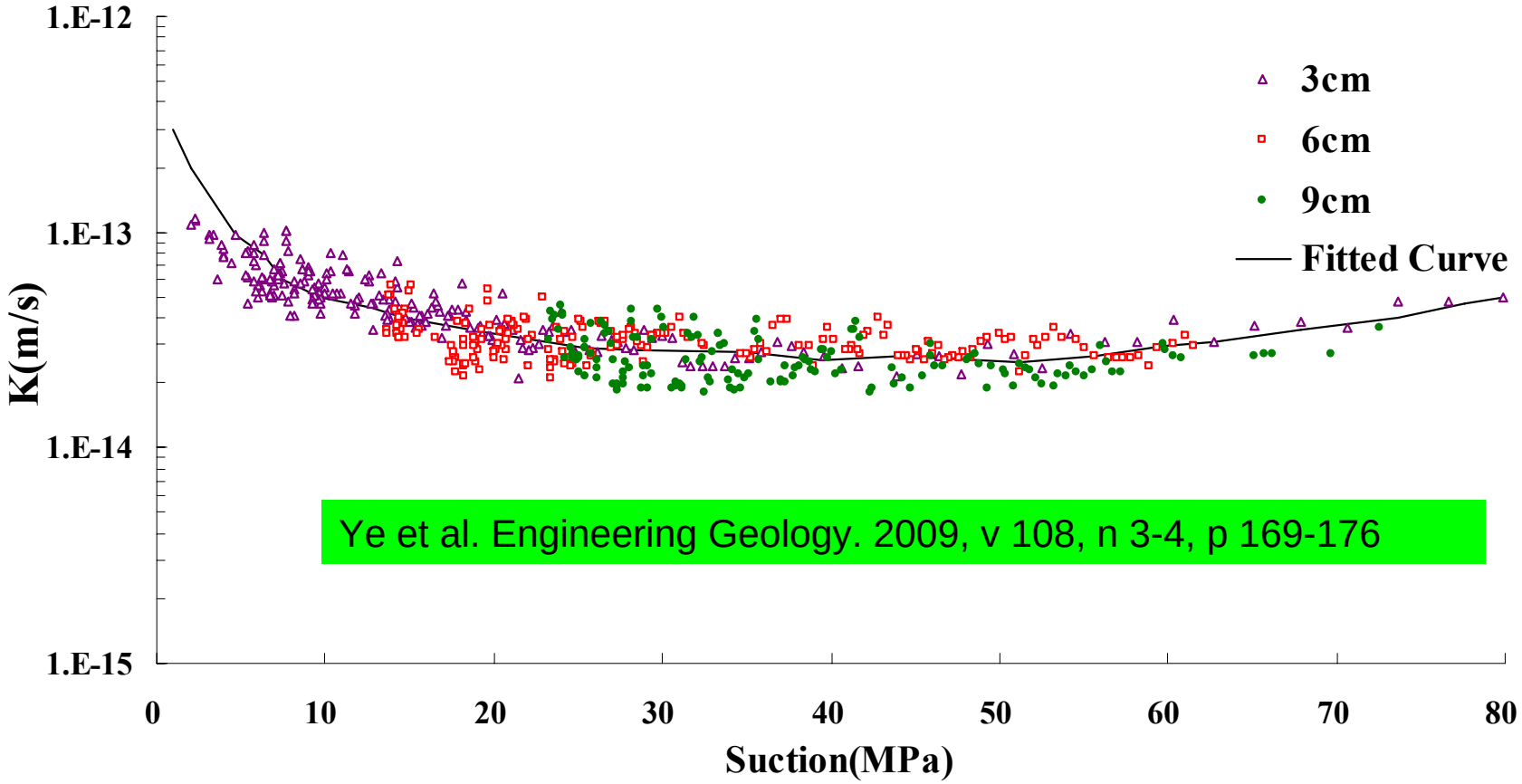

Change of unsaturated hydraulic conductivity with suction for the confined GMZ01 at 60^0C

3.2.2 Infiltration tests at various temperatures

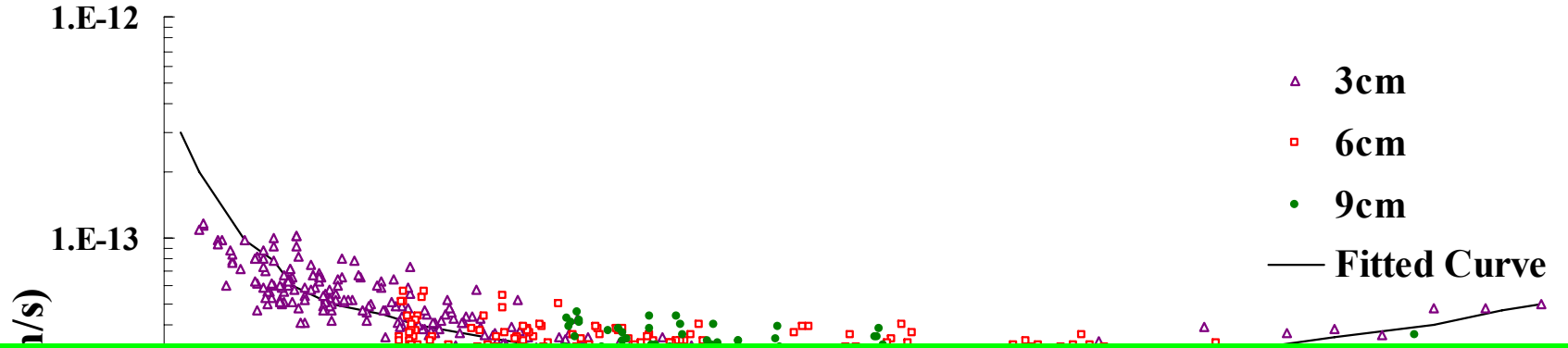

As in the first stage, water transfer is primarily governed by the network of large pores and these large pores are progressively decreasing in quantity and in size, resulting in hydraulic conductivity decreases. After completion of this large-pore clogging by gel creation, a normal conductivity increase with suction decrease is observed (Ye et al., 2009).

GMZ01 at 60^{0}C

3.2.2 Infiltration tests at various temperatures

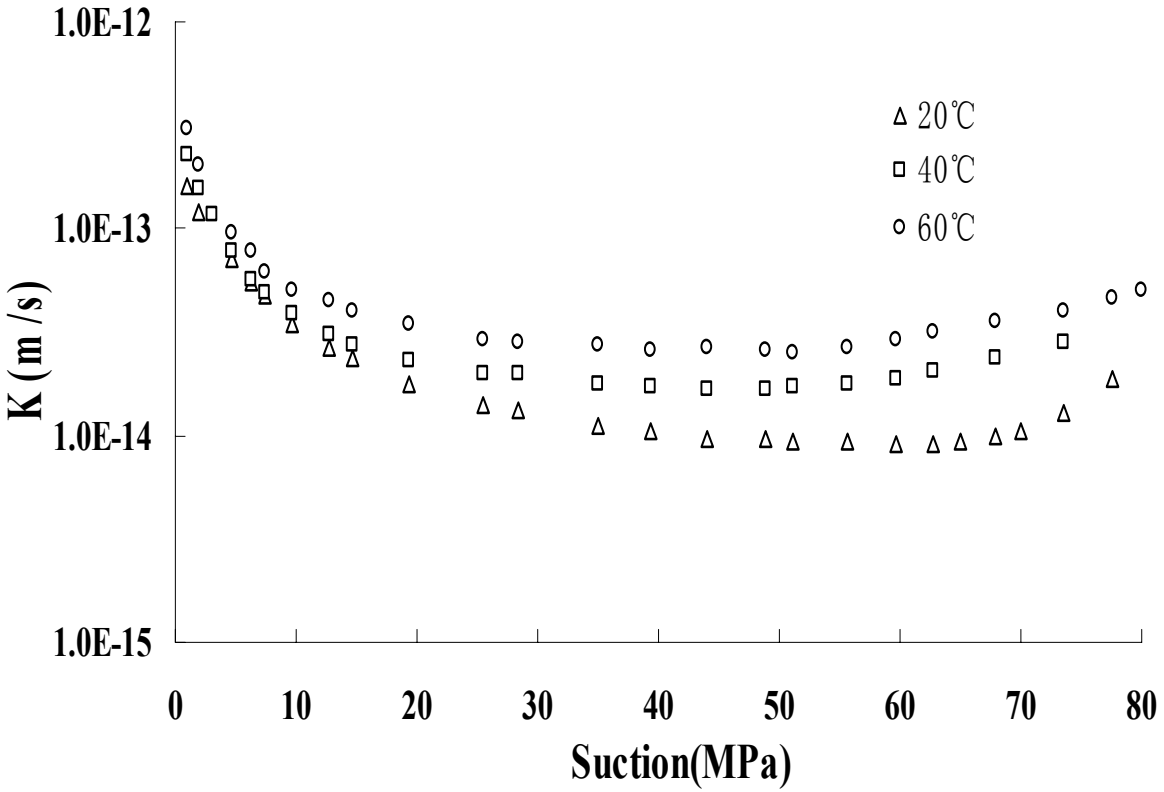

- Hydraulic conductivity increases as temperature rises.
- Temperature influence depends on suction

*Ye et al. , Engineering Geology. 2012. Vol. 126: 1-7

Outline

1 Introduction

2 GMZ bentonite

3 Temperature effects on hydraulic conductivities

3.1 Saturated hydraulic conductivity

3.2 Unsaturated hydraulic conductivity

4 Conclusion

4 Conclusion

- The swelling pressure of the compacted GMZ01 bentonite increases with temperature rise.
- The saturated hydraulic conductivity of the compacted GMZ01 bentonite increases with temperature rise. Temperature changing paths (heating or cooling) have little impact on the saturated hydraulic conductivity.

4 Conclusion

- The revised model accounts for both the water viscosity and effective flow cross area of porous channels can well reflect the temperature influences on saturated flow.
- For all the temperatures considered, the unsaturated hydraulic conductivity decreases slightly in the first stage of hydration. The value of the hydraulic conductivity becomes constant as hydration progresses. Finally, the hydraulic conductivity increases rapidly with suction decreases when saturation is approached.

4 Conclusion

- **Under confined conditions, the hydraulic conductivity increases as temperature increases, at a rate that decreases with temperature rises. Also, the influence of temperature on the hydraulic conductivity is quite suction-dependant.**

http://www.unsat-waste2013.cn

Third International Symposium on Unsaturated Soil Mechanics and Deep Geological Waste Disposal

(UNSAT-WASTE 2013)

7-10 July 2013, Shanghai,

http://www.unsat-waste2013.cn

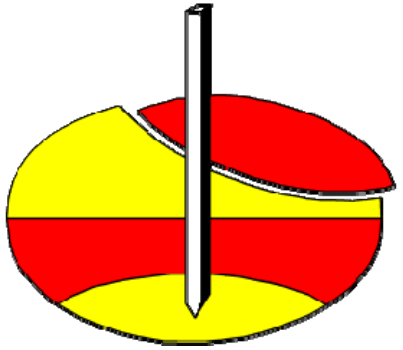

Many thanks for your attention!

Initial Results on Stability of natural GMZ Ca-Bentonite & modified Na- Bentonite under Thermal/Radiation Aging

By : Yang Zhongtian

China Institute for Radiation Protection
(CIRP,CNNC)

E-mail:ztyang@263.net
Mobile phone:13934546499

Contents

1 Introduction
2 Experimental
3 Results
4 Initial conclusion
5 Recent work

1 Introduction

- **GMZ Bentonite from inner Mongolia has been recommended as potential buffer material in china.**
- **Its stability under near field condition shoub be investigated**

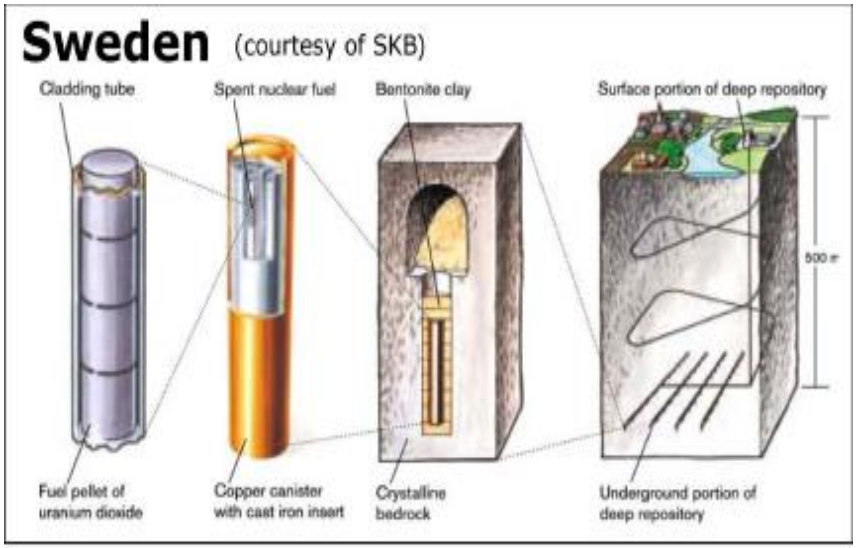

Requirements

- **near field condition**

dose rate: 0.2～2 Gy/h（γ、n）

temp.: 90℃

↓

thermal period lasted:
hundreds ～thousands years
temp.: 90℃→disposal Environment tem.

total dose in thermal period: 0.7 MGy ～ ? MGy

（Applied Clay Science 43 (2009)143-149）

↓

what will happen?

how to simulate and validate?

Methodology

- **problem: Have to make predictions of time-temperature-dose rate superposition at experimentally inaccessible times**
- **How to solve: mainly two experiment methods**

① simulating method

similar to real disposal condition (low temp.、low dose rate short time) → extrapolate to hundreds ～thousands years

② Accelerating method

adopting accelerated condition (high temp.、high dose rate short time) →results stand for the long term effect

How to verify the methods and results with sufficient confidence ?

Which one would be better?

2 Experimental

2.1 Material

- **Ca-bentinote: exploited directly from GMZ mine and prepared by xinghe county dope factory**

  Apparent density: 0.51 g/cm^3

- **Modified-Na-bentonite: prepared by reaction of Ca-bentinote with Na_2CO_3 solution by xinghe county dope factory**

  Apparent density: 0.46 g/cm^3

  water content: 7.3%

- **Bentonite be used as got without any further processing.**

2 Experimental

2.2 Thermal treatment

- Ca-bentinote \M-Na-bentonite was put in PTFE bottles and sealed
- Temp.:

  120℃、150 ℃ 、180 ℃
- Duration:

  3000h、6000h、9000h

2 Experimental

2.3 Irradiation treatment

- **M-Na-bentonite was put in canister made of stainless steel(thickness:1mm; diam.:10cm;Height:60cm) and sealed**
- **γirradiation at R.T.**

  Dose rate:1.7 kGy/h

  Cumulative dose: 1000kGy、2000kGy、3000kGy、4000kGy、5000kGy

2 Experimental

2.4 Irradiation- Thermal sequential treatment

- after γirradiation, canister with **M-Na-bentonite** were put into an oven and treated at following condition

  Temp.: 120℃、150 ℃ 、180 ℃

  Time:3000h、6000h、9000h

2 Experimental

2.5 Analysis

XRD

- qualitative analysis : by both CIRP and zhejiang University
- quantitative analysis: zhejiang University

DX-2700 in CIRP

3 Results

3.1 Comparison of thermal treatment results for M-Na-bentonite & Ca-bentonite

XRD spectrum of M-Na-bentonite aging at 180℃

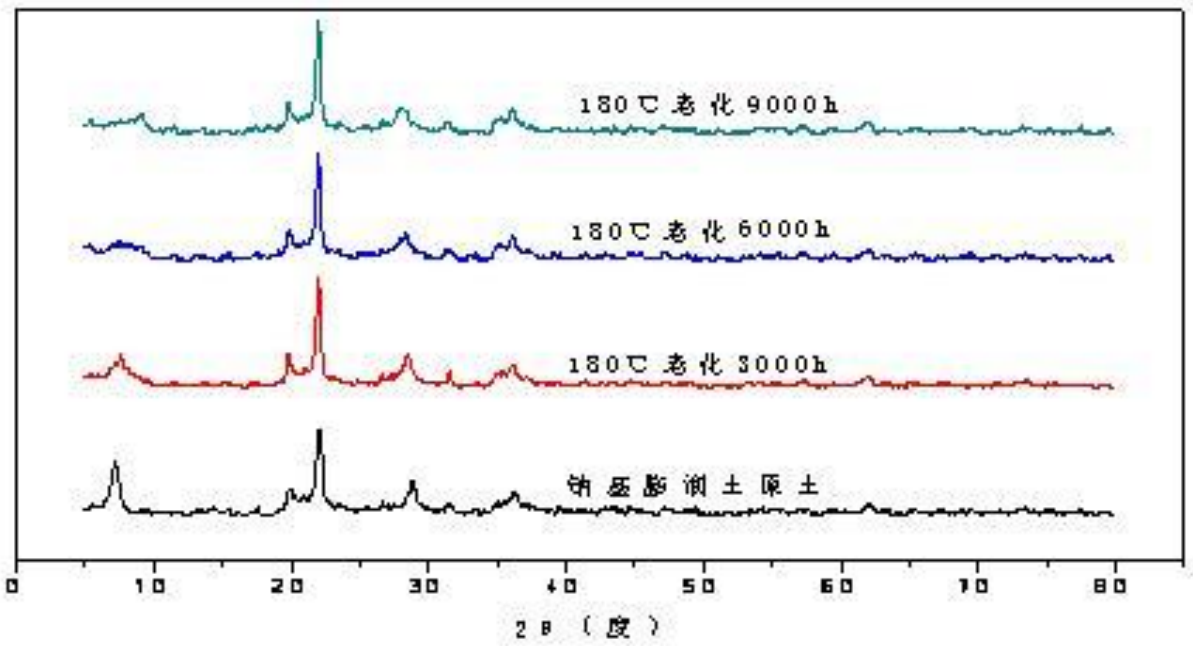

XRD spectrum of Ca-bentonite aging at 120℃、150℃、180℃ for 3000h

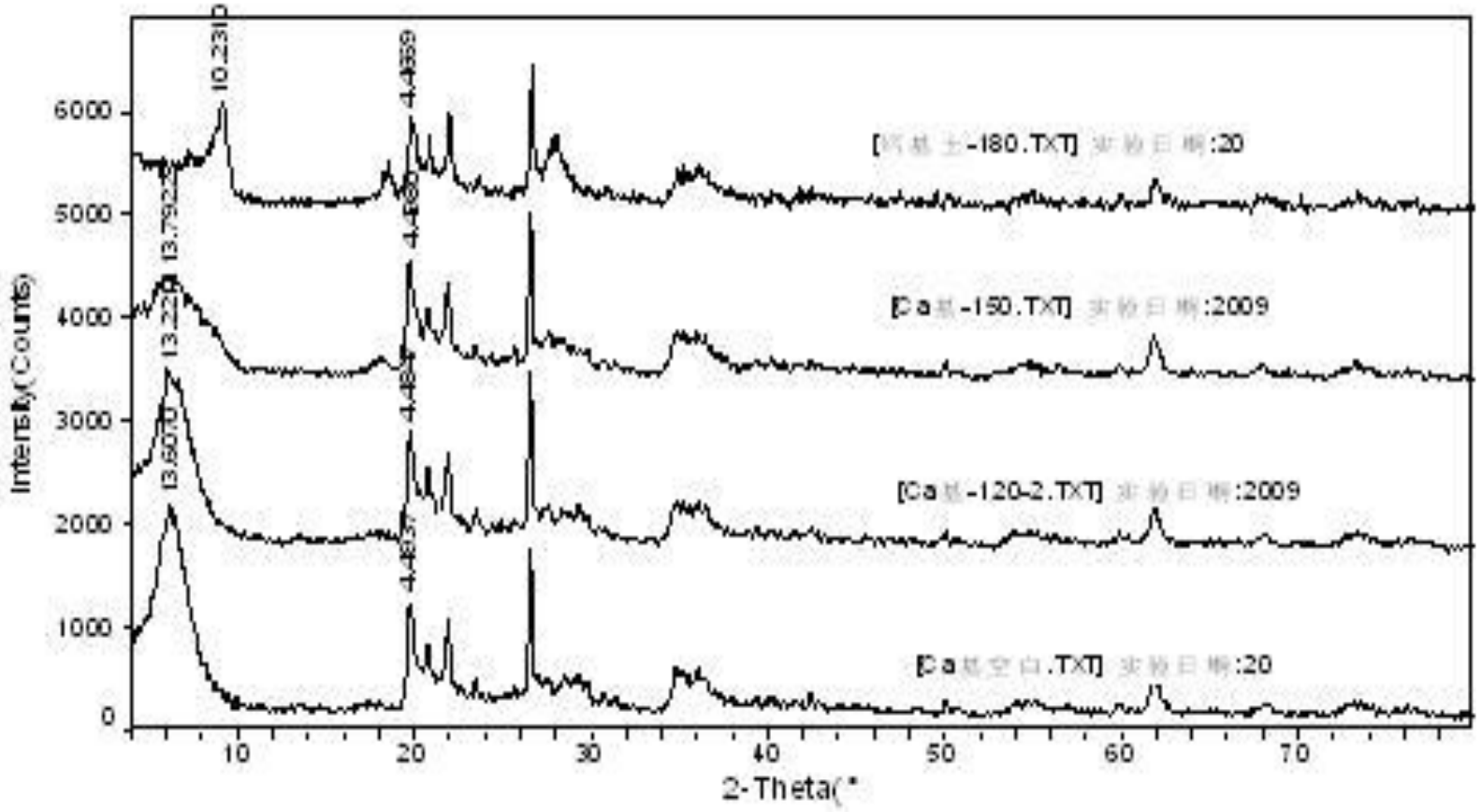

Conclusion: Na-bentonite is more stable than Ca-bentonite under thermal aging.

3 Results

3.2 Thermal treatment of M-Na-bentonite

- For 120℃、150℃、180℃--3000h：small change
- For 120℃、150℃、180℃--6000h：obvious change
- For 120℃、150℃、180℃--9000h：new diffraction peak of illite

Conclusion:

- Temperature effect is small during this interval
- Time effect is more obvious

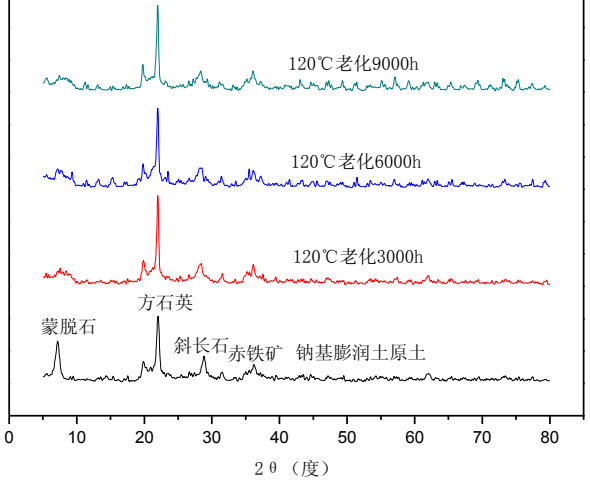

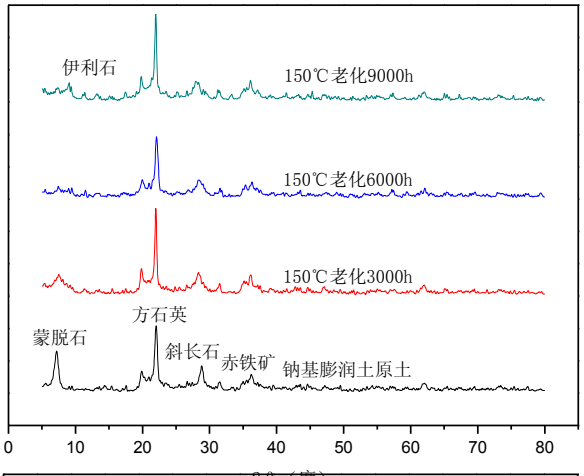

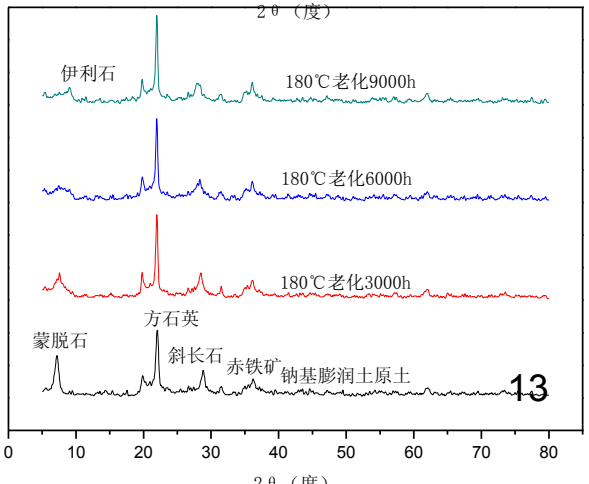

3 Results

3.3 γIrradiation treatment of Na-bentonite

(1) qualitative analysis

- almost no change

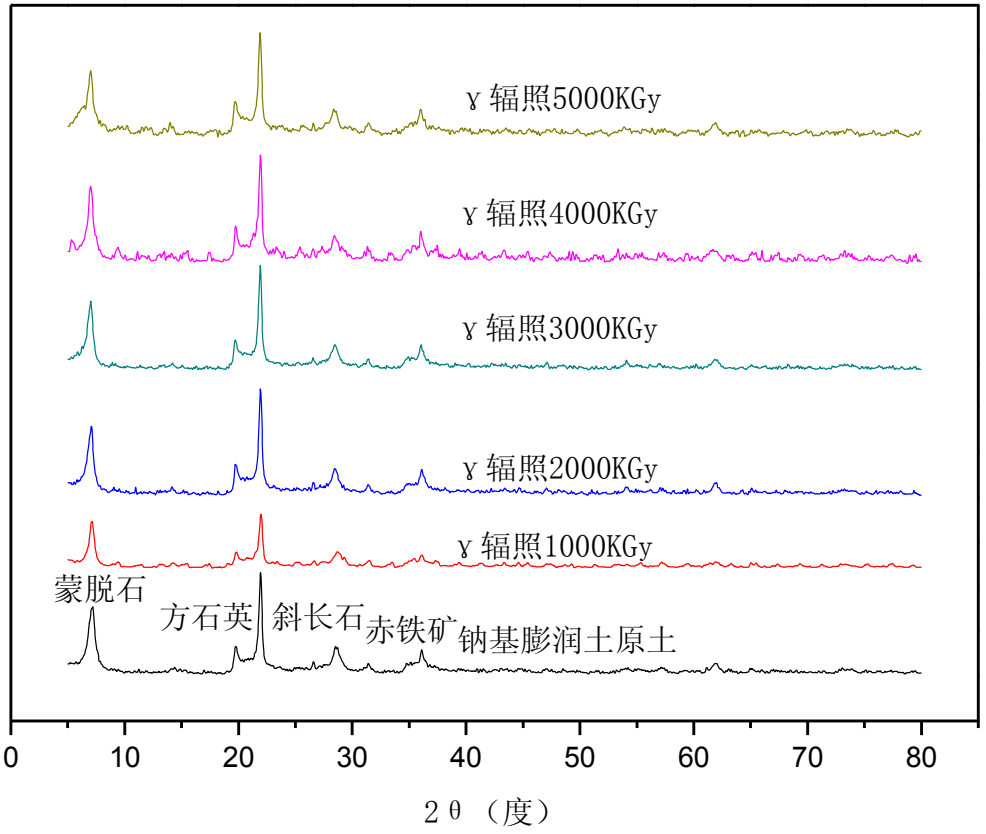

3 Results

(2) quantitative analysis

- similar result as for that of thermal treatment,
- small change of 2-Theta & d value

  decrease of crystal size

No.	condition	2-Theta 衍射角	d （Å） 层间距	Height	Area(a1)	FWHM	XS（Å） 晶胞尺寸
1	blank	7.074	12.4858	7401	139996	0.551	158
2	1000 kGy	7.053	12.5229	6792	150639	0.625	137
3	2000 kGy	7.121	12.4032	11953	256797	0.624	137
4	3000 kGy	7.085	12.4667	7075	143192	0.594	145
5	4000 kGy	7.065	12.5024	7232	145629	0.587	147
6	5000 kGy	7.098	12.4433	7778	160334	0.590	146

3 Results

3.4 Irradiation- Thermal sequential treatment of M-Na-bentonite

(1) qualitative analysis

- 1000kGy-180℃-6000h
  5000kGy-180℃-6000h:
  Obvious change of smectite diffraction peak
- 1000kGy-120℃-9000h
  5000kGy-180℃-9000h :
  Disappear of smectite diffraction peak;
  Formation of new diffraction peak of illite.

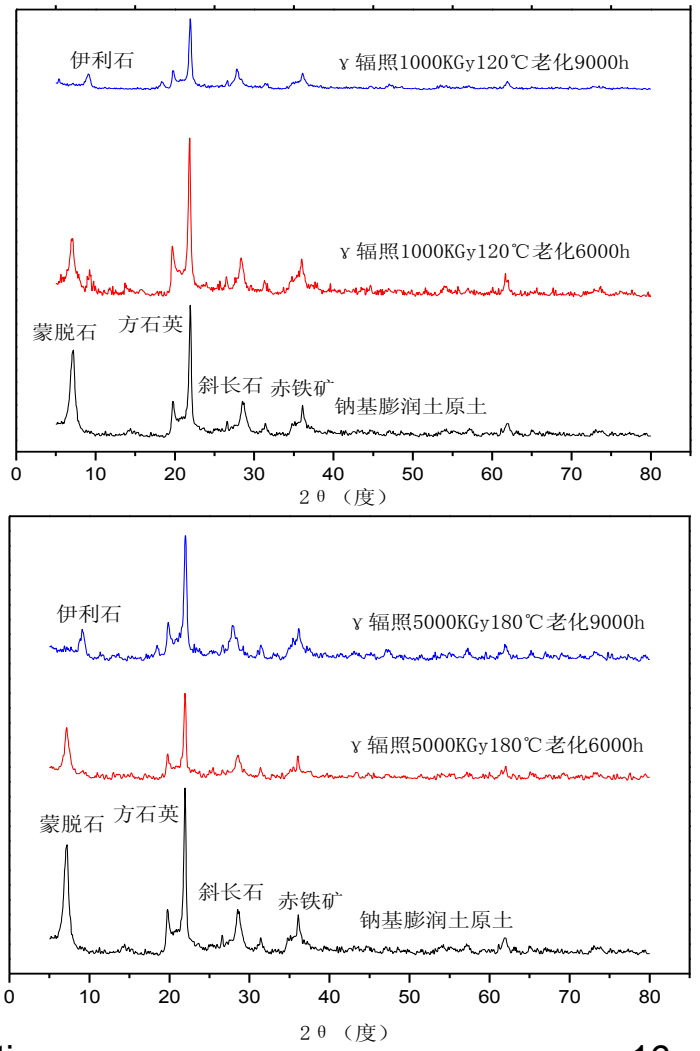

(2) quantitative analysis

No.	Condition	2-Theta 衍射角	d （Å） 层间距	FWHM	XS（Å） 晶胞尺寸
1	Blank	7.074	12.4858	0.551	158
2	1000 kGy	7.053	12.5229	0.625	137
3	1000KGy-120℃-6000h	7.131	12.3869	0.726	116
4	1000KGy-120℃-9000h	7.618	11.5953	1.367	60
5	1000KGy-180℃-9000h	7.370	11.9849	1.454	56
6	5000 kGy	7.098	12.4433	0.590	146
7	5000KGy-120℃-6000h	7.084	12.4676	0.592	146
8	5000KGy-120℃-9000h	7.339	12.0363	1.208	68
9	5000KGy-180℃-9000h	7.315	12.0745	1.407	58

4 Initial conclusions

(1) General effects： γ irradiation-thermal sequential treatment ＞ thermal treatment ＞γ irradiation.

(2) During irradiation- thermal sequential treatment, crystal size decreases with the increase of time and temperature; but the temperature effect is small; time effect is more obvious.

(3) Even for weak aging condition :1000kGy-120℃, diffraction peak of smectite disappear absolutely after 9000h(only more than 1 year) treatment, it means that modified-GMZ Na-bentonite is not stable under such condition.

5 Plan for future work

- **Guess: effects of simultaneous γirradiation /thermal treatment ≥ γirradiation-thermal sequential treatment**

New Experiment : Dose rate effect

simultaneous γirradiation /thermal treatment (~90℃)

Detailed irradiation condition

		Dose Rate		
Cumulative Dose		**610 Gy/h**	**170 Gy/h**	**85 Gy/h**
0.28 MGy	**time**			**3401 h**
	Sample No.			**1 #**
0.37 MGy	**time**	**608 h**	**2180 h**	**4360 h**
	Sample No.	**11 #**	**5 #**	**2 #**
0.74 MGy	**time**		**4360 h**	
	Sample No.		**3 #**	

Diffraction pattern : 0.37MGy（11#-610Gy/h、5#-170Gy/h、2#-85Gy/h）

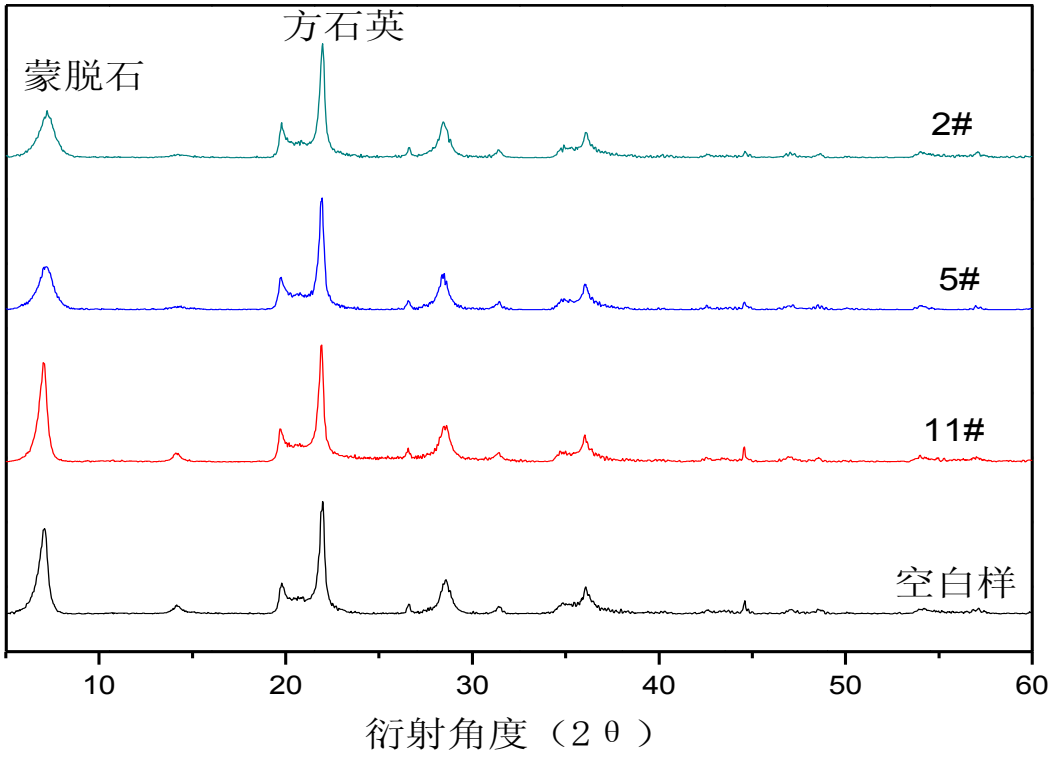

No.	condition	2-Theta（度）	d value（Å）	FWHM	XS（Å）晶胞尺寸	Area	Height 峰高
blank	—	7.096	12.4469	0.632	136	27252	1042
11#	610Gy/h-623h-0.37MGy	7.054	12.5215	0.561	155	28485	1205
5#	170Gy/h-2180h-0.37MGy	7.194	12.2781	1.008	82	22289	541
2#	85Gy/h-4360h-0.37MGy	7.252	12.1798	1.038	80	23290	548

With dose rate ↓: **2-Theta ↑， d value ↓， XS（Å）↓。**

Concl.：There exist dose rate effect.

Diffraction pattern :
85 Gy/h(1#-0.28MGy/2#-0.37MGy）

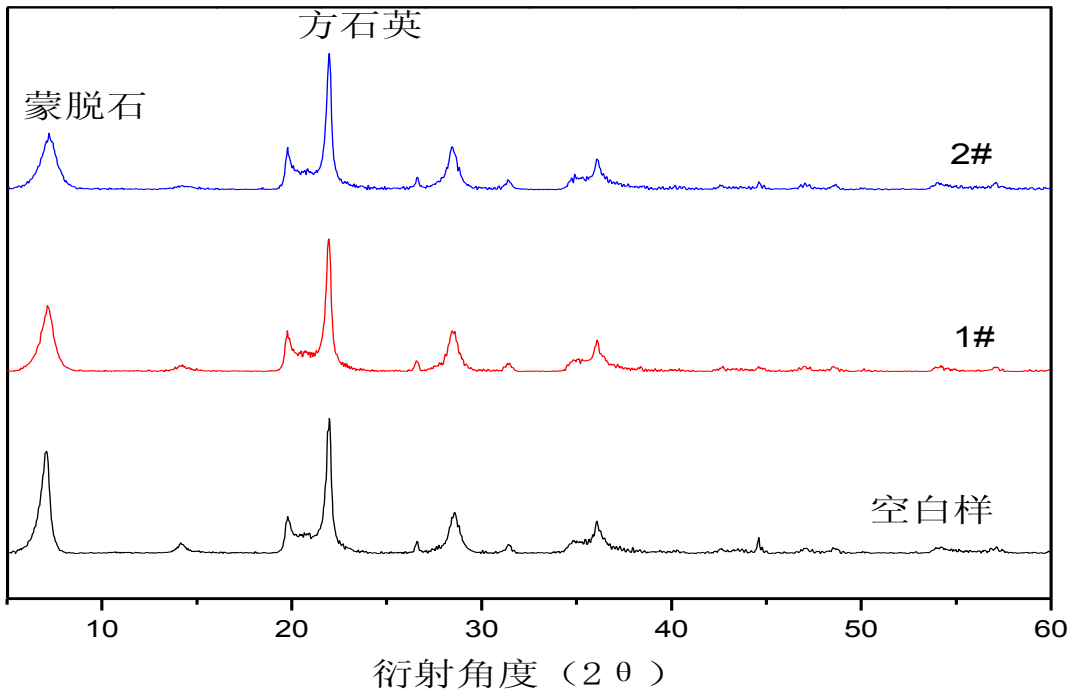

No.	condition	2-Theta（度）	d value（Å）	FWHM	XS（Å）晶胞尺寸	Area	Height 峰高
blank	—	7.096	12.4469	0.632	136	27252	1042
1#	85Gy/h-3401h-0.28MGy	7.199	12.2700	0.888	94	23113	643
2#	85Gy/h-4360h-0.37MGy	7.252	12.1798	1.038	80	23290	548

Diffraction pattern : 170 Gy/h-（5#-0.37MGy/3#-0.74MGy）

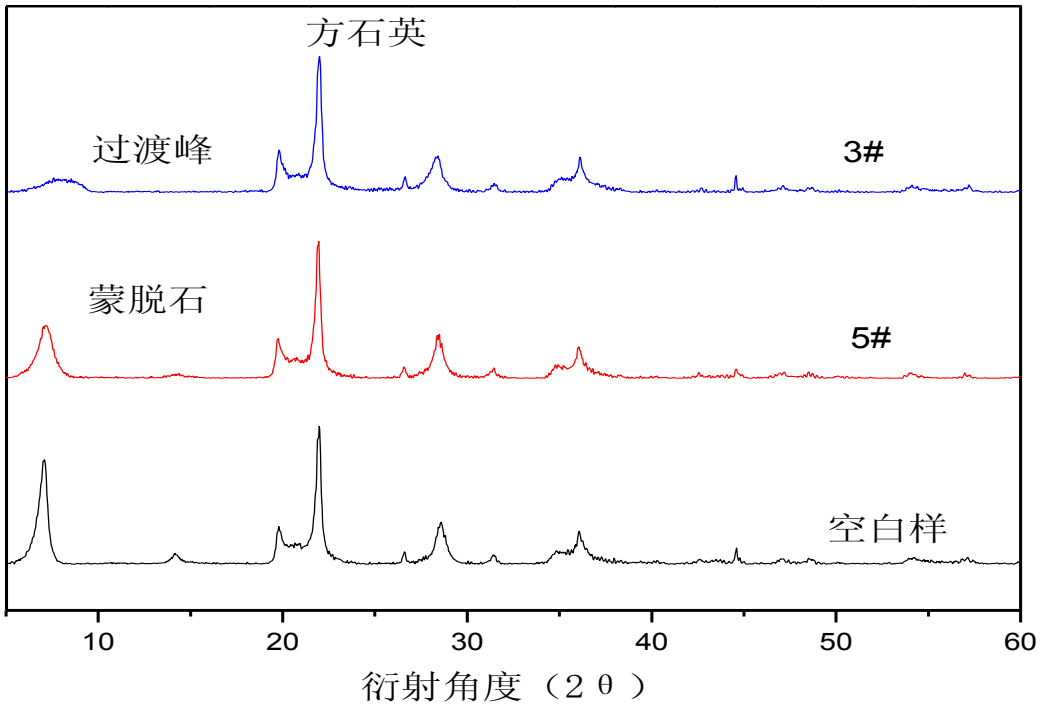

No.	condition	2-Theta（度）	d value（Å）	FWHM	XS（Å）晶胞尺寸	Area	Height 峰高
blank	—	7.096	12.4469	0.632	136	27252	1042
5#	170Gy/h-2180h-0.37MGy	7.194	12.2781	1.008	82	22289	541
3#	170Gy/h-4360h-0.74MGy	7.612	11.6040	1.176	70	1101	26
		8.479	10.4193	2.118	38	8961	120

With dose ↑: **2-Theta ↑， d value ↓， XS（Å）↓。**

Concl.：There exist dose effect.

At condition:

90℃-170Gy/h-0.74MGy, after 4360h(6 months)

there appears an transition diffraction peak

This proves that : GMZ bentonite is not stable under combined radiation/ thermal aging, and montmorillonite will transform to illite in short time

Results: IR、STA、Kd(Cs-137) , till 2013

Thanks for your Attention!

2nd Chinese-German Workshop on Radioactive Waste Disposal
Karlsruhe, 15-16 Oct. 2012

THM Behaviour of Clay Host Rocks for Disposal of Radioactive Waste

Chun-Liang Zhang
Gesellschaft für Anlagen- und Reaktorsicherheit (GRS)
Repository Safety Research Division
Braunschweig, Germany

URLs in clay formations

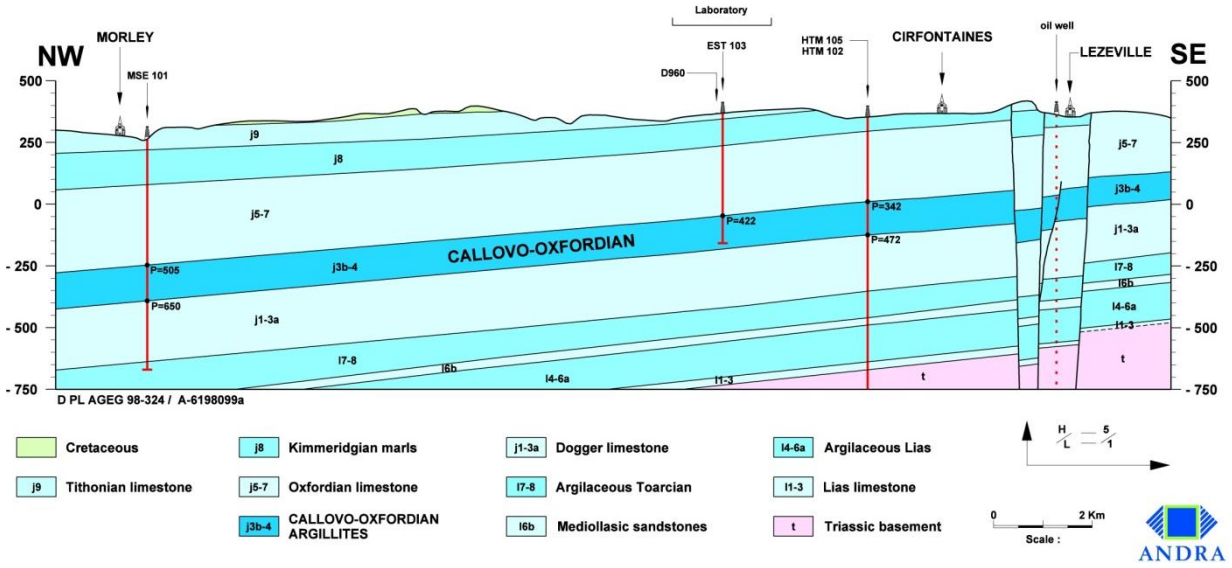

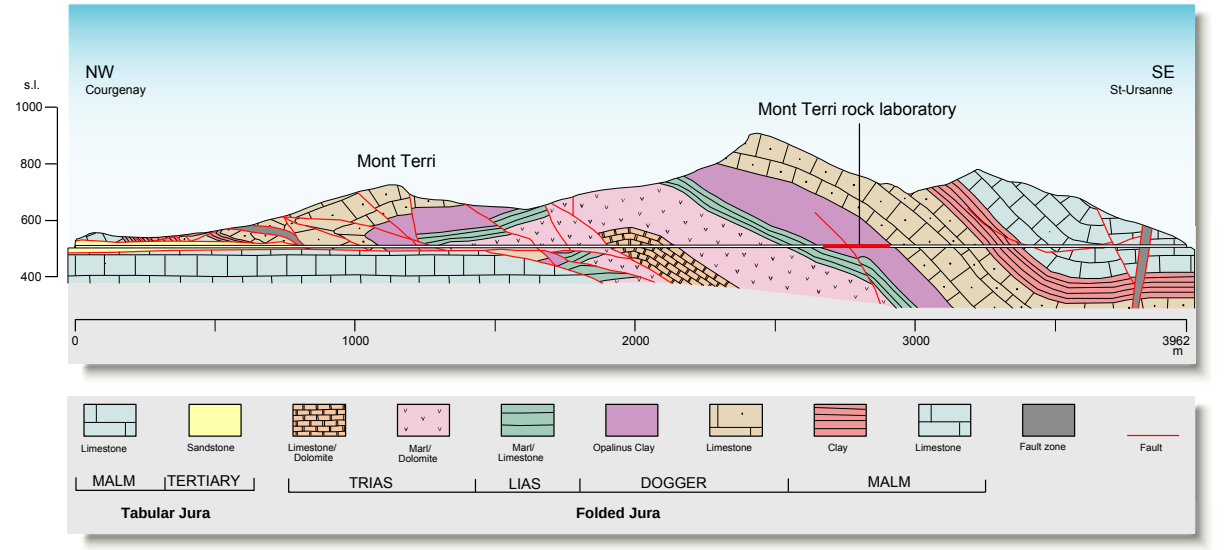

Callovo-Oxfordian Argillite at Bure in France

clay content	40 – 45 %
water content	7.7 %
dry density	2.30 g/cm^3
porosity	16.0 %
uniaxial strength	20 – 30 MPa
permeability	< 10^{-20} m^2

Opalinus Clay at Mont Terri in Switzerland

clay content	58 – 76 %
water content	6.7 %
dry density	2.35 g/cm^3
porosity	15.0 %
uniaxial strength	10 – 15 MPa
permeability	< 10^{-20} m^2

GRS Research Projects (national & international, since 2000)

	Project	Investigations of
Clay host rock	MODEX-REP	HM behaviour of the COX argillite at Bure
	Pre-Project Bure	THM behaviour of the COX argillite at Bure
	HED Experiment	Thermal effects on the Opalinus clay at Mont Terri
	VE Experiment	Ventilation effects on the Opalinus clay at Mont Terri
	NP-PRO	Damage and self-sealing of clay rocks
	TIMODAZ	Thermal impact on long-term development of EDZ
	BET / HG-C	Gas migration in clay formation
	THM-TON	THM-Processes in the COX argillite around HLW
Clay buffer	FEBEX	THM behaviour of bentonite buffer around HLW
	EBS	Hydration of bentonites as sealing material
	SWELLING	Swelling of bentonites under saline conditions
	KENTON	Water/gas two-phase-flow in clay-based mixtures
	SB Experiment	Self-sealing barriers of clay-based mixtures

Field observations ⟺ Laboratory tests ⟺ Numerical modelling

MODEX-REP: GRS lab tests on drilling cores

- Physical properties
- Permeability
- Short-term behaviour
- Long-term behaviour

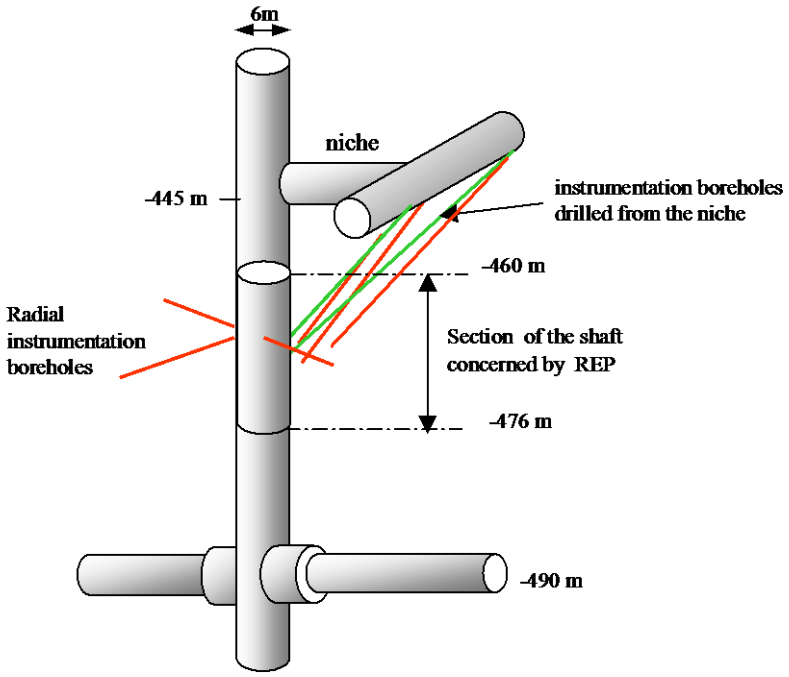

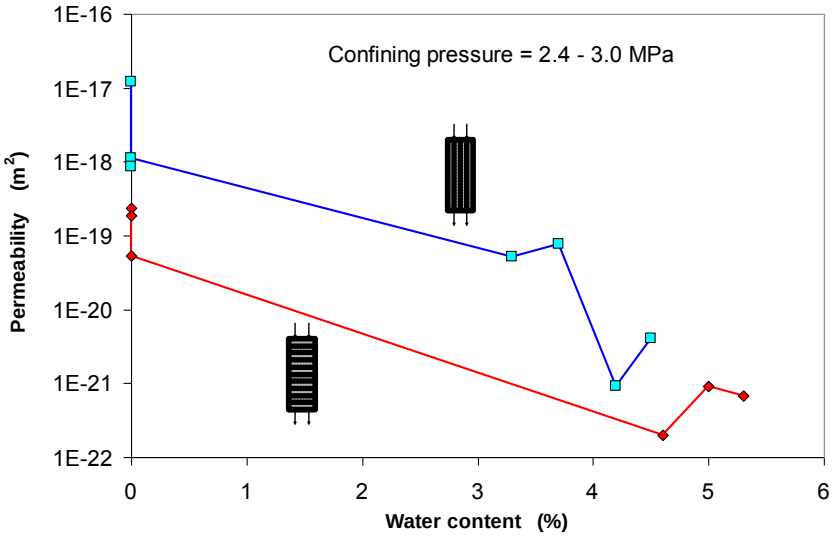

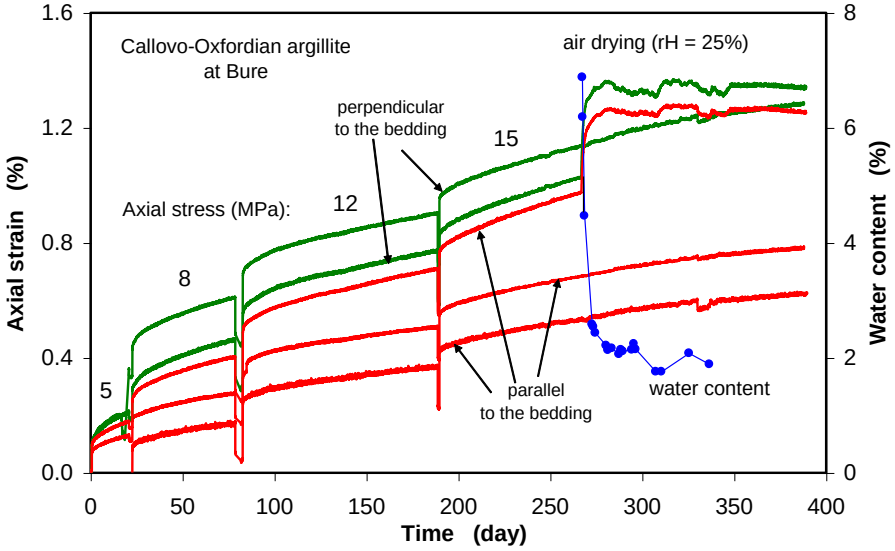

Ventilation Experiment (VE): In-situ measurements

VE Geoelectrics: Electrode Array

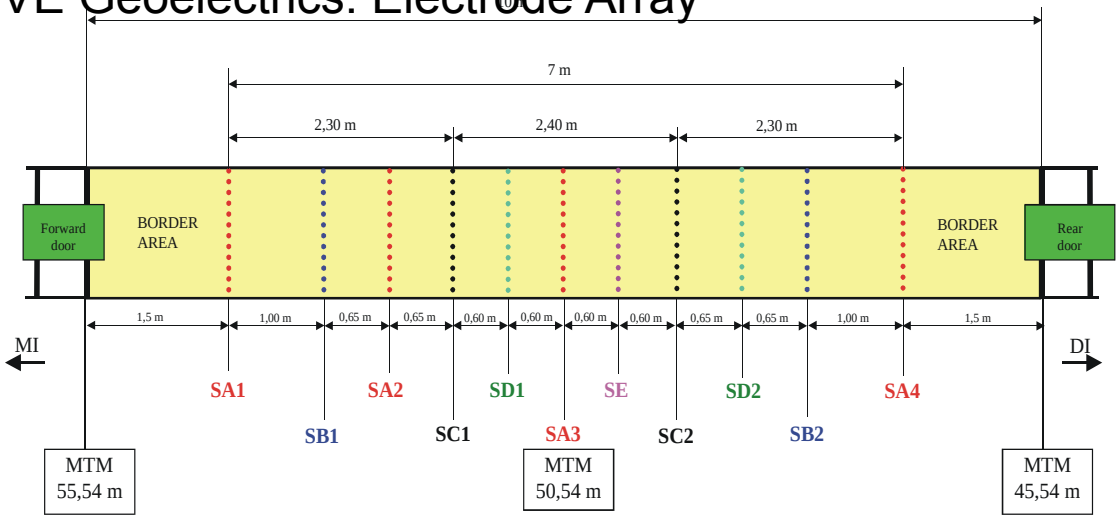

SA: Mini-Piezometers
SB: Humidity sensors
SC: TDRs
SD: Extensometers
SE: Geoelectric

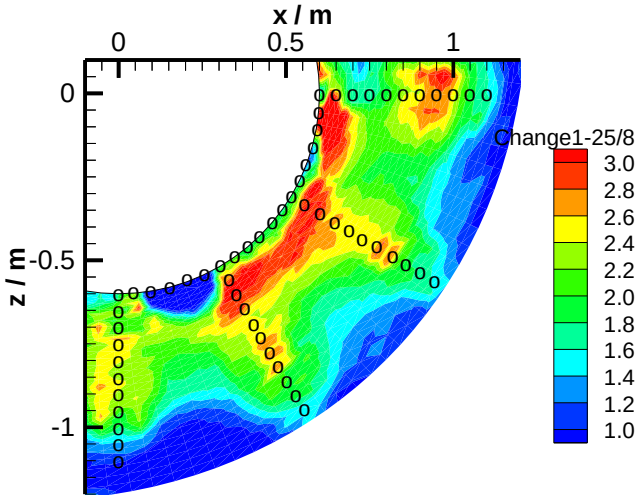

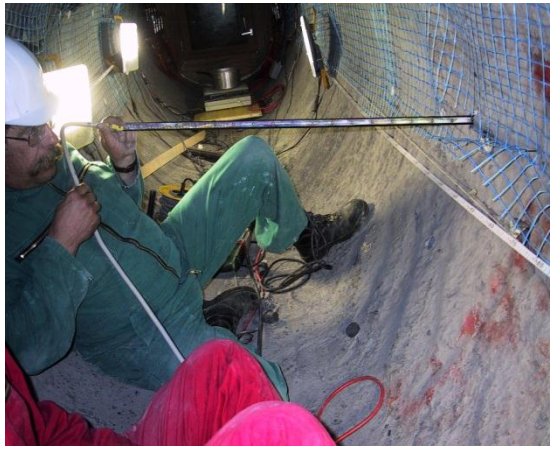

Ventilation Experiment (VE): Lab tests

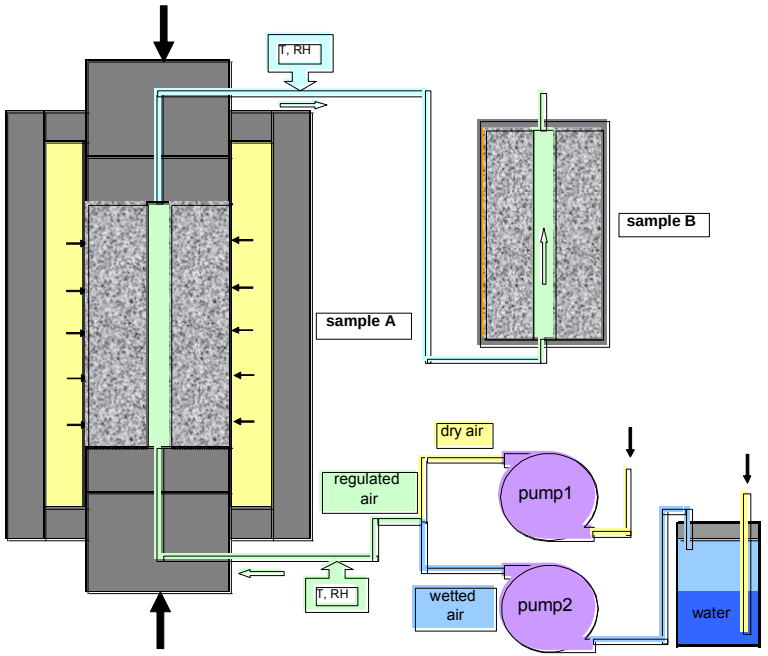

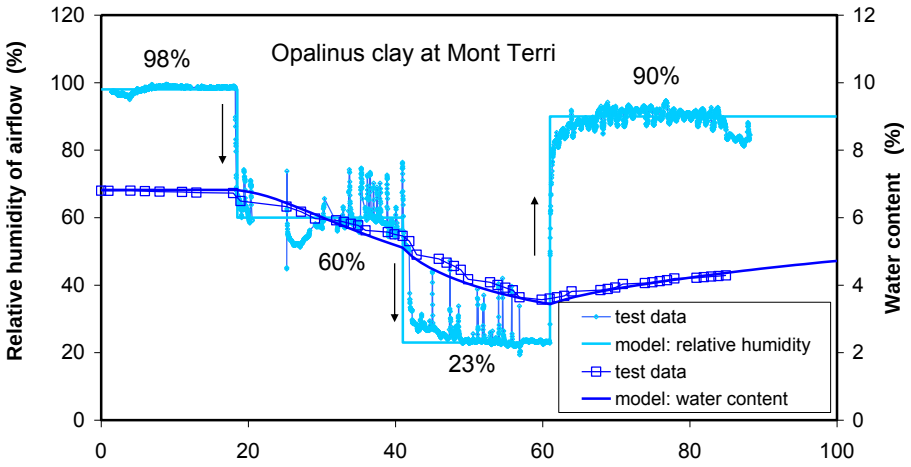

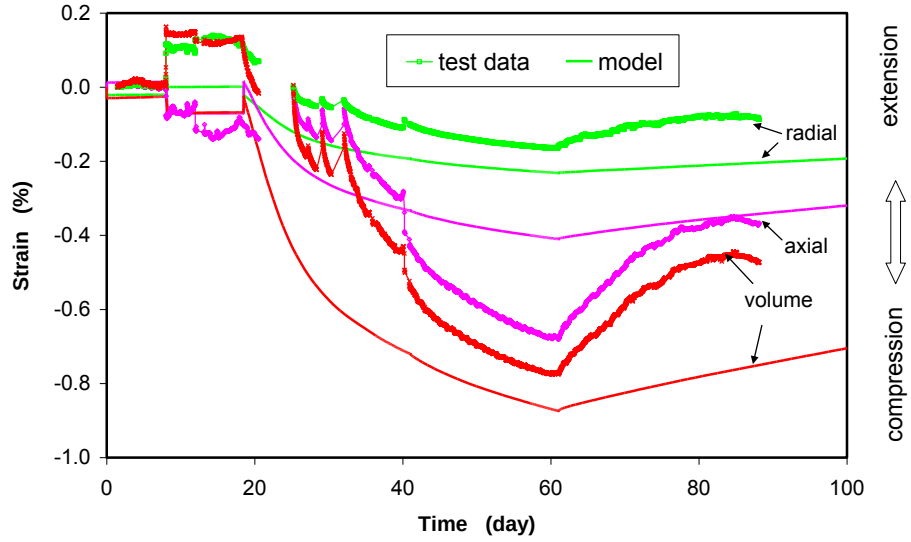

SB Experiment: Self-sealing of clay-based barriers

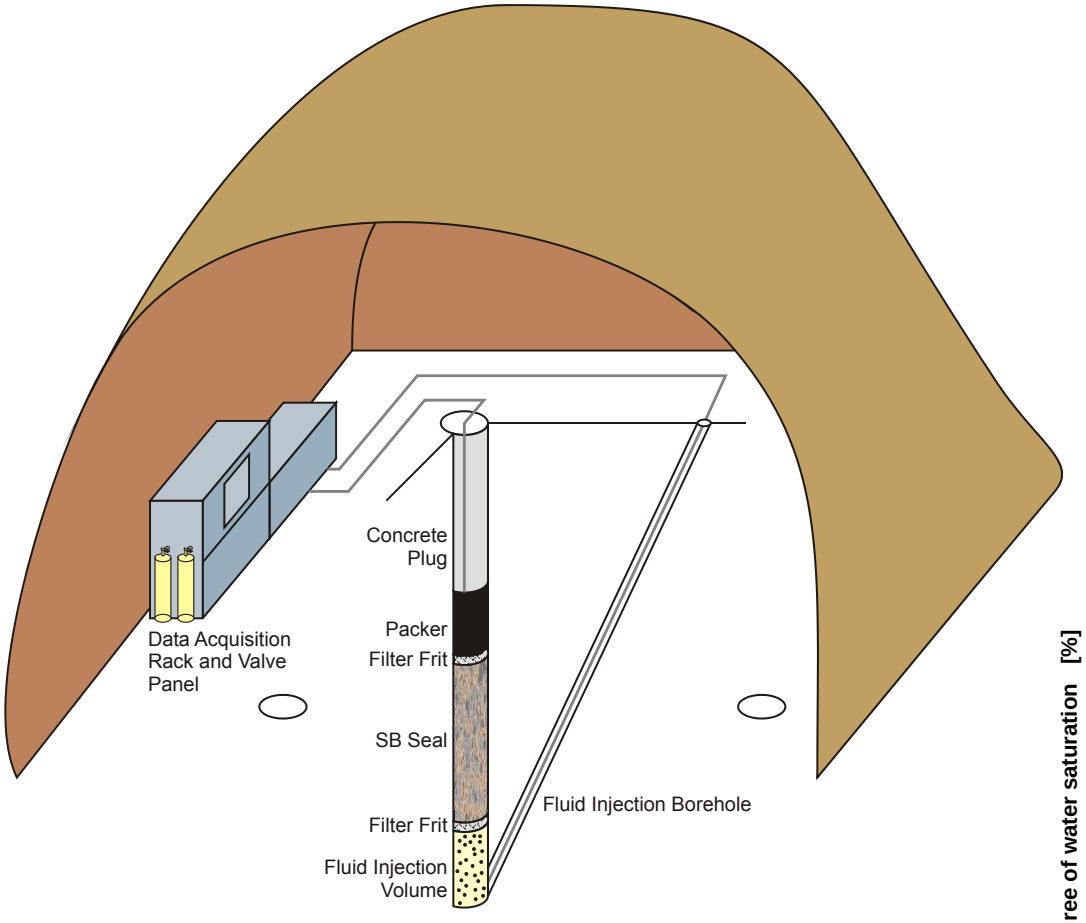

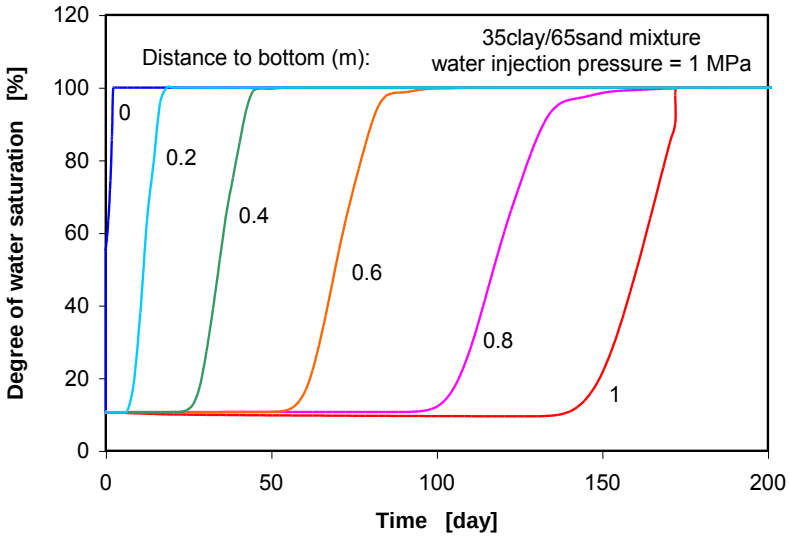

Re-saturation of Clay/Sand Mixtures

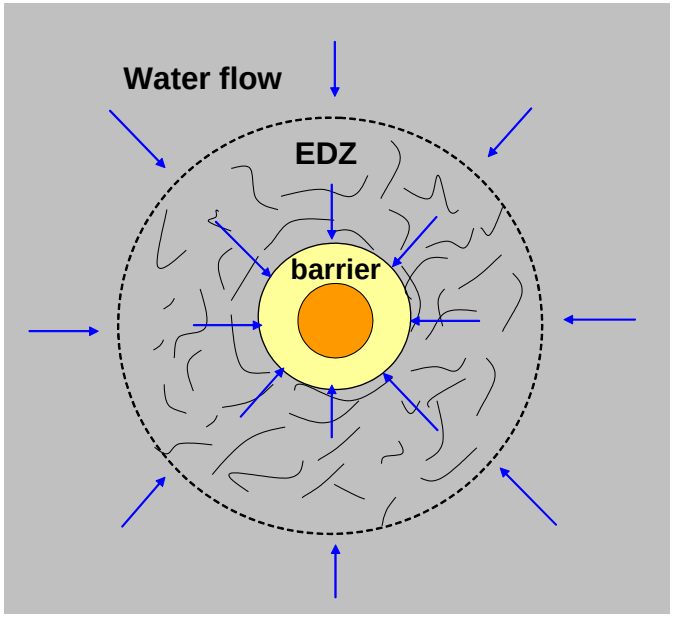

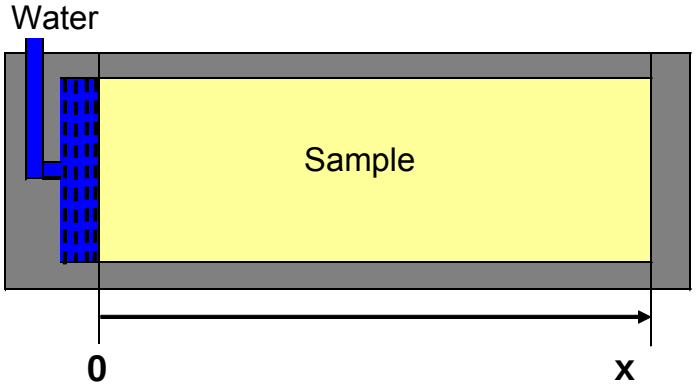

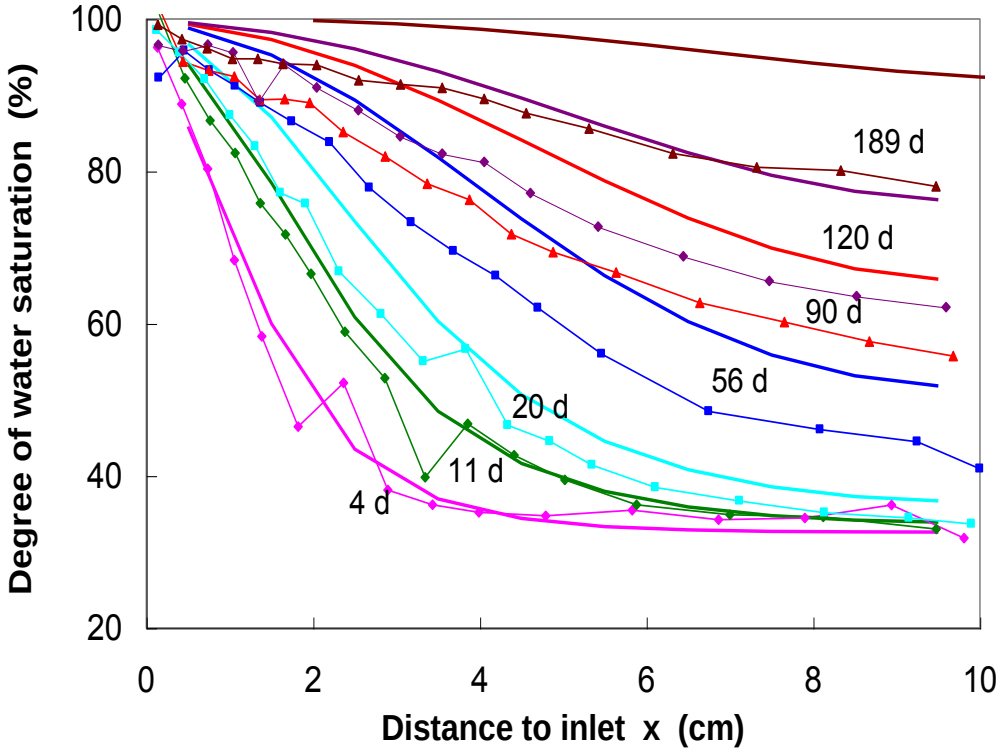

Test data obtained on MX-80 bentonite

Modelling results for FEBEX bentonite (code: CODE-BRIGHT)

HE-D heating experiment

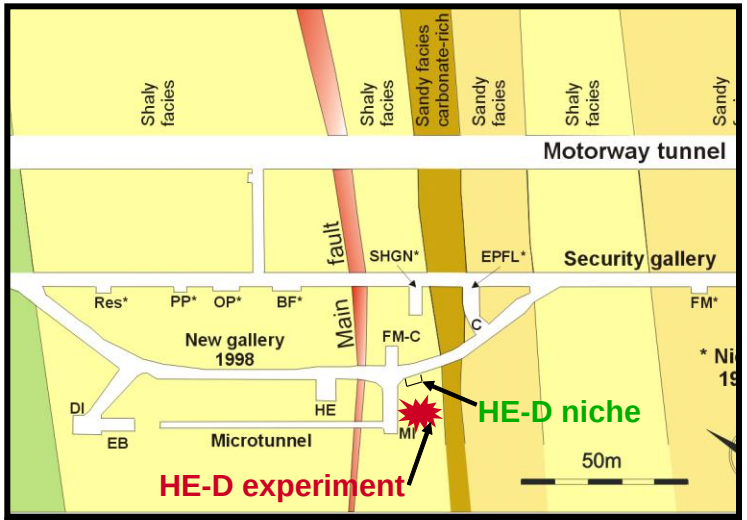

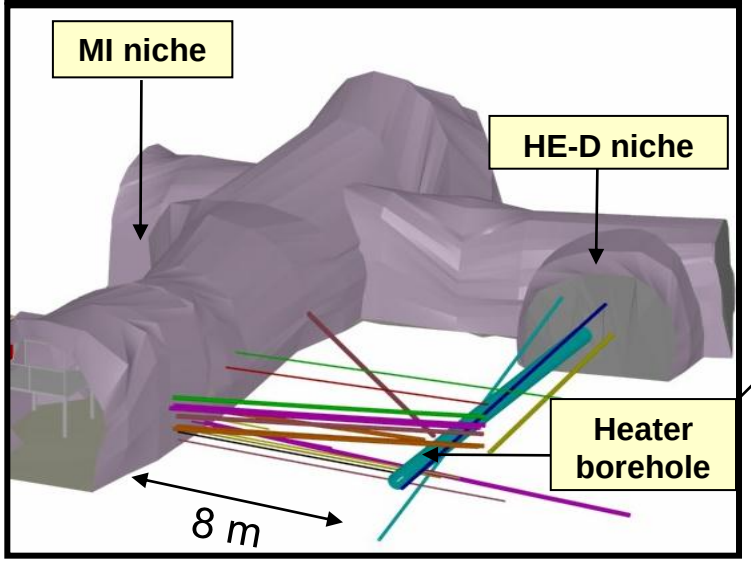

HE-D Experiment at URL Mont Terri

- **Objective:** Understanding of THM processes in clay
- **Measurement:** Temperature
  Pore-water pressure
  Gas migration
  Deformation
- **Modelling**

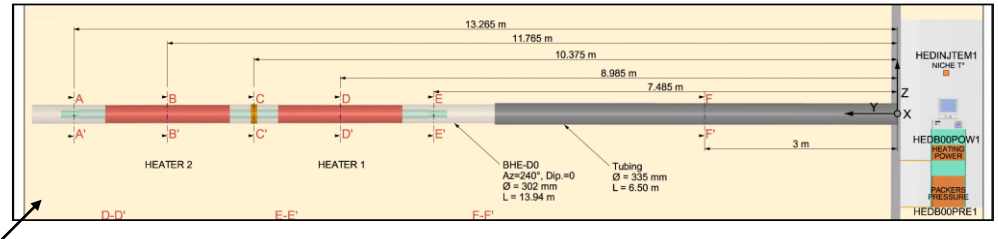

Heater borehole: D = 30 cm, L = 14 m

24 boreholes

more than 80 instruments

HE-D Experiment: temperature and pore-water pressure

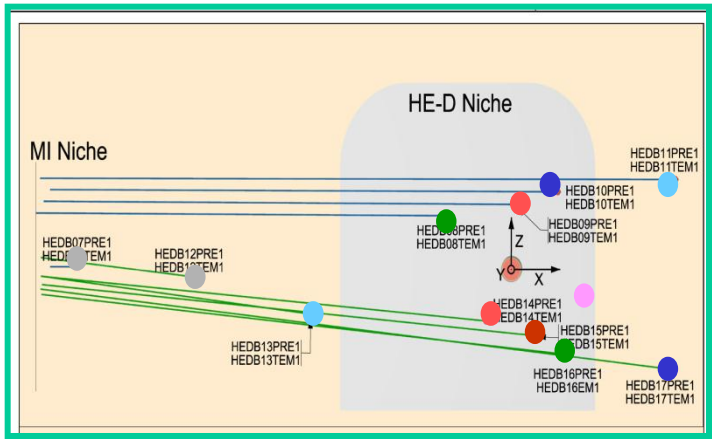

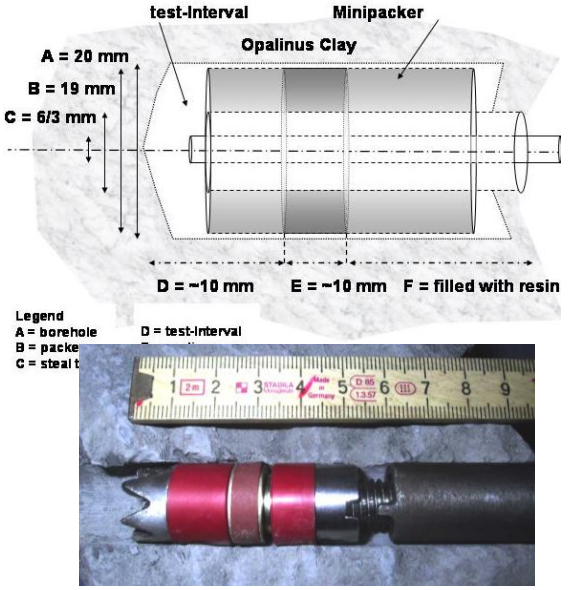

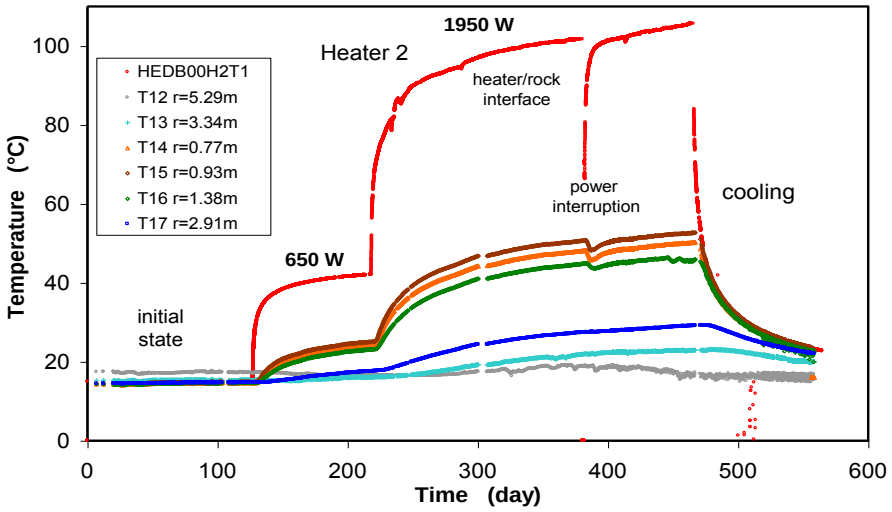

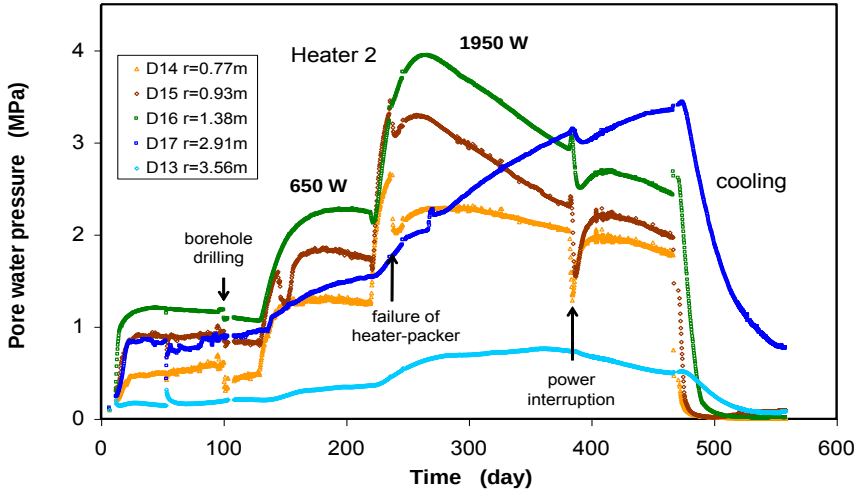

HE-D Experiment: Large-scale heating test

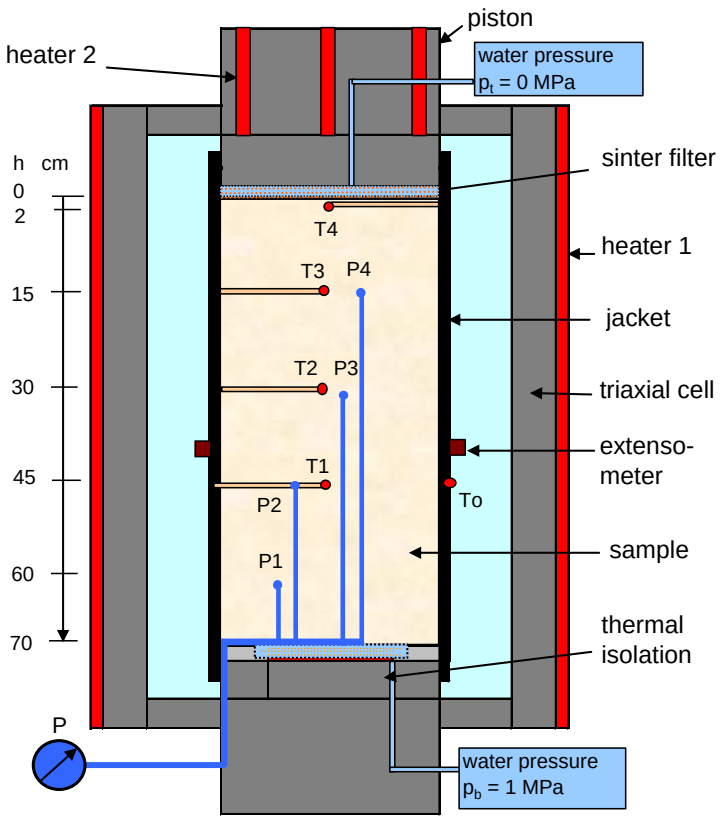

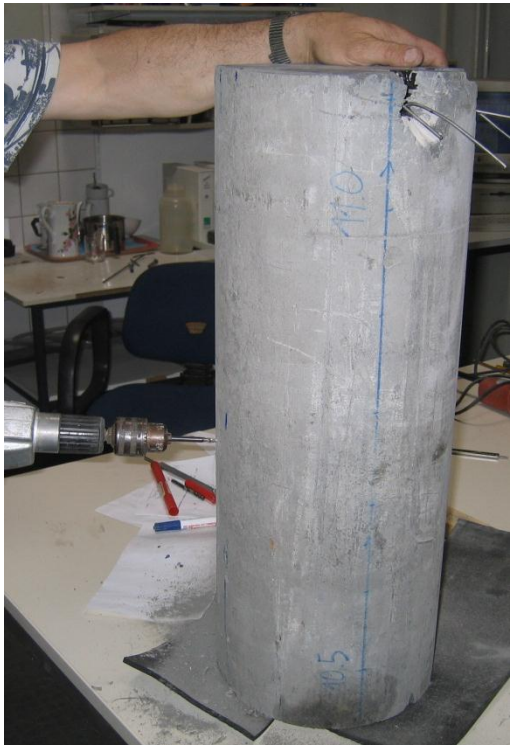

Sample: D=260mm, L=700mm

GRS-mini-packers
(D=10mm, L=30mm)

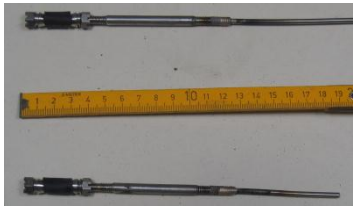

Temperature sensors
PT100

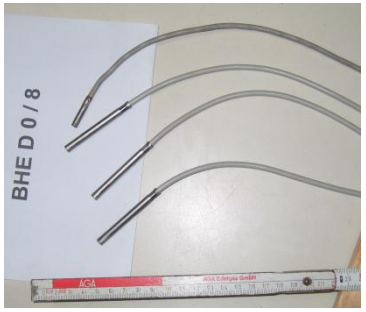

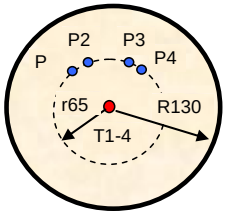

Confining stress = 8 MPa
Heater temperature = 80°C, Boundary temperature = 30°C
Water pressure at top = 0 MPa, Water pressure at bottom = 1 MPa

Results of the large-scale heating test

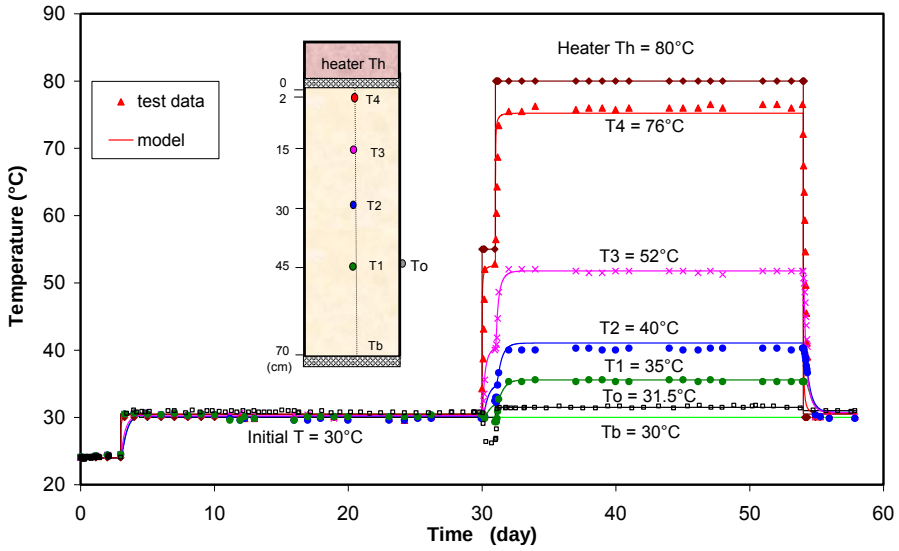

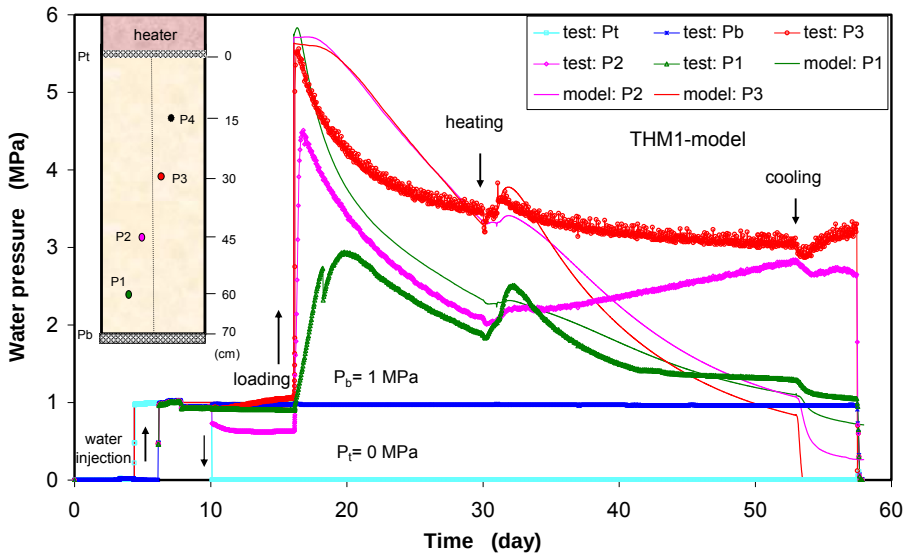

Thermal conductivity	$\lambda = 1.7\ W \cdot m^{-1} \cdot K^{-1}$
Specific heat capacity	$C = 800\ J \cdot kg^{-1} \cdot K^{-1}$
Thermal expansion coefficient of the solid grains	$\alpha_s = 1.5 \cdot 10^{-6}\ K^{-1}$
Thermal expansion coefficient of the pore water	$\alpha_w = 3.4 \cdot 10^{-4}\ K^{-1}$
Thermal expansion coefficient of the rock mass	$\alpha_m = 1.7 \cdot 10^{-5}\ K^{-1}$
Elastic modulus	$E = 6680$ MPa
Poisson's ratio	$\nu = 0.33$
Intrinsic permeability	$k = 2 \cdot 10^{-20}\ m^2$

Coupled THM Modelling (CODE-BRIGHT)

- Balance of energy:

$$\frac{\partial}{\partial t}\left[E_s\rho_s(1-\phi)+E_l\rho_l S_l\phi+E_g\rho_g S_g\phi\right]+\nabla\cdot\left(\mathbf{i}_c+\mathbf{j}_{Es}+\mathbf{j}_{El}+\mathbf{j}_{Eg}\right)=f^E$$

- Balance of water mass:

$$\frac{\partial}{\partial t}\left(\theta_l^w S_l\phi+\theta_g^w S_g\phi\right)+\nabla\cdot\left(\mathbf{j}_l^w+\mathbf{j}_g^w\right)=f^w$$

- Balance of air mass:

$$\frac{\partial}{\partial t}\left(\theta_l^a S_l\phi+\theta_g^a S_g\phi\right)+\nabla\cdot\left(\mathbf{j}_l^a+\mathbf{j}_g^a\right)=f^a$$

- Balance of solid mass:

$$\frac{\partial\theta_s^s(1-\phi)}{\partial t}+\nabla\cdot\left(\mathbf{j}_s^s\right)=0$$

- Stress equilibrium:

$$\nabla\cdot\boldsymbol{\sigma}+\mathbf{b}=\mathbf{0}$$

- **Heat transport:**
  conduction, advection with water/vapour flow
- **Water flow:**
  advection and vapour diffusion
- **Air flow:**
  advection and dissolution in liquid water
- **Thermo-elasto-plastic model:**
  thermal expansion/consolidation, swelling/shrinking

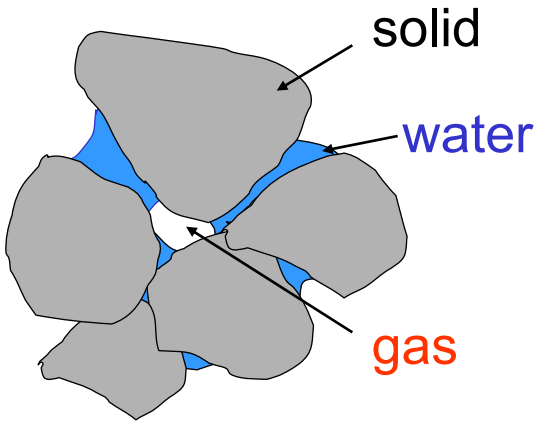

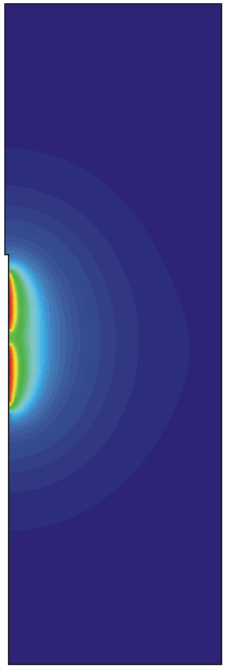

Modelling of the HE-D Heating Experiment

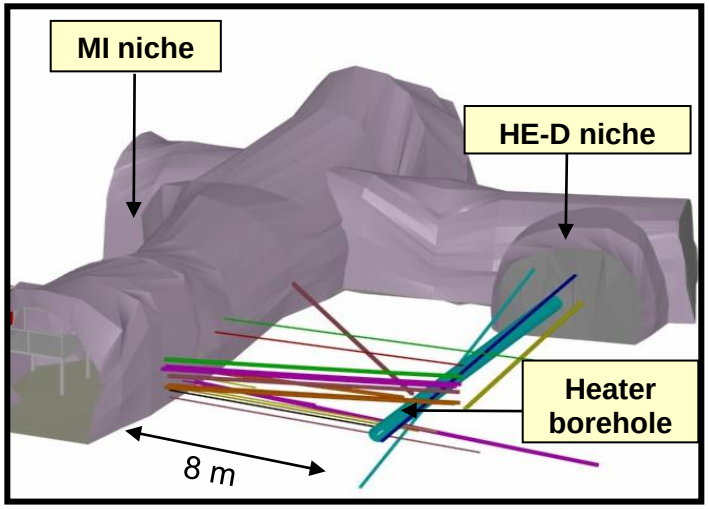

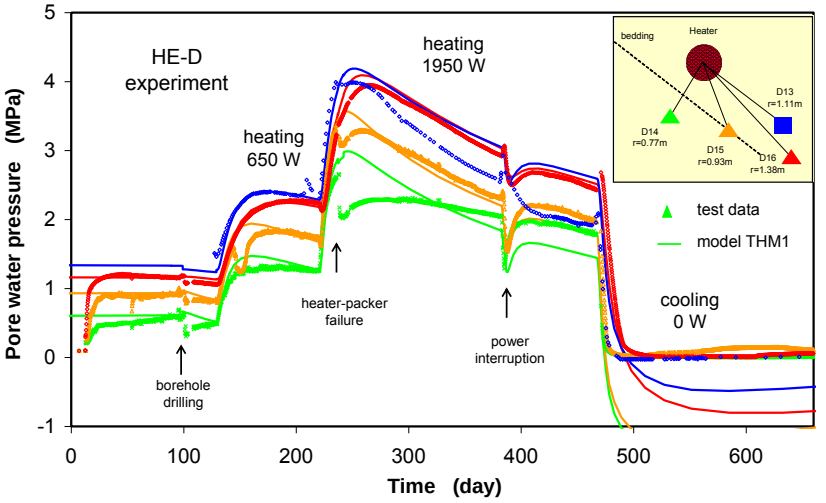

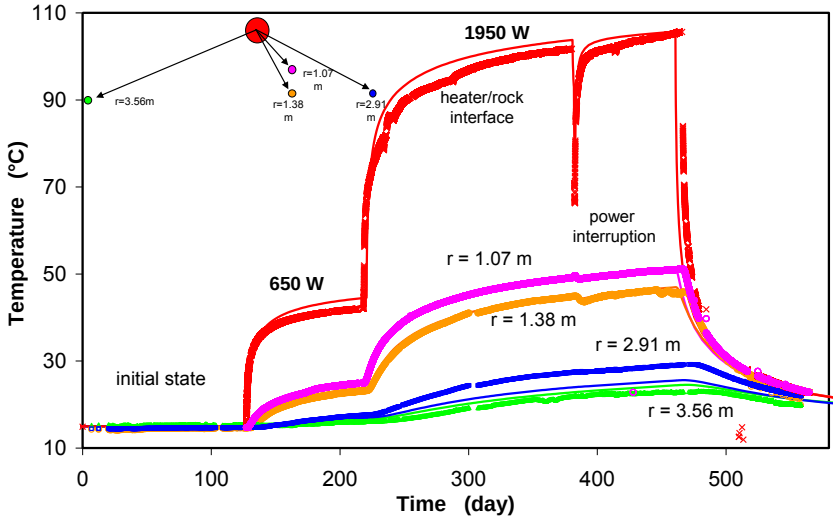

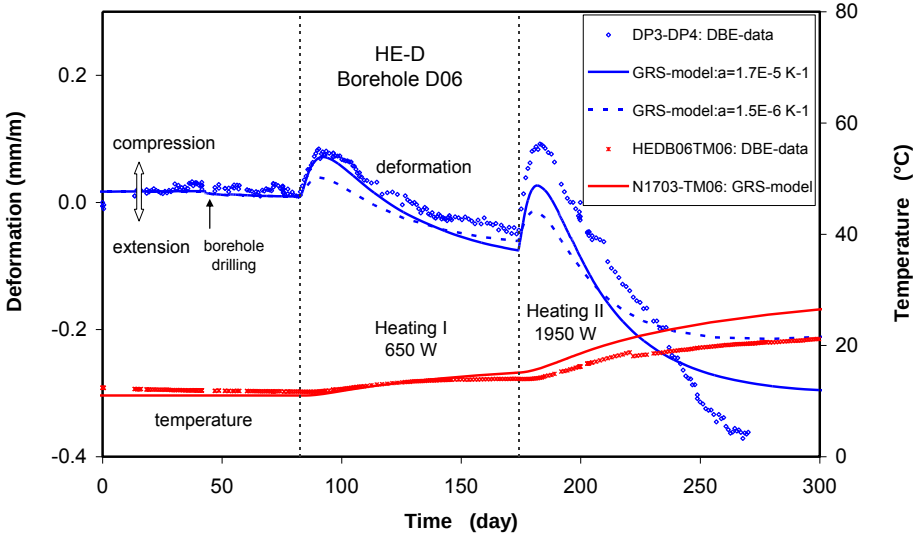

Damage tests

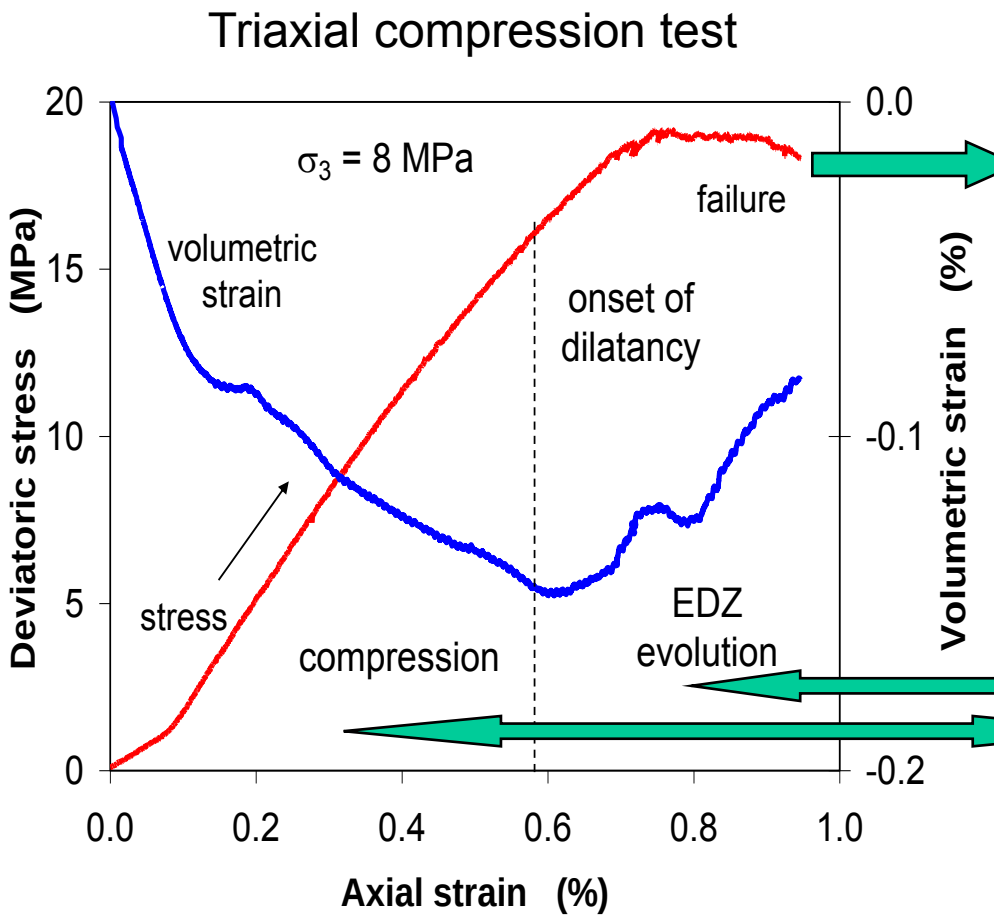

Opalinus clay samples after failure

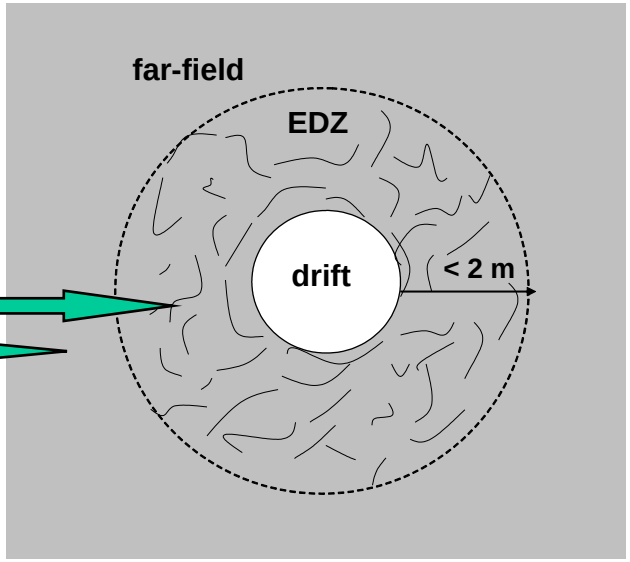

Long-term creep tests

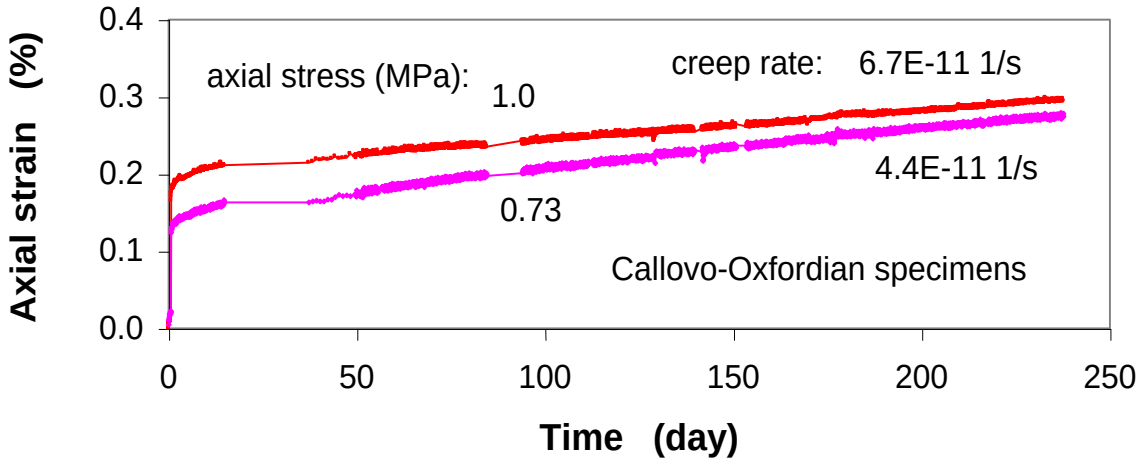

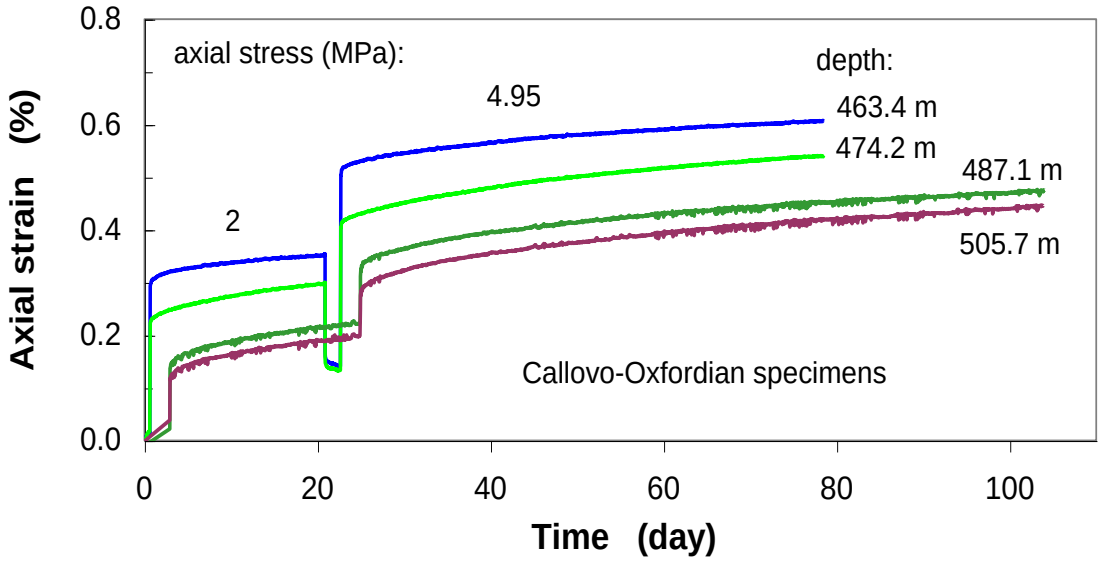

Long-term deformation
→ drift convergence
→ compaction of barriers
→ re-healing of EDZ

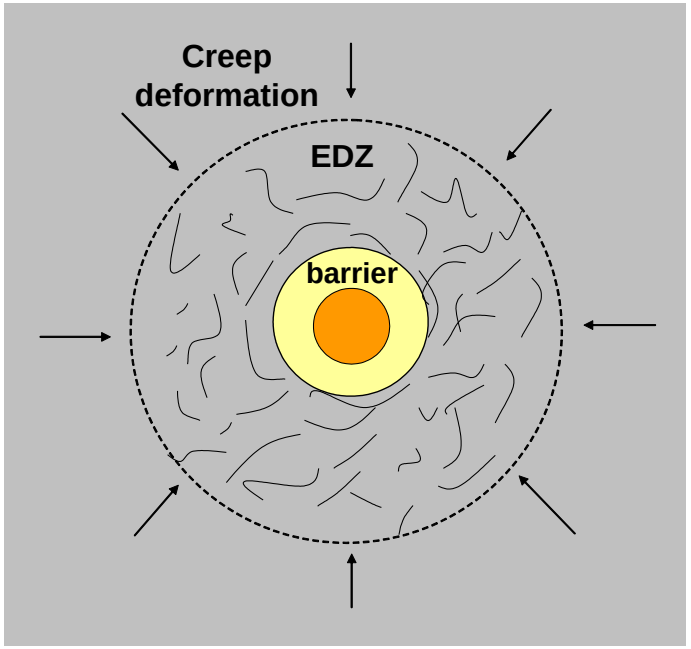

Sealing tests on damaged samples by re-compaction

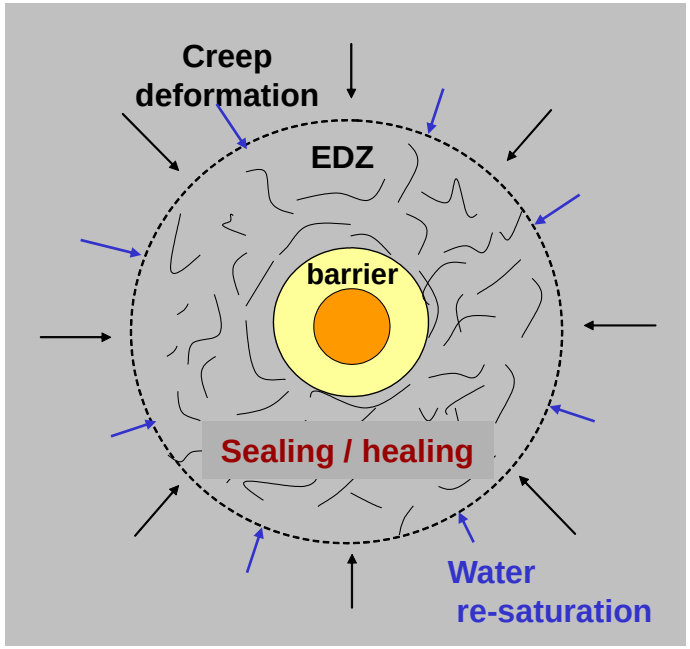

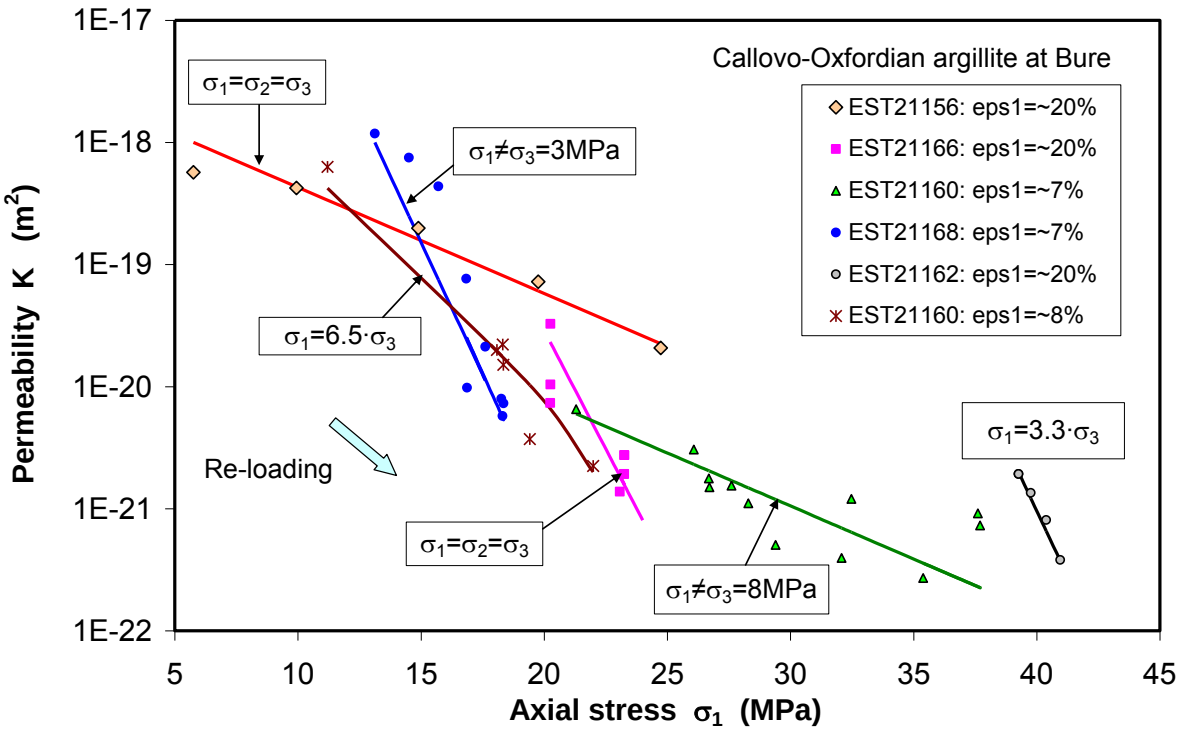

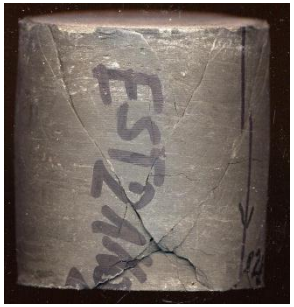

Sealing tests by water re-saturation

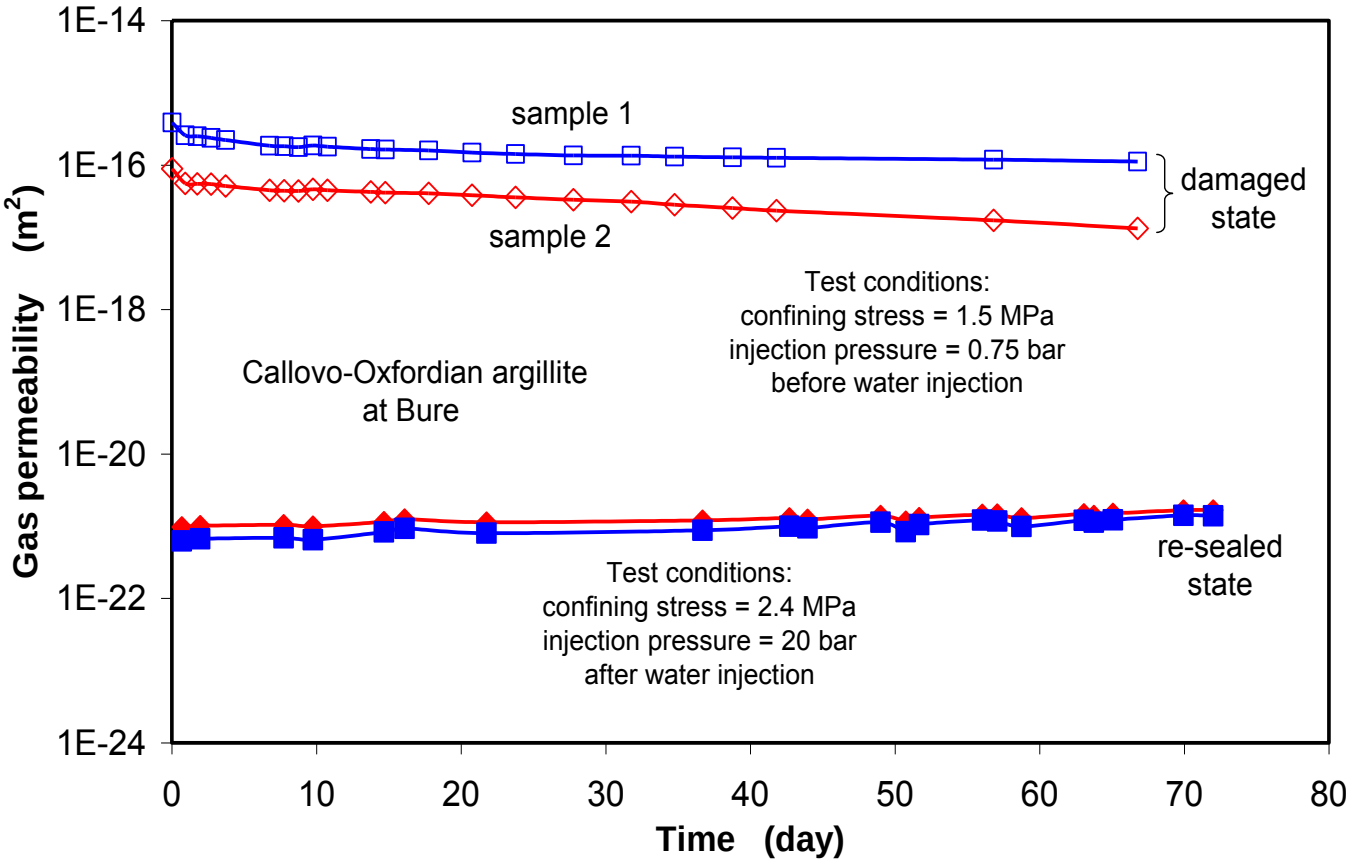

Sample 1

Sample 2

Re-sealed samples show the same permeability as that of intact clay rock

$K = 10^{-21}\ m^2$

Conclusions

The studied clay rocks exhibit that

- The deformation is dominated by elasto-plasticity with dilatancy at high stresses
- Above the damage boundary, shear and tensile fracturing leads to failure
- The damage-induced permeability increase occurs only at low confining stresses
- The fracture closure & permeability decrease is dominated by the normal stress
- The effective stress is dominated by the swelling pressure acting in bound porewater
- The swelling pressure & strain depends on water saturation & confining conditions
- The sealing fractures is strongly enhanced by water flow and can be resealed to the intact rock state under the repository conditions
- Only positive rather than negative thermal effects are observed with respect to the integrity and stability of the clay host formations

Bentonites in HLRW systems

Stephan Kaufhold

Reiner Dohrmann

One of todays big challanges:

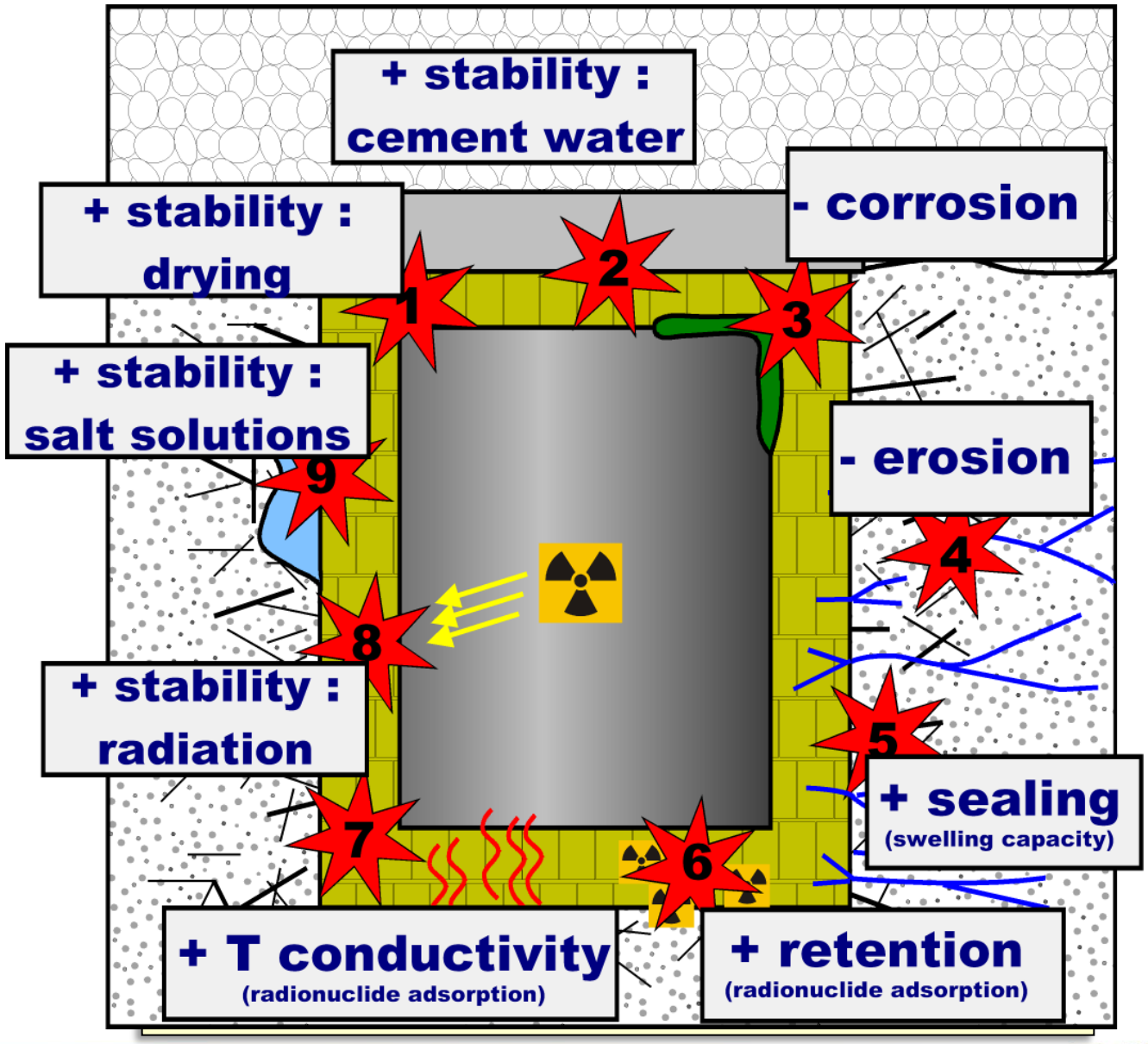

BGR Bundesanstalt für Geowissenschaften und Rohstoffe
GEOZENTRUM HANNOVER

Introduction – aim of BGR bentonite study

Bentonites are rather different !!!!!!

Bentonites cannot be generalized,
e.g. the corrosion rate determined with one bentonite does not apply to all others

For the determination of the actual ranges of e.g. corrosion rates (or whatever) different bentonites have to be compared.

Therefore, BGR established a significant sample set which is used to compare performance and properties

e.g.: compare Fe content with a specific performance parameter (e.g. temperature stability)

Introduction - Sample base

Introduction - Sample base

All samples (except for 4) were available as raw materials

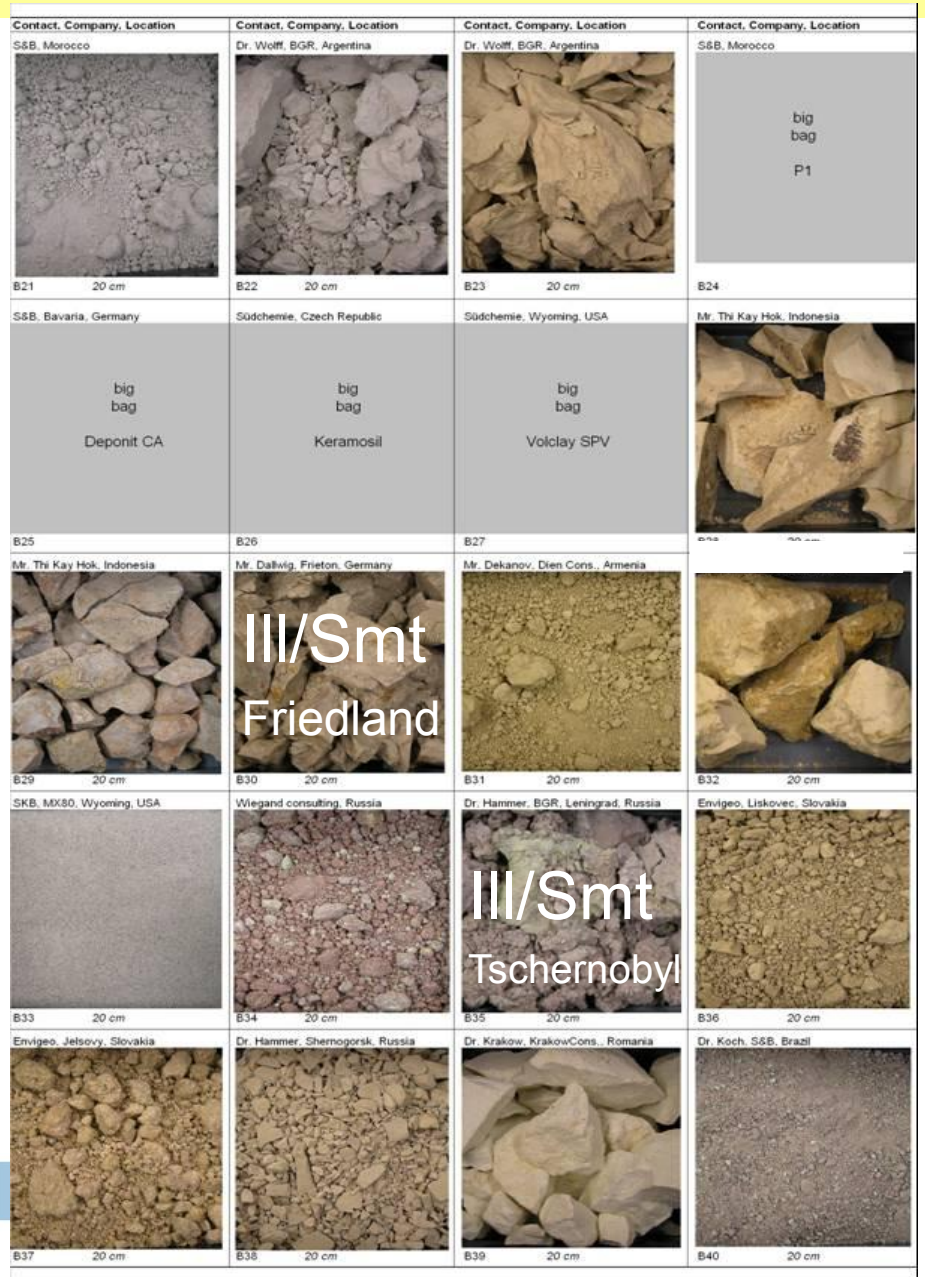

Characterisation– mineralogical composition (charge 1)

Common minor components: quartz, feldspar, carbonates

often: kaolinite, cristob., gypsum, musc/illite, dolom., TiO_2

Rarely: apatite, baryte, pyrite, zeolite, chlorite, hem/ilm/goe,

	B-1	B-2	B-3	B-4	B-5	B-6	B-7	B-8	B-9	B-10	B-11	B-12	B-13	B-14	B-15	B-16	B-17	B-18	B-19	B-20	B-21	B-22	B-23	B-24	B-25	B-26	B-27	B-28	B-29	B-30	B-31	B-32	B-33	B-34	B-35	B-36	B-37	B-38	B-37	B-38
smectite	78	77	89	91	88	91	91	67	74	89	89	91	84	88	79	70	88	92	75	86	80	76	80	80	61	86	84	69	89	37	81	92	88	77	41	75	80	63	n.d	n.d
musc./illite		3						2	2							19	5		4	3				4	17					29					31		6	9		
kaolinite													3	3	4	3									4				5	3				4		2				
chlorite																														2							0			
quartz	3	1	1	2	1		2	17	5	6	1	1	6	3	7	7	1	2	10	2	1	4	10	1	13	1	4	2	6	23	7	0	3	16	22	11	6	11		
cristobalite	0		2					1	6											2	1	12		3		8	5	8			9	0	1			3				
hematite										1	0	2																												
ilmenite										1	0																													
rutile+ anatase	0		1	1	1	1				2	3		2	2	3															1			1	1	0		0			
goethite											6																													
calcite	1	0	0		5	0	1	2	2	1	1	1	4	1	4		2	1	3	2		0			0	1	1			0	1	0	1				1	7		
dolomite							1										1															1			1			1		
feldspars	18	19	7	5	2	8	4	8	9		0	0	1	3	2		2	5	8	5	18	8	10	12	5	4	5	4	0	4	1	2	7	2	6	8	8	8		
heulandite								1	1																															
analcime								1	1																															
clinopt																												17			1	5								
pyrite					1																									1										
barite				1											1									0																	
gypsum					1			1	1			0				1				1							1						0							
fluorapatite												4	1		1																									

Ufer, K., Stanjek, H., Roth, G., Dohrmann, R., Kleeberg, R., Kaufhold, S., 2008. Quantitative phase analysis of bentonites by the Rietveld method. Clays and Clay Minerals 56 (2), 272–282.

Kaufhold, S., Hein, M., Dohrmann, R., Ufer, K. (2012) Quantification of the mineralogical composition of clays using FTIR spectroscopy. – Journal of Vibrational Spectroscopy, 59, 29 - 39.

Characterisation – chemical composition (charge 2), XRF

	SiO_2	TiO_2	Al_2O_3	Fe_2O_3	MnO	MgO	CaO	Na_2O	K_2O	P_2O_5	LOI	sum
	[mass%]	[mass%]	[mass%]	[mass%]	[mass%]	[mass%]	[mass%]	[mass%]	[mass%]	[mass%]	[mass%]	[mass%]
B1	53.3	0.2	16.6	2.8	0.1	4.1	1.7	1.3	0.9	0.0	18.7	99.7
B2	52.0	0.6	15.4	5.0	0.1	4.4	1.7	0.9	1.1	0.1	18.5	99.6
B3	52.1	0.7	16.6	4.9	0.1	3.1	1.6	0.6	0.3	0.1	19.5	99.7
B4	49.4	0.7	15.6	8.0	0.0	3.1	0.9	0.6	0.4	0.1	19.5	98.7
B5	47.6	0.7	15.9	6.0	0.0	3.0	4.4	0.4	0.5	0.1	20.2	99.7
B6	52.8	0.7	18.0	3.4	0.0	3.5	1.5	0.5	0.5	0.2	18.7	99.7
B7	54.8	0.3	17.0	3.2	0.1	4.5	1.5	2.0	1.5	0.1	14.5	99.6
B8	66.8	0.1	15.7	3.1	0.0	1.5	0.9	2.6	0.4	0.0	8.3	99.7
B9	59.6	0.1	14.7	3.0	0.3	1.4	5.4	2.2	0.4	0.0	12.2	99.7
B10	49.4	1.9	13.9	11.4	0.0	2.6	1.5	0.8	0.5	0.1	17.5	99.6
B11	46.1	2.4	14.4	15.7	0.1	2.5	0.9	1.8	0.1	0.0	15.9	99.7
B12	47.9	0.6	13.6	9.8	0.0	3.9	3.1	1.6	0.1	1.4	17.7	99.7
B13	44.6	2.0	16.2	10.1	0.1	2.1	3.1	0.1	0.6	0.3	20.4	99.6
B14	45.8	2.1	16.8	9.9	0.0	2.2	1.6	0.1	0.7	0.4	20.3	99.6
B15	38.3	1.7	13.8	8.8	0.2	2.0	10.2	0.2	0.5	0.5	23.0	99.2
B16	51.5	0.4	20.1	5.9	0.0	2.9	1.4	0.1	1.7	0.1	15.5	99.7
B17	54.5	0.3	17.4	3.2	0.1	4.2	1.9	2.0	1.0	0.1	14.6	99.6
B18	53.6	0.2	16.7	3.1	0.0	4.2	1.7	1.2	0.9	0.0	18.1	99.7
B19	54.1	0.2	15.5	3.4	0.0	4.3	2.9	1.2	1.2	0.1	16.7	99.7
B20	60.8	0.1	19.0	3.6	0.0	2.3	1.2	2.0	0.5	0.1	9.9	99.7
B21	54.2	0.2	20.7	2.2	0.0	2.0	1.2	2.0	1.1	0.0	15.8	99.6
B22	62.4	0.2	15.0	1.1	0.0	3.3	1.0	2.3	0.4	0.1	13.9	99.8
B23	58.7	0.2	17.5	1.1	0.0	3.1	1.2	2.5	0.5	0.1	14.8	99.7
B24	53.2	0.2	21.2	2.0	0.0	2.1	1.3	2.0	1.0	0.0	16.6	99.6
B25	55.0	0.5	18.1	5.8	0.0	2.3	1.2	0.3	1.7	0.1	14.8	99.7
B26	62.3	0.1	14.0	1.1	0.0	3.0	1.7	0.8	0.7	0.0	15.9	99.8
B27	59.2	0.2	19.2	3.7	0.0	2.3	1.3	2.3	0.5	0.1	10.7	99.7
B28	58.8	0.2	13.5	2.1	0.0	3.1	2.7	0.1	0.5	0.1	18.4	99.6
B29	49.8	1.2	21.0	5.4	0.0	1.9	1.1	0.0	0.1	0.0	19.3	99.7
B30	58.9	0.9	17.9	6.3	0.0	2.0	0.3	1.1	3.0	0.1	9.0	99.7
B31	59.7	0.7	13.7	4.7	0.0	3.2	1.8	2.0	0.7	0.2	13.1	99.7
B32	52.1	0.4	12.8	8.4	0.0	2.7	1.9	0.4	0.5	0.1	20.1	99.5
B33	58.6	0.1	19.5	3.6	0.0	2.4	1.2	2.1	0.5	0.0	11.4	99.7
B34	57.9	0.6	15.5	7.2	0.0	2.4	1.6	0.2	0.6	0.1	13.4	99.7
B35	59.8	1.1	16.7	5.9	0.0	2.1	1.1	0.0	3.9	0.0	8.9	99.7
B36	61.7	0.8	17.5	8.1	0.1	1.6	1.3	0.4	1.4	0.1	6.7	99.7
B37	63.3	0.1	20.1	2.4	0.1	3.4	1.9	0.5	0.8	0.0	7.0	99.6
B38	54.6	0.7	16.0	3.1	0.1	2.5	5.8	1.0	0.9	0.1	14.7	99.7
B39	69.1	0.2	15.6	1.9	0.0	0.6	1.3	0.0	0.2	0.0	10.9	99.8
B40	51.7	0.4	20.2	7.6	0.0	3.0	0.1	0.0	0.1	0.0	16.6	99.7

- SiO_2: quartz/cristob
- Al/Mg/Fe: variable smectite composition and minor components as kaolinite, goethite
- Ca/Na/K: variable interlayer composition and minor components as feldspar/illite

Kaufhold, S., Dohrmann, R. (2008) Detachment of colloidal particles from bentonites in water. - Applied Clay Science, 39, p. 50–59..

Characterisation – LECO analysis (C, S)

	organic C [mass%]	inorganic C [mass%]	total C [mass%]	total S [mass%]
B1	0.0	0.1	0.2	0.0
B2	0.0	0.0	0.1	0.0
B3	0.0	0.0	0.0	0.0
B4	0.0	0.0	0.0	0.1
B5	0.0	0.6	0.6	0.7
B6	0.0	0.0	0.0	0.0
B7	0.0	0.2	0.2	0.1
B8	0.0	0.2	0.2	0.1
B9	0.1	0.3	0.3	0.2
B10	0.1	0.1	0.1	0.0
B11	0.0	0.1	0.1	0.0
B12	0.0	0.1	0.1	0.1
B13	0.1	0.5	0.5	0.0
B14	0.1	0.1	0.2	0.0
B15	0.1	0.4	0.4	0.0
B16	0.1	0.0	0.1	0.1
B17	0.1	0.3	0.4	0.1
B18	0.1	0.1	0.2	0.0
B19	0.0	0.3	0.4	0.0
B20	0.1	0.2	0.3	0.3
B21	0.0	0.0	0.0	0.0
B22	0.0	0.0	0.0	0.0
B23	0.0	0.0	0.0	0.0
B24	0.0	0.0	0.1	0.1
B25	0.1	0.0	0.1	0.0
B26	0.1	0.1	0.2	0.0
B27	0.8	0.1	0.9	0.2
B28	0.1	0.0	0.1	0.0
B29	0.1	0.0	0.1	0.0
B30	0.4	0.1	0.5	0.1
B31	0.0	0.2	0.2	0.0
B32	0.1	0.0	0.1	0.0
B33	0.1	0.1	0.1	0.0
B34	0.1	0.0	0.1	0.0
B35	0.0	0.0	0.0	0.0
B36	0.1	0.0	0.1	0.0
B37	0.2	0.1	0.3	0.2
B38	0.3	1.0	1.3	0.0
B39	0.0	0.0	0.0	0.0
B40	0.0	0.0	0.0	0.0

- C_{org} is commonly low (0.1 or lower, largest content in VolclaySPV (Wyo-product)
- Approximately half of the bentonites are free of C_{inorg} (below 0.0 mass%)
- Approximately 70% of the bentonites are free of S (below 0.0 mass%)

Kaufhold, S., Dohrmann, R. (2008) Detachment of colloidal particles from bentonites in water. - Applied Clay Science, 39, p. 50–59..

Results – variability of the BGR bentonite sample set

Smectite content: 60 – 95 mass% (without ill/smt clays)

LCD: 0.18 – 0.38 eq/FU

CEC: 65 – 110 meq/100 g

% Na: 0 – 100 %

pH: 4 - 10

%tet charge: 10 – 65 %

Fe content: 1 – 16 mass%

Carbonates: 0 – 10 mass% (Cc-eq)

SSA: 7 – 130 m^2/g

Different smectite morphology (sample with fibrous smt)

Different submicron particle size distribution

1 - drying

Kaufhold & Dohrmann (2010): all sampels dried at 90° and 120°C up to 4.5 years !

CEC decreased by ca. 10 %

Process is limited

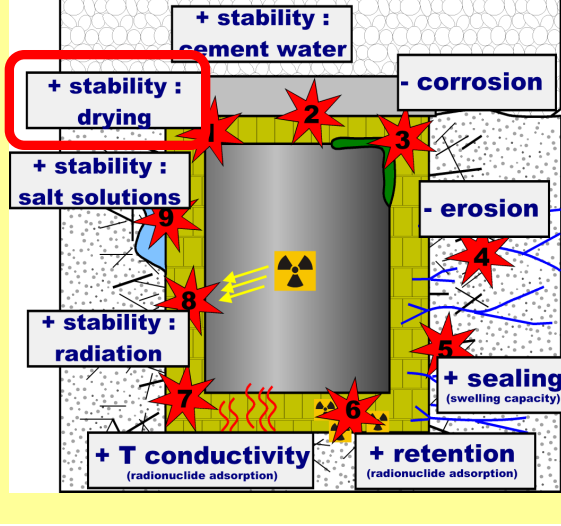

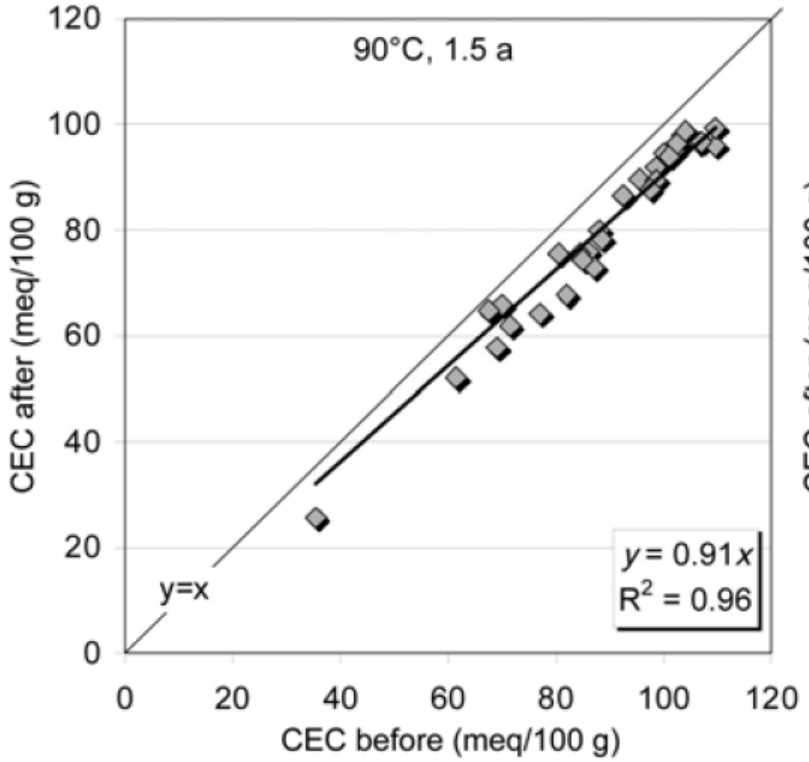

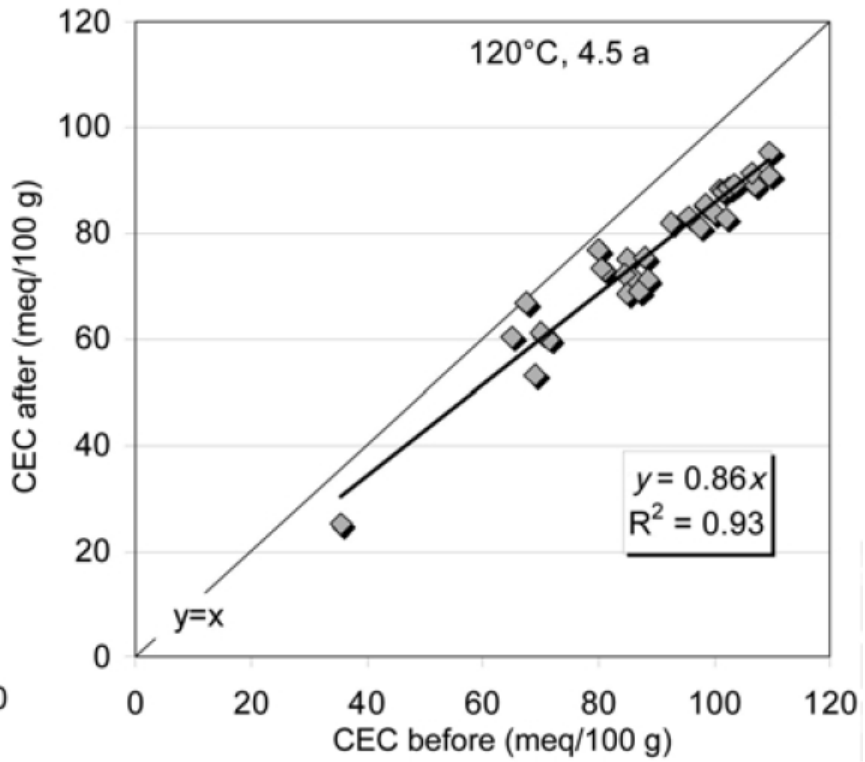

Kaufhold, S., Dohrmann, R. (2010a) Effect of extensive drying on the cation exchange capacity of bentonites. – Clay Minerals, Vol. 45, No. 4, p. 441 – 448.

1 - drying

Ca/Mg decreased from 90° to 120°C

Na did not change to the same extend

90°C (1.5a) -> 120°C (4.5a)

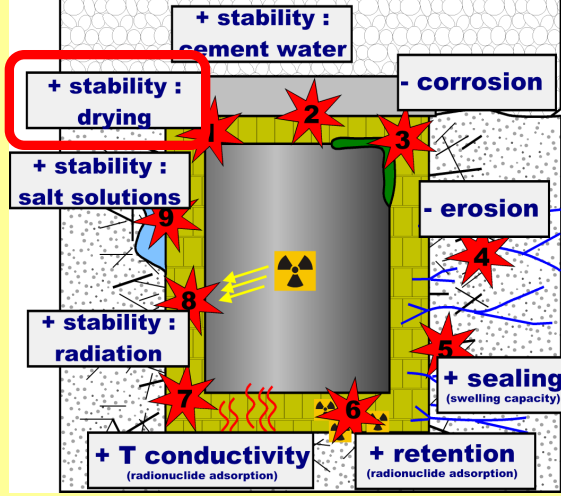

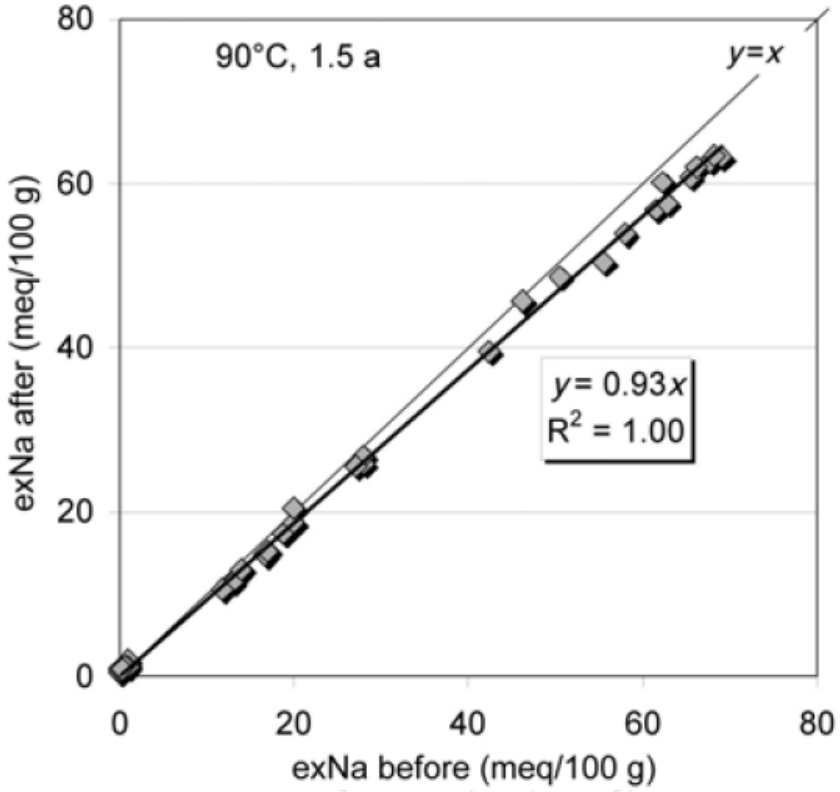

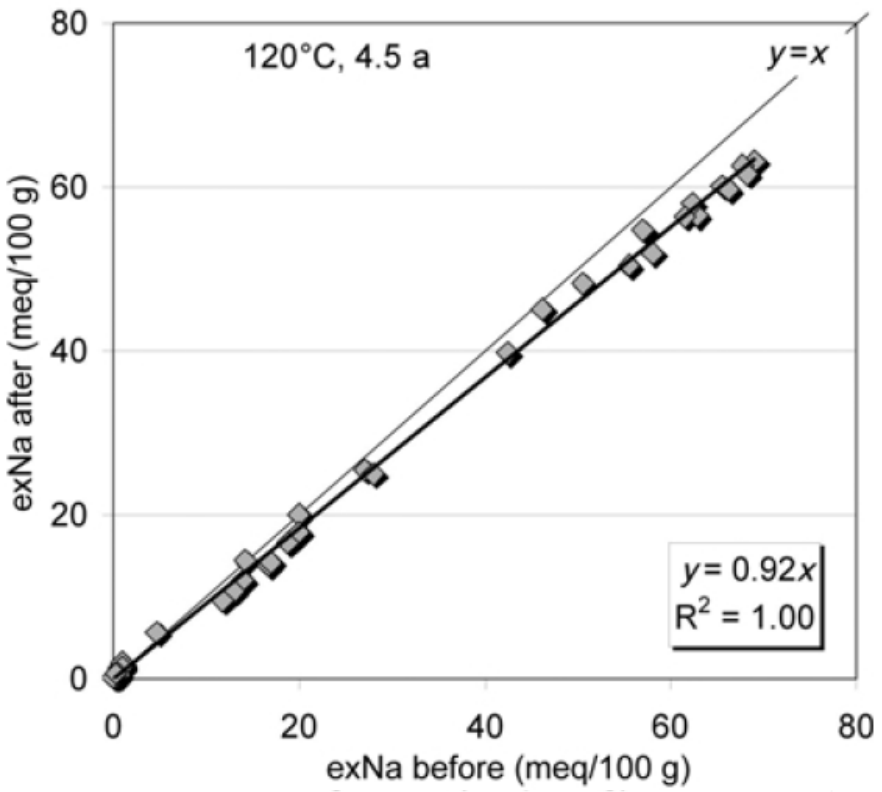

Kaufhold, S., Dohrmann, R. (2010a) Effect of extensive drying on the cation exchange capacity of bentonites. – Clay Minerals, Vol. 45, No. 4, p. 441 – 448.

1 - drying

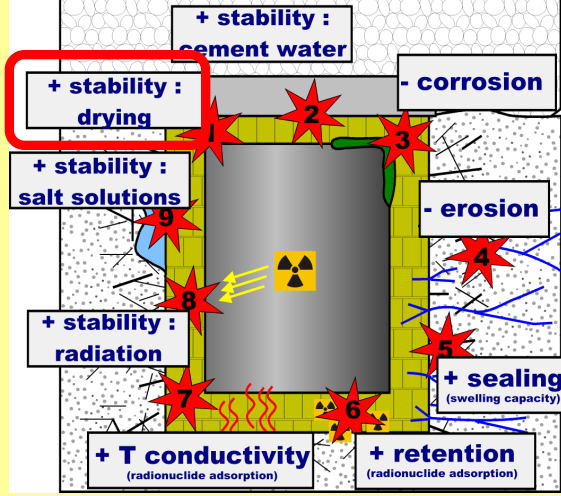

A model for explaining this was developed

Bivalent cations migrate towards sites where they are bound more strongly – possibly opposing charges?

Conclusions: loss of swelling capacity upon drying only is a limited process

Kaufhold, S., Dohrmann, R. (2010a) Effect of extensive drying on the cation exchange capacity of bentonites. – Clay Minerals, Vol. 45, No. 4, p. 441 – 448.

2 – cement

Batch experiments with different conditions (60 – 90°C, with and without excess of $Ca(OH)_2$, diffferent shaking intensity; Kaufhold & Dohrmann, 2011)

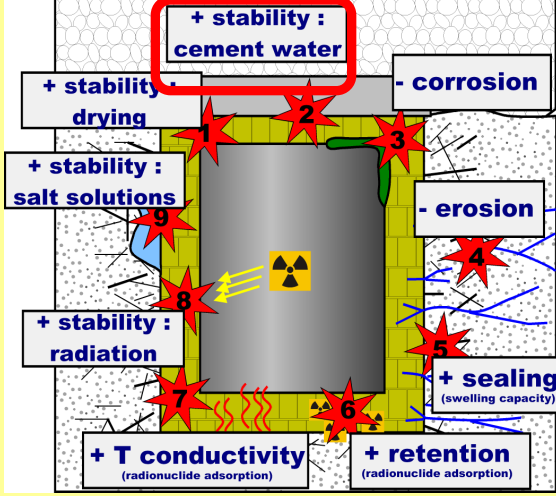

reference	sample	solution	pH	T [°C]	t [months]	type of experiment	Conclusions
Cuevas et al., 2007	Mg-FEBEX	K-, Na-, Ca-OHx	12.5/13.5	60°	6-12	batch	At pH 12.5, 60°C no significant reaction, alteration products at pH 13.5
Bauer et al., 2006	Na-SAz-1	1 M KOH		80°	≈ 6	batch	KOH induces solid state transformation towards illite (high charged smectite)
Turrero et al., 2007	FEBEX	mixed	13.5	100°	6-12	column, incl. cement block	formation of cement minerals (portlandite, CSH,..) at cement block contact
Cuisinier et al., 2008	COX	portland cement sol.	12.4	60°	6-12	column	microstructure is affected (macroporosity increased)
Kamland et al., 2007	MX80	NaOH/ $Ca(OH)_2$	12.4-13.8	RT?	1.5	column	pH < 13 has no effect on swelling pressure
Melkior et al., 2004	COX+MX80	mixed	12.5	RT?	1-12	diffusion	alkaline solution increases the diffusion coefficients
Mosser-Ruck & Cathelineux, 2004	Wyom. + Texas	K-, Na-, Ca-OH_x/CO_3	12-12	150°	2	batch	smectite alteration and precipitation of secondary minerals in case of KOH/CO_3
Claret et al., 2002	COX	SYF	13.2	60°	12	batch	smectite is altered (towards mixed layer minerals) and organic matter might preserve some smectites
Pusch et al., 2003	Friedland	extracted cement water	8-9.4	RT?	5	batch	hydraulic concuctivity slightly increased
Ramirez et al. 2002	Almeria Bentonite	K-, Na-, Ca-OH_x	10-13.5	-90°C	12	batch	the bentonite is stable up to pH 12.6
Savage et al., 1992	different silicates	K-, Na-, Ca-OH_x	13	70°	3	batch	silicates dissolve and secondary phases precipitate
SYF = simple young fluid, NAGRA, 1995							

Clear: smectites dissolve congruently at high pH > 13

2 – cement

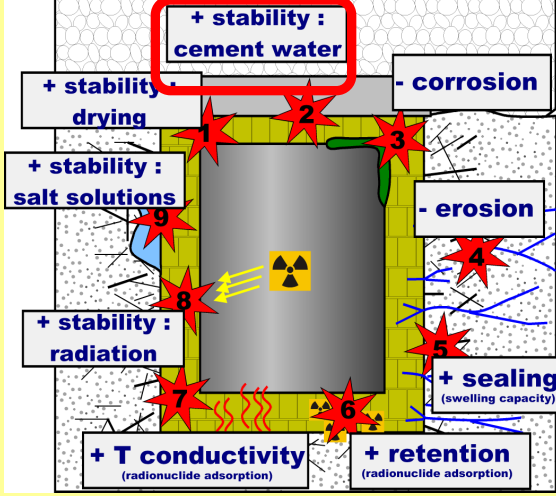

Rather different elemental concentrations were obtained which indicates different dissolution/precipitation processes

Excess $Ca(OH)_2$ led to carbonate precipitation, a saturated $Ca(OH)_2$ solution was effectivley buffered by bentonite

Smectite dissolution at large pH is supposed to be congruent, Si concentration affected by SiO_2 phases, solubility difficult to determine because of precipitation of .. (zeolites…)

For HLRW repositories low pH cements are recommended

Kaufhold, S., Dohrmann, R. (2011) Stability of bentonites in salt solutions III Ca-hydroxide solutions. – Applied Clay Science 51, 300–307.

3 – corrosion

Aerobic corrosion is limited (even in lab)

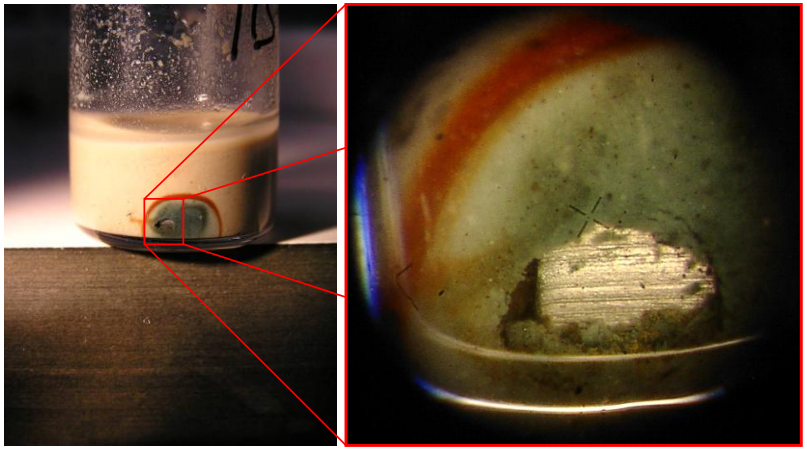

Corrosion proceeds anaerobically

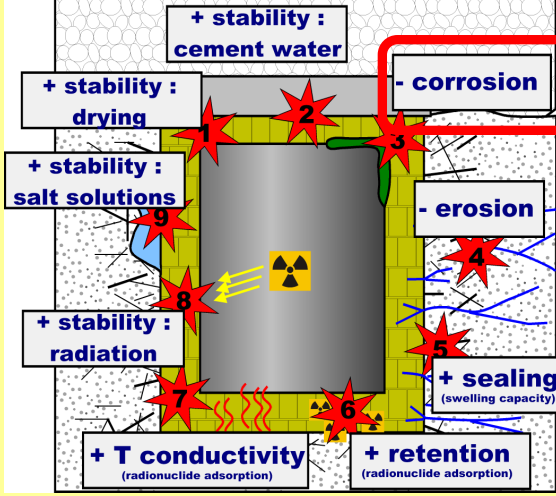

Corrosion products are 1:1 or 2:1:1 Fe-clay minerals

	experiment	T / t	observation	Model 1	Model 2	Model 3
Guillaume et al., (2003)	Fe powder / plate in MX80 + water	300°C / 9 months	formation of new Fe/Mg-layer silicates (chlorite, saponite), zeolites, quartz	dissolution - precipitation + solid state reaction		
Lantenois et al., (2005)	Fe powder with suspensions of different smectites	80°C / 1.5 - 4 months	formation of new phases depends on di/trioctahedral smectite, exchangeable cations, pH	corrosion of metal Fe results from its interaction with protons liberated from the clay surface = Fe^{2+} forms	Fe^{2+} migrates into interlayer and from there into octahedral layer	the new octahedral sheet and old tetrahedral sheet do not fit together anymore = separation
Wilson et al. (2006b)	Fe powder with Kunipia F suspension	80 - 250°C / 3 months	formation of magnetite and analcime, smectite alteration (amongst others)	TEM indicates: loss of tetrahedral sheet = isolated 7 A layers	the 7 A units are supposed to be the precursor of berthierine and/or chlorite	
Perronnet et al. (2007)	Fe powder with suspensions of different smectites	80°C / 3 months	different reaction products, CEC de- and increase	reduction of structural Fe = increase of LCD = uptake of protons = increase of pH	alkalinity causes smectite destabilization = formation of Si-Al-Fe gels	Fe^{2+} from corrosion migrates into gel = formation of 7 or 14 A non swellable clay minerals
Carlson et al. (2007)	carbon steel wires embedded in compacted MX80	50°C / appr. 2 years	reduction of structural Fe but no secondary phases observed			

Corrosion rate = f(bentonite) is currently investigated at BGR

4 – erosion

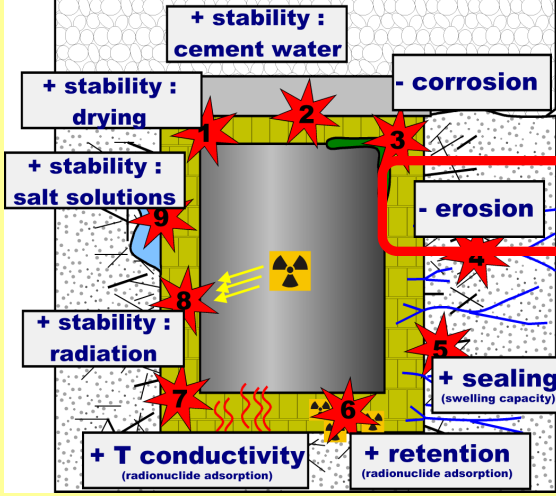

Detachment of colloidal particles mainly depends on exchangeable Na^+

Detached colloids (which “survived” 46,000 g centrifugation) were mainly smectite

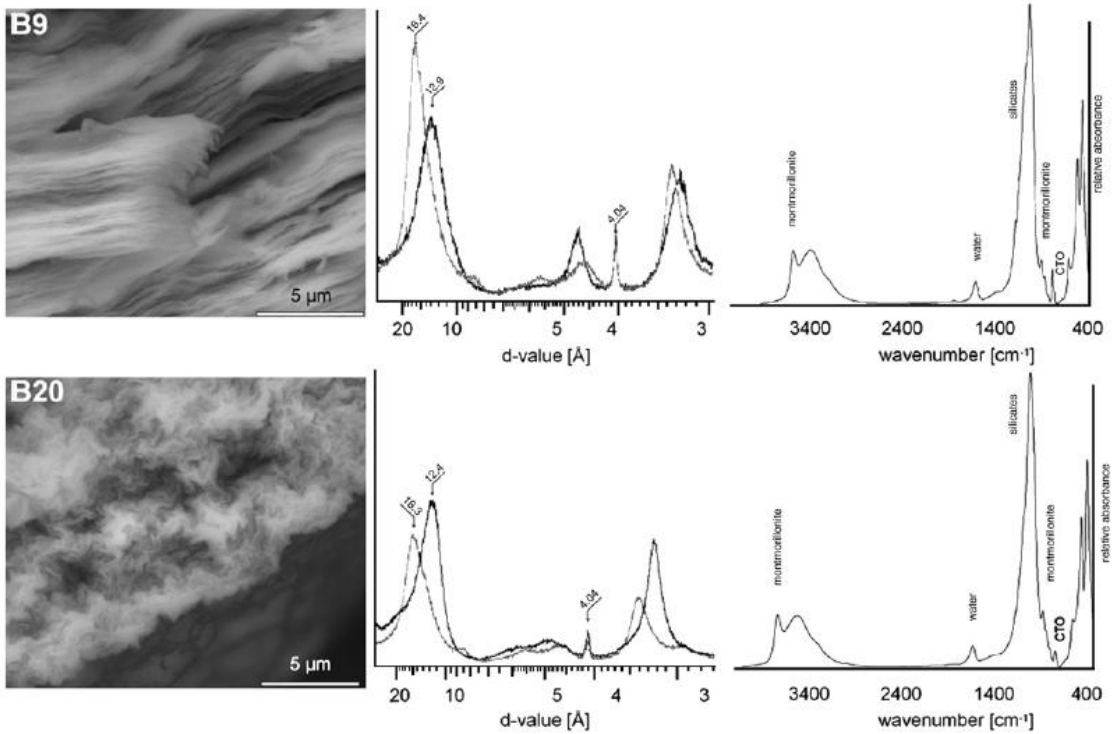

pH may also play a role but Na^+ and pH are systematically related

Kaufhold, S., Dohrmann, R. (2008) Detachment of colloidal particles from bentonites in water. - Applied Clay Science, 39, p. 50–59.

Sealing depends on swelling pressure,

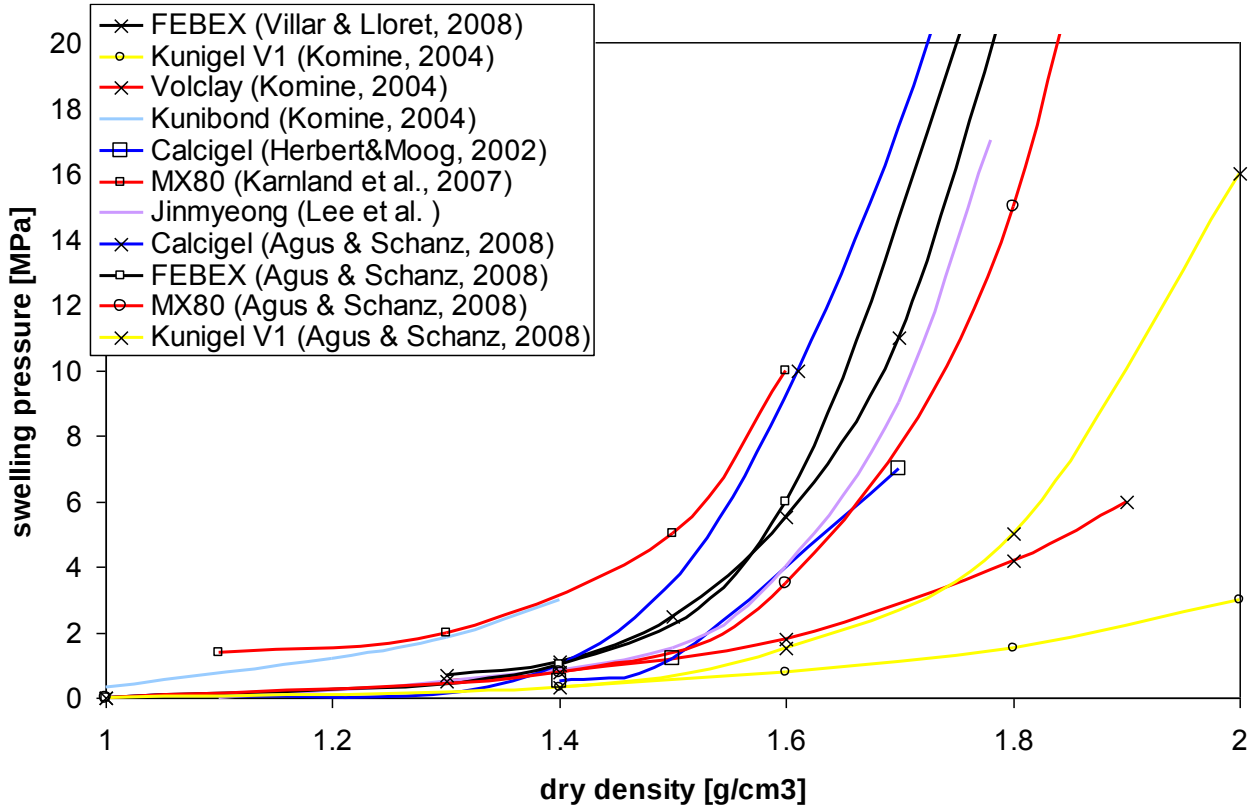

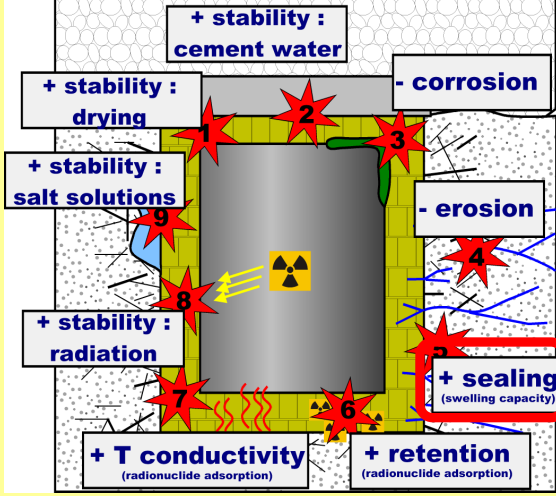

Swelling pressure depends on dry density

What determines the variability? Ex. cation, microstructure?

Currently investigated at BGR

6 retention

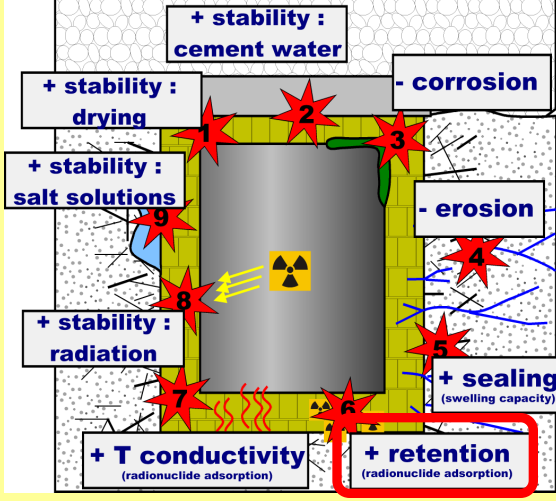

Radionuclide retention depends on adsorption sites

Possible adsorption sites are interlayer or edge surface

Yet, retention capacity of different bentonites is supposed to be similar, despite possible slight differences of selectivities

However, bentonites can be modified with respect to the retention of certain radionuclides (e.g. ^{129}I, Kaufhold et al., 2007)

Kaufhold, S., Pohlmann-Lortz, M., Dohrmann, R., Nüesch, R. (2007) About the possible upgrade of bentonite with respect to iodide retention capacity. - Applied Clay Science, 35, 39–46

7 T conductivity

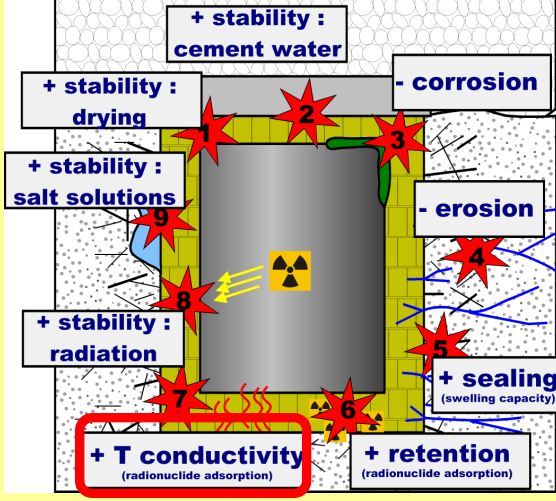

T conductivity depends on

- Quartz+illite / smectite ratio
- Water content
- porosity (compaction)
- microstructure

Details still have to be investigated

8 radiation stability

Radiation may cause structural degradation

but

Few studies were conducted:

- Rather large dosis required for serious structural damage (e.g. Allard et al., 2012)
- Structural Fe particularly sensitive towards radiation

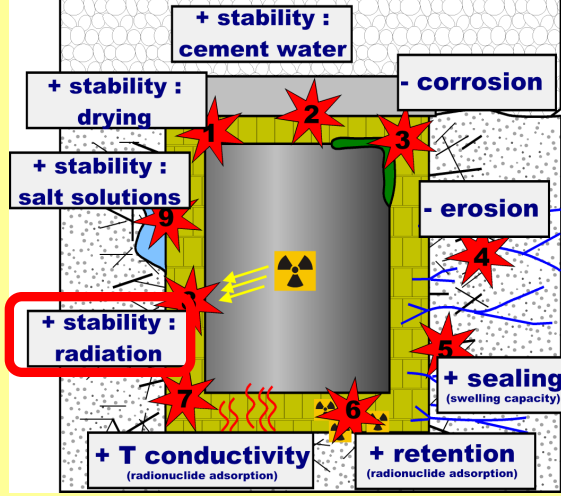

Allard, Balan, Calas, Fourdrin, Morichon, Sorieul (2012) Radiation induced defects in clay minerals: a review. - Nuclear Instruments and Methods in Physics Research Section B: Beam Interactions with Materials and Atoms, Volume 277, 15 April 2012, Pages 112–120

9 salt stabilty - NaCl

Two different batch tests 3 and 5 months

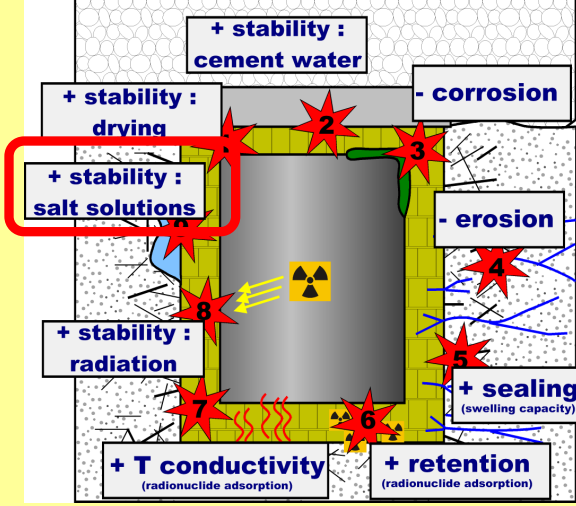

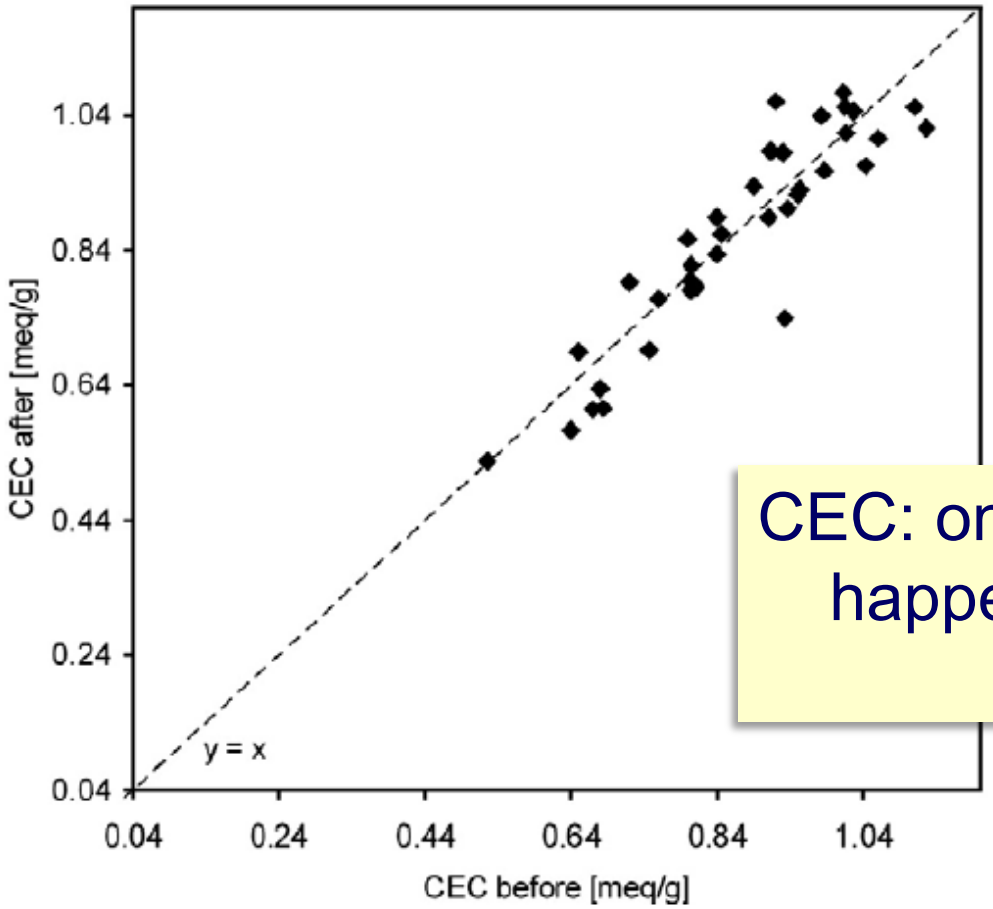

CEC: on average nothing happened

Fig. 5. Comparison of the CEC of all bentonites before and after 5 months reaction with NaCl solution.

9 salt stabilty - KCl

again cation exchange + carbonate exchange buffer observed

BUT !!

1) More silica was dissolved
2) The CEC slightly decreased
3) The amount of soluble silica (Na_2CO_3 extractable) increased
4) Water uptake capacity significantly decreased

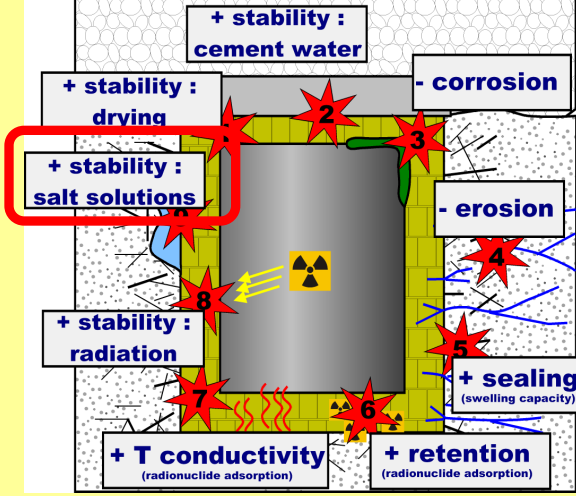

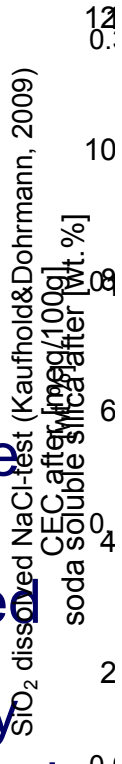

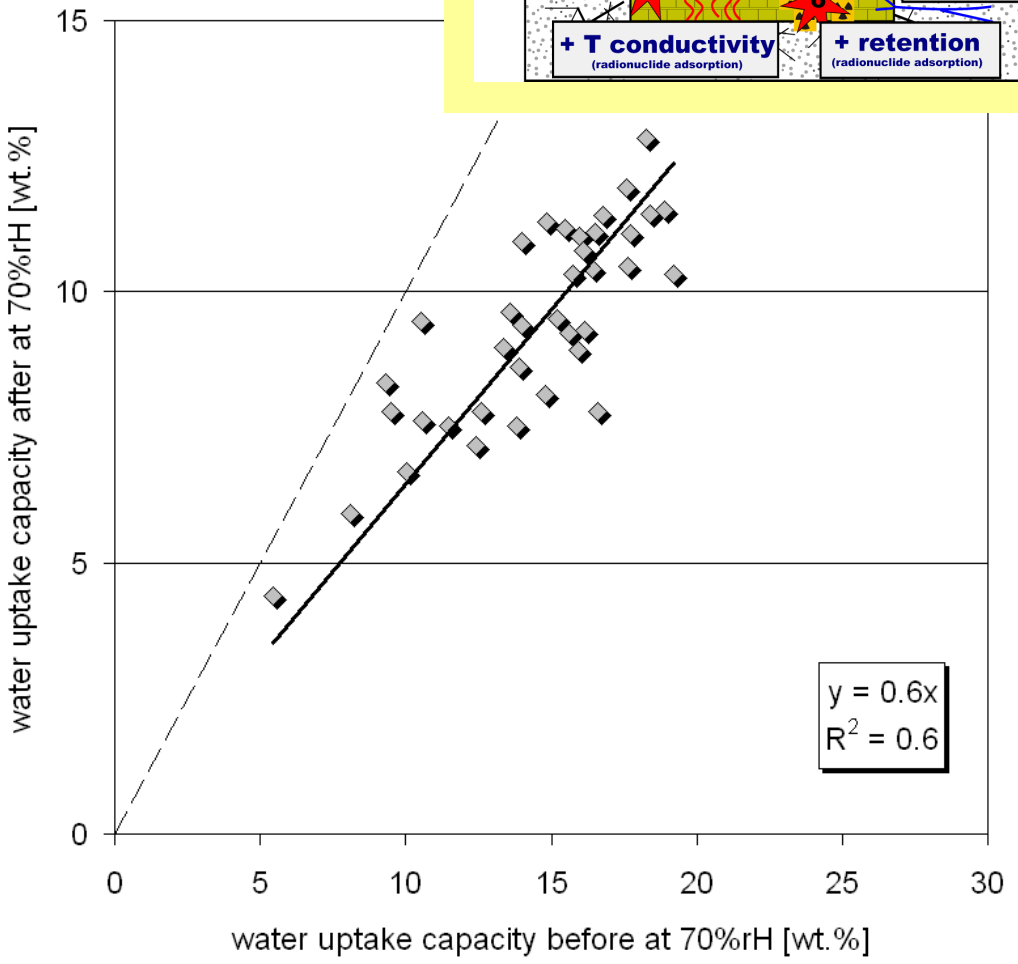

Kaufhold, S., Dohrmann, R. (2010) Stability of bentonites in salt solutions II. Potassium chloride solution — Initial step of illitization? – Applied Clay Science, 49, 98 – 107.

9 salt stabilty - KCl

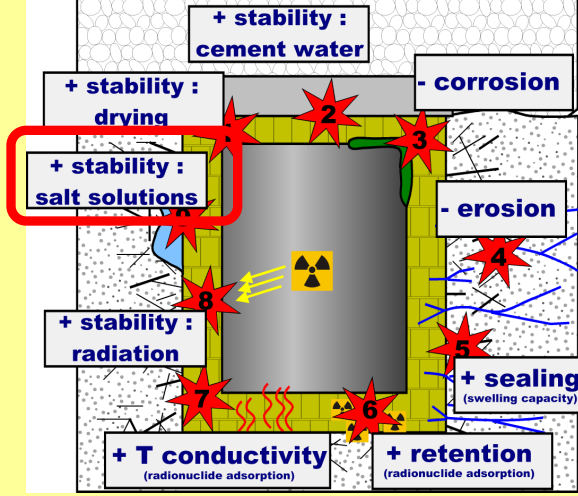

Products were characterized:

Real Illitization (appr. 5 %)
soda soluble silica increase

Non-swelling smectite (45 %)
loss of water/EG-swelling capacity (may be reversible)
– 50% of which with fixed K (no exchange in CEC tests)

Swellable K smectite (50 %)
normal smectites with exchangeable K

stability tests - conclusions

In the stability tests some bentonites lost more of their swelling capacity and some less (in % of cause, to eliminate the effect of different CECs)

!! Interestingly, in all stability tests the bentonites showed the same trend: Some lost more % of their CEC (in all tests) and some less (were more stable in all tests)

The reason could not be found in the basic parameter set (Fe-content, LCD, BET, %Na,..)

The reason may be the different solubilities..

However, determination of the smectite solubility is not trivial, this will be investigated in an upcoming project together with GRS and TUM

Overall conclusions

Process is limited, bentonites different

All bentonites dissolve at high pH => low pH cement

Under construction

Cation exchange fast, K induces illitization, some bentonites are more reactive than others – maybe solubility?

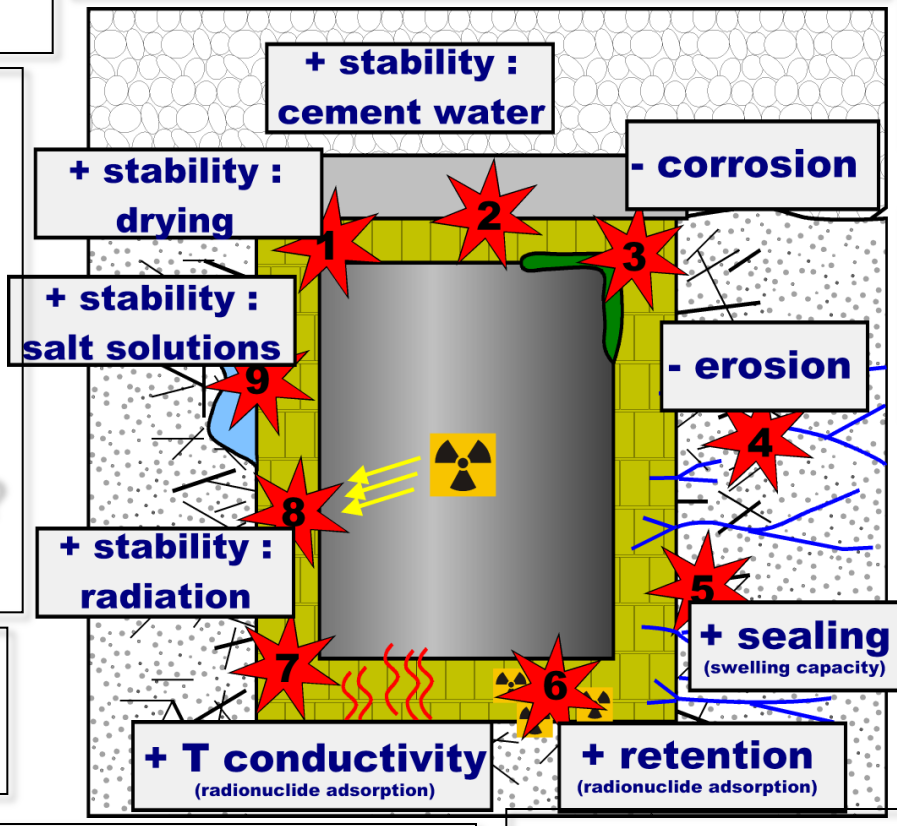

Na bentonites less suitable

Under construction

Fe rich are less stable

Quartz + illite content increases T-cond.

Normal bentonites are similar, bentonites can be upgrades, e.g. for I^{129} retention..

Overall conclusions

Results obtained, yet, already help to identify suitable or less suitable HLRW bentonites

However, for a final recommendation all parameters have to be considered

For 2 + 9: Batch experiments

Batch tests at 60°C, 3 – 5 months

4 g bentonite with 40 mL solution -> centrifuge -> dialysis

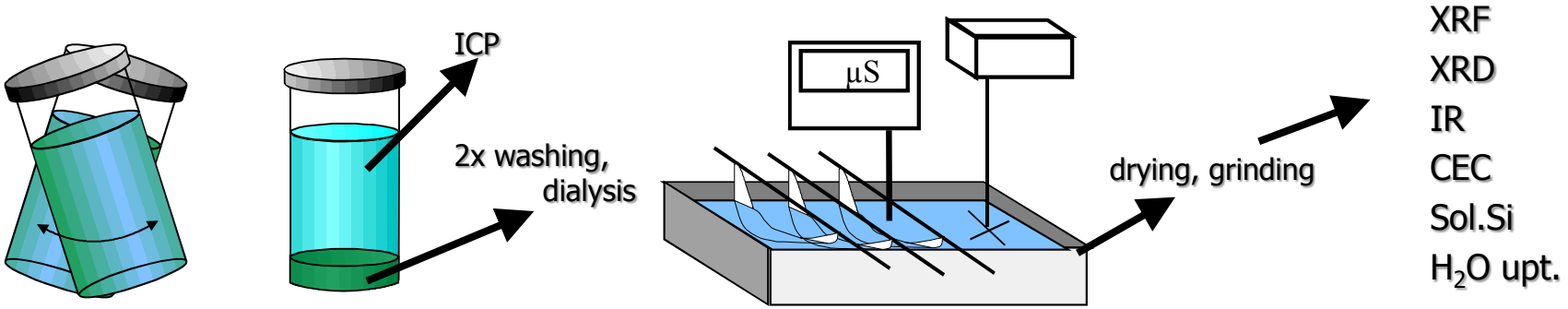

Analysis of solid products by: XRD (AD, EG, oriented), XRF, IR, DTA, CEC, soluble silica, water uptake capacity

!! Important to use different methods before interpretation !!
(particularly XRD alone is insufficient – because of effect of texture, layer per stack – which can change upon dispersion)

Experimental conditions

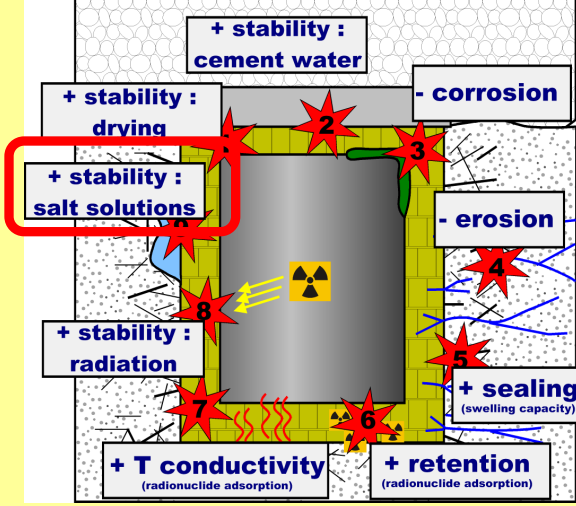

NaCl

(4 g, 40 mL 6 M NaCl, 60°C shaking, 3, 5 months)

KCl

(4 g, 40 mL 1 M KCl, 60°C shaking, 5 months)

9 salt stabilty - NaCl

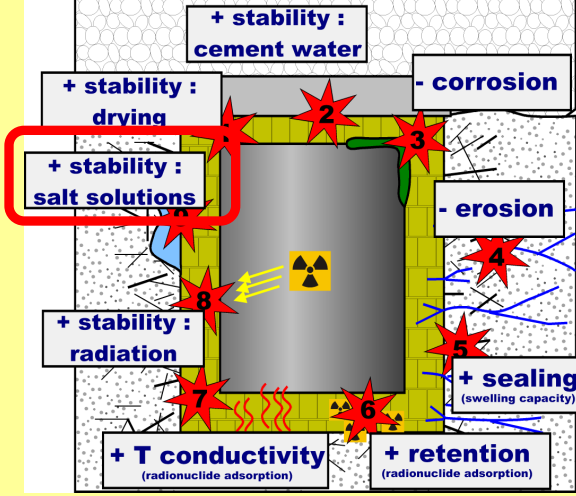

Carbonates buffered the cation exchange. Some Wyoming bentonites even took up Ca^{2+} from the NaCl solution because of Ca-carbonate and gypsum dissolution

No specific irreversible reactions of bentonite with NaCl solutions were found

However, Na^{+} exchange facilitates colloid detachment which indirectly affects bentonite stability

Kaufhold, S., Dohrmann, R. (2009) Stability of bentonites in salt solutions I sodium chloride. – Applied Clay Science, 45, 3, p. 171 – 177.

Kaufhold, S., Dohrmann, R. (2008) Detachment of colloidal particles from bentonites in water. - Applied Clay Science, 39, p. 50–59.

Long-Term Performance of Engineered Barrier Systems:

The EC Project PEBS

2nd Chinese-German Workshop on Radioactive Waste Disposal
Karlsruhe, October 15-16, 2012

PEBS Long-term Performance of Engineered Barrier Systems

Fig. 1

PEBS Overall Objective and Approach

Objective: Evaluate the sealing and barrier performance of the EBS with time, through development of a **comprehensive approach**, involving experiments, model development, and consideration of the potential impact on safety functions.

- **Experiments** cover the full range of conditions
  - from initial emplacement of wastes (high heat generation and EBS re-saturation)
  - to later stage establishment of near steady-state conditions, i.e. full re-saturation and thermal equilibrium with the host rock
- Results will be **integrated** in a way to connect the initial transient state of the EBS and its long-term state in a more convincing way
- **Models** are developed and improved to provide a more complete description of the THM and THMC behaviour of the EBS system
- The projects aims at providing a more quantitative basis for **relating the evolutionary behaviour to the safety functions** of the system and at further clarifying the significance of residual uncertainties for long-term performance assessment

Fig. 2

Project Partners and Duration

PEBS is an EC co-funded project of

- **BGR, GRS** (Germany)
- **NAGRA, Solexperts, TK Consult** (Switzerland)
- **ENRESA, AITEMIN, CIMNE, UDC, CIEMAT, Golder, UAM** (Spain)
- **SKB, Clay Technology** (Sweden)
- **ANDRA** (France)
- **BRIUG** (China)
- **JAEA** (Japan)

PEBS started on March 1, 2010 and runs for 48 months.

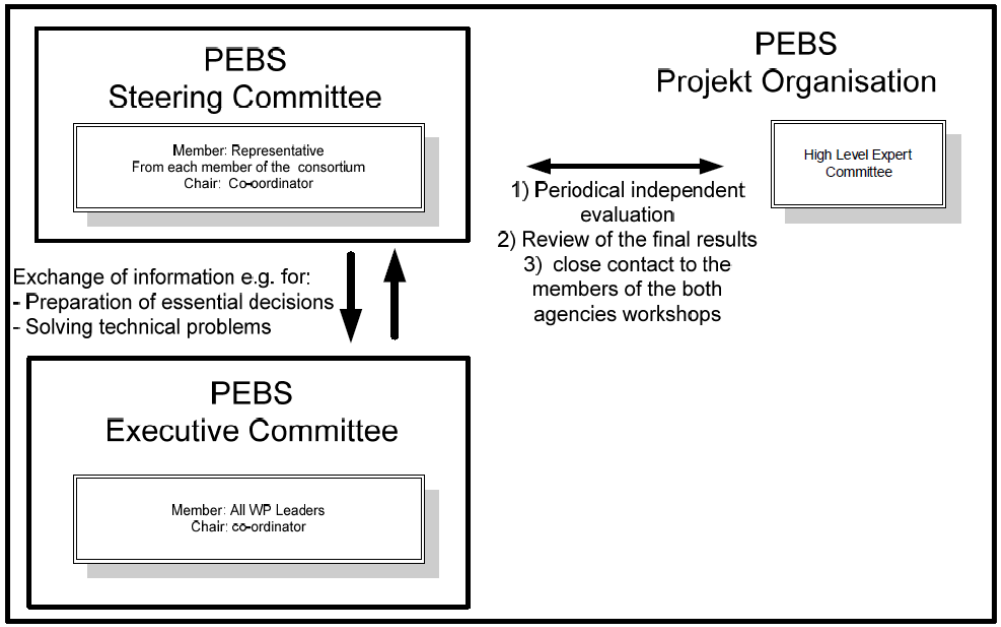

Fig. 3

Work Programme

- WP1: **Analysis of system evolution** during early post closure period: Impact on long-term safety functions
  (WP lead: SKB)
- WP2: **Experimentation** on key EBS processes and parameters
  (WP lead: ENRESA)
- WP3: **Modeling** of short-term effects and extrapolation to long-term evolution
  (WP lead: GRS)
- WP4: Analysis of **impact on long-term safety** and guidance for repository design and construction
  (WP lead: NAGRA)
- WP B: **Chinese mock-up experiment** on compacted bentonite buffer
  (WP lead: BRIUG)
- WP5+6: Dissemination and project management
  (WP lead and project coordinator: BGR)

Experiments Covering Different Stages in Repository Evolution

Early resaturation time 10 years | Resaturation period 50 years | Pressure recovery period 200 years | Long-term evolution

Thermal evolution

High T°

Time after repository closure

Low T°

Buffer resaturation and swelling

Low S

High S

Ongoing chemical effects (corrosion)

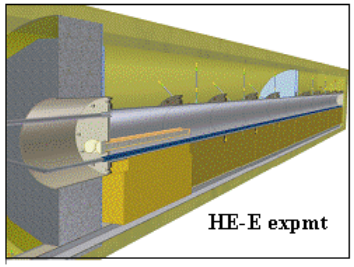

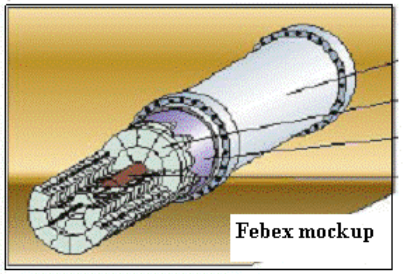

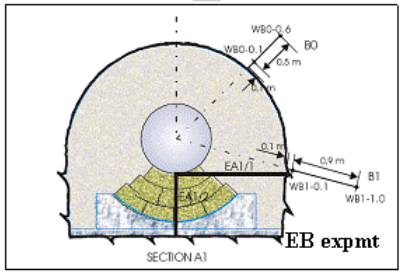

Modeling in Task 3.2 | Task 3.3 | Task 3.1 | Task 3.4

Fig. 5

Immediate Connections Between Tasks

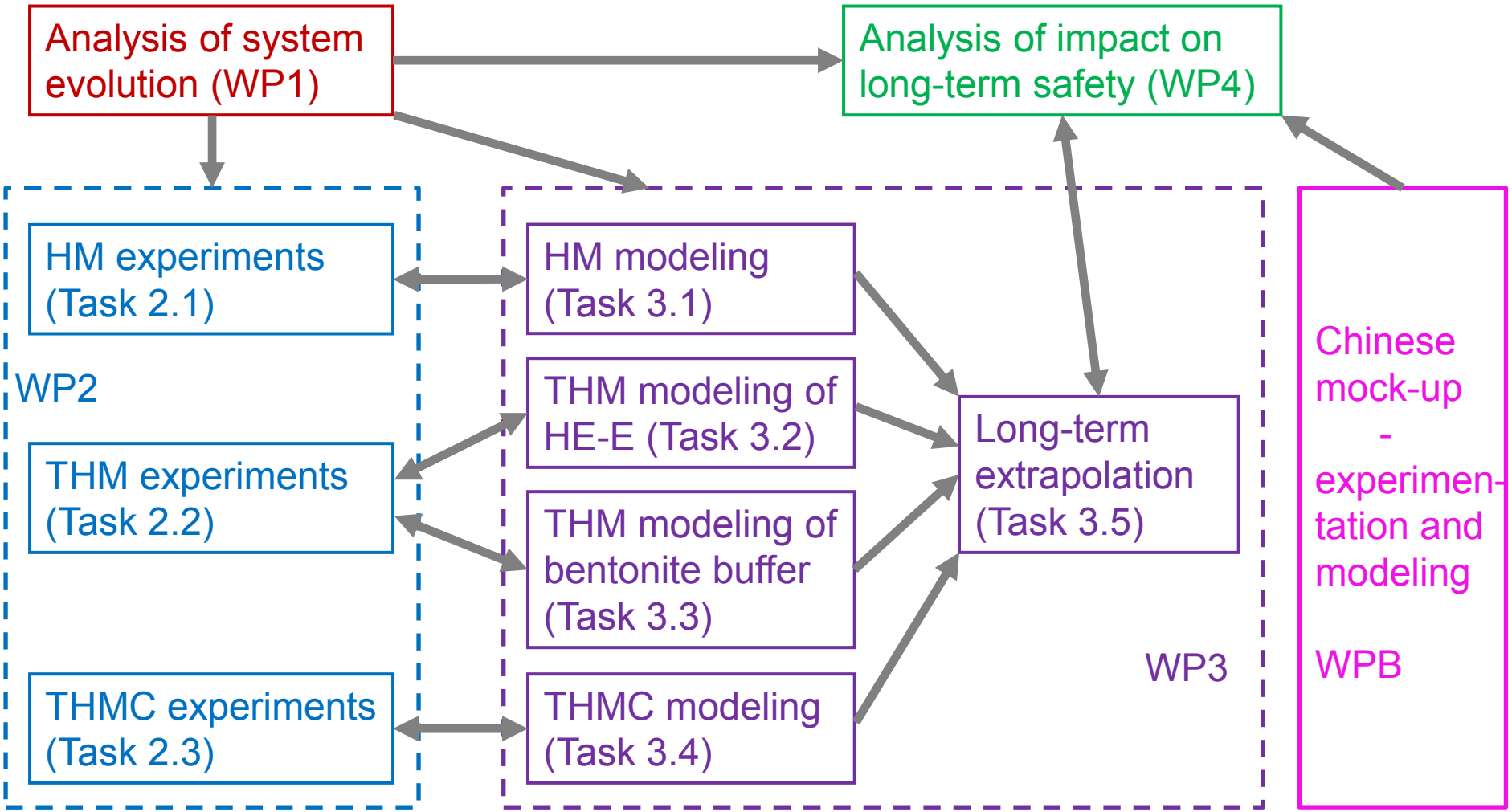

Fig. 6

WP1: Analysis of system evolution during early post closure period

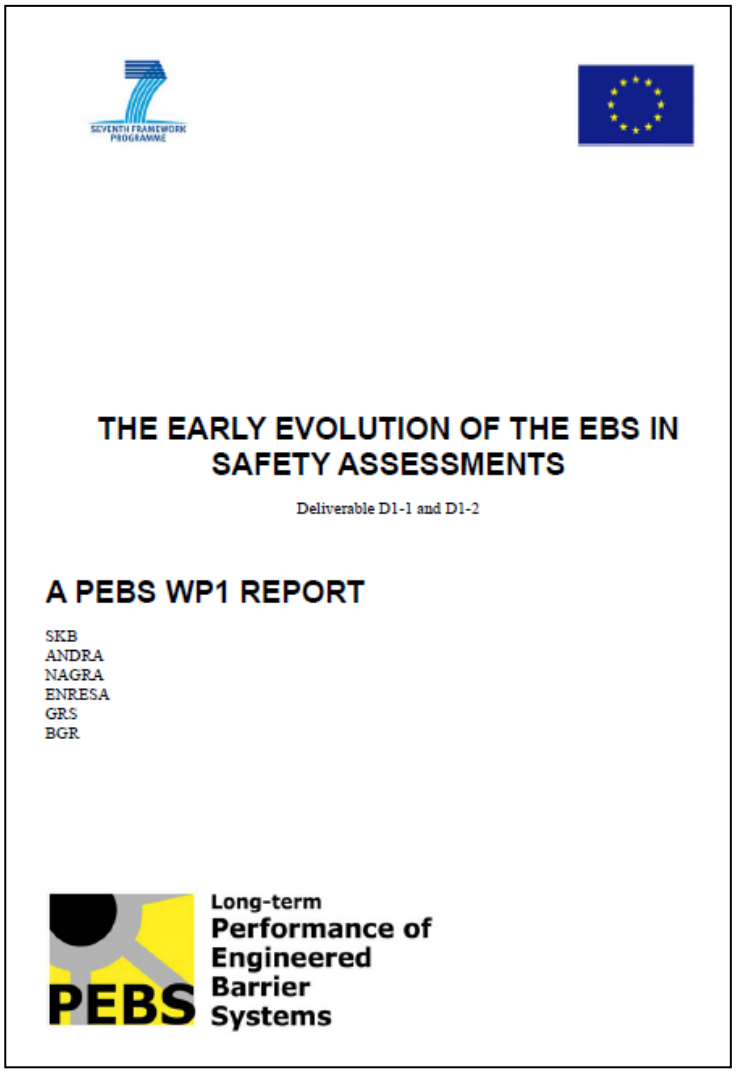

THE EARLY EVOLUTION OF THE EBS IN SAFETY ASSESSMENTS

Deliverable D1-1 and D1-2

A PEBS WP1 REPORT

SKB
ANDRA
NAGRA
ENRESA
GRS
BGR

Long-term Performance of Engineered Barrier Systems

WP1 objectives:

- **Identify important processes** during the early evolution of the EBS
- Discuss how the **short-term transients** will/may **affect the long-term performance** and the safety functions of the repository
- Describe the current treatment of the early evolution of the EBS in long-term safety assessments for spent nuclear fuel/HLW
- Identify the merits and shortcomings of the current treatment
- Discuss the needs for additional studies of these issues and how they can support future assessments – give directions to other WPs
- **Define** “scenarios” (**simulation cases**) related to events in the early evolution of the EBS

Fig. 7

Tasks 2.1/3.1 Dismantling of the Mont Terri EB and related HM modeling

- A controlled **dismantling of the EB bentonite buffer**, for which the artificial hydration process started back in May 2002, after in depth evaluation of the monitoring data to further complete the already gained knowledge on the resaturation and swelling processes is performed. New **lab infiltration tests** provide further data.
- The HM modeling aims at providing a satisfactory scientific representation and a sound basis for **interpretation of the EB hydration phase** and of the dismantling data. New or improved constitutive laws (double structure approach, water density change) are developed and adjusted with the experimental data.

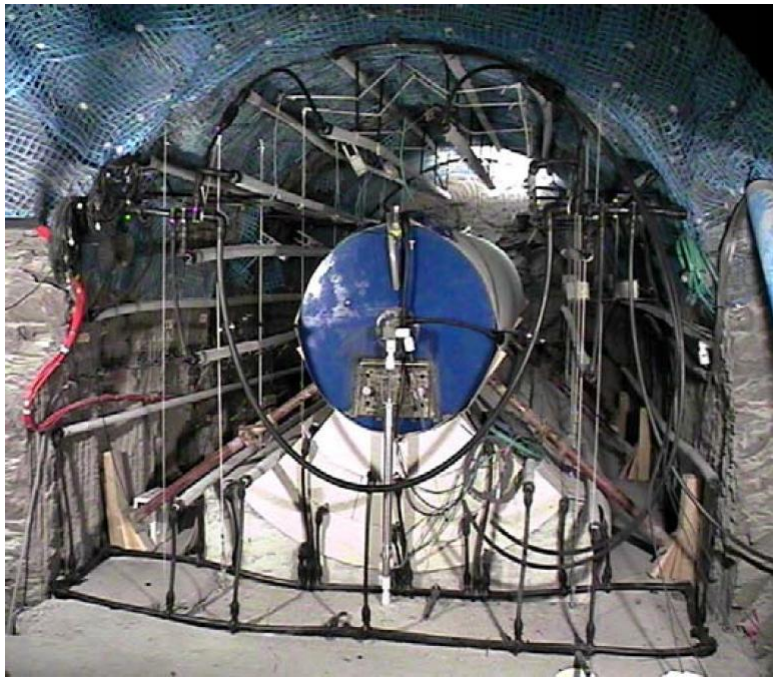

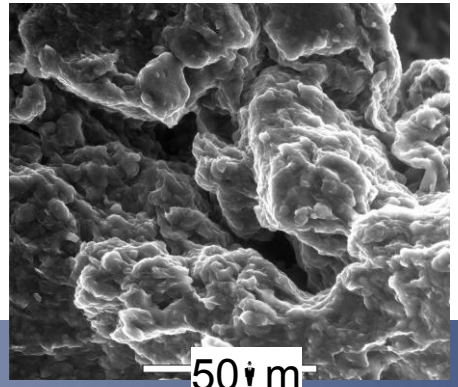

Fig. 8

Tasks 2.2.1/3.3: Lab experiments on key THM processes and THM modeling of buffer

- Experimental tasks comprise the **FEBEX mock-up** and **long-term THM infiltration tests** in cells at CIEMAT with bentonite and sand/bentonite buffer
- Modeling work includes
  - **Evaluation of existing models** for bentonite buffer evolution
  - Incorporation of **new processes** into simulation of long-term lab experiments and development of **enhanced constitutive models**
  - Simulation of long-term lab experiments and **extrapolation to large-scale** in-situ tests

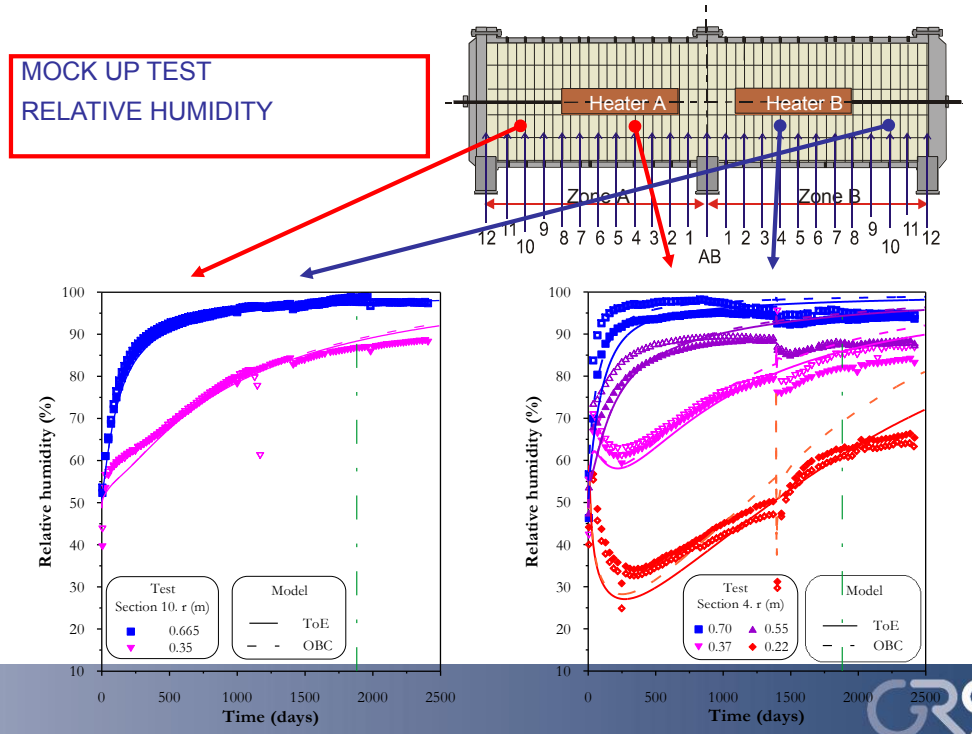

Measured and calculated relative humidity in the FEBEX mock-up taking into account thermo-osmosis

Fig. 9

Tasks 2.2.2/3.2: Mont Terri Heater Experiment HE-E (1)

- **HE-E objective:** Elucidate the early non-isothermal resaturation period and its impact on the THM behaviour
  - provide the experimental data base required for the calibration and validation of existing thermo-hydraulic models of the early resaturation phase
  - upscale thermal conductivity of the partially saturated buffer from laboratory to field scale for pure bentonite and sand-bentonite mixture
- **Characteristics:**
  - 1:2 scale (microtunnel 1.3 m)
  - Natural resaturation from clay host rock
  - Heater surface temperature: 140 C
  - Duration: June 2011 -> 2014
  - Two symmetrical sections - different granular materials

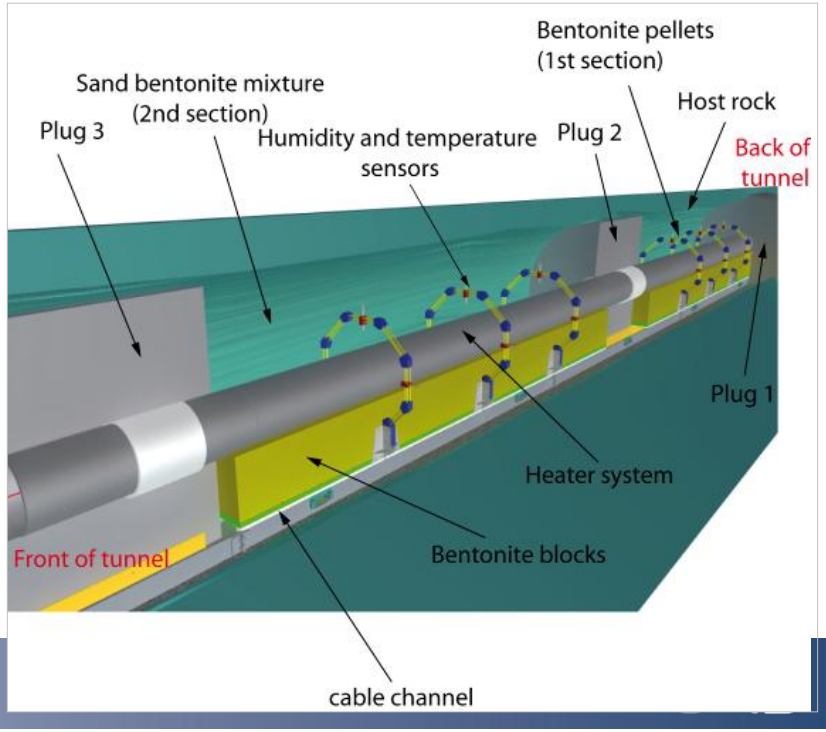

Fig. 10

Tasks 2.2.2/3.2: Mont Terri Heater Experiment HE-E (2)

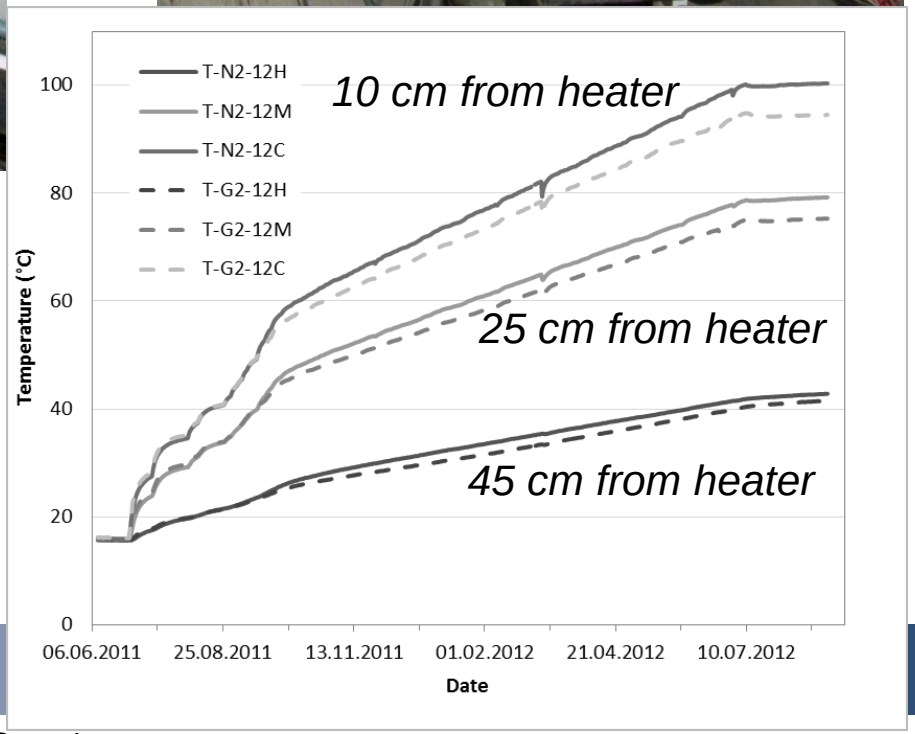

Fig. 11

Tasks 2.2.2/3.2: Mont Terri Heater Experiment HE-E (3)

- **Scoping calculations for the design** of the HE-E to assure that the experiment lay-out meets the requirements regarding temperature evolution and that instrumentation is adequate
- **Interpretative modeling** of the HE-E **by prediction/evaluation cycles** with uncertainty assessment, concentrating on the thermal and thermomechanical behaviour in the early post-closure phase

Design modelling	Calibration/validation	Extrapolation
Purpose: scaling of dimensions, time and processes (scale1:2.5) Requirements: - Use of reference heat output for SF - Use of reference design of SF canisters/tunnel Procedure: - Down scaling to the tunnel size at Mont-Terri - Scaled heat output - Scaled time period for peak T° - System evolution in terms of dimensionless numbers	Purpose: scaling of dimensions, time and processes (scale1:2.5) Procedure: - Blind prediction using the input from the design models - Calibration using the field data of the first 2 years - Refined predictions using the complete dataset - Sensitivity analysis - Evaluation of the results Performance indicators - T° distribution - Saturation - Pore pressure evolution	Purpose: simulation of the PA relevant parameters over a period of 1000 years (early evolution of the SF near field) Procedure: - Simulation of the real scale SF near field using the design model, calibrated model - Inclusion of system understanding from other experimentsl - Sensitivity analysis - Interpretation of the differences between codes/approaches - Conclusions for the PA Performance indicators - T° distribution - Saturation - Pore pressure evolution - Stress/deformation
1- 5 years	1- 5 years	1- 1000 years

Modelled timeframe

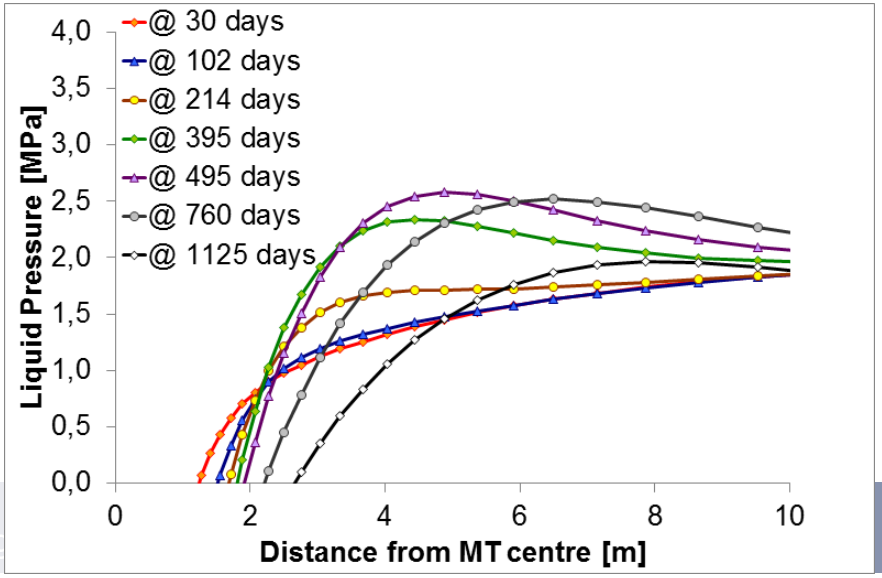

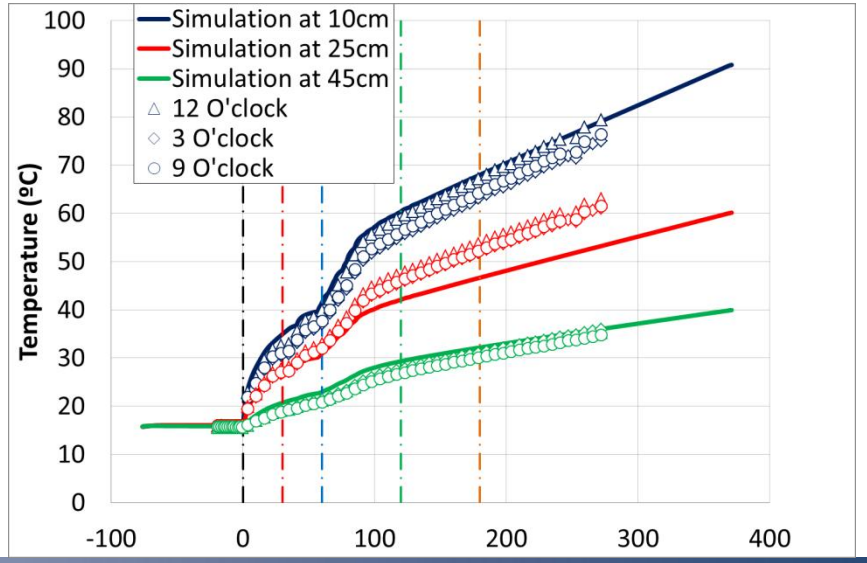

Tasks 2.3/3.4: Experimentation and Modeling of Key THMC Processes

Objectives of THMC experiments

- Investigate corrosion processes, alkaline plumes and interaction of pore water with concrete, bentonite, and C-steel (**GAME tests**: Geochemical Advanced Mock-up Experiments)
- Study processes at the **interfaces** canister/bentonite and concrete/bentonite in dedicated tests

THmC Simulation

- Improve current THC models to account for different types of pores (**dual continua models**), **porosity changes** (m) caused by swelling phenomena, and **reactive gases**: $O_{2(g)}$, $CO_{2(g)}$, $H_{2(g)}$
- **Test THmC model** with previous and ongoing lab and in situ tests

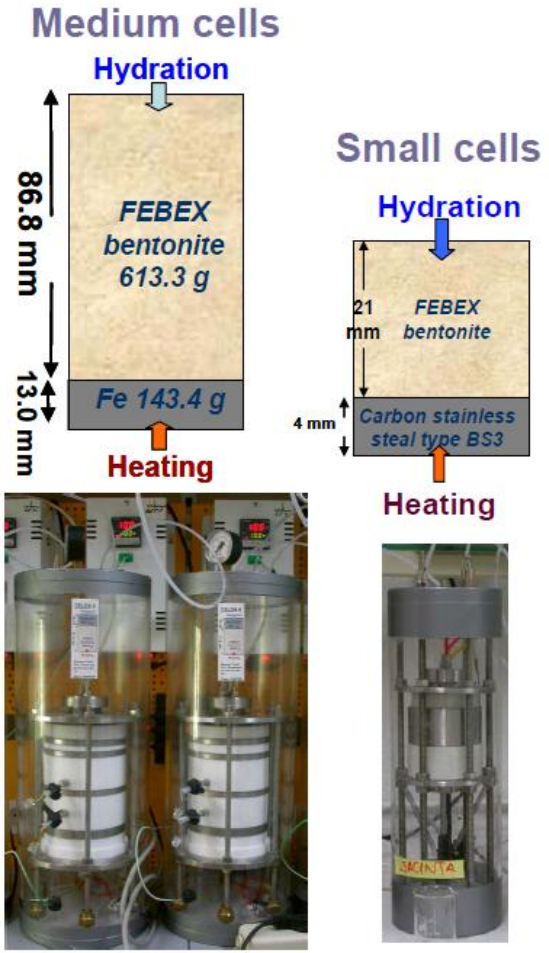

Fig. 13

WPB: The Chinese Mock-up Experiment

Objectives

- To study the property of GMZ Na-bentonite and the bentonite-canister reaction under coupled T-H-M-C conditions
- To simulate vertical placement of a container with radioactive waste
- To monitor the behavior of GMZ Na-bentonite barrier at high temperature and special water
- To provide data for future design for engineered barrier system

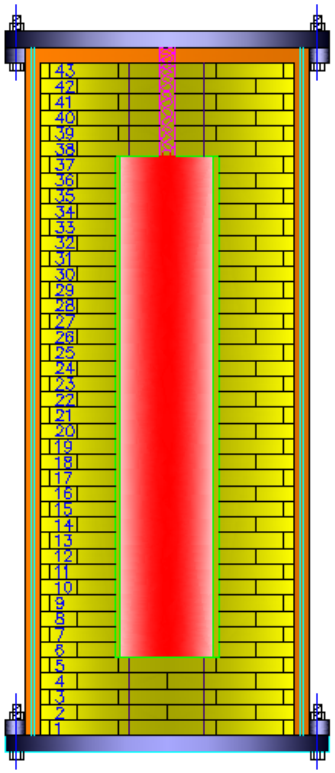

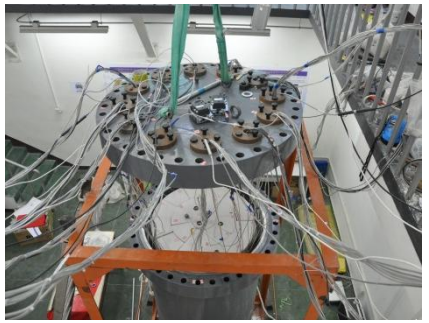

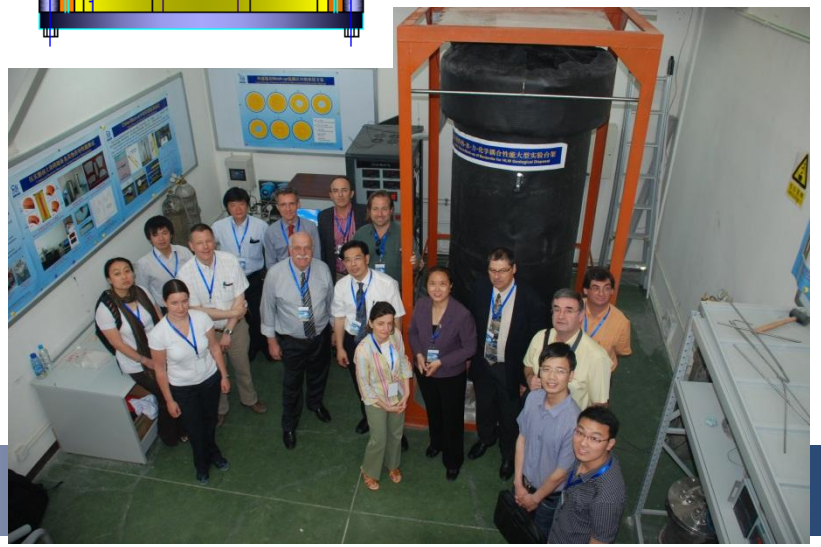

Fig. 14

Task 3.5: Long-Term Extrapolation Objectives

- Assessment of the results of Task 3.1 - 3.4 regarding their implications for different time and space scales
- **Identification of the significant processes** in the resaturation phase & afterwards
- Development or modification of the available **formulations to incorporate phenomena and processes deemed to be relevant** for long-term predictions
- **Performance of coupled numerical analysis** for long-term evolution of the engineered barrier system in the repository
- **Evaluation of the model uncertainty** and its implications for long-term prediction
- Compilation and evaluation of the usefulness of natural analogues for providing support, testing and validation of long-term predictions of current THMC models

Meaning of “long-term”:

- To the end of the resaturation phase (10^2 – 10^3 years)
- To the end of PA-considered time (10^5 – 10^6 years)

Fig. 15

Modeling Cases for Long-Term Extrapolation

- **Water uptake in the buffer (T < 100 C)**
- **Thermal evolution of the buffer (T > 100 C)**
- **Hydro-mechanical evolution of the buffer**
- **Geochemical evolution, especially at interfaces (canister – bentonite and bentonite – concrete)**

- The models for the relevant processes are in principle existing and will be used for long-term simulation. Such models include, e.g.
  - Non-Darcy flow (threshold pressure and critical gradient)
  - Thermo-osmosis
  - Double structure model to account for microfabric evolution
  - Different types of water in macro- and micropores

WP4: Analysis of impact on long-term safety and guidance for repository d. & c.

Objectives:

- **Develop a synthesis** showing how the EBS and near-field rock will behave both during and after the transient period
- **Obtain a fully balanced view of all findings** and relate them to the specific relevant time and spatial domains
- **Give feedback to design** in terms of guidance for performance limits or modifications to design

WP4: Analysis of impact on long-term safety and guidance for repository d. & c.

Tasks 4.1 & 4.2:

- Develop evaluation structure for models and status of process understanding as well as a report structure
- Review the findings in WP2 and WP3 including other relevant experiments, identify information gaps
- Develop qualitative process related description of the early evolution of the EBS
- Quantitative assessment of WP2 and WP3 outcomes and uncertainties involved, identification of disagreements
- Discuss the importance with respect to the performance criteria
- Assess the impact on the safety functions (based on completed SA studies)
- Evaluate the importance of the identified aspects of the early evolution of the EBS based on scenarios for clay and granite host rock at relevant conditions

Fig. 18

WP4: Analysis of impact on long-term safety and guidance for repository d. & c.

Tasks 4.3:

- Propose improved approach for integrating the thermal and resaturation phase with the long term steady state phase for SA
- Identify remaining uncertainties and future R&D needs
- Link the impact on the long term safety requirements to the design requirements in the light of this

Fig. 19

The research leading to these results has received funding from the European Atomic Energy Community's Seventh Framework Programme (FP7/2007-2011) under grant agreement n° 249681

The GRS contribution is co-funded by the German Ministry of Economy and Technology (BMWi), FKZ 02 E 10689

Klaus Wieczorek

klaus.wieczorek@grs.de

Gesellschaft für Anlagen- und Reaktorsicherheit (GRS)
Theodor-Heuss-Strasse 4
38122 Braunschweig
Germany

TU Clausthal

GRS Gesellschaft für Anlagen- und Reaktorsicherheit (GRS) mbH

Numerical Simulations of THM Processes in Rock-Buffer-System surrounding High-Level Radioactive Waste

X.-S. Li[1]; C.-L. Zhang[2]; K.-J Röhlig[1]

1. Institute of Disposal Research, Clausthal University of Technology

2. Gesellschaft für Anlagen- und Reaktorsicherheit (GRS) mbH

2nd Chinese - German Workshop on Radioactive Waste Disposal
Karlsruhe, October 15-16, 2012

HLW Disposal Concept

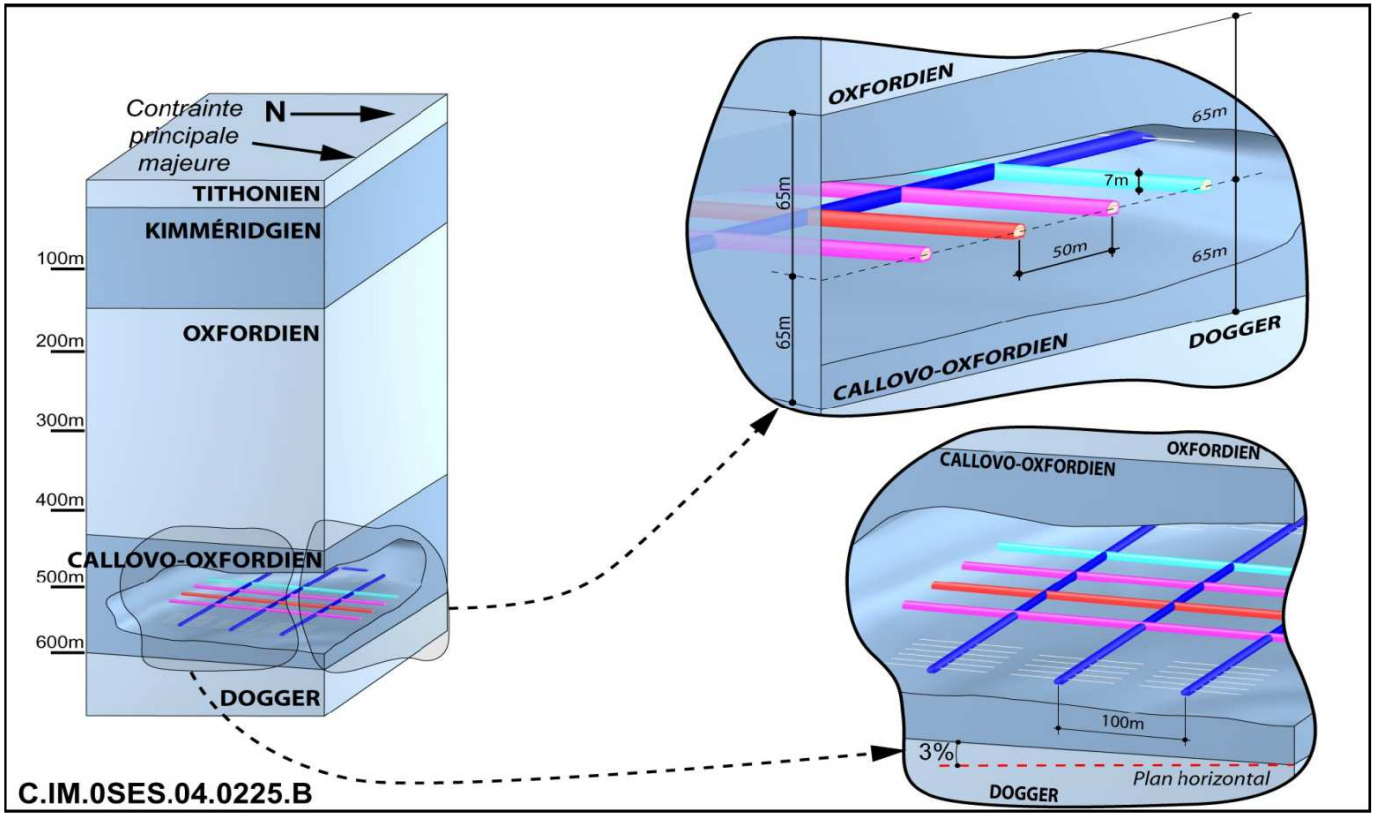

French Disposal Concept (Andra 2005) www.andra.fr 2005

Direct SNF Disposal in Drift

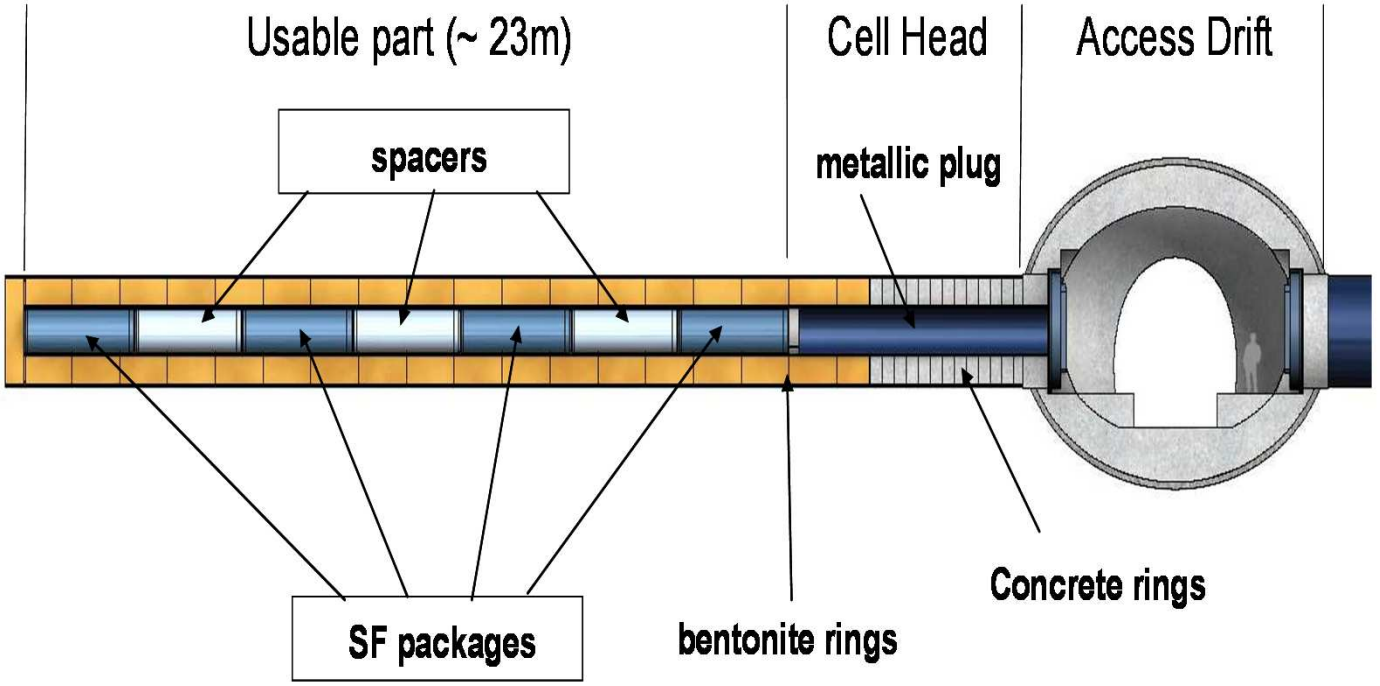

Dossier 2005 www.andra.fr 2005

Axisymmetric model for the rock-buffer-system

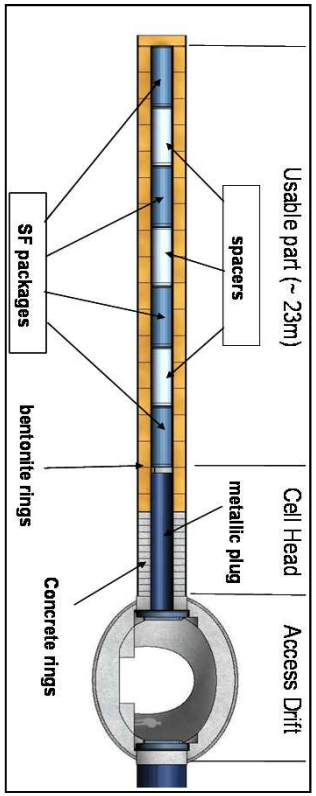

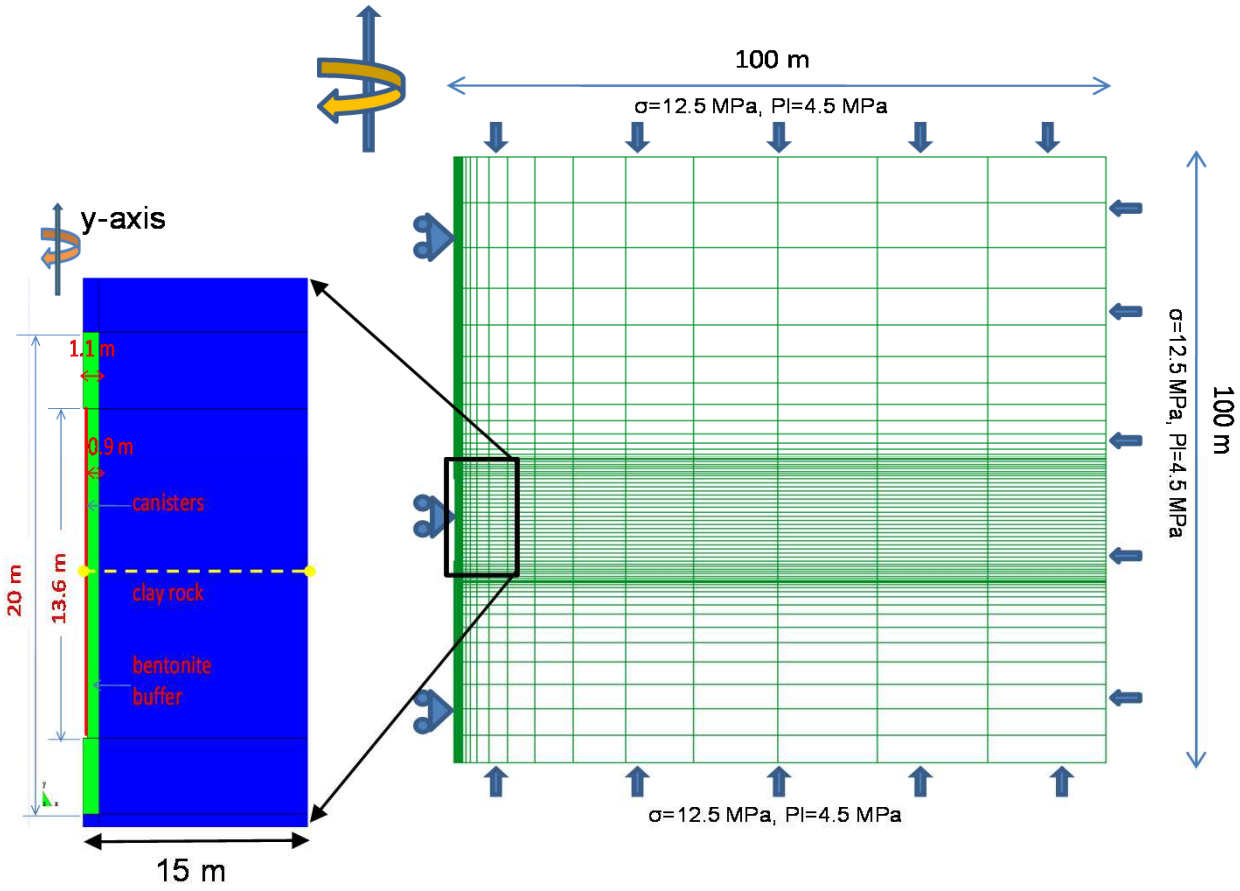

Coupled THM Modelling (CODE-BRIGHT)

- Balance of energy: $\frac{\partial}{\partial t}\left[E_s\rho_s(1-\phi)+E_l\rho_l S_l\phi+E_g\rho_g S_g\phi\right]+\nabla\cdot\left(\mathbf{i}_c+\mathbf{j}_{Es}+\mathbf{j}_{El}+\mathbf{j}_{Eg}\right)=f^E$
- Balance of water mass: $\frac{\partial}{\partial t}\left(\theta_l^w S_l\phi+\theta_g^w S_g\phi\right)+\nabla\cdot\left(\mathbf{j}_l^w+\mathbf{j}_g^w\right)=f^w$
- Balance of air mass: $\frac{\partial}{\partial t}\left(\theta_l^a S_l\phi+\theta_g^a S_g\phi\right)+\nabla\cdot\left(\mathbf{j}_l^a+\mathbf{j}_g^a\right)=f^a$
- Balance of solid mass: $\frac{\partial\theta_s^s(1-\phi)}{\partial t}+\nabla\cdot\left(\mathbf{j}_s^s\right)=0$
- Stress equilibrium: $\nabla\cdot\boldsymbol{\sigma}+\mathbf{b}=\mathbf{0}$

- **Heat transport: conduction, advection with water/vapour flow**
- **Water flow: advection and vapour diffusion**
- **Gas pressure: atmospheric**
- **Mechanical behaviour:**
  - **argillite-damage model for clay rock**
  - **thermo-elasto-plastic model (BBM model) for bentonite**

Thermal Constitutive Equations

- Fourier's law

$$\mathbf{i}_c = -\lambda \nabla T$$

$$\lambda = \lambda_s^{(1-\phi)} \lambda_l^{(\phi \cdot S_l)} \lambda_g^{\phi(1-S_l)} = \lambda_{sat}^{S_l} \lambda_{dry}^{(1-S_l)}$$

- Internal energy of liquid

$$E_l = E_l^w \omega_l^w + E_l^a \omega_l^a$$

- Internal energy of gas

$$E_g = E_g^w \omega_g^w + E_g^a \omega_g^a$$

- Internal energy of solid E_s

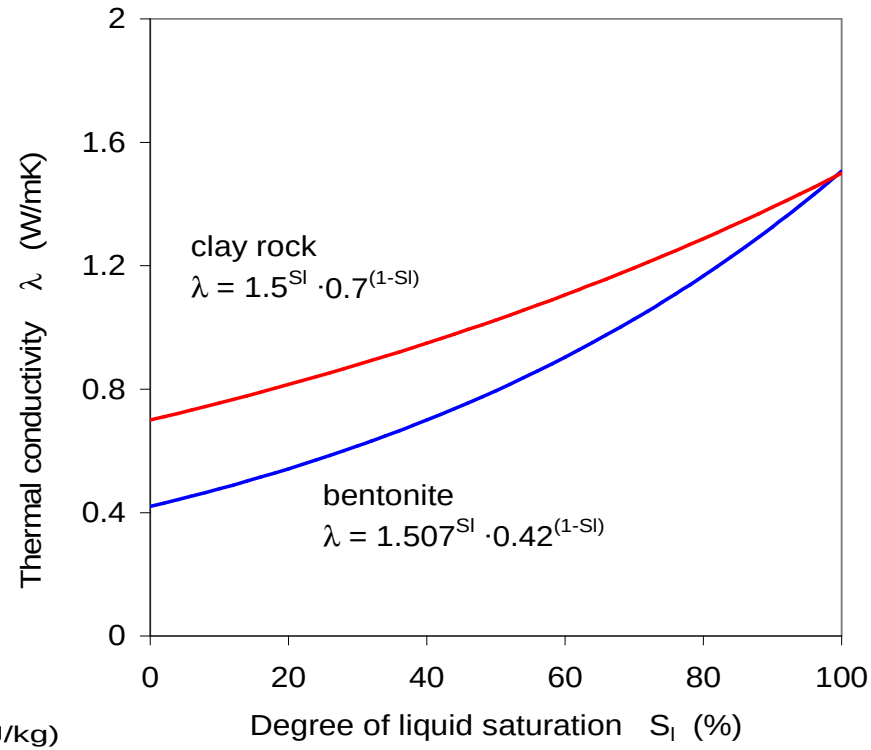

E_l^w = 4180.0 T (J/kg), E_l^a = 1006.0 T (J/kg)

E_g^w = 2.5·10^6 +1900 T (J/kg) E_g^a = 1006 T (J/kg)

E_s = 930 T (J/kg) for the Opalinus clay

Hydraulic Constitutive Equations

- Water/gas two phase Darcy flow

$$\mathbf{q}_\alpha = -\mathbf{K}_\alpha (\nabla P_\alpha - \rho_\alpha \mathbf{g}) \quad \mathbf{K}_\alpha = \mathbf{k}\, k_{r\alpha} / \mu_\alpha$$

- Relative water/gas permeability

$$k_{rl} = S_l^{1/2} \cdot \left[1 - (1 - S_l^{1/\beta})^{\beta}\right]^2 \qquad k_{rg} = 1 - k_{rl}$$

- Water saturation – suction relationship

$$S_l = \left[1 + \left(\frac{s}{P_0}\right)^{1/(1-\beta)}\right]^{-\beta}$$

- Intrinsic permeability related to porosity

$$\mathbf{k} = \mathbf{k}_0 \frac{\phi^3}{(1-\phi)^2} \frac{(1-\phi_0)^2}{\phi_0^3}$$

- Diffusion of water vapour

$$\mathbf{i}_g^w = -\mathbf{D}_g^w \nabla \omega_g^w = -(\phi \rho_g S_g \tau \mathbf{D}_m^w \mathbf{I} + \rho_g \mathbf{D}'_g) \nabla \omega_g^w$$

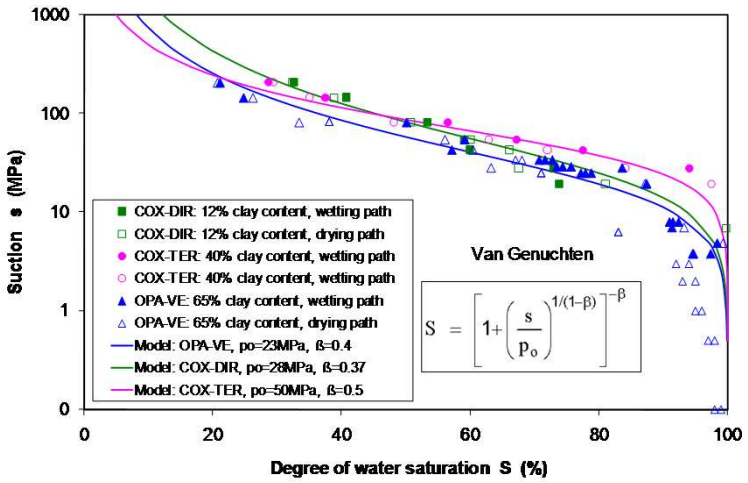

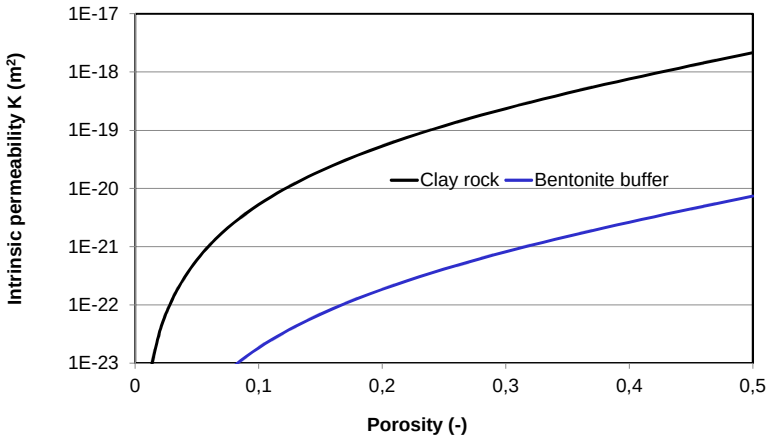

Mechanical Constitutive Equations

Elastoplastic-damage model for clay rock

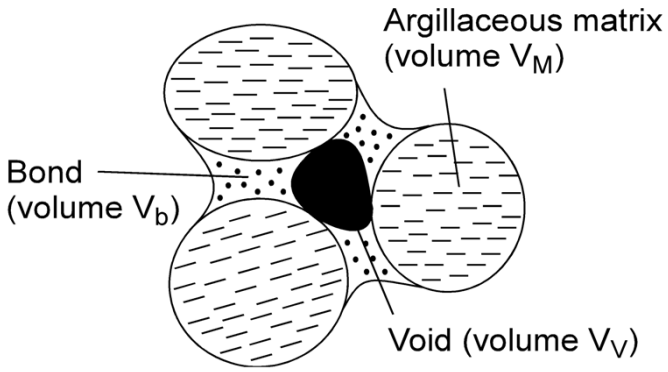

$$d\varepsilon_{ij}^{M} = d\varepsilon_{ij} + d\varepsilon_{ij}^{b}$$

$$\sigma_{ij} = (1+\chi)\sigma_{ij}^{M} + \chi\sigma_{ij}^{b}$$

$$\chi = \frac{\varepsilon_v^b}{\varepsilon_v} = \frac{\varepsilon_q^b}{\varepsilon_q} = \chi_0 \cdot \exp\left(-L/2\right)$$

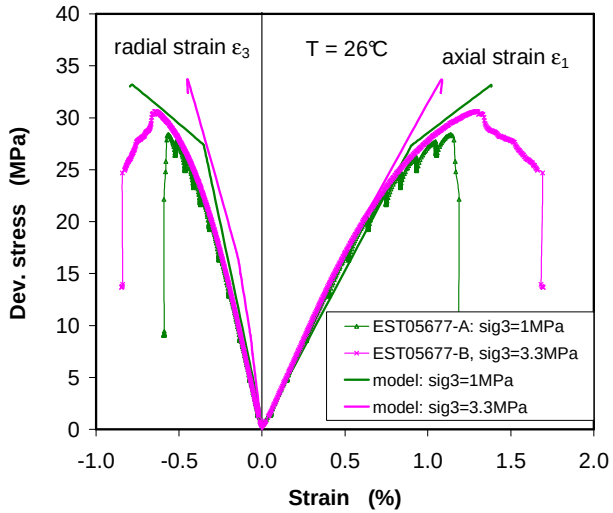

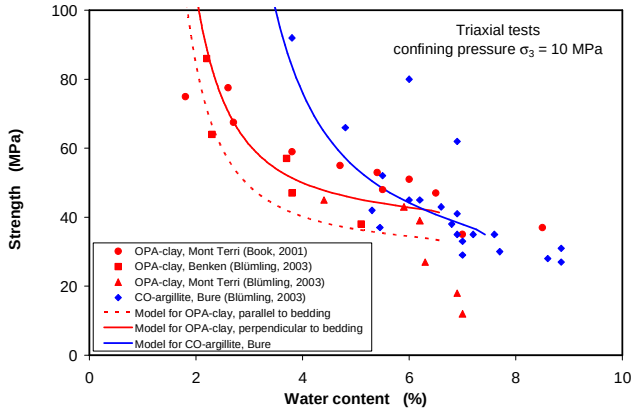

Mechanical Constitutive Equations

Thermo-Elastoplastic model for compacted bentonite

Consolidation

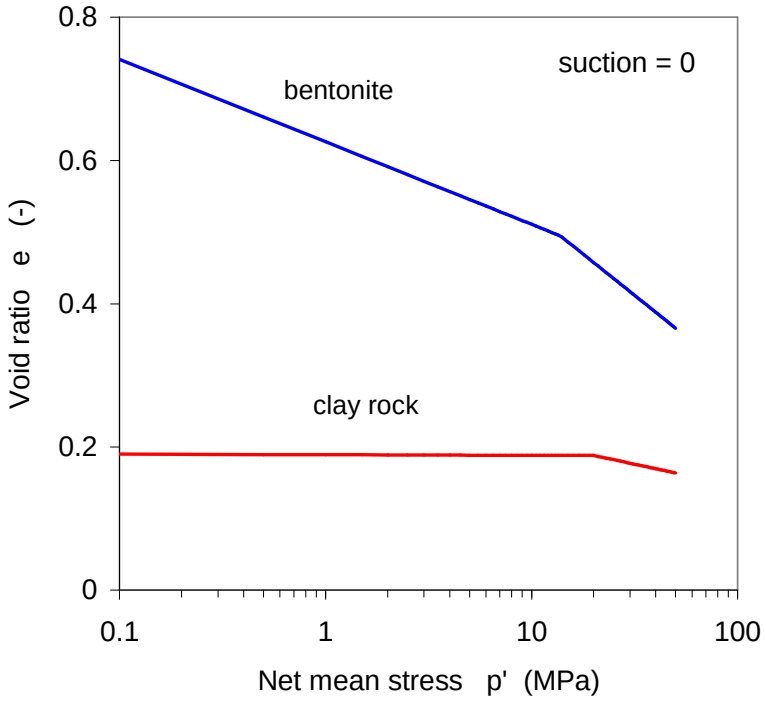

Swelling

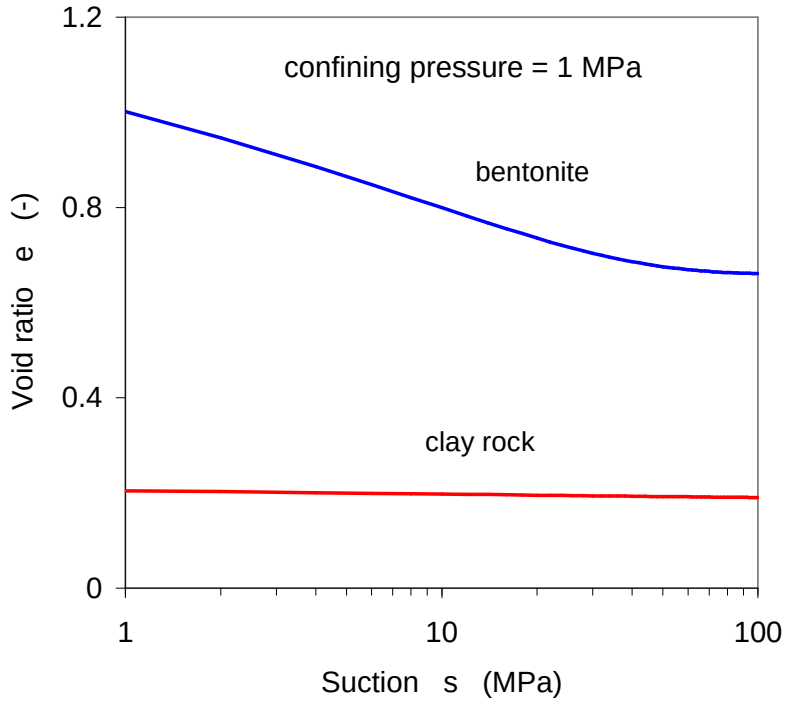

Axisymmetric model for the rock-buffer-system

- **Initial state** before the construction (0-0.1 day)
- **Excavation and ventilation phase** (0,1-100 days):
- The borehole has been drilled and ventilated for 100 days.
- **Backfilled phase** (100 days- 6 years):
- The SNF canisters have been emplaced, the drilled borehole has been backfilled with bentonite buffer and heated by SNF canisters.

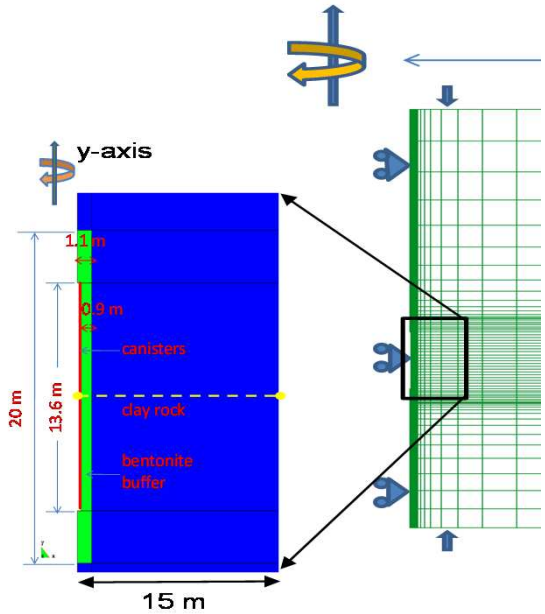

Heat output from HLW

$$j_e = j_{eo} \cdot \exp[-abs(\lambda_e) \cdot t]$$

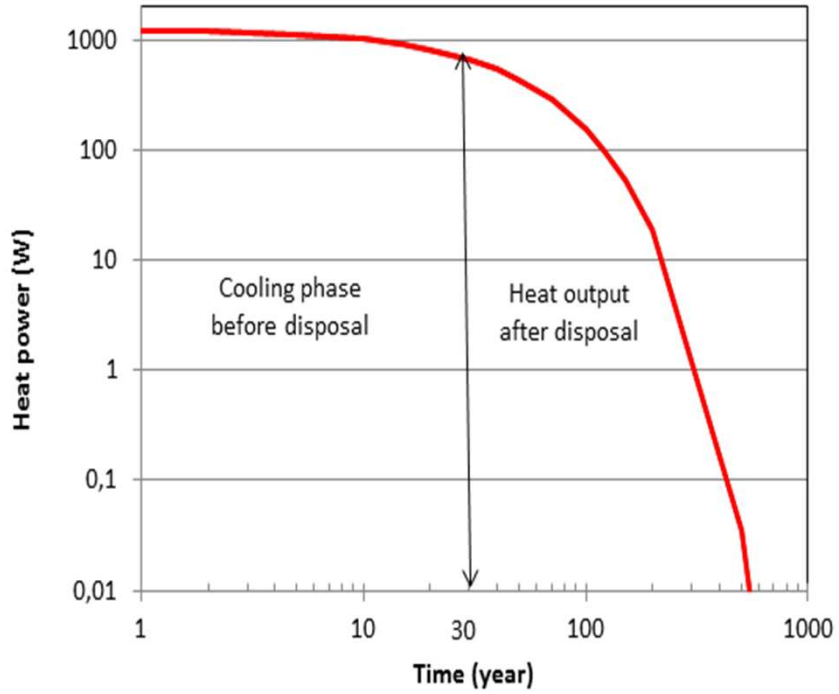

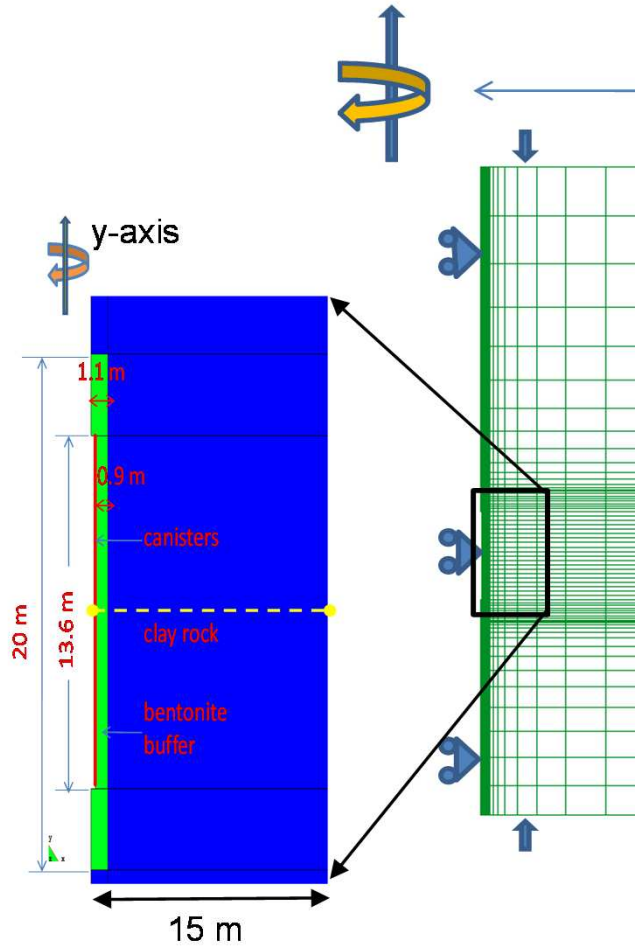

Excavation damaged zone (EDZ)

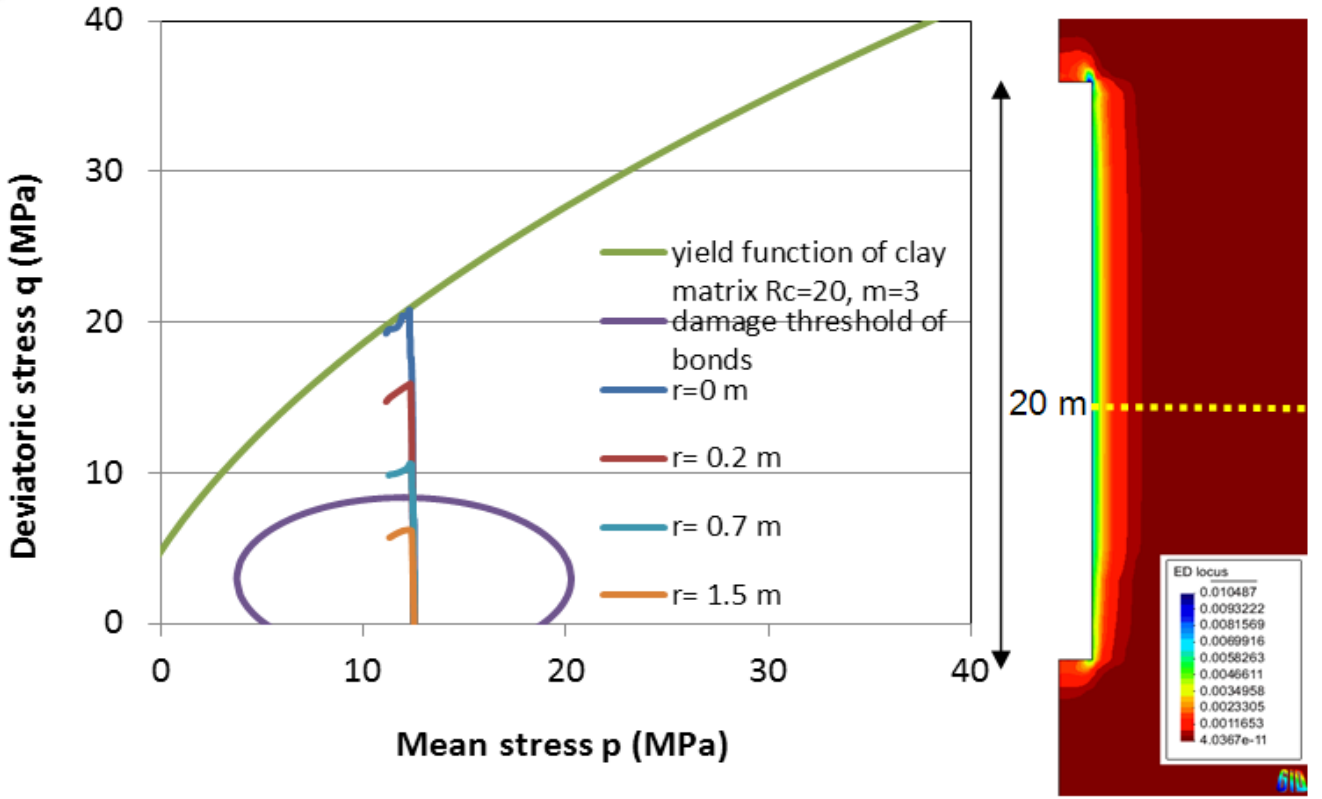

a) stress evolution

b) damaged zone

Temperature evolution

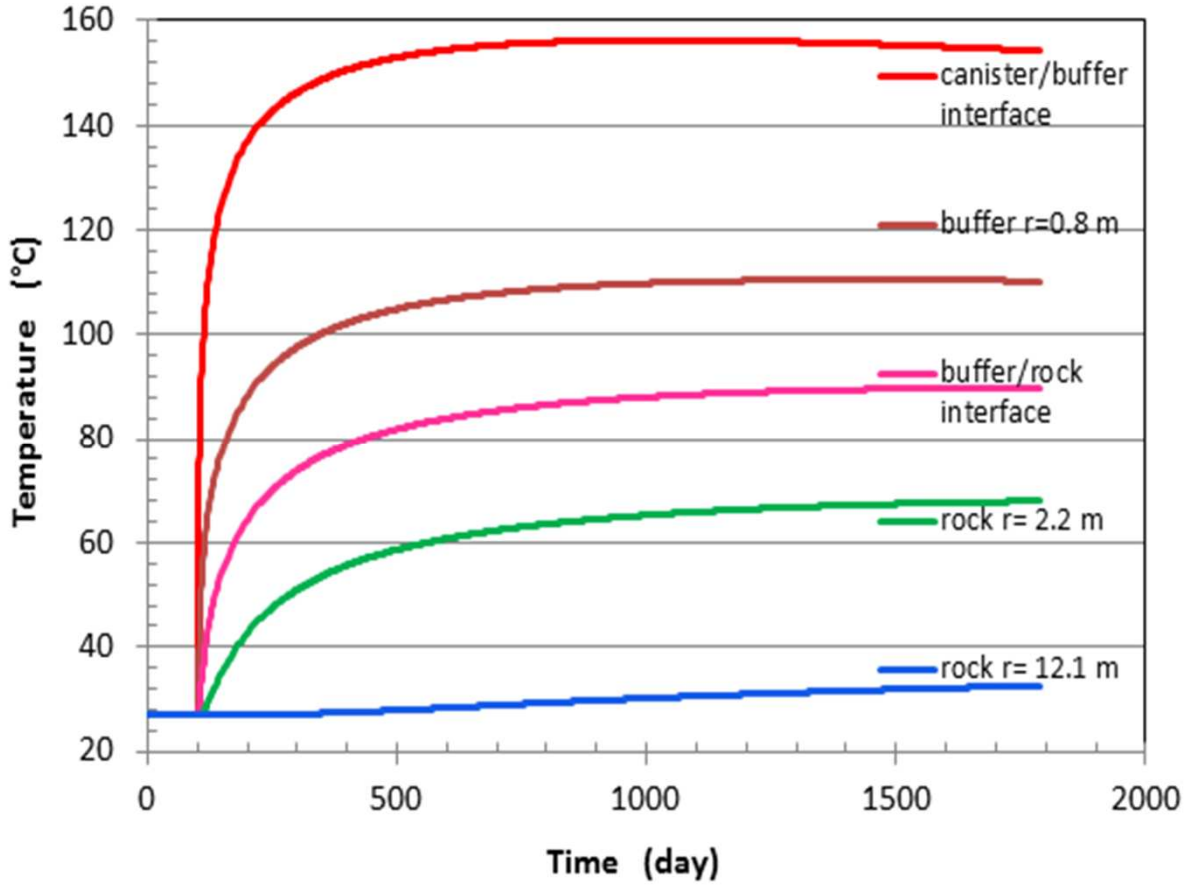

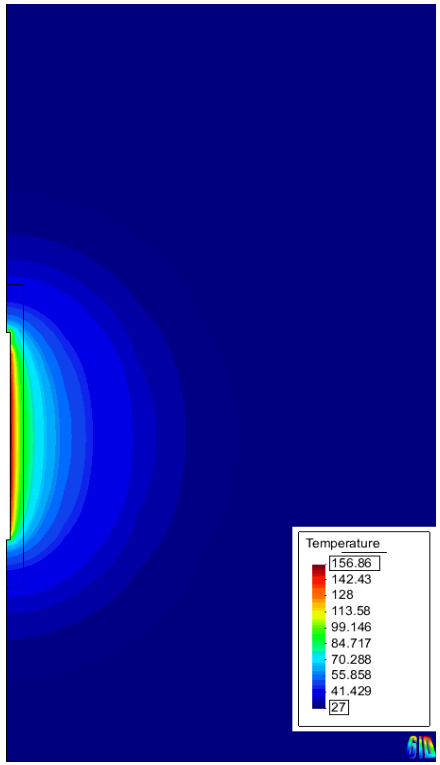

Pore-water pressure changes

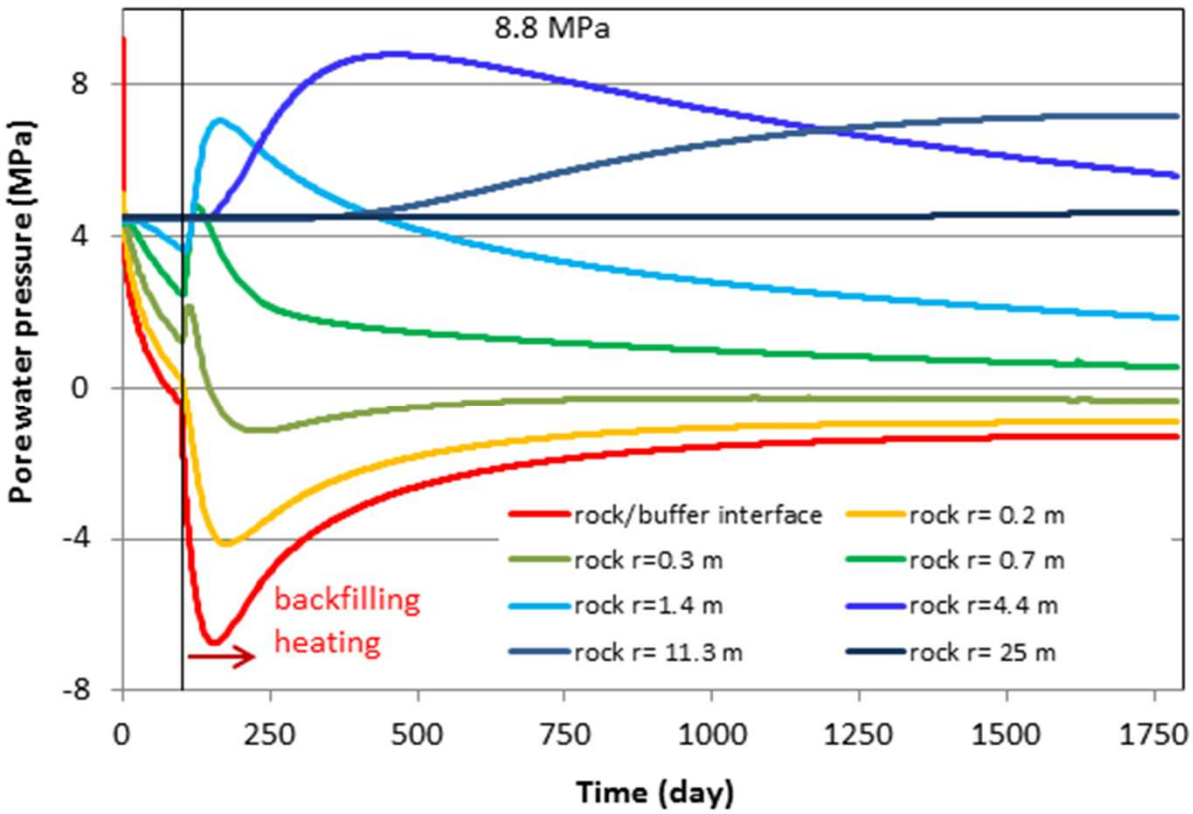

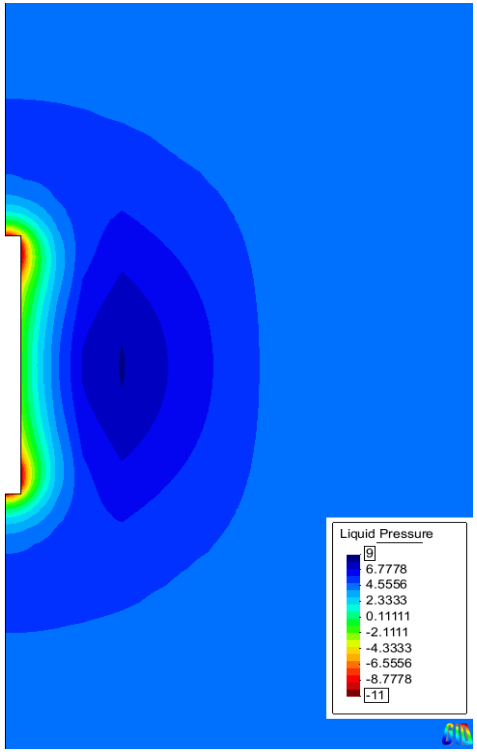

Porosity change in bentonite buffer

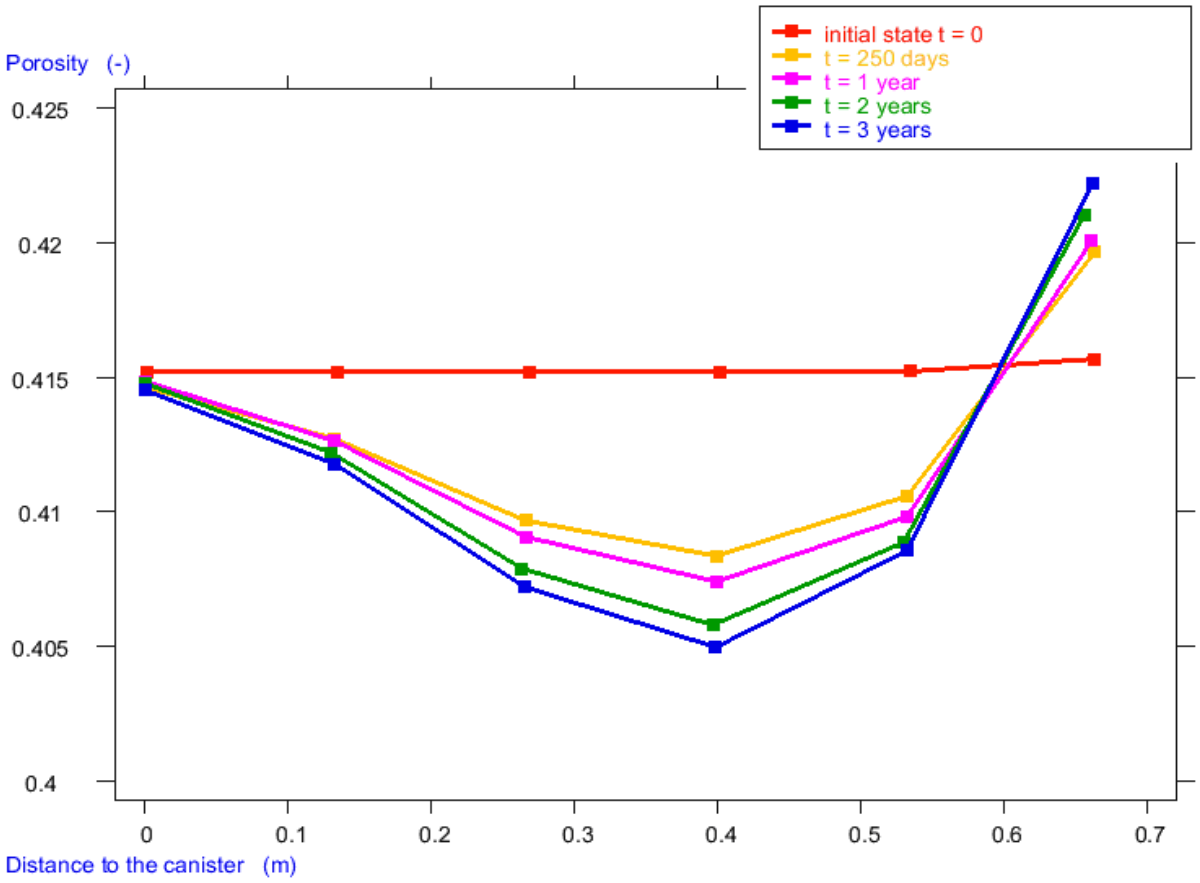

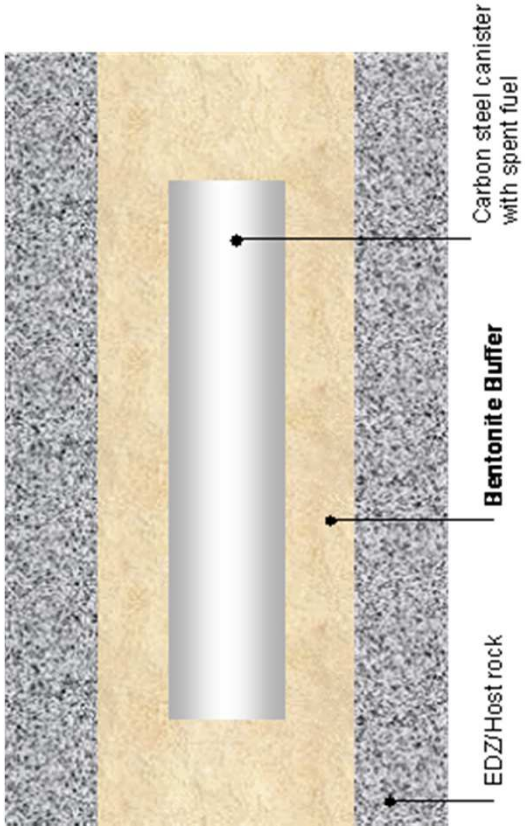

Water saturation in bentonite buffer

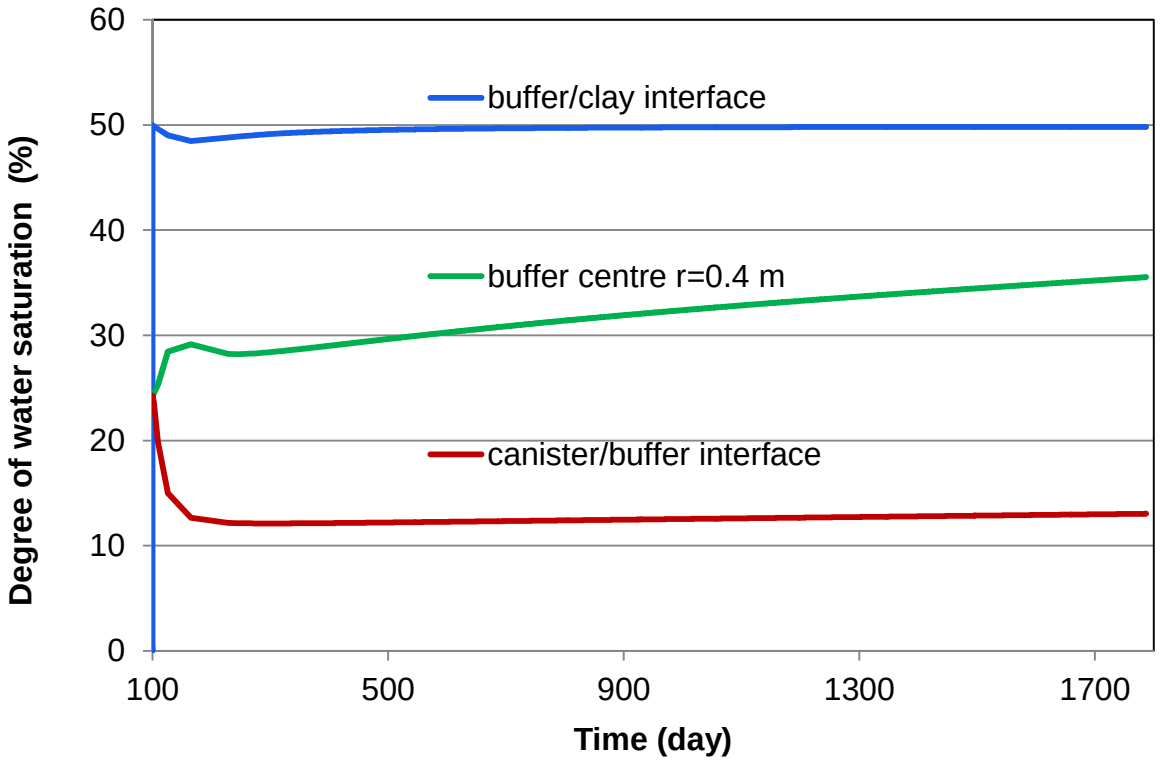

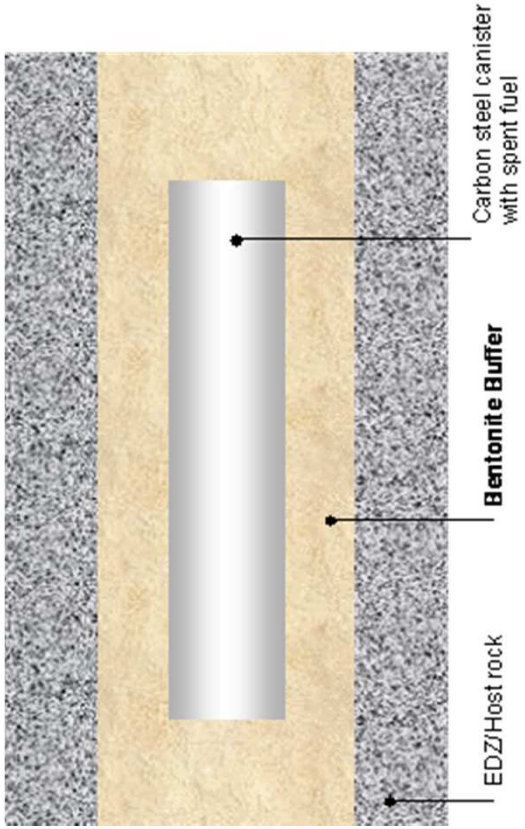

Thermal deformation

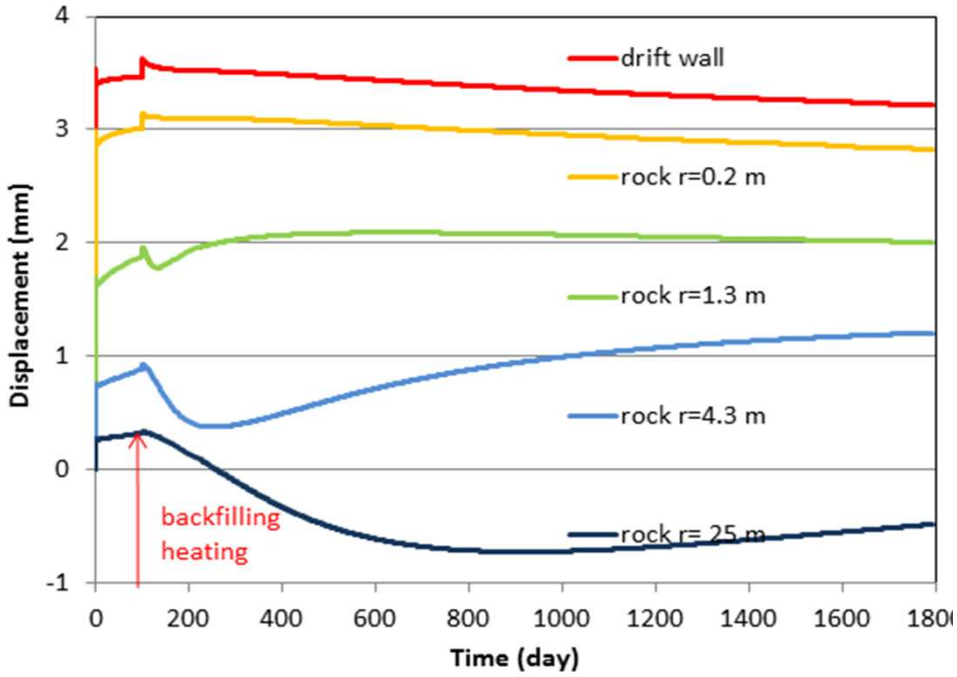

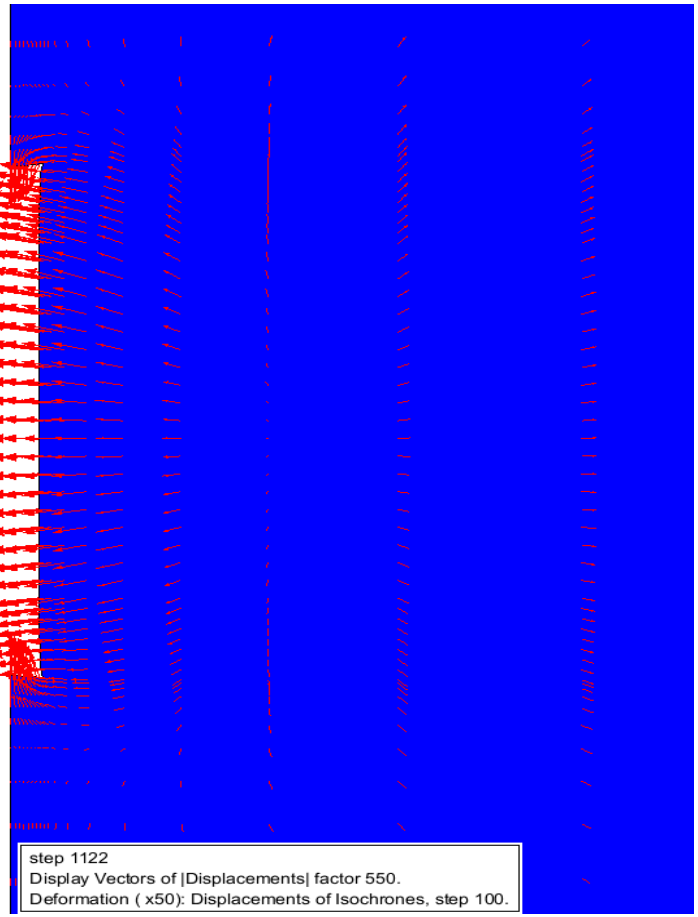

Conclusions

- Temperature:
  - T_{max} = 157 ℃ at the surface of SNF containers at ~3 years
  - T_{max} = 90 ℃ in the host rock
- Water saturation:
  - desaturation in the buffer near the containers due to the thermal evaporation of the pore water
  - resaturation in the buffer near the rock by taking up water from the saturated far-field
- Thermally-induced pore-water pressure is limited below 9 MPa, no fracturing is possible.
- Thermal expansion is revealed in the heated rock mass, while thermal compaction in the buffer occurs.
- Generally, no or little negative thermal effects are given by the modelling

TU Clausthal

Gesellschaft für Anlagen- und Reaktorsicherheit (GRS) mbH

Tuesday, October 16, 2012

TOPIC: RN-BEHAVIOR

R&D on HLW Treatment and Disposal in CIAE

by ZHANG Zhengtao ,WANG Bo

R&D Laboratory on Radioactive Waste Conditioning and Disposal of
China Institute of Atomic Energy (CIAE)

2nd German-Chinese Workshop on Radioactive Waste Disposal
Karlsruhe，Germany
Oct. 15, 2012

CIAE Major Fields of R&D

on Radioactive Waste treatment and Disposal

Reprocessing

HLLW

HLLW Vetrification

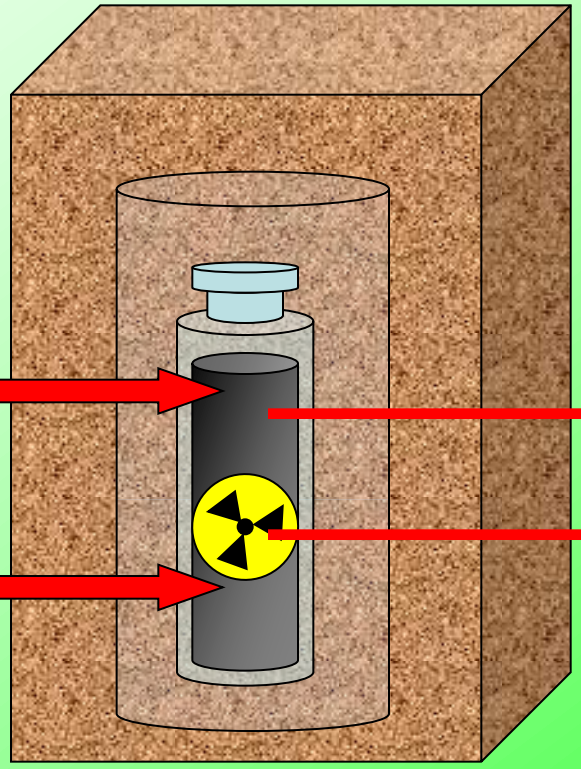

Long-term Behavior of HLW Glass in Geological Repository

Immobilization of Legacy Waste

Chlorine Salt and Graphite Sleeves Of legacy

Chemistry and Migration behavior of Actinide in Geological conditions

R&D Projects, 2010-2015

(1) Cold Crucible Melter for vetrification of HLLW

(2) Long-term Behavior of Simulated HLW-Glass in Geological Repository

(3) Chemistry and Migration behavior of Radionuclides under geological disposal conditions

(4) Immobilization of Legacy Wastes:

Chlorine Salt in Glass-Ceramic

Self-Sustainable Propagating High Temperature Synthesis for Graphite Sleeves

China Institute of Atomic Energy

原子能院

(1) Cold Crucible Melter for HLLW

CCM is a versatile technology for vitrification of HLLW.
The technology is now being used to vitrify the HLLW in Some countries.

CIAE CCM, 2010

Molten glass inside the CIAE cold crucible melter in operation

Molten glass tapping

(1) Cold Crucible Melter for HLLW

Design and optimize a high and middle-frequency converter, 2011

- High-frequency: 592 kHz ; Power: 48.6 KW
- Middle-frequency: 18 KW, **frequency adjusts automatically.**

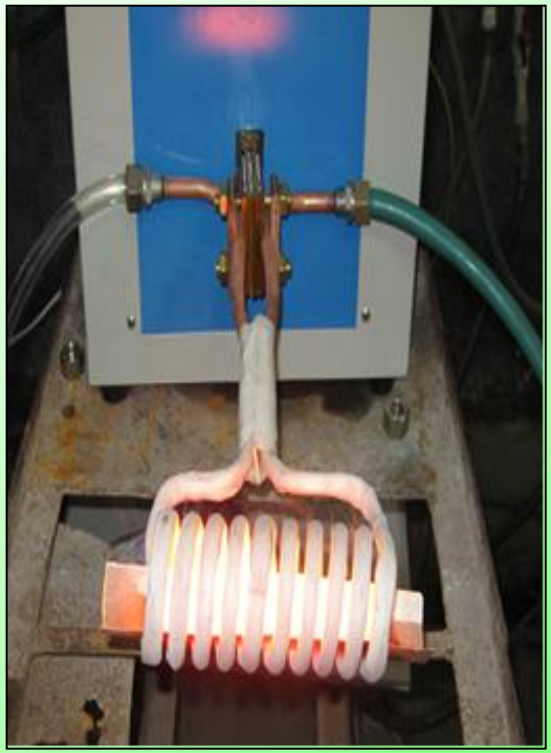

China Institute of Atomic Energy

原子能院

(1) Cold Crucible Melter for HLLW

An integrated CCM prototype will be established in CIAE，2015

CCM Prototype in CIAE

Waste feed component

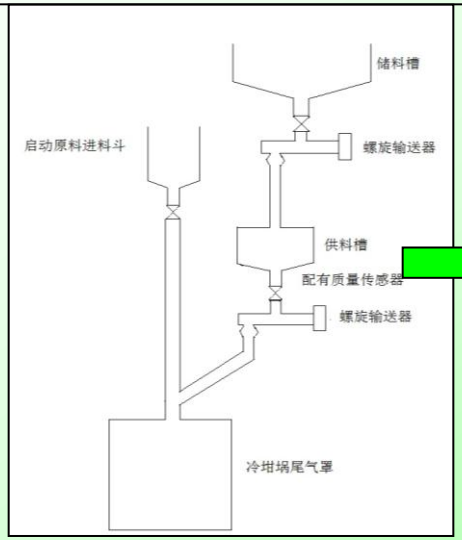

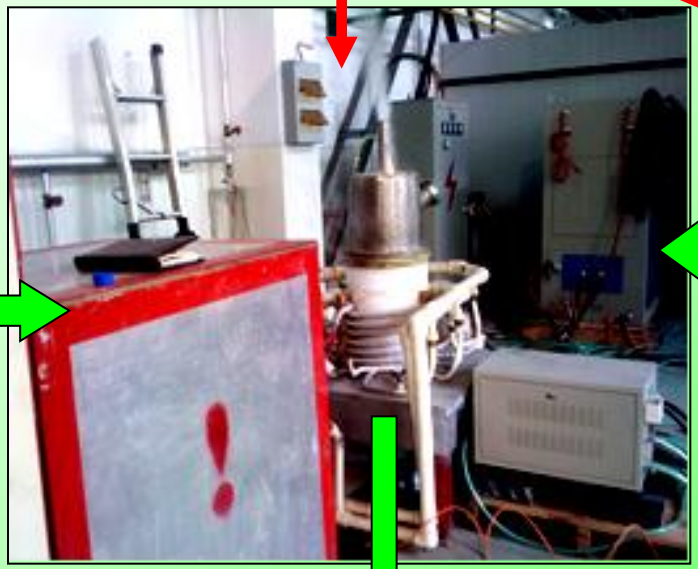

Off-gas treatment system

2013

Vitrification of simulated HLLW in 2015:

- Producing Capacity : 10 kg/h
- Higher Temperature：1500℃；

China Institute of Atomic Energy

原子能院

(2) Long-term Behavior of HLW Glass in Geological Repository

Simulated HLW Glass Leaching experiment has been performed in CIAE, 2010

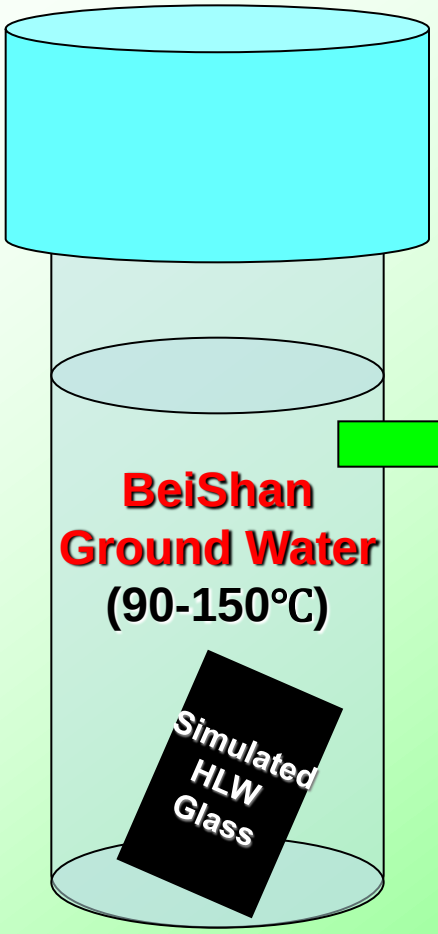

Figure 1: The leaching of the glass modifying elements.

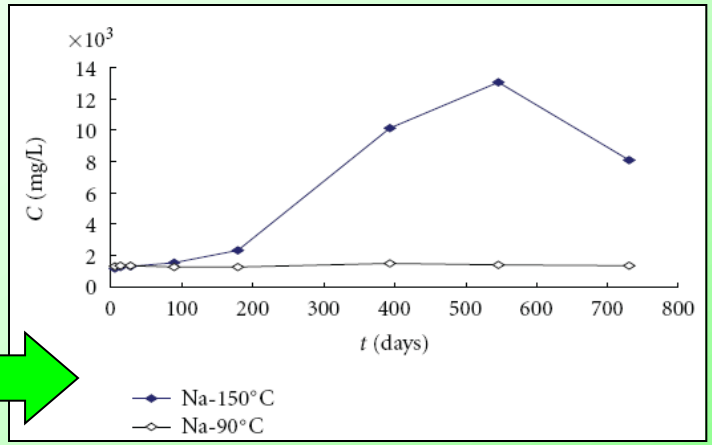

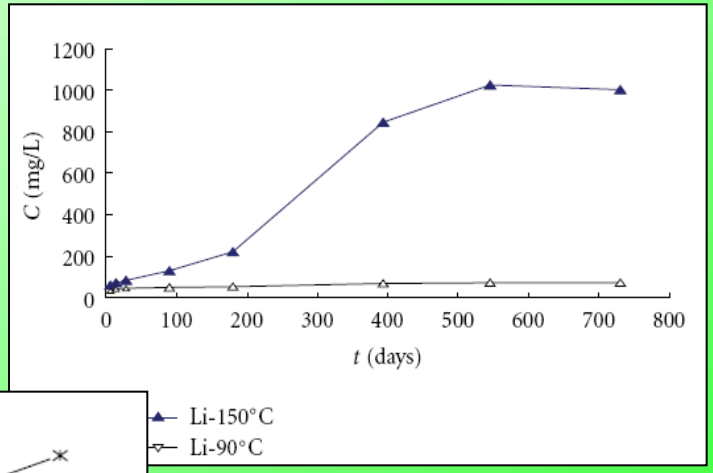

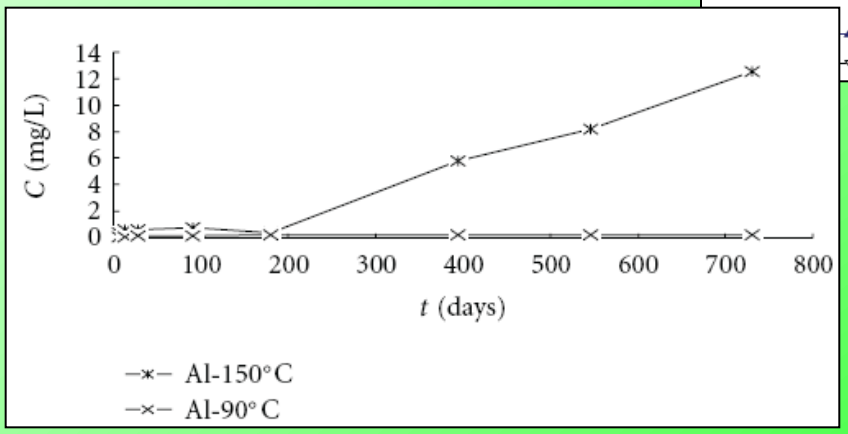

Temperature is a key parameter for the Long-term Behavior of HLW Glass

The secondary products formation of simulated HLW glass at 150 ℃

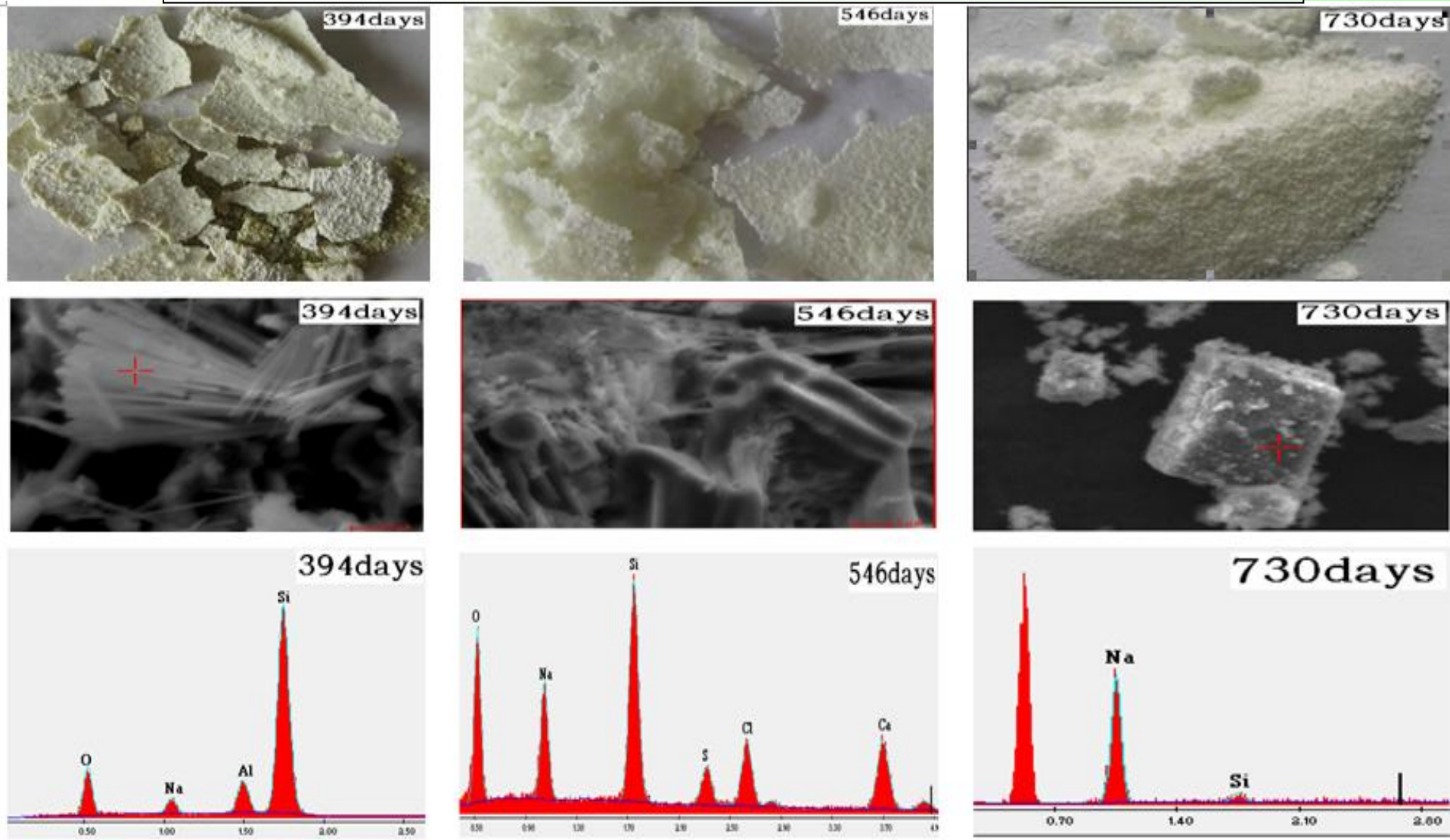

Figure 2: The secondary products (a), their SEM images (b), and their EDS (c).

Table 1: Mineral distribution of secondary products.

Time (d)	Zeolite P	Mordenite	Nontronite	Dickite	Okonite	Quartz	Saponite	Tincalconite
394	12%	28%	25%			35%		
546	2%			6%	1%		55%	35%
730								100%

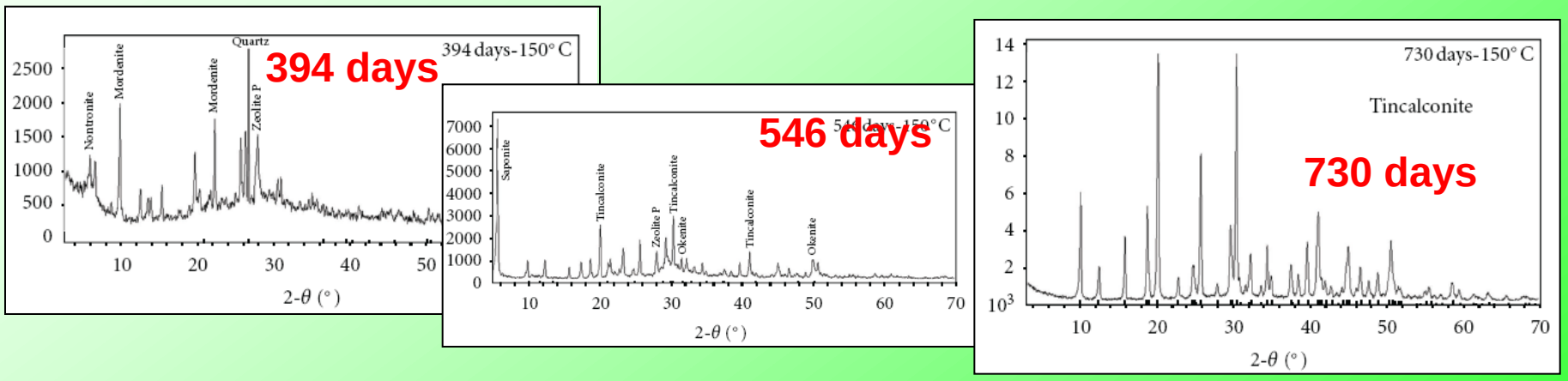

glass was degraded into other minerals at 150℃

$$Glass \leftrightarrow Silica(aqueous) \rightarrow \frac{Quartz}{Zeolite}$$

China Institute of Atomic Energy

(2) Long-term Behavior of HLW Glass in Geological Repository

- Small-scale Interaction equipment of Glass-Container-Back fill materials-Host Rock

- U / Th glass
- Operation Temperature: 20-150℃
- Experimental Period: 4 years

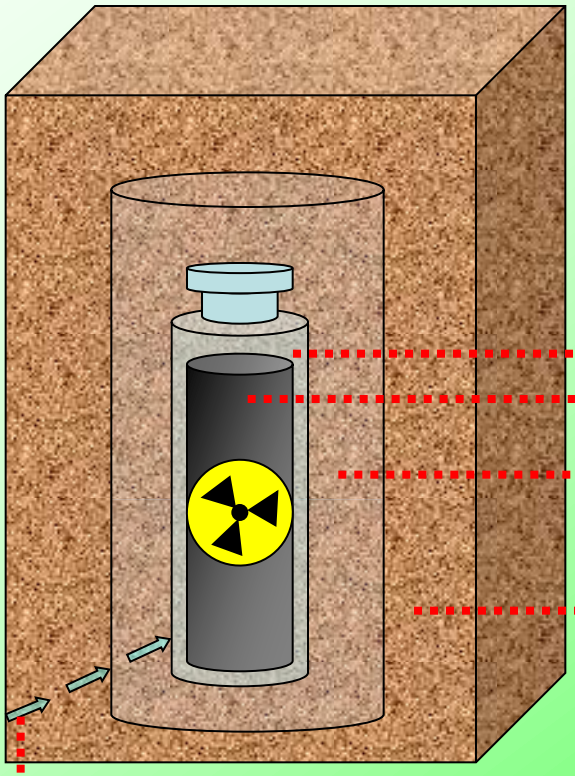

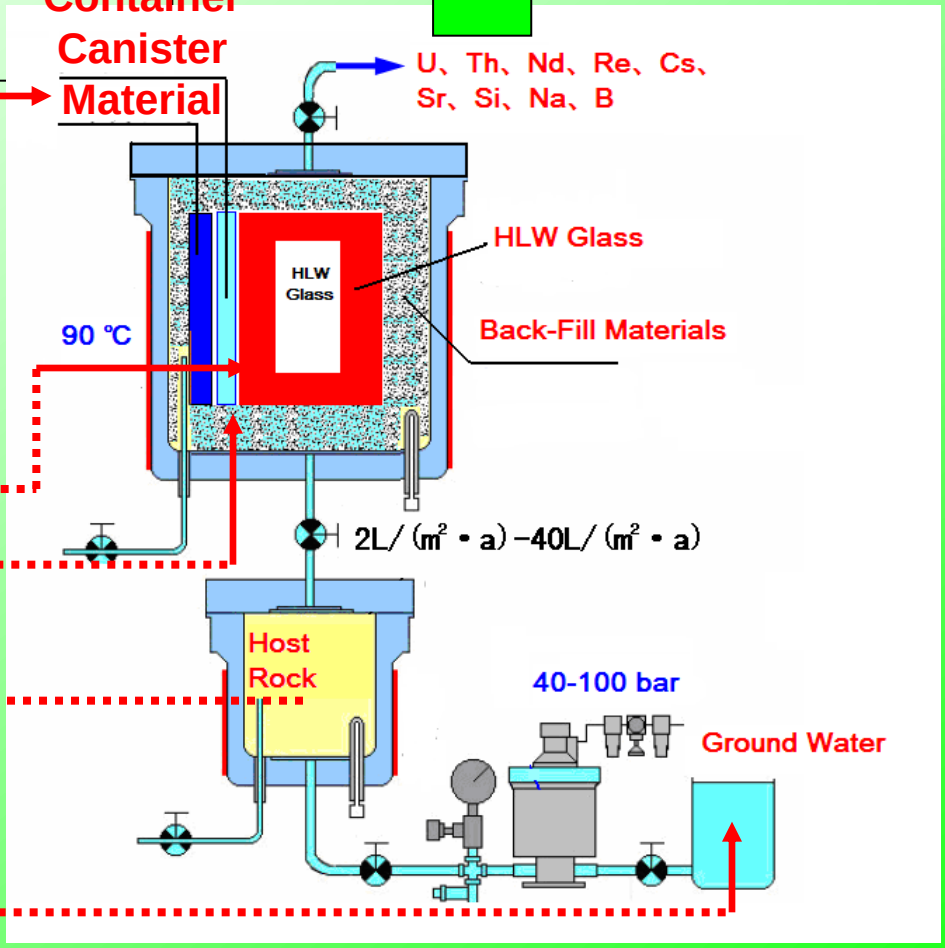

China Institute of Atomic Energy

原子能院

2012-2015

1.Aqueous Solutions

•Sampling period: 3,6,9,12,18,24,30,36,42, 48 months.
•Analysis of U,Th,Nd,Re,Cs,Sr,Si,Na,B with ICP-MS/AES.

2.Canister Metal

3.Simulated HLW Glass

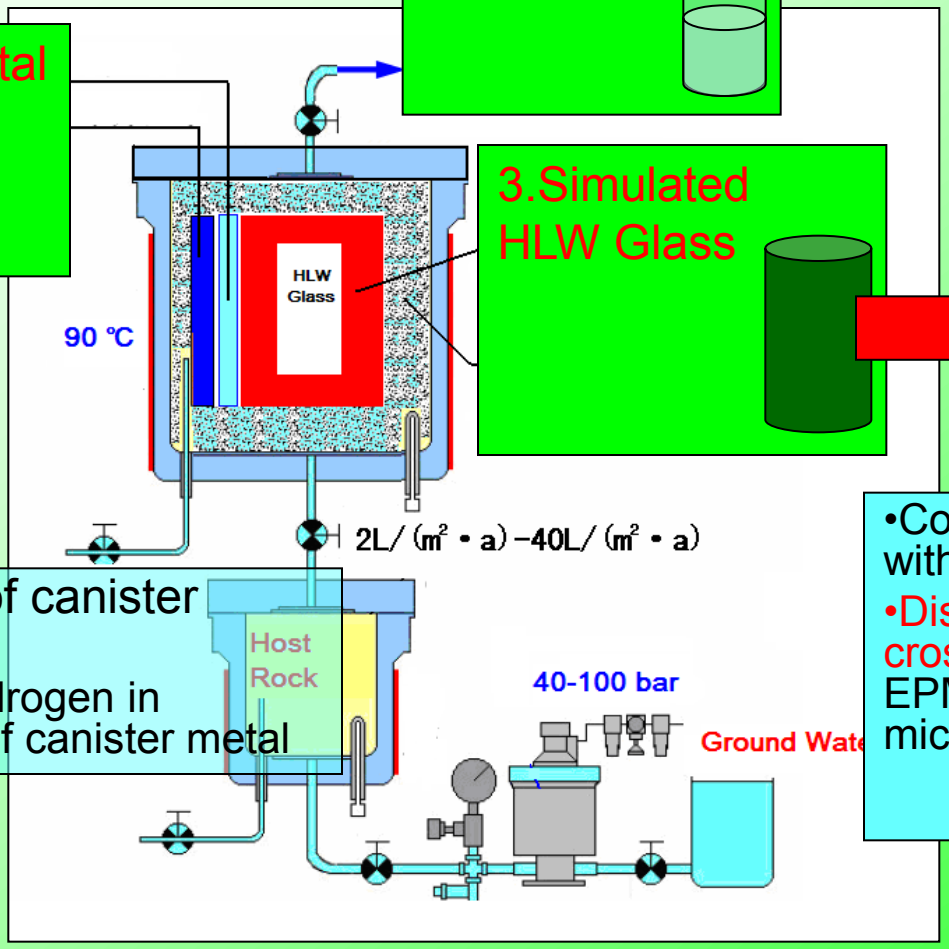

•Corrosion rate of canister metal with SEM
•Distribution of Hydrogen in corrosion section of canister metal

•Corrosion rate of HLW glass with SEM
•Distribution of key elements in crossion layer with EPMA(Electron probe X-ray microanalyser) ;

China Institute of Atomic Energy

原子能院

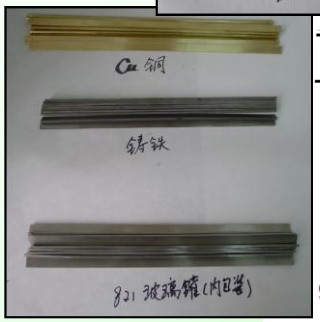

U/Th Simulated HLW Glass

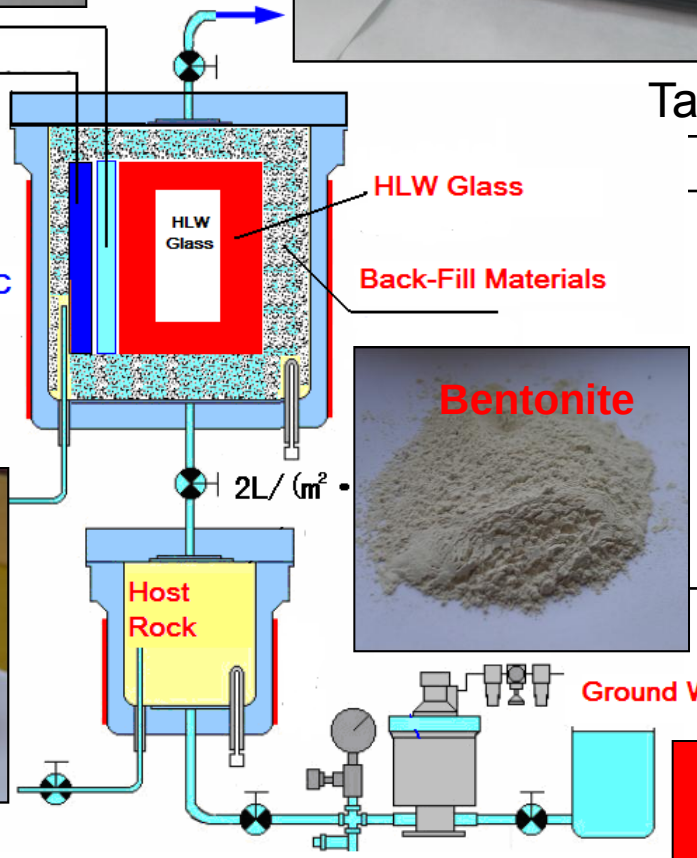

Table 2 Composition of simulated HLW gl

Oxide	wt%	Oxide	wt%	Oxide	wt%
SiO_2	50.232	La_2O_3	0.1326	Fe_2O_3	3.144
B_2O_3	18.48	SrO	0.0368	NiO	0.5728
Na_2O	11.190	Y_2O_3	0.016	K_2O	0.0912
Li_2O	2.94	MoO_3	0.1941	P_2O_5	0.0688
Al_2O_3	3.3816	MnO_2	0.016	SO_3	0.6448
CaO	4.536	Cs_2O	0.1152	Cr_2O_3	0.296
TiO_2	0.9897	BaO	0.0208	Nd_2O_3	0.01
MgO	0.84	U_3O_8	1.9728	ThO_2	0.035
Re_2O_7	0.052				

BeiShan Ground Water

(3).Chemistry and Migration Behavior of Radionuclides

(1)Migration of radionuclide at Room temperature

- **Solubility of Np,Pu, Tc , Am in Beishan underground water**
- **Solubility of actinides and Tc at high temperature**

(2) Migration of radionuclide in mock-up conditions

- **Migration of radionuclide in Backfilling materials**
- **Migration of radionuclide in fracture fill material of host rock(BeiShan Granite)**

(3) Modeling of the migration of radionuclide

(4) Immobilization Chlorine Salts in ceramics

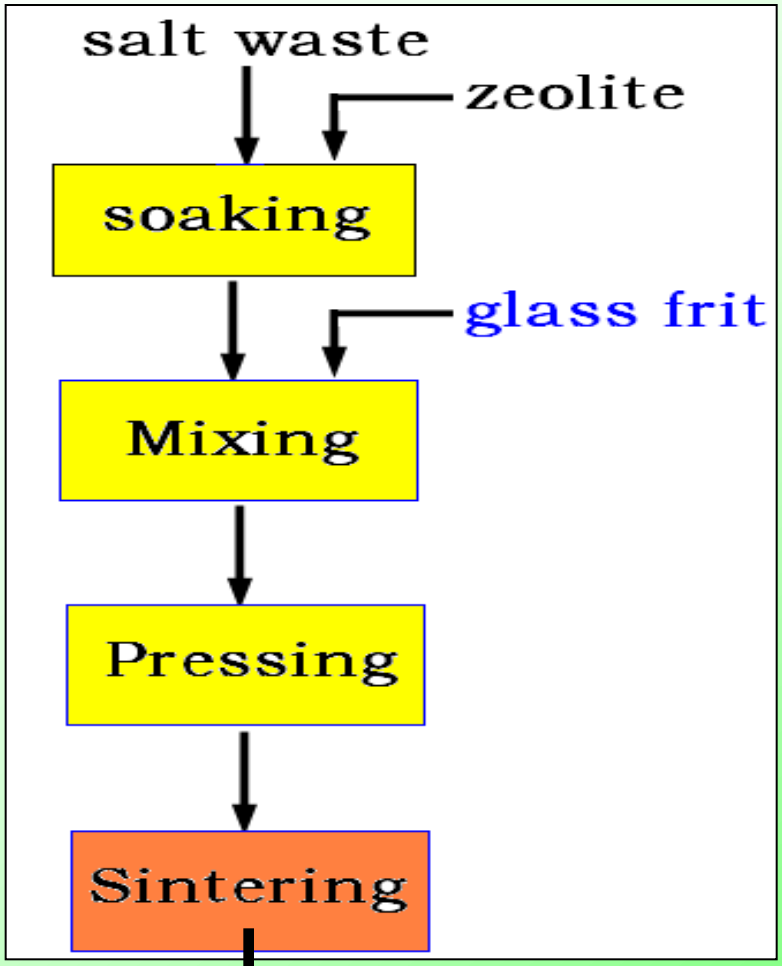

Table 3 Composition of simulated chlorine salts

chlorine salts	wt%	chlorine salts	wt%	chlorine salts	wt%
$BaCl_2$	1.20	KI	0.15	$NdCl_3$	7.71
$CeCl_3$	2.33	LiCl-KCl	69.82	$SrCl_2$	1.00
CsCl	2.84	NaCl	14.95		

Nd and Ce been used to replace the actinides

Leaching rate

XRD

SEM

(4) Immobilization legacy wastes in ceramics

- A bench scale of glass-ceramic fabrication facility to be established
- Demonstration of immobilization of chlorine salt to be performed

(4) Immobilization legacy wastes in ceramics

Table 4 Composition of simulated chlorine salts Ceramics（wt%）：

Simulated Waste	4A-Zeolite	Glass Firt	Zr、Ti、P
24	40-60	15-30	2-6

- HLW Chlorine Salts loading up to 24 wt%，
- HLW HLW Slurry loading up to 50 wt%；

- Ceramic Characterization ：Leaching rate of Cs/Sr/Re/U ＜ 1×10^{-3} g/cm²·d，Th and Nd ＜ 1×10^{-4} g/cm²·d。

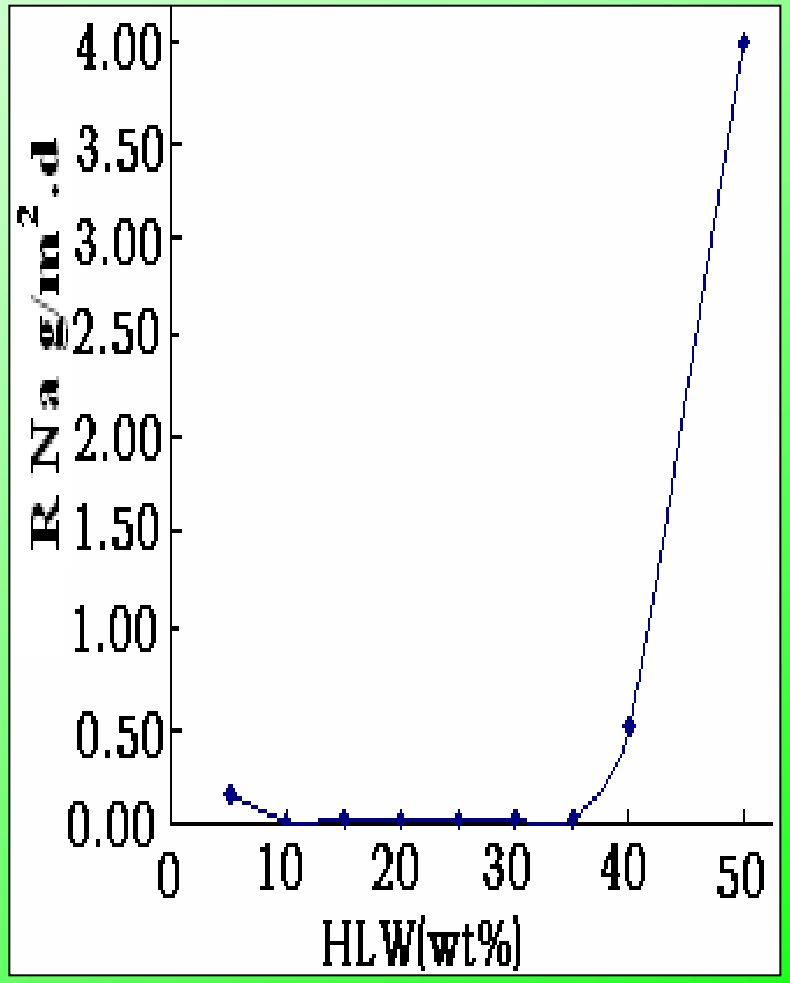

Self-Sustainable Propagating High Temperature Synthesis for Graphite Sleeves

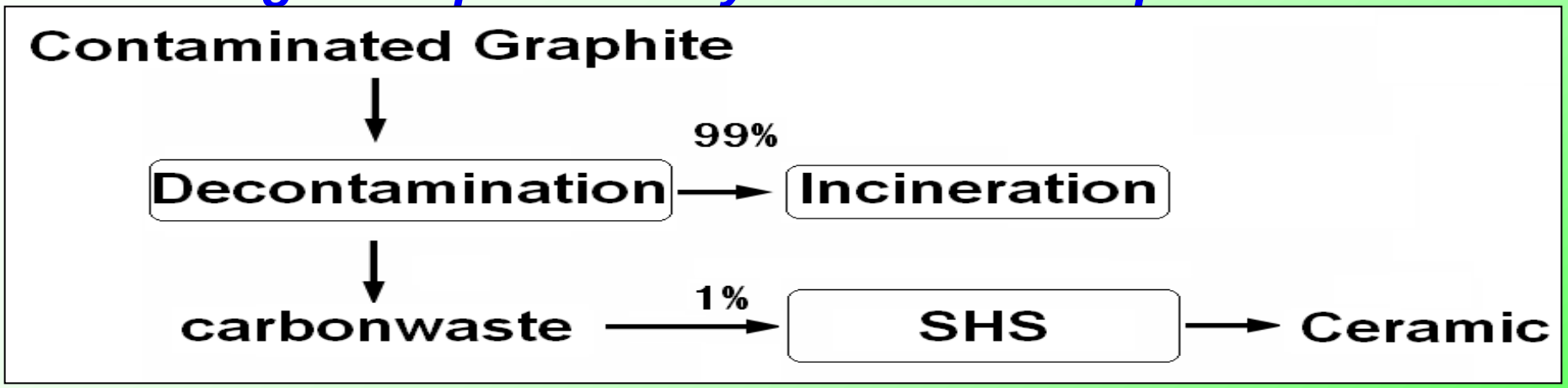

Thank You for Your Attention

Karlsruhe Institute of Technology

Source Terms for Highly Radioactive Waste Forms

2nd Chinese-German Workshop on Radioactive Waste Disposal
Karlsruhe, October 15-16, 2012

Bernhard Kienzler

Institut für Nukleare Entsorgung (INE)

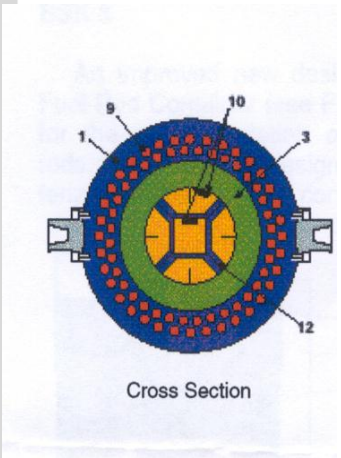

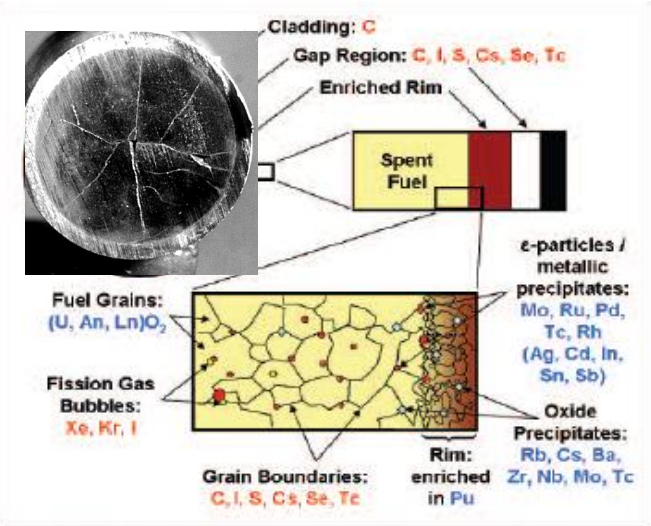

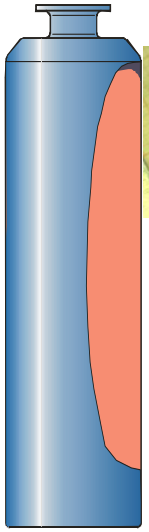

Nuclear Situation in Germany

- Ban on construction of nuclear power plants (2001)
- Ban on reprocessing (since 2005)
- De facto ban on spent fuel element transports (on-site interim storage)
- Complete phase-out until 2022 (2012)

Total Electricity Generation (2011):
612×10^9 kWh

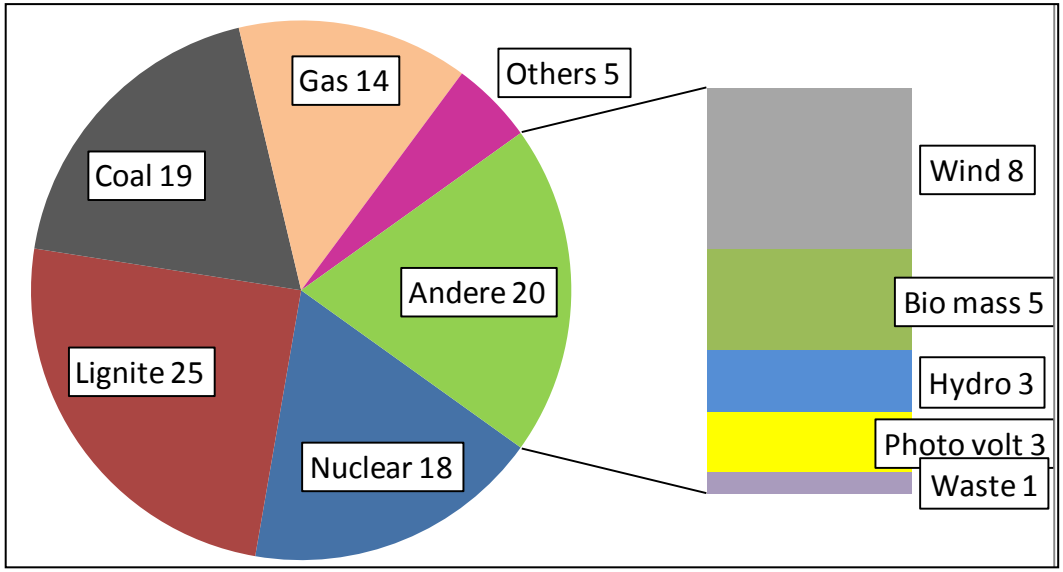

Radioactive Wastes in Germany

Heat producing wastes: ca. 29.030 m³

- **Spent Fuel (disposed directly)**
  - **from power reactors** **21.800 m³**
  - **pilot / test reactors** **5.530 m³**

  (THTR/AVR, PKA/IKA, res. reactors)
- **Reprocessing***
  - **HLW Glass** **670 m³**
  - **CSD-B, CSD-C** (hulls / end pieces) **850 m³**
  - **Others** **180 m³**

Disposal Strategy:

- **Interim Storage** **min. 30 yrs.**
- **Deep underground disposal**
  - since 1977 Gorleben salt dome
  - 2012 "Site Selection Law"

* from LaHague and Sellafield

Non heat producing wastes ca. 280 000 m³

- **NPP operation:** **300 m³/yr**
- **Others**
  - Decommissioning
  - Research
  - Industry
  - Medical applications
  - Scales

Disposal Strategy:

- **Deep underground disposal**
  - Konrad abandoned iron ore mine
  - Licenced since 2002/2006
  - Start of operation 2019

Quelle: BfS 2011

Project: Preliminary safety analysis for Gorleben (vSG)

- **Analysis of the suitability of the Gorleben site on the basis of a preliminary Safety Case**
  basing on:
  1. Preliminary safety analysis with emphasis on **long-term safety**, showing in a comprehensible, documented and traceable way if and under which conditions a safe disposal is possible at the site.
  2. Development of an optimized **disposal concept** under consideration of operational safety.
  3. Determination of additional required (future) **research** and **exploration** needs
- Present state of **science and technology** and all timely available **results of exploration**.

Structure of vSG

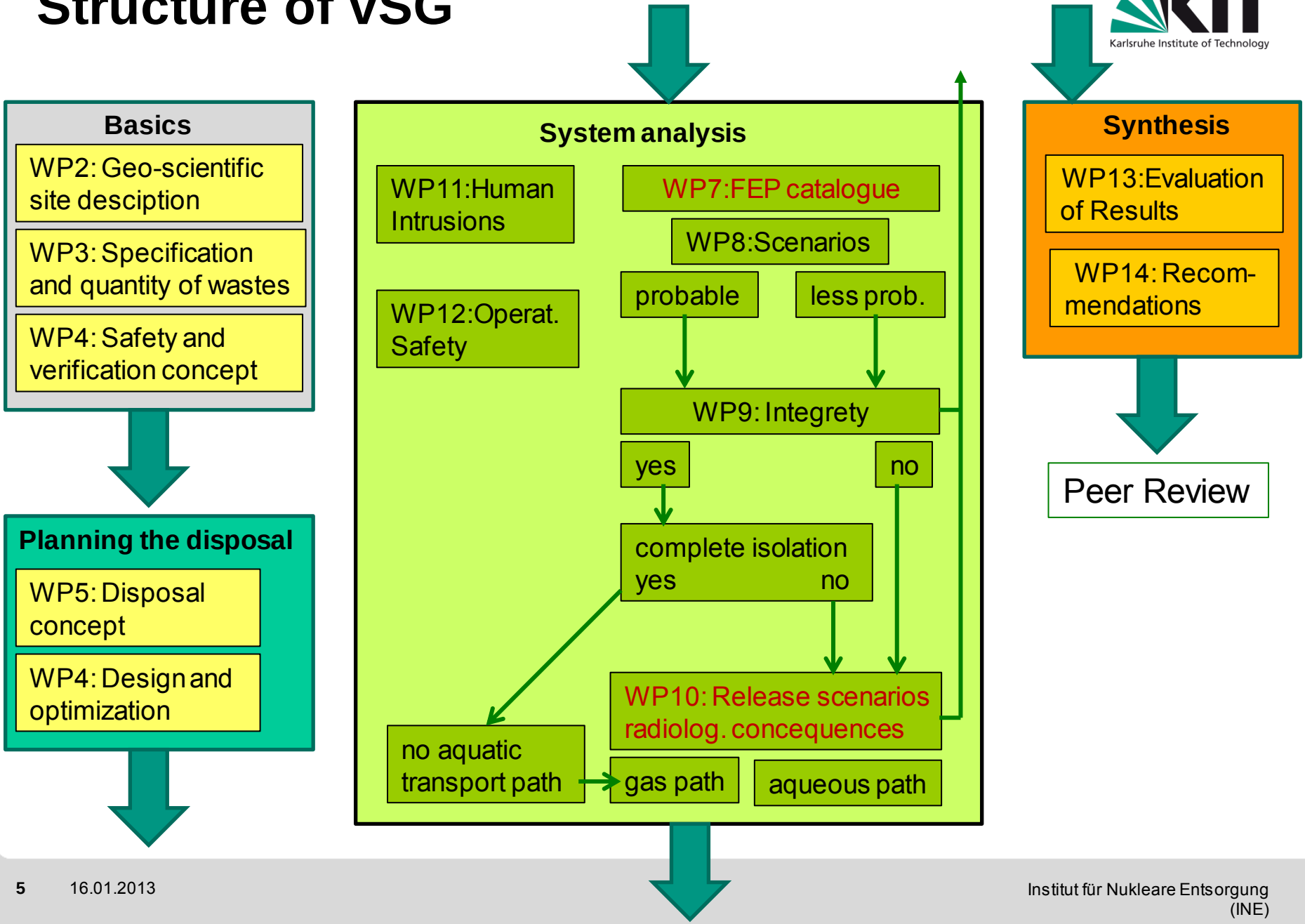

Source term for heat producing wastes

- HLW glass
  - Temperature dependence of HLW glass dissolution
  - Kinetics of HLW glass dissolution
- Spent nuclear fuel from LWRs
  - Instant release fraction
  - Matrix dissolution
- Temperature effects
  - Radiolytic reactions
  - Spent nuclear fuel corrosion
- Compacted hulls, end pieces and spacers (CSD-C waste)
- Boundary Conditions
- Radionuclide source term
  - Kinetically controlled radionuclide mobilization
  - Thermodynamically Controlled Radionuclide Mobilization
- Radionuclide solubility
- Sorption

Boundary conditions

- Inventories
- Types of wastes / canisters / backfill
  - Thick-walled canisters, corrosion allowance by carbon steel
- Disposal concept: Ratio of waste mass / volume to open pore space
- Probable evaluation:
  - Penetration of saturated salt solutions (6m NaCl or 4 m $MgCl_2$ solution)
  - NaCl solution unbuffered
    $6 \leq pH \leq 9$
  - Reducing conditions / consumption of oxygen by steel corrosion
- Hydrocarbon degradation below critical value
- Carbonate-free system

HLW Glass

WAK and Vitrification Plant Karlsruhe (VEK)

WAK (1971-1991)
- Reprocessing of 200 t of spent fuel
- 60 m³ HAWC
- $7.7 \cdot 10^{17}$ Bq

VEK
- 1996 – 1998 constr. mock-up;
- 1999 – 2005 construction VEK
- 2009 – 2010 hot operation;

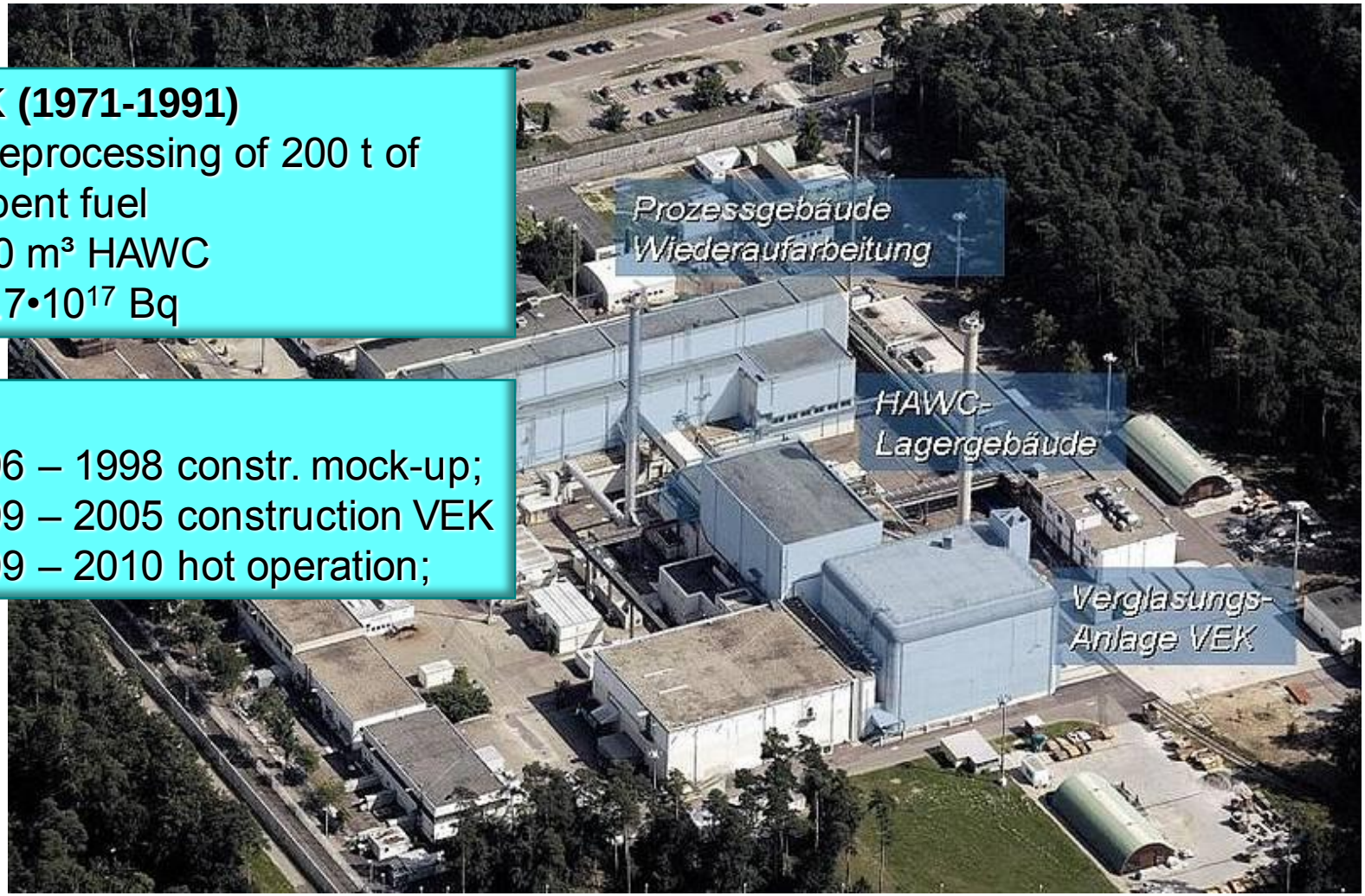

Foto: WAK

Vitrification of High Level Liquid Waste

WAK

60 m³ HLLW

➔ **50 t HLW Glass in**
130 Canisters
5 CASTOR Casks

Operational Data of VEK

- Active operation start: 16.09.2009
- End of vitrification: September 2010
- 130 Canisters filled
- 5 CASTOR containers loaded
- Transport to Interim Storage Facility Febrary 2011
- Decontamination and dismanteling

Glass quality: Test procedures

- **MCC-1** static leaching of monolithic sample at constant temperature (40°C, 90°C), sampling at 3, 7, 14, 28 d
- **MCC-2** static test (elevated temperature)
- MCC-nn ...
- **Soxhlet test** (1879 extraction method)
  evaporation of solvent
  (leaching in distilled water)

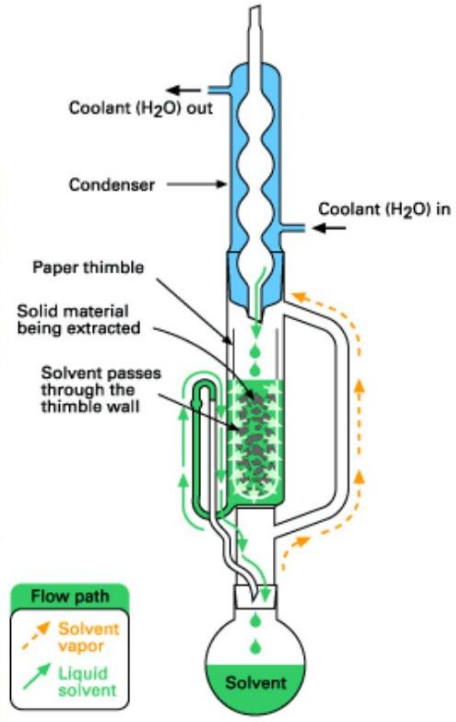

- **Immersion Tests**
  powder, fragments,
  relevant groundwater

Glass Corrosion

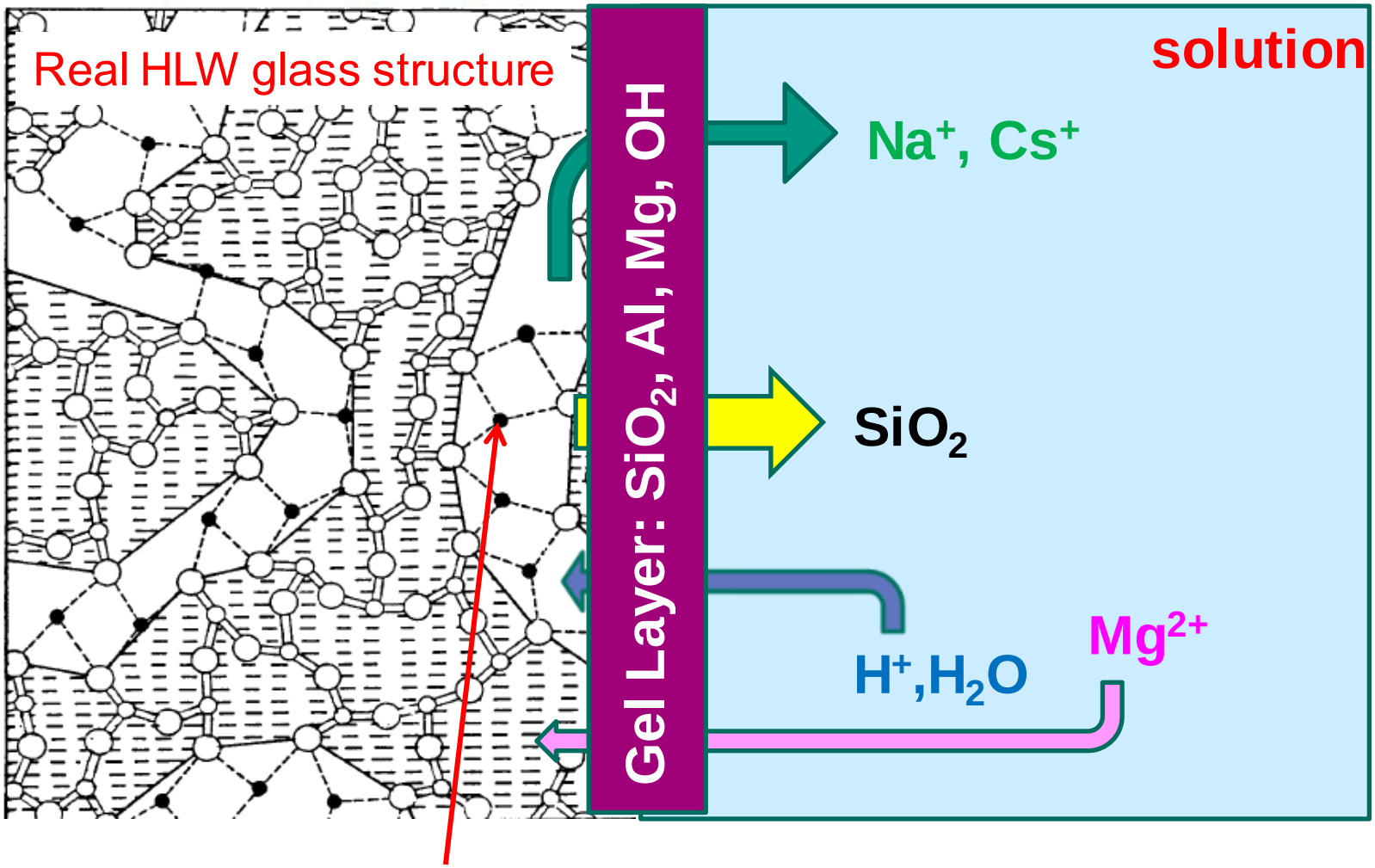

Network formers:
Si, B

Network modifiers:
Na, K, Ca, Cs, ...

Present investigations on HLW glass

Examination of the VEK-glass samples by Raman spectroscopy

Objectives:

- Investigation of homogeneity of VEK glass with respect to RN / glass constituents
- Precipitates of noble metal
- crystalline oxides enriched in radionuclides

Materials:

Sample	Mass / g	Dose rate / mSv/h
#23 (3 fragm.)	0.4365	450
#57 (1 big, 2 small fragm., + particles)	1.033	500
#71 (1 fragm.)	0.750	500

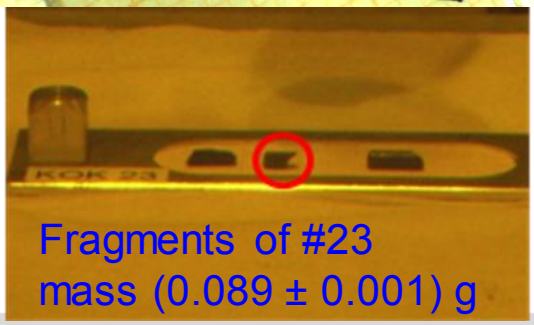

Raman spectroscopy of the VEK-glass

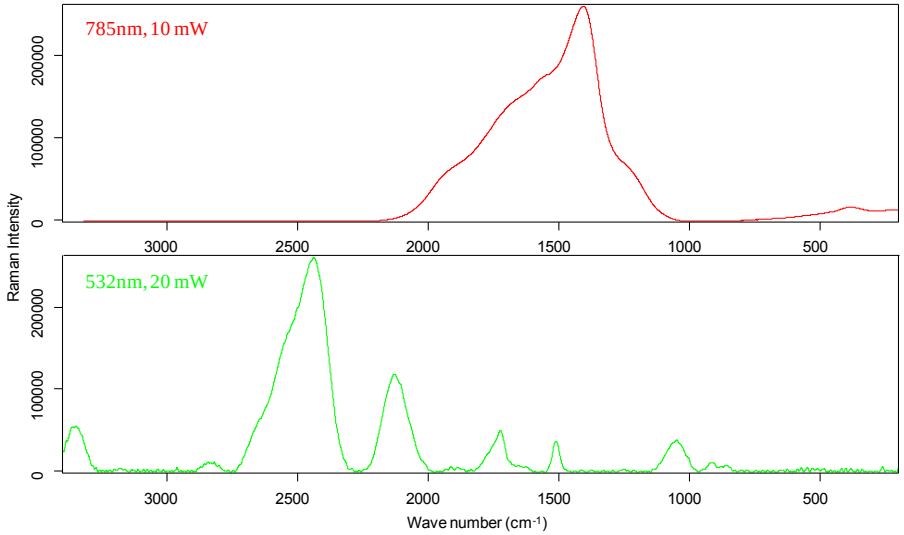

Raman spectra of inactive sample
- laser of 785 nm at 10 mW (red spectra),
- laser of 532 nm at 5 mW (green spectra)

Comparison of Raman spectra @ 785 nm
- VEK 57-2 (blue line)
- VEK 23-1(green line)
- inactive glass (red line) .

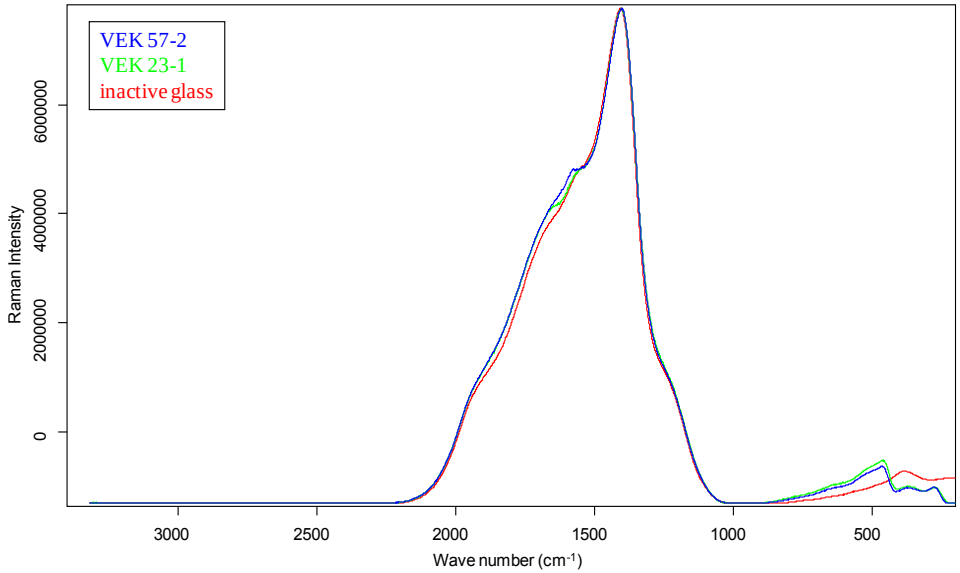

Results:

- high fluorescence intensities @ 785 nm.
- different glass fragments did not reveal significant differences
- and did not allow any conclusion about
  - phase separations or
  - presence of precipitates in the glass.

Spent Nuclear Fuel

Experiments - Disposal

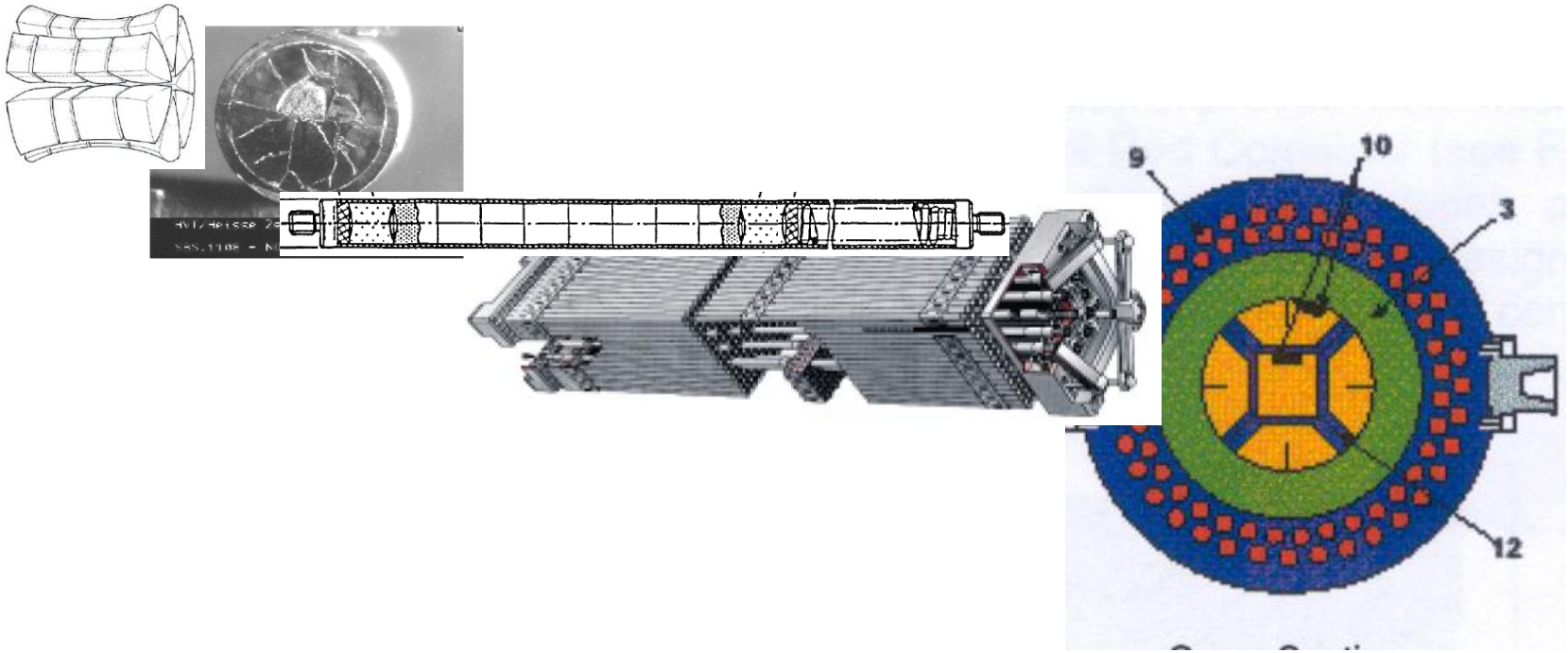

Complex structure of spent fuel

Cladding: C

Gap region: C, I, Cs, Se,

Enriched rim: Pu

Spent fuel

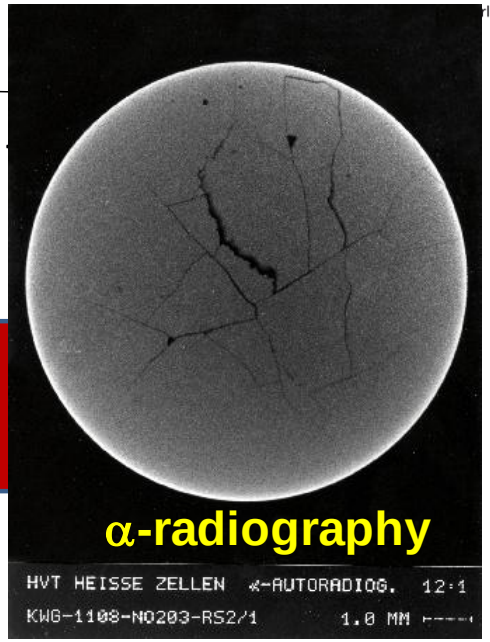

fuel grains
U, Pu, Ln, Sr

fission gas bubbles
Kr, Xe, I

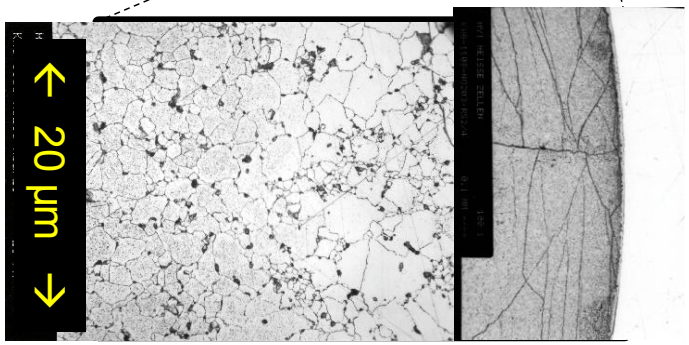

ε-particles
metallic precipitates
Mo, Ru, Pd, Tc, Rh
Ag, Cd, In, Sb, Sb

oxide precipitates
Rb, Cs, Ba, Zr, Nb
Mo, Tc

Grain boundaries
C, I, Cs, Se, Tc

Rim
enriched with Pu

Definition of instant / fast release

Project related definition or PA related definition

RN release by matrix corrosion
controlled by radiolysis,
hydrogen, Cl-....

↔

initial (fast) release of RN
controlled by chemistry of fuel,
spatial distribution,
burn-up, lin. power
(reactor operation)

- gap
- large cracks
- grain boundaries
  - close to surface
  - rim
  - grain boundaries along cracks

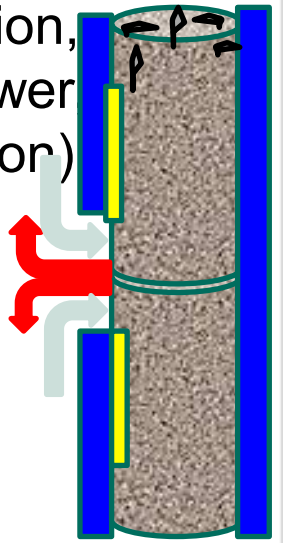

Euratom 7th Framework Programme Collaborative Project "Fast / Instant Release of Safety Relevant Radionuclides from Spent Nuclear Fuel": FIRST-Nuclides

1. Partners / Beneficiaries

Hungarian Academy of Sciences, Centre for Energy Research

2. Associated Groups (AG)

Groups participating at their own costs with specific RTD contributions or particular information exchange functions, or mobility measures (for European AGs only)

Used (spent) nuclear fuel interactions

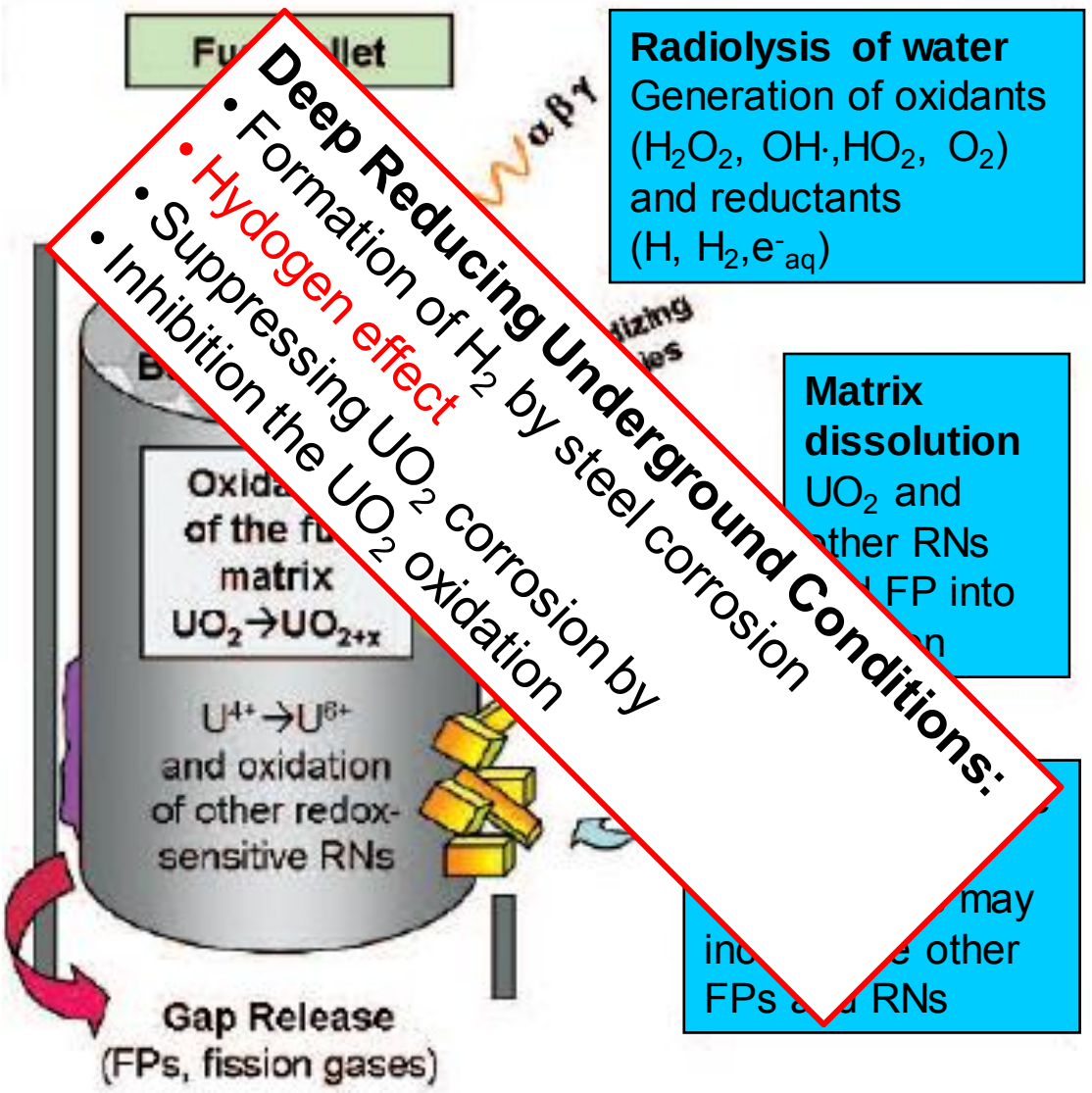

RN Release from Spent Nuclear Fuel: H_2 versus Br^- Effect

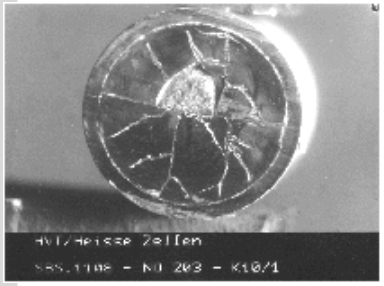

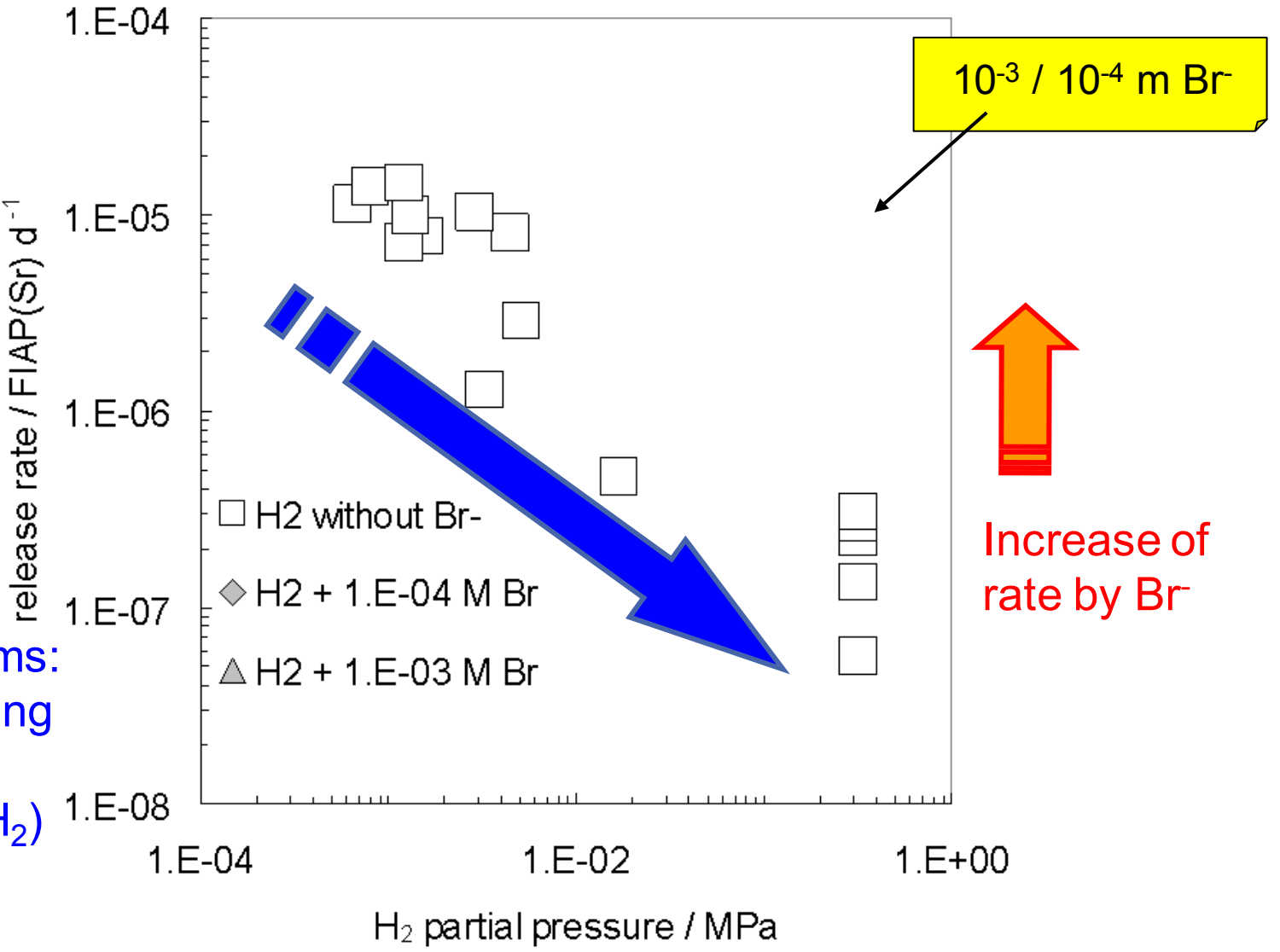

Br^- free systems: Rate decreasing with increasing $p(H_2)$

Metz et al., Radiochim. Acta 96, 1-12 (2008)

Details

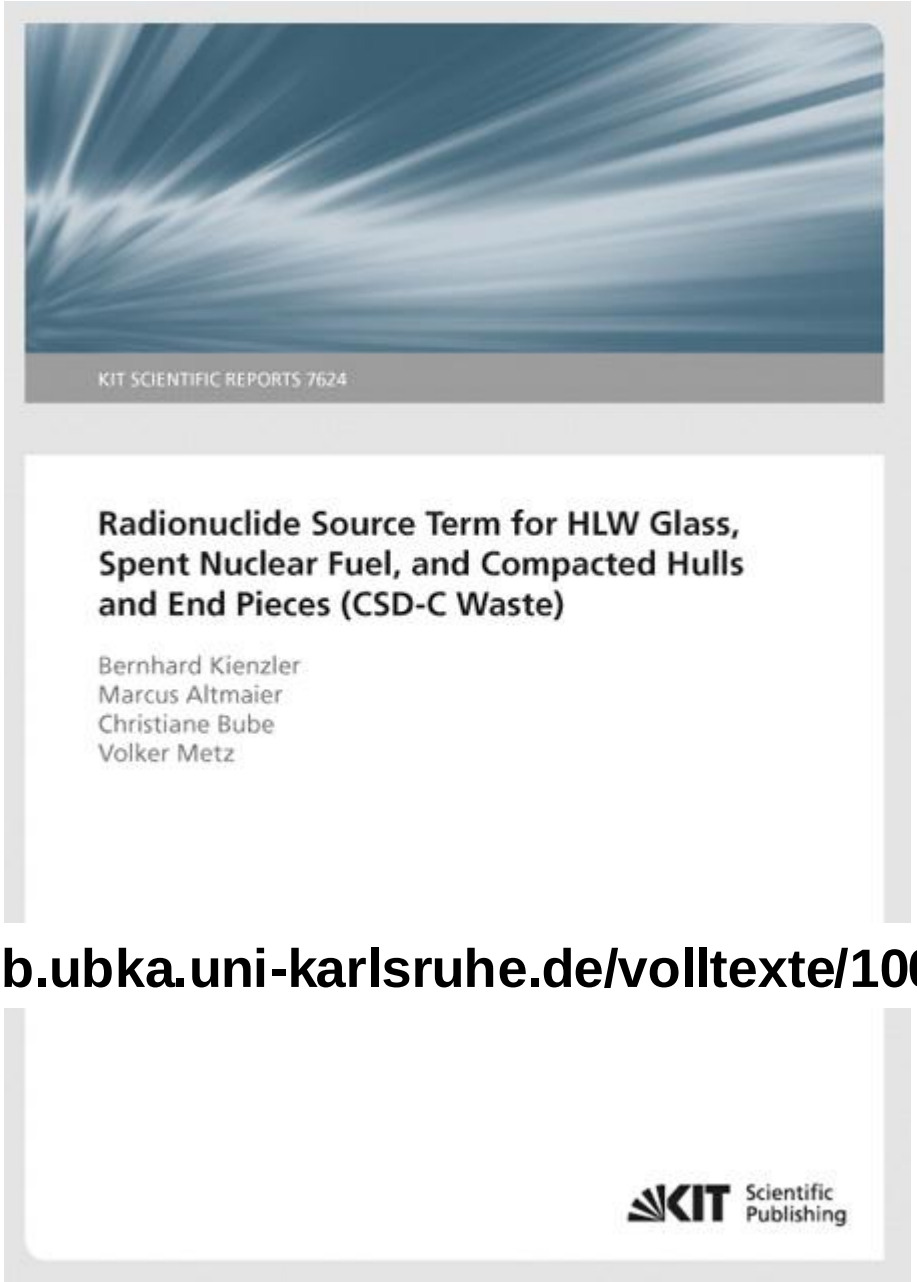

http://digbib.ubka.uni-karlsruhe.de/volltexte/1000029420

Summary

- Source terms for heat producing wastes under potential rocksalt conditions ✓
- Source terms for non-heat producing wastes under potential rocksalt conditions ✓
- Variation of boundary conditions ✓
- Identification of open questions
- Filling the gaps by
  - in-house R&D
  - third party funded R&D projects
  - international projects (EU) and networks

Radio-nuclides Migration Research to Support Geological Disposal of HLW in CIAE

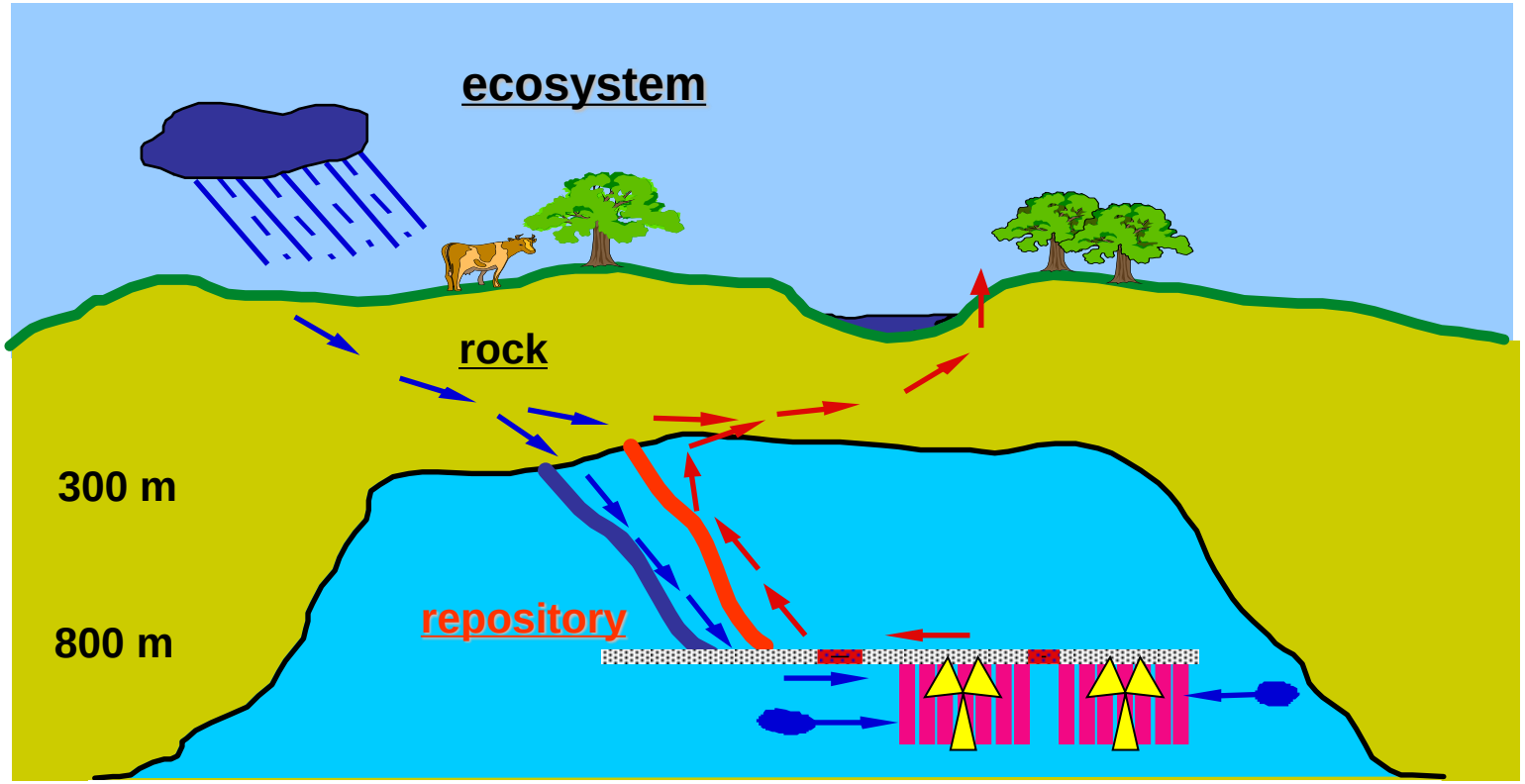

ZHOU Duo，ZHANG Zhen-tao，WANG Bo，LONG Hao-qi，
BAO Liang-jin，CHEN Xi，SONG Zhi-xin，JIANG Tao

原子能院

Outline

1. Introduction
2. Beishan Granite and Groundwater Composition and Properties
3. Disposal Behavior of Simulated Glass
4. Chemical Behavior of Key Nuclides in Groundwater
5. Interaction of Radio-nuclides with Medium
6. Problems of Disposal Chemical Research
7. Consideration and Prospect

1. Introduction

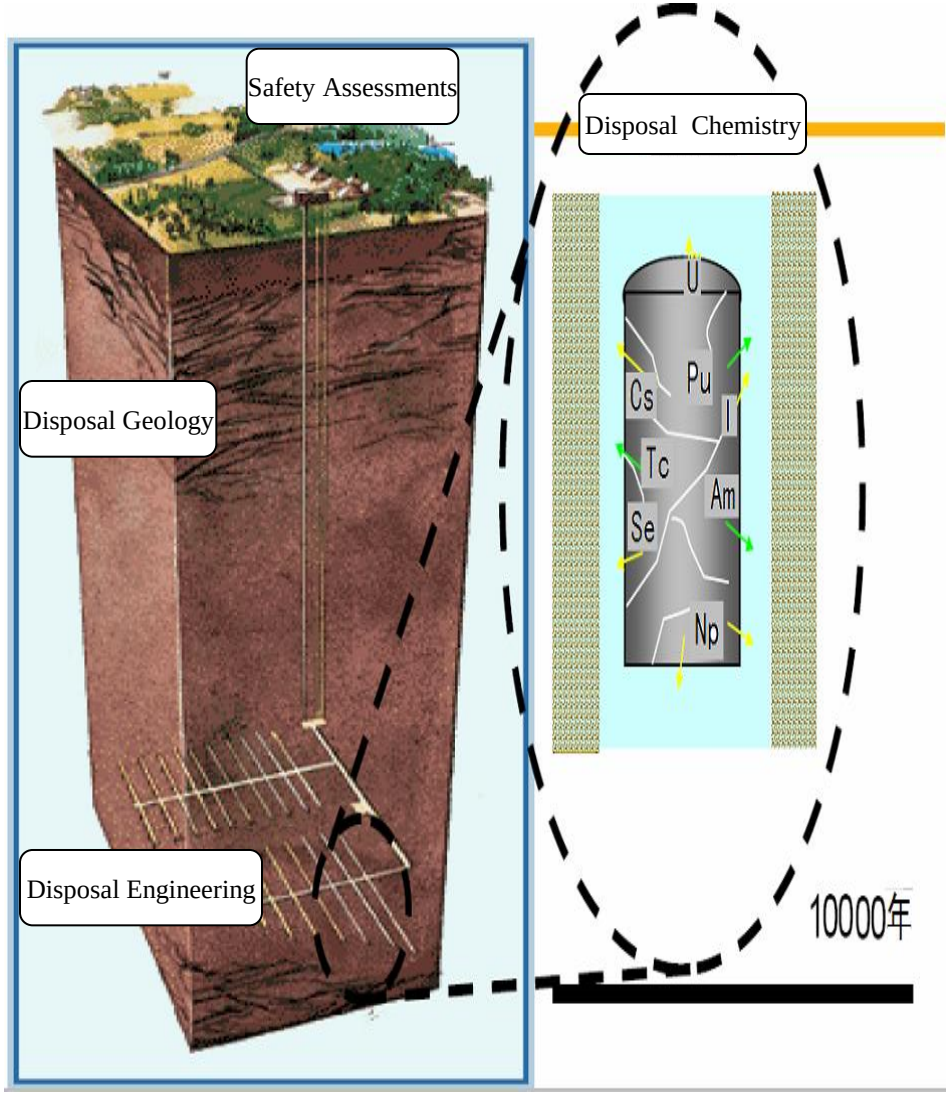

- The deep geological disposal is internationally recognized feasible as a safe disposal of HLW.
- The core task for deep geological disposal of HLW is to contain radio-nuclides as much as possible and to retard the radio-nuclides migration with the help of multiple barrier means.
- Current research in CIAE is more focused on geochemical behavior of key radio-nuclides such as neptunium-237 (^{237}Np), plutonium-239 (^{239}Pu), americium-241 (^{241}Am) and technetium-99 (^{99}Tc) in groundwater intrusion scenario.

2. Beishan Granite and Groundwater Composition and Properties

Table 1. Beishan Granite Component

Species	percent
Na_2O	4.51%
MgO	3.76%
Al_2O_3	16.46%
SiO_2	55.22%
P_2O_5	0.89%
K_2O	3.43%
CaO	6.00%
TiO_2	1.37%
MnO	0.09%
Fe_2O_3	1.50%
FeO	4.35%
CO_2	0.68%
H_2O^+	1.24%

The granite is mainly composed of silicon oxide(SiO_2) and aluminum oxide(Al_2O_3); Ferrous oxide (FeO) and ferric oxide (Fe_2O_3) are minor components.

Properties: Low hydraulic conductivity, low diffusion constant and high sorption

2. Beishan Granite and Groundwater Composition and Properties

Table 2. Beishan Groundwater Composition

Species	Concentration， mM
Na^+	47.89
K^+	0.37
Ca^+	6.02
Mg^+	2.12
HCO_3^-	2.18
Cl^-	50.44
SO_4^{2-}	14.8
F^+	0.17
NO_3^+	0.48
Total Alkalinity	109 mg/L
Total Carbonate	2.32
pH	7.58
Eh(mV)	-200
Ionic Strength (mM)	~130

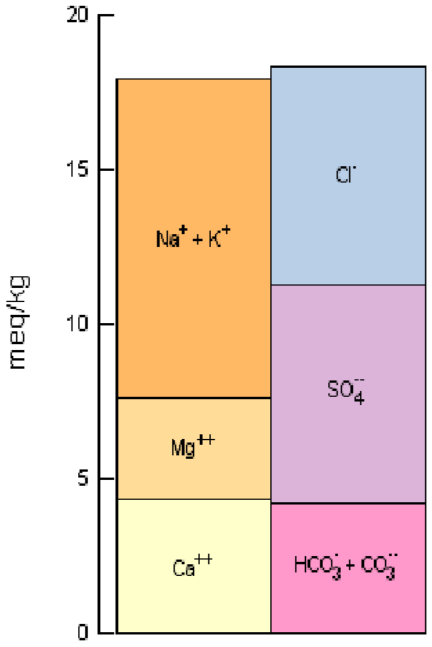

There are several main components of groundwater which is from geological voids,

- Cation： **Na^+, Ca^{2+},** Mg^{2+}, K^+, Fe^{2+}, Fe^{3+};
- Anion： **Cl^-, SO_4^{2-},** HCO_3^-, CO_3^{2-}, F^-, NO_3^-.

Properties: Slightly alkaline and strongly reducing

3. Disposal Behavior of Simulated Glass

Leaching behavior of key frame elements was investigated at 150℃ and 90℃ in our lab.

- At 150℃, sudden alteration phenomenon happened for simulated glass with action of groundwater, which results in **substantial leaching** for key frame elements (Na, Li, Si, Al);
- While at 90℃ corrosion just only happened on the surface of simulated glass, which leads to **gentle leaching**.

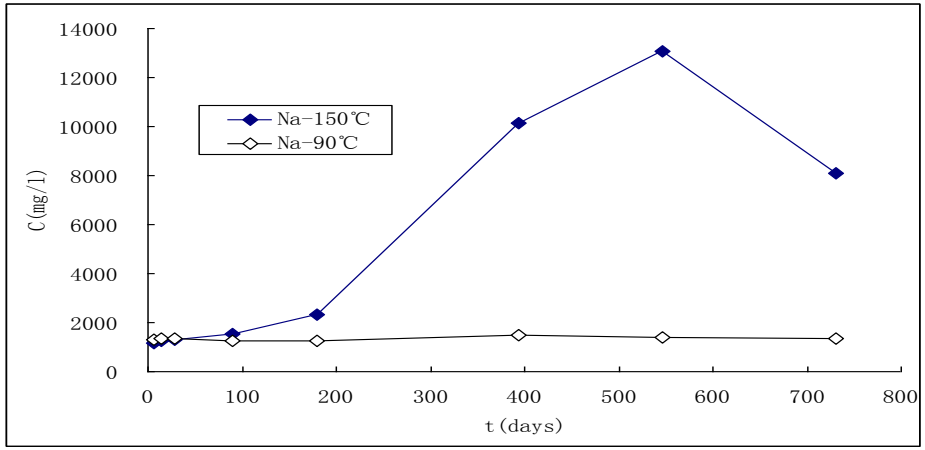

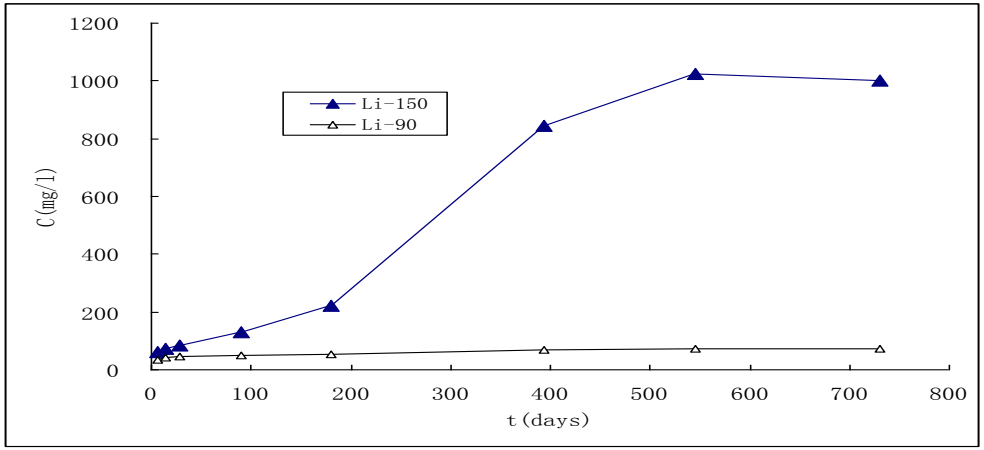

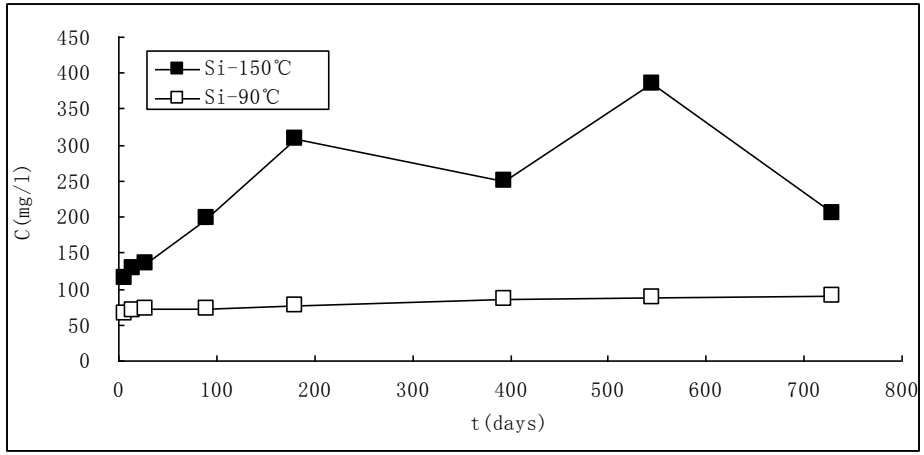

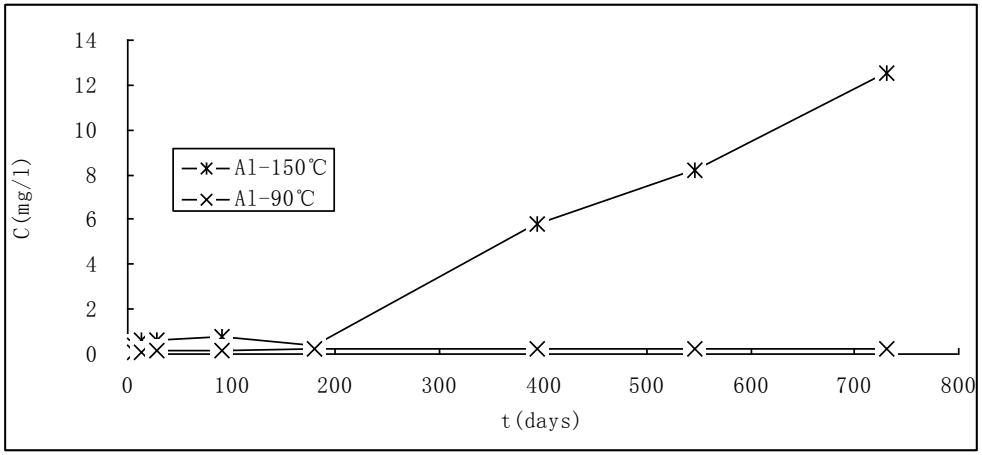

3. Disposal Behavior of Simulated Glass

Leaching behavior of radioactive substitute elements was investigated at 150℃ and 90℃ in our lab.

- At 150℃, **60 percent** of molybdenum(Mo) as Tc substitute is leaching out from simulated glass;
- While at 90℃, **little** Mo only on the glass surface is leaching out.

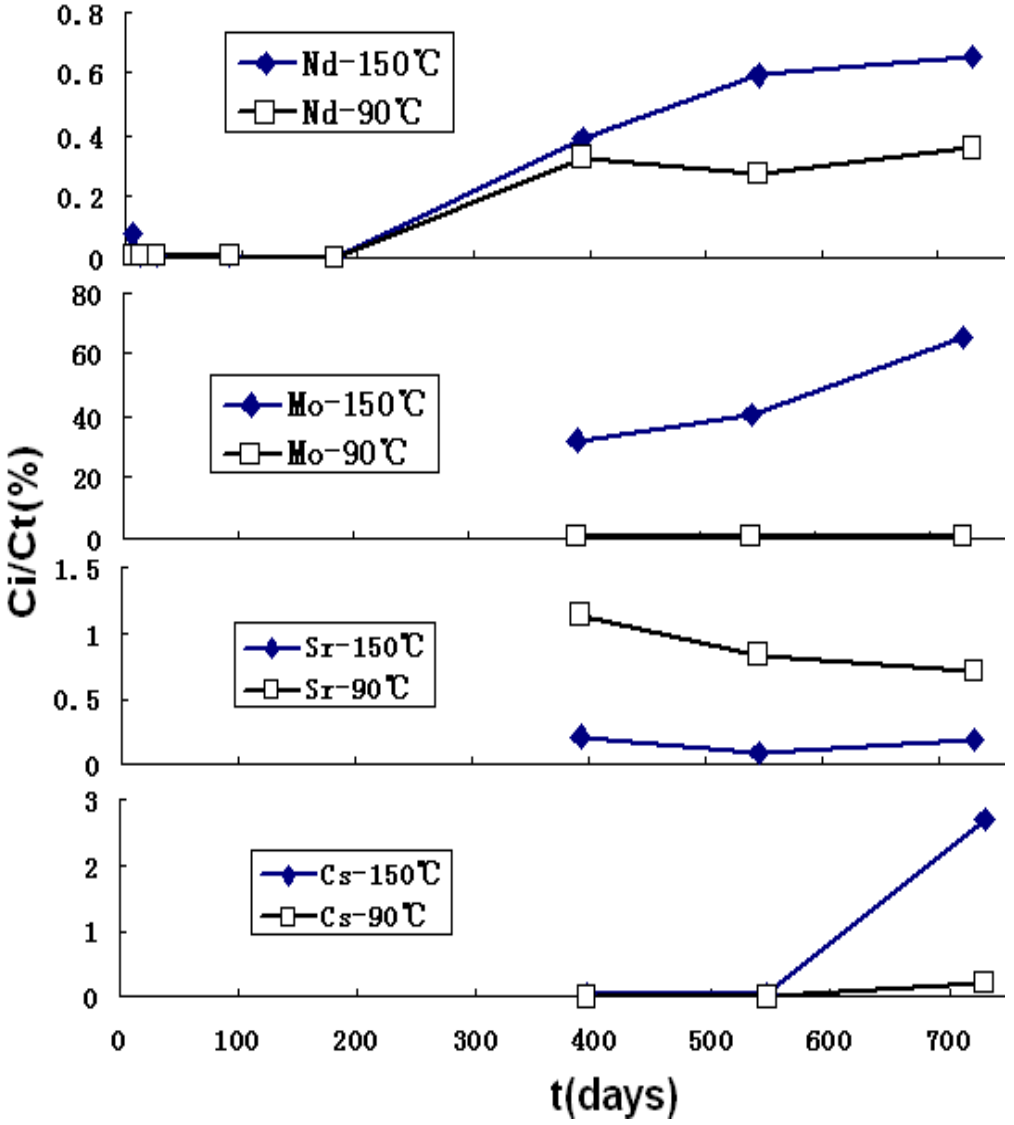

3. Disposal Behavior of Simulated Glass

Corrosion behavior: Large amounts of secondary product formed at high temperature (150℃)

- With simulated glass soaked in groundwater for **394** days, in the soaking liquid emerged **some acicular crystal**, in which silicon (Si) and oxygen (O) are main elements, a preliminary judge for **quartz**;
- With simulated glass soaked in groundwater at for **546** days, in the soaking liquid emerged **some white powder**, in which silicon (Si) , sodium (Na) and oxygen (O) are main elements, a preliminary judge for **zeolite**;
- With the simulated glass soaked in groundwater for **730** days, the bulk glass had altered, **abundant of white powder formed, the crystal shape is cubic**, the main elements of the bulk are sodium (Na) and boron (B), a preliminary judge for borate.

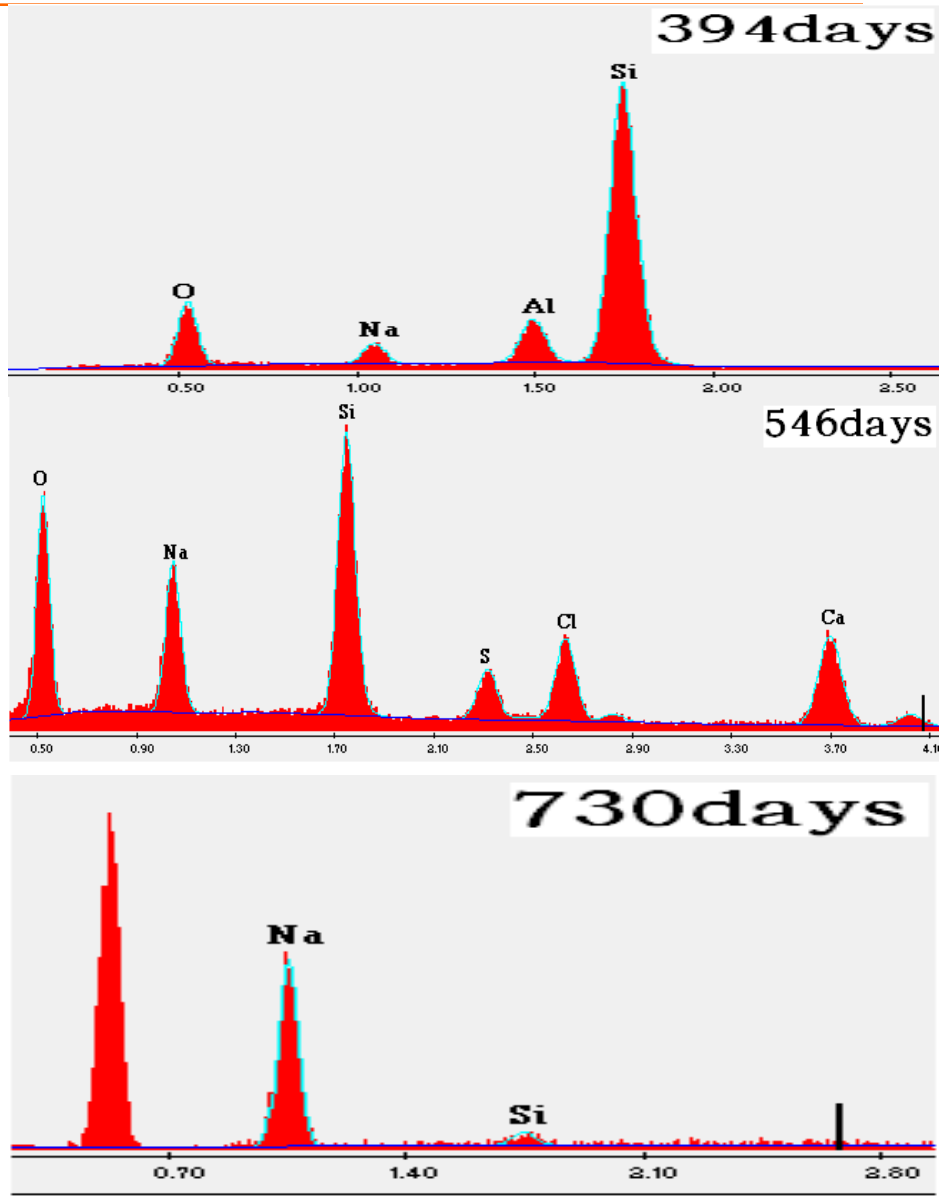

Frame elements spectrogram of secondary product with EDS

3. Disposal Behavior of Simulated Glass

Corrosion behavior: continuous alteration reaction occurred at high temperature (150℃)

- With glass soaked in groundwater at 150℃, a large number of Si is leaching out from glass. When concentration of Si in the soaking liquid reached saturation, **quartz** would form.
- As the reaction progresses, lots of silicate mineral phase such as **zeolite** (which is more stable than glass) would form and the glass would be destroyed.
- At the same time, large amounts of boron (B) and sodium (Na) elements are released, which results in super-saturation for B and Na, so **borate** would form.

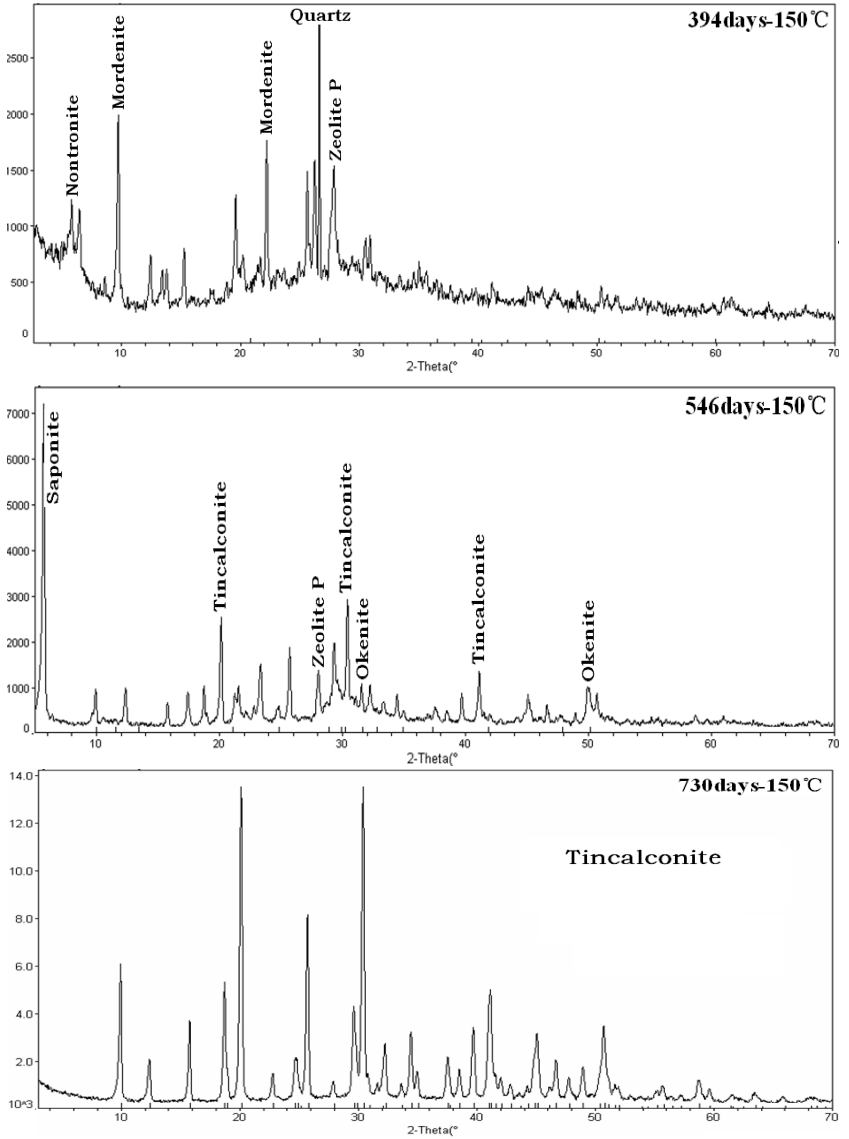

Crystal phase spectrogram of corrosion product with XRD

4. Chemical Behavior of Key Nuclides in Groundwater

Solubility and Species

Table 3. Solubility data of radio-nuclides in underground water

nuclides	pH	Solubility (mol/L)	valence	control phase
Np(Ⅴ)	8.4	5×10^{-5}	98.5% Np(Ⅴ)	NpO_2OH
Np(Ⅳ)	8.0	1×10^{-8}	100% Np(Ⅳ)	$Np(OH)_4$
Pu(Ⅳ)	8.4	1×10^{-8}	100% Pu(Ⅳ)	$Pu(OH)_4$
Tc(Ⅳ)	8.0	3×10^{-9}	100% Tc(Ⅳ)	$TcO(OH)_2$
Am	8.1	5×10^{-10}	100% Am(Ⅲ)	$Am(OH)_3$

- Neptunium, plutonium and technetium exist as tetra-valent species in reducing environment, which results in low solubility. Control phase in Table 3 is speculated by authors.
- The pH and carbonate concentration become the main factors affecting solubility through hydrolysis and complex reaction.
- In the range of pH 7-10, pH variation has little effect on solubility of tetra-valent species such as Np(Ⅳ), Pu(Ⅳ), Tc(Ⅳ).
- Complex reaction of Pu(Ⅳ) and Am(Ⅲ) with CO_3^{2-} ion results in increased solubility; There is no obvious increase for solubility of Np(Ⅳ) and Tc(Ⅳ) with the concentration of CO_3^{2-} increasing.
- Solubility of Pu(Ⅳ) and Am(Ⅲ) decreases remarkably with temperature increasing.
- Solubility of Np(Ⅳ) both in pure water system and in the Beishan groundwater increases with temperature increasing.

4. Chemical Behavior of Key Nuclides in Groundwater

Colloidal Behavior-Ultracentrifugation Method

	storage time	ionic strength	pH	humic acid	centrifugal speed/rpm	stacking density /(kg/m^3)
Np colloidal quantity	↗	↗	↗	↗	60000-100000	2150
Pu colloidal quantity	↗	no significant effect	↗	no effect	80000-100000	8896
Tc colloidal quantity	↘	↘	no significant effect	↗	40000-100000	5485

Colloidal stacking density of Np is far less than that of Pu and Tc, which shows Np colloid is mainly pseudo colloid.

Humic acid concentration has almost no effect on the formation of colloidal Pu, which illuminates that real colloid come into being.

4. Chemical Behavior of Key Nuclides in Groundwater

Colloidal Behavior-Ultrafiltration Method for Pu, Am Colloidal Research

- Tetra-valent Pu(Ⅳ) mainly exists as ionic form in pure water, while in groundwater colloid is main existent form of Pu(Ⅳ).
- Existence of Pu (IV) colloid makes concentration 2 orders of magnitude higher than solubility of Pu(Ⅳ) in groundwater.
- Colloidal granularity of Pu(Ⅳ) is mainly distributed between 100 nm and 450 nm, the proportion of Pu(Ⅳ) colloidal quantity in groundwater is about 85%.

- Am mainly exists as large colloidal form in groundwater, while in pure water, Am exists as small colloidal form.

- Colloidal research with membrane filter method for Am and Pu in groundwater, shows that Am mainly exists as pseudo colloidal form, Pu mainly exists in the form of real colloid.

4. Chemical Behavior of Key Nuclides in Groundwater

Redox Behavior

Pu

- Hydrogen peroxide (H_2O_2) can reduce penta-valent Pu(Ⅴ) into tetra-valent Pu(Ⅳ) which further hydrolyzes to form colloid;
- The increase of pH, temperature and concentration of H_2O_2 leads to increase of reductive rate;
- The existence of cations such as K^+, Ca^{2+}, Mg^{2+} has no significant effect on reductive rate of Pu(Ⅴ), while existence of anions leads to increase of reductive rate of Pu(Ⅴ). (sequence of ability: F^-〉 SO_4^{2-}〉 HCO_3^-〉 Cl^-)
- Granite powder can reduce penta-valent Pu(Ⅴ) into tetra-valent Pu(Ⅳ) most of which is adsorbed on surface of granite, reductive rate increases with pH and temperature increasing.

Tc

- In alkaline water, iron powder can reduce pertechnetate (TcO_4^-) into technetium dioxide dihydrate ($TcO_2 \cdot 2H_2O$) which is easily oxidized to TcO_4^- by solution of hydrogen peroxide (H_2O_2).
- TcO_4^- in distilled water can be reduced to tetravalent Tc(Ⅳ) by bivalent tin (Sn(Ⅱ)), the redox reaction equation can be expressed as: 3Sn(Ⅱ) + 2Tc(Ⅶ)→3Sn(Ⅳ) + 2Tc(Ⅳ).
- In alkaline water, activation energy Ea for reduction of TcO_4^- by Sn(Ⅱ) is 29.08 kJ/mol, the reaction rate equation is: $-dc_{(TcO4-)}/dt = k \cdot c_{(TcO4-)} \cdot c_{(OH-)} - 0.478 \cdot c_{(Sn(Ⅱ))} \cdot 0.629$.

5. Interaction of Radio-nuclides with Medium

Adsorption Kd of Np, Pu, Am and Tc in various medium was determined with batch experimental under anoxia atmosphere at normal temperature, which results are listed in table 4.

Table 4. Adsorption Kd (ml/g) value of Np, Pu, Am, Tc in various medium

	Iron powder	Ferrous oxide (FeO)	Ferric oxide (Fe_2O_3)	Ferroferric oxide (Fe_3O_4)	bentonite	granodiorite	crack infilling
Np	**~3×10³**	-	-	**~1×10³**	30~90	**~1×10³**	~8×10²
Pu	**~2×10⁴**	**~1×10⁴**	**~2×10⁴**	**~1×10⁴**	**~3×10³**	**~2×10³**	-
Am	-	-	-	-	**~1×10⁴**	**~3×10³**	-
Tc	**~2×10³**	~500	~3	~7	10~80	**~3×10³**	-

Adsorption Kd of Pu and Am on bentonite and granite is vary large, so that Pu and Am in repository can be strongly blocked and contained in the near field and far field of repository;

Adsorption Kd of Np and Tc on granite is vary large, while that on bentonite is smaller, which indicates the near field has weak blockade and tolerance for Np and Tc.

With strong adsorption properties, Fe can strong block migration of Np, Pu and Tc.

5. Interaction of Radio-nuclides with Medium

Effect of Temperature on Sorption of Np

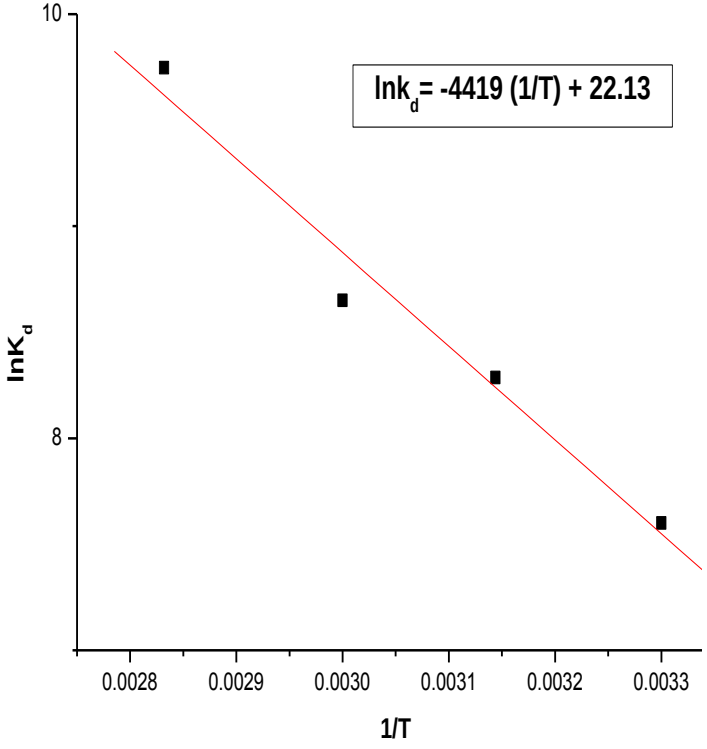

Table 5. Adsorption Kd of Np(Ⅳ) on Granite at different Temperature

Np（Ⅳ）	30℃	45℃	60℃	80℃
Kd(ml/g)	1593	1711	2152	2183
△H^o （KJ·mol^{-1}）	36.7	36.7	36.7	36.7
△S^o （J·mol^{-1}·K^{-1}）	184.0	184.0	184.0	184.0
△G^o （KJ·mol^{-1}）	－19.0	－21.7	－24.5	－28.2

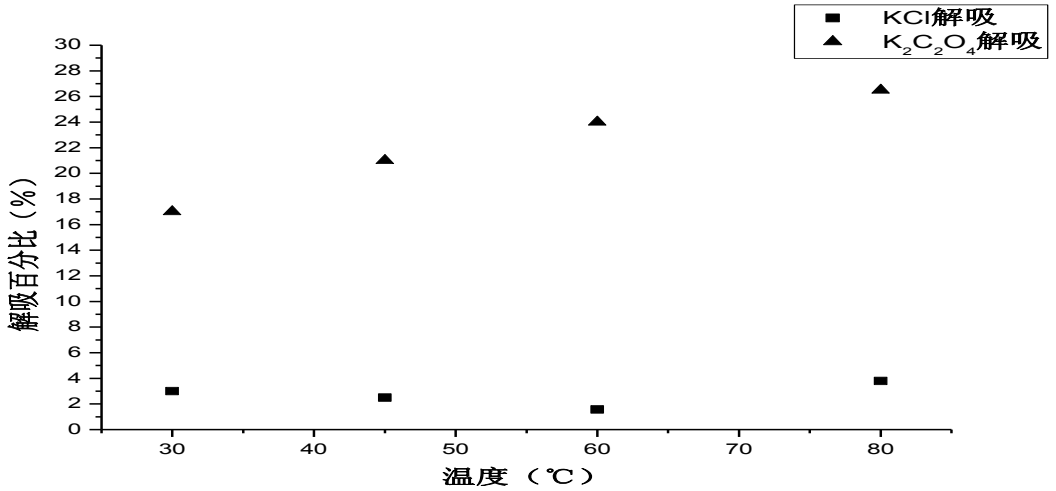

- Kd values of Np adsorbed on granite samples increase with temperature increasing.
- Temperature has little effect on the desorption percentage (1.6%~3.8%) in potassium chloride (KCl) solution which can desorb Np(Ⅳ) adsorbed electro-statically on granite samples.
- Desorption percentage (17%～26.5%) in potassium oxalate($K_2C_2O_4$) solution increases with temperature increasing, $K_2C_2O_4$ solution can desorb Np(Ⅳ) in amorphous phase minerals.

5. Interaction of Radio-nuclides with Medium

Effect of Temperature on Adsorption of Am

Table 6. Adsorption Kd and desorption Kd' of Am in granite

t (℃)	30℃	45℃	60℃	80℃
Kd (10^4ml/g)	0.28±0.02	0.62±0.03	2.60±0.43	8.20±0.54
Kd' (10^5ml/g)	0.14±0.01	0.80±0.06	2.28±0.13	3.12±0.23

Table 7. $\triangle H^o$、$\triangle S^o$、$\triangle G^o$ for adsorption of Am on granite

T（℃）	30℃	45℃	60℃	80℃
$\triangle H^o$ (kJ/mol)	60.0	60.0	60.0	60.0
$\triangle S^o$ (kJ•K^{-1}/mol)	0.27	0.27	0.27	0.27
$\triangle G^o$（kJ·mol^{-1}）	-19.7	-23. 7	-27. 8	-33. 2

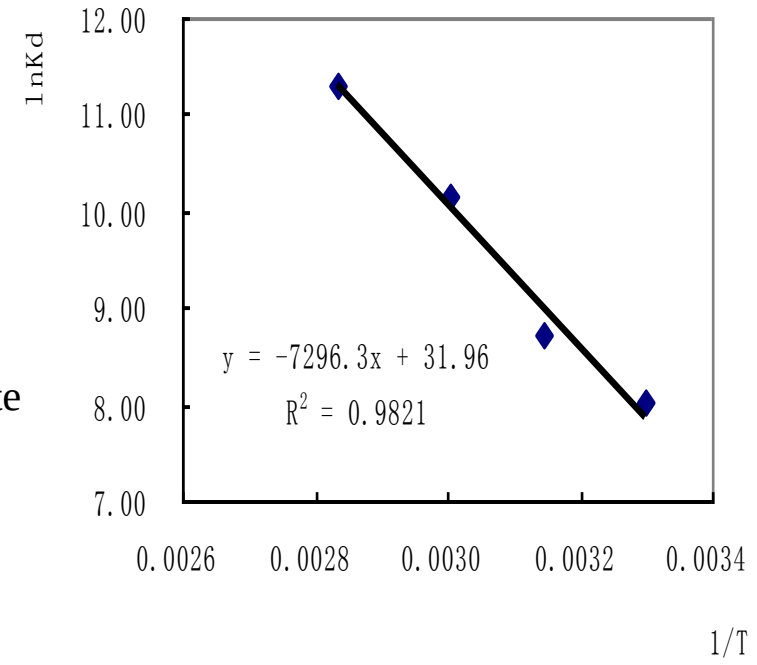

Kd values of Am adsorbed on granite samples increase with temperature increasing.

High temperature is favorable for the adsorption of Am on granite.

Adsorption Kd of Am on granite samples at different temperatures are less than desorption Kd' value, which indicates the adsorption is irreversible.

5. Interaction of Radio-nuclides with Medium

Effect of Temperature on Adsorption of Tc

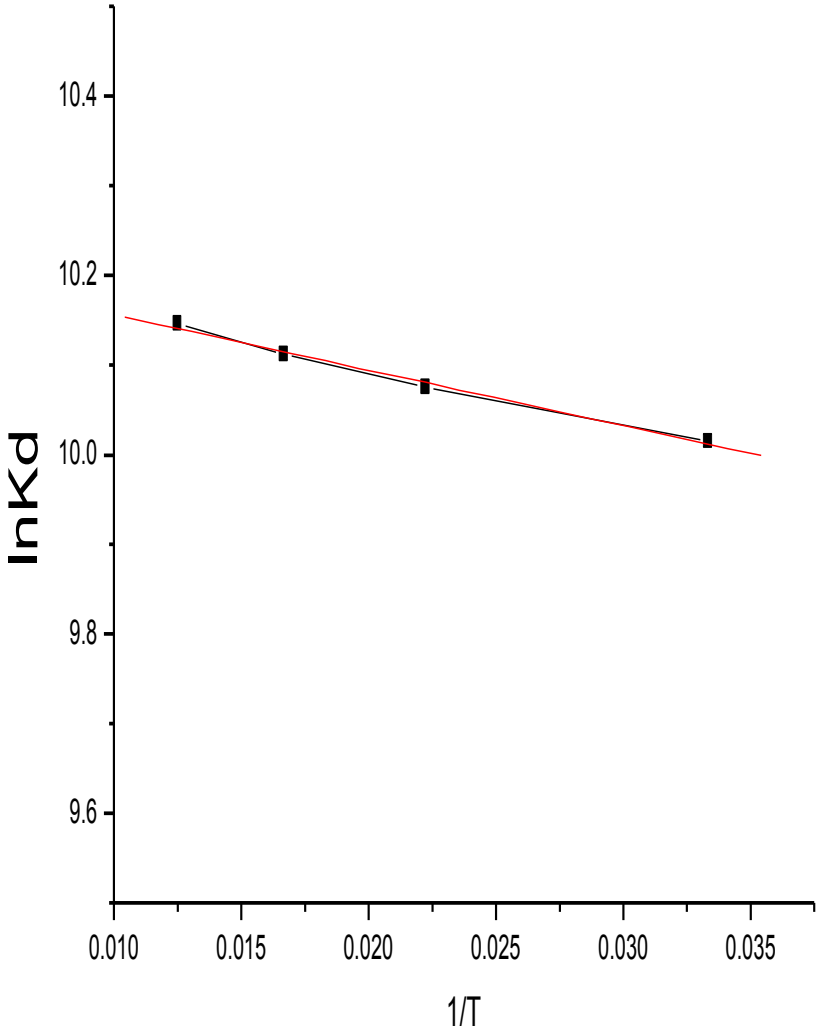

Table 8. Adsorption Kd and ΔG of ^{99}Tc on granite

temperature	30℃	45℃	60℃	80℃
Kd(ml/g)	1439.82	2306.17	2849.50	3079.50
ΔG(kJ/mol)	-25.68	-26.96	-28.23	-29.92

Kd of hepta-valent Tc(Ⅶ) in granite samples increases with temperature increasing.

On the large area of mineral surface, hepta-valent Tc(Ⅶ) is reduced into tetra-valent Tc(Ⅳ) which has low solubility.

The free energy is negative, which indicates that the adsorption reaction is a spontaneous reaction.

5. Interaction of Radio-nuclides with Medium

Free-aqueous Diffusion Coefficient of Np, Pu, Tc

Table 9. Effect diffusion coefficient of Np, Pu, Tc and its influence factors

pH=8.46	D(m^2/s)	Activation energy (kJ/mol)	Temperature	Viscosity	pH	Concentration of Fe^{2+} or Sn^{2+}
Np(35℃)	1.32×10^{-10}	49.80	T↑D↑	η↑D↓	pH↑D↓	Fe^{2+}↑D↓
Pu(35℃)	1.32×10^{-10}	150.6	T↑D↑	η↑D↓	pH↑D↑	Fe^{2+}↑D↑
Tc(30℃)	2.92×10^{-9}	15.42	T↑D↑	η↑D↓	pH↑D↓	Sn^{2+}↑D↓

Free-aqueous diffusion coefficients of Np, Pu, Tc increase with temperature increasing.

Free-aqueous diffusion coefficients of Np, Pu, Tc decrease with viscosity increasing.

5. Interaction of Radio-nuclides with Medium

Diffusion Coefficient within Matrix

Table 10. Diffusion coefficients of Np, Pu, Tc in bentonite and granite

	atmosphere	groundwater	bentonite		granite
		capillary	static back-to-back	dynamic constant source	dynamic constant source
$D_{Tc}(m^2/s)$	air	2.9×10^{-9}	1.1×10^{-10}	**1.6×10^{-9}**	**$(1\text{-}4)\times10^{-11}$**
	anoxic	-	9.7×10^{-11}	7.1×10^{-11}	-
$D_{Np}(m^2/s)$	air	1.3×10^{-10}	$(4\text{-}8)\times10^{-13}$	**8.2×10^{-12}**	**1×10^{-14}**
	anoxic	-	$(3\text{-}5)\times10^{-13}$	-	-
$D_{Pu}(m^2/s)$	air	1.3×10^{-10}	**2.5×10^{-14}**	-	-
$D_{Am}(m^2/s)$	air	-	**2.5×10^{-14}**	-	-
$D_{Sr}(m^2/s)$	air	-	2.4×10^{-11}	1.6×10^{-12}	-
$D_{Cs}(m^2/s)$	air	-	1.5×10^{-12}	1.4×10^{-11}	-

The diffusion coefficients of Am and Pu in bentonite and granite are very low due to strong adsorption properties of bentonite and granite;

The diffusion coefficients of Tc and Np are relatively bigger, depending on chemical speciation in medium.

Technetium is dominated by pertechnetate (TcO_4^-) in aqueous phase, Neptunium is dominated by penta-valent neptunyl (NpO_2^+).

The negatively charged TcO_4^- diffuses more fast than the positively charged NpO_2^+, due to electrostatic repulsion of negatively charged surface of geological medium.

6. Problems of Disposal Chemical Research

Long-Term Disposal Properties of Glass

(1) Leaching source parameters for glass are seriously lack, which neesd for us to strengthen the research in this field.

(2) Materials of HLW packaging body and disposal container are not identified, the comprehensive research about interaction between glass with buffer backfill materials and groundwater is still very weak;

(3) Certain progress about buffer backfill has been made, but research about material which weakens corrosion of HLW glass and packaging body is vary lack and need to be strengthen.

6. Problems of Disposal Chemical Research

Chemistry of Nuclides in Groundwater

(1) The lack of direct and rapid detection means for nuclide species;

(2) The lack of means for analysis of precipitation or solid phase;

(3) Lack of research for colloid system;

(4) Lack of dissolution and precipitation kinetics.

6. Problems of Disposal Chemical Research

Radionuclide - Medium Interaction

(1) Lack of research on microcosmic interfacial chemistry;

(2) Basic data are scarce;

(3) The adsorption mechanism is not studied enough;

(4) The coupling effect of multiple factors is less studied;

(5) Coexistence system of radio-nuclides is less studied.

7. Consideration and Prospect

(1) Establish sophisticated equipment and optimize analysis means to improve chemical behavior research of actinides and fission product elements in groundwater;

(2) To carry out research on the chemical behavior of key nuclides in solid-liquid interface;

(3) Under thermo-hydro-mechanical-chemical-radical coupling condition，strengthen research on migration behavior of key nuclides in backfill material and undisturbing surrounding rock;

(4) Research on mechanism of gas release, impact of microorganism and organic matter on radionuclide migration, radiolysis effect in geological disposal environment;

(5) Develop long-term chemical stability study and corrosion behavior study for HLW package, HLW glass and spent fuel under disposal;

(6) Research and develop corrosion inhibitor for glass and packaging materials;

(7) Establishment geological chemical databases for disposal of HLW and develop migration model for HLW repository.

thank you for your attention!

PTKA
Project Management Agency Karlsruhe
Karlsruhe Institute of Technology

BGR Bundesanstalt für Geowissenschaften und Rohstoffe

BRIUG

2nd Chinese-German Workshop on Radioactive Waste Disposal, Karlsruhe

Chemical Behavior of Plutonium in Groundwater

J. Y. Xu

Chengdu University of Technology, Chengdu, China

October, 2012

Outline

- introduction
- Prior research in China
- Our current & future work

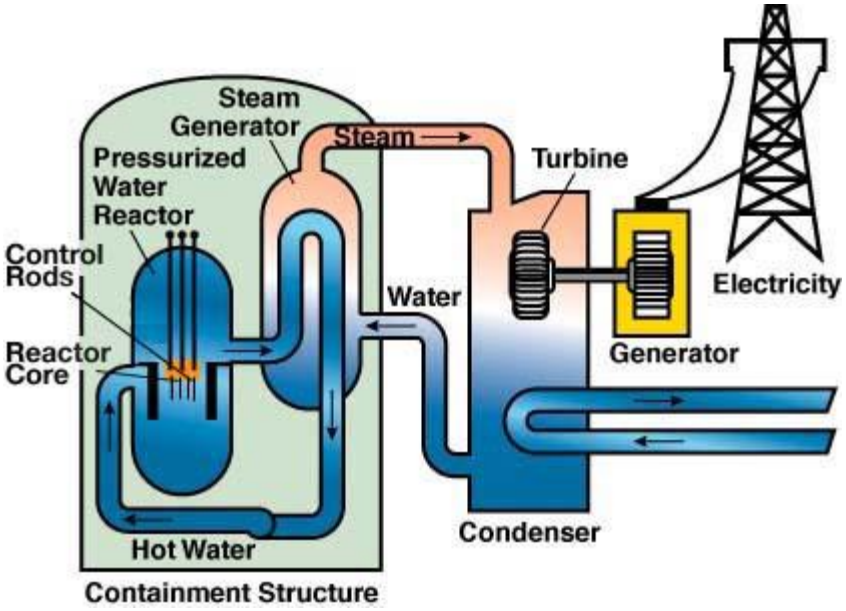

The Plutonium is a word from the Latin “pluto”

Pluto, Greek god of wealth, ruled the dark underworld of myth.

This shows that Pu is one of the toxic elements in nature.

So, The Putonium was under the spotlight attract much attention in HLW.

What is the fate of plutonium?

Biological Uptake and Biotransformations

"Hot particle" and Fission Product Contamination

Thermal and Photochemical Reactions

Gaseous and Aerosol Release

Radiocolloid Formation

hydrosphere

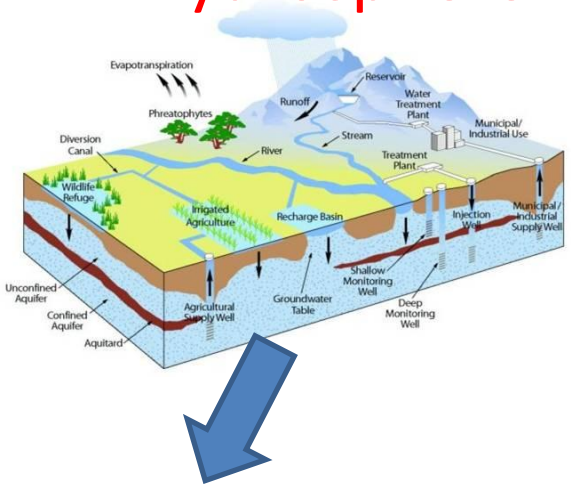

Plutonium Cycling in the Environment

Precipitation, Polymerization and Dissolution

Coprecipitation And Release Upon Dissolution

Aqueous Transport

Complexation And Hydrolysis

Oxidation Reduction and Disproportionation

Sorption/Ion Exchange and Desorption on Inorganic, Organic and Colloidal Materials

Prior Work on Pu chemical behavior in groundwater, in China

(1) Pu speciation

Added Pu	Pu(Ⅲ) %	Pu(Ⅳ) %	Pu(Ⅴ) %	Pu(Ⅵ) %
Pu(Ⅲ) 100%	2.76	82.52	10.43	0.65
Pu(Ⅳ) 100%	2.89	82.27	13.17	0.81
Pu(Ⅴ) 100%	2.01	82.49	10.53	0.87
Pu(Ⅵ) 100%	2.23	81.05	12.12	1.08

1.Initially, we put the *tervalent /tetravalent/ pentavalent/ hexavalent* Pu into the groundwater, respectively.

2. After 60 days balance, the *tetravalent* plutonium is dominant specation in the goundwater.

3. As the table shows: the equilibrium concentration of *tetravalent* plutonium is from eighty-one point zero five to eighty-two point five two percent.

(2) Solubility of $Pu(OH)_4$ (am)

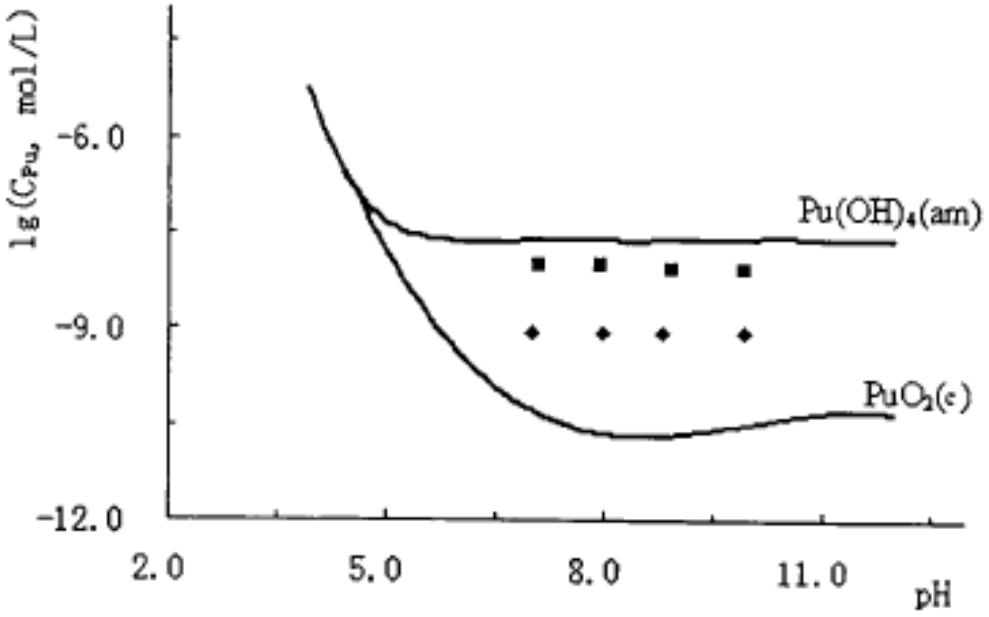

■ without $NaNO_2$
◆ with $NaNO_2$
— calculated

1. The figure shows that the experimental solubility of amorphous plutonium tetra hydroxide compare with results by computational simulation.
2. The square shape(■) denotes “in absence of sodium nitrite”. The diamond shape (◆) denotes “in presence of sodium nitrite”. The line (—) denotes results by computational simulation.
3. The experimental results shows that the solubility of plutonium is basically consistent with the results simulated by software in absence of sodium nitrite.
4. At the same time， amorphous plutonium tetra hydroxide is controlling phase of plutonium solubility in groundwater.

(3) The effect of H_2O_2 on Pu(V) reduction

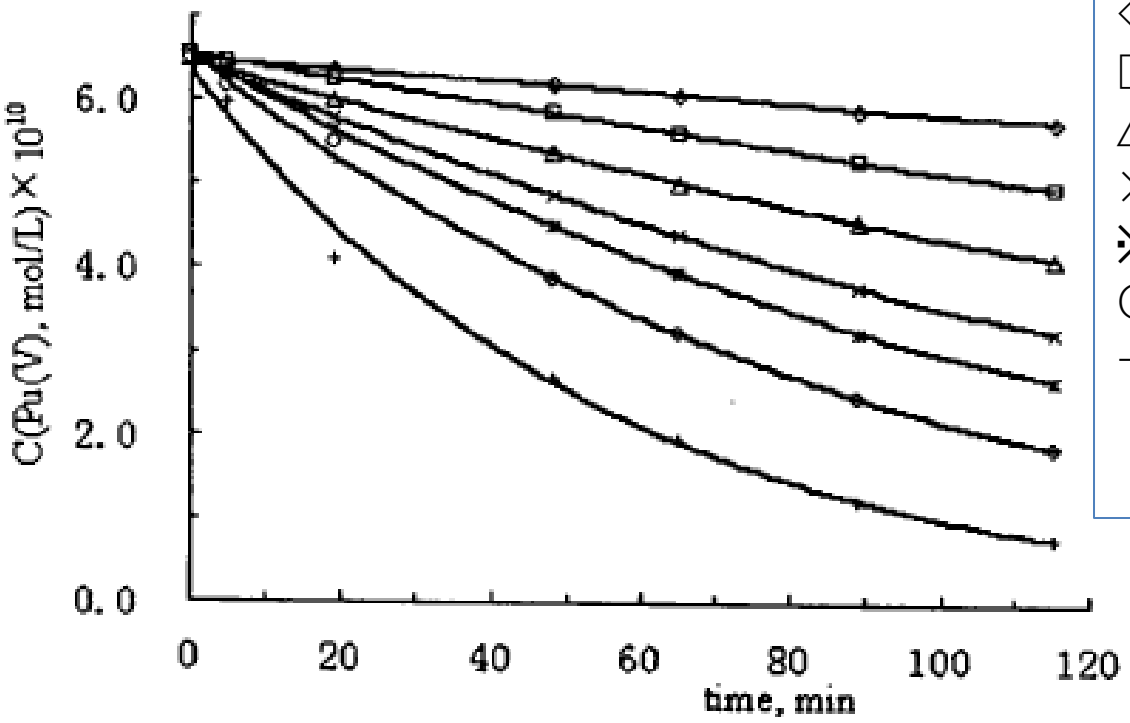

◇ 1.29×10^{-3} mol/L
□ 3.30×10^{-3} mol/L
△ 5.50×10^{-3} mol/L
× 7.40×10^{-3} mol/L
※ 9.05×10^{-3} mol/L
○ 1.25×10^{-3} mol/L
＋ 2.55×10^{-3} mol/L

T=20.0±0.1 ℃

1. Hydrogen peroxide (H_2O_2) is a stable radiolysis product in groundwater.
2. *Pentavalent* plutonium can be reduced to *tetravalent* plutonium by hydrogen peroxide.
3. *Tetravalent* plutonium dominates the solubility of plutonium in groundwater.
4. So, the effect of hydrogen peroxide (H_2O_2) on *pentavalent* plutonium reduction is very important.
5. As shown in the figure, the rate of *pentavalent* plutonium is gradually increasing with the increased concentration of hydrogen peroxide.

(4) The effect of pH on Pu(V) reduction

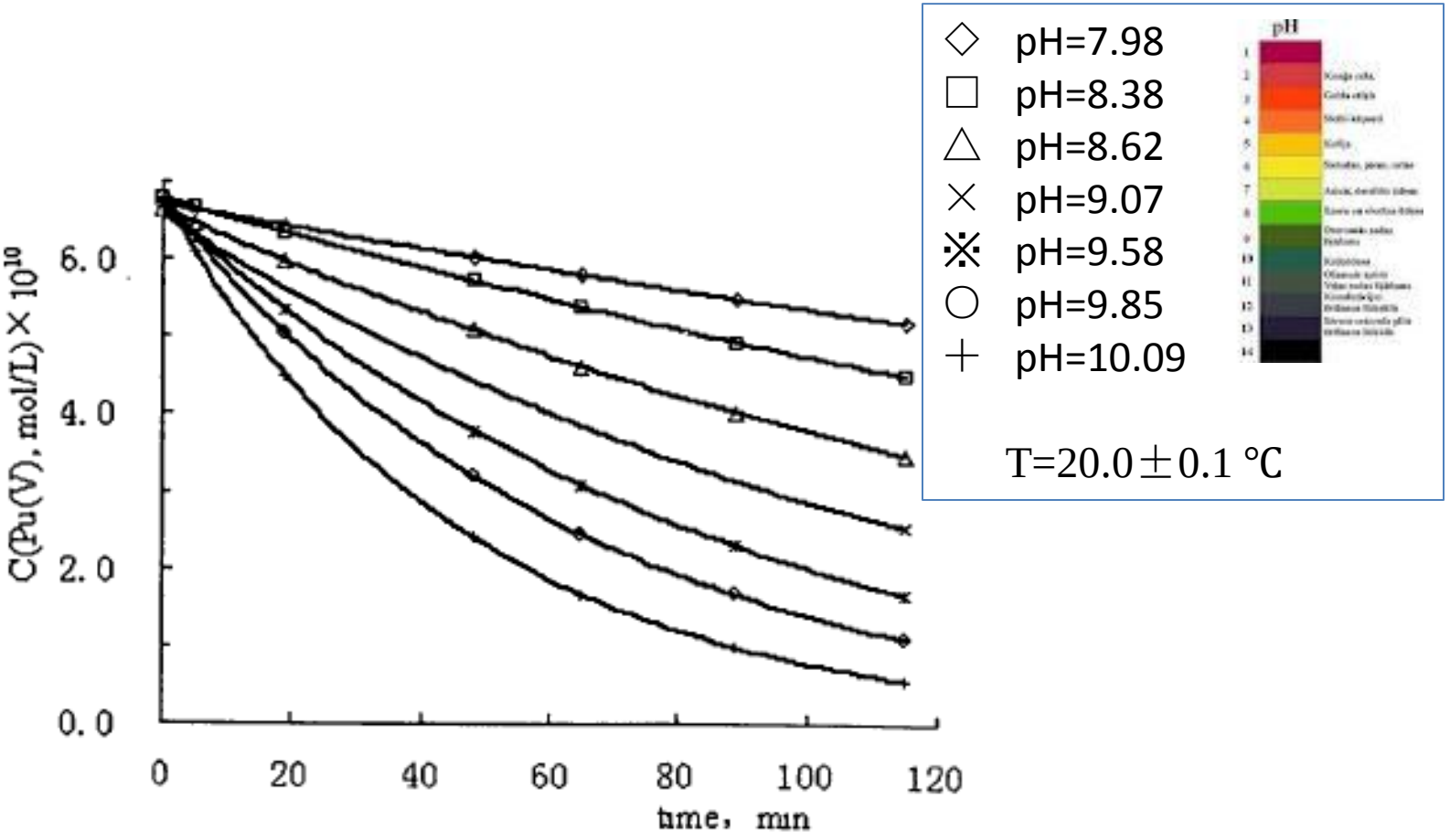

1. The pH of groundwater have a significant impact on the stability of *pentavalent* plutonium.
2. The rate of *pentavalent* plutonium reduction is significantly increasing with the increase of pH value.

(5) The effect of temperature on Pu (V) reduction

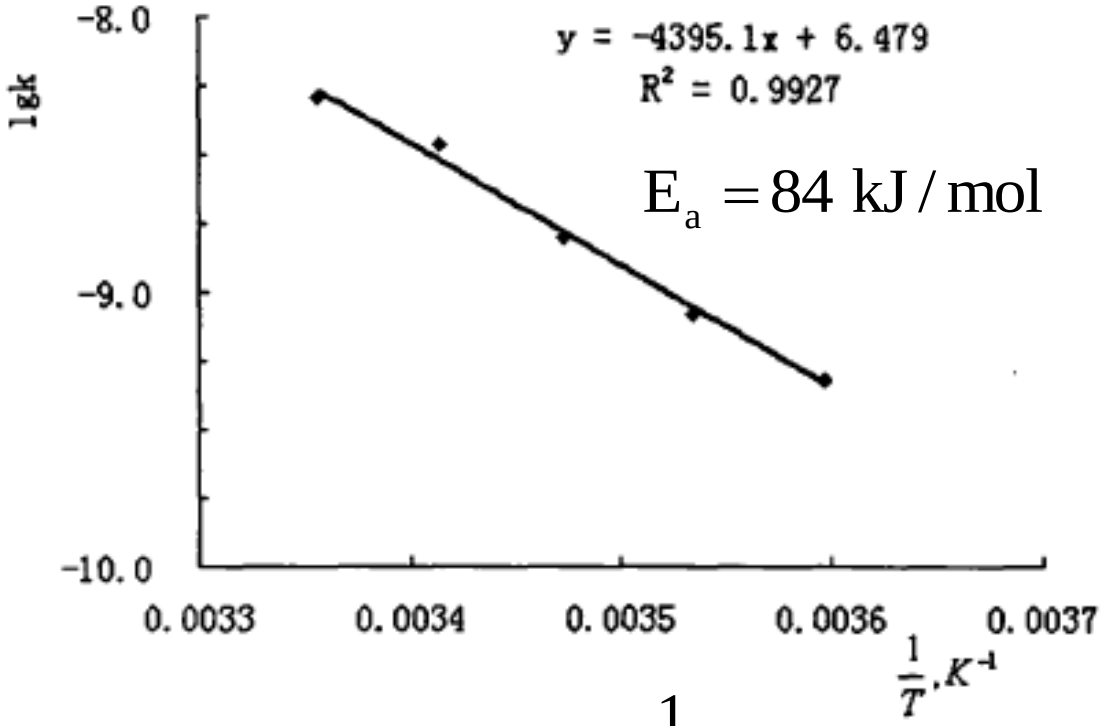

$$E_a = 84\ \text{kJ/mol}$$

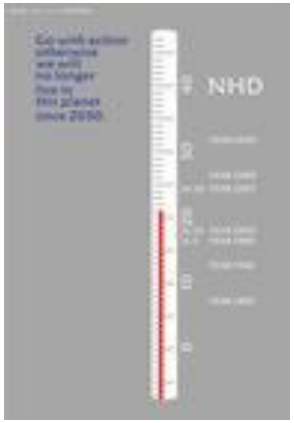

$$\lg k \sim \frac{1}{T}$$

1.The reaction temperature of *pentavalent* plutonium and hydrogen peroxide was studied.
2.The activation energy of the reduction reaction is eighty-four kilo-joule per mole.

(6) The reaction mechanism of H_2O_2 and Pu(V)

Possible mechanism:

$$H_2O_2 \overset{k_1}{\longleftrightarrow} H^+ + HO_2^- \qquad (1)$$

$$PuO_2^+ + HO_2^- \overset{k_2}{\longleftrightarrow} PuO_2O_2H \qquad (2)$$

$$PuO_2O_2H \overset{k_3}{\longleftrightarrow} PuO_2O_2H^{\neq} \qquad (3)$$ ← Rate-controlling reaction

$$PuO_2O_2H^{\neq} \overset{k_3}{\longleftrightarrow} Pu^{4+} + \text{reductant} \qquad (4)$$

Rate equation :

$$\text{rate} = (3.93 \pm 1.93) \times 10^{-9} \times c(Pu) \times c(H_2O_2) \times c(H^+)^{-1}$$

(7) The effect of inorganic cation on Pu(V) reduction

* No cation
◇ K^+ (0.005mol/L)
△ Mg^{2+} (2.16×10^{-4}mol/L)
○ Ca^{2+} (6.25×10^{-4}mol/L)

□ Fe^{2+} (4.48×10^{-5}mol/L)

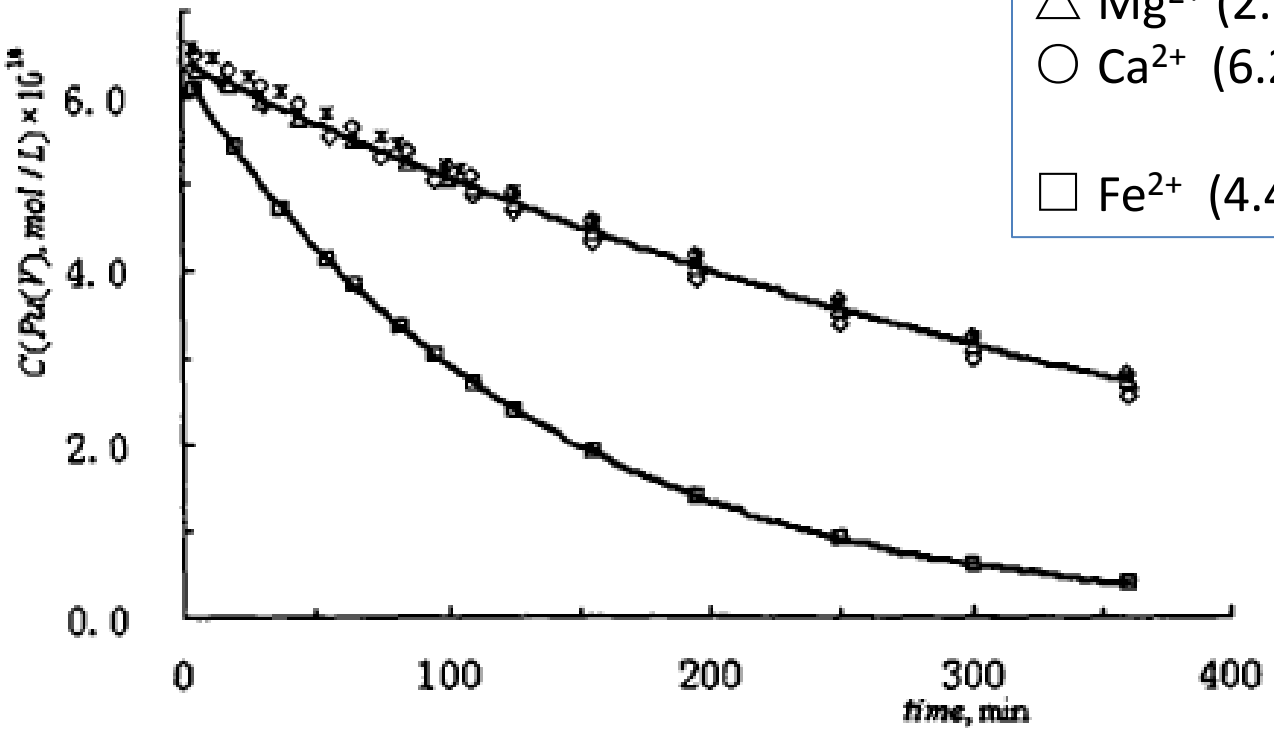

1. potassium, sodium, calcium, magnesium and ferrous cations commonly exist in groundwater.
2. The reaction rate of *pentavalent* plutonium and hydrogen peroxide have no significant change in presence of potassium, sodium, calcium, magnesium.
3. However, Iron ion significantly accelerates the reaction rate of *pentavalent* plutonium and hydrogen peroxide.

(8) The effect of inorganic anion on Pu(v) reduction

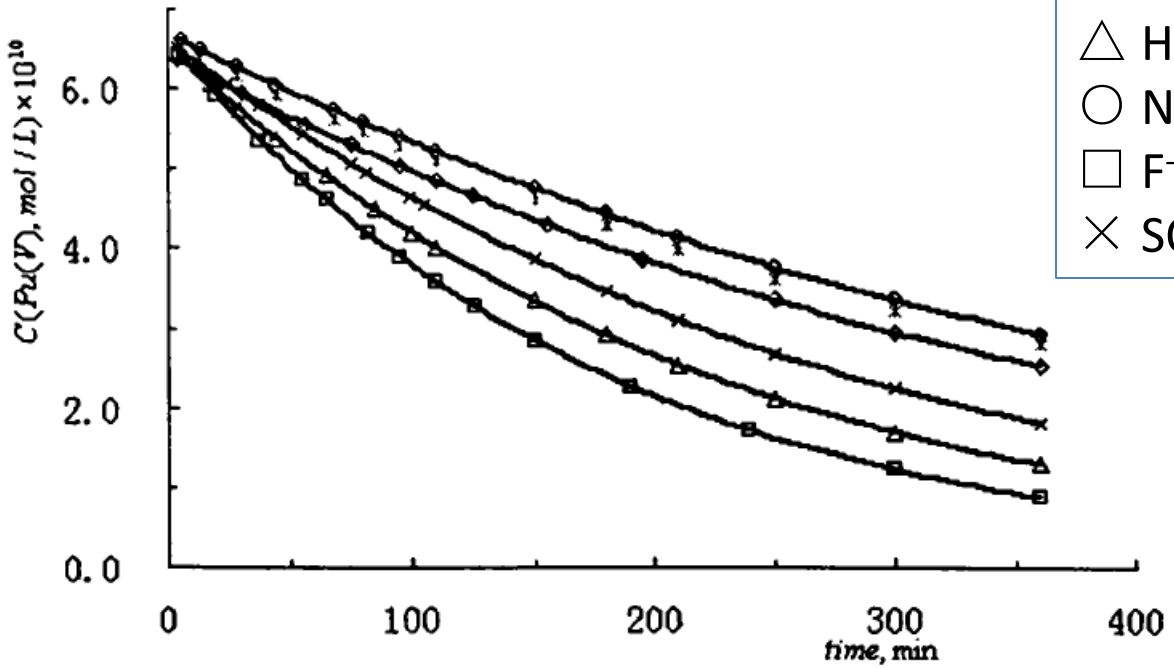

※ no anion
◇ Cl^- (5×10^{-2}mol/L)
△ HCO_3^- (2.26×10^{-3}mol/L)
○ NO_3^- (2.25×10^{-4}mol/L)
□ F^- (9.94×10^{-4}mol/L)
× SO_4^{2-} (1.25×10^{-2}mol/L)

1. Bicarbonate, nitrate, fluoride, chloride and sulphate ions also commonly exist in groundwater.
2. The reaction rate of *pentavalent* plutonium and hydrogen peroxide is accelerated in the presence of these inorganic anion.
3. It is fact that different anions will have different influence on the reaction rate.

(9) Stability of Pu(v) in groundwater somewhere

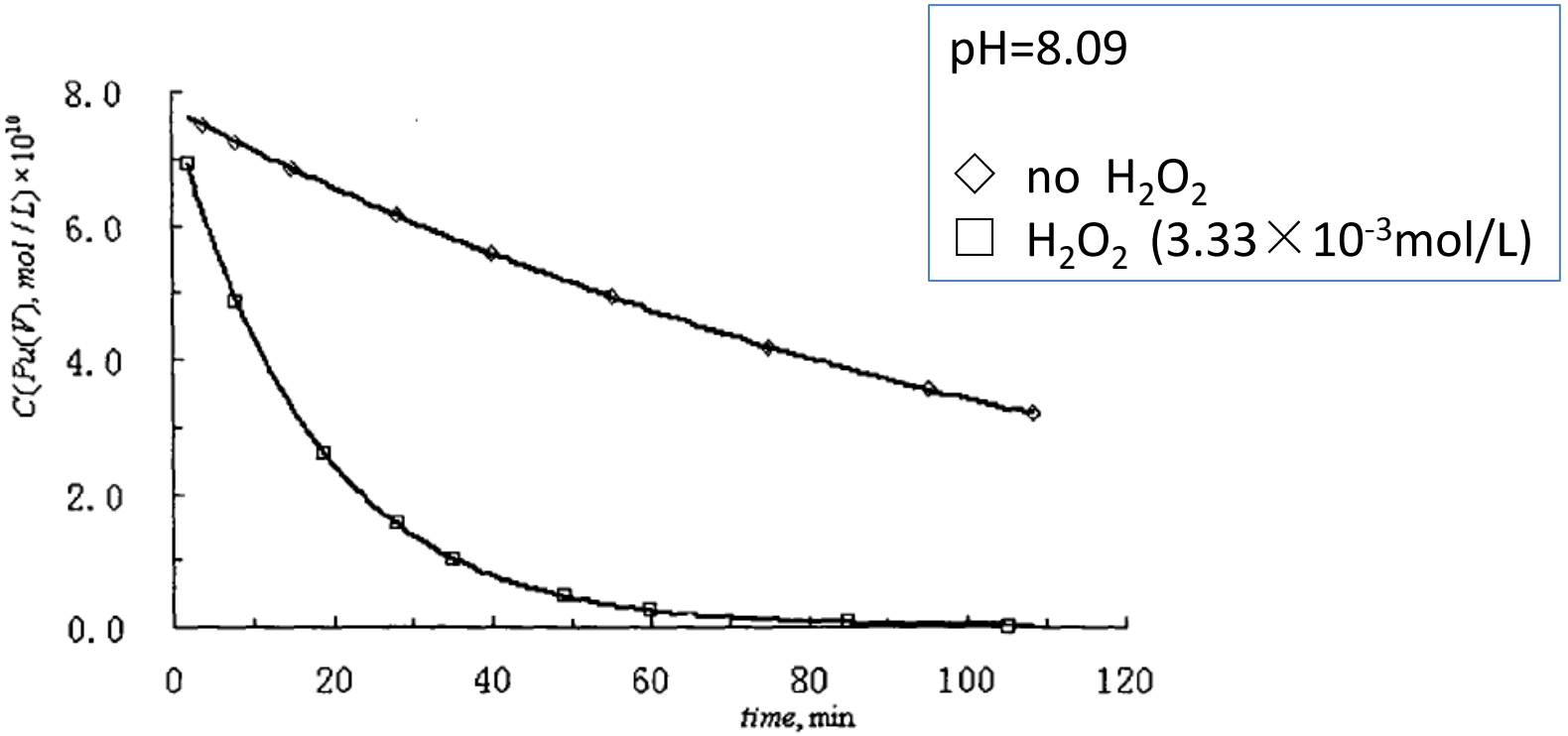

1. The groundwater show some reduction capability to *pentavalent* plutonium, itself.
2. Ferrous, sulfide and nitrous ions, goethite, iron sulfide and humic acid may coexist in the groundwater.
3. Hydrogen peroxide is more conducive to the reduction of *pentavalent* plutonium.

(10) The effect HCO_3^- and CO_3^{2-} ion on the solubility of $Pu(OH)_4(am)$

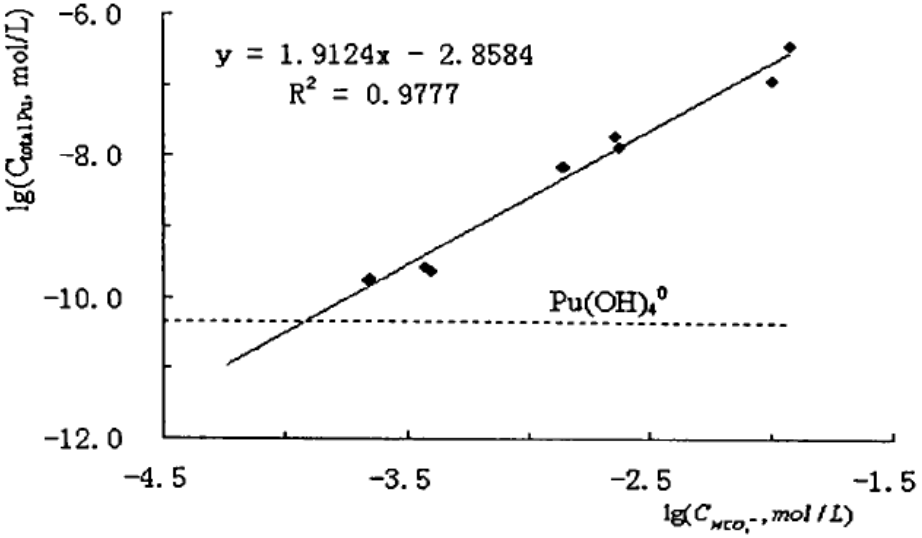

lgc(Pu,aq)—HCO_3^-

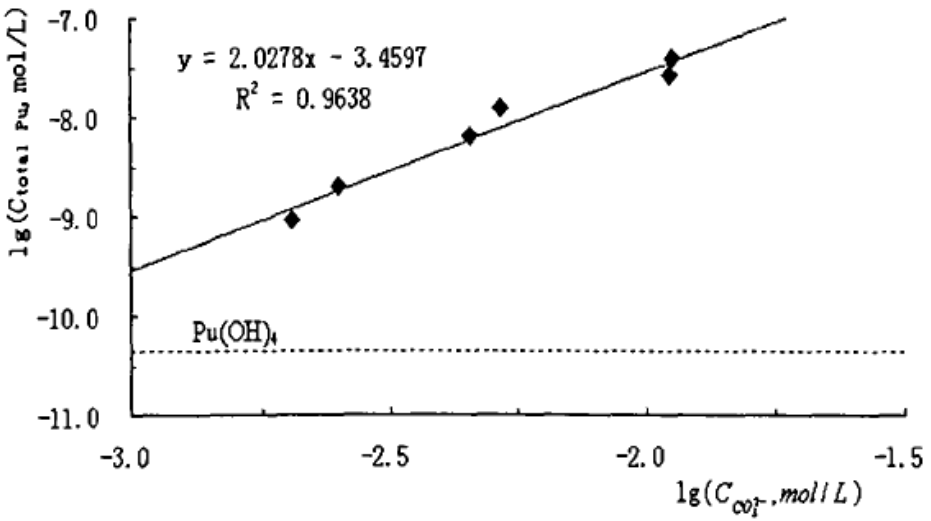

lgc(Pu,aq)—CO_3^{2-}

1. Amorphous plutonium can form complex with bicarbonate.
2. So, the solubility of amorphous plutonium in the groundwater is increasing with bicarbonate levels increased
3. Carbonate has also a similar effect to amorphous plutonium.
4. The solubility of amorphous plutonium in groundwater is increasing linearly with bicarbonate or carbonate ion concentration.

(11) Possible complex reaction of HCO_3^- , CO_3^{2-} and $Pu(OH)_4(am)$

$$Pu(OH)_4(am) + 2HCO_3^- = Pu(OH)_4(HCO_3)_2^{2-} \quad (1)$$

$$Pu(OH)_4(am) + 2HCO_3^- = Pu(OH)_2(HCO_3)_2^{2-} + 2H_2O \quad (2)$$

$$Pu(OH)_4(am) + 2CO_3^{2-} = Pu(OH)_4(CO_3)_2^{4-} \quad (3)$$

1. Possible complex reaction of bicarbonate (HCO_3^-) , carbonate (CO_3^{2-}) and amorphous plutonium is as follow: reaction one (1), two(2) and reaction three (3).
2. So, these complex reaction increase solubility of amorphous plutonium tetra hydroxide in the groundwater.

(12) Pu adsorption behavior on the surface of granite

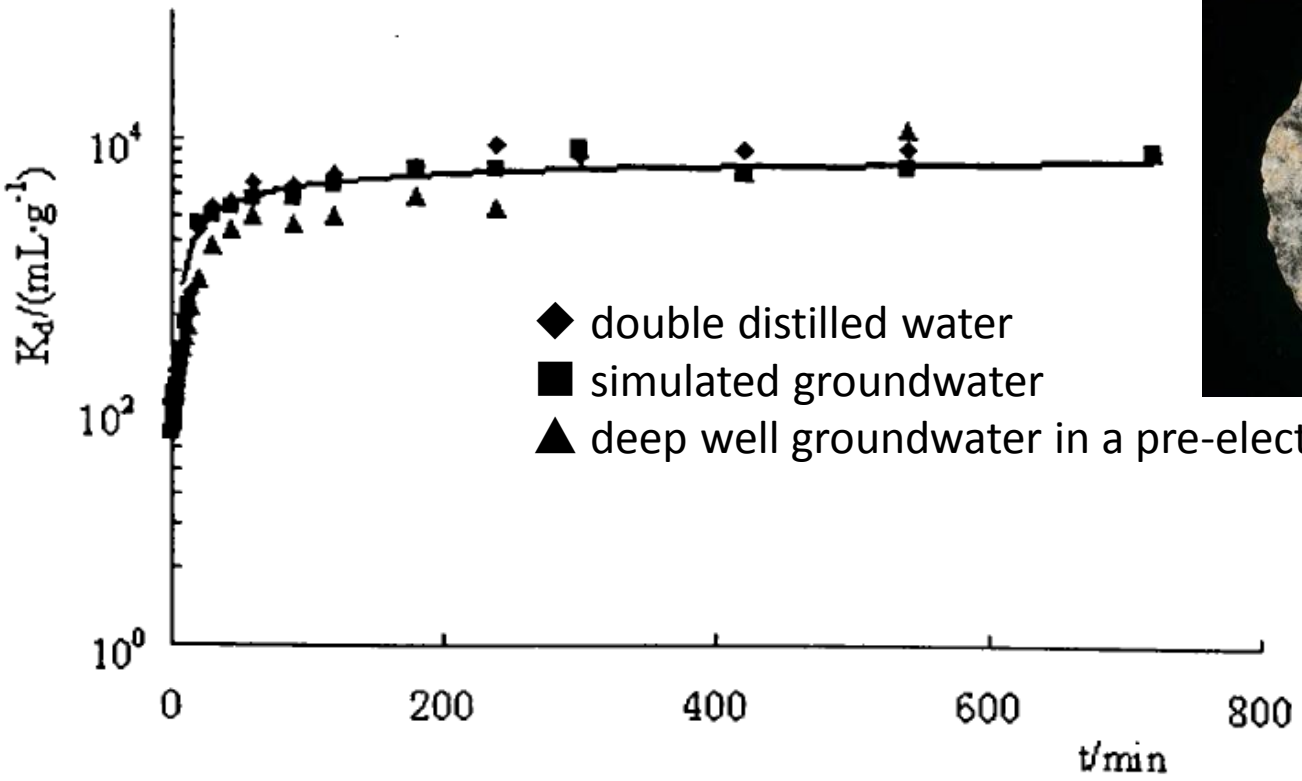

1. The plutonium adsorption behavior on the surface of the rock influences the migration in the groundwater.
2. The plutonium adsorption behavior has been esearched on the surface of the granite in the groundwater.
3. The results show that plutonium adsorption reach balance on the surface of granite in the groundwater after about six hundred minutes.

(13) Pu adsorption and desorption behavior on granite surface

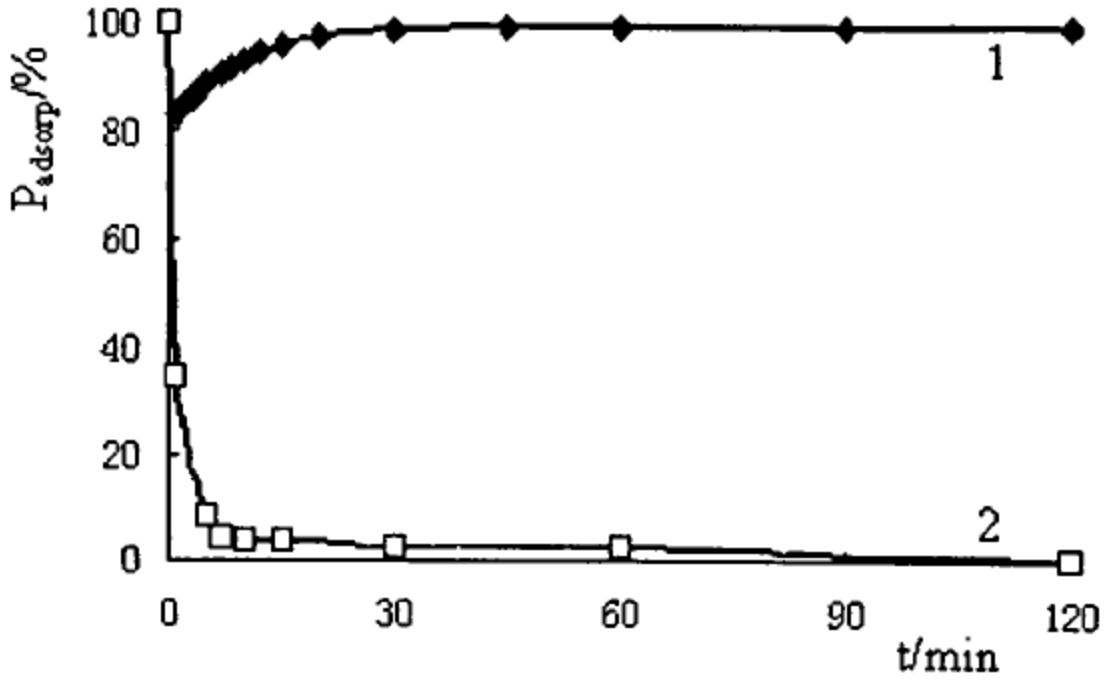

1. The pH of groundwater is the key factor of plutonium adsorption on surface of the granite.
2. The lower the pH of groundwater, the more detrimental to the adsorption of plutonium.

(14) Pu adsorption behavior on surface pyrrhotite

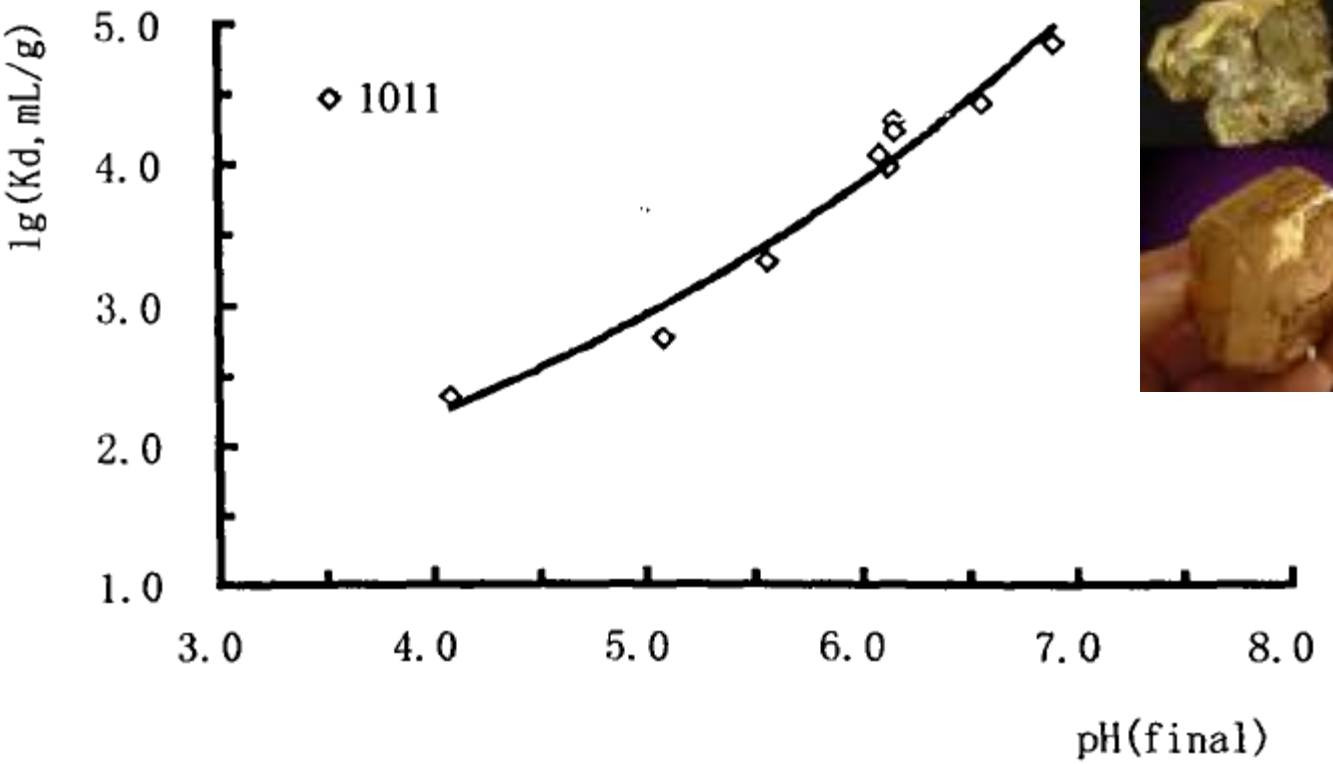

◇ 75% pyrrhotite, 15% (kaolinite + feldspar + quartz)

1. The pyrrhotite is the key mineral influencing plutonium adsorption on granite.
2. The pyrrhotite was separated from the granite.
3. There are seventy-five percent pyrrhotite and kaolinite, feldspar, quartz fifteen percent in selected mineral.
4. Plutonium adsorption capacity on the pyrrhotite surface is increasing with the pH of groundwater.

(15) Pu adsorption behavior on surface clay minerals

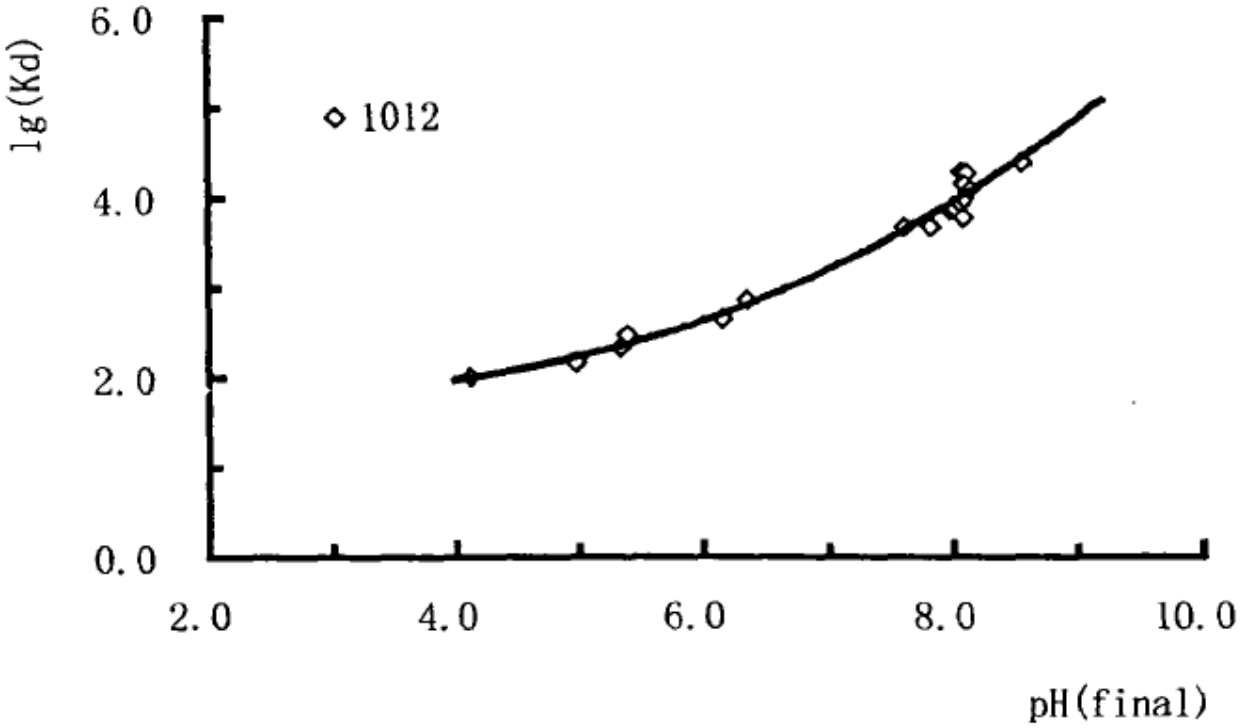

◇ kaolinite , feldspar, quartz, mica, and so on

1. The clay mineral is also the key mineral influencing plutonium adsorption on granite.
2. The clay mineral was separated from the granite.
3. Plutonium adsorption capacity on the surface of clay is increasing with the pH of groundwater.

Focus of our further research--*isolate plutonium from biosphere*

Migration behavior of plutonium in the groundwater around clay rock region

- **Colloid transport**
- **humic acid**

Establish optimal migration model for migration of Pu in clay rock region

Thanks for your attention

Tuesday, October 16, 2012

TOPIC: TECHNICAL/ENGINEERING

2nd Chinese-German Workshop on Radioactive Waste Disposal
Karlsruhe, German
October 15-16, 2012

Feasibility of CS Canister Used for HLW Geological Disposal

Junhua Dong, Wei Ke
Institute of Metal Research, Chinese Academy of Sciences
Shenyang, China

Background

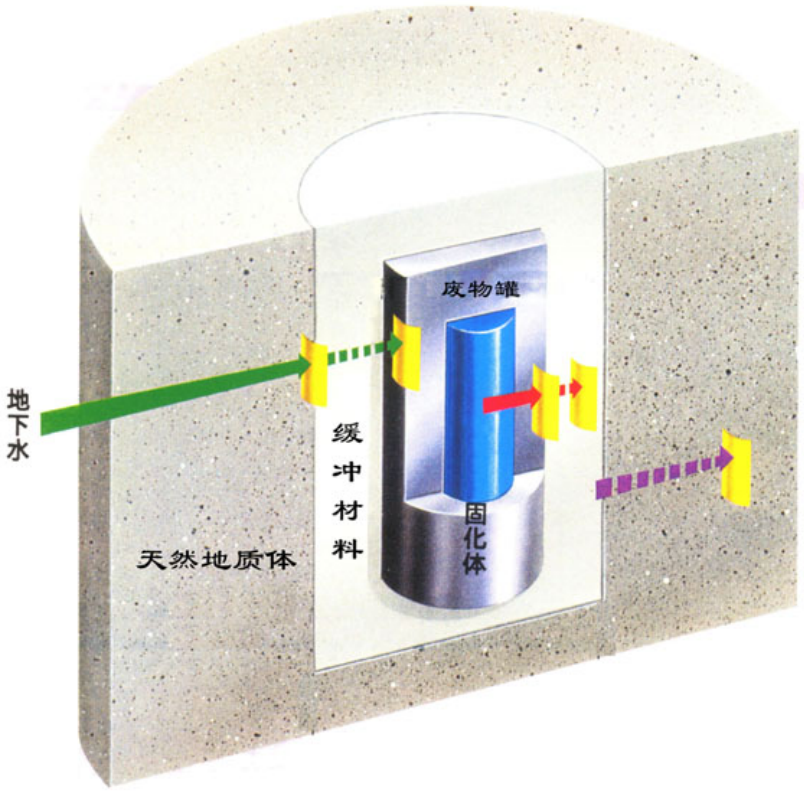

- Geological disposal of HLW include multi-barriers, which is known as the natural barrier and the engineering barrier.
- the engineering barrier includes glass solidification, canister, overpack and buffer material.

Overpack is the first barrier to isolate the radionuclide from human being. Its corrosion mode determines its serving life.

Background

- In the oxygen free underground water for HLW geological disposal, carbon steel was thought to satisfy the most technical criterions for isolating the HLW besides some low corrosion resistance.
- Corrosion of CS canister **was thought to obey** the anodic dissolution galvanized by the hydrogen evolving reaction mode, which occurred as general corrosion.
- Passivation mode was thought to be ease of pitting corrosion caused by chloride ion, which induce the stress corrosion cracking of CS canister.
- Anodic active dissolution / Passivation / Local corrosion? What will happen for the CS canister in the underground water during more than thousand years disposal? It needs a correct answer for HLW geological disposal engineering design.

Background

Thermodynamics of CS Canister Corrosion

$3Fe + 4H_2O = Fe_3O_4 + 8H^+ + 8e$ (1)

$E=-0.08664-0.05916pH$ (2)

$3\alpha\text{-}FeOOH + H^+ + e = Fe_3O_4 + 2H_2O$ (3)

$E=0.2845-0.05916pH$ (4)

$Fe + 2H_2O = \alpha\text{-}FeOOH + 3H^+ + 3e$ (5)

$E=-0.04540-0.05916pH$ (6)

$Fe^{2+} + 8\alpha\text{-}FeOOH + 2e = 3Fe_3O_4 + 4H_2O$ (7)

$E=0.08609+0.02958lg[Fe^{2+}]$ (8)

$Fe^{3+} + 8\alpha\text{-}FeOOH + 3e = 3Fe_3O_4 + 4H_2O$ (9)

$E=0.3137+0.01972lg[Fe^{3+}]$ (10)

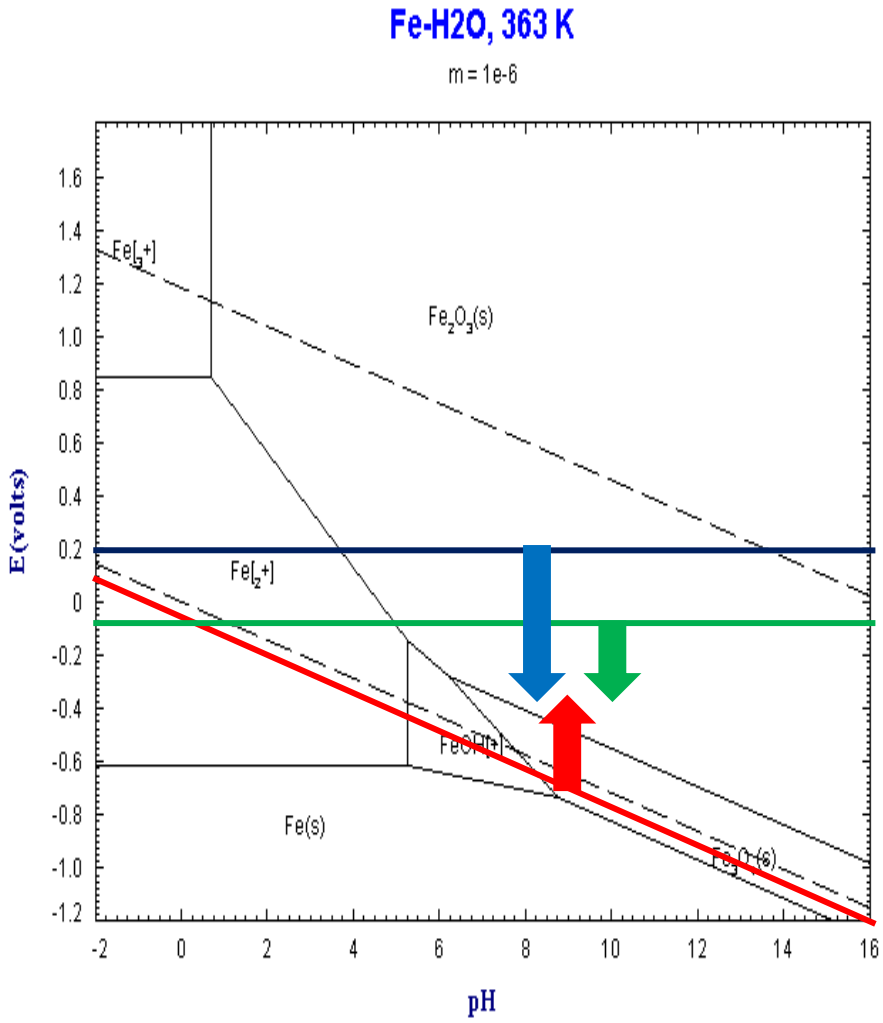

Background

Kinetics of CS Canister Corrosion

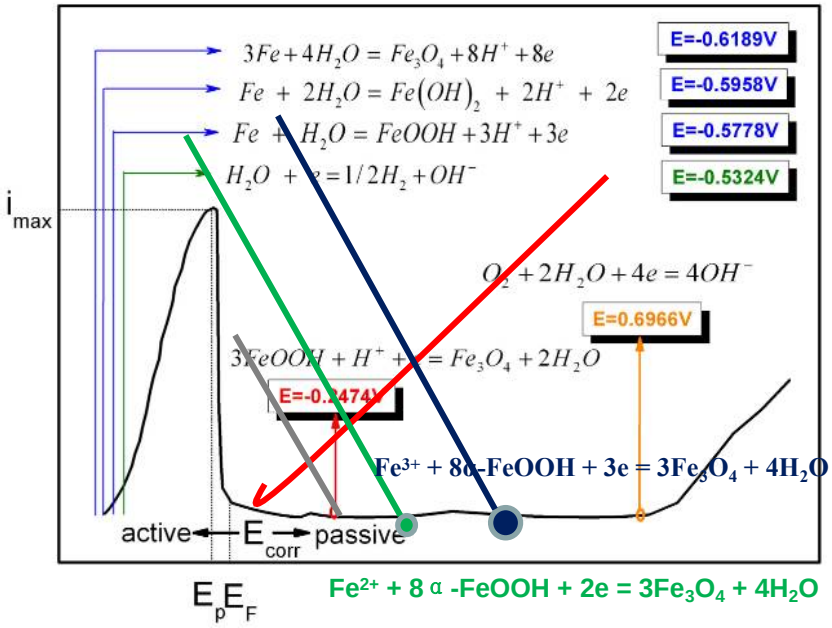

- The open circuit potential determines the corrosion mode of anodic dissolution or passivation.
- the chemical compositions of the ground water and the corrosion products make effects on localized corrosion potential and dissolving mode of the passive film during the long term disposal.

Background

Chemicals contained in the underground water

Beishan, China

ion	mol/L	ion	mol/L
F^-	1.31×10^{-4}	Na^+	5.42×10^{-2}
Cl^-	3.39×10^{-2}	K^+	6.36×10^{-4}
NO_3^-	**3.08×10^{-4}**	Ca^{2+}	1.54×10^{-3}
SO_4^{2-}	1.39×10^{-2}	Mg^{2+}	1.01×10^{-2}
CO_3^{2-}	0.84×10^{-4}	pH	
HCO_3^-	1.90×10^{-3}	TDS	

Calculated by Japanese

chemicals	mol/L
$HCO_3^-/CO_3^{2-}/H_2CO_3$	$<7.3\times10^{-2}$
SO_4^{2-}	$<6.1\times10^{-2}$
HS^-/H_2S	$<9.2\times10^{-1}$
Cl^-	$<5.9\times10^{-1}$
P（Title）	$<2.9\times10^{-6}$
NO_3^-	0.0
NH_3	$<1.6\times10^{-4}$
NH_4^+	$<5.1\times10^{-3}$
B(Totle)	$<1.7\times10^{-3}$
pH	5.9~8.4

Target of the present study

- What is the corrosion mode of CS canister?

  Anodic active dissolution or passivation?
- What is the effect of the chemicals in the underground water ?

  $HCO_3^-/Cl^-/SO_4^{2-}/pH$
- Does the CS canister satisfy the technical request for HLW geological disposal?

Experiment

- Polarization curves
- Potentiostatic current decay
- Corrosion potential monitoring
- EIS measurement
- XRD detection and SEM observation

Electrolyte	C/mol/L
HCO_3^-	0.01 ~ 0.1
$HCO_3^-+Cl^-$	0.01 ~ 0.5
$HCO_3^-+SO_4^{2-}$	0.01 ~ 0.5
$HCO_3^-+ Cl^- +SO_4^{2-}$	Σ=0.1

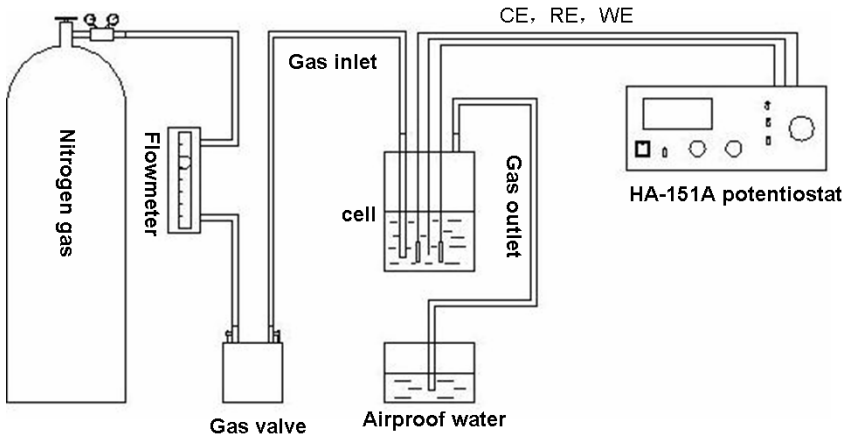

Results and discussions

Polarization behaviors and corrosion potentials of CS immersed in HCO_3^- solutions

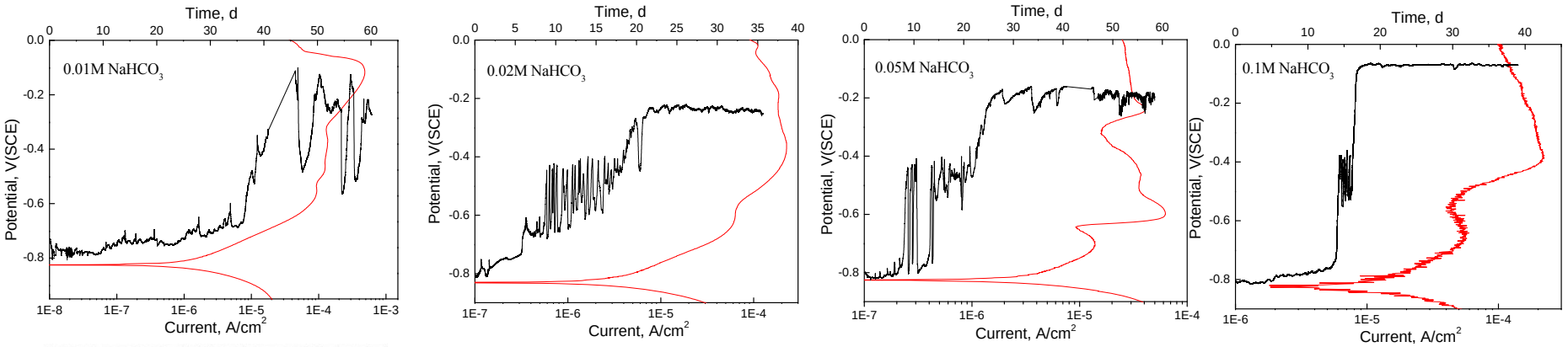

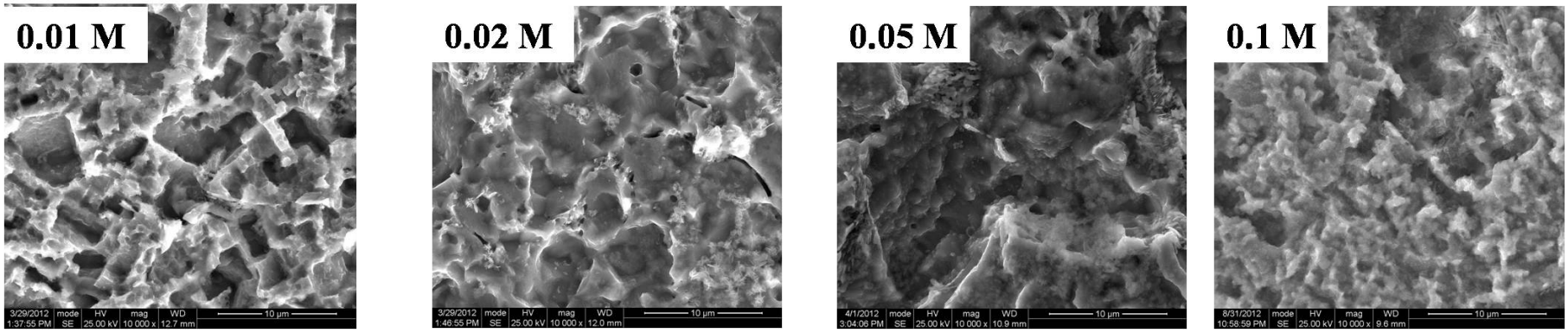

1.CS keeps same anodic dissolution at low potential in all HCO_3^- solution, but changes from limited diffusion to passivation and transpassivation at high potential with increasing HCO_3^- concentration.

2.The corrosion potential of CS increases from active to passive during the immersion

Results and discussions

XRD patterns of the corrosion products of CS immersed in HCO_3^- solutions and the corrosion potential of CS drawn in Pourbaix diagram

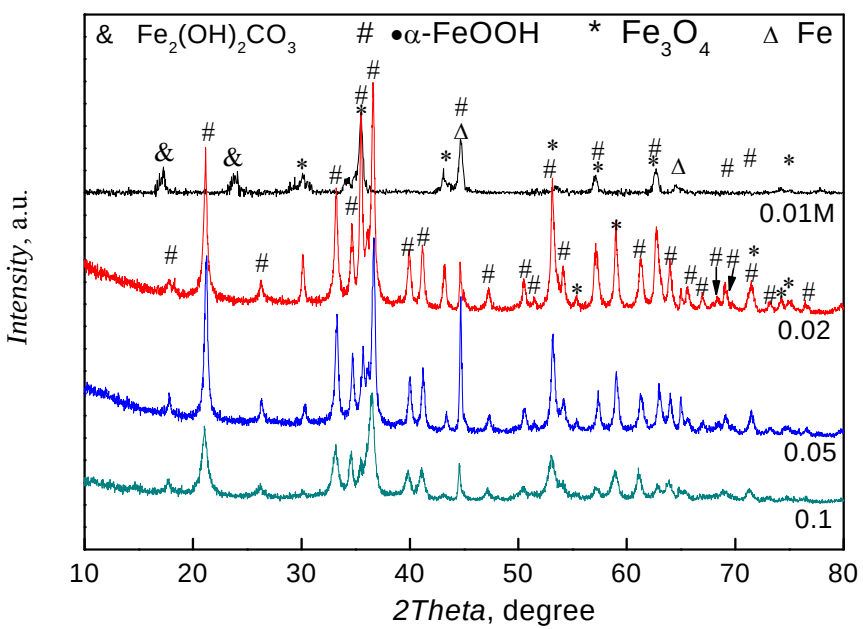

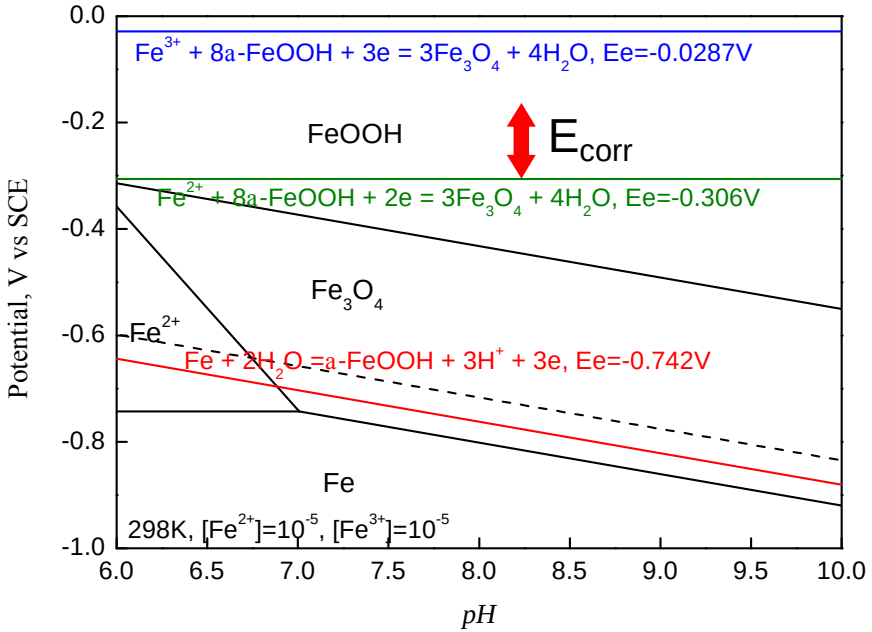

Anode: $Fe + 2H_2O = \alpha\text{-}FeOOH + 3H^+ + 3e$, E_e=-0.742V, pH=8.33

Cathode: $Fe^{3+} + 8\alpha\text{-}FeOOH + 3e = 3Fe_3O_4 + 4H_2O$, E_e= -0.0287V

Results and discussions

Polarization behaviors and corrosion potentials of CS in 0.01M HCO_3^- solutions containing Cl^-

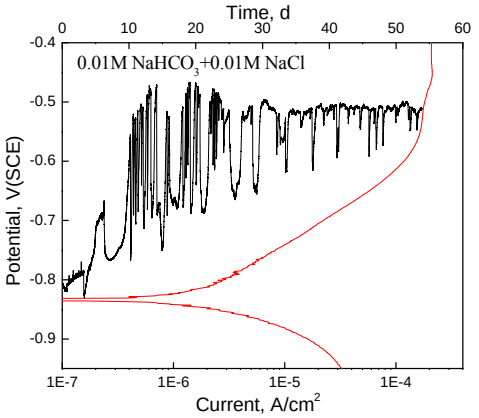

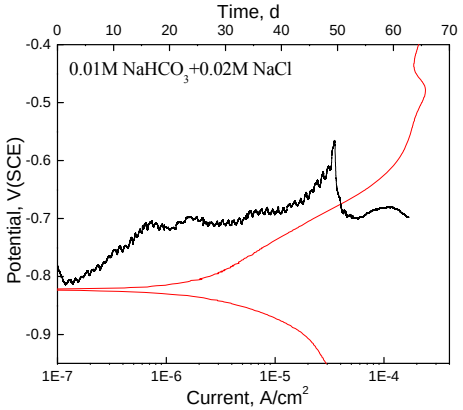

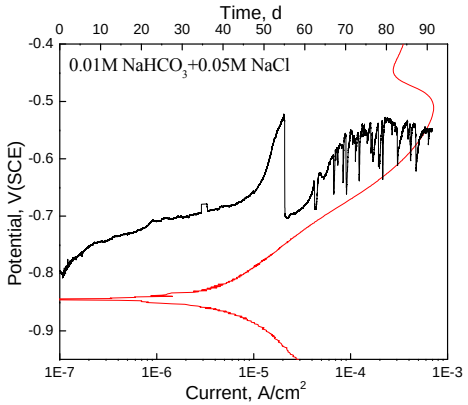

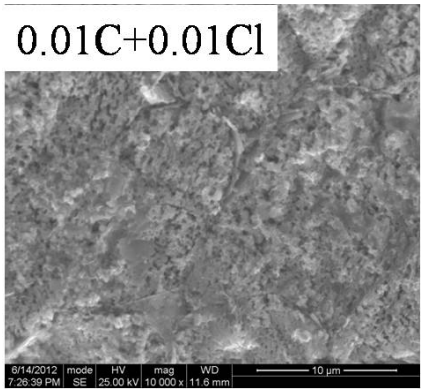

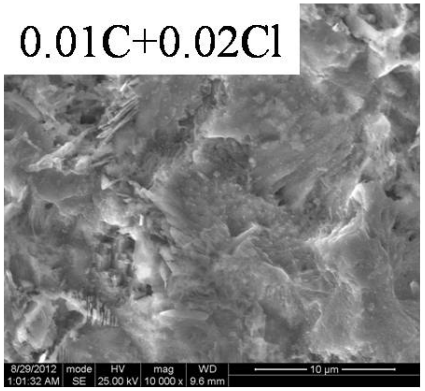

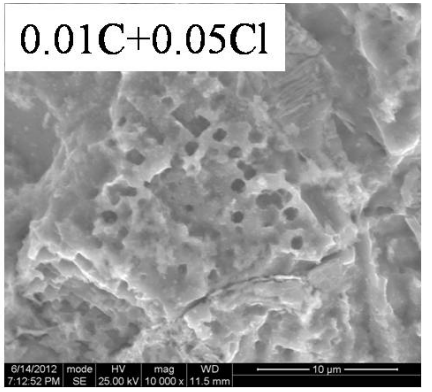

CS keeps anodic active dissolution in 0.01M HCO_3^- solutions containing Cl^-, morphologies after long term immersion show a general corrosion.

Results and discussions

Polarization behaviors and corrosion potentials of CS in 0.01M HCO_3^- solutions containing Cl^-

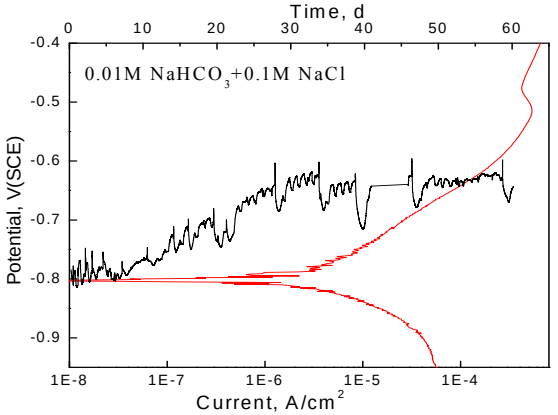

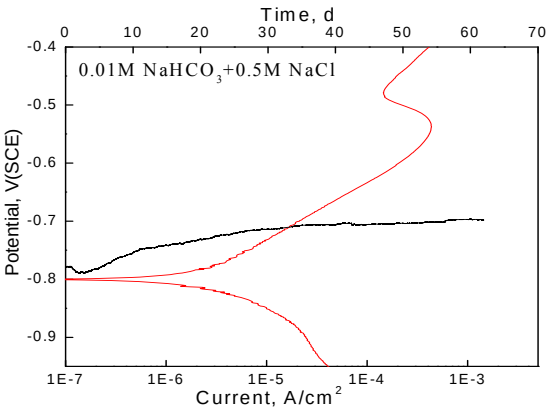

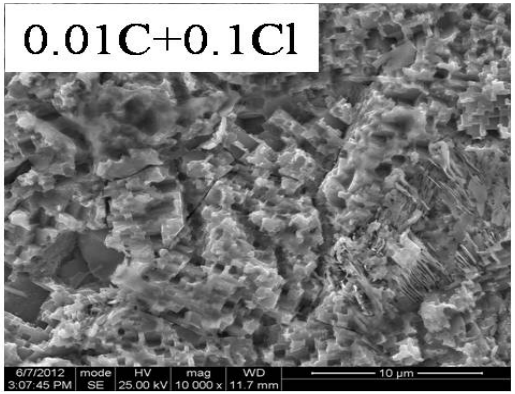

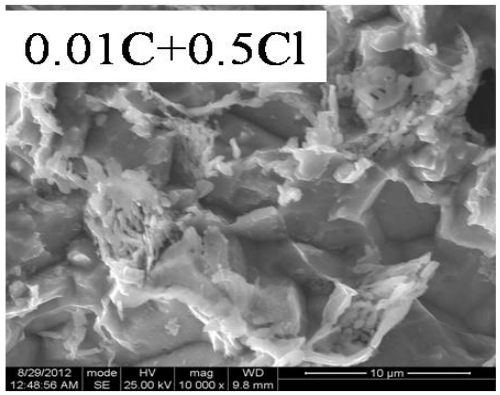

Increase of Cl^- concentration decreases the corrosion potential; morphologies after long term immersion show a general corrosion.

Results and discussions

XRD patterns of the corrosion products of CS immersed in 0.01M HCO_3^- solutions containing Cl^- and the corrosion potential of CS drawn in Pourbaix diagram

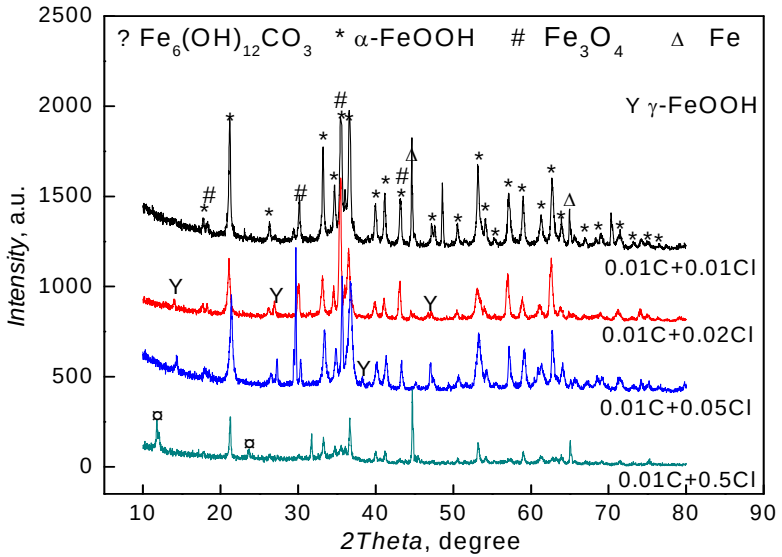

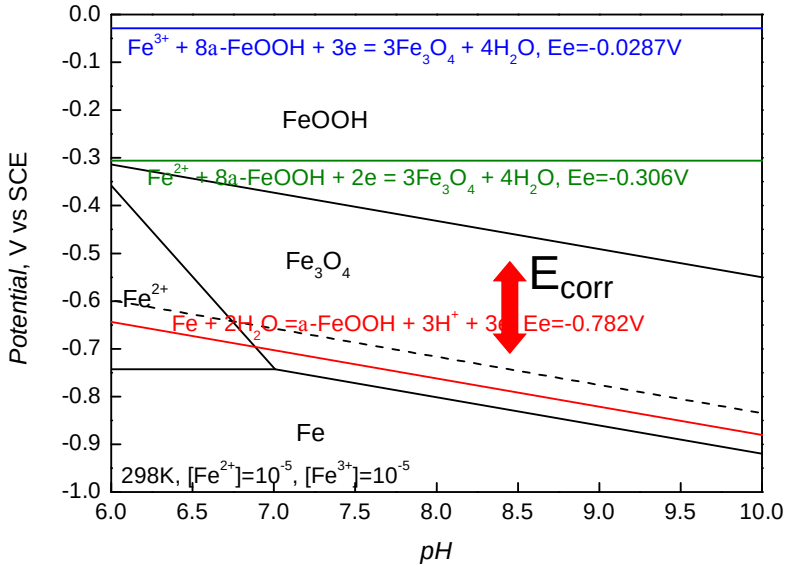

Anode: $Fe + 2H_2O = \alpha\text{-}FeOOH + 3H^+ + 3e$, pH=8.33, E_e=-0.742V

Cathode: $Fe^{2+} + 8\alpha\text{-}FeOOH + 2e = 3Fe_3O_4 + 4H_2O$, E_e= -0.306V

$3\,\alpha\text{-}FeOOH + H^+ + e = Fe_3O_4 + 2H_2O$

Results and discussions

Polarization behaviors and corrosion potentials of CS in 0.01M HCO_3^- solutions containing SO_4^{2-}

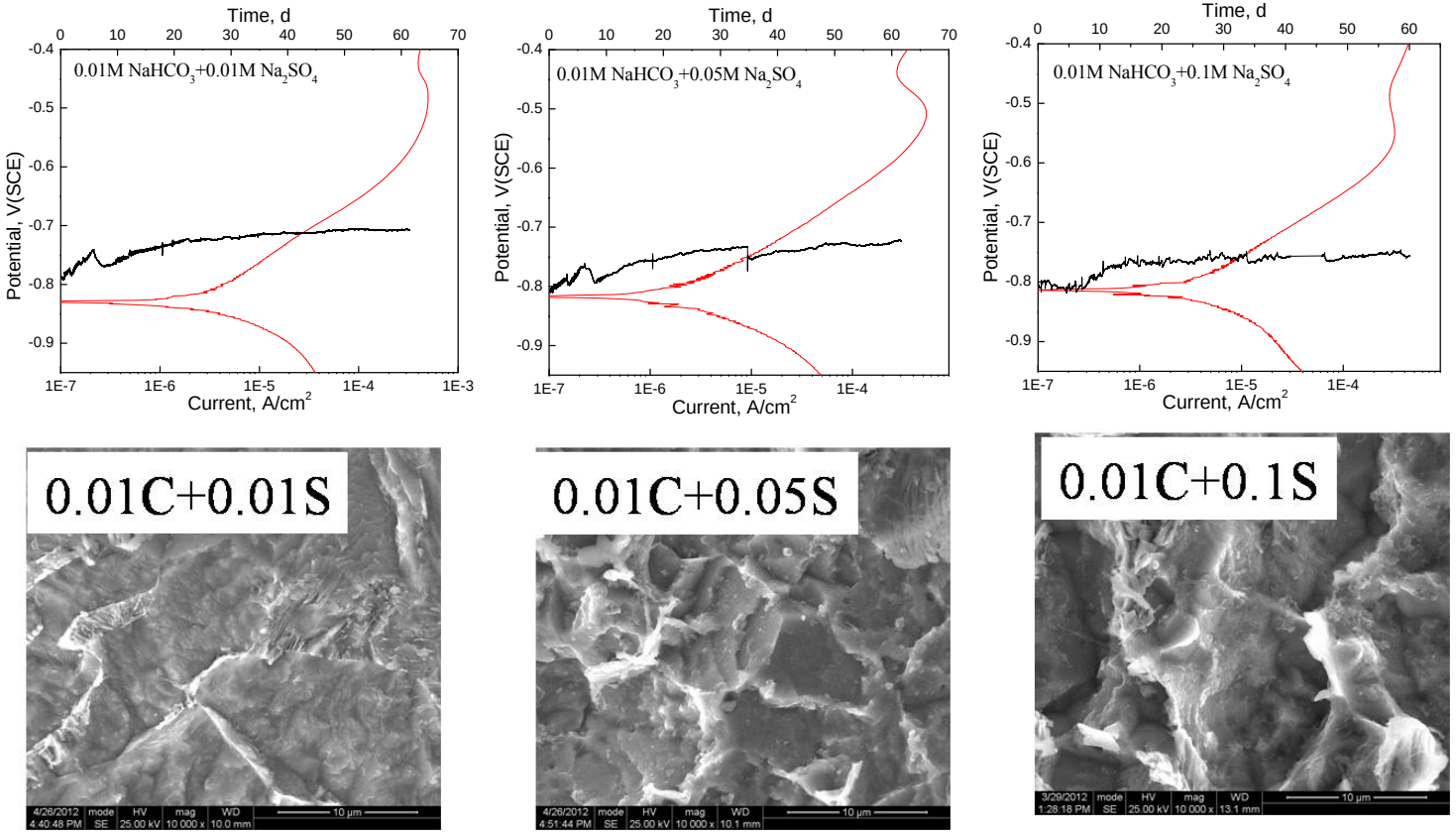

CS keeps anodic active dissolution in 0.01M HCO_3^- solutions containing SO_4^{2-}. Increase of SO_4^{2-} concentration decreases the corrosion potential; morphologies after long term immersion show a general corrosion.

Results and discussions

XRD patterns of the corrosion products of CS immersed in 0.01M HCO_3^- solutions containing SO_4^{2-} and the corrosion potential of CS drawn in Pourbaix diagram

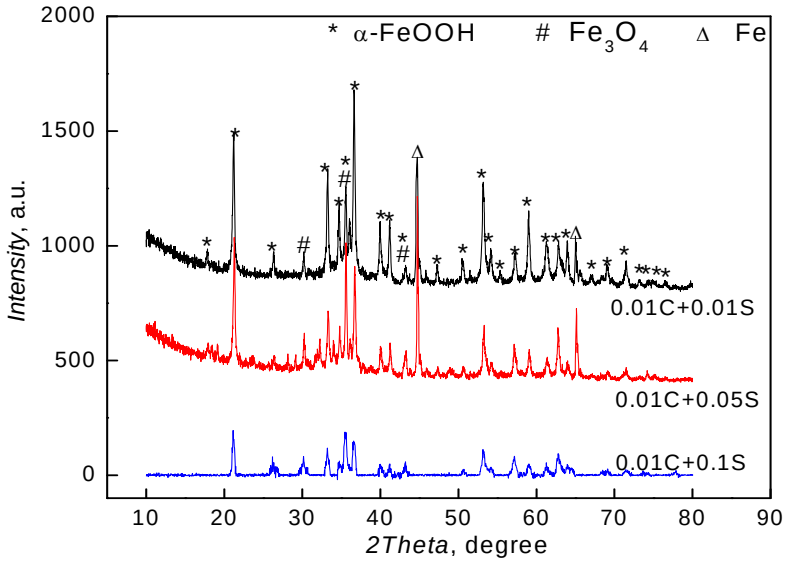

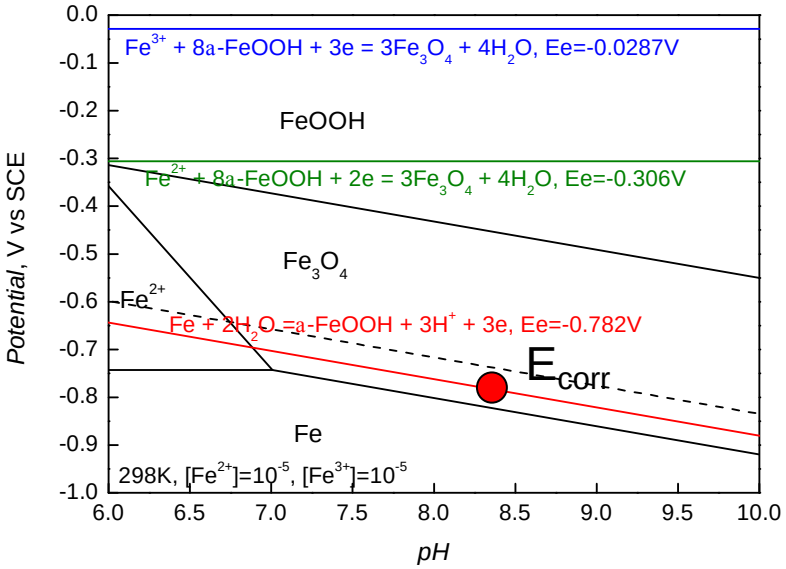

Anode: $Fe + 2H_2O = \alpha\text{-}FeOOH + 3H^+ + 3e$, pH=8.33, E_e=-0.742V

Cathode: $Fe^{2+} + 8\alpha\text{-}FeOOH + 2e = 3Fe_3O_4 + 4H_2O$, E_e= -0.306V

$3\,\alpha\text{-}FeOOH + H^+ + e = Fe_3O_4 + 2H_2O$, Ee= -0.4521V

$2H^+ + 2e = H_2$, E_e= -0.7366V

Results and discussions

Polarization behaviors and corrosion potentials of CS in 0.01M HCO_3^- solutions containing both SO_4^{2-} and Cl^-

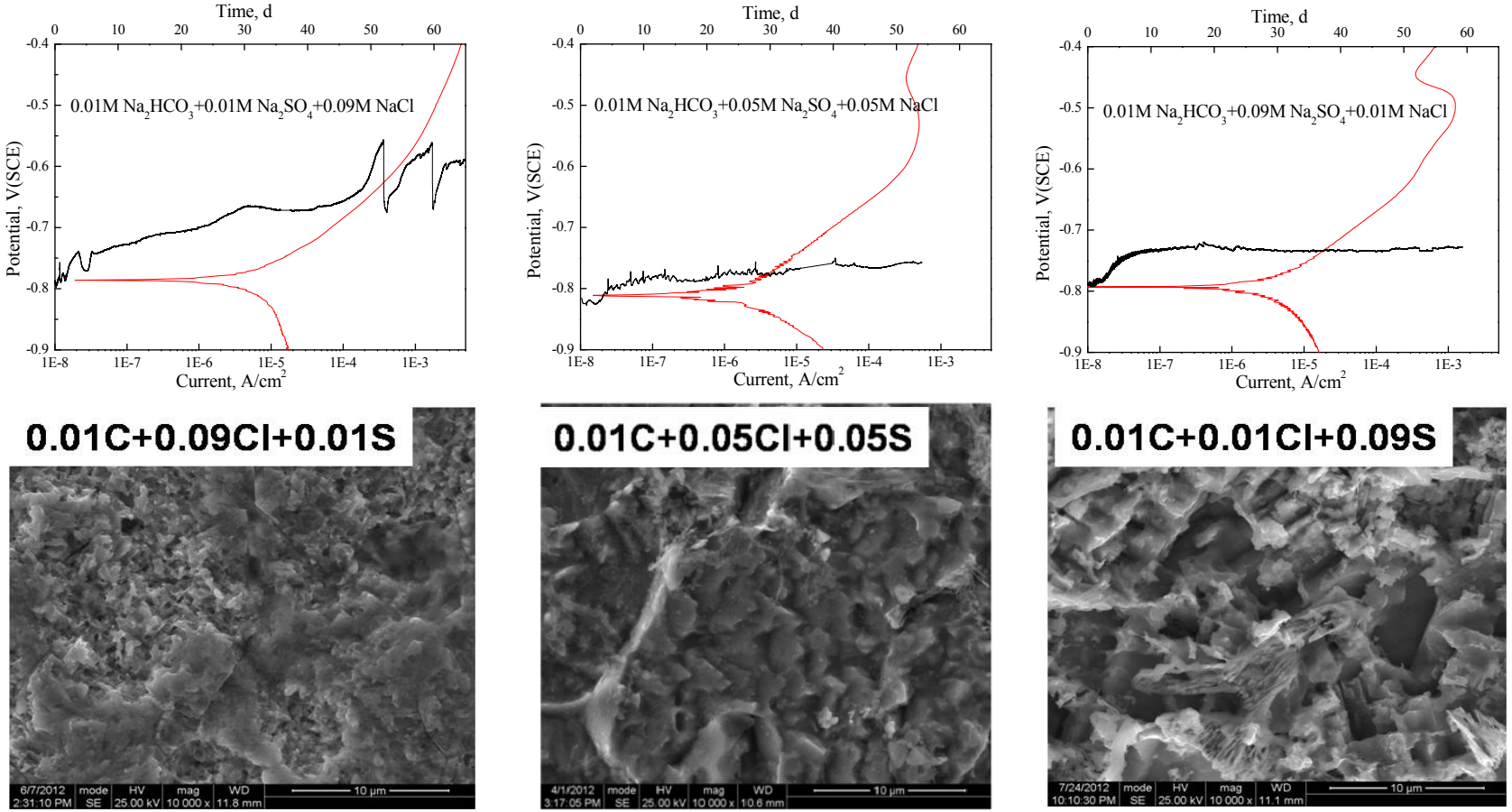

CS keeps anodic active dissolution in 0.01M HCO_3^- solutions containing both SO_4^{2-} and Cl^-, morphologies after long term immersion show a general corrosion.

Results and discussions

XRD patterns of the corrosion products of CS immersed in 0.01M HCO_3^- solutions containing both SO_4^{2-} and Cl^- and the corrosion potential of CS in Pourbaix diagram

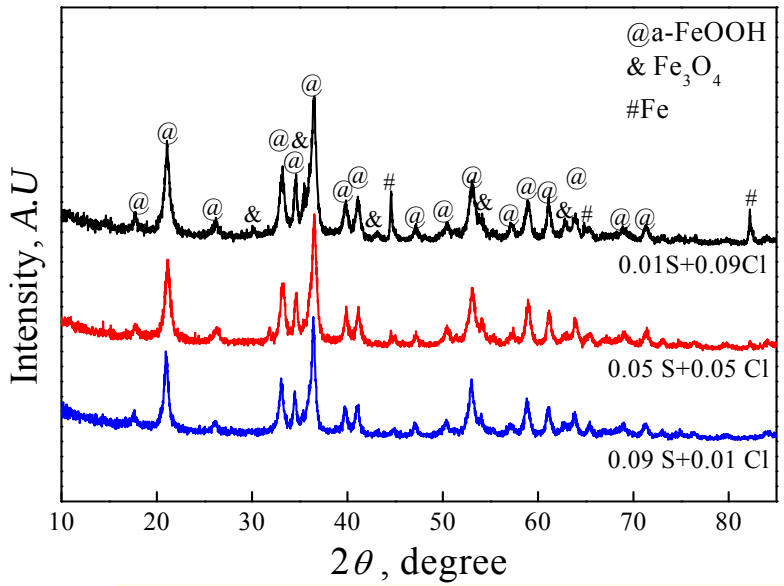

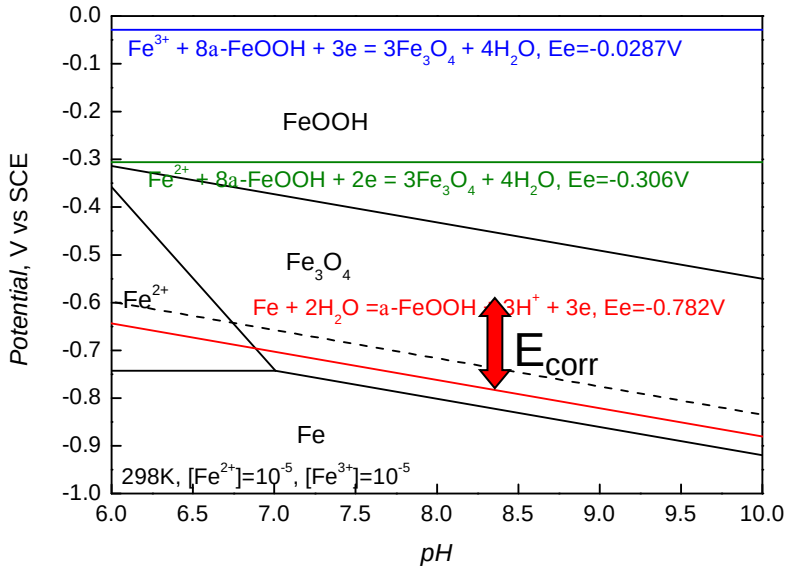

Anode: $Fe + 2H_2O = \alpha\text{-}FeOOH + 3H^+ + 3e$, pH=8.33, E_e=-0.742V

Cathode: $Fe^{2+} + 8\alpha\text{-}FeOOH + 2e = 3Fe_3O_4 + 4H_2O$, E_e= -0.306V

$3\,\alpha\text{-}FeOOH + H^+ + e = Fe_3O_4 + 2H_2O$, Ee= -0.4521V

$2H^+ + 2e = H_2$, E_e= -0.7366V

Results and discussions

Polarization behaviors and corrosion potentials of CS in 0.05M HCO_3^- solutions containing Cl^-

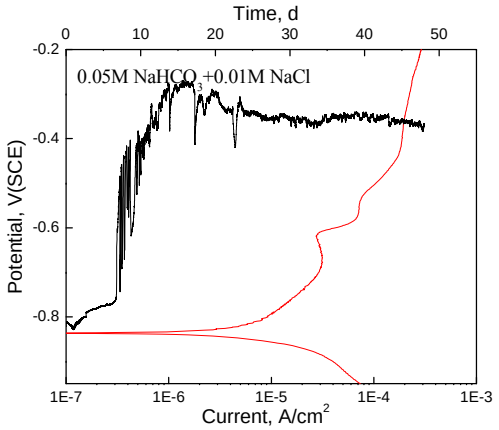

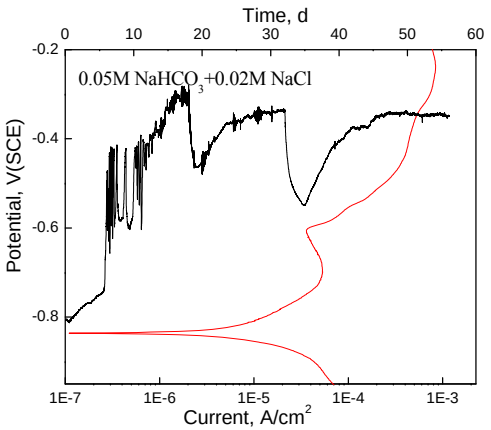

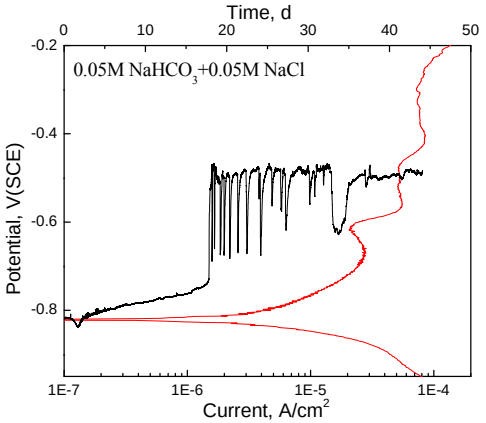

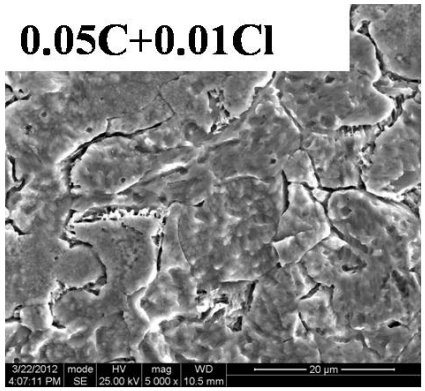

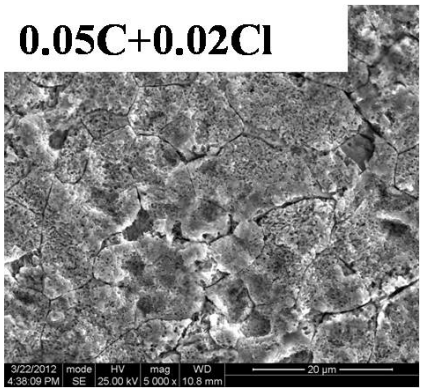

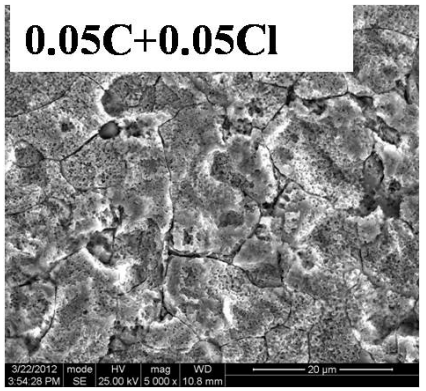

CS conducts anodic transpassivation in 0.05M HCO_3^- solutions containing Cl^-, morphologies after long term immersion show a localized corrosion.

Results and discussions

Polarization behaviors and corrosion potentials of CS in 0.05M HCO_3^- solutions containing Cl^-

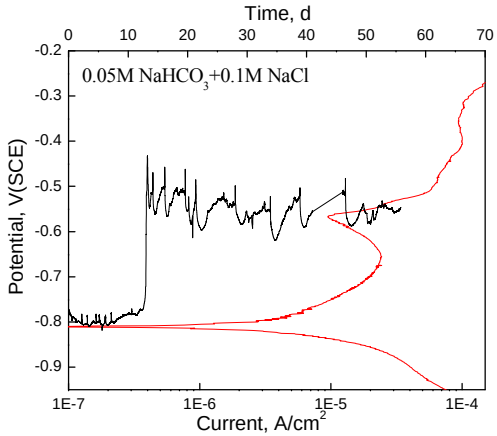

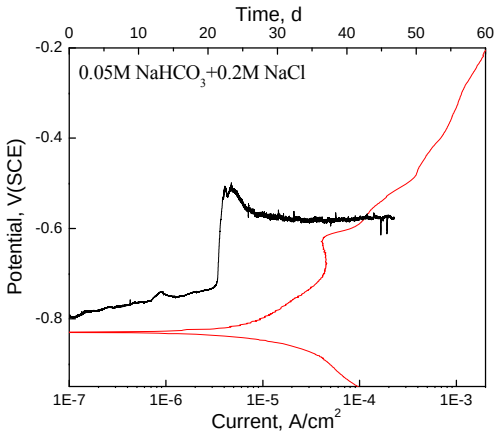

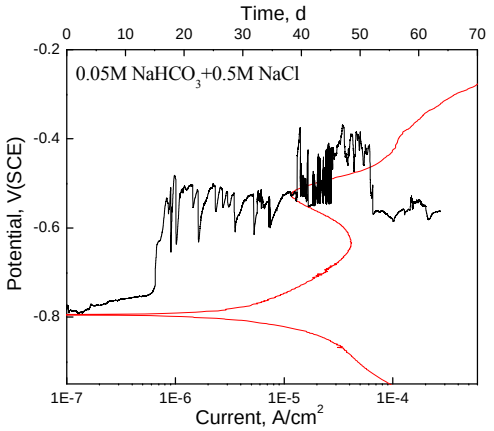

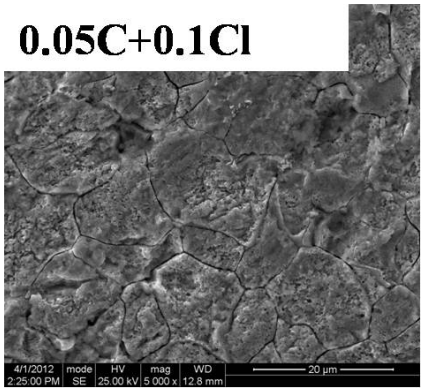

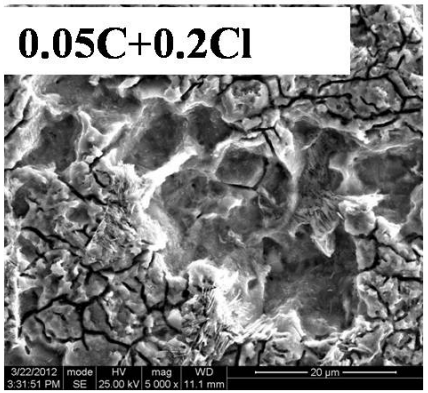

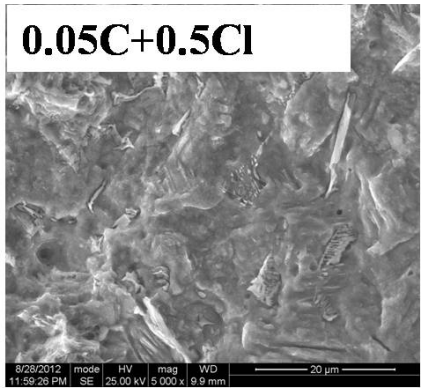

CS conducts anodic transpassivation in 0.05M HCO_3^- solutions containing Cl^-, morphologies after long term immersion show a localized corrosion.

Results and discussions

XRD patterns of the corrosion products of CS immersed in 0.05M HCO_3^- solutions containing Cl^- and the corrosion potential of CS drawn in Pourbaix diagram

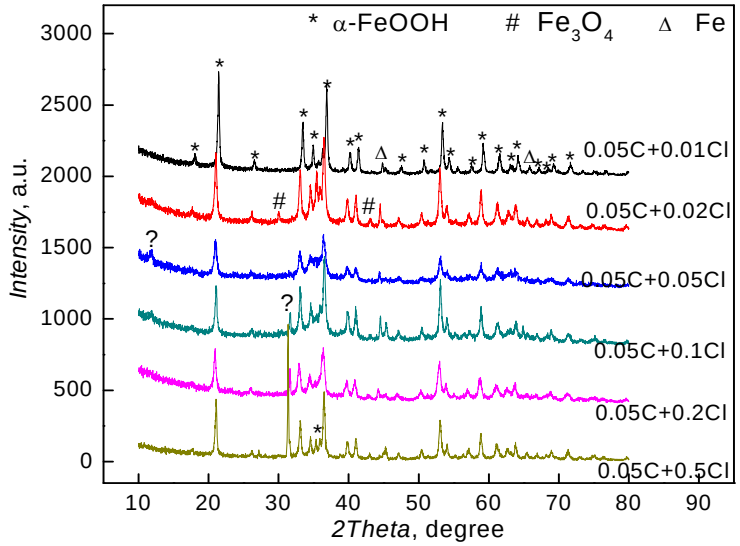

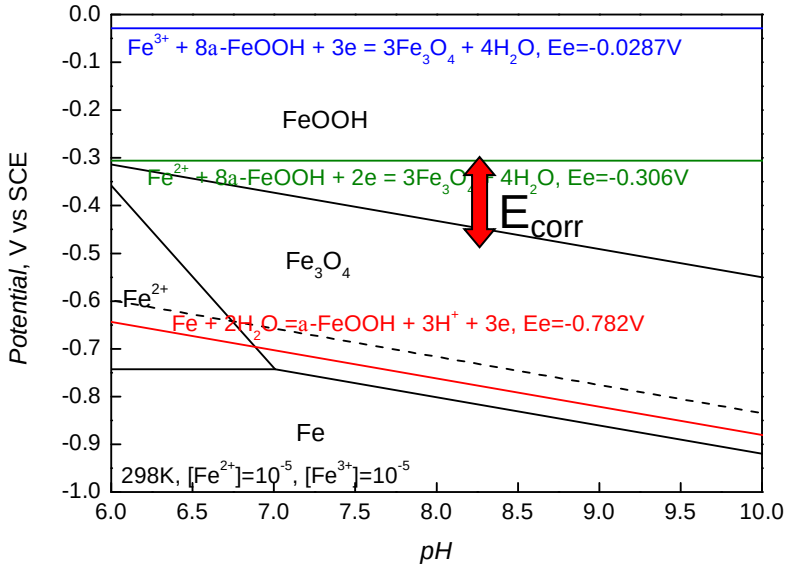

Anode: $Fe + 2H_2O = \alpha\text{-}FeOOH + 3H^+ + 3e$, pH=8.33, E_e=-0.742V

Cathode: $Fe^{2+} + 8\alpha\text{-}FeOOH + 2e = 3Fe_3O_4 + 4H_2O$, E_e= -0.306V

Results and discussions

Polarization behaviors and corrosion potentials of CS in 0.05M HCO_3^- solutions containing SO_4^{2-}

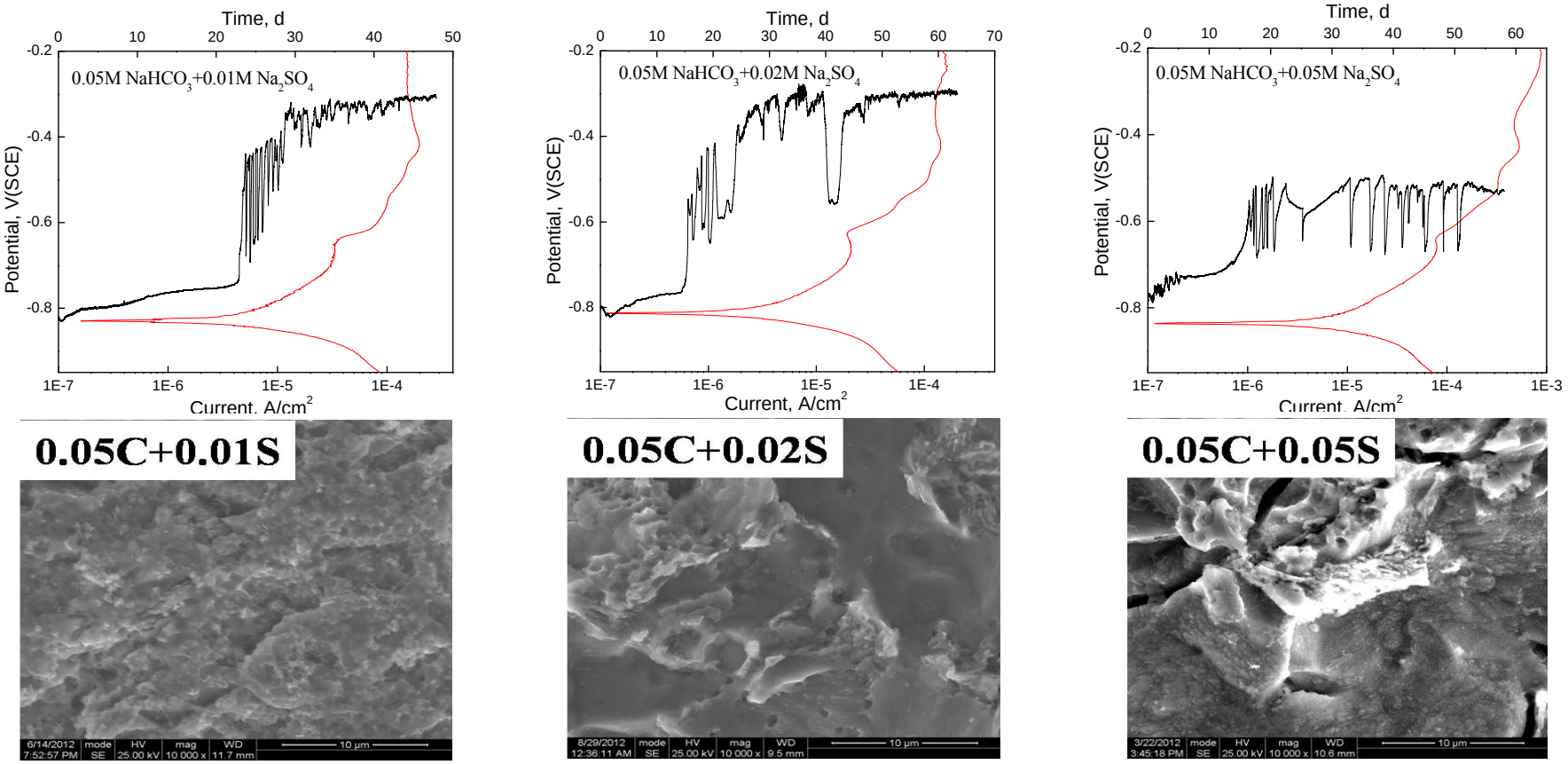

CS conducts anodic transpassivation in 0.05M HCO_3^- solutions containing high SO_4^{2-} concentration.

Results and discussions

Polarization behaviors and corrosion potentials of CS in 0.05M HCO_3^- solutions containing SO_4^{2-}

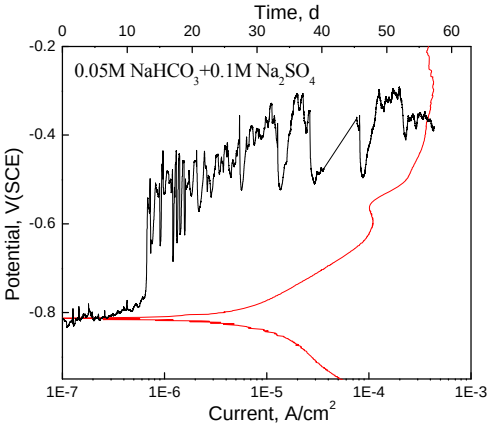

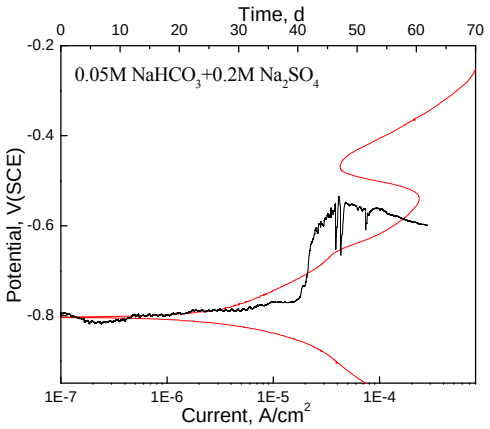

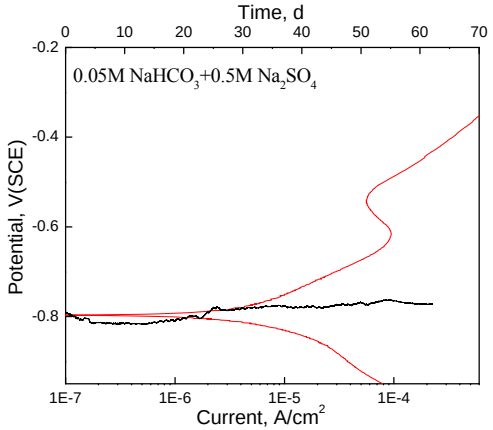

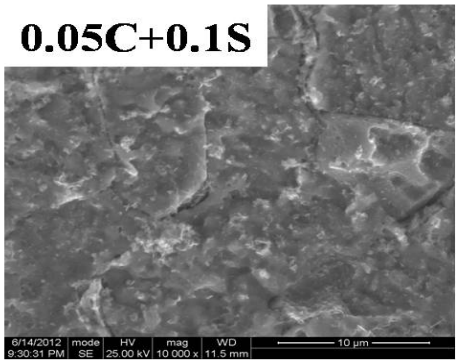

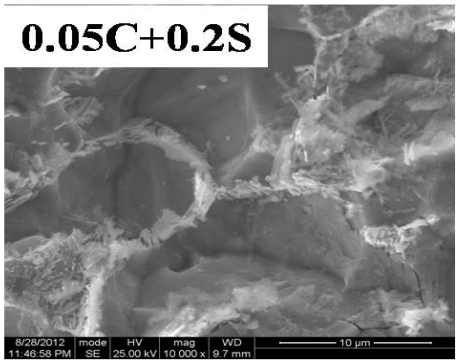

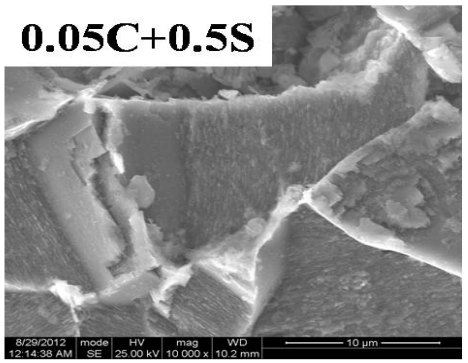

CS conducts anodic active dissolution in 0.05M HCO_3^- solutions containing low SO_4^{2-} concentration. Increase of SO_4^{2-} concentration decreases the corrosion potential; morphologies after long term immersion show a general corrosion.

Results and discussions

XRD patterns of the corrosion products of CS immersed in 0.05M HCO_3^- solutions containing SO_4^{2-} and the corrosion potential of CS drawn in Pourbaix diagram

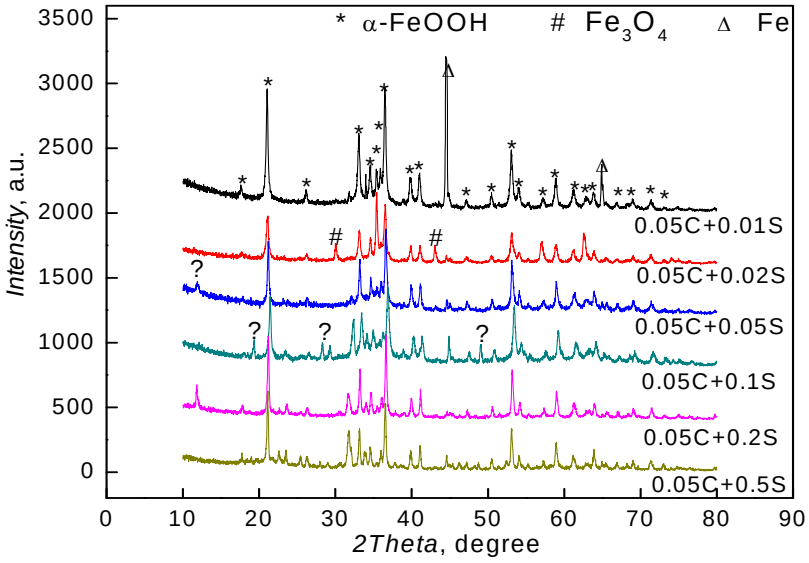

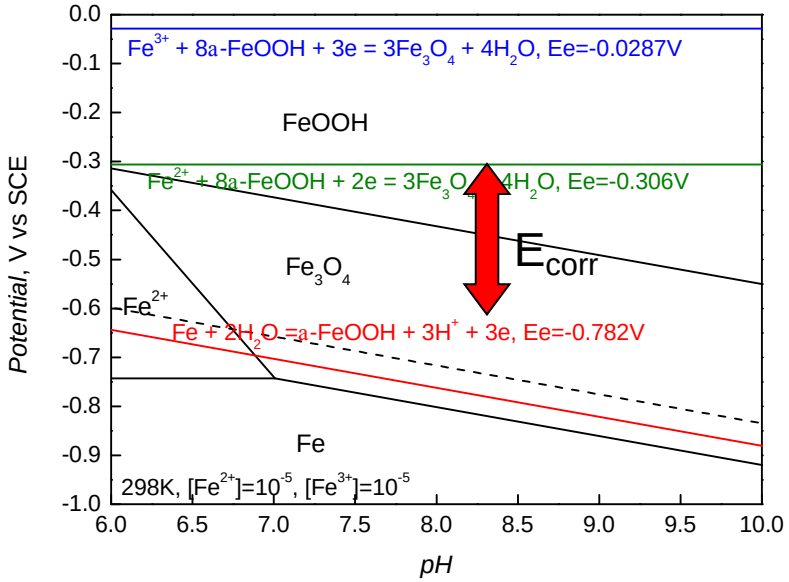

Anode: $Fe + 2H_2O = \alpha\text{-}FeOOH + 3H^+ + 3e$, pH=8.33, E_e=-0.742V

Cathode: $Fe^{2+} + 8\alpha\text{-}FeOOH + 2e = 3Fe_3O_4 + 4H_2O$, E_e= -0.306V

$3\,\alpha\text{-}FeOOH + H^+ + e = Fe_3O_4 + 2H_2O$, Ee= -0.4521V

Results and discussions

Polarization behaviors and corrosion potentials of CS in 0.05M HCO_3^- solutions containing both SO_4^{2-} and Cl^-

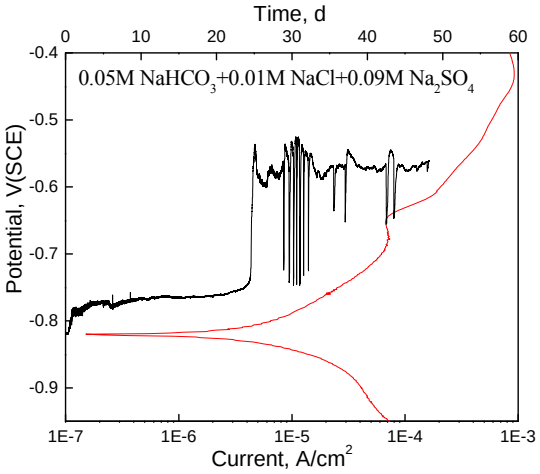

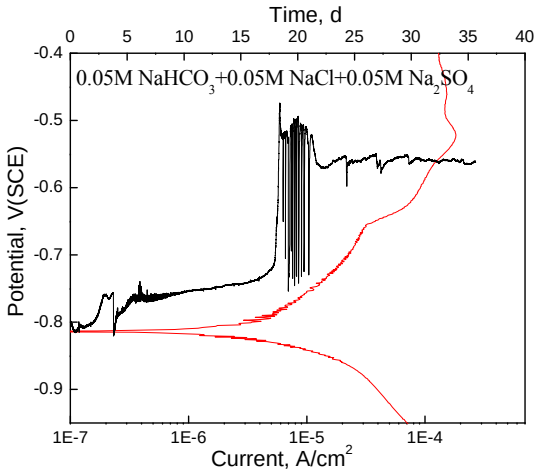

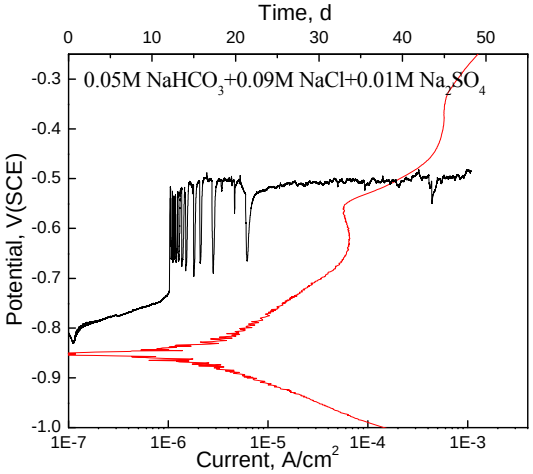

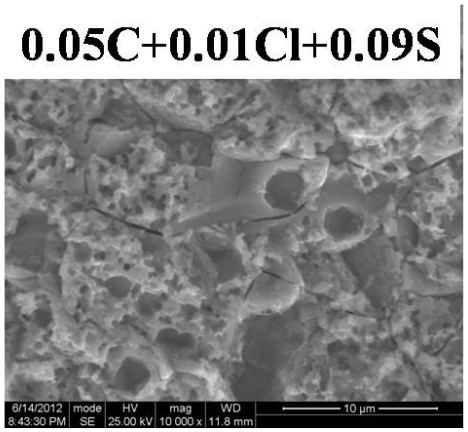

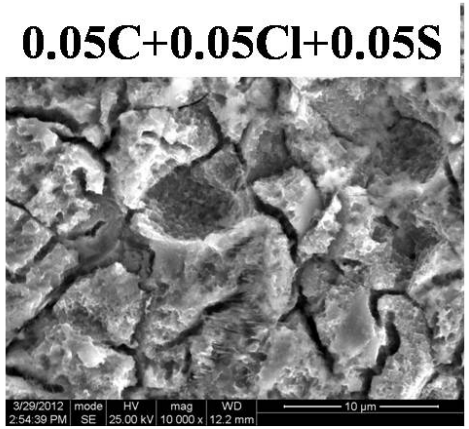

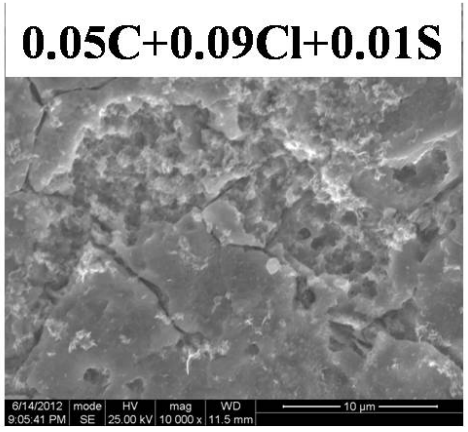

CS conducts localized anodic dissolution in 0.05M HCO_3^- solutions containing both SO_4^{2-} and Cl^-, morphologies after long term immersion show a pitting corrosion.

Results and discussions

XRD patterns of the corrosion products of CS immersed in 0.05M HCO_3^- solutions containing both SO_4^{2-} and Cl^- and the corrosion potential of CS in Pourbaix diagram

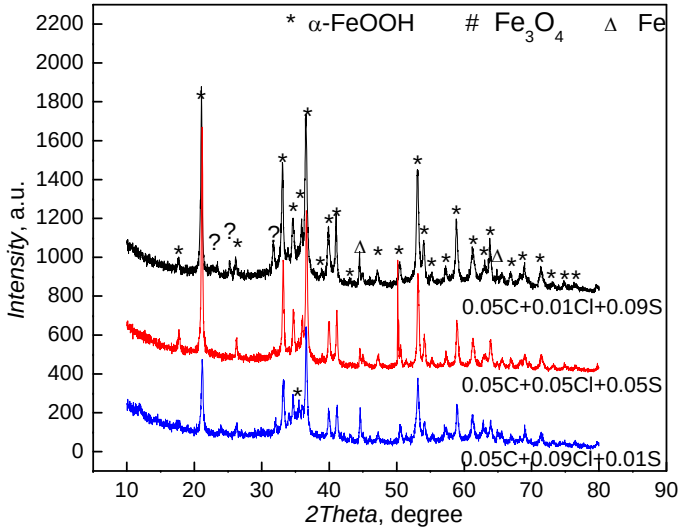

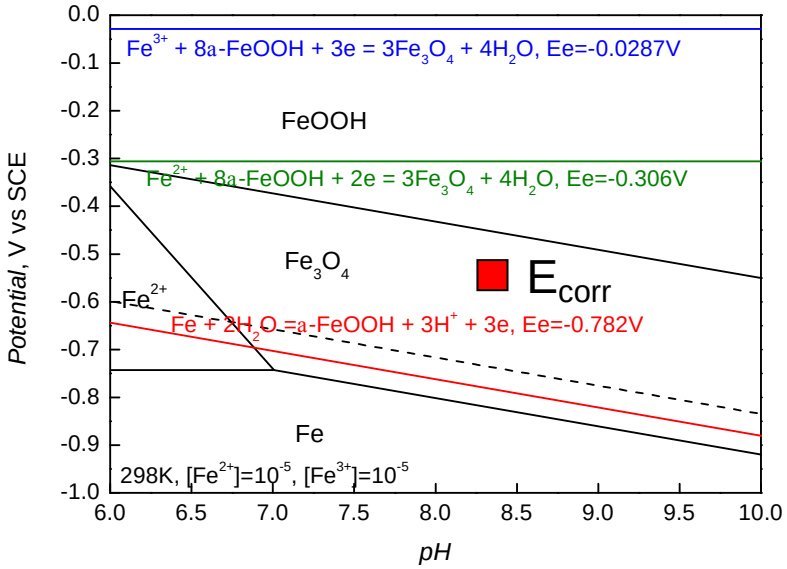

Anode: $Fe + 2H_2O = \alpha\text{-}FeOOH + 3H^+ + 3e$, pH=8.33, E_e=-0.742V

Cathode: $Fe^{2+} + 8\alpha\text{-}FeOOH + 2e = 3Fe_3O_4 + 4H_2O$, E_e= -0.306V

$3\,\alpha\text{-}FeOOH + H^+ + e = Fe_3O_4 + 2H_2O$, Ee= -0.4521V

Results and discussions

Polarization behaviors and corrosion potentials of CS in 0.1M HCO_3^- solutions containing Cl^-

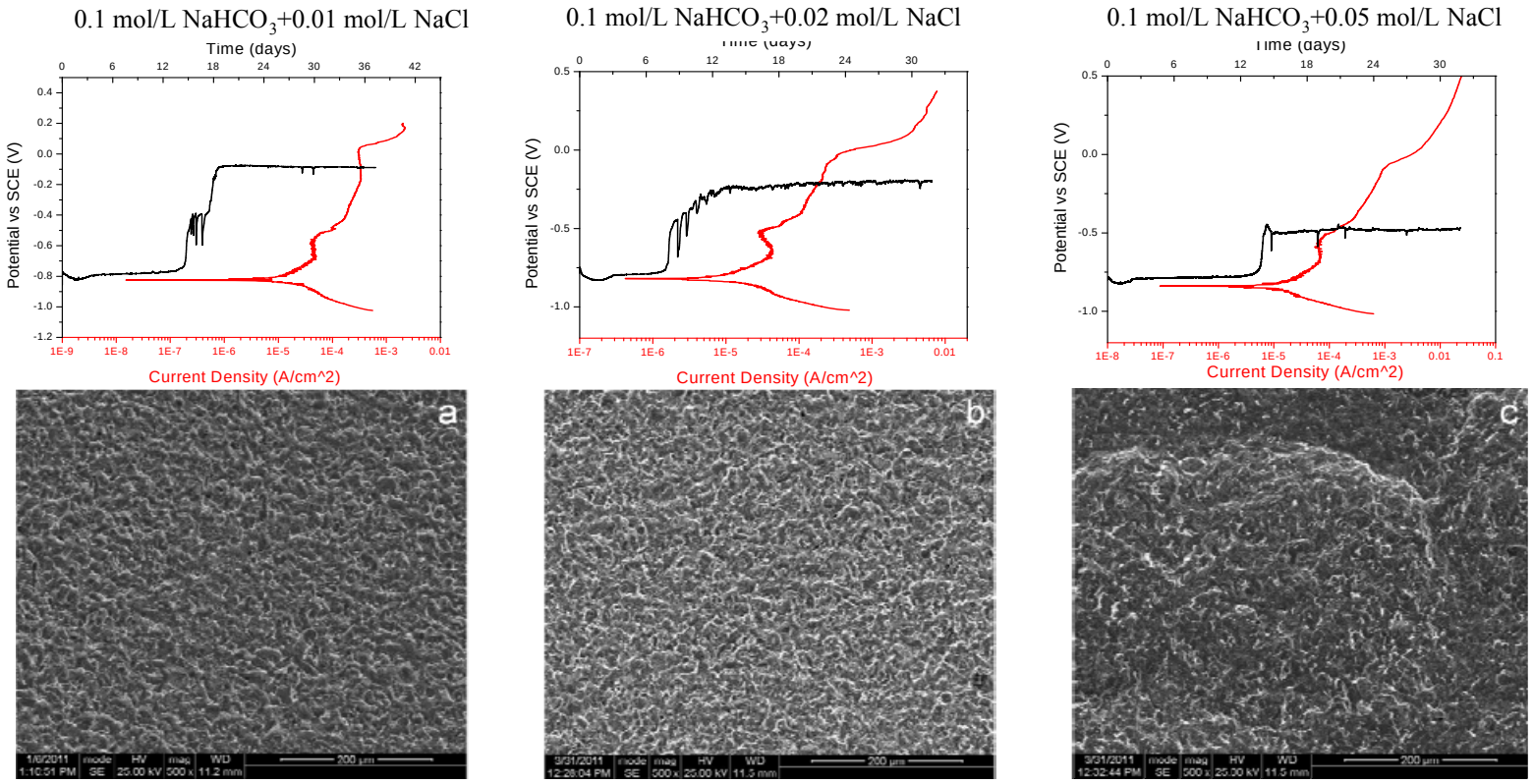

CS conducts transpassivation corrosion at low Cl- concentration, morphologies show general corrosion; but converts to localized corrosion at higher than 0.05M

Results and discussions

Polarization behaviors and corrosion potentials of CS in 0.1M HCO_3^- solutions containing Cl^-

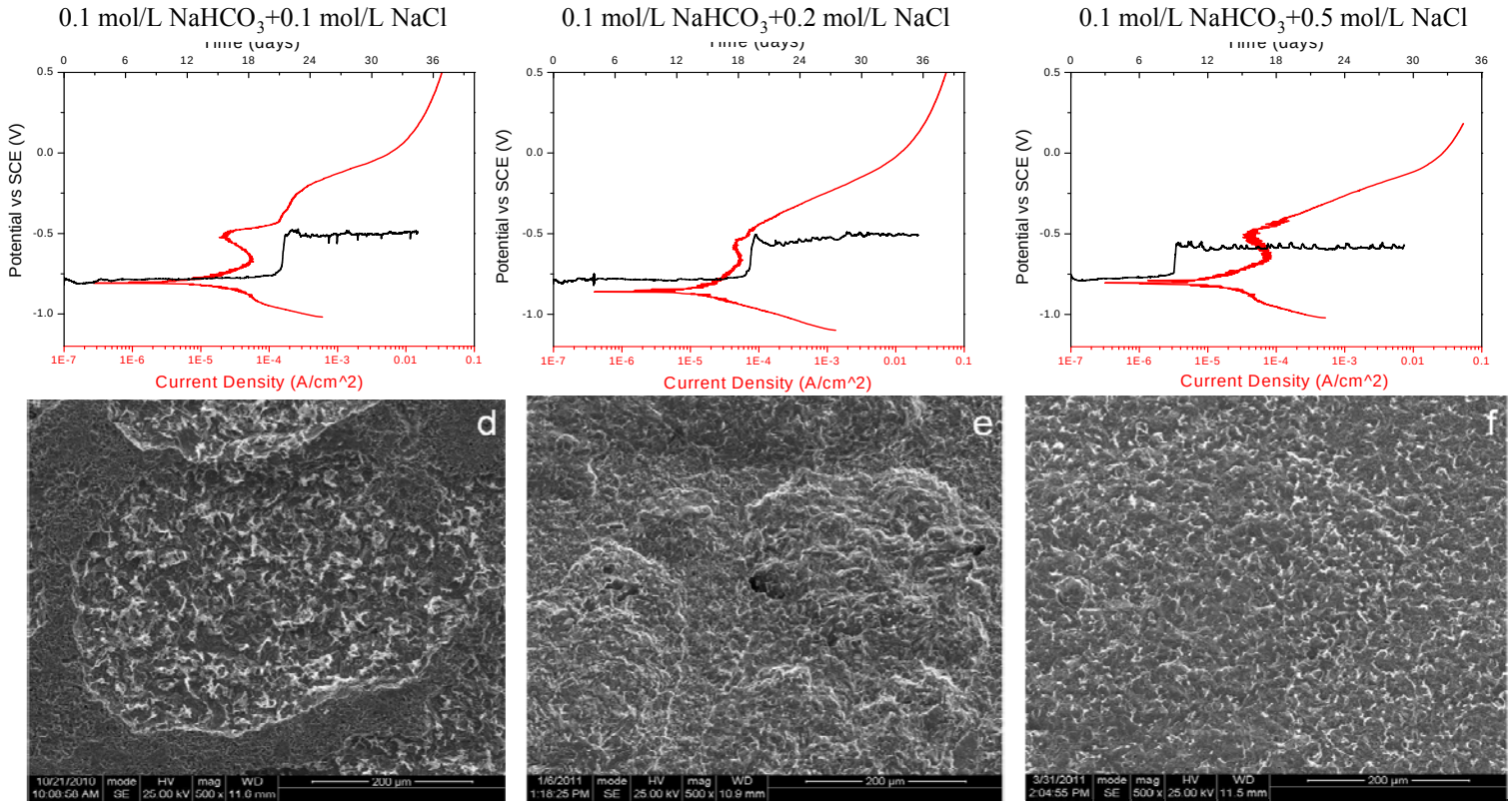

The corrosion potential of CS decreases with increasing Cl- concentration, corrosion mode converts from transpassivation to passivation.

Results and discussions

XRD patterns of the corrosion products after the immersion

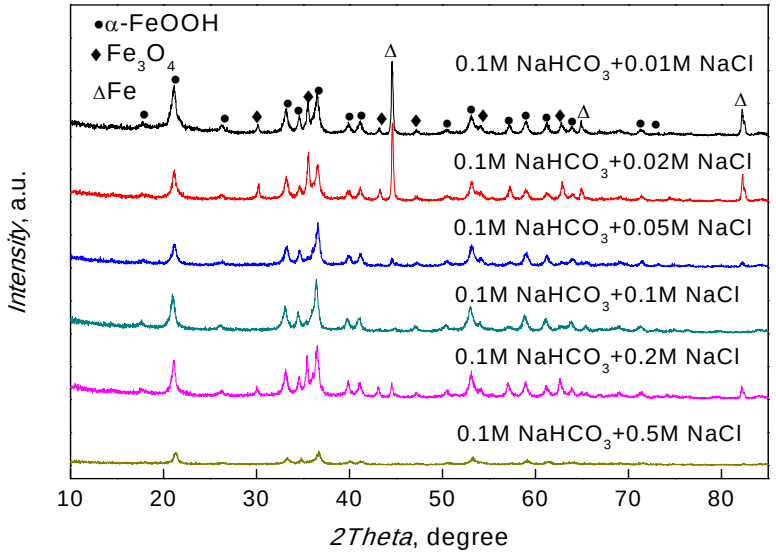

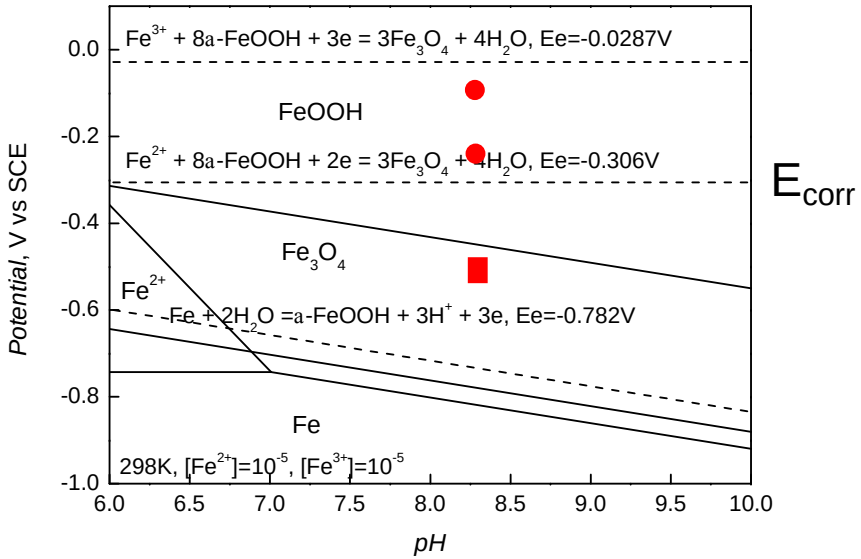

Anode: $Fe + 2H_2O = \alpha\text{-}FeOOH + 3H^+ + 3e$, pH=8.33, E_e=-0.742V

Cathode: $Fe^{3+} + 8\alpha\text{-}FeOOH + 3e = 3Fe_3O_4 + 4H_2O$, Ee= -0.0287V

$Fe^{2+} + 8\alpha\text{-}FeOOH + 2e = 3Fe_3O_4 + 4H_2O$, E_e= -0.306V

$3\,\alpha\text{-}FeOOH + H^+ + e = Fe_3O_4 + 2H_2O$, Ee= -0.4521V

Results and discussions

Polarization behaviors and corrosion potentials of CS in 0.1M HCO_3^- solutions containing SO_4^{2-}

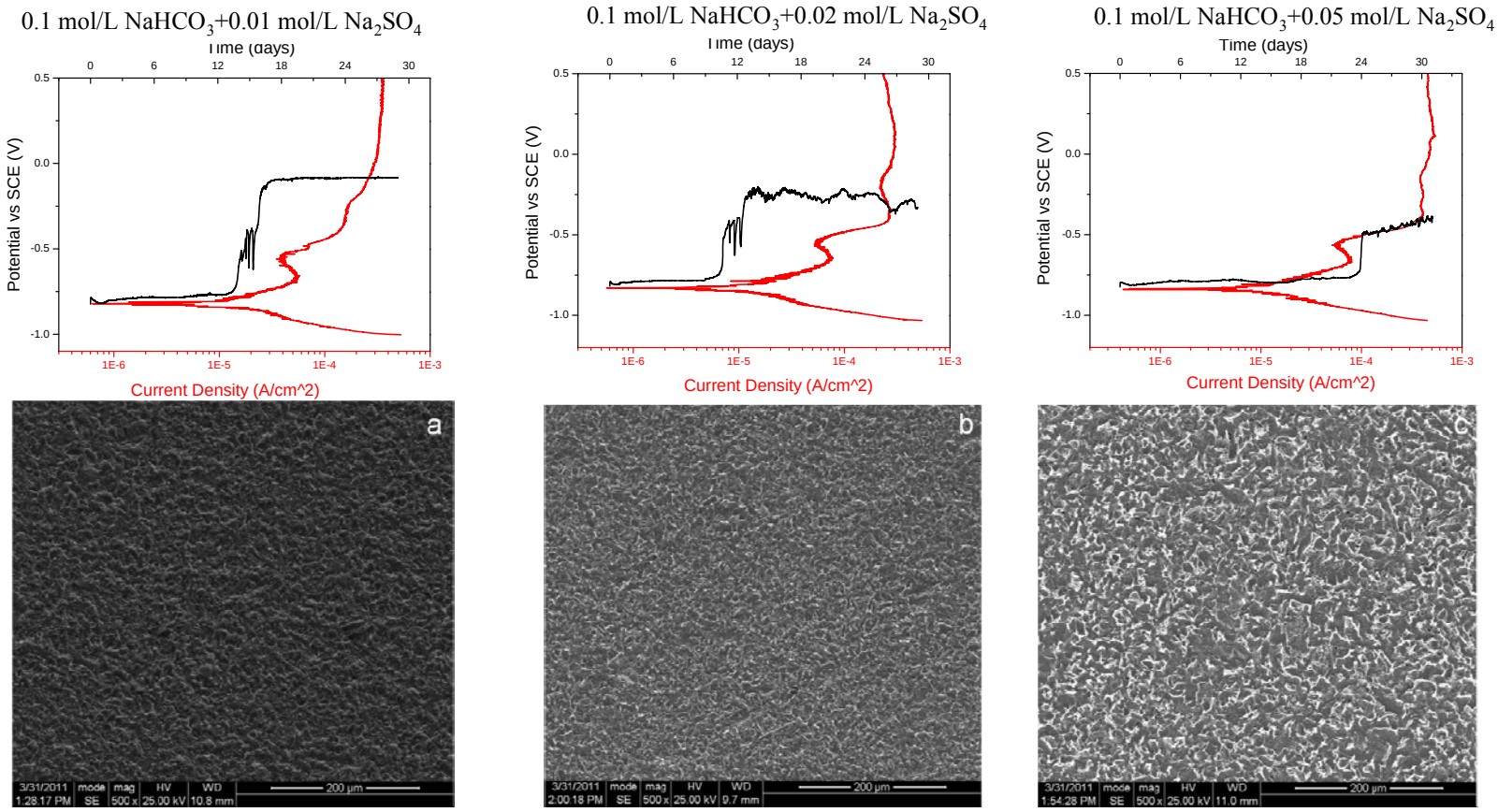

CS conducts anodic transpassivation in 0.1 HCO_3^- solutions containing high SO_4^{2-} concentration. morphologies after long term immersion show a general corrosion.

Results and discussions

Polarization behaviors and corrosion potentials of CS in 0.1M HCO_3^- solutions containing SO_4^{2-}

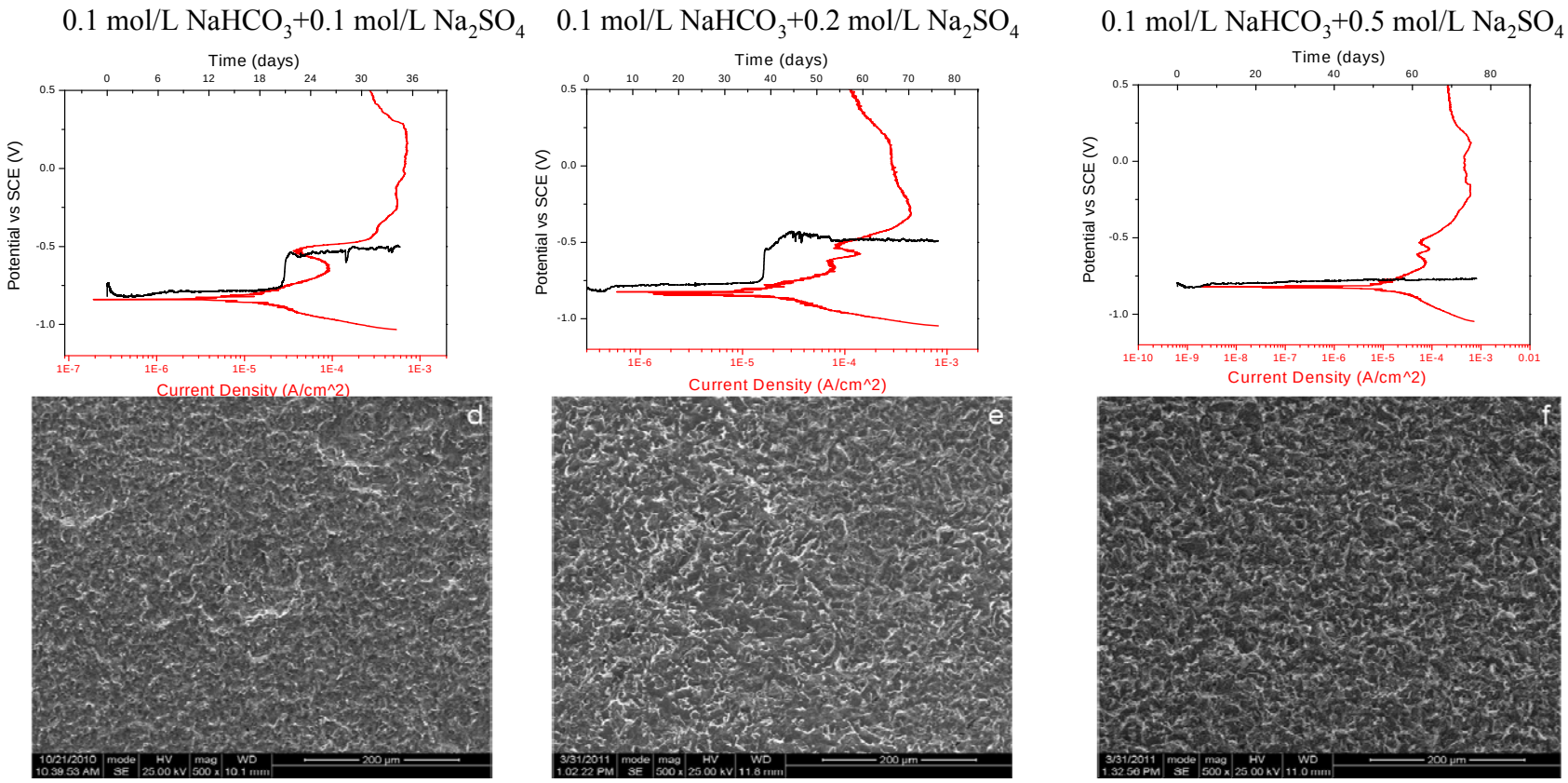

CS conducts anodic transpassivation in 0.1M HCO_3^- solutions containing low SO_4^{2-} concentration. morphologies after long term immersion show a general corrosion.

Results and discussions

XRD patterns of the corrosion products after the immersion

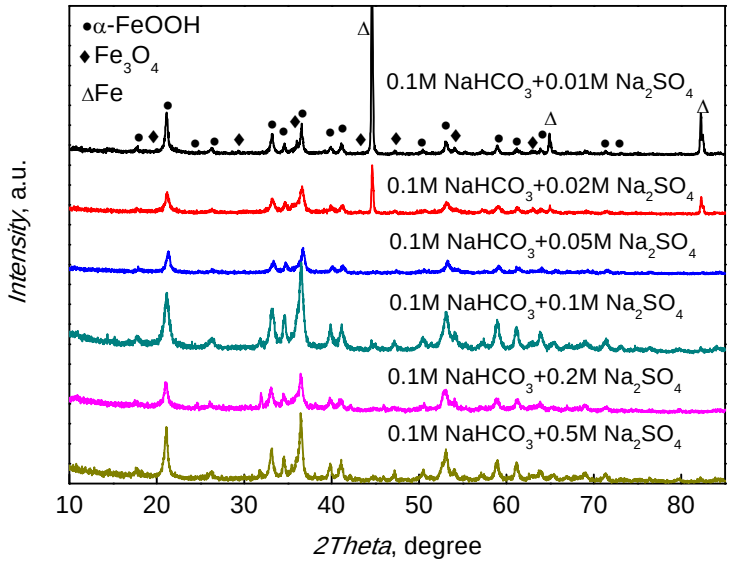

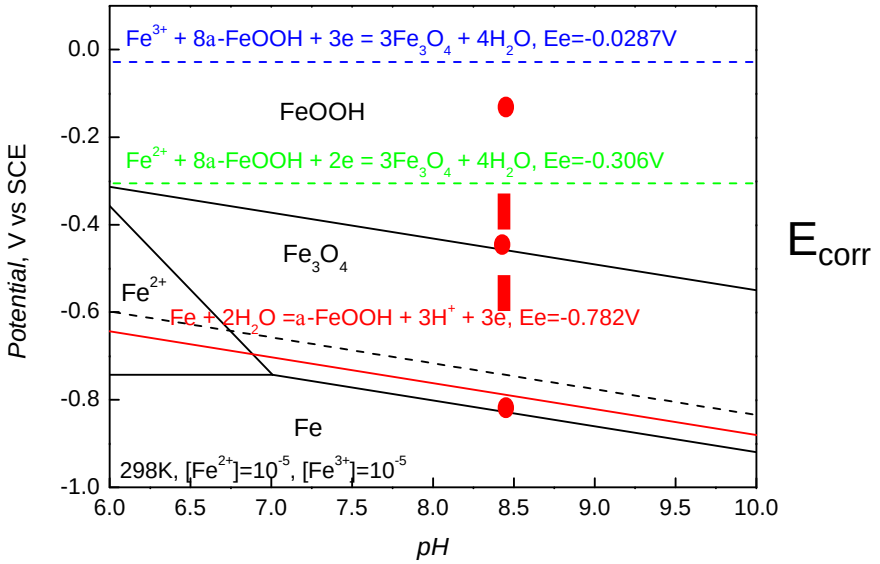

E_{corr}

Anode: $Fe + 2H_2O = \alpha\text{-}FeOOH + 3H^+ + 3e$, pH=8.33, E_e=-0.742V

Cathode: $Fe^{3+} + 8\alpha\text{-}FeOOH + 3e = 3Fe_3O_4 + 4H_2O$, Ee= -0.0287V

$Fe^{2+} + 8\alpha\text{-}FeOOH + 2e = 3Fe_3O_4 + 4H_2O$, E_e= -0.306V

$3\,\alpha\text{-}FeOOH + H^+ + e = Fe_3O_4 + 2H_2O$, Ee= -0.4521V

Results and discussions

Polarization behaviors and corrosion potentials of CS in 0.1M HCO_3^- solutions containing both SO_4^{2-} and Cl^-

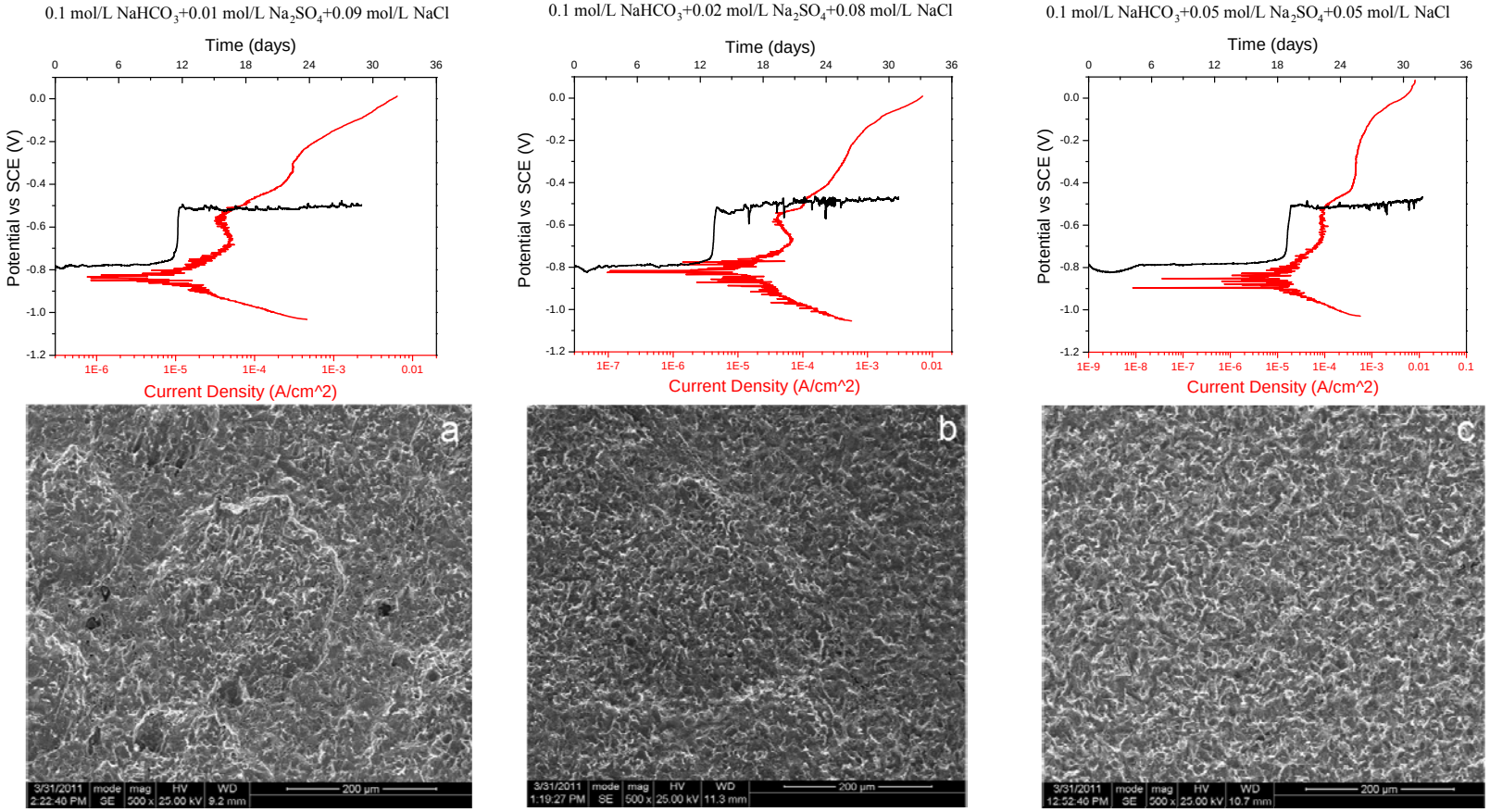

CS conducts transpassivation corrosion in 0.1M HCO_3^- solutions containing both SO_4^{2-} and Cl^-, localized corrosion morphologies were shown in high Cl^- and low SO_4^{2-} concentrations but general corrosion morphologies in low Cl^- and high SO_4^{2-}.

Results and discussions

Polarization behaviors and corrosion potentials of CS in 0.1M HCO_3^- solutions containing both SO_4^{2-} and Cl^-

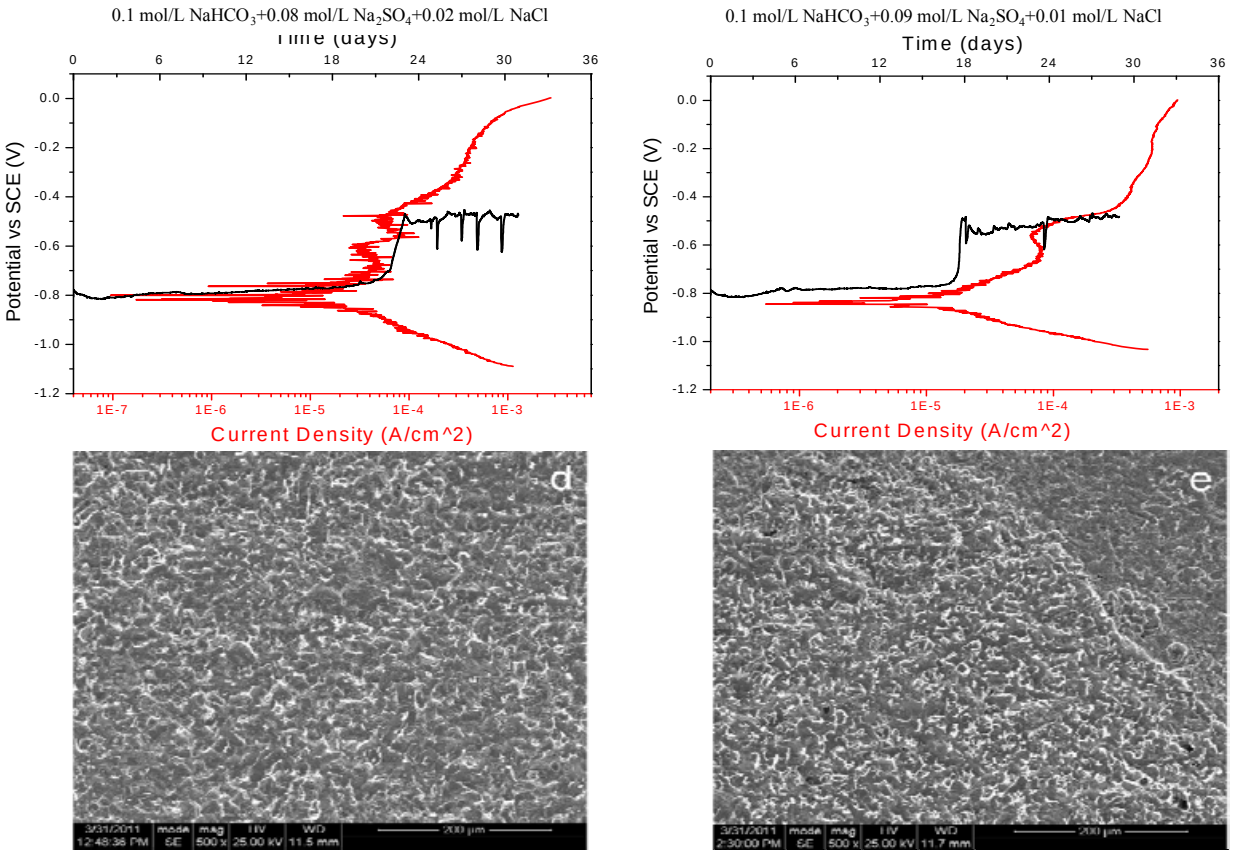

Results and discussions

XRD patterns of the corrosion products after the immersion

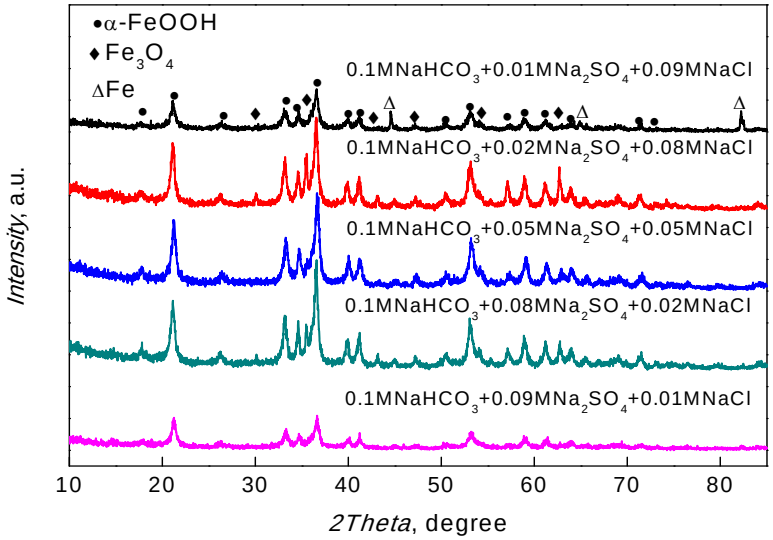

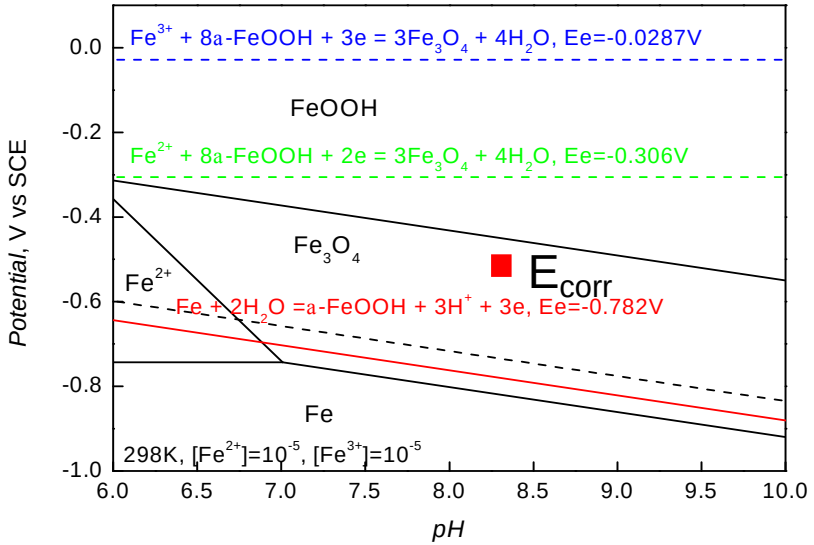

Anode: $Fe + 2H_2O = \alpha\text{-}FeOOH + 3H^+ + 3e$, pH=8.33, E_e=-0.742V

Cathode: $Fe^{2+} + 8\alpha\text{-}FeOOH + 2e = 3Fe_3O_4 + 4H_2O$, E_e= -0.306V

$3\,\alpha\text{-}FeOOH + H^+ + e = Fe_3O_4 + 2H_2O$, Ee= -0.4521V

Corrosion modes of CS in the underground water

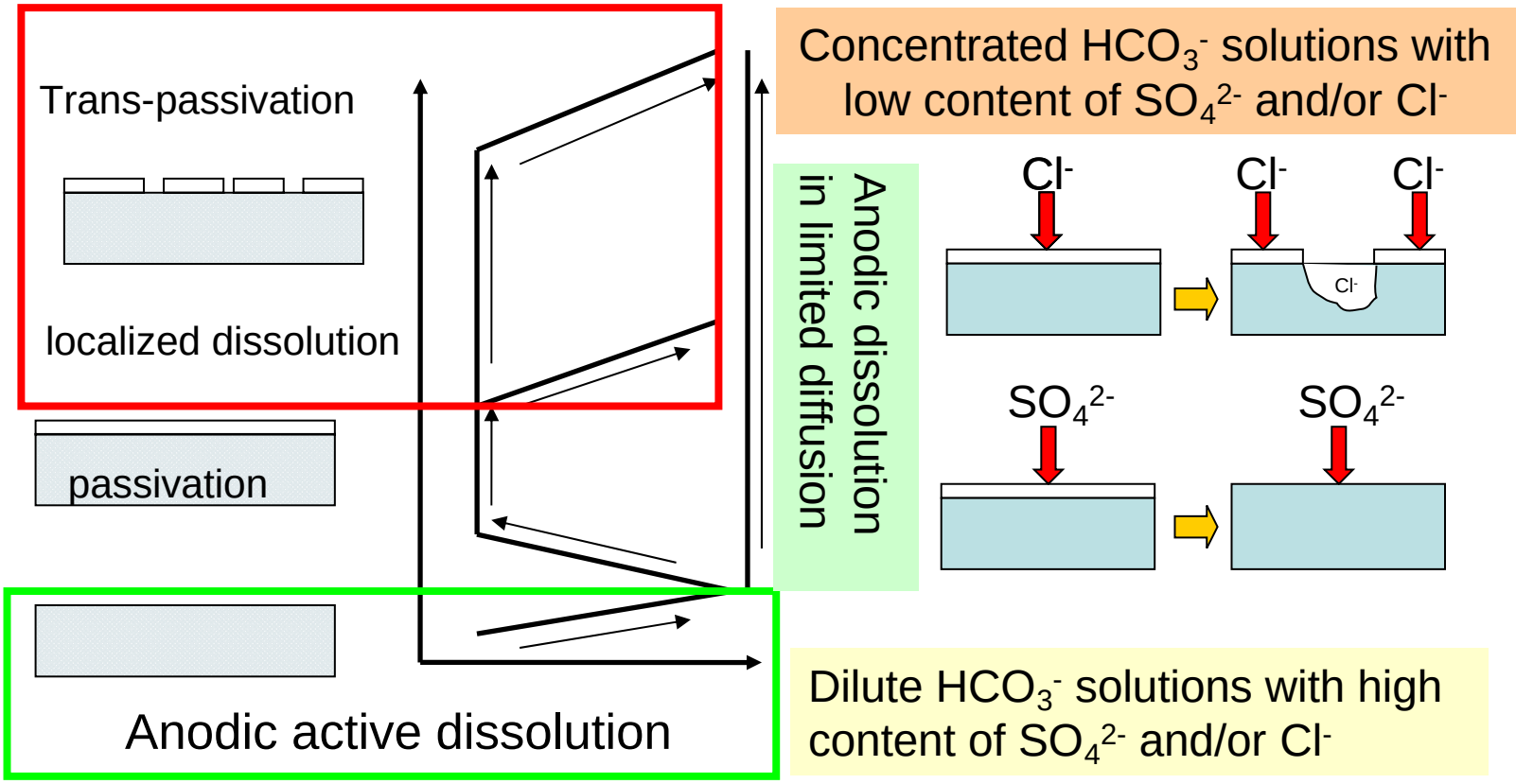

Effect of the ground water on the corrosion behavior of CS canister

- In pure HCO_3^- solution, the corrosion potential of the immersed CS locates in limited diffusion range at low concentration but trans-passivation range at high concentration
- Ether increasing Cl^- or SO_4^{2-} concentration in HCO_3^- solutions can decrease the corrosion potentials of the immersed CS, which can converts corrosion mode from trans-passivation to localized corrosion even general corrosion
- Cl^- can cause pitting corrosion under proper conditions; SO_4^{2-} just causes general corrosion;
- The mixture of Cl^- and SO_4^{2-} in HCO_3^- solutions can also decrease the corrosion potentials of the immersed CS, , high ratio of $[Cl^-]$ to $[SO_4^{2-}]$ causes pitting corrosion, low ratio of $[Cl^-]$ to $[SO_4^{2-}]$ causes general corrosion.

Results and discussions

Evolution of the Nyquist plots of low carbon steel during immersion

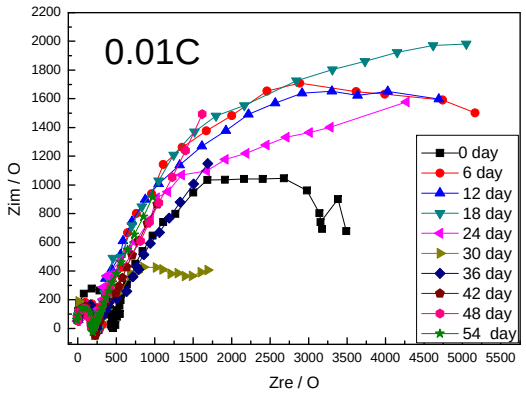

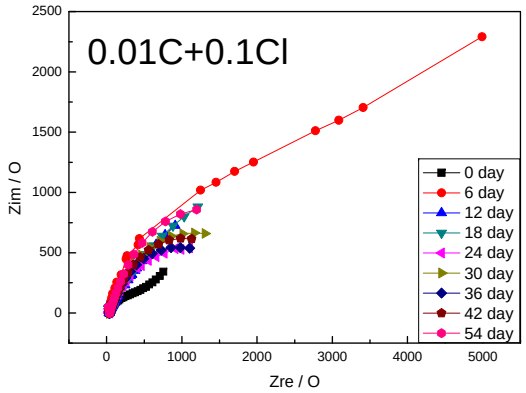

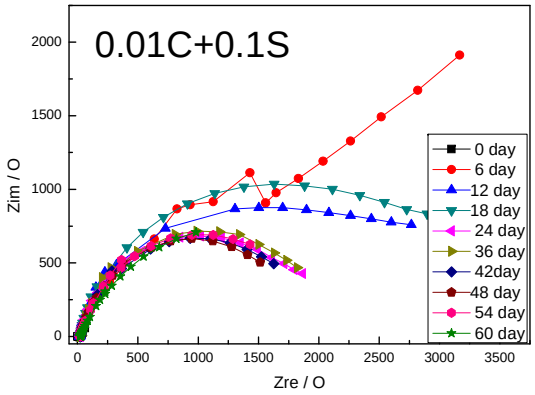

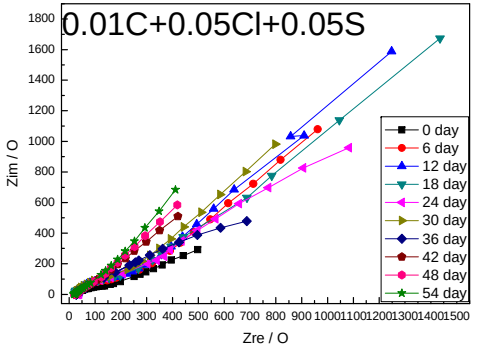

Results and discussions

Evolution of the Nyquist plots of low carbon steel during immersion

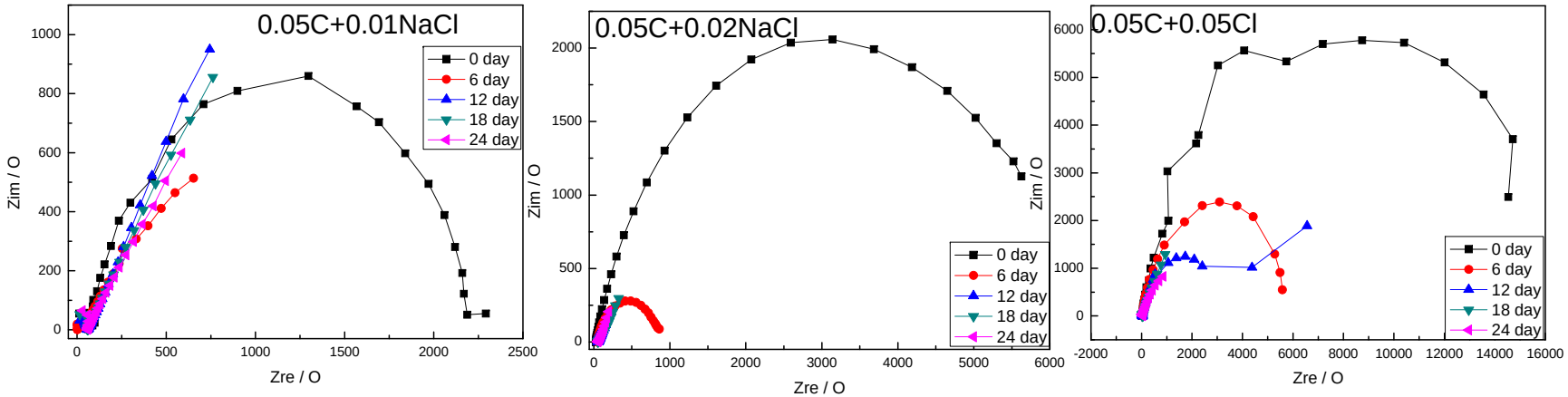

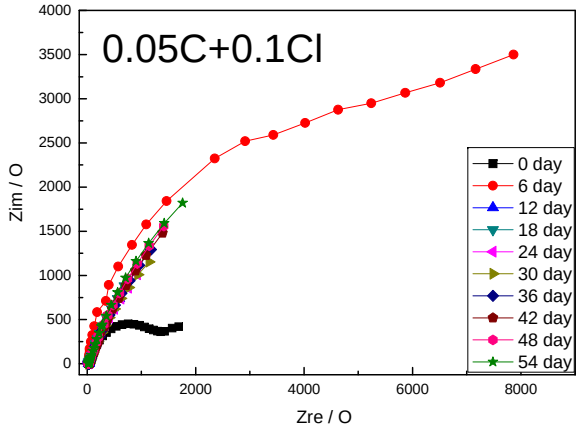

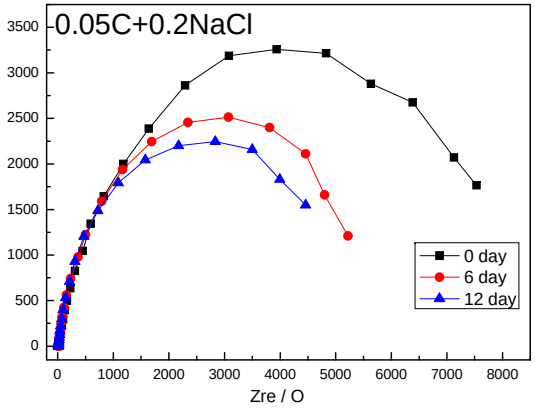

Results and discussions

Evolution of the Nyquist plots of low carbon steel during immersion

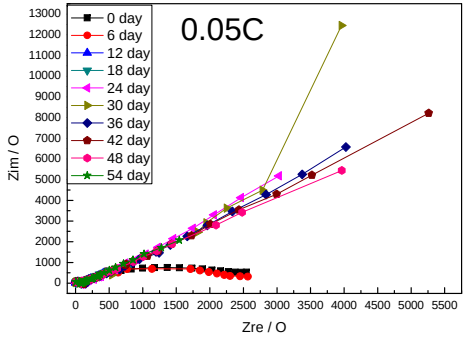

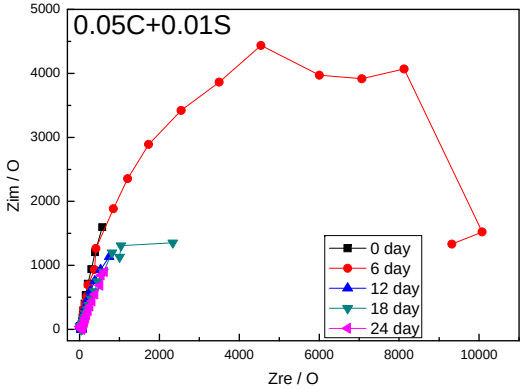

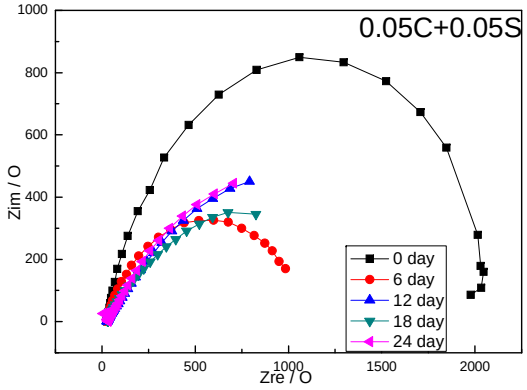

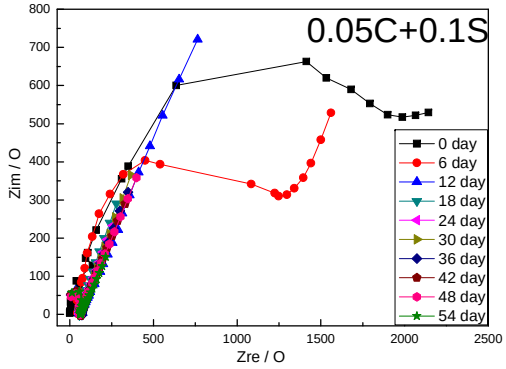

Results and discussions

Evolution of the Nyquist plots of low carbon steel during immersion

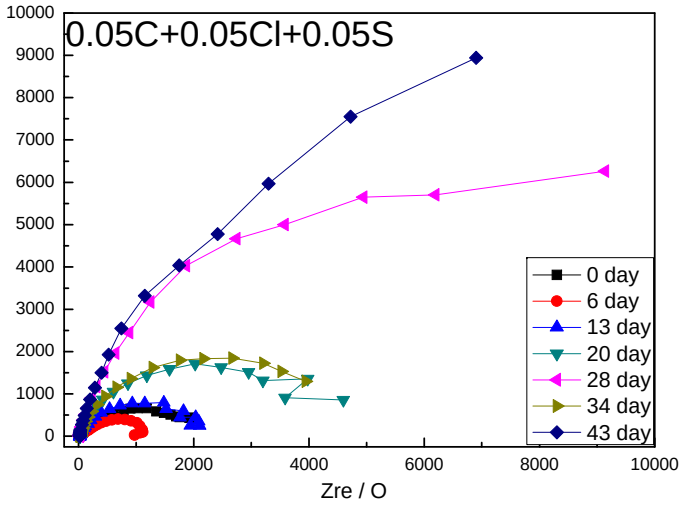

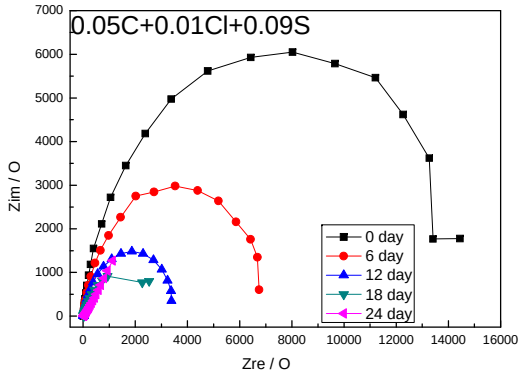

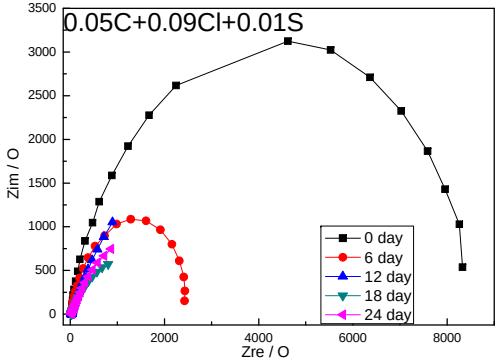

Results and discussions

Evolution of the Nyquist plots of low carbon steel during the immersion

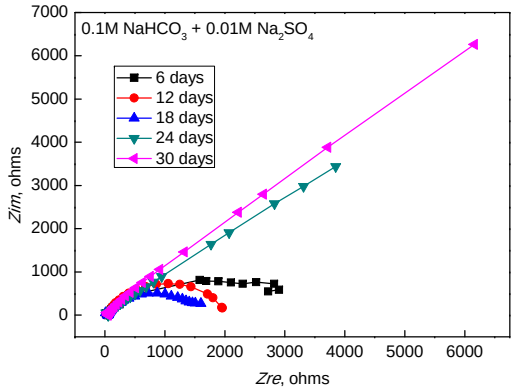

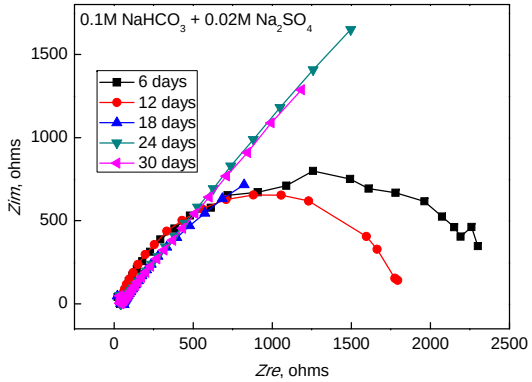

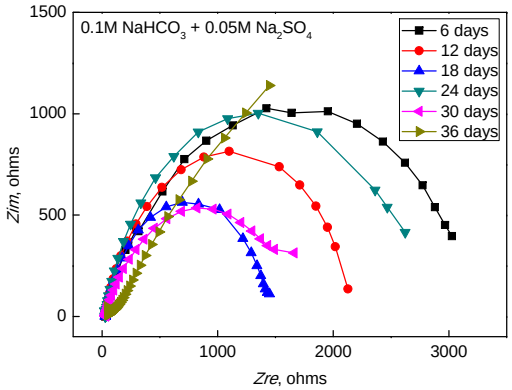

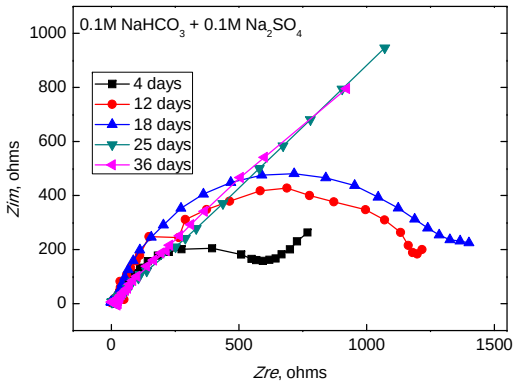

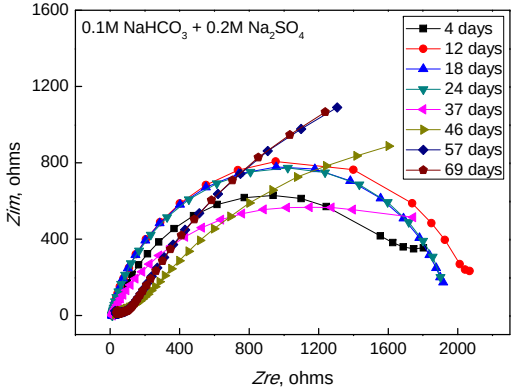

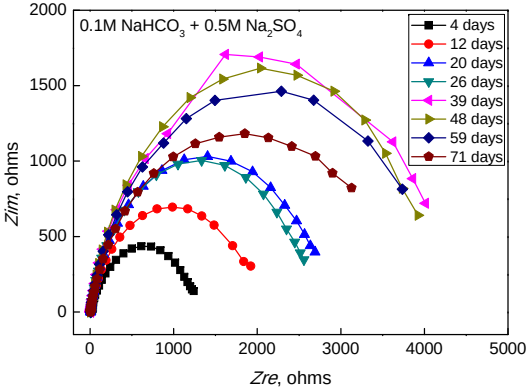

Results and discussions

Evolution of the Nyquist plots of low carbon steel during immersion

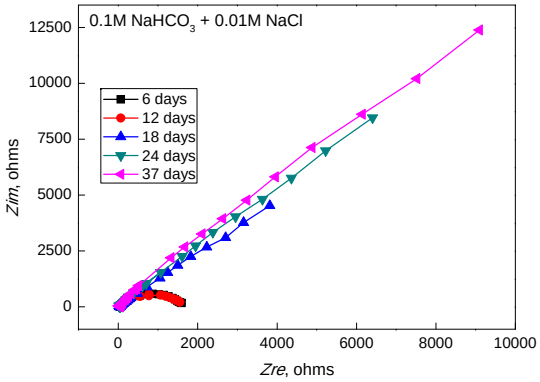

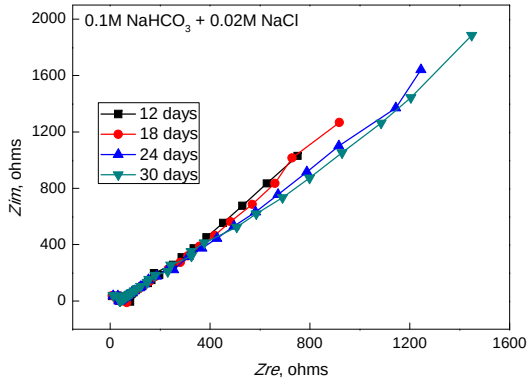

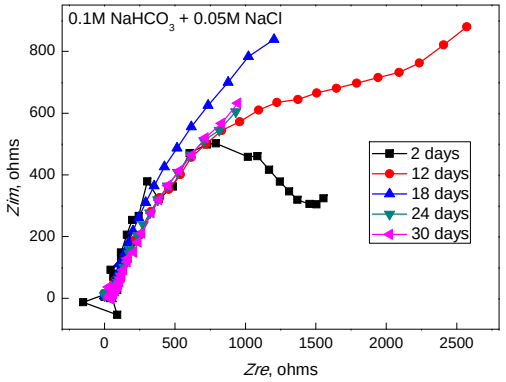

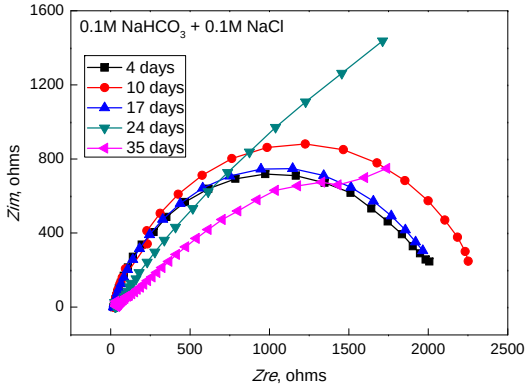

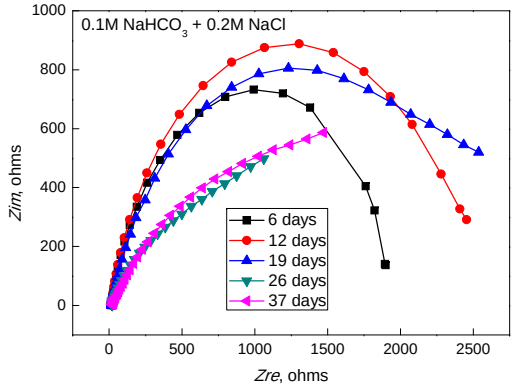

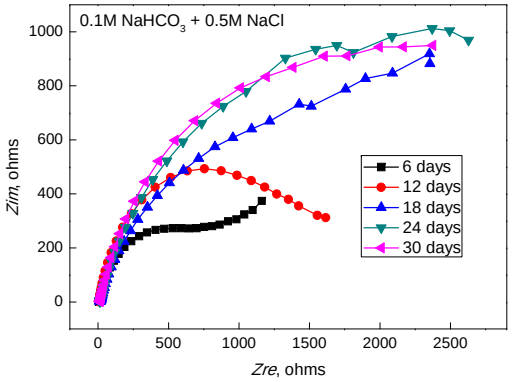

Results and discussions

Evolution of the Nyquist plots of low carbon steel during immersion

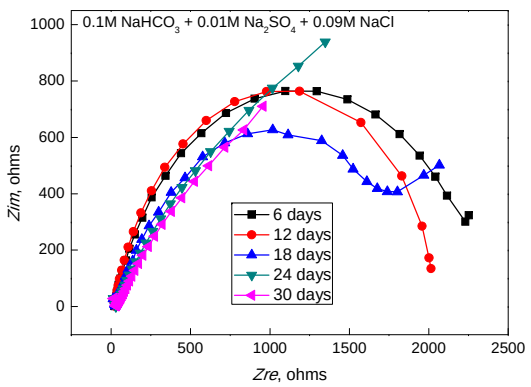

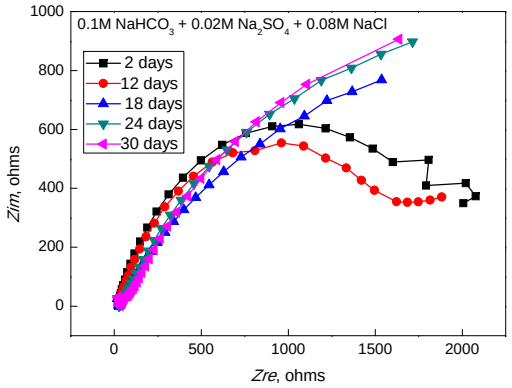

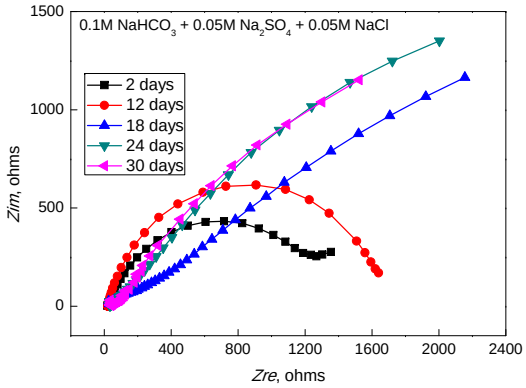

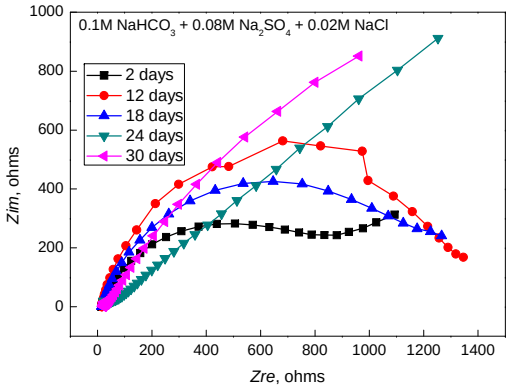

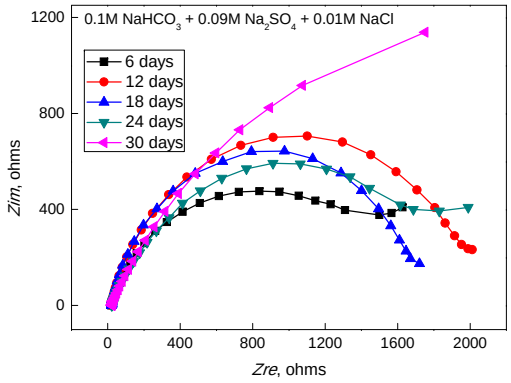

Corrosion rate of CS

- In 0.01MHCO_3^- solution with Cl^- and SO_4^{2-}, the corrosion rate is about 100μm/a.
- When HCO_3^- concentration is higher than 0.05M, whether it contains Cl^- or SO_4^{2-}, the corrosion rate will increase to about 1000μm/a.
- Relationship between corrosion current density and thickness loss for steel:

  $100\mu A/cm^2=1.13mm/a$

- If 1000a are required for the life time of CS canister during the disposal, the thickness design will be more than 1000mm, which meets a big problem!

Feasibility of CS Canister Used for HLW Geological Disposal

- The corrosion mode of CS canister will be observably influenced by the chemicals and concentrations in the underground water.
- In dilute HCO_3^- solutions with Cl^- and SO_4^{2-}, CS conducts anodic active dissolution, and may satisfy the requests for HLW geological disposal
- In more concentrated HCO_3^- solutions with Cl^- and SO_4^{2-}, CS conducts anodic trans-passivation or localized corrosion, and the corrosion rate is close to 1000μm/a, which may cause big difficulties for design and manufacture of the CS canisters.

谢谢垂听，欢迎光临

中国科学院金属研究所

Institute of Metal Research, Chinese Academy of Sciences

Direct Disposal of
Casks for Transportation and Storage CASTOR®

Enrique Biurrun

DBE TECHNOLOGY GmbH, Peine

Hoisting Cage for 85t Payload

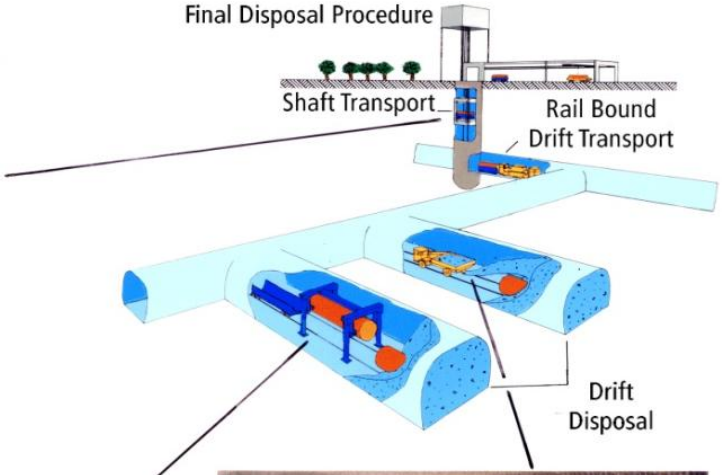

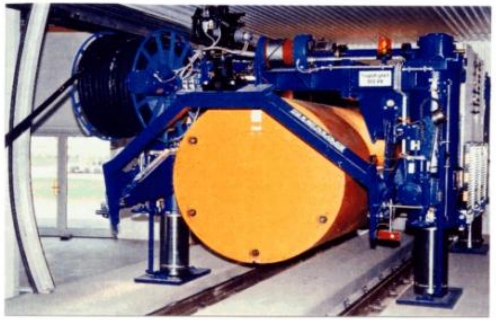

Waste Emplacement Machine

Backfilling Slinger Truck in a Disposal Drift

The Task

Feasibility of Cask Direct Disposal

- **Repository Design (thermal, mechanical)**

- **Handling and Disposal Design**
  - *Cask and cart loading into the shaft cage*
  - *Shaft hoisting to the underground disposal level*
  - *Cask and cart unloading from the shaft cage*
  - *Cask transfer in the shaft station to the transport and disposal vehicle*
  - *Transport to the disposal borehole with a battery driven locomotive*
  - *Cask disposal*

Handling and Transport of 12 different casks

Transport and Storage Cask –Types
CASTOR® V/19 (up to Series Nr. 005)
CASTOR® V/19* (from Series Nr. 006)
CASTOR® V/52
CASTOR® Iia
CASTOR® Ic (Series Nr. 02)
CASTOR® 440/84
CASTOR® HAW 20 / 28 CG (up to Series Nr. 015)
CASTOR® HAW 20 / 28 CG (from Series Nr. 016)
CASTOR® HAW 28 M
CASTOR® TS 28 V
TN 24 E / TN 85

Cask Masses up to 160 t

Cask Variants

CASTOR® V/19

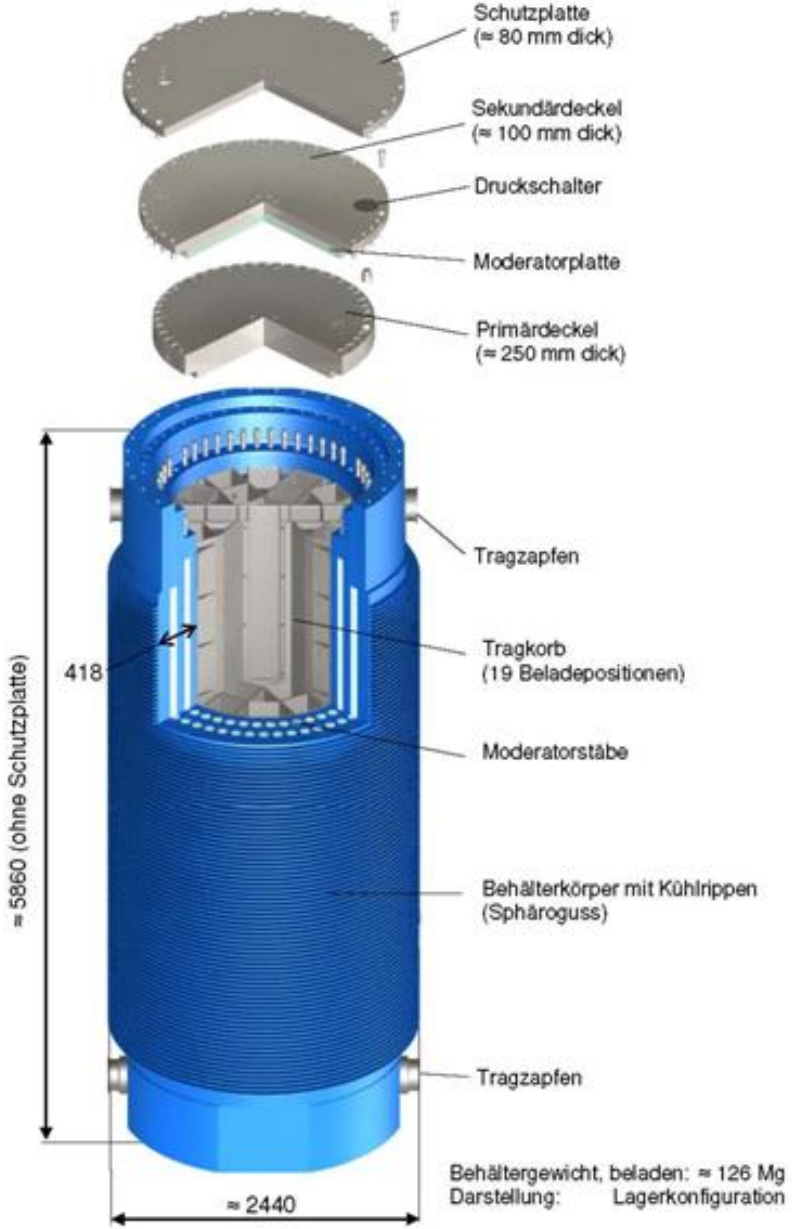

Source: GNS

Cask Variants

CASTOR® HAW 28 M

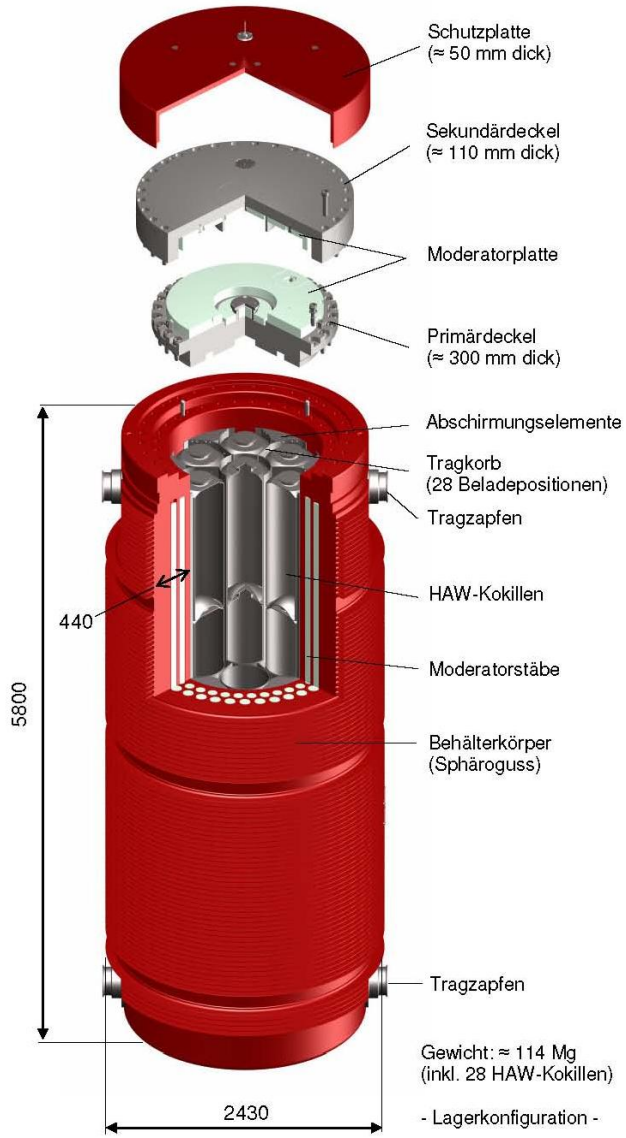

Quelle: GNS

Cask Example

Features to consider in the design

- *7 different distances between trunnions*
- *(4.720 mm – 5.200 mm)*
- *Different trunnion geometries at the cask head (lid) end*
- *Different trunnion geometries at the cask bottom end*
- *Different diametrical distances between trunnions, (2.395 mm - 2.720 mm) at the head end*
- *Different diametrical distances between trunnions, (2.395 mm - 2.720 mm) at the bottom end*

- *Different position of the cask's centers of gravity*

Hoisting System Design Data

Schacht Hoist with 175 t payload

Shaft diameter	7.5 m
Disposal horizon	870 m
Shaft depth	950 m
Cask weight (max.)	160 t
Transport cart weight	15 t
Cage weight including floating floor	48 t
Counterweight	133 t
Ropes (6) diameter	66 mm
Maximum unbalance	90 t
Hoisting speed	1m/s

Shaft Cage

Shaft Cage for 175 t Payload

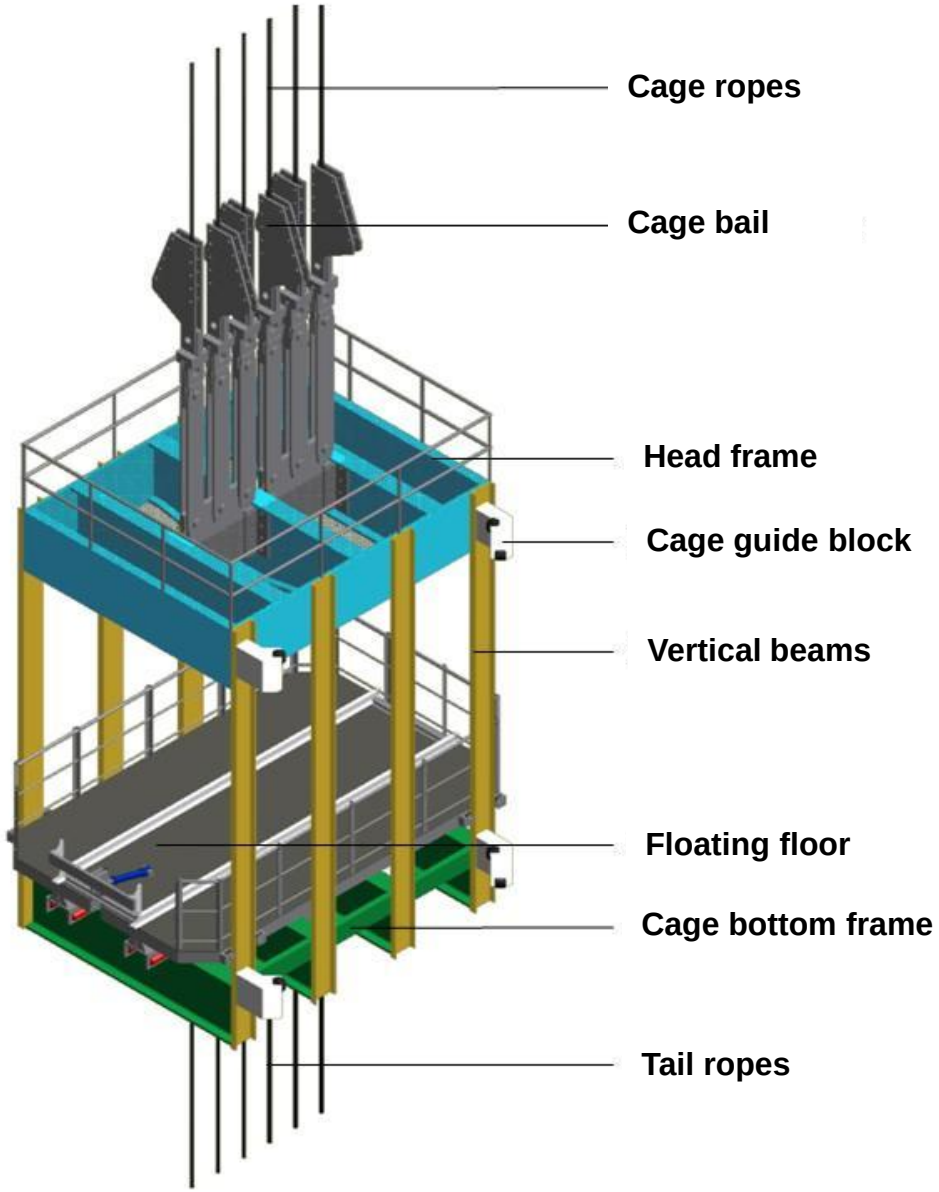

Shaft Cage

Shaft Cage
for 175 t Payload

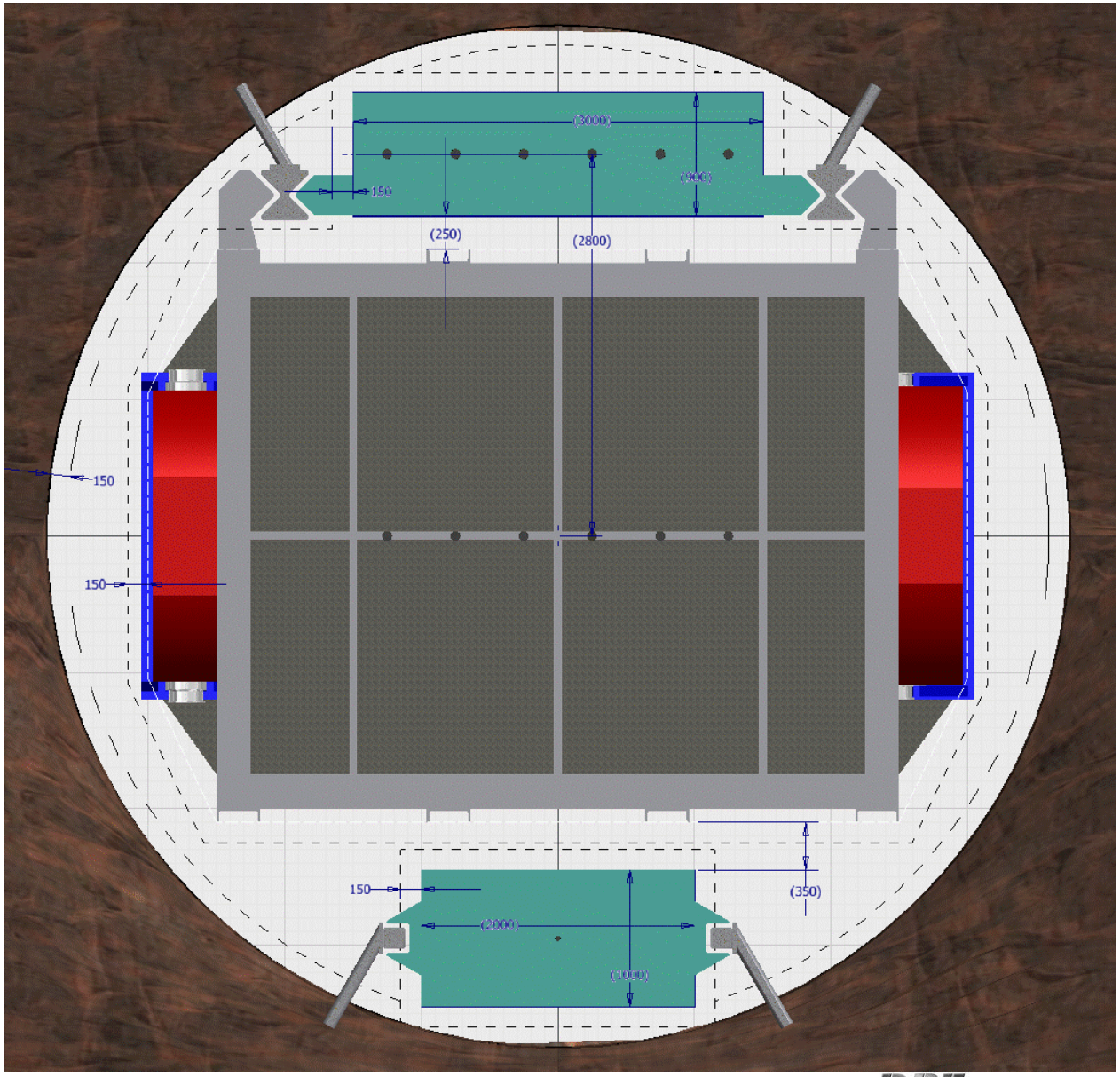

Shaft Hoisting System

25t Crane

Machine floor
Hoisting machine and
Auxiliary hoist

Gripping and lifting device

Bumper for hoisting cage and counter weight
Gripper
Selda-system

Hoisting Cage
Shaft station at 0 m

Shaft cellar

Fire doors

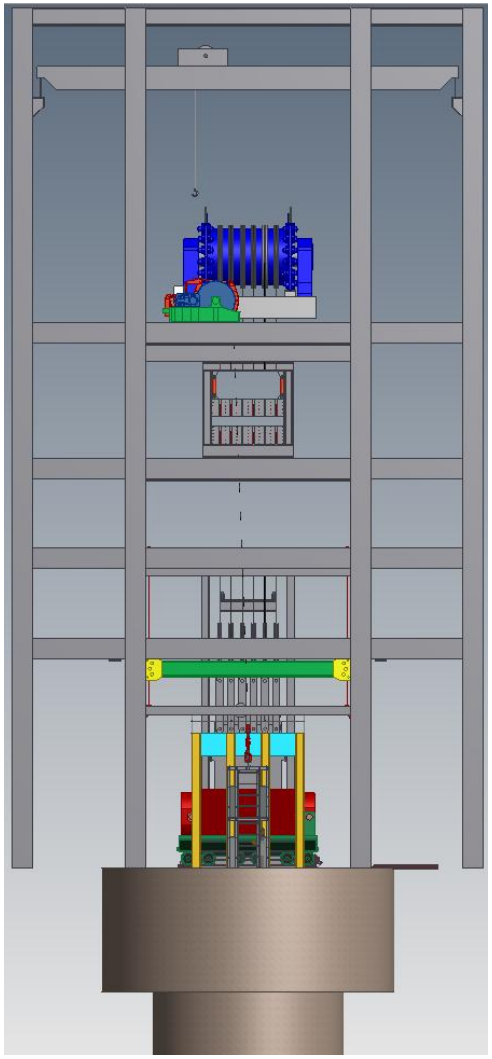

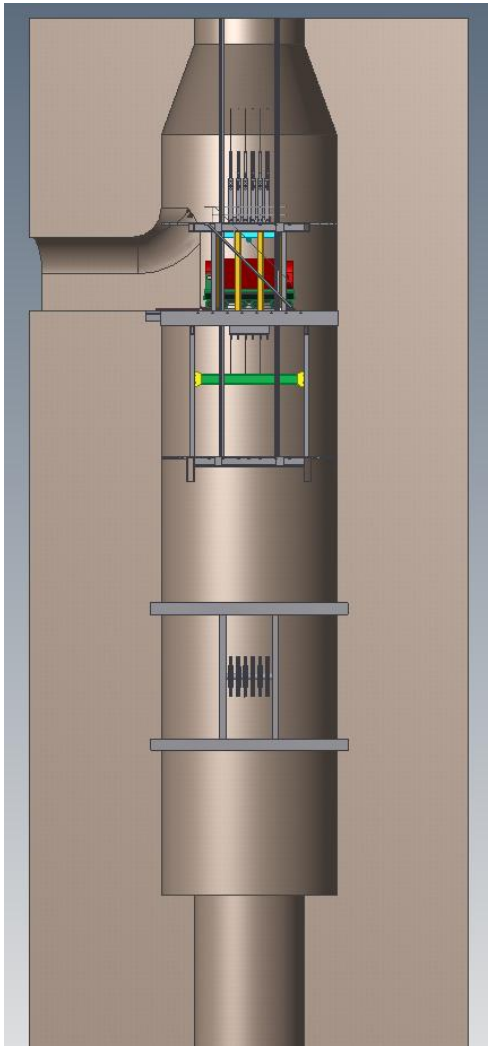

Shaft diameter enlargement to 12m

Shaft station at disposal level - 870m

Rope deflector at Level - 895m

Handling Steps Underground

- Unloading from the shaft cage
- Transfer in the shaft station to transport and disposal vehicle
- Transport to the disposal borehole with a battery driven locomotive
- Disposal

Shaft Hoisting Cart

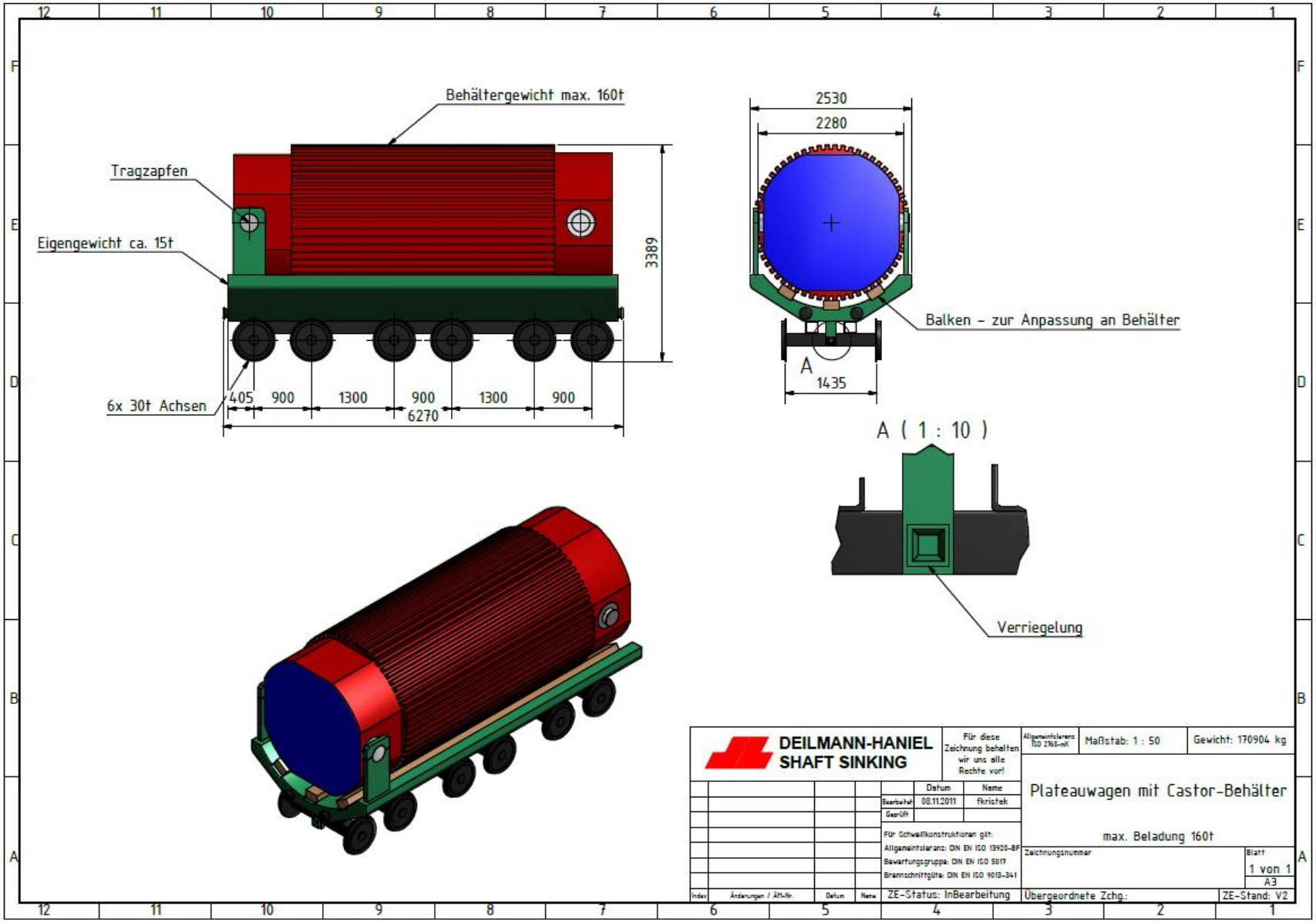

Shaft Station at the 870 m-Level

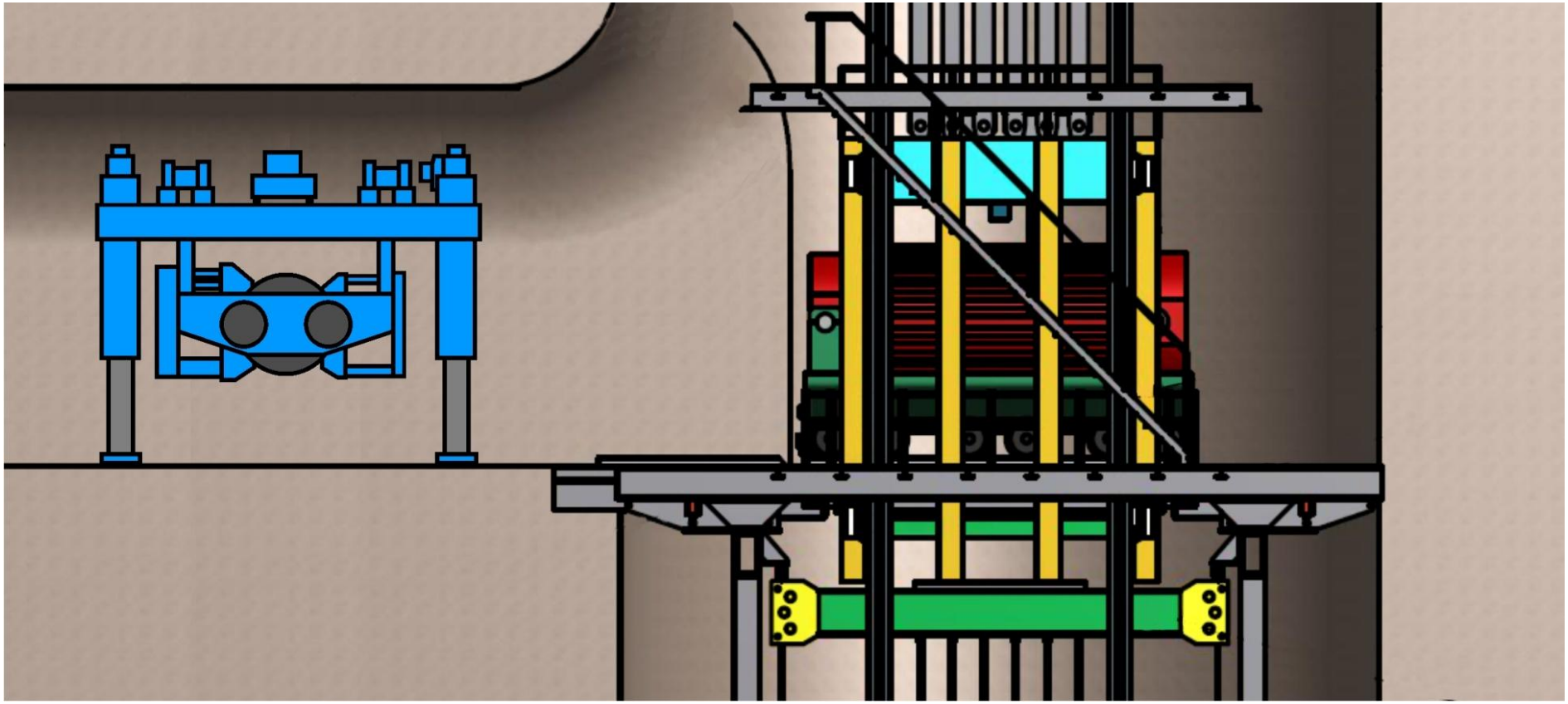

Requirements on the Gantry Crane

- Operational
  - Cask lifting from the shaft hoisting cart
  - Cask loading onto disposal device (optionally in slightly inclined position as the borehole
  - Handling of different cask types without backfitting

- Regulatory
  - KTA 3902 4.3 Lastaufnahmevorrichtung mit erhöhten Anforderungen – Status 06/1999 (lifting equipment for higher requirements)
  - According to 7.4.1.1 und 7.4.2.1 lifting capacity design with 1.25-times factored load
  - DIN 15018 Krane (11/1984)

Gantry Crane

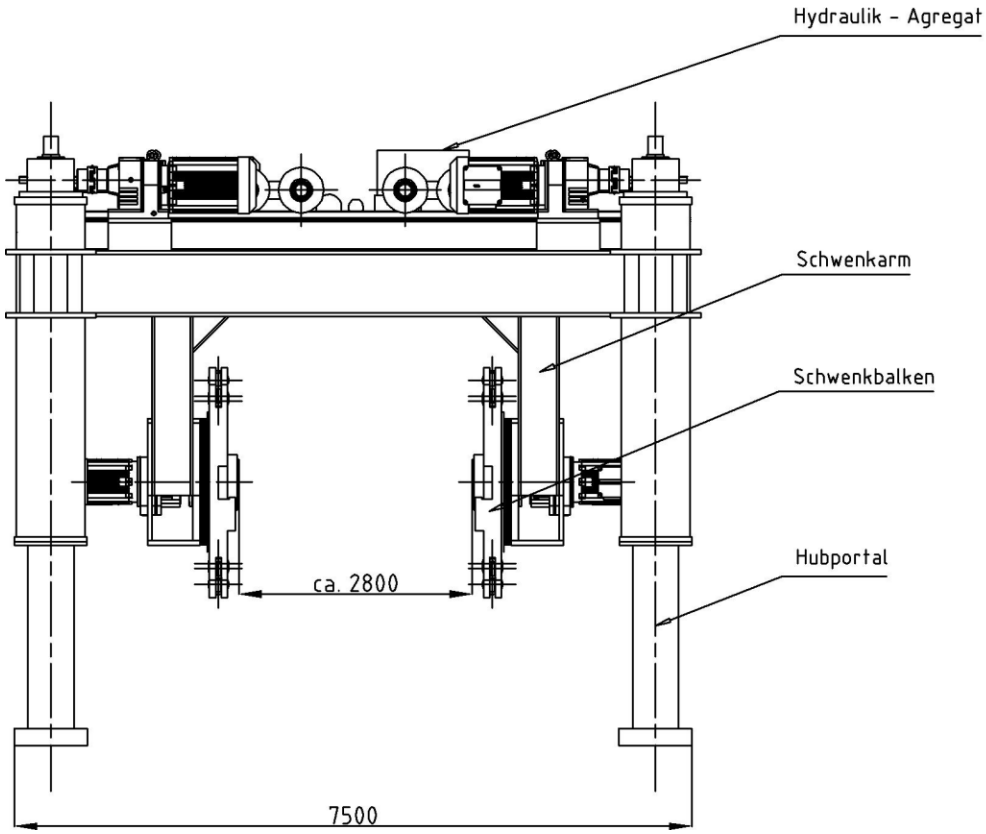

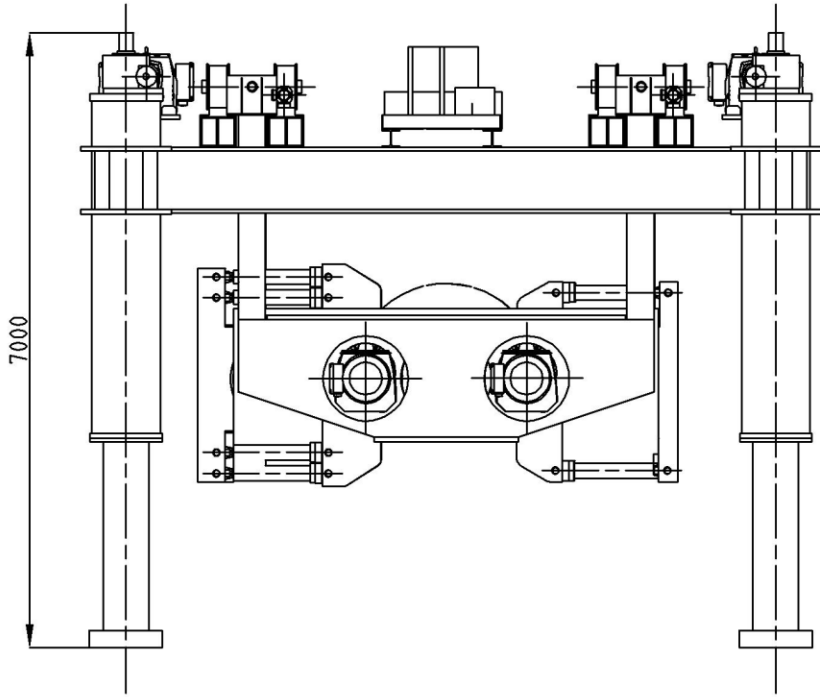

Hoist and Swing Gear

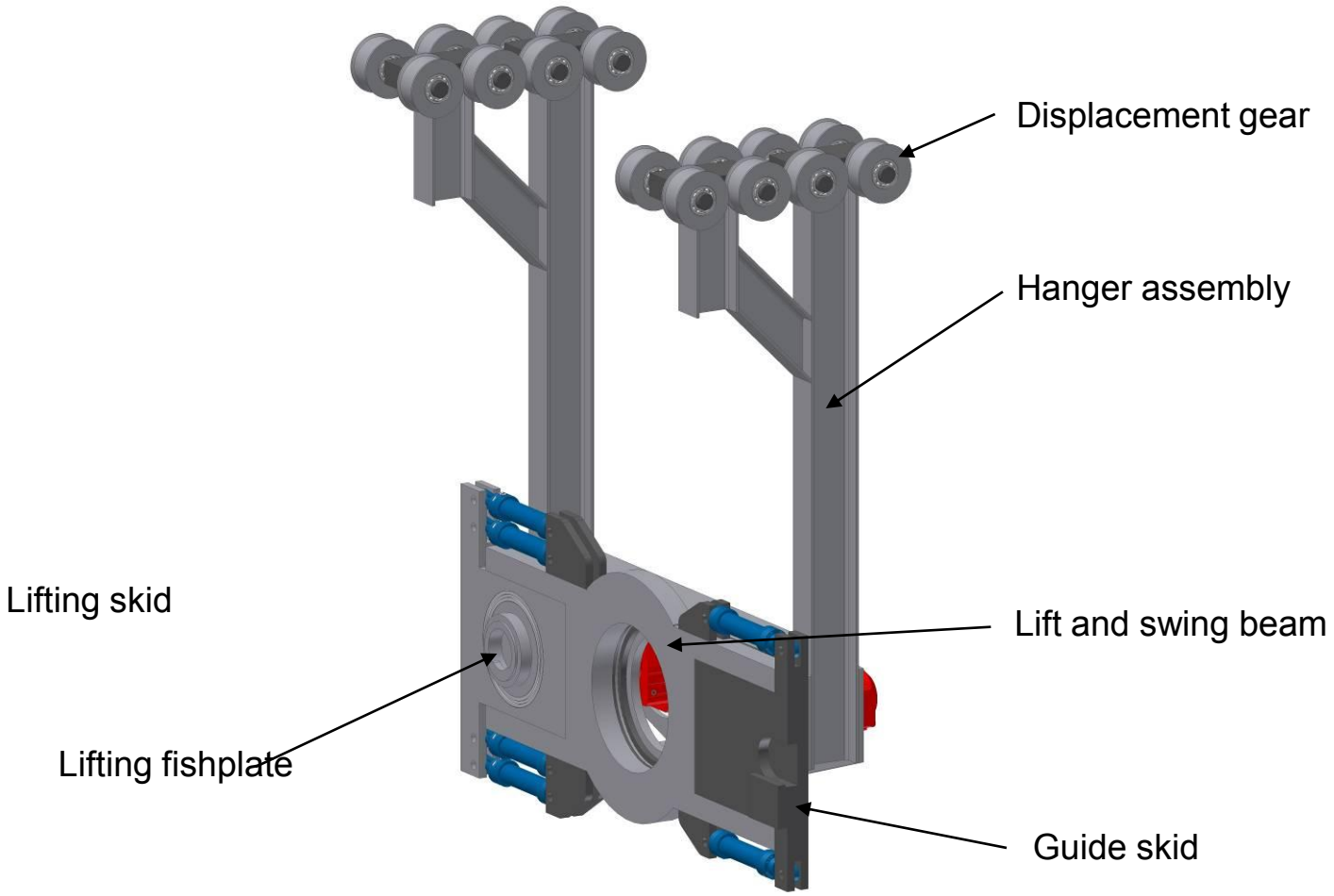

Gantry Crane Technical Data

Weight	=	ca. 130 t	
Payload	=	max. 160 t	
Length	=	ca. 8 m	
Width	=	ca. 7,5 m	With electric engine for turning beam
Width	=	ca. 7 m	With electro-hydraulic engine for turning beam
Height	=	ca. 7 m	
Height max.	=	ca. 8 m	

CASTOR® Cask Disposal Field

Disposal field for 70 casks

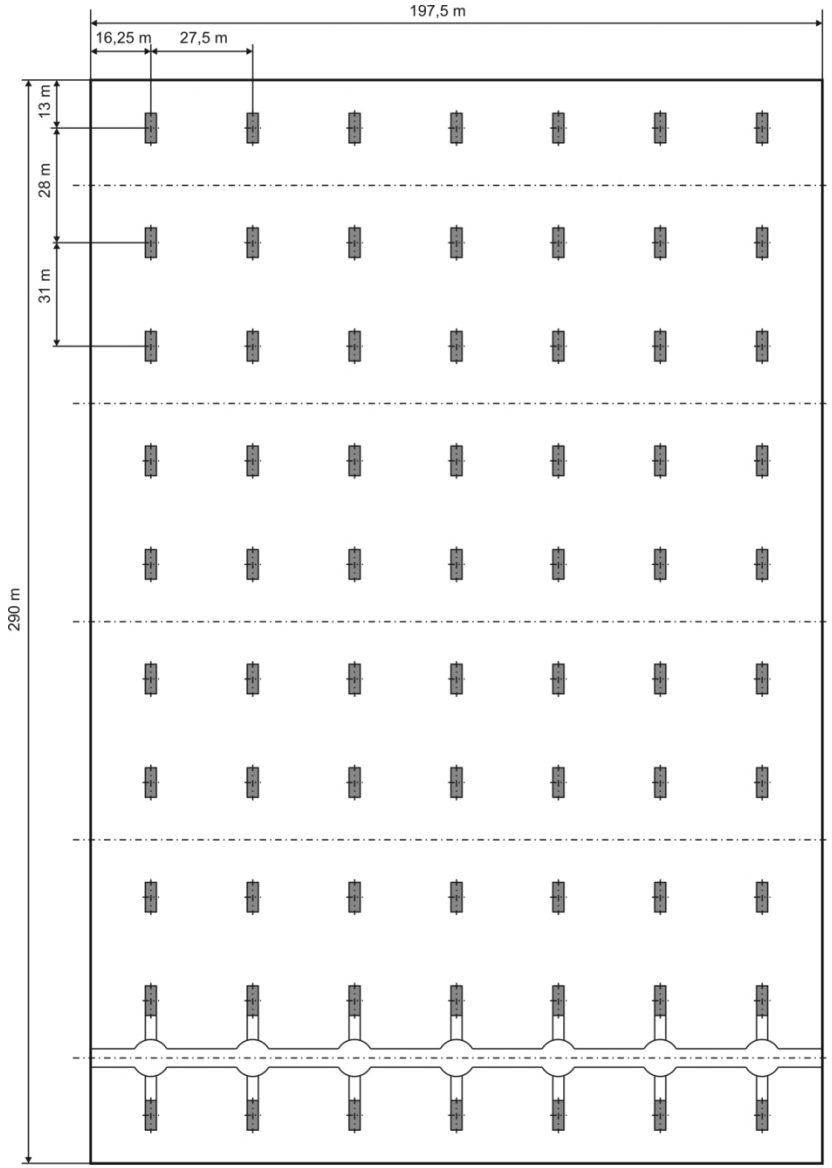

Disposal Machine

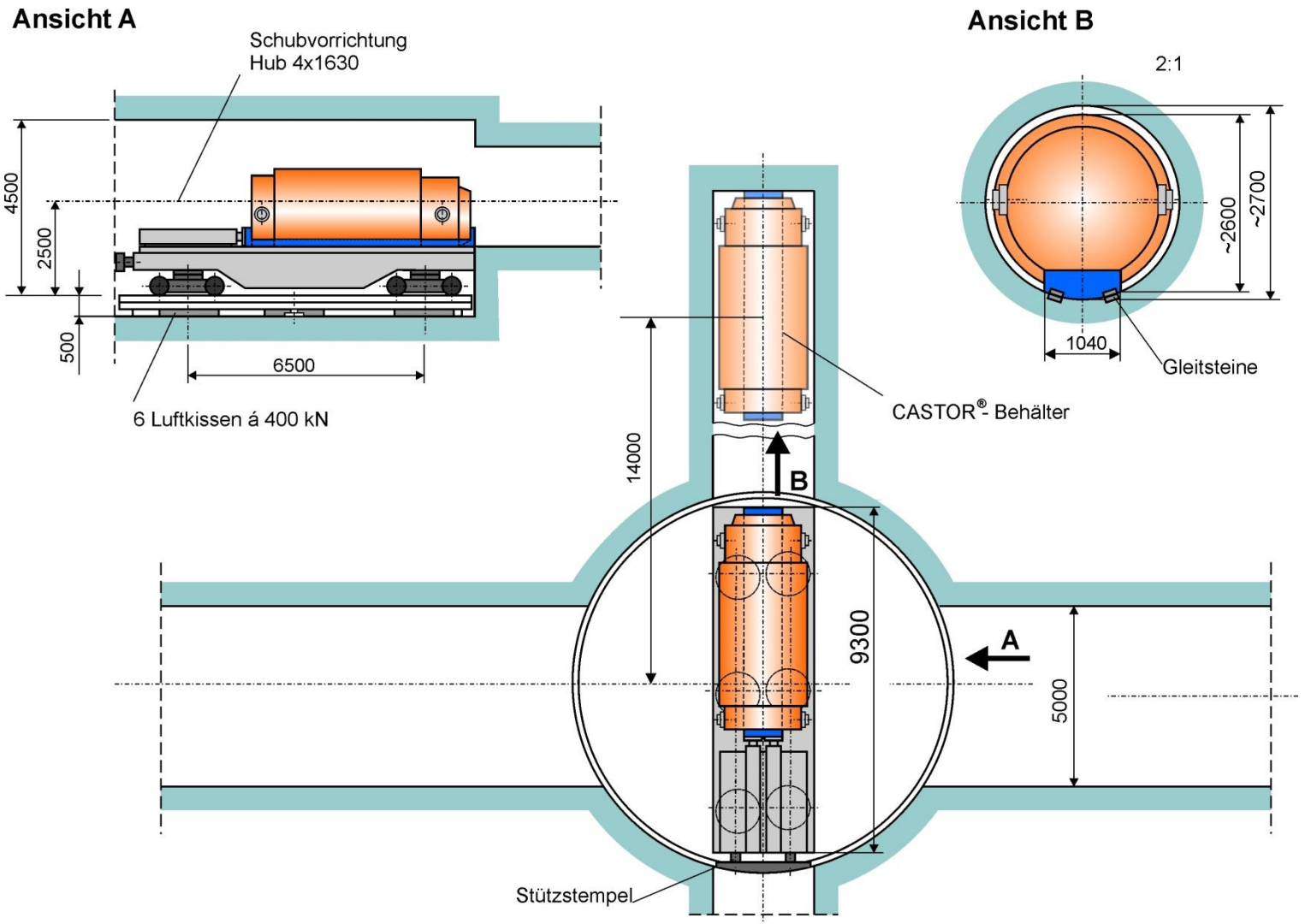

Cask on Lost Skid

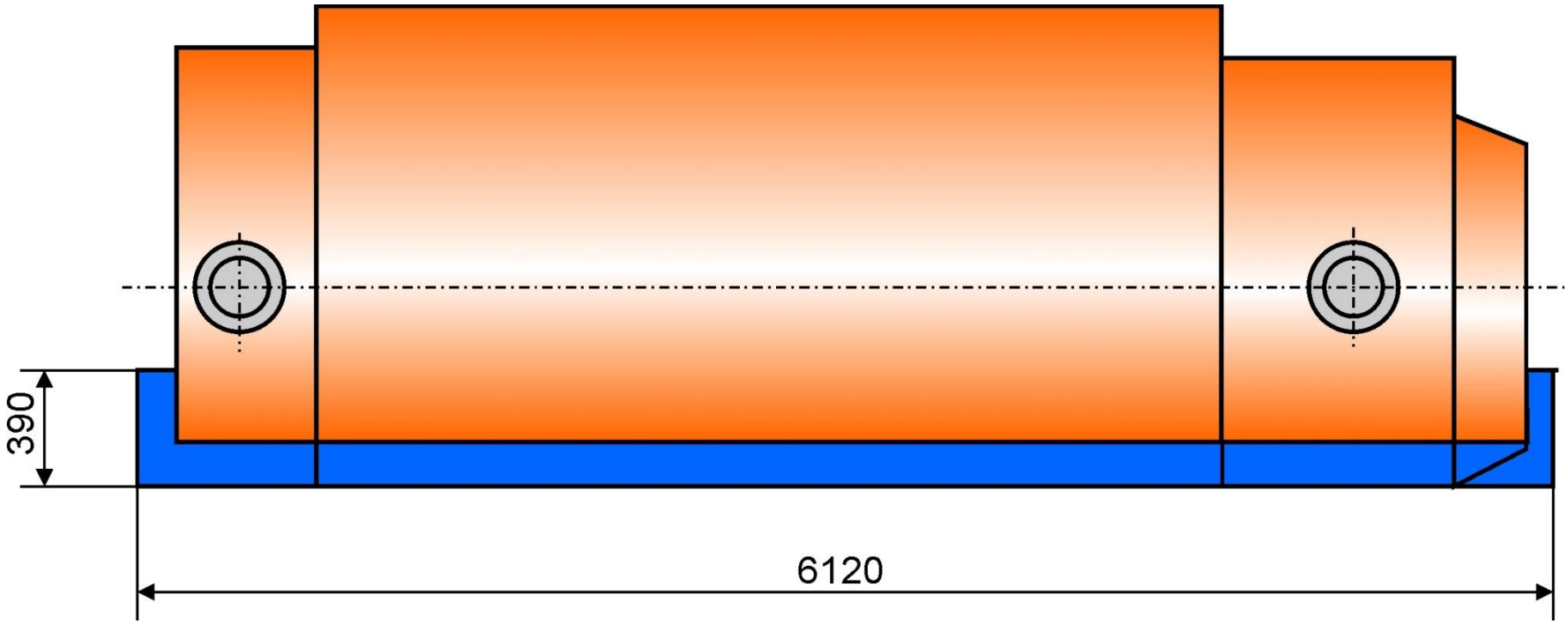

DBE TECHNOLOGY GmbH

Thank you
for your attention!

PTKA
Project Management Agency Karlsruhe
Karlsruhe Institute of Technology

BGR Bundesanstalt für Geowissenschaften und Rohstoffe

BRIUG

AGENDA

2nd Chinese-German Workshop on Radioactive Waste Disposal

Karlsruhe
October 15-16, 2012

Venue
Karlsruhe Institute of Technology (KIT)
Campus North, Building 419

Monday, October 15

11:30 - 13:00 Arrival & Registration & refreshment & Kantine

13:00 Welcome address KIT and PTKA/BGR/BMWi
13:15 Welcome address Mr. Lin, CNNC

13:30 Geological Disposal of high-level radioactive waste in China: update 2012 (Wang, BRIUG)
14:00 A new approach for siting a repository for HLW in Germany (Bräuer, BGR)

Topic: Host rock characterization (rock mechanics / hydrogeology)

14:30 Rock mass characterization for the preselected Beishan area, Gansu province of China´s HLW radioactive waste repository (Wang, CAS, Institute of Soil & Rock Mechanics)
15:00 Multi-scale applications of electrical resistivity tomography in the site characterization for HLW disposal (Zhou, Nanjing University)
15:30 Characterization of fracture networks on different scales (Li, Nanjing University)

16:00 Break

16:30 German experience & investigations regarding host rock characterization (Shao, Sönnke, BGR)
17:00 Radionuclide transport in crystalline formations: laboratory and field experiments (Schäfer, KIT-INE)
17:30 A fractional derivative approach to creep of rock salt (Zhou, CU of Mining & Technology)
18:00 Basics of waste disposal in rock salt mass (Lux, TUC)

19:00 Dinner

21:30 Bus transport to hotels

PTKA
Project Management Agency Karlsruhe
Karlsruhe Institute of Technology

BGR Bundesanstalt für Geowissenschaften und Rohstoffe

BRIUG

Tuesday, October 16

Topic: Technical / geotechnical barriers

08:30 THMC-testing of expandable clays for potential use in HLW disposal repository (Liu, East China Institute of Technology)
09:00 Experimental investigation on thermo-hydraulic behavior of compacted GMZ02 bentonite (Ye, Tongji University)
09:30 Initial results on stability of natural GMZ Ca-Bentonite & modified Na-Bentonite under Thermal/radiation Aging (Yang, China Institute for Radiation Protection)
10:00 THM-Behavior of clay (Zhang, GRS)

Break 10:30

11:00 Bentonit characterization / behavior (Kaufhold/Dohrmann , BGR)
11:30 Project "PEBS" (Wiezcorek, GRS)
Modeling of Bentonite behavior (Li, TU Clausthal)

12:00 – 13:00 Lunch

Topic: RN-Behavior

13:00 Study on the long-term behavior of HLW glass in geological conditions (Wang, CAEA)
13:30 Source Terms for highly radioactive wastes (HLW glass and spent fuel) (Geckeis, Kienzler, KIT/INE)
14:00 RN migration research to support geological disposal of HLW in China (Zhou, CAEA)
14:30 Critical issues for Pu239 in geological disposal (Tuo, Chendu University)
Chemical behavior of 239Pu in the groundwater solution (Huang, Chendu University)

Topic: Technical/Engineering

15:00 Feasibility of CS canister used for HLW geological disposal (Dong, CAS, Inst. of Metal Research)
15:30 German concepts for containers/casks for HLW-disposal (Filbert, Bollingerfehr, Biurrun, DBE Tec)
16:00 Summary

Adjourn 17:00
Transport to Karlsruhe Main Station / Hotels

Optional: Technical visit Schachtanlage Konrad, October 18, 2012

Wednesday, October 17
Transport by bus from Karlsruhe to Wolfenbüttel (Parkhotel)
Thursday, October 18
Technical Visit "Schachtanlage Konrad", bus to Frankfurt

List of participants

Name	Organization	Address	Email
Junhua DONG	Institute of Metal Research, CAS	62, Wencui Road, Shenyang, 110016, China	jhdong@imr.ac.cn
Bo WANG	China Institute of Atomic Energy (CIAE)	P.O. Box 275-93, Xin Zhen, Fang Shan District, Beijing 102413	yyxwb4672@163.com
Duo ZHOU	China Institute of Atomic Energy (CIAE)	P.O. Box 275-93, Xin Zhen, Fang Shan District, Beijing 102413	zd-ciae@163.com
Hongwei ZHOU	China University of Mining and Technology (Beijing)	Xueyuan Road D11, Beijing 100083	zhw@cumtb.edu.cn
Xiaozhao LI	Nanjing University	Han Kou Road #22, Nanjing 210093	lixz@nju.edu.cn
Weimin YE	Tongji University	1239 Siping Road, Shanghai	Ye_tju@tongji.edu.cn
Tao LIU	Southwest university of science and technology	59, Mid-section of Quinglong Road, Fucheng district, Mianyang, Sichuan, China, 621010	swust_lt@sina.com
Jinyong XU	Chengdu University of Technology	No. 1, Dongsan Road, Erxianqiao, Chenghua District, Chengdu	xujinyong@cdut.cn
Lin Sen	CNNC, Department of International Business	No.1, Nansanxiang, Sanlihe, Xicheng	Lins8080@163.com
Ning LI	China Nuclear Power Engineering Co., Ltd.	No. 117, Xisanhuanbeilu, Haidian District, Beijing, 100840	lininga@cnpe.cc
Xuhong WANG	China Nuclear Power Engineering Co. Ltd.	No. 117, Xisanhuanbeilu, Haidian District, Beijing, 100840	wangxh@cnpe.cc
Qiuyu YANG	China Nuclear Power Engineering Co. Ltd.	No. 117, Xisanhuanbeilu, Haidian District, Beijing, 100840	yangqy@cnpe.cc
Liang XIE	China Nuclear Power Engineering Co. Ltd.	No. 117, Xisanhuanbeilu, Haidian District, Beijing, 100840	xieliang@cnpe.cc
Hongbin MA	China Nuclear Power Engineering Co. Ltd.	No. 117, Xisanhuanbeilu, Haidian District, Beijing, 100840	anhuima@yahoo.cn
Zhongtian YANG	China Institute for Radiation Pro-tection	Xuefu street, P.O. Box 120, 030006, T aiyuan, Shanxi Province	ztyang@263.net
Qiyou ZHOU	Nanjing University	Han Kou Road #22, Nanjing 210093	zhouqy@nju.edu.cn
Pinghui LIU	East China Institute of Technology	No. 56 Xuefu Road, Fuzhou City, Jiangxi Province, 344000	pinghui_liu@126.com
Guibin WANG	Institute of Rock and Soil Mechanics, Chinese Academy of Science	Xiao Hong Shan, Wuchang District, Wuhan, Hubei, China, 40071	gbwang@whrsm.ac.cn
Taian LUO	East China Institute of Technology	No. 56 Xuefu Road, Fuzhou City, Jiangxi	taluo@ecit.cn

Name	Organization	Address	Email
		Province, 344000	
Ju WANG	Beijing Research Institute of Uranium Geology	10 Xiaoguandongli, Anwai, Beijing 100029	Wangju@briug.cn
Nana LI	Beijing Research Institute of Uranium Geology	10 Xiaoguandongli, Anwai, Beijing 100029	linana@briug.cn
Yuanxin JIN	Beijing Research Institute of Uranium Geology	10 Xiaoguandongli, Anwai, Beijing 100029	jinyuanxin@briug.cn
Xiyong WANG	Beijing Research Institute of Uranium Geology	10 Xiaoguandongli, Anwai, Beijing 100029	wangxiyong@briug.cn
Yu TAO	CNNC, Department of International Cooperation	No.1, Nansanxiang, Sanlihe, Xicheng	549502986@qq.com
STEININGER Walter	KIT/PTKA-WTE	Karlsruhe Institut für Technologie, Hermann-von-Helmholtz-Platz 1, 76344 Eggenstein-Leopoldshafen	Walter.steininger@kit.edu
BRÄUER Volkmar	BGR	Bundesanstalt für Geowissenschaften und Rohstoffe (BGR), Geozentrum Hannover Stilleweg 2, 30655 Hannover	Volkmar.braeuer@bgr.de
SHAO Hua	BGR	Bundesanstalt für Geowissenschaften und Rohstoffe (BGR), Geozentrum Hannover Stilleweg 2, 30655 Hannover	shao@bgr.de
SÖNNKE Jürgen	BGR	Bundesanstalt für Geowissenschaften und Rohstoffe (BGR), Geozentrum Hannover Stilleweg 2, 30655 Hannover	Juergen.soennke@bgr.de
DOHRMANN Reiner	BGR	Bundesanstalt für Geowissenschaften und Rohstoffe (BGR), Geozentrum Hannover Stilleweg 2, 30655 Hannover	Reiner.dohrmann@bgr.de
KAUFHOLD Stephan	BGR	Bundesanstalt für Geowissenschaften und Rohstoffe (BGR), Geozentrum Hannover	Stephan.kaufhold@bgr.de
MENTE Michael	BGR	Bundesanstalt für Geowissenschaften und Rohstoffe (BGR), Geozentrum Hannover Stilleweg 2, 30655 Hannover	Michael.mente@bgr.de
LUX Karl-Heinz	TU Clausthal	Institut für Aufbereitung, Deponietechnik und Geomechanik, Lehrstuhl für Deponietechnik und Geomechanik, Erzstraße 20, 38678 Clausthal-Zellerfeld	lux@tu-clausthal.de
HERCHEN Kai	TU Clausthal	Institut für Aufbereitung, Deponietechnik und Geomechanik, Erzstraße 20, 38678 Clausthal-Zellerfeld	Kai.Herchen@tu-clausthal.de
HOU Michael	TU Clausthal	Technische Universität Clausthal, Institut für Erdöl- und Erdgastechnik, Agricolastraße 10 38678 Clausthal-Zellerfeld	hou@tu-clausthal.de

Name	Organization	Address	Email
LI Xiaoshuo	TU Clausthal	Technische Universität Clausthal, Institut für Endlagerforschung, Adolph-Roemer-Straße 2A, 38678 Clausthal-Zellerfeld	xiaoshuo.li@tu-clausthal.de
ROTHFUCHS Tilmann	GRS	Gesellschaft für Anlagen- und Reaktorsicherheit mbH, FB Endlagersicherheitsforschung, Theodor-Heuss-Str. 4, 38122 Braunschweig	Tilmann.rothfuchs@grs.de
MÖNIG Jörg	GRS	Gesellschaft für Anlagen- und Reaktorsicherheit mbH, FB Endlagersicherheitsforschung, Theodor-Heuss-Str. 4, 38122 Braunschweig	Joerg.moenig@grs.de
ZHANG Chun-Liang	GRS	Gesellschaft für Anlagen- und Reaktorsicherheit mbH, FB Endlagersicherheitsforschung, Theodor-Heuss-Str. 4, 38122 Braunschweig	Chun-Liang.zhang@grs.de
WIECZOREK Klaus	GRS	Gesellschaft für Anlagen- und Reaktorsicherheit mbH, FB Endlagersicherheitsforschung, Theodor-Heuss-Str. 4, 38122 Braunschweig	Klaus.wieczorek@grs.de
BREUSTEDT Michael	DBE TECHNOLOGY	Eschenstraße 55, D-31224 Peine	breustedt@dbe.de
BÜHLER Michael	KIT/PTKA-WTE	KIT, Hermann-von-Helmholtz-Platz 1,	Michael.buehler@kit.edu
BITTDORF Holger	KIT/PTKA-WTE	KIT, Hermann-von-Helmholtz-Platz 1,	holger.bittdorf@kit.edu
STACHEDER Markus	KIT/PTKA-WTE		Markus.stacheder@kit.edu
KIENZLER Bernhard	KIT/INE	KIT, Hermann-von-Helmholtz-Platz 1,	Bernhard.kienzler@kit.edu
GECKEIS Horst	KIT/INE	KIT, Hermann-von-Helmholtz-Platz 1,	Horst.geckeis@kit.edu
SCHÄFER Thorsten	KIT/INE	KIT, Hermann-von-Helmholtz-Platz 1,	Thorsten.schäfer@kit.edu

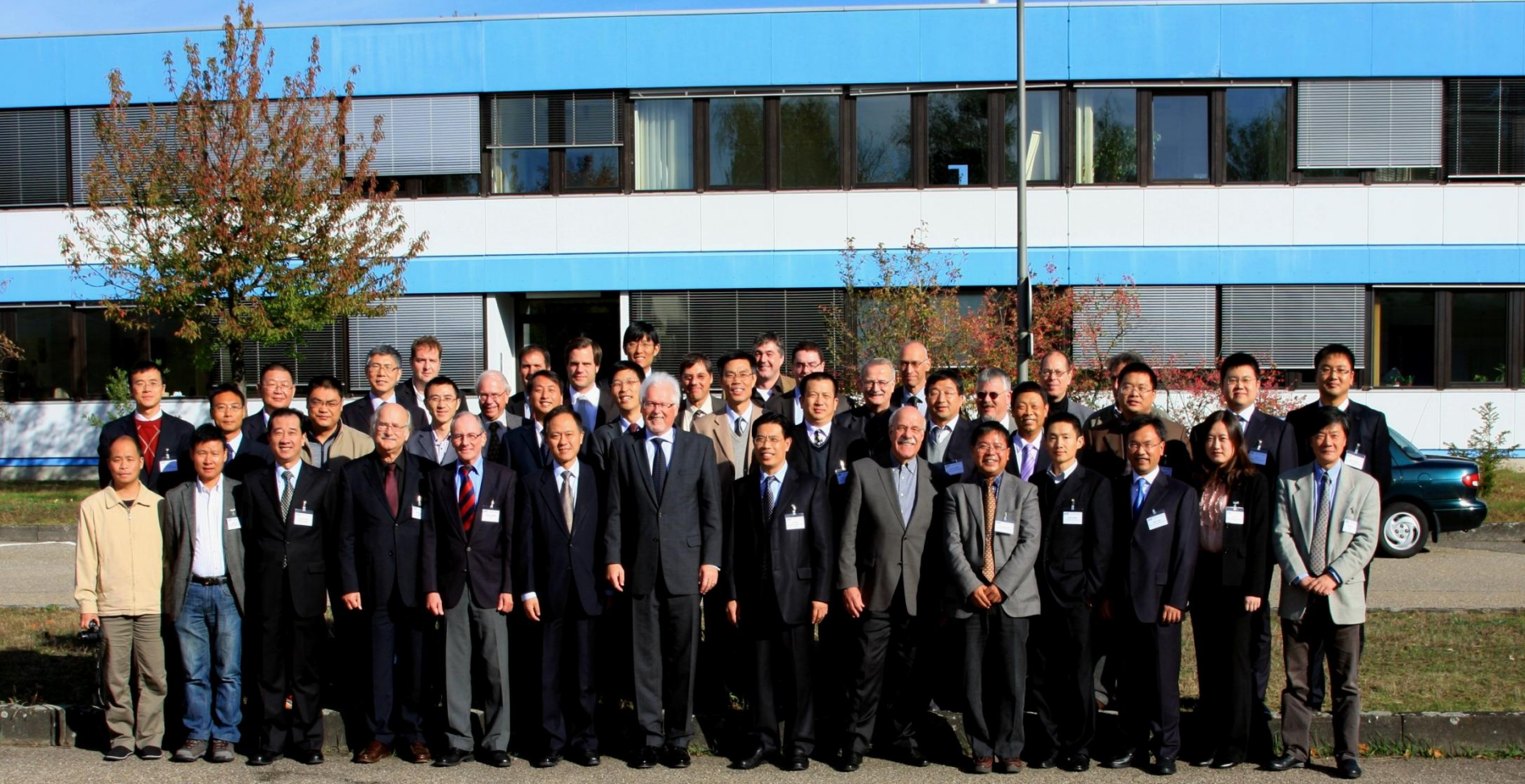

2nd- Chinese-German Workshop on Radioactive Waste Disposal

Karlsruhe, October 15 -16, 2012